PERFORMANCE IMPROVEMENT OF WEAK CLAY FOUNDATION USING STONE COLUMN AND GEOCELL-SAND MATTRESS

A THESIS

submitted by

MUKUL CHANDRA BORA

for the award of the degree

of

DOCTOR OF PHILOSOPHY

DEPARTMENT OF CIVIL ENGINEERING
INDIAN INSTITUTE OF TECHNOLOGY GUWAHATI

NOVEMBER 2010

Dedicated to my heavenly parents
whose inspiration and blessings
brought me to this stage

THESIS CERTIFICATE

This is to certify that the thesis entitled **PERFORMANCE IMPROVEMENT OF WEAK CLAY FOUNDATION USING STONE COLUMN AND GEOCELL-SAND MATTRESS** submitted by Mukul Chandra Bora to the Indian Institute of Technology Guwahati for the award of the degree of Doctor of Philosophy is a bonafide record of research work carried out by him under my supervision. The contents of this thesis, in full or in parts, have not been submitted to any other Institute or University for the award of any degree or diploma.

Guwahati - 781 039
Date:

Dr. Sujit Kumar Dash
Associate Professor

STATEMENT

I do hereby declare that the matter embodied in this thesis is the result of investigations carried out by me in the Department of Civil Engineering, Indian Institute of Technology Guwahati, Guwahati, Assam, India.

In keeping with the general practice of reporting scientific observations, due acknowledgements have been made wherever the work described is based on the findings of other investigators.

Guwahati - 781 039 **Mukul Chandra Bora**
Date:

AKNOWLEDGEMENTS

I have great pleasure in expressing my deep sense of gratitude to my thesis supervisor, Dr. Sujit Kumar Dash for his inspiring guidance and constant encouragement throughout the course of my research work. I am grateful to him for sparing his valuable time and effort at all stages upto the completion of the work. I am very much obliged to him for all the help, affection and kind words, which helped me to complete the work successfully.

I am thankful to Prof. S. K. Deb, Head Civil Engineering Department for all the help rendered to me during my research. I am indebted to the all the Doctoral Committee members for sparing their valuable time in reviewing my work. I also thank Prof. S. Talukdar for his suggestions for the research work.

The study leave provided by the Department of Higher and Technical Education, Government of Assam, Dispur is gratefully acknowledged.

I extend my thanks to Mr. A. Borsaikia, Mr. Kumar Pallav, scientific officer; Mr. H. R. Upadhaya, technical assistant; Md. Bajal, project staff; workshop instructor; Mr. Gohain and Mr. Mrinal Sharma for their help in carrying out the experimental work.

My sincere thanks to my fellow research scholars Miss Minaxi and Md. Monowar Hussain for their consistent companionship. I thank all the M. Tech. students for their cheerful company.

I deeply express my heartfelt gratitude and thanks to my wife Runmi whose support is highly solicited.

MUKUL CHANDRA BORA

ABSTRACT

Keywords: Bearing capacity, soft clay, stone column, geocell-sand mattress, circular footing.

Due to the ever increasing demand for land space because of increased construction activity world wide, there is an increasing need to improve soft soil grounds which otherwise are deemed to be unsuitable. Ground improvement technique is a potential alternative to mitigate this problem. Amongst the various ground improvement techniques used for improving the in-situ ground conditions, geosynthetics reinforcement and stone column technique are the widely used ones. The three dimensional geocells are the latest adaptation in the avenues of geosynthetic reinforcements. It is a three dimensional, polymeric, honeycomb like structure of cells interconnected at joints. The reinforcement mechanism in the geocells is by all-round confinement of soil within its pockets. The stone columns are formed by compacting stones into the cylindrical hole formed in soft clay bed, generally by vibro-floatation technique. When load is applied the stone column develops end bearing and skin friction resistance as in piles. Their individual application of both these techniques has been studied well. However, combined application of both, has remained unexplored.

Under the present study a series of experiments have been carried out to develop an understanding of the behaviour of foundation systems having geocell-sand mattress overlying stone column reinforced clay beds. The model tests were conducted in a test bed-cum-loading frame assembly in the laboratory. The influence of various parameters, such as; length and spacing of stone columns; pocket size, height, density of fill soil in geocell mattress; base geogrid and encasement of stone columns were systematically studied.

The test results indicate that, with the provision stone columns, of adequate length and spacing, 3.5 fold increases in bearing capacity of soft clay foundations can be achieved. With geocell mattress of optimum geometry and dense soil infill, seven fold increase in bearing capacity of the clay foundation can be achieved. While, the geocell mattress-stone column composite reinforcement can increase the bearing capacity of clay bed by ten fold. The increase in the load carrying capacity and reduction in settlement, of the composite reinforced foundation bed, increases with increase in length of stone columns till 5_{dc}, beyond which further improvement is marginal. The optimum spacing of stone columns in composite foundation beds is $2.5d_{sc}$. With further reduction in spacing, the stone columns do not produce much of additional performance improvement. The critical height of geocell mattress, giving optimum performance of stone columns in the composite foundation bed, is equal to about the diameter of the footing.

A layer of planar geogrid at the interface between the geocell mattress and stone column reinforced clay bed can bring an improvement in bearing capacity as high as 30% more than that with the geocell mattress-stone column reinforcement alone. Encasement of stone columns further improves the performance, with the bearing capacity increasing with the increase in the length of encasement. However, with full length encasement of the floating stone columns the performance improvement reduces substantially. Combined application of base geogrid and encasement of stone columns is an added advantage that brings further improvement in load carrying capacity of the composite foundation bed.

Dimensional analysis shows that, the results of the present study to be applicable in practice, the strength of the prototype geocell should be of N^2 times the strength of the model geocells, where N is the model scale.

TABLE OF CONTENTS

Table of Contents (continued) **Page**

CHAPTER 3 EXPERIMENTAL INVESTIGATIONS

CHAPTER 4 STONE COLUMN REINFORCED CLAY BED

CHAPTER 5 GEOCELL SAND MATTRESS REINFORCED CLAY BED

Table of Contents (continued) **Page**

Table of Contents (continued) **Page**

CHAPTER 9 SUMMARY AND CONCLUSIONS

LIST OF TABLES

LIST OF FIGURES

List of Figures (continued) **Page**

List of Figures (continued) **Page**

List of Figures (continued) **Page**

List of Figures (continued) **Page**

List of Figures (continued) **Page**

List of Figures (continued) **Page**

List of Figures (continued) **Page**

List of Figures (continued) **Page**

List of Figures (continued) **Page**

List of Figures (continued) **Page**

List of Figures (continued) **Page**

List of Figures (continued) **Page**

List of Figures (continued) **Page**

GLOSSARY

Base geogrid	geogrid provided at the base of the geocell layer
Bodkin	plastic strip used to connect geogrids in a geocell structure
Infill soil	soil filled in the geocell pockets
Pocket size	equivalent diameter of the geocell pockets

ABBREVIATIONS

ASTM	American Society of Testing Materials
BG	base geogrid
BX	biaxial Geogrid
DT	displacement transducer
ESC	encased stone column
GC	geocell
GI	galvenised iron
IF	improvement factor
LVDT	linear variable displacement transducer
PRS	Percentage Reduction in footing settlement
SC	stone column

NOTATION

English Symbols

c_u	undrained strength of the clay
C_c	coefficient of curvature
C_u	coefficient of uniformity
d_{gc}	equivalent diameter of geocell pockets
d_{sc}	diameter of stone column
D	diameter of circular footing
D_{10}	grain size corresponding to 10% finer
D_{30}	grain size corresponding to 30% finer
D_{50}	grain size corresponding to 50% finer
D_{60}	grain size corresponding to 60% finer
h	height of geocell mattress
IF_{sc}	improvement factor with stone column
IF_{gc}	improvement factor with geocell sand mattress
IF_{gesc}	improvement factor with stone column and geocell sand mattress
IF_{gescbg}	improvement factor with stone column, geocell sand mattress and base geogrid
IF_{esc}	improvement factor with encased stone column
IF_{gcesc}	improvement factor with encased stone column and geocell sand mattress
$IF_{gcescbg}$	improvement factor with encased stone column, geocell sand mattress and base geogrid
ID	relative density of sand
L	length of stone column
L_{esc}	length of encasement of stone column
q_{sc}	footing pressure with stone column
q_{gc}	footing pressure with geocell sand mattress
q_{gcsc}	footing pressure with stone column and geocell sand mattress
q_{gcscbg}	footing pressure with geocell sand mattress, stone column and base geogrid
q_{esc}	footing pressure with encased stone column
q_{gcesc}	footing pressure with geocell sand mattress and encased stone column

$q_{gcescbg}$	footing pressure with geocell sand mattress, encased stone column and base geogrid
q	footing pressure on unreinforced clay bed
q_{gc}	footing pressure with additional geogrid
q_{ult}	ultimate footing pressure on reinforced sand bed
S	spacing of stone columns
S_r	degree of saturation
s	footing settlement
u	depth to the top of reinforcement layer
x	distance from center of footing

Greek Symbols

δ	surface deformation
γ_{dmax}	Maximum dry density
γ_{dmin}	Minimum dry density
γ_b	Bulk density of clay
ϕ	angle of internal friction of the soil
ψ	dilation angle

CHAPTER 1

INTRODUCTION

1.1 BACKGROUND

Due to the ever increasing demand for land space because of increased construction activity world wide, there is an increasing need to improve soft soil grounds which otherwise are unsuitable for adopting the conventional shallow foundations. Using deep foundations, such as pile, to bypass the weak soil is often costly. Ground improvement technique is a potential alternative to mitigate this problem. Amongst the various ground improvement techniques used for improving the in-situ ground conditions, geosynthetics reinforcement and stone column technique are probably the most versatile ones. This is primarily due to their simplicity, ease of construction and overall economy that finds favour with the practicing engineers.

1.2 GEOCELL REINFORCED SOIL

The techniques of reinforcing the earth have been used for centuries. Use of timbers for construction of roads over peat bogs dates back to 3000 B.C. (Dewar, 1962). Recently there has been a major growth of interest in this subject due in part to the pioneering work of Henri Vidal in the development of 'Reinforced Earth' (Vidal, 1969) a term which is now used as a general description of this form of constructions.

In early days, the concept of reinforcing the earth was mainly pertaining to the use of metallic reinforcements (Sridharan 1990). Over the past two decades this concept has been extended to other materials like fabrics and grids, often termed as geotextiles and geogrids (Das and Khing 1994, Das et al. 1996), randomly distributed fibers (Puppala

and Musenda 2007); manufactured mainly from polypropylene materials. The geocell reinforcement is a recently developed reinforcing technique, which is a three dimensional, polymeric, honeycomb like structure of cells interconnected at joints (Bush et al 1990). The structure of a typical geocell readily available in the market is shown in Fig.1.1.

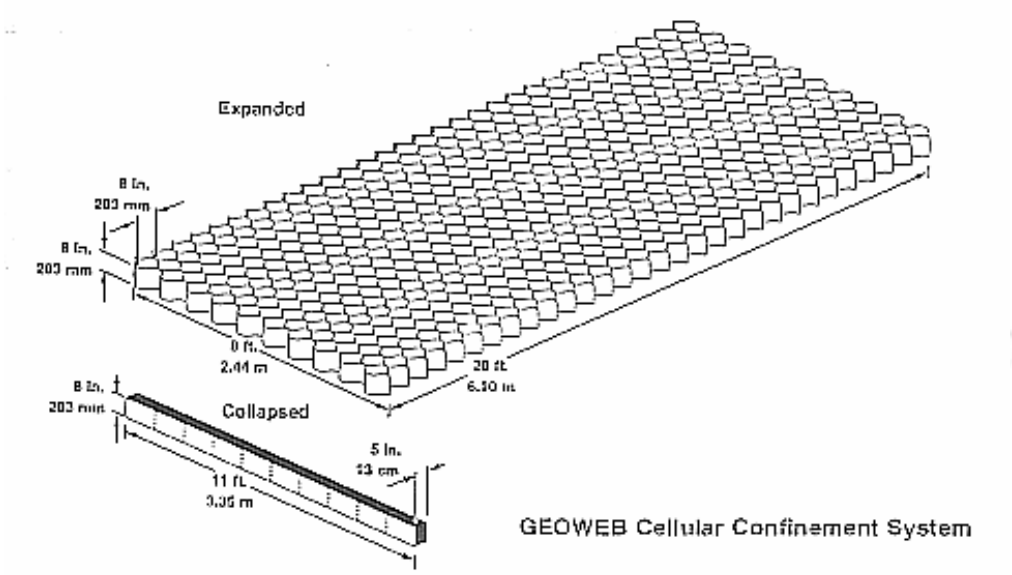

Fig. 1.1 Typical readymade geocell structure

For the construction of embankments, roadways etc. on extremely soft clay soils, where geocell mattresses of much higher height are required, they are fabricated at the site by joining various geogrids cut into the required size. The geocell mattresses are constructed in two phases. First, strips of geogrids having width equal to the height of the proposed geocell are cut from rolls and joined together in a definite pattern (Fig. 1.2). In the second phase, the pockets of these geocells are filled with granular materials to form the geocell-soil mattress.

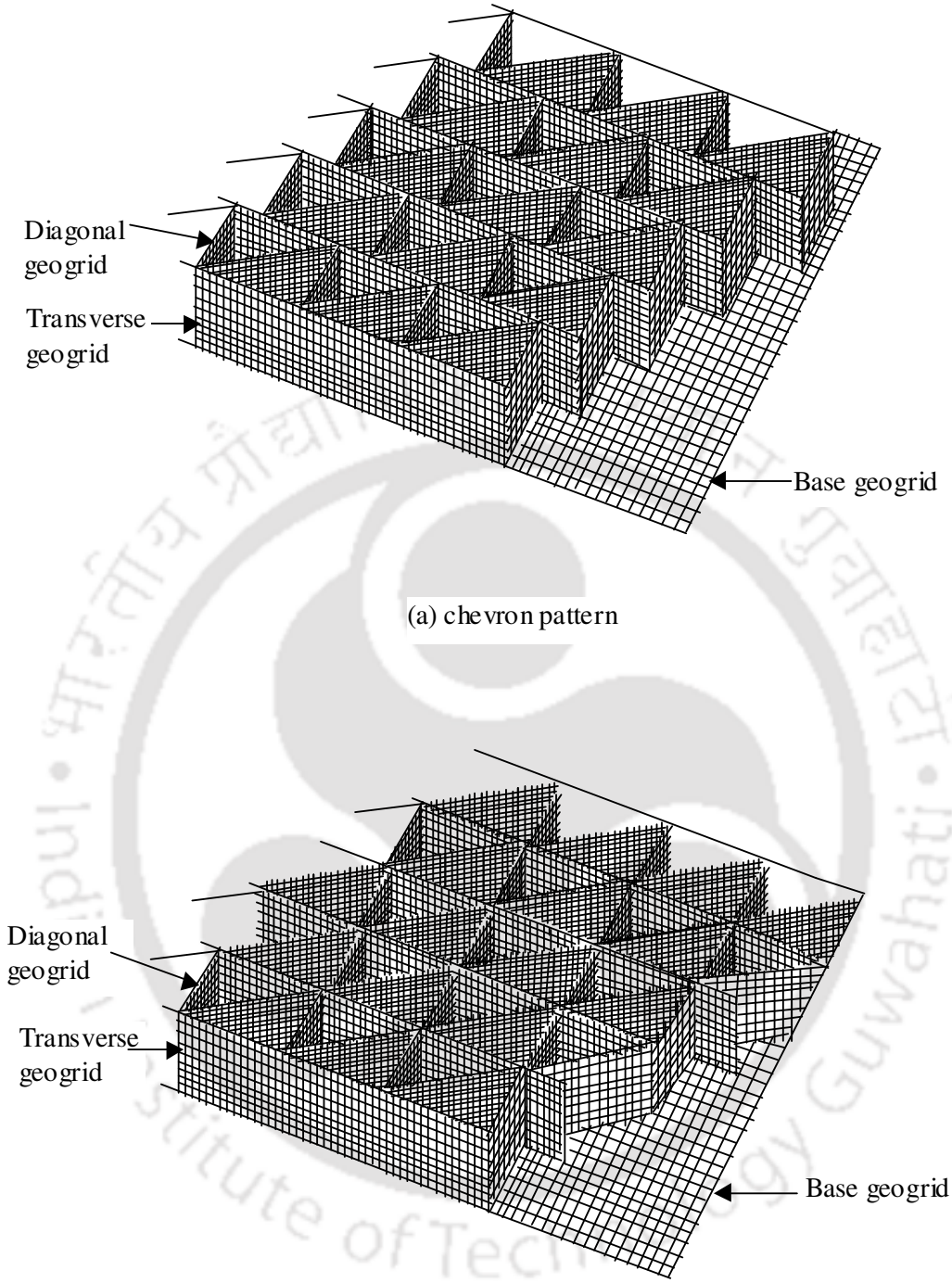

Fig 1.2 Patterns used for the formation of geocell mattress

The reinforcement mechanism in the geocells is by all-round confinement of soil within its pockets (see Fig.1.3). Unlike planar reinforcement, the geocell confinement reduces lateral spreading of the in fill soil and thereby increases the overall rigidity of the reinforced foundation bed. It intersects the potential failure planes and its rigidity forces them deeper into the foundation soil. This induces a higher surcharge loading on the failure plane thereby leading to a higher load carrying capacity.

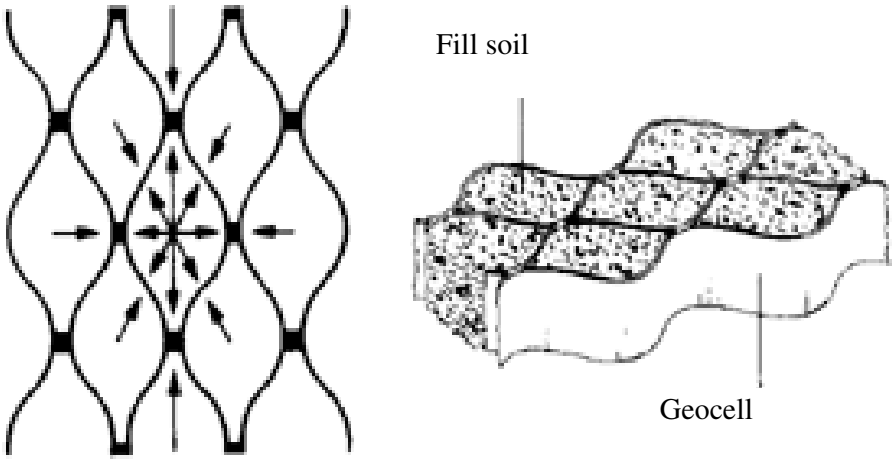

Fig.1.3 Soil confinement by geocell reinforcement

1.3 STONE COLUMN REINFORCED SOIL

The stone column technique was initially used in 1960, in Europe, and thereafter has been successfully used worldwide. The stone columns are formed by compacting stones into the cylindrical hole formed in soft clay bed, generally by vibro-floatation technique. When load is applied the stone column develops end bearing and skin friction resistance as in piles. Besides, the stone column being a flexible structure

expands under loading and thereby derives lateral support from the surrounding soil leading to increased load carrying capacity (Fig. 1.4).

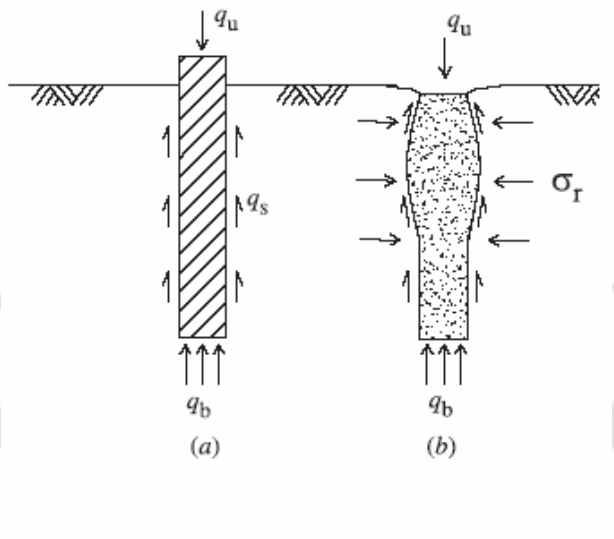

Fig. 1.4 Load carrying mechanism of stone column (Hughes and Withers 1974)

The stone column, apart from increasing the bearing capacity and reducing settlement, acts as a drain that accelerates consolidation of the soft clay.

1.4 OBJECTIVE OF THE PRESENT STUDY

The objective of the present study is to develop an understanding of the behaviour of geocell sand mattress-stone column reinforced weak clay beds, under monotonous circular loading.

1.5 ORGANISATION OF THE THESIS

This thesis comprises of eight different chapters, including the present introductory one. Chapter 2 presents a review of literature on geocell reinforcement; stone column reinforcement and combined use of geosynthetics-cum-stone column reinforcement.

Summary of the reported research works and scope of present study have been brought out at the end of this chapter. Planning of experiments, characterisation of the materials used, details of test setup and test procedures are discussed in Chapter 3. The obtained results are presented and discussed in Chapter 4-7. Chapter 4 deals with stone column reinforced clay beds. Chapter 5 presents the results of load tests on geocell mattress overlying clay bed. Chapter 6 brings out the performance improvement of clay bed due to the combined application of geocell-sand mattress and stone column reinforcement. Chapter 7 depicts the additional performance improvement due to encasement of stone columns with geomesh and provision of basal geogrid at base of the geocell mattress. Regression models to predict the load carrying capacity of the reinforced foundation beds and dimensional analysis to extrapolate model test data to full scale are attempted in Chapter 8. Chapter 9 summarises the results obtained and major conclusions drawn from the present study.

CHAPTER 2

REVIEW OF LITERATURE AND SCOPE OF PRESENT STUDY

2.1 INTRODUCTION

This chapter presents a review of the reported research works on soil reinforcement using geocells, stone columns, for the reduction of settlement and improvement of bearing capacity. The literature review is presented in three different sections. The first section is on geocell reinforced ground. The second is on stone column reinforced soil beds. The third section presents work on geosynthetics reinforced soil mattress overlying stone column/pile reinforced soil bed. Scope of the present research work has been brought out in the last section of this chapter.

2.2 STUDIES ON GEOCELL REINFORCED SOIL BEDS

Geocell reinforcement is a three dimensional honey-comb like structure formed from a series of interlocking cells. The United States Corps of Engineers (Webster and Watkins 1977, Rea and Mitchell 1978, Webster and Alford 1978) were the pioneer in the development of this concept of cellular reinforcement for the stabilization of granular materials for the construction of roads in beach sand. The initial work performed at the United States Army Engineers Waterways Experimental Station led to the development of commercially available geocells. Two types of geocell systems are referred in the literature. The first type of geocell system, mostly used for the reinforcement of road bases and ballast track, slope protection, channel protection and retaining walls; are made of polymer sheets welded together to form a mattress of interconnected cells (Bathurst and Crowe, 1994). This is popularly called geoweb mattress.

Another type of geocells referred to in the literature consists of strips of geogrid connected to form three dimensional cells. This type of geocell system has primarily been used in making foundations over soft soils for embankments, roads and marine structures etc (Bush et. al. 1990). However, tests are also reported where geocell reinforcement is used in homogenous sand beds and homogenous clay beds. The review of literature has therefore been presented under three different sections dealing with geocells; in sand beds, in sand layer overlying clay beds and in clay beds.

2.2.1 Sand beds

Mitchell et al. (1979) conducted model tests on geogrid cell reinforced sand in a square box of 915mm size. In order to back calculate the equivalent elastic modulus (E_r) for the reinforced layer, with help of the elastic theory solutions for homogeneous elastic layers overlying rigid base, the grid cell reinforced sand layer was placed directly on a rigid concrete floor. The influence of specific variables such as, ratio of radius of loaded area to cell height and ratio of loaded area to cell width were studied by varying the cell height and the diameter of the loaded area. An approximate formulation has been proposed to find out the equivalent elastic modulus (E_r) of the reinforced layer.

$$E_r = E_u f_1\left(\frac{E_g}{E_m}\right) f_2\left(\frac{a}{B}\right) f_3\left(\frac{h}{B}\right) f_4\left(\frac{a}{h}\right) f5\left(N_j\right) f_6\left(E_s\right) \quad (2.1)$$

where a/h, is the layer geometry ratio; h/B, the grid geometry ratio; a/B, the loaded area-grid geometry ratio; E_m, the modulus of the cell fill material; E_g, the modulus of the grid material; E_s, the modulus of the subgrade; E_u is the modulus of the unreinforced sand layer and N_j is the number of grid joints per unit area. The test results indicate that bearing capacity increases with size of loaded area and thickness

of grid cell layer. Grid cell reinforcement can lead to many fold increase in the effective modulus of a sand layer.

Experimentally, Khay et al. (1986) studied the reinforcing efficiency of various geotextile structures in the performance improvement of sand subgrade. The geotextiles included, cell, fibers and prefabricated sheets of polyamide threads. Geocells used had an a/b (cell width to depth) ratio of 0.5 with varying depth of 10, 15 and 20 cm. The geocell reinforcement showed considerable performance improvement. The settlement of geocell mattress was appreciably low which suggests that it behaves as a slab.

Guido et al. (1989) conducted a parametric study using laboratory plate load tests on geoweb reinforced sand beds. The parameters studied were the texturisation roughness of the geoweb wall, number of layers of the geoweb reinforcement (N), depth of placement of the first layer of the reinforcement below the loaded plate (u), size (extent) of the geoweb reinforcement (b) and relative density (ID) of the fill material. The plate load tests were conducted in a square wooden box. Test results indicated that for untextured geowebs, at N = 4 or more, the bearing capacity ratio (BCR) did not show any increase indicating that, N = 4 is an optimum value. However, for medium texturised cells, at N = 4, the BCR was still increasing. As the depth of placement decreased the BCR increased and settlement decreased. For the untextured geoweb at u/B ratio (i.e. B is the width of the footing) of 1.0, while for texturised geocell at u/B ratio of 1.25; the reinforced structure behaved like an unreinforced case. The optimum b/B ratio beyond which the increase in BCR is marginal was found to be 2 and 3 for untextured and medium textured case respectively. Studies carried out on the effect of relative density indicated that for loose soil the percentage improvement in load carrying capacity is relatively higher.

Koerner (1990) proposed a failure mechanism for the geocell reinforced foundation bed, based on plastic limit equilibrium theory as used for estimating the bearing capacity of shallow foundation. Since slip lines are interrupted by the vertical walls of the mattress, for such a failure to occur, the sand in particular cell must punch out of it, thereby loading the sand beneath the level of the geocell. This in turn fails in bearing capacity, but now with the positive effects of a surcharge loading and higher density conditions. Thus the increase in bearing capacity due to the provision of geocell can be taken as 2τ where, τ is the shear strength between geocell wall and soil contained within it and is defined as

$$\tau = \sigma_h \tan\delta \qquad (2.2)$$

Where, σ_h is the average horizontal force within the geocell = qK_a, q is the applied vertical pressure, K_a is the coefficient of active earth pressure, δ the angle of shearing resistance between soil and cell wall material.

Dash et.al. (2001a) reported the results of laboratory-model tests on a strip footing supported by a sand bed reinforced with a geocell mattress. The parameters varied in the testing program include pattern of geocell formation, pocket size, height and width of geocell mattress, the depth to the top of geocell mattress, tensile stiffness of the geogrids used to fabricate geocell mattress and the relative density of the sand. With the provision of geocell reinforcement, failure was not observed even at a settlement equal to 50% of the footing width and a load as high as 8 times the ultimate bearing capacity of the unreinforced sand. In addition to the tensile strength of reinforcement, the aperture size and orientation of ribs of the geogrid used to fabricate the geocell mattress substantially influence the improvement in the performance due to the reinforcement.

The results from laboratory model tests conducted by Dash et.al (2001b) on strip footings supported by geocell reinforced sand beds with additional planar reinforcement show that a layer of planar geogrid placed at the base of the geocell mattress further enhances the performance of the footing in terms of the load-carrying capacity and the stability against rotation. The beneficial effect of this planar reinforcement becomes negligible at higher heights of geocell mattress.

Dash et. al. (2003a) through laboratory model tests studied the bearing capacity of circular footings supported by geocell-reinforced homogenous sand beds. Footing load–settlement response, deformations at the fill surface, strains in the geocell wall and pressure distributions below the geocell mattress were measured. The test results demonstrate that by providing geocell reinforcement in the sand bed, significant performance improvement in terms of increased bearing capacity and reduced surface deformation can be obtained. Measurements indicate that the footing pressure is redistributed more uniformly over a wider area on the subgrade soil, indicating that the geocell-reinforced sand bed behaves as a composite mass.

Dash et. al. (2004) have studied the relative performance of different forms of reinforcement (i.e. geocell, planar and randomly distributed mesh elements) in sand beds under strip loading. The results demonstrate that geocell reinforcement is the most advantageous form of soil reinforcement technique amongst the three. With the provision of geocell reinforcement, failure was not observed even at a settlement equal to about 45% of the footing width and a load as high as eight times the ultimate capacity of the unreinforced soil, whereas, with planar reinforcement, failure took place at a settlement of about 15% of the footing width and a load of about four times the ultimate capacity of the unreinforced soil. For the case with randomly distributed mesh reinforcement, failure was recorded at a load of about 1.8 times the ultimate

capacity of the unreinforced soil and at a settlement of about 10% of the footing width.

Dash et. al. (2008) have observed that with the provision of geocell reinforcement, the subgrade modulus of sand bed can be increased as high as eight times that of unreinforced case. A multiple-variable data regression is performed on the experimental data to establish the relation between the effect of reinforcing in terms of subgrade modulus improvement factor and the parameters that control the scheme of reinforcement. This equation will be of use in predicting the subgrade modulus of geocell-reinforced sand beds, and effective utilisation of geocell reinforcement in increasing the performance of sand foundations.

Wesseloo et. al. (2009) reported the results of uniaxial compression tests performed on geocell packs of different sizes comprising of single and multiple geocells. The packs were fully instrumented to record the deformations within. They observed that the strength of the geocell composite structure is indirectly proportional to the size of the individual cells and that the strength of the packs reduces with an increase in the number of cells in the structure.

2.2.2 Sand bed over weak clay bed

Broms and Massarach (1977) suggested the use of metallic grid mat consisting of rectangular and triangular cells for different offshore structures. Failure of such cells could be either due to penetration failure or due to bearing capacity failure. Penetration failure occurs when the height of the cells is smaller than the circumference, where as, bearing capacity failure governs when height of the cells is relatively large. Penetration resistance was calculated by considering vertical force equilibrium on the cell wall and bearing capacity was calculated using Terzaghi's bearing capacity equation. It was concluded that the penetration resistance increased

rapidly with increased height of cells. The bearing capacity for cells with triangular shape was larger than that with the rectangular cells, both taken at equal settlement.

Webster and Watkins (1977), Webster and Alford (1978) have conducted full scale traffic, field tests on, interconnected, shallow, thin-walled aluminium cells placed over soft subgrade, with cell axes oriented vertically and filled with sand. It has been found that the geocell reinforced sand can provide significantly greater load carrying capacity than the compacted soil alone. The behaviour of the grid cell mattress resembles that of a slab. Based on the findings it is concluded that the performance of sand-filled grid cells, when used over very soft subgrade, is equivalent to that of a layer of crushed stone that is as much as 1.6 times thicker than the height of the cells.

Rea and Mitchell (1978) conducted a series of laboratory model tests to investigate the performance of interconnected paper cells filled with sand as reinforced layer for application in low cost highway construction. The cells were made of 0.008inch (0.203 mm) thick paper and were square in shape when expanded. The width was kept constant as 2 inches (51mm). The subgrade was simulated using springs. The influences of the parameters investigated are,

- the ratio of radius of loaded area(a) to cell width(B)
- the ratio of the cell width(B) to cell height(h)
- the influence of subgrade stiffness and
- effect of repeated loading.

Based on the test results the various modes of failure were identified as: 1. Cell penetration 2. Cell bursting 3. Cell wall buckling 4. Bearing capacity failure 5. Bending failure 6. Excessive rutting.

Maximum bearing capacity under static load was found for a/B ratio in the range of 0.75 to 1.0. The optimum h/B ratio was about 2.25. The cell reinforced sand showed better resistance to repeated loading. The mechanism of resistance to soil shearing was summarised as:

1. The sand gets confined and restricted against lateral movement, till strength of the reinforcement reaches ultimate value.
2. Tension in the reinforcement gave a corresponding compression on the sand encapsulated in the cells, thus giving increased stiffness.
3. Development of slip surfaces (shear planes) through the reinforcement is inhibited.

Johnson (1982) have used geocell mattress concept at Great-ham-Creek bridge, England. The geocell mattress was placed under the 5 meter high approach embankment over soft estuarine silts running up to 7 meter depth. It was observed that the settlements measured were less than 50% of the predicted values. The lateral strains were also found to be very small.

De Garidel and Morel (1986) have carried out field tests to find out the suitability of continuous filaments, micro-geogrids and geotextile cells filled by soils for road construction. Geocells used in these tests had a/b (cell width to depth) ratios of 0.5 and 0.1. Test results indicate that the reinforced structures do not show increased rigidity at small displacements. However, at large displacement the strengthening effect is remarkable, especially for honeycomb geocell structures.

Robertson and Gilchrist (1987) reported the selection of the geocell mattress for Auchenhowie road as the most cost effective solution and practical way of constructing a 4 meter high embankment over a 4 meter deep soft clay overlying

mudstone. The average undrained shear strength of the clay was 15kPa. The selection of the geocell mattress was made after an economical appraisal of both excavation-replacement and geocell mattress, after other methods had been rejected on the ground of practical difficulty or a much longer construction period. Cost estimation showed that the geocell mattress method of construction can save 31% of the cost of conventional solutions.

Jenner et al. (1988) proposed the use of slip line fields in determining the increased bearing capacity of soft ground due to cellular foundation mattress installed at the base of an embankment. The ultimate bearing capacity of the soft layer was analysed with the help of the theory proposed by Johnson and Melor (1983). The bearing capacity diagram was developed by working from the outer edge of the slip line field inwards to the boundary of the 'rigid head'. Where 'rigid head' is the term used to denote the soil zone, which remains in the active condition and so, does not experience plasticity. Thus the slip line field was used to define the maximum allowable pressure distribution within a zone of limiting plasticity. The following equation was given for calculating the value of average bearing pressure over the rigid head zone ($\overline{P}$), Johnson and Mellor (1983)

$$\frac{\overline{P}}{C_u} = \frac{2(2\times I + 0.5\times d)}{2\times X} + \frac{P}{C_u} \qquad (2.3)$$

where C_u is the undrained shear strength of the soft layer, I is the sum of (Rotation of slip line × Horizontal chord length), X is the sum of horizontal chord length, d is the depth of the soft layer and P is the pressure read at the extreme end of the 'rigid head' of the slip line field.

Bush et al. (1990) reported the use of geocell foundation mattress (a honeycombed structure formed from a series of interlocking cells). These cells were fabricated directly on a soft foundation soil from polymer grid reinforcement and then filled with granular material resulting in a rigid base of 1 meter deep. Apart from, providing a working area for the construction of the geocell itself and subsequent embanking, it serves as a drainage blanket to assist the consolidation of the underlying soft foundation. The incorporation of a geocell mattress induces a rough interface between the soft foundation and the contained granular fill of the mattress. Besides, its rigidity evenly distributes the load onto the foundation bringing forth a regular stress field within the soft foundation layer. These features enabled the geocell mattress to exert a degree of restraining influence on the deformation in the soft foundation. It also rotated the principal stress direction in the embankment fill up to 45 degree inclined inward at the top of the foundation soil. This altered the potential slip mechanisms in the foundation soil and resulted in an enhanced bearing capacity.

Dean and Lothin (1990) have reported the construction of an embankment over a deep soft deposit using a geocell mattress. The geocell layer was fabricated using uniaxial geogrid and the lower mat of the geocell mattress was a biaxial geogrid. The geocell pockets were filled with crushed rock. Among all other alternatives (i.e. construction of a viaduct, replacement of the soft deposit with rock fill, preconsolidation of the soft soil) the geocell mattress option was found to be cheapest and most practical solution. The geocell was found to be effective in reinforcing the base of the embankment while, the settlement took place. It enabled the embankment to be constructed more rapidly than any of the alternatives.

Cowland and Wong (1993) have reported the construction of a five kilometer-long road, part of which crossed an alluvial plain on embankment. At two locations on the

alluvial plain this embankment was underlain by soft clay deposits. A geocell mattress was used as the means of supporting the embankment on these soft clay deposits. Wick drains were installed beneath the embankment to speed up consolidation of the soft clays, and using staged construction the embankment was built up to a maximum height of 10m. The embankment was fully instrumented with pneumatic piezometers, inclinometers, hydrostatic profile gauges, settlement plates, surface settlement markers, and lateral movement blocks. The data from these were used to monitor the performance of the geocell mattress foundation during the construction of the embankment. It was observed that the geocell mattress underwent very small lateral extension. The deflected shape of the geocell mattress indicated that it has behaved as a raft foundation to the embankment.

Mandal and Gupta (1994) carried out experiments to study the stability of a geocell-reinforced soft soil structure, on the bearing capacity and the failure settlement of a two-layer system. Series of laboratory model load tests on marine clay beds overlain by sand layer with and without the geocells were performed. It is observed that load-settlement characteristics are substantially improved owing to the use of geocell reinforcement.

Mhaiskar and Mandal (1996) investigated the efficacy of the geocell structure on a soft clay subgrade by performing laboratory model tests as well as finite-element analysis. The geocells were filled with sand. Parameters studied are the width, height of geocell, strength of geocell material and relative density of the fill in the geocell. The experimental results were simulated using ANSYS (a general purpose Finite Element programme). The geocell layer was considered as a layer with an equivalent stiffness. Close agreement has been found between the experimental and the finite

element analysis results. Considerable amount of improvement in the ultimate load and reduction in settlement was obtained due to the geocell reinforcement.

Knight and Bathurst (1997) and Bathurst and Knight (1998) have carried out numerical simulations of cover soil layers used over flexible long span soil-steel bridge conduits for the case with and without geocell reinforcement. The simulations were done by using a nonlinear finite element program GEOFEM. A parametric finite element analysis shows that with the provision of geocell reinforcement, the minimum specified soil cover can be reduced by 60% without any loss of initial stiffness. Besides, the geocell reinforcement is found to have increased the ultimate bearing capacity of the system significantly.

Forsman et al. (1998) have reported a case study on the performance of a geocell reinforced road over deep peat deposit. The geocells were fabricated using Tensar SS_{30} and SR_{55} geogrids. The geocell pockets were filled with light expanded clay aggregate. This lightweight fill was used because of expected large settlements in the peat deposit. The test structures were experimentally instrumented using vertical magnetic probe extensometers, horizontal hydrostatic profile gauges, settlement plates, horizontal extensometers and strain gauges. Plate load tests and falling weight deflectometer tests were conducted to measure the modulus of the subgrade. The results indicate that the tension is concentrated quite near the loading point. The geocell layer was found to be effective in increasing the bearing capacity and reducing differences in settlements. Even after one and half years after the construction, no significant differential settlement was noticed on the road surface.

Krishnaswamy et al. (1998, 2000) conducted a series of laboratory model tests on geocell supported earth embankments constructed over soft clay bed. The soft clay bed was prepared in a large test tank to a depth of 600mm. The geocell layers were

fabricated using different type of uniaxial and biaxial geogrids. The embankments were subjected to uniform surcharge pressure, on the crest, until failure. Test results indicated that the provision of a geocell layer at the base of the embankment improves the performance of the embankment to a large extent. The parametric study shows that the surcharge capacity of the embankment depends on the stiffness of the geogrid, pocket opening size, height of geocell, type of soil filled inside the geocell and the pattern used to form the geocells.

Dash et. al. (2003b) have brought out the effectiveness of geocell reinforcement placed in the granular fill overlying soft clay beds. The test beds were subjected to monotonic loading by a rigid circular footing. Footing load, footing settlement and deformations on the fill surface were measured during these tests. The influence of width and height of geocell mattress as well as that of a planar geogrid layer at the base of the geocell mattress on the overall performance of the system has been systematically studied through a series of tests. The test results indicate that with the provision of geocell reinforcement in the overlying sand layer, a substantial improvement in the performance of the system can be obtained in terms of increase in the load carrying capacity and reduction in surface heaving of the foundation bed. An additional layer of geogrid placed at the base of the geocell mattress further enhances the load carrying capacity and stiffness of the foundation bed. A seven-fold increase in the bearing capacity of the circular footing can be obtained by providing geocell reinforcement along with a basal geogrid layer in the sand bed overlying the soft clay.

Madhavi Latha et. al. (2006) have studied the influence of geocell reinforcement on the performance of earth embankments constructed over weak foundation soil. Model embankments were constructed above a layer of geocells formed using geogrids, on top of a soft clay bed prepared in a steel test tank. Uniform surcharge pressure was

applied on the crest and pressure-deformation behavior of the embankment and strains in the walls of geocells were monitored continuously until failure was reached. The influence of various parameters like tensile stiffness of geocell material, height and length of geocell layer, pocket-size of the cell, pattern of formation of geocells, and type of fill material inside the cells was studied. Geocell reinforcement was found to be advantageous in increasing the load-bearing capacity and reducing the deformations of the embankments. The experimental results were validated using a general purpose slope-stability program and a simple design procedure has been brought out for the preliminary design of geocell-supported embankments.

Zhou and Wen (2008) reported that one or two layers of geosynthetic materials placed in a sand cushion over a soft-soil foundation can create composite layers with improved bearing capacity. The results indicate that with the provision of a geocell-reinforced sand cushion, there is substantial reduction in settlement of the underlying soft soil. The subgrade reaction coefficient is improved by 3000%, and the deformation is reduced by 44%. The earth pressure on the soft soil beds, with the non-reinforced sand cushion is much larger than that with the geocell-reinforced sand cushion.

Through a series of laboratory scale model tests, Sireesh et. al. (2009) have brought out the potential benefits of using geocell reinforced sand mattress over clay subgrade with void. The parameters investigated in the test programme include, thickness of unreinforced sand layer above clay bed, width and height of geocell mattress, relative density of the infill sand in the geocells, and the influence of an additional layer of planar geogrid placed at the base of the geocell mattress. The test results indicate that with the provision of geocell mattress of adequate size, over the clay subgrade with void, can substantially improve the performance of the foundation bed. The optimum

beneficial effect of providing geocell mattress can be achieved by extending the geocell mattress beyond the void at least a distance equal to the diameter of the void. The influence of the void, over the performance of the footing reduces for height of geocell mattress greater than 1.8 times the diameter of the footing. Better improvement in performance is obtained for geocells filled with dense soil.

Zhang et. al. (2009) using Winkler foundation model have developed a theoretical model to estimate the deformations of the geocell reinforced mattress under vertical symmetric loads. The influences of various factors such as load, length and flexural rigidity of geocell reinforcement, coefficient of subgrade reaction and the interface resistance on the stress-deformation characteristic of geocell reinforcement are brought out. The obtained results indicate that the effect of interface resistance at the soil-geocell interface is an important parameter to be considered in the designs.

2.2.3 Clay beds

Sitharam et. al. (2005) investigated the possibility of using geocell reinforcement in soft clay foundations. A series of laboratory-scale static load tests were carried out on a rigid circular footing placed on geocell reinforced and unreinforced clay beds. Parameters of the test program included depth of placement of the geocell layer, width and height of the geocell layer, and influence of an additional layer of planar geogrid at the base of the geocell mattress. With the provision of geocell reinforcement, the load carrying capacity of the soft clay foundation can be improved by a factor of up to 4.8 times that of the unreinforced soil. Heaving in the soil surface can be reduced substantially by providing geocell reinforcement of sufficient height and width. Further improvement in performance could be obtained with the provision of an additional layer of planar geogrid at the base of the geocell mattress.

Sitharam et. al. (2007) presented the results of laboratory model tests carried out to develop an understanding of the behaviour of geocell-reinforced soft clay foundations under circular loading. Natural silty clay was used in this study. The geocells were prepared using biaxial polymer grid. The performance of the reinforced bed is quantified using non-dimensional factors; bearing capacity improvement factor (I_f) and percentage reduction in footing settlement (PRS). The test results demonstrate that the geocell mattress redistributes the footing load over a wider area thereby improving the performance of the footing. The load carrying capacity of the clay bed is increased by a factor of up to about 4.5 times that of unreinforced bed. From the pressure-settlement responses, it is observed that the geocell-reinforced foundation bed behaves as a much stiffer system compared to the unreinforced case indicating that a substantial reduction in footing settlement can be achieved by providing geocell reinforcement even in soft clay. The maximum reduction in footing settlement obtained with the provision of geocell mattress of optimum size placed close to the footing is around 90%. Further improvement in performance is obtained with provision of an additional planar geogrid layer at the base of the geocell mattress.

2.3 STONE COLUMN REINFORCED GROUND

The stone column is a relatively new addition to the existing ground improvement technique for soft cohesive soil. A stone column is a column of stones made by vertical cylindrical hole in the soft clay bed and subsequently filling it with compacted stone aggregates. Given the higher strength and stiffness of the stone columns they carry a substantially larger proportion of the applied load than their soft soil counterpart leading to overall performance improvement of the clay foundation in terms of increased bearing capacity and reduced settlement. Besides, the granular stone column material having high permeability, the columns act as vertical drains

facilitating consolidation of the soft clay thus providing long term increase in strength. Hughes and Withers (1974) reported that stone columns were first used in France in 1830 to support the ironworks at an artillery arsenal (Moreau et. al., 1835). The method was later used in Germany in the year 1936 after a gap of more than 100 years of its first use. But the application of stone column became popular after the invention of Vibrofloatation technique for densifying granular soils which later extended for construction of vibro-displacement stone column in soft cohesive soil. Over the last three decades several research works have been reported highlighting the beneficial effects of stone columns in improving the performance of weak ground. It was observed that in very soft soil, due to lack of confinement the stone columns underwent premature bulging leading to failure. To overcome this problem stone columns were reinforced, thus began the technology of reinforced stone columns. The literatures relevant to the present study are presented in the following two subsections; i.e. unreinforced stone column, reinforced stone columns.

2.3.1 Unreinforced stone column

Mitchell and Huber (1985) carried out load tests on full scale stone columns constructed in field. Finite element simulation too was carried out for prediction of the load settlement behaviour of the stone columns. It was observed that the installation of stone columns led to reduction in settlements to about 30-40% of that of the unimproved ground.

Juran and Guermazi (1988) reported the results of laboratory parametric study conducted to investigate the response of a soft foundation soil reinforced by compacted sand columns. Triaxial compression tests under different boundary conditions were performed on composite soil specimens made of annular silty soil samples with a central, compacted river-sand column. The test results show that the

group effect of stone columns, the clay/stone replacement factor, and the consolidation of the soft soil have a significant effect on the vertical stress concentration on the column and on the settlement reduction of the foundation soil.

Juran and Riccobono (1991) carried out an experimental study to study the feasibility of using artificially cemented, compacted-sand columns for reinforcing soft cohesive soils. Triaxial compression tests were conducted on composite-reinforced soil samples made of normally consolidated, kaolinite, reinforced by both cemented and untreated columns of river sand. The test results indicate that low-level cementation in compacted-sand columns can significantly improve the settlement response and load-carrying capacity of reinforced soft foundation soils. The inter granular cementation provides an effective cohesion to the compacted-sand column, rendering its behavior more independent of the confining pressure mobilized in the surrounding soft soil. Therefore, low-level cementation can be used efficiently to extend the range of application of the sand-column technique in soft, compressible clayey soils.

Alamgir et. al. (1996) developed a theoretical model to study the deformation behaviour of soft ground reinforced by columnar inclusions. The analysis is performed based on the deformation properties of the column material and the surrounding soil. The interaction shear stresses between the column and the surrounding soil are considered to account for the stress transfer between the column and the soil. The solution is obtained by imposing compatibility between the displacements of the column and the soil for each element of the column-soil system. The parametric analysis shows that shear stress is maximum at the top and at the column-soil interface and they decrease with depth and radial distance. At the surface, the stresses on the column and the soil are the same. They increase in the column and decrease in the soil, with depth. The stress in the soil is small adjacent to the column

and increases with radial distance towards the outer boundary of the unit cell. Besides it is found that the relative stiffness of the column and soil plays a significant role in controlling the settlement reduction of soil bed while the influence of Poisson's ratio of soil is marginal. .

Poorooshasb and Meyerhof (1997) analysed the efficiency of end bearing stone columns and end bearing lime columns in reducing the settlement of foundation system. The foundation system was assumed to consist of a large number of regularly spaced stone columns of equal length installed in a weak soil layer and supporting a rigid mat. The analysis examines the influence of such factors as the column spacing, the weak soil properties, properties of the granular medium used in constructing the column, the in situ stresses caused by the installation technique, the depth of the bedrock relative to the tip of the columns and the magnitude of the load carried by the supported raft foundation. It is observed that the spacing of the stone columns and the degree of compaction of the materials in the columns are the most important factors that affect the performance of the stone column foundation system prominently.

Rao et al. (1997) carried out load tests on stone column reinforced soft clay bed. Tests were carried out for both single and groups of stone columns. The test results showed that the stone columns can be satisfactorily used to increase the load bearing capacity of the soft formation by 2 to 3 times that of unreinforced one.

Christoulas et. al (2000) carried out instrumented axial loading tests on large scale model stone columns. Kaolin was used to simulate the natural soil conditions. The deformed shape of the stone columns is found to be independent of method of construction of stone columns i.e. via pile driving equipment or by vibro-replacement technique. The upper parts of the stone columns are found to have bulged due to the applied loading over a length of about 2.5 to 3 times the diameter of the column.

Based on the test data a trilinear load settlement relation is proposed for design purposes.

Wood et. al. (2000) performed model tests to determine the mechanism and response of beds of clay reinforced with stone columns, subjected to surface footing loads. An exhumation technique was used to map the deformed shape of the model stone column and using the same the way in which the columns have transferred load to the surrounding clay were deciphered. It was observed that the diameter, length and spacing of the stone columns, control the response of the system, whether the columns act as rigid inclusions transferring load to their tips and eventually deforming either by buldging or by the formation of a failure plane, or whether they are able to compress axially or even, bend if sufficiently slender, to undergo significant lateral deformation. Pressure transducers have been used to record the distribution of contact pressure between columns and soil which indicates that the columns at mid radius of the footing are typically the most heavily loaded ones.

Bae et. al (2002) studied the failure mechanism and various parameters responsible for the behaviour of end-bearing column groups through loading tests and unit cell consolidation tests. Results of model tests are simulated by a finite element model analysis. The obtained results from tests and analysis indicate that bearing capacity of stone column is affected by undrained strength of surrounding ground and area replacement ratio of composite ground. The behaviour of foundation bed is affected by diameter and spacing of stone columns rather than their embedment ratio. The critical length of the stone columns to mobilize maximum performance improvement is of the order of 2.3 to 3.8 times its diameter.

McKelvey et. al. (2004) carried out a series of laboratory model tests on stone column reinforced clay bed. Two different materials; a transparent material with 'clay like'

properties, and white kaolin were used to prepare the foundations beds. The tests on the transparent material permitted visual examination of deforming granular columns during loading. It was observed that bulging was significant in long columns, whereas punching was prominent in shorter columns. The presence of the stone columns greatly improved the load-carrying capacity of the soft clay bed. However, columns longer than about six times their diameter did not lead to further increases in the load-carrying capacity. This suggests that the optimum length of the stone column is about six times its diameter.

Ambily and Gandhi (2007) carried out experiments on behaviour of single stone column and group of columns by varying parameters like spacing between the columns, shear strength of soft clay and loading conditions. The columns were of 100 mm diameter surrounded by soft clay of varying consistency. In some of these tests the entire equivalent area was loaded to estimate the stiffness of improved ground while in others only single column was loaded to estimate the limiting axial capacity. During the group experiments, the actual stress on column and clay were measured by fixing pressure cells in the loading plate. Finite-element analyses were also performed using 15-noded triangular elements with the software package PLAXIS. A drained analysis was carried out using Mohr-Coulomb's criteria for soft soils, stones and sand. The results indicate that columns arranged with spacing more than 3 times the diameter of the column does not give any significant improvement. The stiffness improvement factor is found to be independent of the shear strength of the surrounding clay soil, however depends very much on spacing of the stone columns and friction angle of the stone aggregates.

Black et. al. (2007) reported an experimental study, wherein, soft Kaolin clay was reinforced with vertical columns of sand and loaded under triaxial conditions. The test

results indicate that with single sand column the strength of clay mass increases by 33%. However, installing a group of columns with similar area replacement ratio did not make much difference in the load carrying capacity.

Rao et.al. (2008) investigated the use of granular pile anchor (GPA) for mitigating heave of expansive clay beds and improving their engineering behaviour. It is a modified form of the conventional granular pile, wherein, an additional anchor is provided in the pile. Plate load tests were conducted on unreinforced expansive clay beds and clay beds reinforced with GPAs, to compare the compressive load response. It was found that expansive clay beds reinforced with GPAs showed higher load-carrying capacity and improved compressive load response compared to that of the unreinforced clay beds. While, the stress required to cause a settlement of 25 mm in the unreinforced expansive clay bed was 200 kN/m^2, the clay bed reinforced with a GPA of 1000 mm long and 150 mm in diameter required 500 kN/m^2 to cause similar settlement, showing an improvement of 150%. The critical length of the granular pile anchor given maximum performance improvement (i.e. of the order of 440%) is about 10 times of its diameter. The maximum bulge diameter increased with increasing diameter and length of the GPA. However, the effect of GPA length is relatively more pronounced on the increase in maximum bulge length, than that of diameter.

2.3.2 Reinforced stone column

Sharma et. al. (2004) carried out model tests on geogrid reinforced granular pile in soft clay. The geogrid reinforcement layers were provided at different depths along the length of the stone column. It was observed that the load carrying capacity was enhanced due to geogrid reinforcement in the stone column. The performance improvement increases with increase in number of geogrid layers and decrease in

their spacing. Bulge length and diameter of the stone column reduced due to the reinforcement.

Ayadat and Hanna (2005) studied the efficacy of geofabric encapsulated stone column to transmit foundation loads in a collapsible soil mass to the underlying bearing strata. Load tests performed on geofabric encapsulated stone columns, installed in a collapsible soil layer subjected to inundation. Parameters varied are length of columns, degree of inundation and strengths of geofabric. The test results indicate that unreinforced sand columns in collapsible soil did not contribute significantly as it failed prematurely. Whereas, the load carrying capacity of encapsulated sand columns was substantial and increases with increase in strength of the geofabric material and/or increase in column length. The settlement of the column due to external loading and inundation decreased owing with increase in column rigidity and length (up to a maximum value equal to the thickness of the collapsible soil layer).

Murugesan and Rajagopal (2006) investigated the improvement in load capacity of the stone column due to encasement through finite element analysis. The analysis shows that the encased stone columns have much higher load carrying capacities and undergo lesser compressions and lesser lateral bulging as compared to conventional stone columns. Lateral confining stresses developed in the stone columns are found to be higher with encasement. With encasement in the top portion of the stone column, up to twice the diameter of the column is found to be adequate in improving its load carrying capacity. As the stiffness of the encasement increases, the lateral stresses transferred to the surrounding soil are found to decrease. This phenomenon makes the load carrying capacity of encased columns less dependent on the strength of the surrounding soil as compared to the ordinary stone columns.

Murugesan and Rajagopal (2007) carried out laboratory model tests to investigate the qualitative and quantitative improvement of load supporting capacity of soft ground due to single encased stone column. The tests were performed on a rigid unit cell that represents the stone column and the soil within the tributary area around the stone column. The load tests indicated a clear improvement in the load carrying capacity of the stone column due to encasement. Encasement with geosynthetics having higher modulus resulted in stiffer response. The effect of encasement was found to decrease with increase in the diameter of the stone column. The improvement in the performance of stone columns was found to be significant, even with partial encasement.

Malarvizhi and Ilamparuthi (2007) have studied the behaviour of the encased stone column stabilized bed both through experiments and numerical modelling. A parametric study was carried out by varying the L/D ratio (L = length, D = diameter) of the stone columns, stiffness of geogrid and angle of internal friction of the stone aggregate. It was found that encasing stone column with geogrid improved the load carrying capacity of the stone column reinforced clay bed substantially. This performance improvement increases with increase in stiffness of the encasing geogrid. This is attributed to the increased stress concentration on the column leading to reduced load transferred to the clay mass. The angle of shearing resistance of the column material too influences the performance of the encased stone column but to a lesser degree as compared to that of the stiffness of the encasing geogrid.

Black et. al. (2007a) carried out load tests on stone columns in a weak deposit of peat to evaluate the effects of reinforcing the stone columns by jacketing with a tubular wire mesh and bridging reinforcement with a metal rod and a concrete plug. The load was applied to a circular plate supported on untreated soil, soil treated with stone

column and soil treated with reinforced stone columns. The results show that the settlement characteristics of the soil can be improved by installing stone columns and that a significant enhancement in the load–settlement response is achieved when the columns are reinforced.

Ayadat et. al. (2008) reported results of an experimental investigation on sand columns internally reinforced with horizontal wire meshes made of plastic, steel and aluminium materials. Loading tests were performed on prototype reinforced sand columns in a stress-controlled chamber that contained normally consolidated clay. The load carrying capacity of the clay is found to be enhanced due to the provision of the reinforcement. For columns reinforced with three aluminium meshes the load carrying capacity has increased up to 75% as compared to 54% and 38% for two and single mesh reinforcement respectively. This performance improvement was found to be relatively lower for steel and much lower for plastic meshes.

Murugesan and Rajagopal (2008) carried out laboratory model tests to investigate the shear load capacity of stone columns, with and without geosynthetic encasement. The tests were performed by inducing lateral soil movements in a stone column treated soft soil. The test results have shown that while the unreinforced stone columns offered very limited resistance to shear movements, the geosynthetics encased stone columns had a much higher resistance. This is attributed to the confining effect of the aggregates by the geosynthetics.

Wu et. al. (2009) have studied the axial stress–strain responses of embedded granular columns encapsulated with flexible reinforcement, using an analytical procedure based on the cavity expansion method. The results have shown that the reinforced granular columns embedded in clay behave differently from granular columns subjected only to a constant confining pressure. Reinforcing the column with a sleeve

at the top portion is found to be adequate to prevent the column from bulging and thereby improve its load carrying capacity. The optimum skirting length that a sleeve can deter a granular column from bulging depends on the characteristics of the in situ soil as well as the stiffness and yield strength of the sleeve.

Gniel and Bouazza (2009) carried out a series of small-scale model column tests that were undertaken to investigate the behaviour of geogrid encased columns. The tests focused on studying the effect of varying the length of encasement and investigating whether a column that was partially encased with geogrid would behave similarly to a fully-encased column. In addition, isolated column behaviour was compared to group column behaviour. The results of partially encased column tests indicated a steady reduction in vertical strain with increase in the encased length of both isolated columns and group columns. Bulging of the column was observed to occur directly beneath the base of the encasement. A significant increase in column stiffness and further reduction in column strain was observed for fully-encased columns, with strain reductions in the order of 80%. This range of performance indicates that the techniques of partial and full geogrid encasement can be applied to potential site applications.

Wu and Hong (2009) have studied the performance improvement of soft clay due to inclusion of encapsulated sand column. The sand columns were encapsulated by geotextiles. The tests consisted of triaxial compression tests on sand columns with two different densities and encapsulated by sleeves fabricated from three different geotextiles. The test results indicate that stiffer the encasing reinforcement lower is the axial strain at which slippage occurs. Slippage results in flatter stress-strain response and thereby lower axial strength, indicating that stiffer reinforcement gives higher performance improvement. Higher the confining pressure lesser is the

interfacial slippage. Under large confining pressure the granular material is more intensely bonded to the geosynthetic encasement leading to steep increase in load carrying capacity.

Murugesan and Rajagopal (2010) conducted laboratory model tests conducted on stone columns installed in clay bed prepared in controlled condition in a large scale testing tank. The load tests were performed on single as well as group of stone columns with and without encasement. Tests were performed with different geosynthetics for the encasement of stone column. The results from the load tests indicated a clear improvement in the load carrying capacity of the stone column due to encasement. The increase in the axial load carrying capacity depends very much upon the modulus of the encasement and the diameter of the stone column.

2.4 GEOSYNTHETIC REINFORCED SOIL MATTRESS OVERLYING STONE COLUMN/ PILE REINFORCED CLAY

Gupta and Somnath (1994) used the concept of geocell in the construction of box culverts over marine clay deposits in New Bombay area. Since the depth of marine clay was more than 6 meters, first tubular gabions were constructed in the soft soil with ends resting on hard moorum layer underlying the soft clay. Next the geocell mattress was constructed on the clay surface. In this arrangement the gabions serve as granular piles and the geocell mattress as flexible pile cap. The performance of the geocell mattress has been reported to be satisfactory.

Han and Gabr (2002) carried out a numerical study to investigate pile-soil-geosynthetics interactions by considering three major influence factors: the height of the fill, the tensile stiffness of geosynthetic, and the elastic modulus of pile material. The obtained results have shown that inclusion of geosynthetics in the earth platform can reduce the settlements above the pile head. The stress concentration ratio and the

maximum tension in geosynthetic increase with the height of the embankment fill, the tensile stiffness of geosynthetic, and the elastic modulus of the pile material. The distribution of tension force in the geosynthetic reinforcement indicated that the maximum tension occurs near the edge of the pile.

Deb et. al. (2007) have developed a mechanical model to predict the behavior of a geosynthetic-reinforced granular fill over soft soil improved with stone columns. The saturated soft soils were idealized by Kelvin–Voight model to represent its consolidation behavior. The stone columns were idealized by stiffer springs. Pasternak shear layer and rough elastic membrane represented the granular fill and geosynthetic reinforcement layer, respectively. The nonlinear behavior of the granular fill and the soft soil was considered. Effect of consolidation of the soft soil due to inclusion of the stone columns had also been included in the model. An iterative finite difference scheme was applied for obtaining the solution. The results indicate that inclusion of the geosynthetic layer effectively reduces the settlement. Nonlinearity in the behavior of the soft soil and the granular fill is reduced due to the use of geosynthetic reinforcement layer.

Abdullah and Edil (2007) carried out a series of tests on embankment constructed over soft ground to evaluate the performance of different types of load transfer platform (LTP) placed at interface of embankment and clay bed reinforced with rammed aggregate piers (called 'geopiers'). Three types of LTP were constructed in accordance with the recommended design for each: a geosynthetic-reinforced LTP with two layers of geogrid (catanary LTP), a geosynthetic reinforced LTP with three or more layers of geogrid (beam LTP), and a reinforced concrete LTP. The results indicate that the differential settlement between the geopiers and the matrix soil is relatively small in all LTP sections, with the smallest in the beam LTP. The tensile

strain in the geogrid was approximately 60% of the allowable design strain of 5% in the beam LTP. In the central LTP, the tensile strain in the geogrid was approximately 20% of the allowable design strain of 6%, although the differential settlement was larger than the beam LTP. The total and differential settlements observed indicate that the use of low stiff geopier column together with LTPs provide an attractive option for supporting low embankments on soft ground with tolerable total and differential settlements. The presence of LTPs and the supporting columns also tend to reduce the lateral movement of the foundation soil. The cost analysis of the different LTPs indicates that construction cost for geosynthetic-reinforced LTPs are likely to vary with locality, however, it appears that beam LTPs offer a less costly approach, with enhanced performance.

Madhav et. al. (2009) studied the interaction between granular pile and the overlying raft using continuum approach. Results show that consideration of radial displacement compatibility does not influence the settlement response or sharing of the applied load between the granular pile and the raft. The percentage of load carried by the granular pile increases with the increase in its stiffness and decreases with the increase of relative size of the raft. The normal stresses at the raft soil interface decreases with the increase of stiffness of granular pile and/or relative length of granular pile. The influences of granular pile stiffness and relative length of the granular pile are found to be more for relatively large size of raft. The percentage of load transferred to the base of granular pile increases with increase in size of raft.

Arulrajah et. al. (2009) reported that the construction of a high speed railway project for trains of speed of upto 160km/hr, between Rawang and Bidor (110km long) in Peninsular Malaysia. The ground improvement methods adopted in the project were vibro-replacement with stone column, dry deep soil mixing (cement columns),

geogrid reinforced pile embankments with individual pile caps. It was observed that where a geogrid layer was laid over the pile caps its tension provides additional support and prevents lateral spreading of the embankment.

2.5 SCOPE OF PRESENT STUDY

The literature review reveals that both geocell-sand mattress and stone columns are effective means for performance improvement of soft clay foundation, primarily, in terms of increase in bearing capacity and reduction in settlements. Their individual applications though have been intensely studied by many researchers but combined application of both has remained unexplored. Conventionally a layer of sand cushion is provided over the stone columns in clay beds. Limited research reported in literature shows that this sand layer when reinforced with planar geosynthetics further improves the performance of the system. Geocells, being three dimensional confining structures would prevent lateral squeezing of sand thereby giving rise to a coherent body called geocell-sand mattress. This relatively rigid geocell-sand mattress is expected to serve as a better platform to support the structure and redistribute its load, onto the stone column reinforced clay bed, in a more uniform manner over a much wider area compared to the case of sand cushion alone. In view of this, under the present investigation a comprehensive experimental research work has been envisaged to study the behaviour of the systems having geocell-sand mattress overlying stone column reinforced clay beds subjected to monotonic circular loading.

CHAPTER 3

EXPERIMENTAL INVESTIGATIONS

3.1 INTRODUCTION

The aim of the present investigation is to study the behaviour of the composite foundation system that comprises of geocell sand mattress overlying stone column reinforced soft clay bed, under circular loading. The details of the materials used, their properties and the model tests are presented in this chapter.

3.2 MATERIALS USED

3.2.1 Clay

A locally available natural silty clay soil was used to prepare the clay subgrades. The specific gravity of this soil is found to be 2.63 (ASTM D 0854 – 02). The particle size distribution was determined as per ASTM D 6913-04.

For particles coarser than 75μm, sieve analysis was carried out and for particles smaller than 75μm; hydrometer test was performed as per ASTM D 4221-99. The particle size distribution of this soil is presented in Fig.3.1. The soil has 20% fraction by weight, finer than 75 μm sieve size.

The liquid limit, plastic limit and plasticity index of the soil are found to be 40%, 21% and 19% respectively (ASTM D 4318-05). As per the Unified Soil Classification System (USCS) [ASTM D2487-06] the soil can be classified as clay with low plasticity (CL).

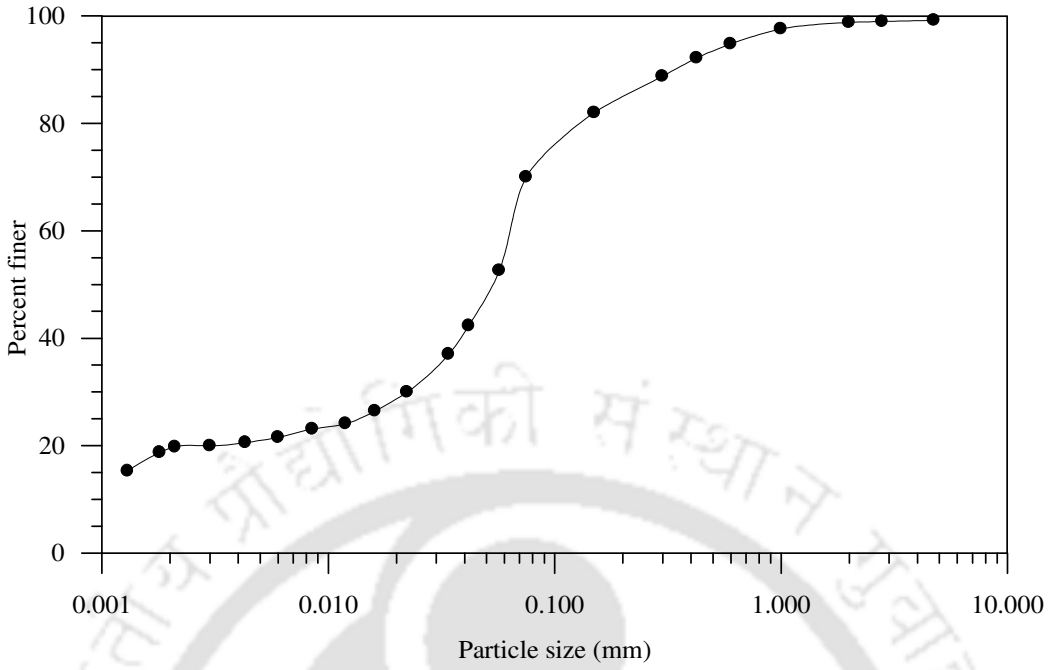

Fig: 3.1 Grain size distribution of the clay used in the experiments

3.2.2 Sand

The sand used for preparing geocell-sand mattress in the model tests is a locally available river sand. The sand was first air dried in the laboratory before it was used in the experimental work. The specific gravity of this sand is found to be 2.68 (ASTM D 0854–06). Its particle size distribution, determined by dry sieve analysis as per ASTM D 6913-04 is shown in Fig. 3.2. The different particle sizes D_{10}, D_{30}, D_{50} and D_{60} are found to be 0.19mm, 0.31mm, 0.44mm and 0.48mm respectively. The Coefficient of uniformity (C_u) and Coefficient of curvature (C_c) are obtained as 2.52 and 1.05 respectively. As per Unified Soil Classification System (USCS) [ASTM D 2487-06], the soil is classified as poorly graded sand (SP). The maximum dry density (γ_{dmax}) as determined using a vibratory table (ASTM-D 4253-00) is 16.51kN/m^3. The minimum dry density (γ_{dmin}) is found to be 13.94 kN/m^3 (ASTM D 4254-00). The maximum void ratio (e_{max}) and minimum void ratio (e_{min}) are 0.89 and 0.59 respectively.

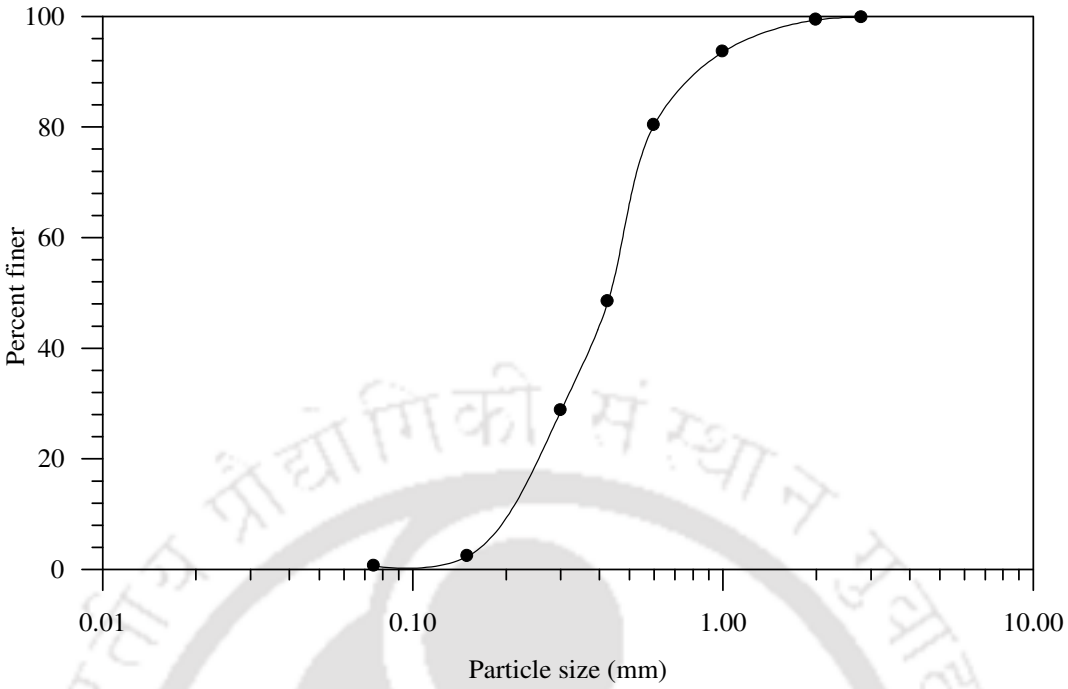

Fig: 3.2. Grain size distribution of sand used in the experiments

The friction angle of the sand at different relative densities was determined using both the triaxial compression tests and direct shear tests. The triaxial compression tests were conducted on dry sand samples of 38 mm in diameter and 76 mm in height under three different confining pressures (i.e.; 100 kPa, 150 kPa and 200 kPa) as per ASTM D 2850. The preparations of the sand samples were done by dry vibratory method as per ASTM 5311-92(04). Weight of dry sand required to obtain a specimen of desired density was determined based on the volume of the spilt mould. The soil was divided into six equal parts and each part was spooned into the membrane lined split mould attached to the bottom plates of the triaxial cell. The soil in each lift was compacted to the desired dry unit weight by vibration. The stress strain responses of the soil at relative densities of 35%, 50% and 80% are shown in Fig.3.3, Fig.3.4 and Fig.3.5 respectively. The corresponding p-q [i.e., $p = (\sigma_1 + \sigma_3)/2$, $q = (\sigma_1 - \sigma_3)/2$] diagram is presented in Fig. 3.6.

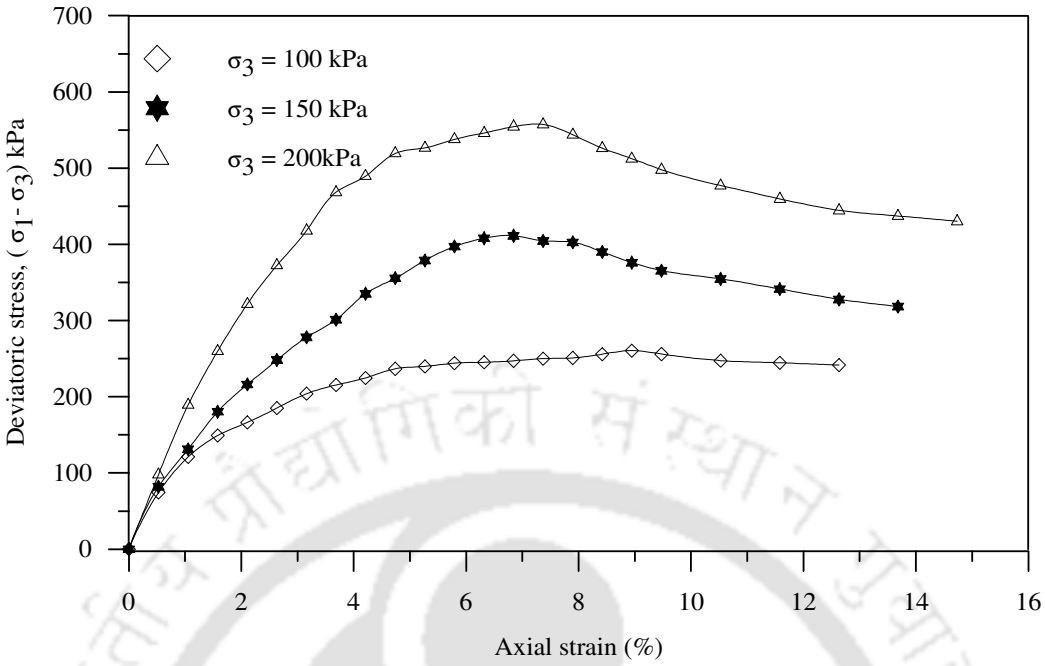

Fig.3.3: Stress-strain curves for sand under triaxial compression tests (ID = 35%)

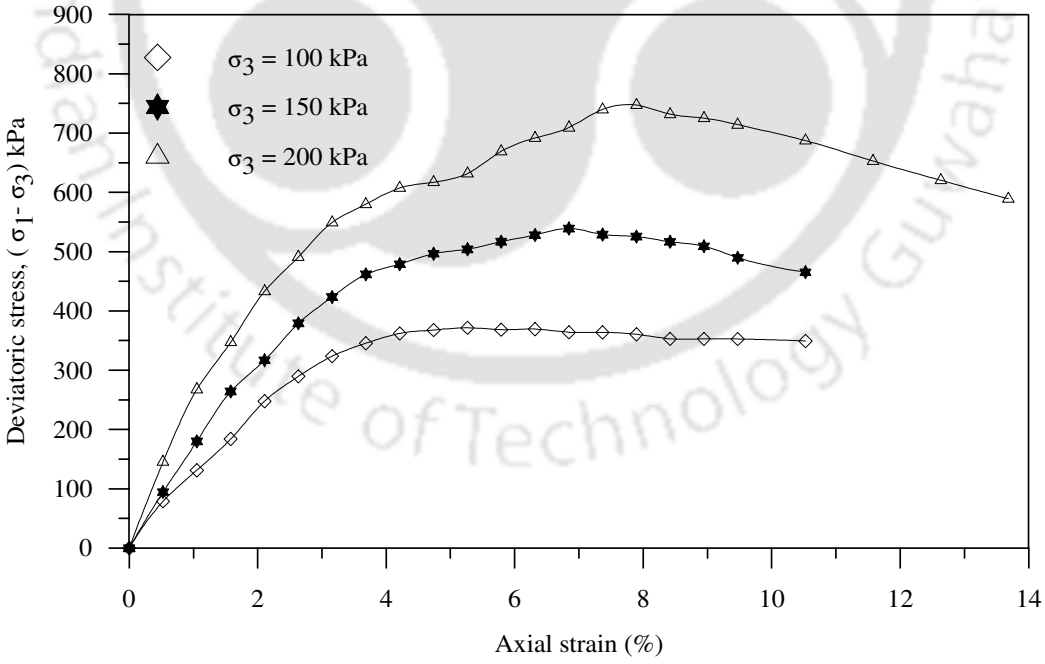

Fig.3.4: Stress-strain curves for sand under triaxial compression tests (ID = 50%)

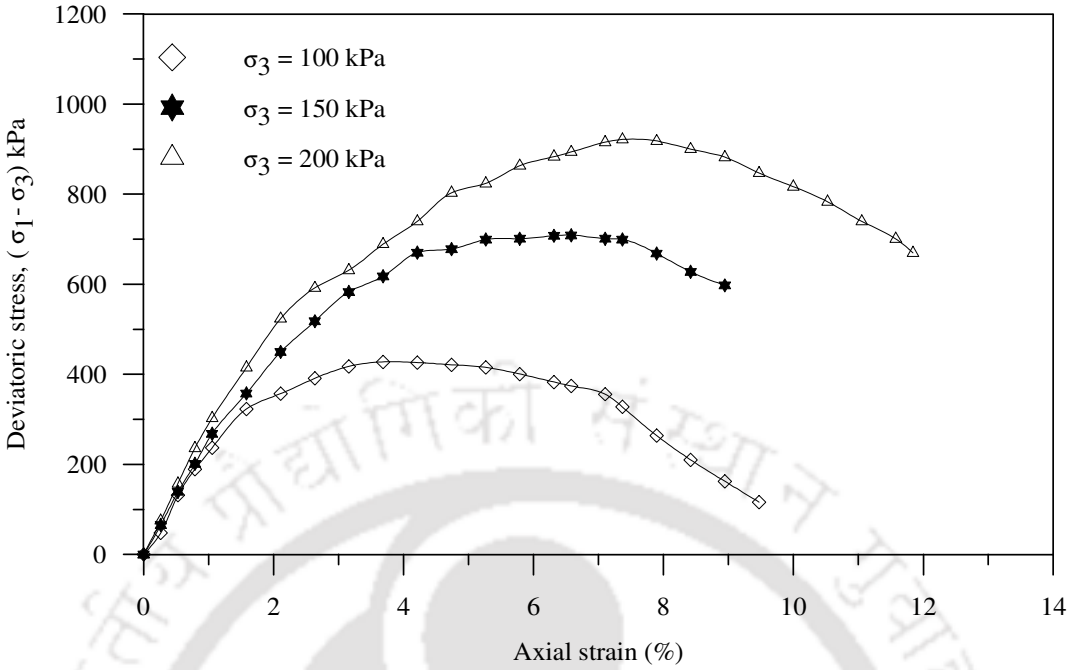

Fig.3.5: Stress-strain curves for sand under triaxial compression test (ID = 80%)

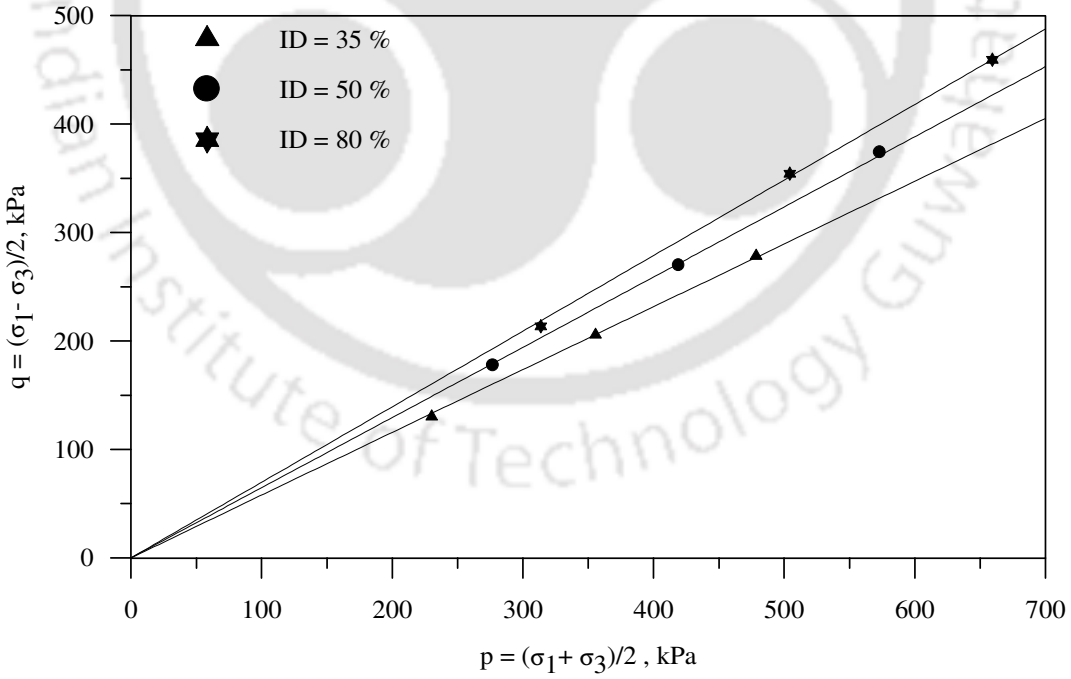

Fig. 3.6: p-q diagram for sand under triaxial compression test for different relative densities

The angles of shearing resistance obtained from the triaxial test are 35°, 40° and 44° for relative densities of 35%, 50%, and 80% respectively.

Direct shear tests were carried out at relative densities of 35%, 50% and 80% as per ASTM D 6528-07. The shear stress versus shear strain responses are presented in Fig. 3.7, 3.8 and 3.9 respectively. The corresponding horizontal versus vertical deformation responses of the soils are depicted in Fig. 3.11. The peak shear stress versus normal stress plots are shown in Fig. 3.10. The friction angles of the sand, at these relative densities, are obtained as 36°, 43°, and 46° respectively.

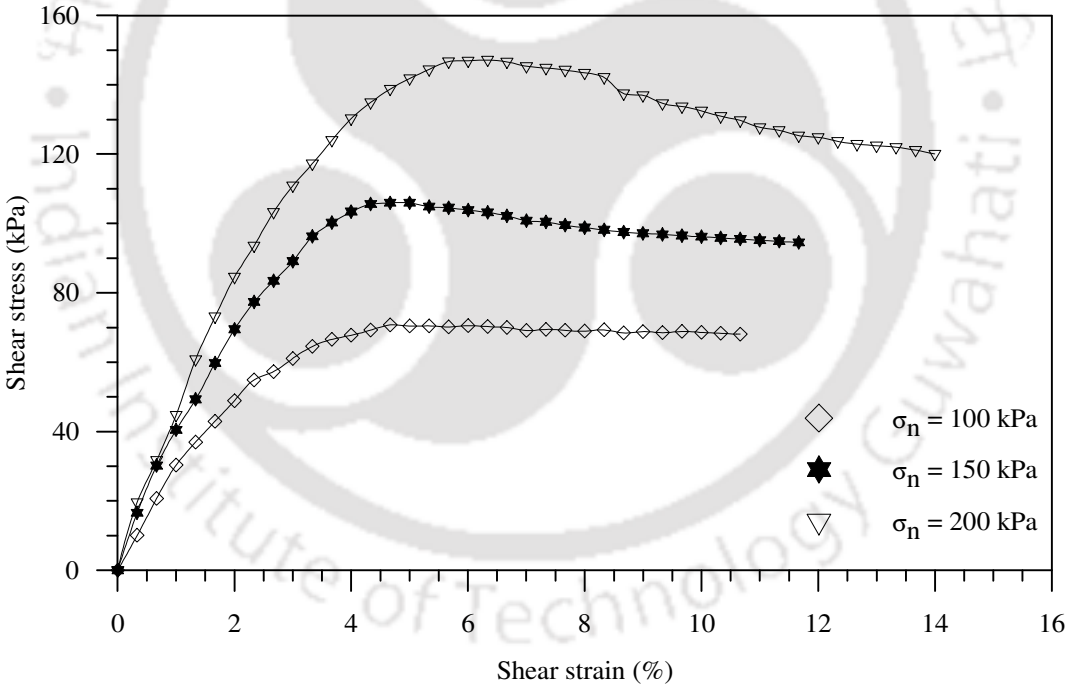

Fig.3.7: Shear stress-shear strain response of sand under direct shear (ID = 35 %)

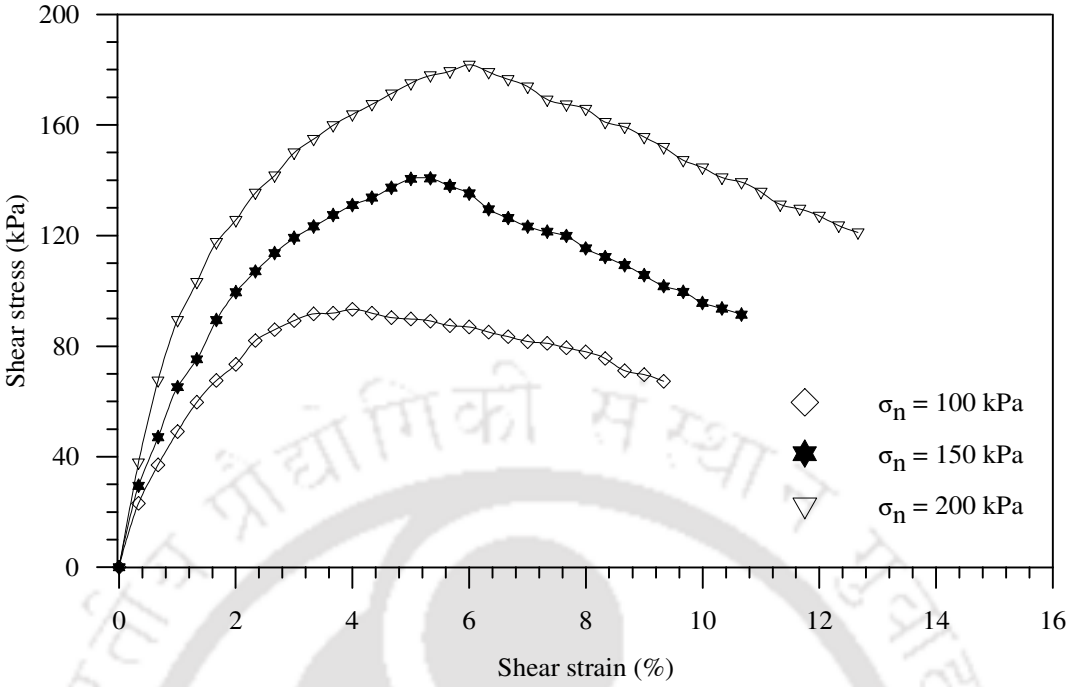

Fig.3.8: Shear stress-shear strain response of sand under direct shear (ID = 50%)

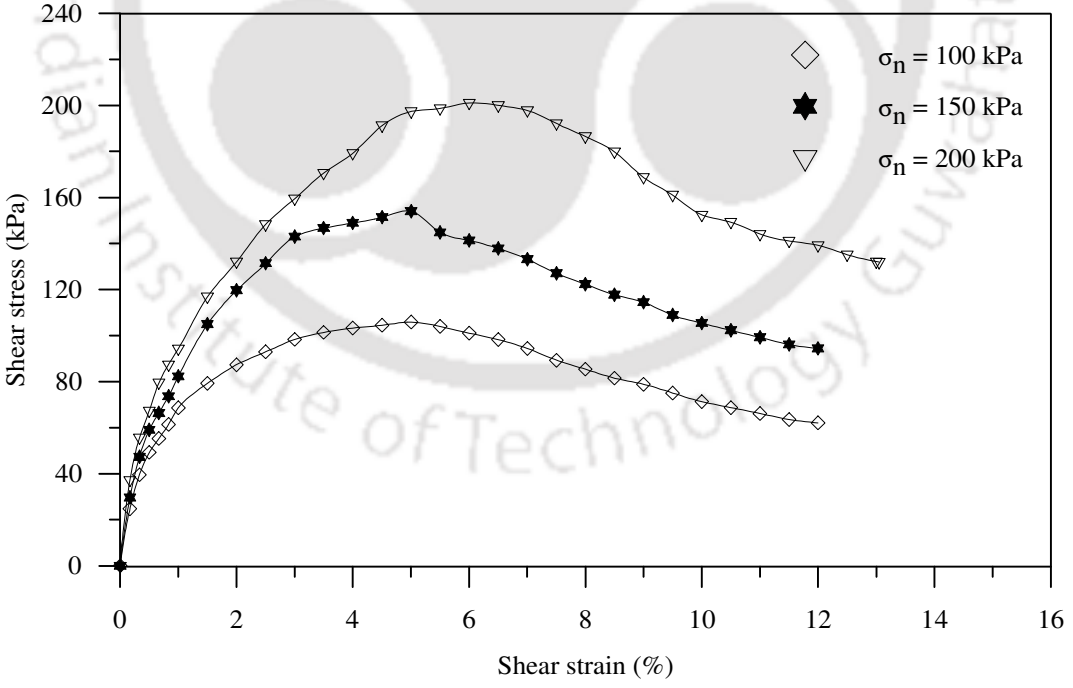

Fig.3.9: Shear stress-shear strain response of sand under direct shear (ID = 80 %)

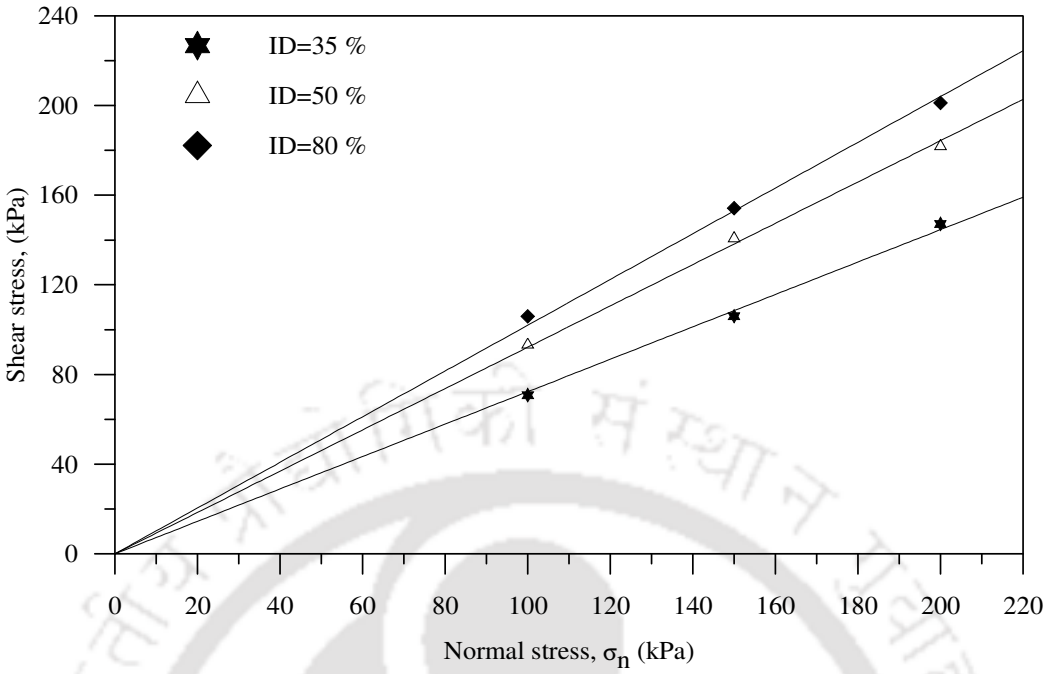

Fig.3.10: Normal stress-shear stress response of sand in direct shear for different relative densities

The dilation angles of the sand at these relative densities, were obtained as per Gibson (1953), according to which, dilation angle is the peak slope of increase in thickness of the sample (i.e., vertical deformation) versus shearing displacement (i.e., horizontal deformation). The increase in thickness of soil sample versus shearing displacement responses for soils at different relative densities, observed from direct shear tests conducted at different normal pressures are depicted in Fig.3.11-3.13. Since dilation decreases with the increase in normal stress (reported by Panda, 2000 and observed in the present study) to have a clear observation of dilation, tests were carried out at relatively lower normal stresses (i.e., 40kPa, 50kPa and 70Kpa). The maximum dilation angles (ψ) observed are 2º, 12º and 20º for relative densities of 35%, 50% and 80% respectively.

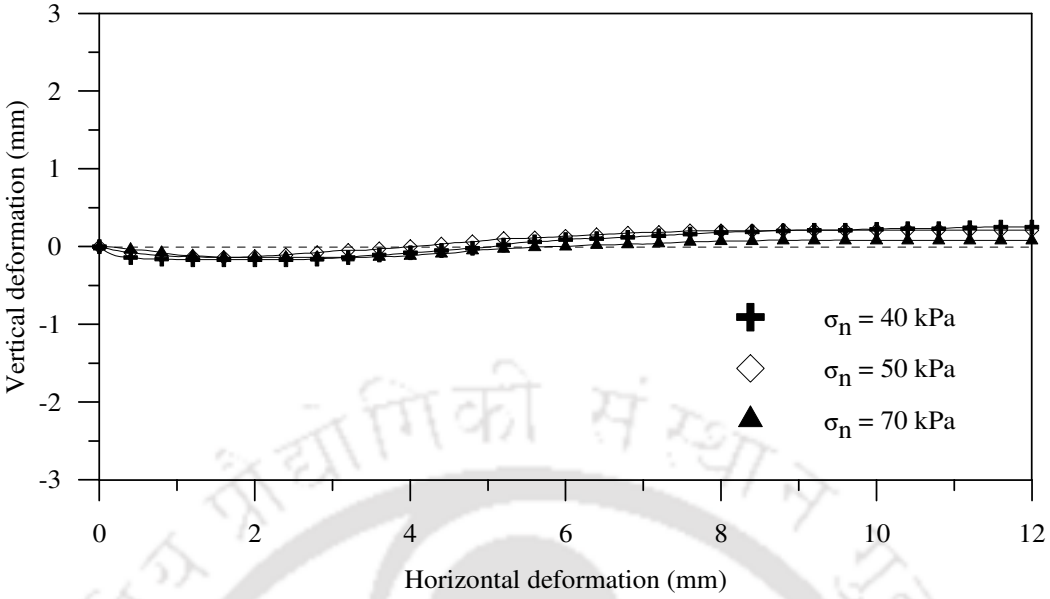

Fig.3.11: Horizontal deformation-vertical deformation response of sand from direct shear test (ID = 35%)

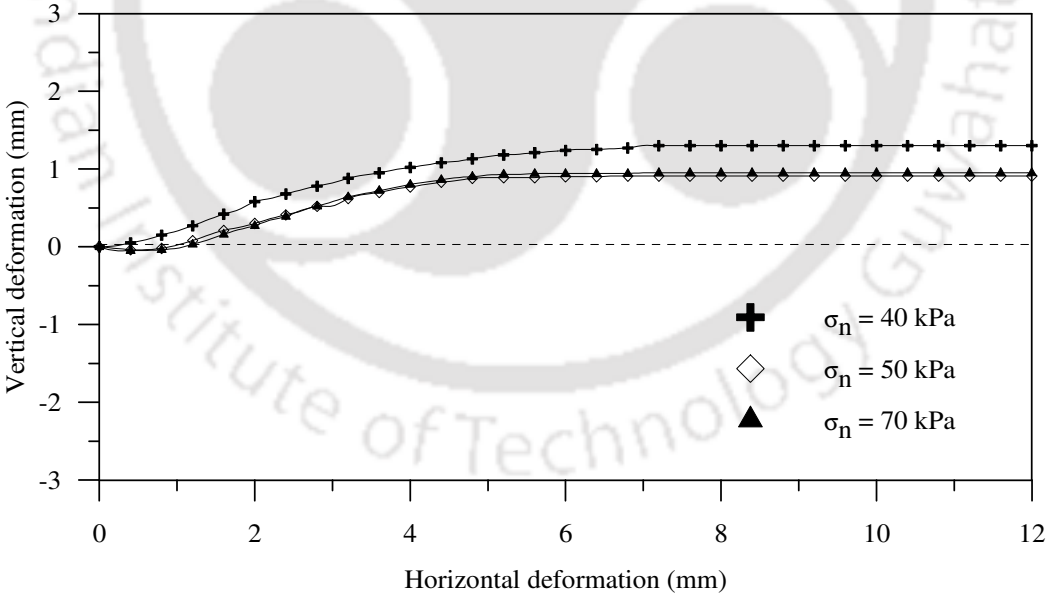

Fig.3.12: Horizontal deformation-vertical deformation response of sand from direct shear test (ID = 50%)

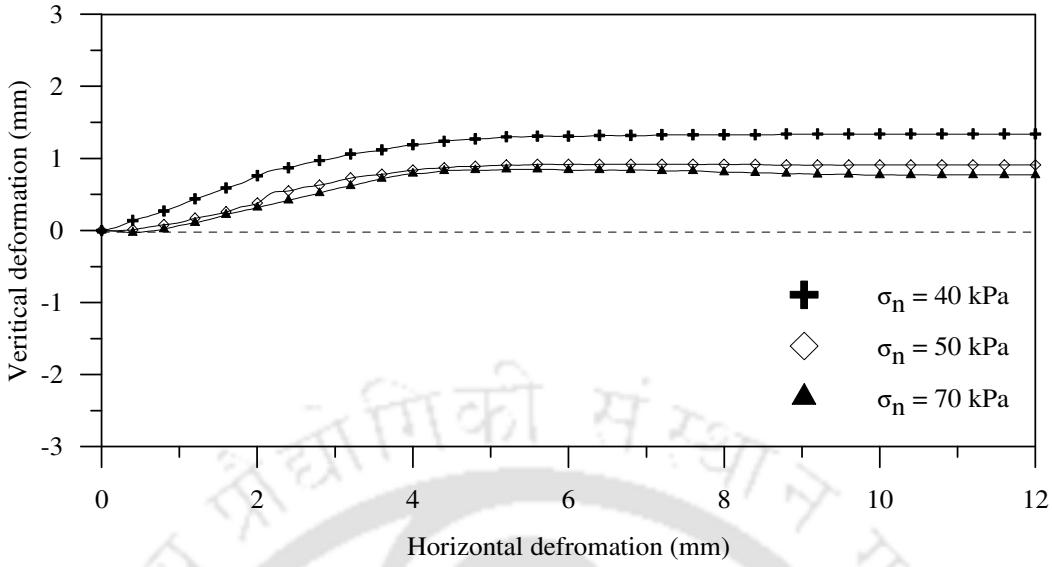

Fig.3.13: Horizontal deformation-vertical deformation response of sand from direct shear test (ID = 80%)

3.2.3 Crushed stone aggregate

The stone columns were formed using crushed stone aggregate with particle size varying in the range of 2mm to 10mm. The particle size distribution of the crushed stone is shown in Fig.3.14. The D_{10}, D_{30} and D_{60} sizes of the stone aggregate are 2.20mm, 3.15mm and 5.11mm respectively. The average particle size of the material (D_{50}) is 4.9mm. The crushed stone aggregate used has Coefficient of uniformity (C_u) of 2.32 and Coefficient of curvature (C_c) of 0.88 and is classified as poorly graded gravel (GP) as per Unified Soil Classification System (USCS).

The specific gravity, maximum dry density (γ_{dmax}) and minimum dry density (γ_{dmin}) of the aggregate are found to be 2.69, 16.83 kN/m^3 and 14.17 kN/m^3 respectively. The aggregate density in the stone columns was maintained as 15.95 kN/m^3 (ID = 71%). The angle of internal friction has been obtained through large size direct shear test setup wherein the test specimen dimension was 300mm × 300mm × 150 mm. The stone aggregate was compacted inside the shear box; at density same as the placement

density in stone columns (i.e., 15.95 kN/m^3). Tests were conducted under normal pressure of 100kPa, 150kPa and 200kPa respectively. The shear stress–shear strain response is shown in Fig.3.15. The corresponding peak shear stress versus normal stress is depicted in Fig. 3.16. The peak friction angle of the aggregate is found to be 48°. The horizontal deformation-vertical deformation response is plotted in Fig. 3.17. The dilation angle (ψ) (i.e.; peak slope of the vertical deformation-horizontal deformation response, Gibson 1953) is found to be 15°.

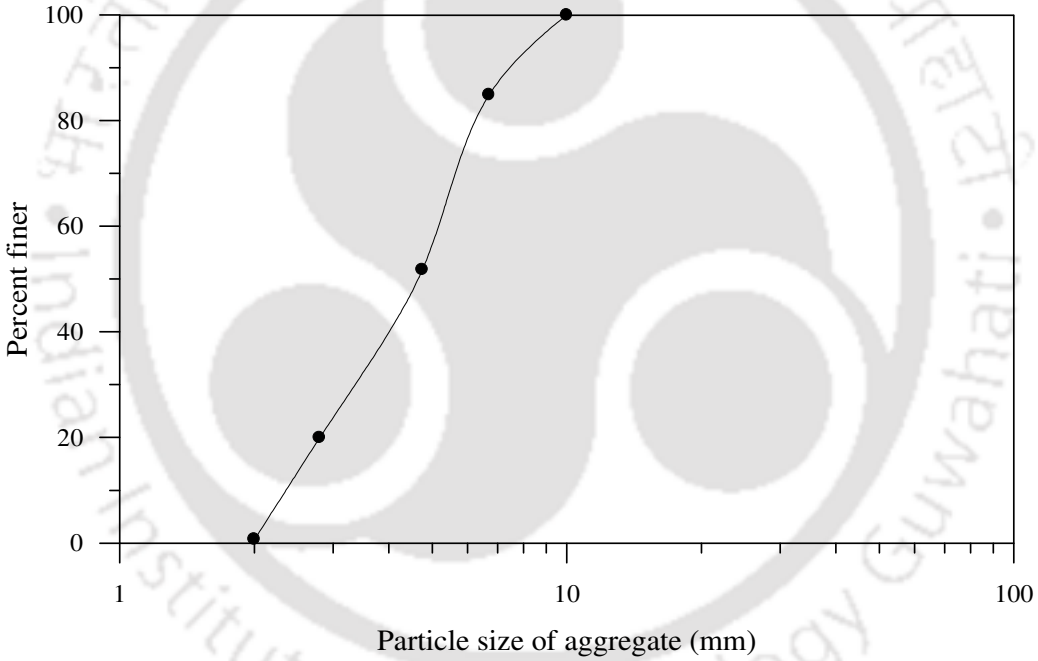

Fig.3.14: Particle size distribution of the aggregate used in stone columns.

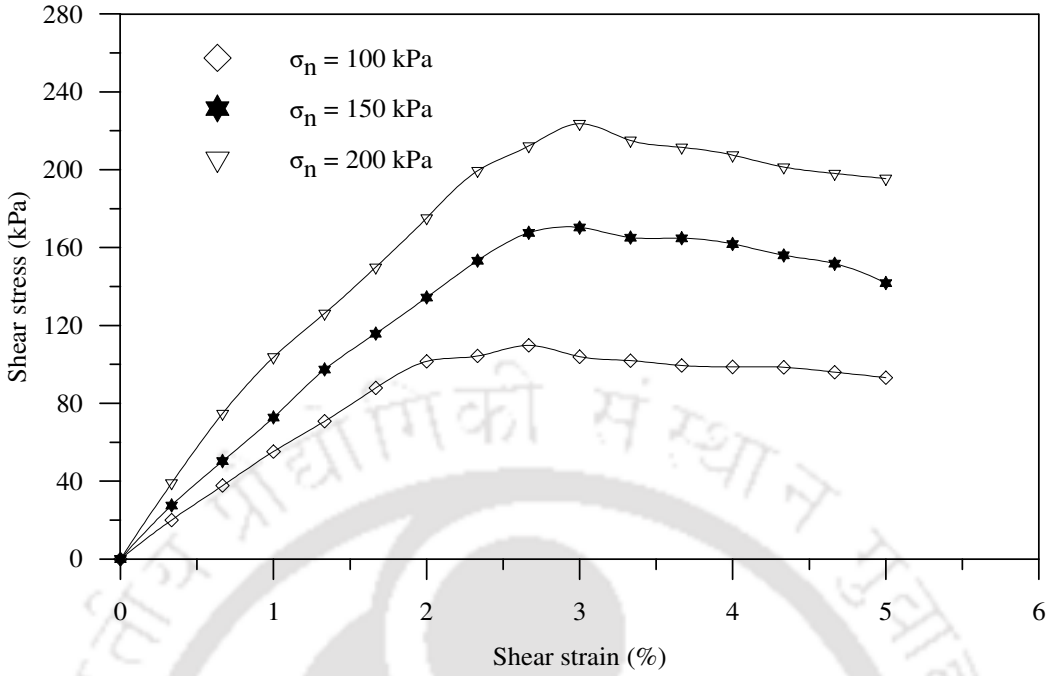

Fig.3.15: Shear stress-shear strain response of stone aggregate in direct shear (ID = 71 %).

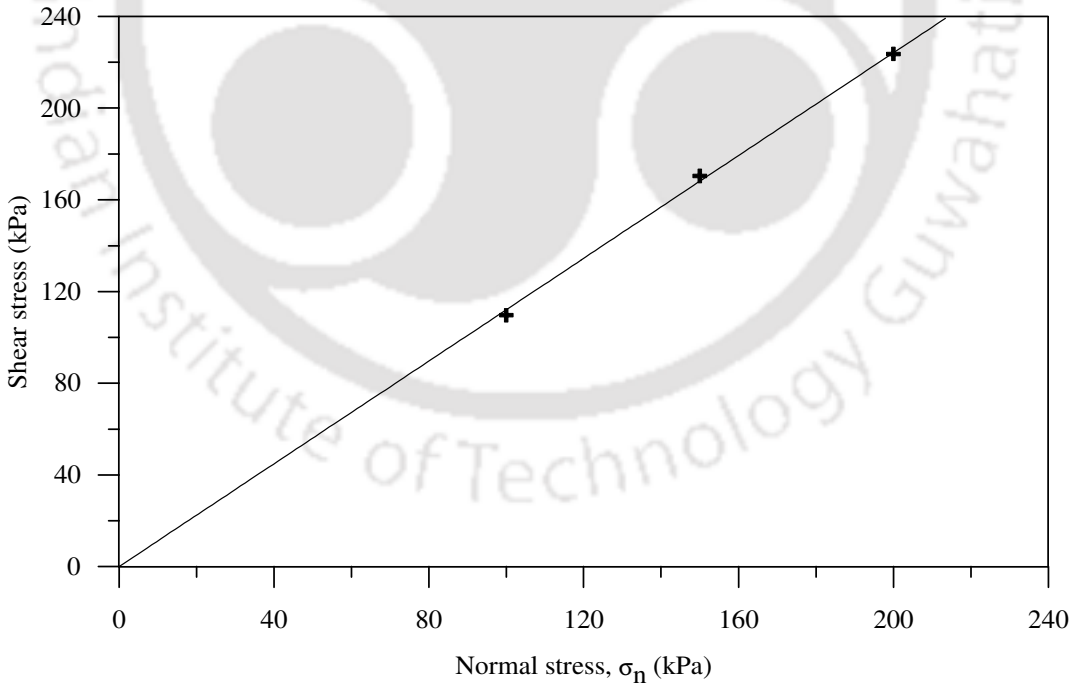

Fig.3.16: Normal stress-peak shear stress response of stone aggregate (ID = 71 %)

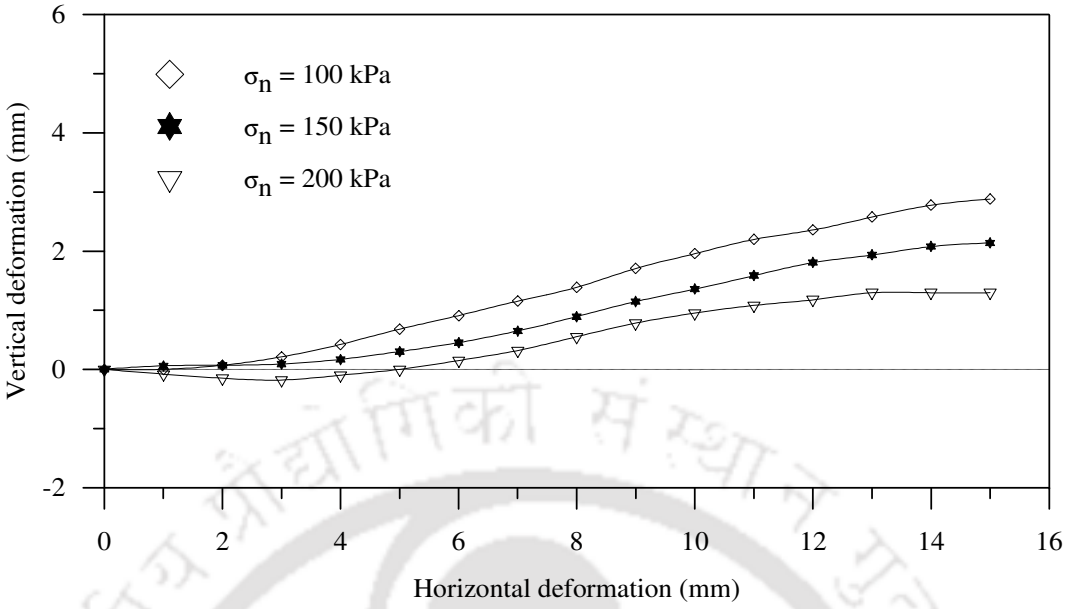

Fig.3.17: Horizontal deformation-vertical deformation response of stone aggregate under direct shear (ID = 71 %)

3.2.4. Geogrid

The geocells used were formed, using a biaxial geogrid (BX) made of oriented polymer having square shaped aperture with opening size of 36mm × 36mm. The photographic view and geometry of the geogrid are shown in Fig. 3.18 and Fig.3.19 respectively.

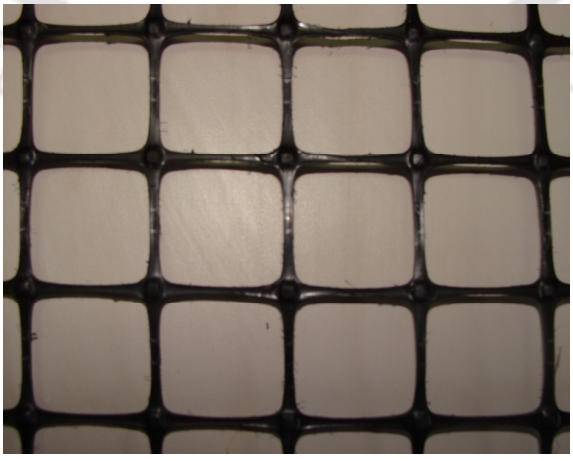

Fig.3.18: Photograph of the geogrid (BX)

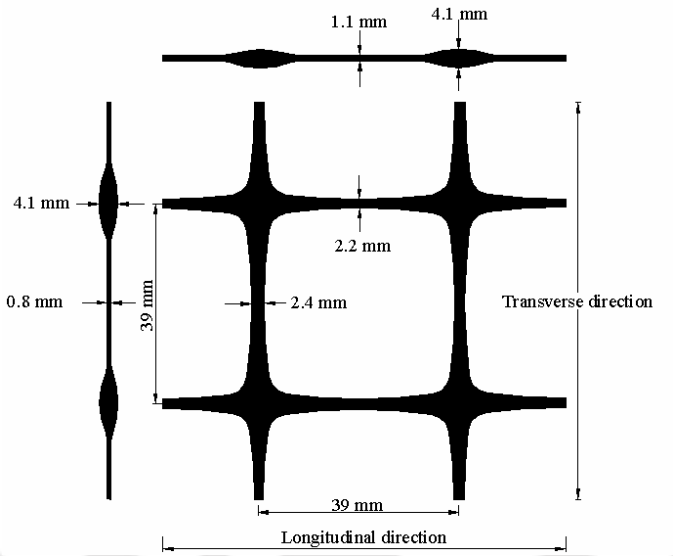

Fig. 3.19 Geometry of the geogrid (BX)

The load strain behaviour of the geogrid as obtained from the standard multi-rib tension test (ASTM D 6637-01) is shown in Fig. 3.20. Different properties of the geogrid obtained from the load strain response are, ultimate tensile strength = 19.3 kN/m, failure strain = 28%, secant modulus at 5% strain = 135kN/m and secant modulus at 10% strain = 108 kN/m.

The joints of the geocells were formed using 6mm wide and 3mm thick plastic strips made of low density polypropylene. The details of the geocell joints are presented in a later section (Section 3.5.3, Fig. 3.40). The geocell joint was tested as per ASTM D 4884, with geogrid specimens having a horizontal bodkin joint at mid length. The load deformation response of the joint is shown in Fig. 3.21. Since the joint is just a plastic strip the strain could not be obtained. Hence the response is presented in terms of axial deformation. The tensile strength of the joint is found to be 4.75 kN/m.

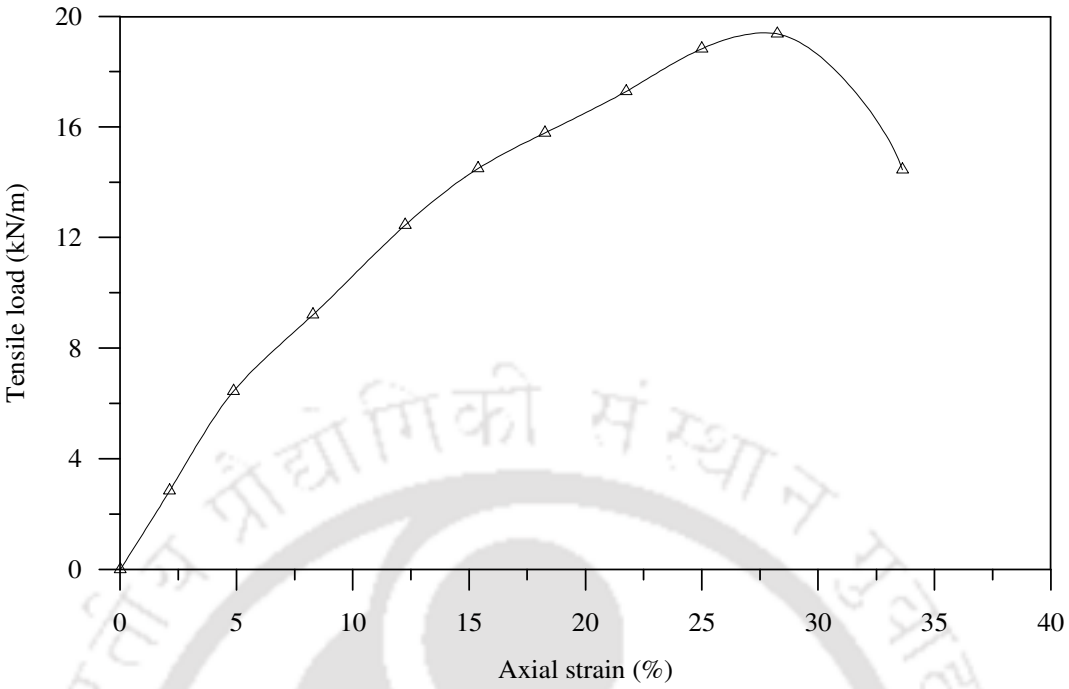

Fig. 3.20: Load-strain behaviour of geogrid (BX)

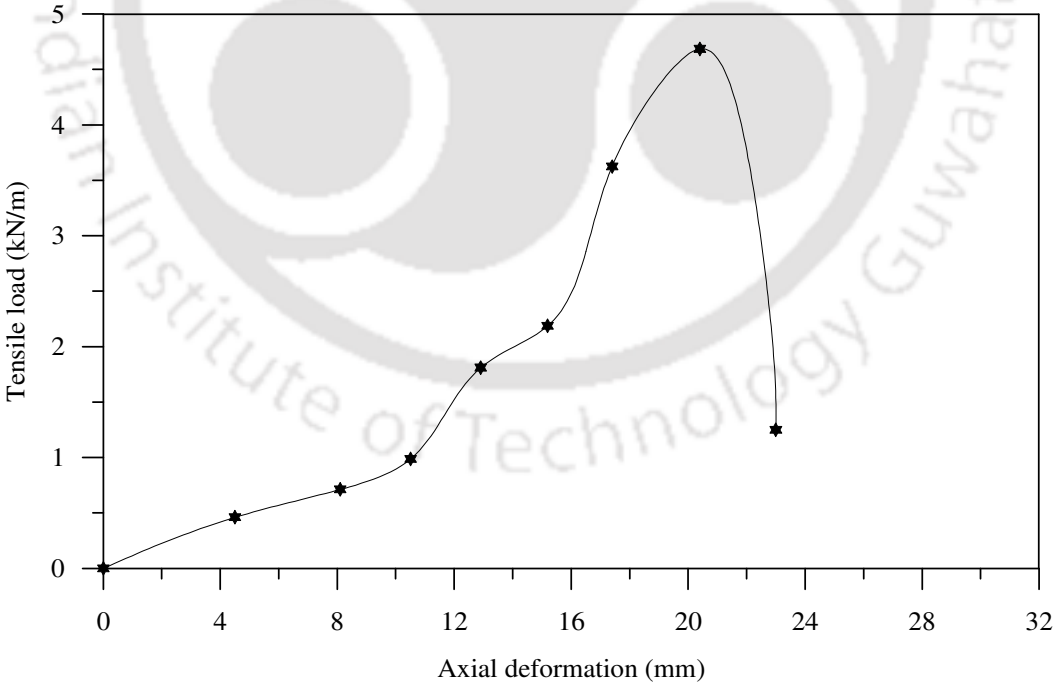

Fig. 3.21: Load-deformation behaviour of the bodkin joint.

The interfacial frictional properties of the geogrid were determined through pullout test as per ASTM D 6706-01, for different relative densities of sand (i.e., 35%, 50% and 80%). The obtained responses for the cases of ID = 35%, 50% and 80% are shown in Fig. 3.22, 3.23 and 3.24 respectively. In the Fig. 3.25 ultimate pullout resistance is plotted against applied normal stress to obtain the peak friction angle of the geogrid–soil interface (δ). The interfacial friction angle (δ) for soil relative density of 35%, 50% and 80% are found to be 24º, 27º and 30º respectively.

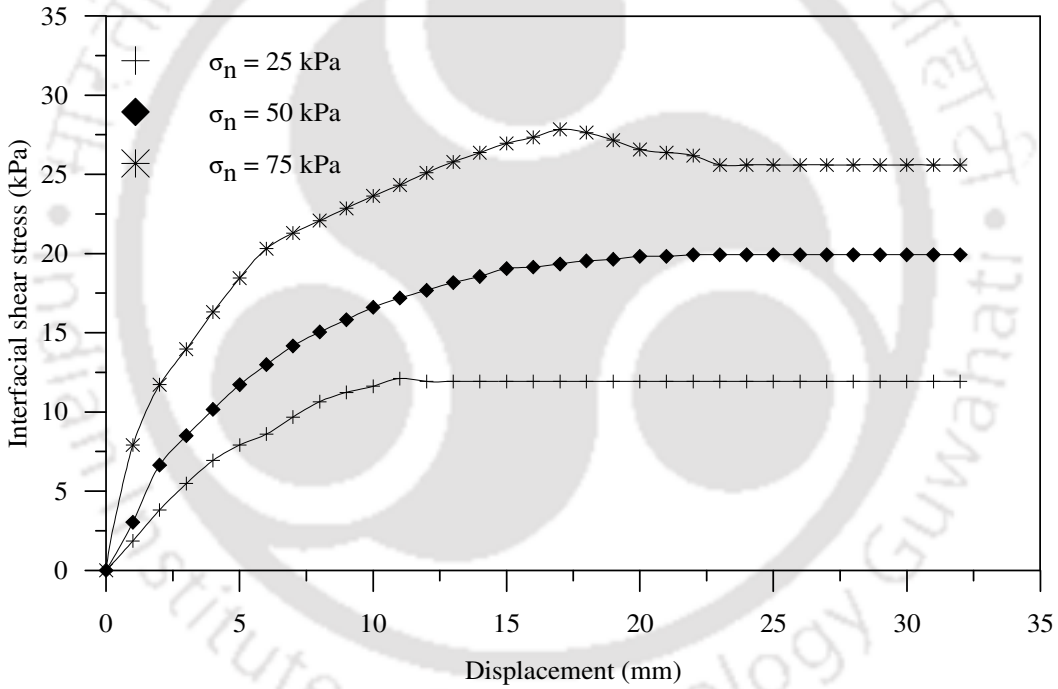

Fig. 3.22: Interfacial shear stress-horizontal displacement response of geogrid in pullout test (ID = 35%)

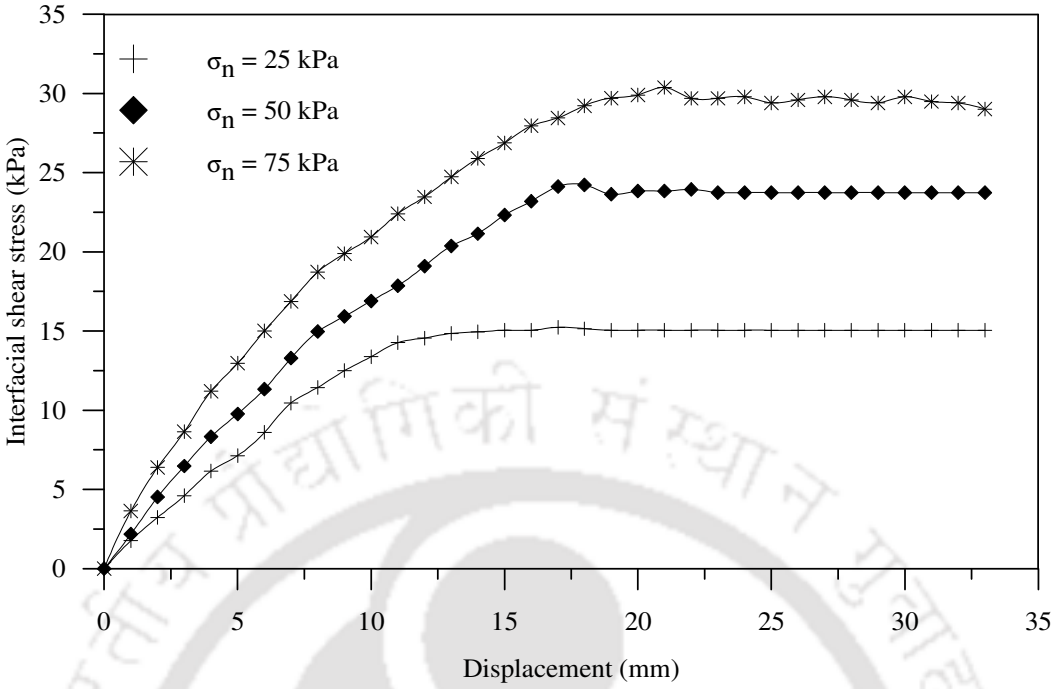

Fig. 3.23: Interfacial shear stress-horizontal displacement response of geogrid in pullout test (ID = 50%)

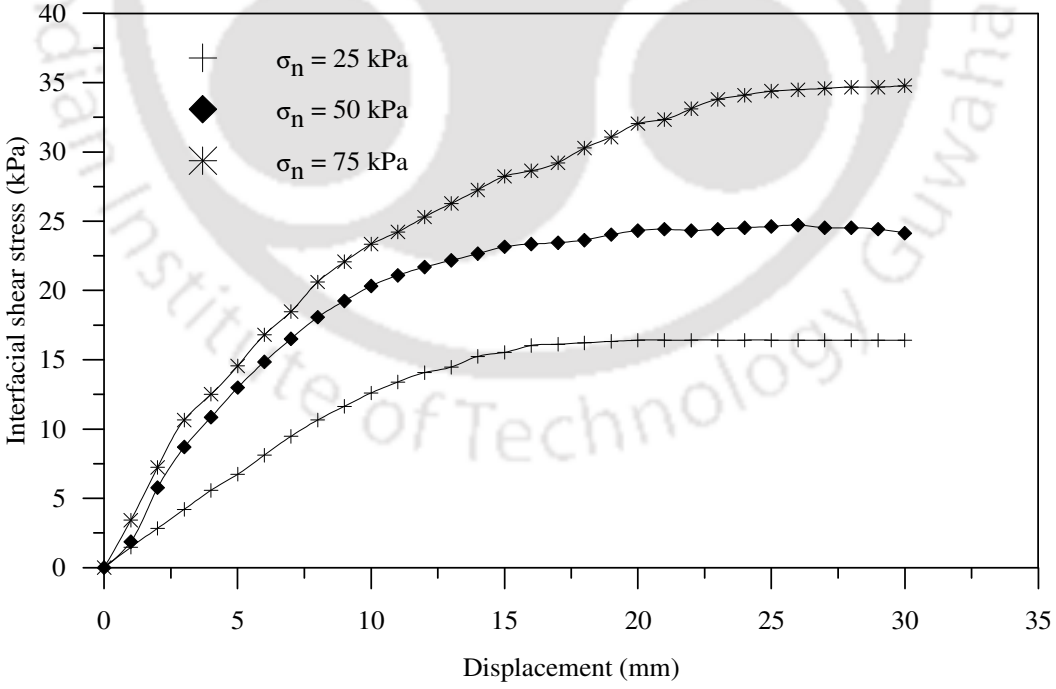

Fig. 3.24: Interfacial shear stress-horizontal displacement response of geogrid in pullout test (ID = 80%)

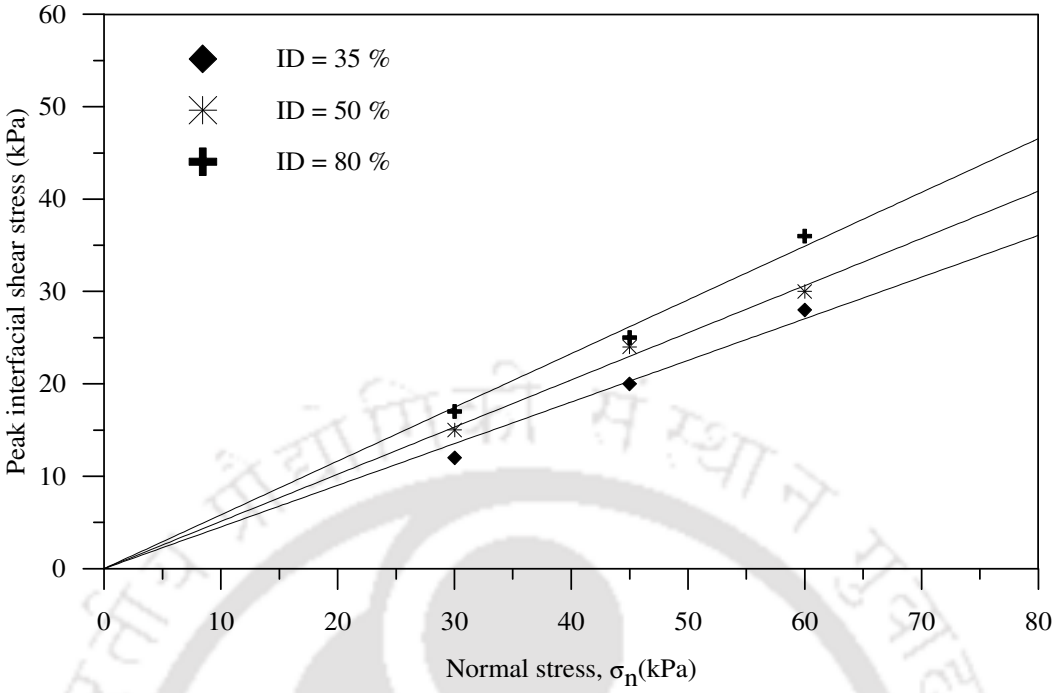

Fig.3.25: Normal stress-peak interfacial shear stress response of the geogrid.

3.2.5 Geomesh

In some experiments the stone columns were encased with geomesh. The geomesh used is relatively soft, which is a commercially available window mesh made of unoriented polymer. It has diamond shaped aperture with aperture opening size of 2mm×2mm. The photograph of the geomesh is shown in Fig.3.26. The load-strain behaviour of the soft geomesh as determined using standard wide width tension tests (ASTM D 6637-01) is shown in Fig.3.27. Beyond 45% axial strain, the load strain response shows large deformation, without further increase in strength. The ultimate tensile strength of the geomesh is found to be 2.9 kN/m

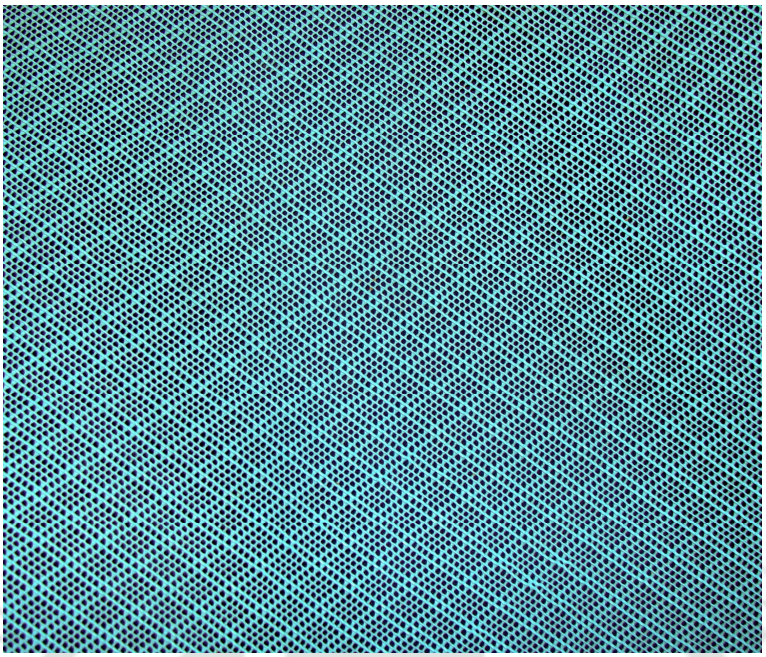

Fig.3.26: Photograph of the geomesh

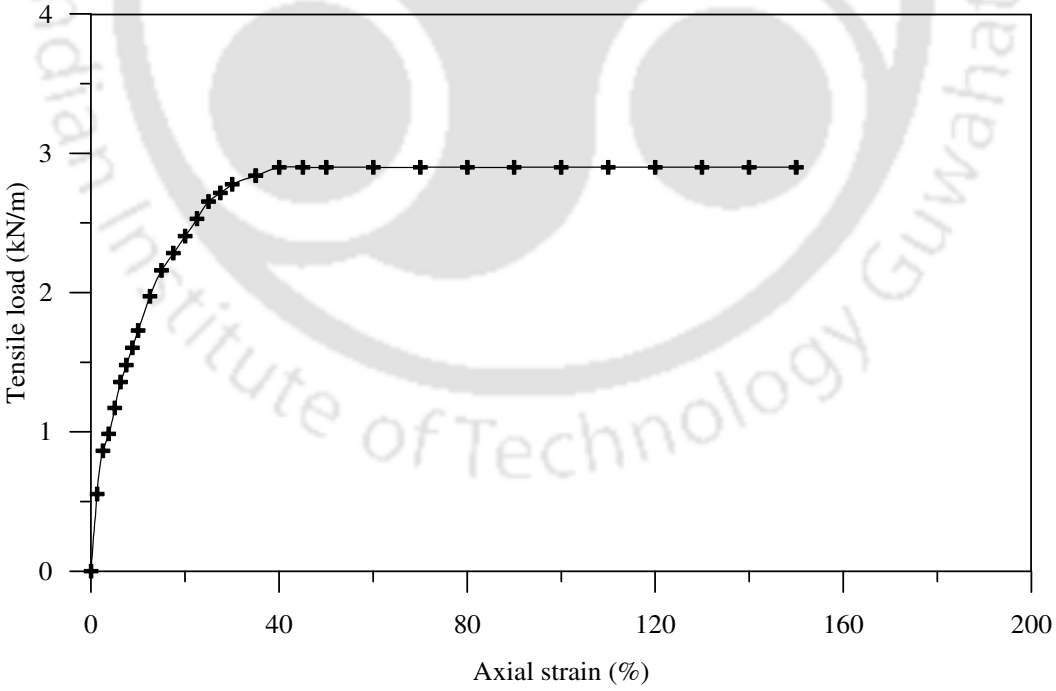

Fig.3.27: Load-strain behaviour of the geomesh

The cylindrical encasement sleeve was formed by overlapping the geomesh to required diameter over 10mm wide section and then stitching over it. The number of stitches and the thread used was kept same for all the tests. The strength of the seam was tested through wide width tensile test (ASTM D 4884), with the specimens having the horizontal seam at mid depth. The load deformation response is shown in Fig. 3.28. The seam strength is found to be 2.45 kN/m.

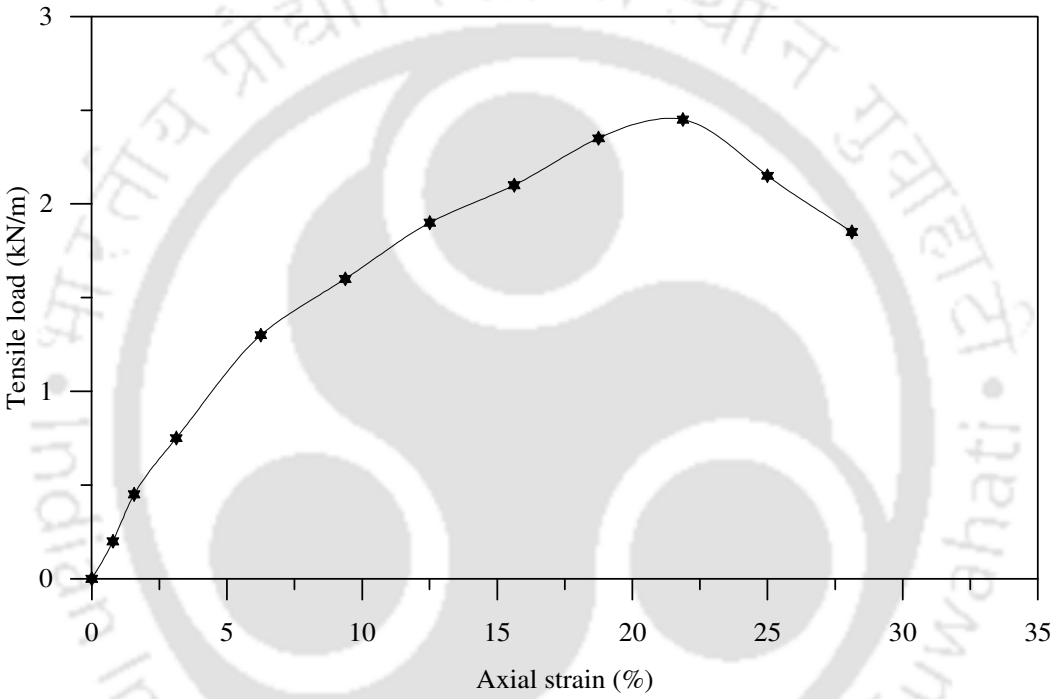

Fig.3.28: Tensile load-strain behaviour of the geomesh seam

3.3 PLANNING OF EXPERIMENTS

The experiments in this investigation were carried out systematically under various series to examine the influence of different parameters of stone column and geocell reinforced sand mattress on the overall response of the geocell–stone column reinforced clay bed under rigid circular footing. Within each series, only one parameter was varied, while the others were kept constant, to understand the influence

of that particular parameter on the overall behaviour. The geometry of the composite foundation system and the parameters considered in the test programme are illustrated in Figs. 3.29, 3.30 and 3.31. Diameter of geocell (d_{gc}) is taken as the equivalent diameter of the geocell pocket opening shown through hatch mark in Fig.3.31. As per the findings of Dash et. al. (2001a), in all tests, the geocell mattress was kept at a depth (u) of 0.1D from the base of the footing to get maximum performance improvement.

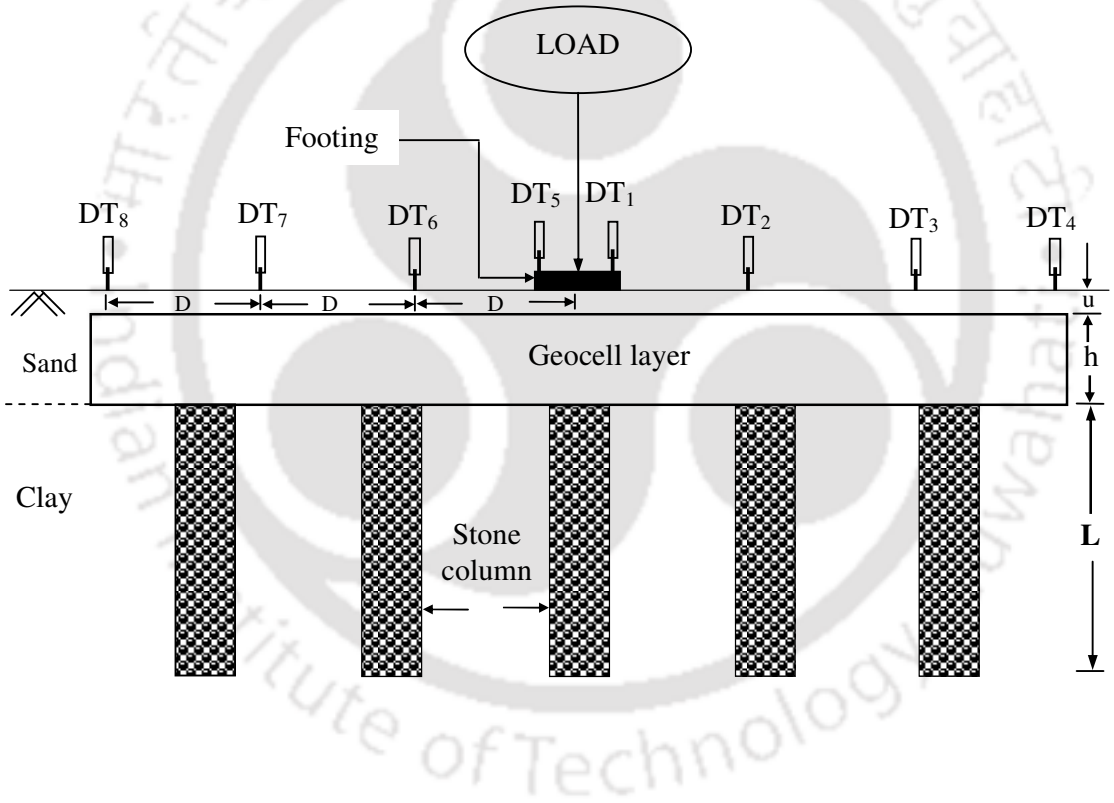

Fig. 3.29: Geometry of stone column-clay bed-geocell mattress foundation system (sectional view)

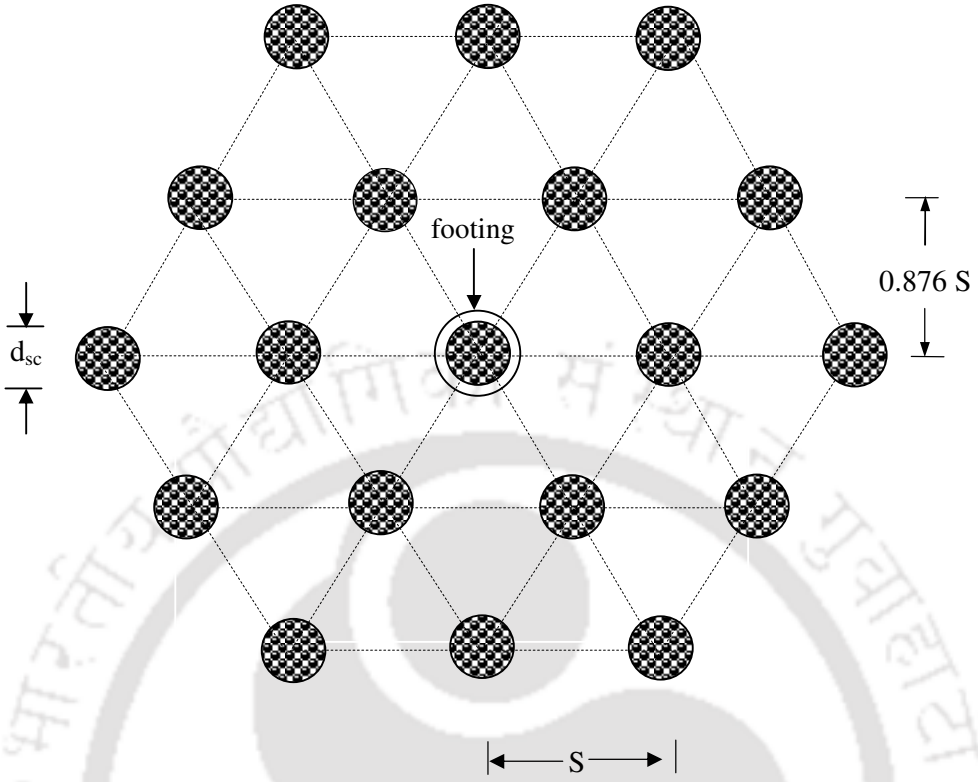

Fig. 3.30: Layout of stone column (plan view)

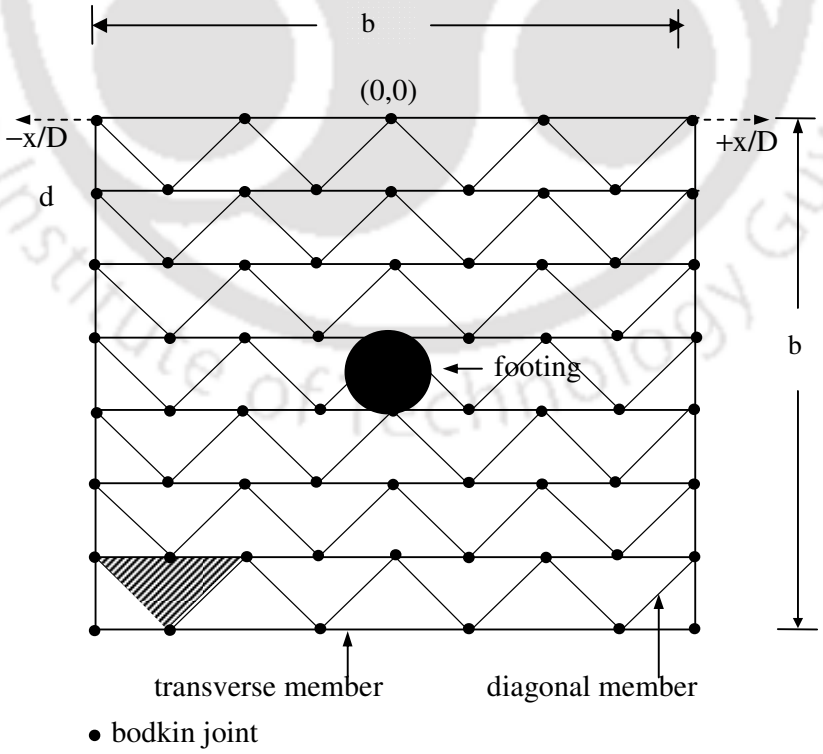

Fig. 3.31: Plan view of a typical geocell layer in chevron pattern.

In total 25 series of model load tests were conducted to establish the influence of the different parameters pertaining to the stone column-clay-geocell mattress, foundation system. The details of these test series are presented in Table 3.1. Tests in series 1 were performed on unreinforced soft clay bed. In series 2 and 3, tests were performed on stone column reinforced clay beds. In these tests the length (L) and spacing (S) of the stone columns were varied.

Under series 4-8 tests were carried out on geocell-sand mattress overlying clay bed. The parameters studied in these tests include the height of the geocell mattress, pocket size and the relative density of infill sand. Based on the results from these tests, optimum dimensions of the geocell mattress giving maximum performance improvement are determined.

The tests in series 9-12 were carried out on the composite foundation system comprising of geocell-sand mattress overlying stone column reinforced soft clay bed. In these tests, length of the stone column was varied for different height of the geocell mattress. In test series 13-16, tests were performed on composite foundation system by varying the spacing of the stone column for different height of geocell mattress.

Under series 17-18, tests were conducted to study the influence of the pocket size of geocells on the overall performance of the composite foundation system (i.e., clay bed-stone column-geocell mattress). Tests in series 19 and 20 were conducted on composite foundation bed by varying the relative density of sand in the geocell sand mattress.

Table 3.1 Details of laboratory model tests

Test Series	Type of reinforcement	Details of parameters investigated
1	Clay Bed	Constant parameter: c_u = 5kPa
2	Clay + SC	Constant parameter : c_u = 5kPa, S/d_{sc} = 2.5 Variable parameter: L/d_{sc} =1,3,5,7
3	Clay + SC	Constant parameter: c_u = 5kPa , L/d_{sc} = 5 Variable parameter: S/d_{sc} = 1.5, 2.5, 3.5
4	Clay + GC	Constant parameter: c_u = 5kPa, u/D = 0.1, d_{gc}/D = 0.8, b/D = 6, ID = 80% Variable parameter: h/D = 0.53, 0.9, 1.1, 1.6
5	Clay + GC	Constant parameter: c_u = 5kPa, d_{gc}/D = 0.8, h/D = 0.53, b/D = 6, u/D=0.1 Variable parameter: ID = 35%, 50%, 80 %
6	Clay + GC	Constant parameter: c_u = 5kPa, d_{gc}/D = 0.8, h/D = 0.9, b/D = 6, u/D = 0.1 Variable parameter: ID = 35%, 50%, 80 %
7	Clay + GC	Constant parameter: c_u = 5kPa, ID = 80 %, h/D = 0.53, b/D = 6, u/D = 0.1 Variable parameter: d_{gc}/D = 0.8, 1.1,1.33
8	Clay + GC	Constant parameter: c_u = 5kPa, ID = 80 %, h/D = 0.9, b/D = 6, u/D = 0.1 Variable parameter: d_{gc}/D = 0.8, 1.1, 1.33
9	Clay + GC + SC	Constant parameter: c_u = 5kPa, h/D = 0.53, b/D = 6, d_{gc}/D = 0.8, S/d_{sc} = 2.5, ID = 80 % Variable parameter: L/d_{sc} = 1, 3, 5, 7
10	Clay + GC + SC	Constant parameter: c_u = 5kPa, h/D = 0.9, d_{gc}/D = 0.8, b/D = 6, S/d_{sc} = 2.5, ID = 80 % Variable parameter: L/d_{sc} = 1, 3, 5, 7
11	Clay + GC + SC	Constant parameter: c_u = 5kPa, h/D = 1.1, b/D = 6, d_{gc}/D = 0.8, S/d_{sc} = 2.5, ID = 80 % Variable parameter: L/d_{sc} = 1, 3, 5, 7
12	Clay + GC + SC	Constant parameter: c_u = 5kPa, h/D = 1.6, d_{gc}/D = 0.8, b/D = 6, S/d_{sc} =2.5, ID = 80 % Variable parameter : L/d_{sc} = 1, 3, 5, 7
13	Clay + GC + SC	Constant parameter: c_u = 5 kPa, L/d_{sc} = 5, h/D = 0.53, b/D = 6, d_{gc}/D = 0.8, ID = 80% Variable parameter : S/d_{sc} = 1.5, 2.5, 3.5

Cont…

14	Clay + GC + SC	Constant parameter: c_u = 5 kPa, L/d_{sc} = 5 , h/D = 0.9, d_{gc}/D = 0.8, b/D = 6, ID = 80% Variable parameter : S/d_{sc} = 1.5, 2.5, 3.5
15	Clay + GC + SC	Constant parameter: c_u = 5 kPa, L/d_{sc} = 5 , h/D = 1.1, b/D = 6, d_{gc}/D = 0.8, ID = 80% Variable parameter : S/d_{sc} = 1.5, 2.5, 3.5
16	Clay + GC + SC	Constant parameter: c_u = 5 kPa, L/d_{sc} = 5 , h/D = 1.6, b/D = 6, d_{gc}/D = 0.8, ID = 80% Variable parameter : S/d_{sc} = 1.5, 2.5, 3.5
17	Clay + GC + SC	Constant parameter: c_u = 5kPa, L/d_{sc} = 5, S/d_{sc} = 2.5, b/D = 6, h/D = 0.53, ID = 80% Variable parameter: d_{gc}/D = 0.8, 1.1,1.33
18	Clay + GC + SC	Constant parameter: c_u = 5kPa, L/d_{sc} = 5, S/d_{sc} = 2.5, b/D = 6, h/D = 0.9, ID = 80% Variable parameter: d_{gc}/D = 0.8, 1.1, 1.33
19	Clay + GC + SC	Constant parameter: c_u = 5kPa, L/d_{sc} = 5,S/d_{sc} = 2.5, b/D = 6, h/D = 0.53, d_{gc}/D = 0.8 Variable parameter: ID = 35%, 50%, 80%
20	Clay + GC + SC	Constant parameter: c_u = 5kPa, L/d_{sc} = 5, S/d_{sc} = 2.5, b/D = 6, h/D = 0.9,d_{gc}/D = 0.8 Variable parameter: ID = 35%, 50%, 80%
21	Clay + GC + BG +SC	Constant parameter: c_u = 5kPa, L/d_{sc} = 5, S/d_{sc} = 2.5, u/D = 0.1, d_{gc}/D = 0.8 , ID = 80%, Variable parameter: h/D = 0.53, 0.9
22	Clay + ESC	Constant parameter: c_u = 5kPa, $L/d_{s\,c}$ = 5, $S/d_{s\,c}$ = 2.5 Variable parameter: L_{esc}/d_{sc} = 1, 3, 5
23	Clay + GC + ESC	Constant parameter: c_u = 5kPa, L/d_{sc} = 5, S/d_{sc} = 2.5, b/D = 6, d_{gc}/D = 0.8 , ID = 80%, h/D = 0.53 Variable parameter: L_{esc}/d_{sc} = 1, 3, 5
24	Clay + GC + ESC	Constant parameter: c_u = 5kPa, L/d_{sc} = 5, S/d_{sc} = 2.5, b/D = 6, d_{gc}/D = 0.8 , ID = 80%, h/D = 0.9 Variable parameter: L_{esc}/d_{sc} = 1, 3, 5
25	Clay + GC + BG + ESC	Constant parameter: c_u = 5kPa, L/d_{sc} = 5, S/d_{sc} = 2.5, L_{esc}/d_{sc} = 3, b/D = 6, d_{gc}/D = 0.8, ID = 80% Variable parameter: h/D = 0.53, 0.9

Note. *GC: Geocell, SC: Stone column, BG: Base geogrid, ESC: Encased stone column*

The influence of a layer of geogrid at the base of the geocell mattress, on the overall performance of composite foundation system was studied under test series 21. Performance of clay bed with encased stone columns was investigated under series 22. Tests under series 23 and 24 were carried out with encased stone columns in the clay bed, underlying geocell mattress.

To understand the combined influence of geocell mattress, base geogrid and encased stone columns, tests in series 25 were carried out, by using all these reinforcements together i.e. geocell-sand mattress, base geogrid, encased stone columns.

3.4 TEST DESCRIPTION

3.4.1 Test Set-up

The model tests were conducted in a test bed-cum-loading frame assembly in the laboratory. Schematic diagram of the test set-up are shown in Fig.3.32. Photographic views of the same are depicted in Fig. 3.33-35. General arrangement of the experimental setup is shown in Fig. 3.36. The soil beds were prepared in a steel tank with inside dimensions of 1000 mm × 1000 mm × 1300 mm (depth). The four sides of the tank are made of thick mild steel sheet and are braced laterally on the outer surface with steel channels to avoid yielding during the tests. The model foundation used is made of a steel plate of 150mm in diameter and 30 mm in thickness. It is attached to the spindle of the hydraulic actuator. A rough-base condition was achieved by cementing a thin layer of sand onto the base of the model foundation with epoxy glue. In all tests the footing was placed at the centre of the tank. The footing was loaded with a computer controlled motorised hydraulic system, wherein, the actuator is supported against the upper cross head of the reaction frame, with the load cell in-between (Fig.3.32a).

The depth of the test tank is 8.6 times the diameter of the footing and the minimum distance from the centre of the footing to the side walls of the tank is 3.3 times the footing diameter. Selig and Mckee (1961) and Chummar (1972) have observed that the failure wedge below a surface footing extends around 2 to 2.5B (B is the width of the footing) on either side of the footing and a depth of around 1.1B from the bottom of the footing.

The longest stone column in the present investigation is 700 mm in length and 100 mm in diameter ($L/d_{sc} = 7$). The maximum height of geocell-sand mattress is 255mm (i.e., 1.7 D). Therefore the clear spacing between the base of the stone column and the bottom of the test tank is 345mm [i.e. 1300 - (700+255)]. This is about 3.45 times the diameter of the stone column (d_{sc}). Mayerhof and Sastry (1978) have observed that the failure zone below a pile extends over a depth of about 2 times the diameter of the pile. In the present case, it being a flexible granular pile, this depth would be further less.

From these observations, it can be concluded that the tank used in the current investigation is considerably large enough and is not likely to interfere with the failure zones and hence the experimental results. Besides, the confinement of the tank wall represents the actual field condition for the interior columns of a large group of stone columns (Ambily and Gandhi 2007).

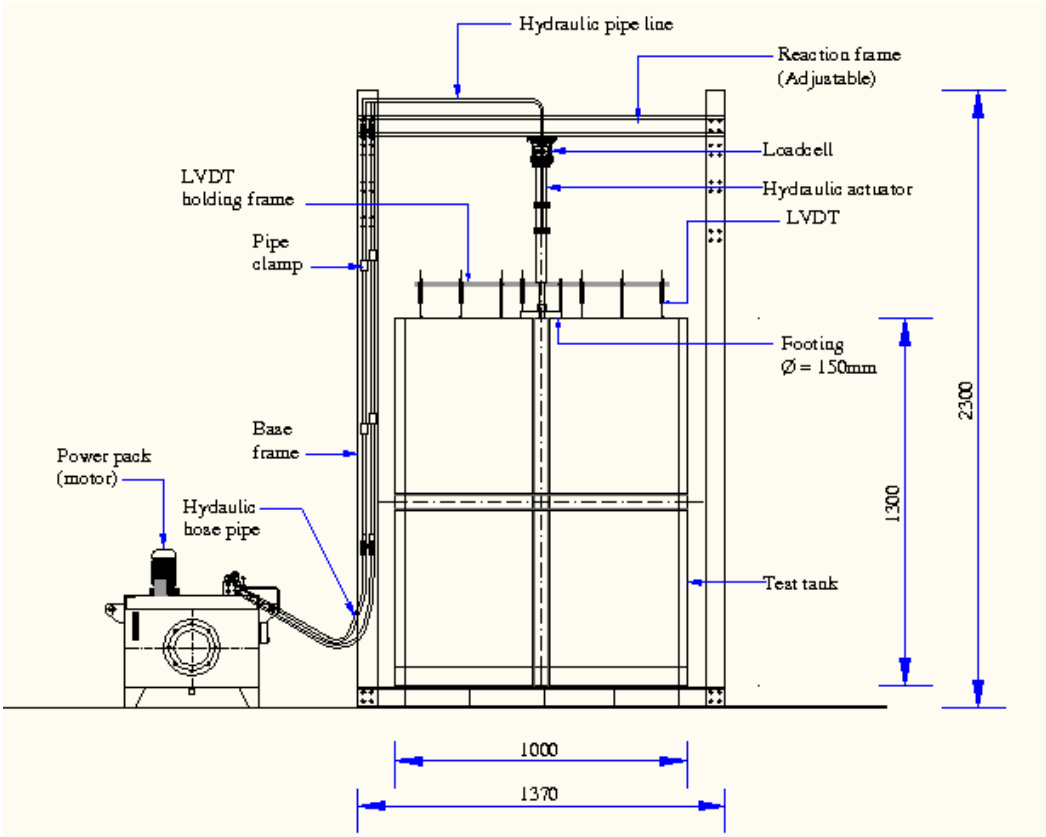

(a) Elevation

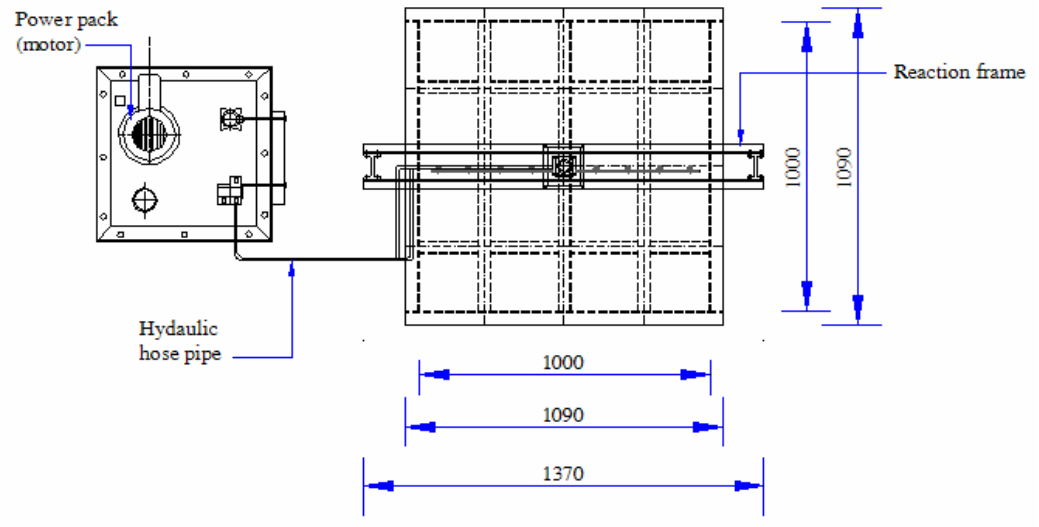

(b) Plan

Fig. 3.32: Schematic diagram of the test setup (All dimensions are in mm)

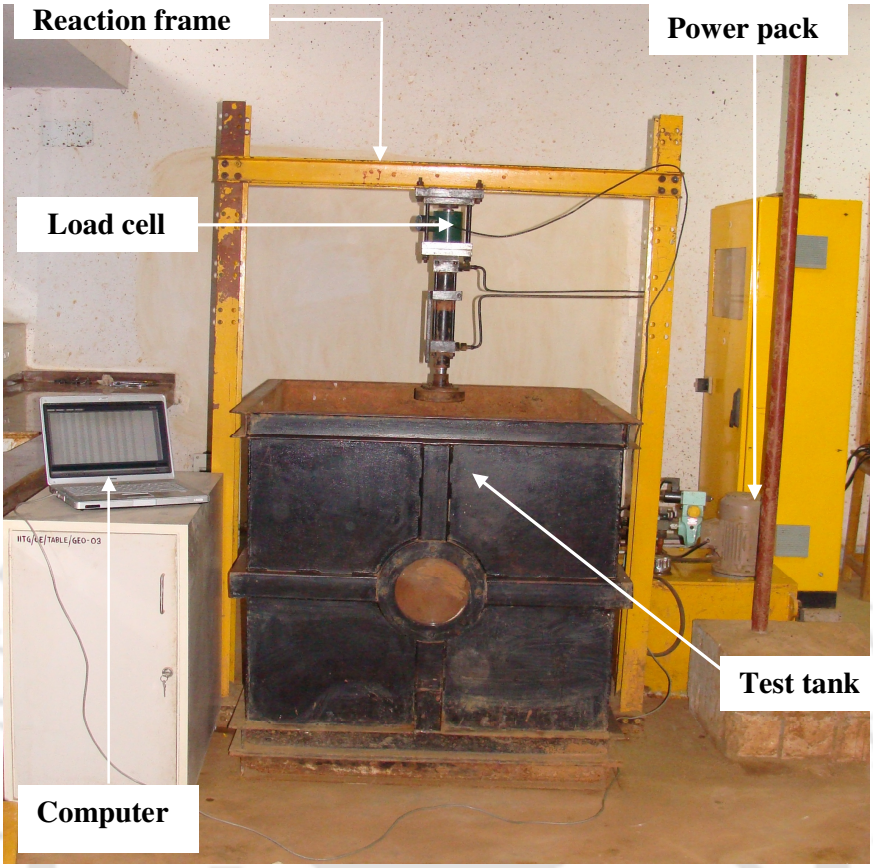

Fig.3.33: Photographic view of the different components of the experimental setup

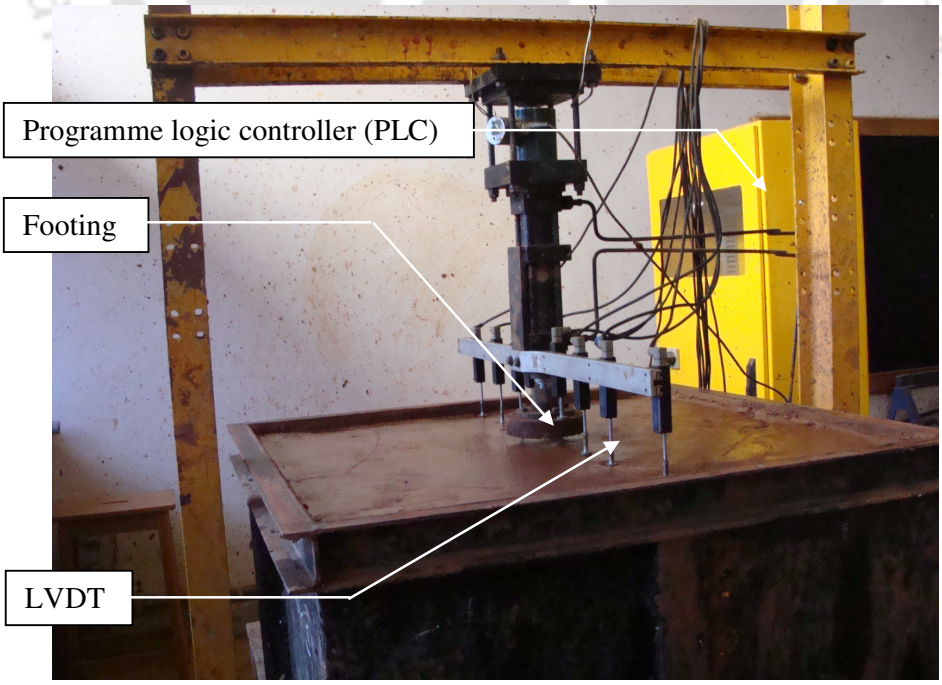

Fig. 3.34: Photograph showing the Programme logic controller, footing and LVDT.

Fig.3.35: Close up view of the programme logic controller (PLC).

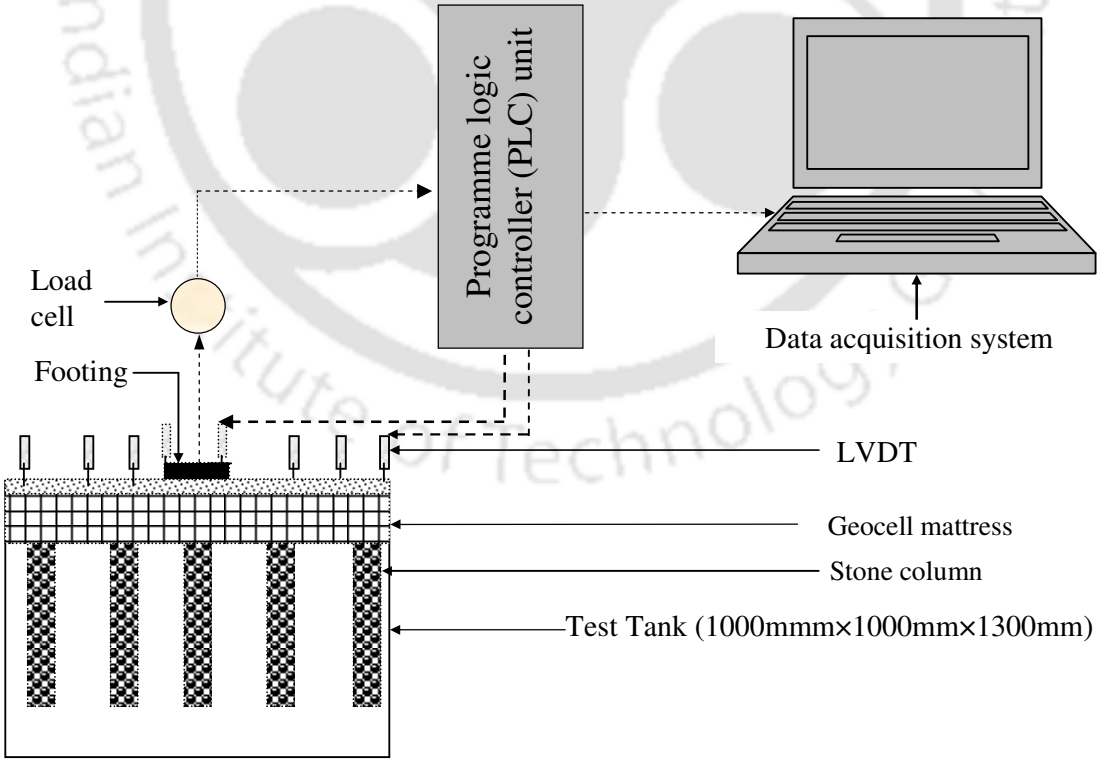

Fig.3.36: General arrangement of different units of the experimental setup.

3.4.2 Instrumentation of the Models

The load applied to the footing was measured through a load cell of 20kN capacity placed between the hydraulic actuator and the reaction frame. The load cell is of strain gauge type with least count of 0.01N. It was calibrated with known loads to develop the calibration curve which was used for the model tests.

The settlement of the footing and deformation on the fill surface were measured using Linear Variable Differential Transducer (LVDT). The LVDTs are of potentiometer type having least count of 3 microns. The settlements of the footing were measured using two LVDTs, one at each end, placed in diagonally opposite sides. The surface settlement/heave of the soil surface was recorded through small settlement plates made from Perspex sheet. These settlement plates were placed on the surface of the foundation bed at the desired locations where surface deformation is to be recorded. The LVDT rested over this settlement plate.

The surface deformations were measured at places 1D, 2D and 3D distance from the centre of the footing, on both sides of the footing. The load and displacement transducers were connected to an automated control system. The data were recorded through computerised data acquisition system. A close up view of the transducers in the test setup is shown in Fig. 3.37.

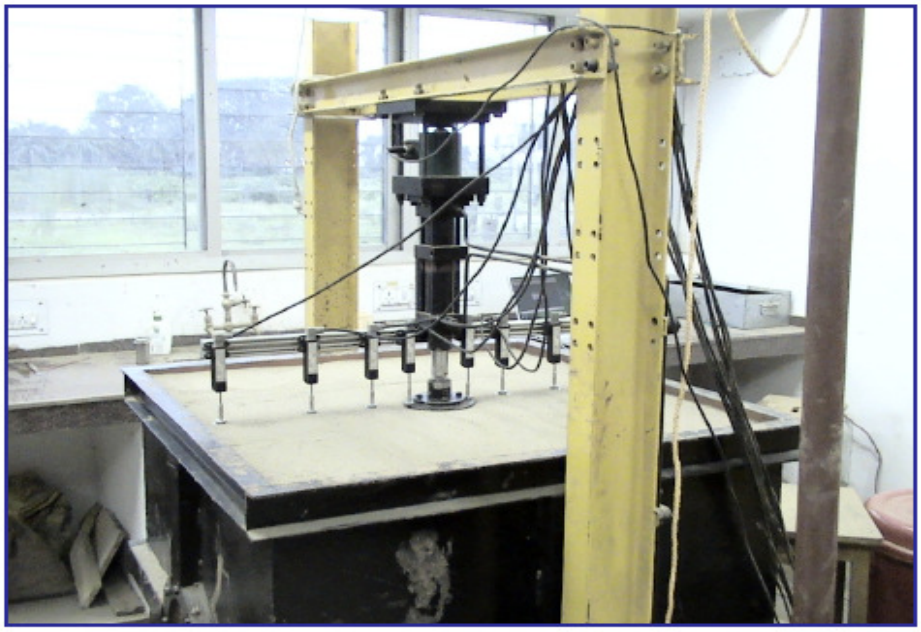

Fig. 3.37: Close up view of the instrumentation in the test set-up

3.5 TEST BED PREPARATION

3.5.1 Preparation of the soft clay bed

The clayey soil was first pulverised and then mixed with predetermined amount of water. In order to achieve moisture equilibrium the moist soil was kept in airtight containers for about a week. To prepare the test bed, the moist soil was placed in the test box and compacted in 0.05 m thick layers till the desired height was reached. For each layer the required amount of soil to produce a desired bulk density was weighted out and placed in the test box making use of a metal scoop. The soil was then gently levelled out and compacted to proper depth by placing a wooden board on the surface and hitting the board with a drop hammer, using depth marking on the sides of the tank as guide. Through a series of trials, the amount of soil, water content of soil, height of fall and number of blows of the drop hammer required to achieve the desired density for each lift were determined a priori. The compaction energy was about

299 kJ/m^3. By carefully controlling the water content and compaction, a fairly uniform test condition was achieved throughout the test programme. In order to verify the uniformity of the test bed, undisturbed samples were collected from different locations in the test bed to determine the in situ unit weight, moisture content and vane shear strength of the clay soil. For each vane shear test, undisturbed soil sample was collected from the test bed through a cylindrical container, by pressing the container through its open end into the soil bed. For passage of air, to avoid air locking, the container base had a hole of about 1 mm diameter. The container with soil was mounted in the vane shear apparatus. The shear vane was gently lowered into the soil and the test was carried out. Table 3.2 presents the average values of different properties of the compacted moist clay and their ranges measured in the test bed. The coefficient of variability of these test data, pertaining to soil samples collected from different locations in the test bed, is found to be within 1.5 %. Using the measured value of water content and bulk density, the degree of saturation (S_r) of the soil is back calculated. The average degree of saturation is found to be in the order of 100%. A typical clay bed prepared in the test tank as described above is shown in Fig.3.38.

Table 3.2. Properties of clay in the foundation bed

Property	Range	Average Value
Moisture Content	35.8-36.5 %	36 %
Bulk Unit weight (γ_b)	18-18.1 kN/m^3	18.05 kN/m^3
Vane shear strength (c_u)	4.8-5.2 kPa	5 kPa

Fig. 3.38: Photograph of a typical clay bed in the test tank

3.5.2 Stone column installation

3.5.2.1 Stone column

The diameter of the stone column in the model tests was kept as 100mm. The diameter of the stone column and size of the aggregate used in the present investigation are approximately a one-seventh scale representation of a prototype stone column of 700mm in diameter with aggregates having average size of about 35mm. The stone columns were constructed by replacement method. A thin open-ended stainless steel pipe of 100 mm outer diameter and wall thickness of 1.5 mm was pushed into the clay bed (Fig.3.38) at the predetermined position till it penetrates upto the desired depth conforming to the length (L) of the column to be formed. Grease was applied on both inner and outer surface of the steel pipe to reduce friction and adhesion, that the pipe can be easily penetrated and withdrawn without any significant

disturbance to the surrounding soil. The clay within the pipe was then gradually scooped out in stages using a helical auger of 90 mm diameter. A maximum height of 100 mm was removed at a time to minimise the suction effect.

After the target depth is reached the internal wall of the pipe was checked for any clay sticking into it, if so, was cleaned. The stone aggregate were then charged into the hole in batches with a measured quantity of 0.6 kg of per batch and were compacted to a height of 50 mm. To achieve a uniform density, compaction was given with a 0.9 kg circular steel tamper with 30 blows of 200 mm drop, to each layer. The pipe was then raised in stages ensuring a minimum of 25 mm penetration below the top level of the placed gravel. This technique of filling the hole was verified through several trials to ensure that there is no significant disturbance to the surrounding clay during construction of the stone column.

The procedure was repeated until the column is completed to the full height. The average density of the stone in the stone column is found to be 15.3 kN/m^3. A typical layout of stone columns in the test bed is shown in Fig. 3.39. The stone column reinforced clay bed thus prepared was loaded with a seating pressure of 2.5 kN/m^2 over the entire area of the bed, for 4 hours, to achieve uniformity in the test bed.

Fig.3.39: Photograph showing the construction of stone column

To check how the stone column is formed, with the present method of installation, stone pieces were removed just after formation (i.e., before load test was done) and Plaster of Paris paste was poured in. The Plaster of Paris ($CaSO_4 \cdot 0.5H_2O$) is available in powder form which when mixed with water forms a thick paste. This paste is poured into the stone column shaft formed due to removal of stones. As the viscosity of the paste of Plaster of Paris is very high, it cannot penetrate into the clay. It gets solidified within a day. After the Plaster of Paris column gets hardened it is removed from its position by removing the surrounding clay. Fig. 3.40 shows a typical hardened Plaster of Paris column. It could be observed from the photograph that the stone column is properly formed.

Fig.3.40: Stone columns in a typical test bed

Fig.3.41: Pre-test shape of a typical stone column ($L/d_{sc} = 5$, $S/d_{sc} = 2.5$)

3.5.2.2 Geomesh encased stone column

For construction of geomesh encased stone columns, the geomesh was first stitched to form a cylindrical sleeve of diameter equal to the diameter of the stone column, as explained earlier. The geomesh sleeve was then put around the thin open ended stainless steel pipe and pushed into the soil along with the pipe. The casing pipe was gradually pulled out as the stone column is formed in lifts, leaving the geomesh sleeve in place, that it encases the aggregates in the stone column.

3.5.3 Formation of sand beds

3.5.3.1 Unreinforced

The sand mattress over the clay bed was formed using raining technique (Fig.3.42). Schematic diagram of the sand raining device is shown in Fig.3.43. It has a hopper connected to a 690 mm long pipe with an inverted cone at the bottom. The hopper has a capacity of holding about 25 kg mass of sand. The sand passes through the 31 mm internal diameter pipe and disperses at bottom by a 60° inverted cone. By varying the height of free fall of dispersed sand particles, the placement density of the sand is varied. The height of free fall is measured from the bottom of the pipe, using a pointer of adjustable length tied at bottom. This device was calibrated by a number of trial fills. Through this device it was not possible to obtain relative density of lower range. To achieve still lower relative density, the bottom cone was removed which allowed interference of sand particles, producing loss of kinetic energy of impact and hence, a lower placement density. The calibration of the device for the case with geocell reinforcement was done to see if there is any effect due to geocell walls. The calibration chart showing the relation between the height of fall and the corresponding relative density for different cases is shown in Fig.3.43. The difference is found to be small. This is because the geocells, being made of geogrids having percent open area

of more than 80%, do not affect much the free flow of sand during raining leading to this small reduction in placement density. In fact, for the case without cone the difference is practically negligible. This is because the sand in the cone does not get dispersed and falls vertical, thereby, does not get interfered by the geocell wall. Based on this calibration curve, the height of fall corresponding to the required relative density was adopted, while raining, to form the test beds. The accuracy of sand placement and consistency of the placement density were checked during raining by placing small aluminium cans of known volumes at different locations in the test tank. The difference in densities measured at various locations in the test tank was found to be less than 1.5 %.

Fig.3.42: Photograph of sand raining for filling up geocell pockets

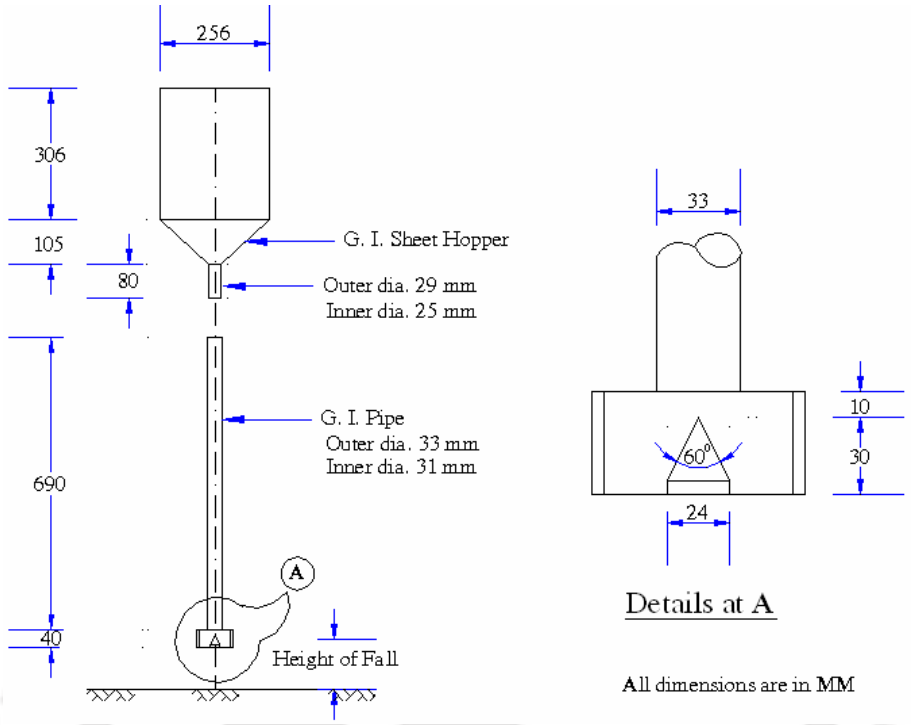

Fig.3.43: Schematic diagram of sand raining device used in the experimental work

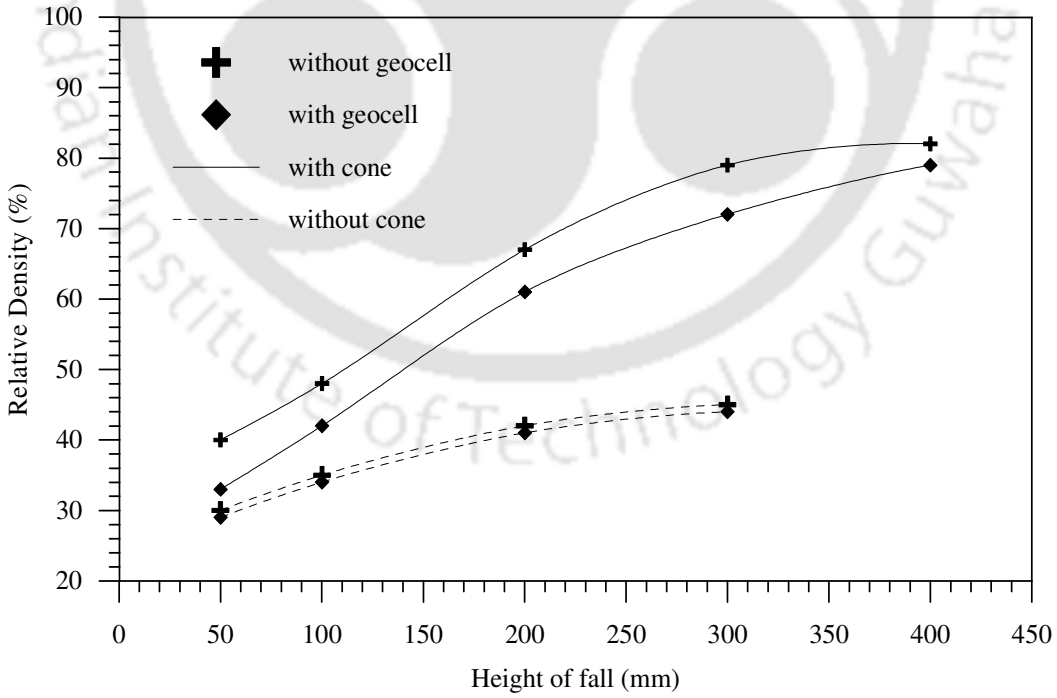

Fig. 3.44: Height of fall versus relative density of sand

3.5.3.2 Geocell reinforced sand bed

The geocell layer, which is a continuous cellular structure, was prepared by cutting the biaxial geogrids to required length and height from full rolls and placing them in transverse and diagonal directions with bodkin joints at the connections (Bush et.al. 1990). The bodkin joint is formed by pulling the ribs of the diagonal geogrid, up through the transverse geogrid and slipping a dowel through the loop created (Fig.3.45).

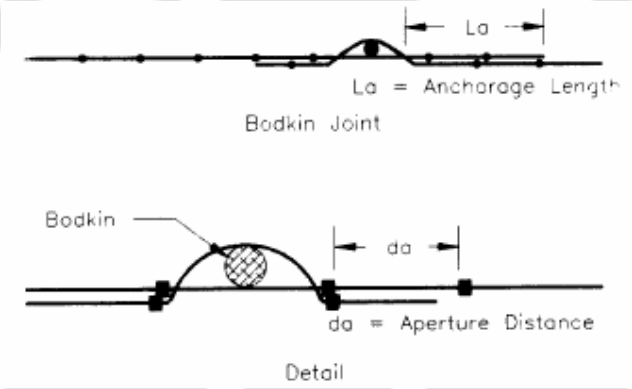

(a) Simac (1990)

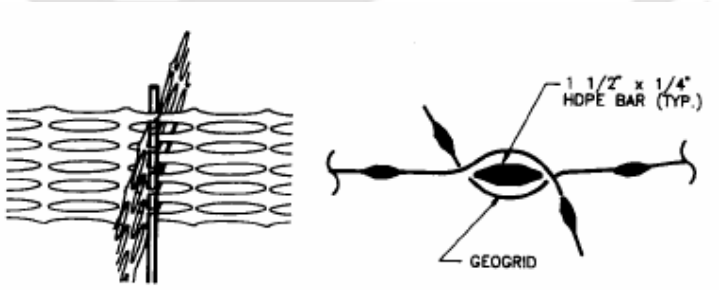

(b) Carroll Jr and Curtis (1990)

Fig.3.45: Details of Bodkin joint (Carroll Jr. and Curtis 1990)

The dowels used for making geocell joints, in the present study, were plastic strips of 8 mm width and 3 mm thickness cut from commercially available plastic sheets made of low density polymer. In all the tests under present investigation, geocells were prepared in chevron pattern as shown in Fig. 3.31, as it gives better performance improvement over diamond pattern (Krishnaswamy et al. 2000; Dash et al. 2001a).

After formation, the geocell cage was kept on the clay surface in the desired alignment. Then the geocell pockets were filled with sand, using sand raining technique. It should be mentioned here that the height of raining to achieve a certain relative density is higher in this case (i.e. with geocells) for higher relative density of soil (Fig.3.40) The difference in density at different places in the test tank is found to be 1.5 %. Photographic view of a typical geocell layer in test bed is shown in Fig. 3.46.

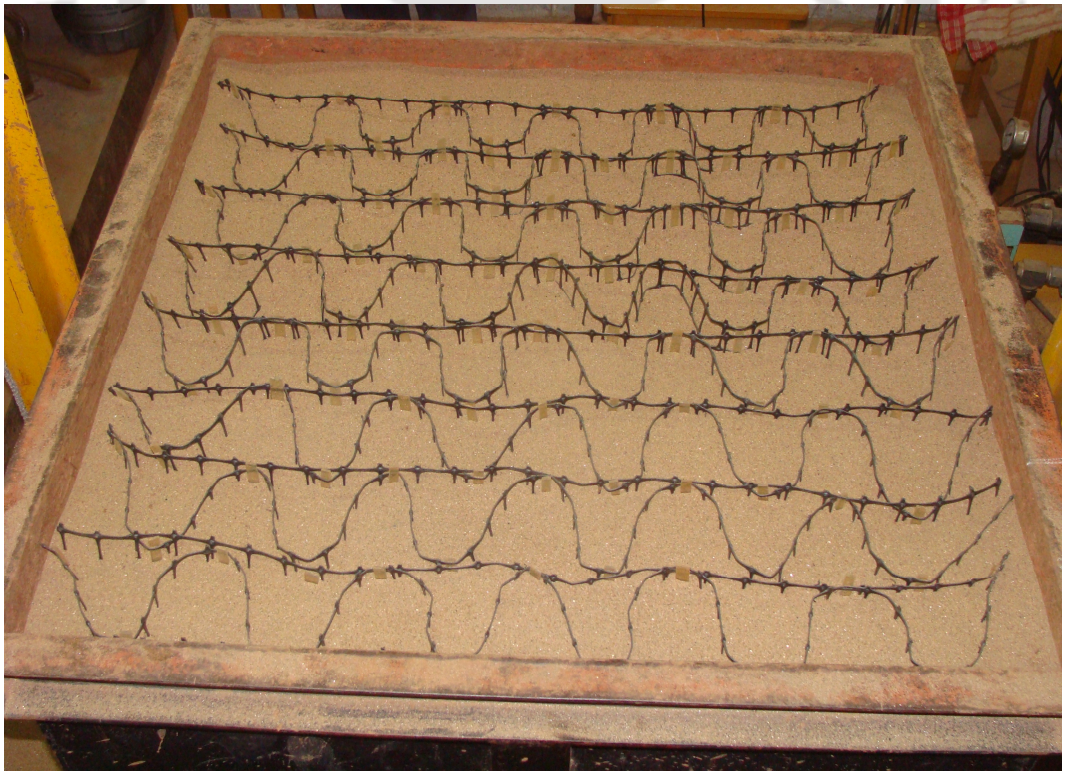

Fig.3.46: A typical geocell layer in test bed.

3.5.4 Test procedure

Loading was applied on the footing through the computer controlled hydraulic system. The footing was pushed at the rate of 2mm/min. This relatively faster rate of loading would produce undrained response in the saturated clay bed, which is one of the worst field conditions expected, because in this case the angle of friction of soil is zero. Such phenomenon is common in case of railways and highways, where the loading is transient in nature. The load deformation data was acquired by the computerised data acquisition system. In all the tests, the footing loading was applied until a footing settlement of 40 mm is reached.

After the test was over the sand was scooped out and the geocell mattress was carefully removed to observe the pattern of distortion in it due to the footing loading. The post test deformed shape of the stone column is obtained by carefully removing the aggregate from the stone column and filling the cylindrical hole with Plaster of Paris paste. After the Plaster of Paris gets hardened it is brought out from the clay bed. The external size and shape of the Plaster of Paris column which is the deformed shape of the stone column was mapped. For each test, the test bed was prepared afresh with new reinforcement. The results obtained are presented and discussed in the following chapters.

CHAPTER 4

STONE COLUMN REINFORCED CLAY BED

4.1 INTRODUCTION

In this chapter the results obtained from the model load tests on stone column reinforced clay beds along with the unreinforced one are presented and discussed. The influence of various parameters of stone columns on the overall performance of the foundation system has been brought out.

4.2 UNREINFORCED CLAY BED

The variation of bearing pressure with footing settlement for footing on unreinforced clay bed (Test series 1) is presented in Fig. 4.1. The footing settlement 's' is the average of the readings of the two LVDTs placed in diagonally opposite sides on the footing. It could be observed that there is no pronounced peak and the slope of the pressure-settlement response continues to decrease, till settlement about 6% of the footing diameter, and thereafter tends to become nearly vertical. This indicates that the soil has undergone failure and hence is unable to support additional pressure.

The deformation (i.e. heave/settlement, δ) profiles on the fill surface at different levels of footing settlement are shown in Fig. 4.2. The downward deformation (i.e. settlement) is considered as (+) and upward deformation (i.e. heave) is taken as (-). The corresponding variations of average surface deformation (δ/D%) with footing settlement (s/D%), at distance (x) of D, 2D and 3D from the centre of footing is depicted in Fig. 4.3. The average surface deformation (δ) is the average of the values recorded on both sides of the footing.

It could be observed that at x = D the fill surface has undergone settlement. This is due to stress dispersion from the footing that an additional mass of soil, other than that below the footing, settles along with the footing. As the soil is fully saturated and the loading rate is faster, therefore, undrained condition prevails, leading to heaving of clay surface beyond the settlement zone (i.e., x > D).

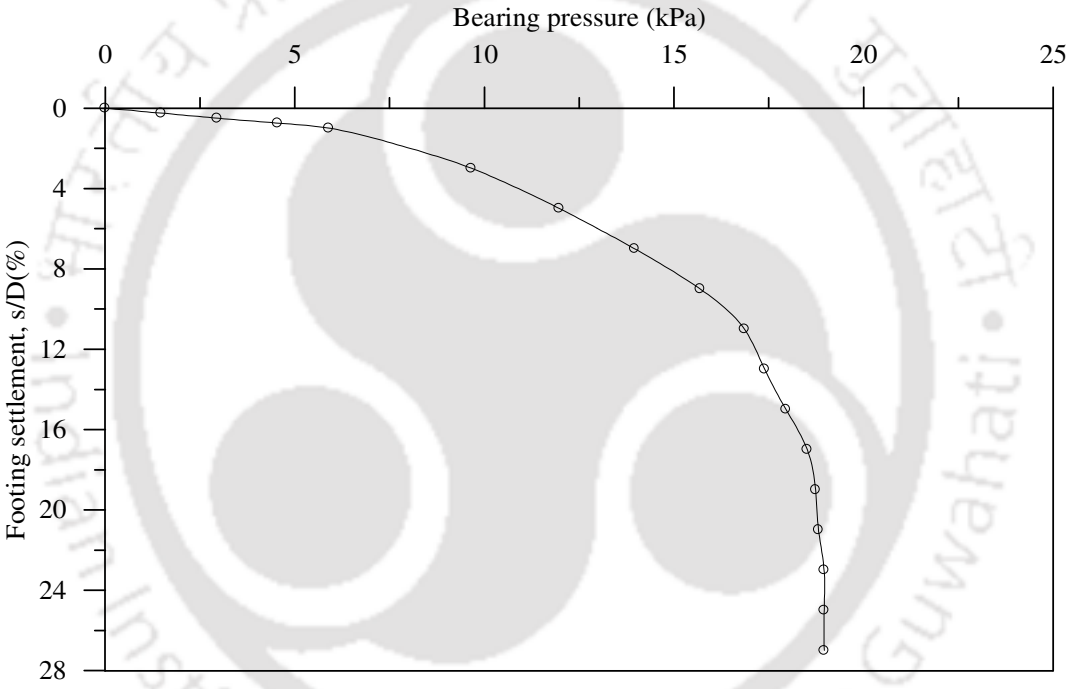

Fig. 4.1: Bearing pressure footing settlement response of unreinforced clay-Test series 1

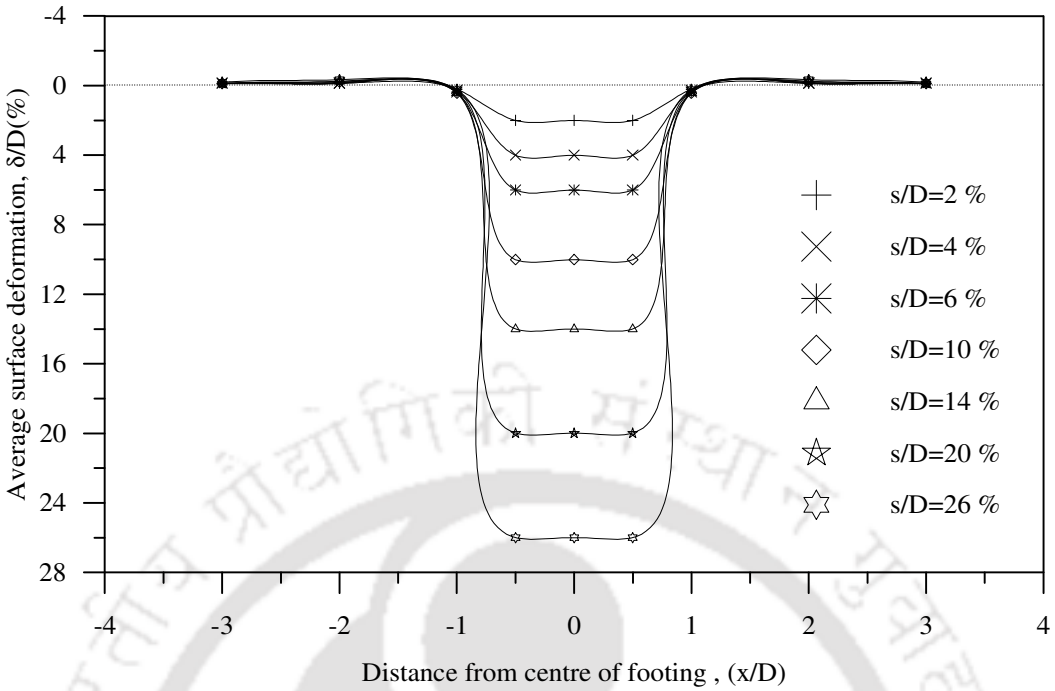

Fig. 4.2: Surface deformation profile of clay bed - Test series 1

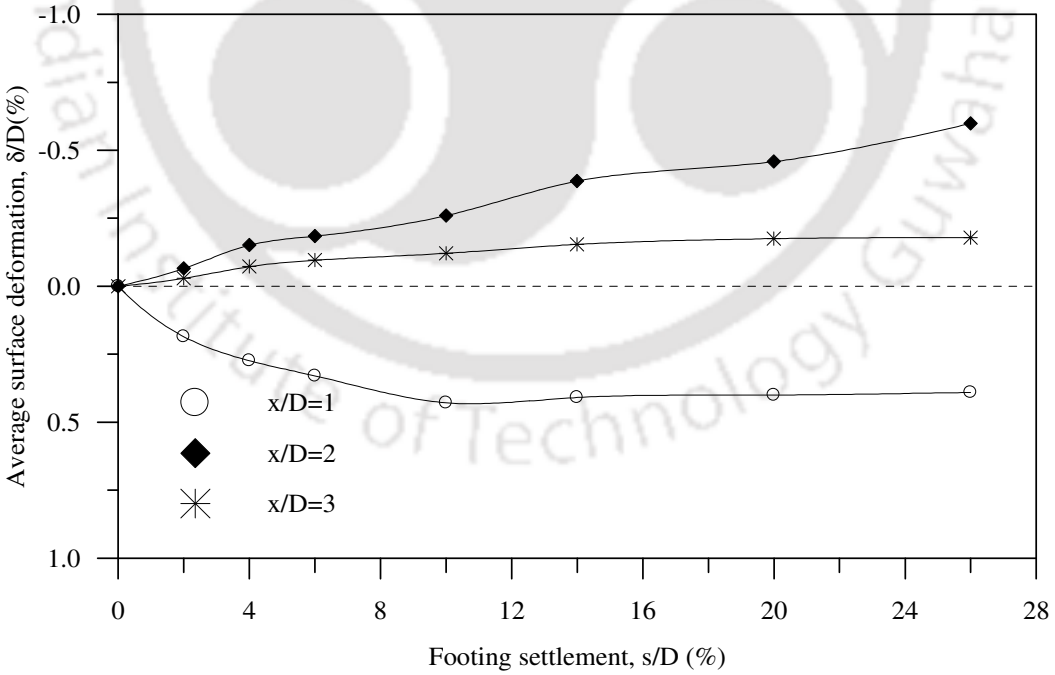

Fig. 4.3: Variation of surface deformation with footing settlement for unreinforced clay bed at different distance from centre of footing - Test series 1

4.3 STONE COLUMN REINFORCED CLAY BED

Tests under series 2 and 3 were carried out to study the behaviour of the stone column reinforced clay foundation system, for different length and spacing of stone columns. In each series only one parameter was varied while others were kept constant. The bearing pressure and settlement responses of the footing, with and without stone columns in the clay beds, are depicted in Fig.4.6 and 4.15. The performance improvement in terms of load carrying capacity of the footing due to provision of stone columns is quantified using a non dimensional factor called bearing capacity improvement factor for stone columns (IF_{sc}).

The *Improvement Factor* (IF_{sc}) is defined as the ratio of the bearing pressure of the stone column reinforced foundation bed, $(q_r)_{sc}$, at a given settlement, to that of the unreinforced clay bed, (q_u), at the same settlement (Eq. 4.1). These terms are shown in Fig. 4.4

$$IF_{sc} = \frac{bearing\ pressure\ with\ stone\ column\ reinforcement\ [q_r]_{sc}}{bearing\ pressure\ on\ unreinforced\ clay\ [q_u]} \quad (4.1)$$

Where,

$(q_r)_{sc}$ = Bearing pressure of the stone column foundation bed at a given settlement

(q_u) = Bearing pressure of the unreinforced clay bed at the same settlement

The performance improvement in terms of reduction in footing settlement due to provision of stone columns in clay bed is quantified through the non dimensional parameter called Percentage Reduction in Footing Settlement (PRS_{sc}). The PRS_{sc} is calculated as explained in Equation 4.2.

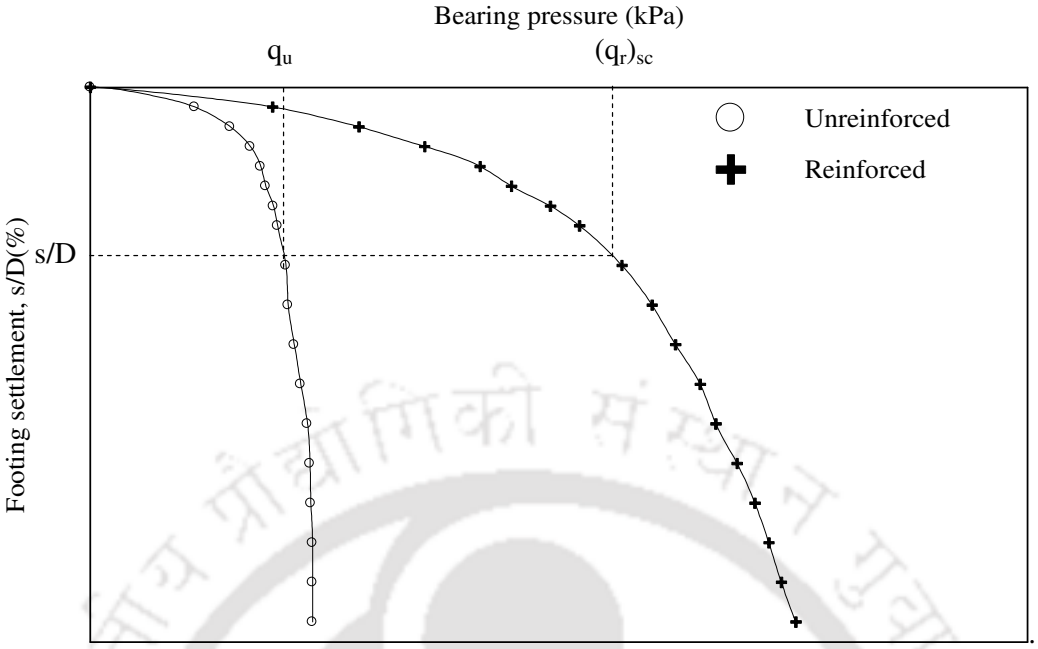

Fig. 4.4: Definition sketch for bearing capacity improvement factor, IF_{sc}

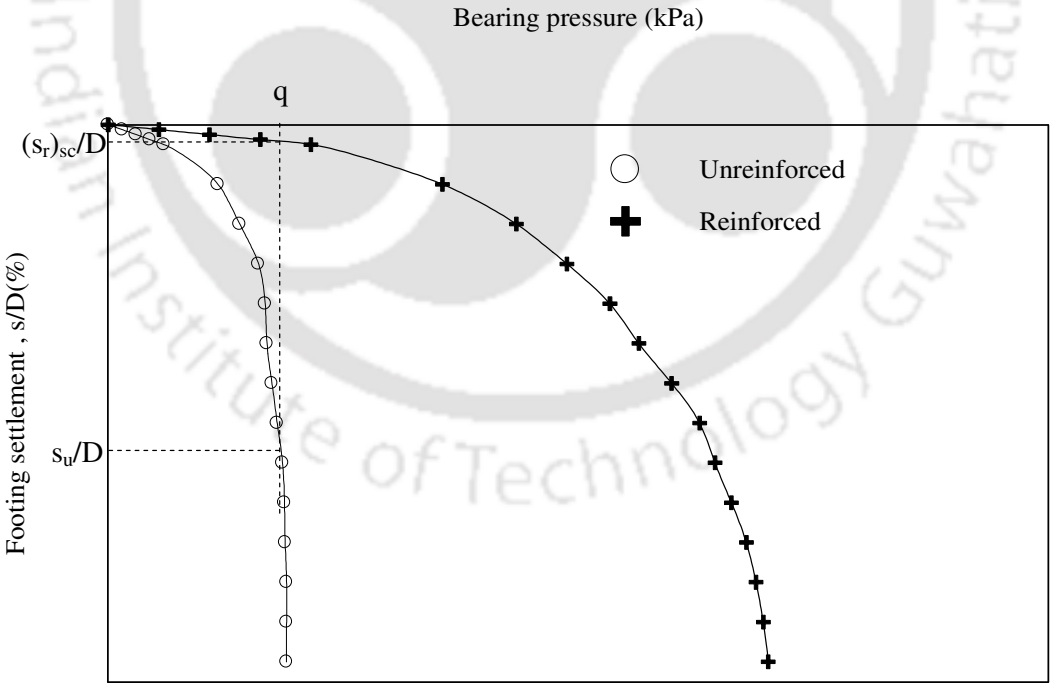

Fig. 4.5: Definition sketch for Percentage Reduction in footing Settlement, PRS_{sc}

$$PRS_{sc} = \frac{s_u - (s_r)_{sc}}{s_u} \times 100 \quad (4.2)$$

Where, s_u is the settlement of unreinforced clay bed, $(s_r)_{sc}$ is the settlement of the stone column reinforced clay bed; both taken at a given bearing pressure q (Fig.4.5). The footing settlement (s) and surface deformation (δ, heave/settlement) are expressed in non dimensional form, in terms of footing diameter as s/D (%) and δ/D (%).

The post test deformed shape of the stone columns mapped through plaster of paris (Fig.4.12) is made use of to study the bulging pattern of the stone columns. The bulge diameter was measured at different depths, from top of the post test exhumed stone columns (plaster of Paris column). Using the bulge profile (Fig. 4.13) radial strain in the stone columns, due to deformation, was obtained as $[(r_d-r_0)/r_0]\times100$, where r_d is the radius of the deformed stone column and r_0 is the radius of the original undeformed stone column. A typical plot of the radial strain in the stone column at different depths of stone column (i.e. over its length, L/d_{sc}) can be seen in Fig. 4.14. The influences of different parameters of stone columns (i.e. length, diameter and spacing) on the overall performance of the foundation system are brought out in the following sections.

4.3.1 Effect of length of stone column

Fig 4.6 depicts the bearing pressure versus footing settlement responses for different lengths of stone column, expressed in non dimensional form with respect to its diameter (L/d_{sc}). It could be observed that even with stone columns having length as small as its diameter (L/d_{sc} = 1), the performance of the clay bed, both in terms of increase in bearing capacity and reduction in settlement, can be increased substantially. The performance improvement continues to increase with increase in length of stone columns. It is of interest to note that with the stone column length varying from $3d_{sc}$ to

$5d_{sc}$ there is substantial improvement in bearing capacity and reduction in settlement of the foundation bed, beyond which further improvement is marginal. The variation of bearing capacity improvement factor IF_{sc} with footing settlement for different lengths of stone column is depicted in Fig. 4.7. It could be observed that with the provision of stone columns the bearing capacity can be increased by 3.5 times that of the clay bed alone (i.e., $IF_{sc} = 3.5$).

For all cases, initially the value of IF_{sc} is high but it reduces with increased footing settlement. However, for settlement (s/D) beyond 3% it continues to increase with increase in settlement. The initially high improvement in bearing capacity is due to stiffening effect of the stone columns. This effect reduces as the stone column deforms under footing penetration. However, after a threshold limit of deformation, the shear resistance of the soil starts getting mobilized substantially, leading to increased load carrying capacity.

Fig. 4.8 presents the stone column induced reduction in footing settlement $(PRS)_{sc}$, at different levels of footing pressure, $(q_r)_{sc}/(q_u)_{ult}$. Where, $(q_r)_{sc}$ is the footing pressure on stone column-clay bed at a given settlement and $(q_u)_{ult}$ is the ultimate pressure of the unreinforced clay bed. With stone column the footing settlement can be reduced to less than 5% that of unreinforced soil (PRS > 95%). The reduction in footing settlement increases with increase in stone column length (L) till 5 times of its diameter (d_{sc}), beyond which further reduction is practically negligible. This is because further resistance of the stone columns brought by increased length remains unmobilised due to excessive bulging at upper layers of the stone columns.

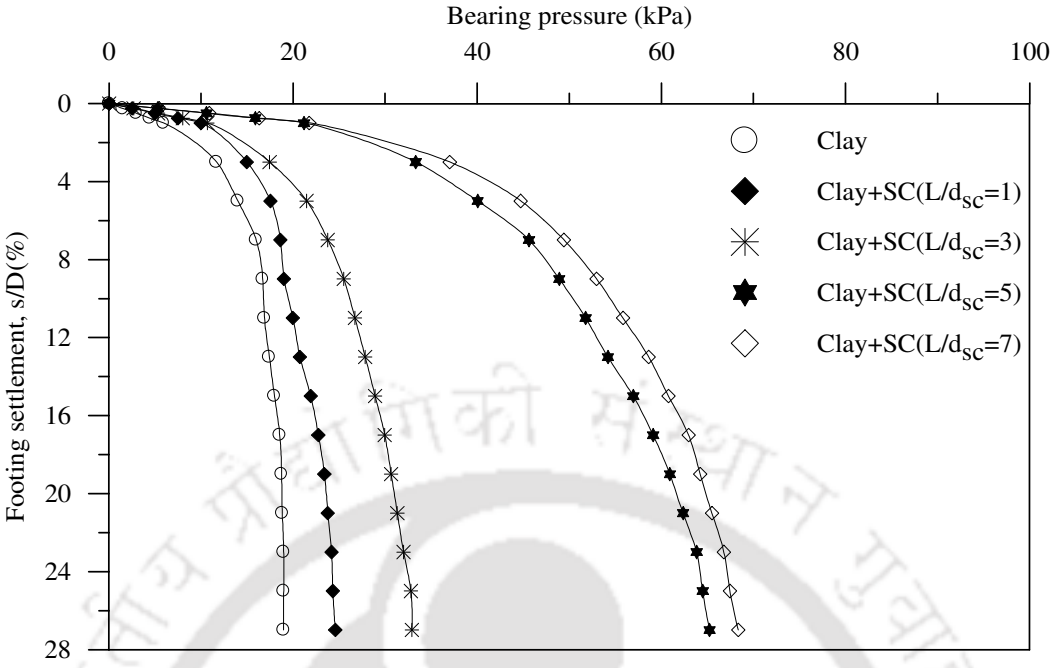

Fig.4.6: Variation of bearing pressure with footing settlement for different length of stone columns (S/d_{sc} = 2.5) - Test series 2

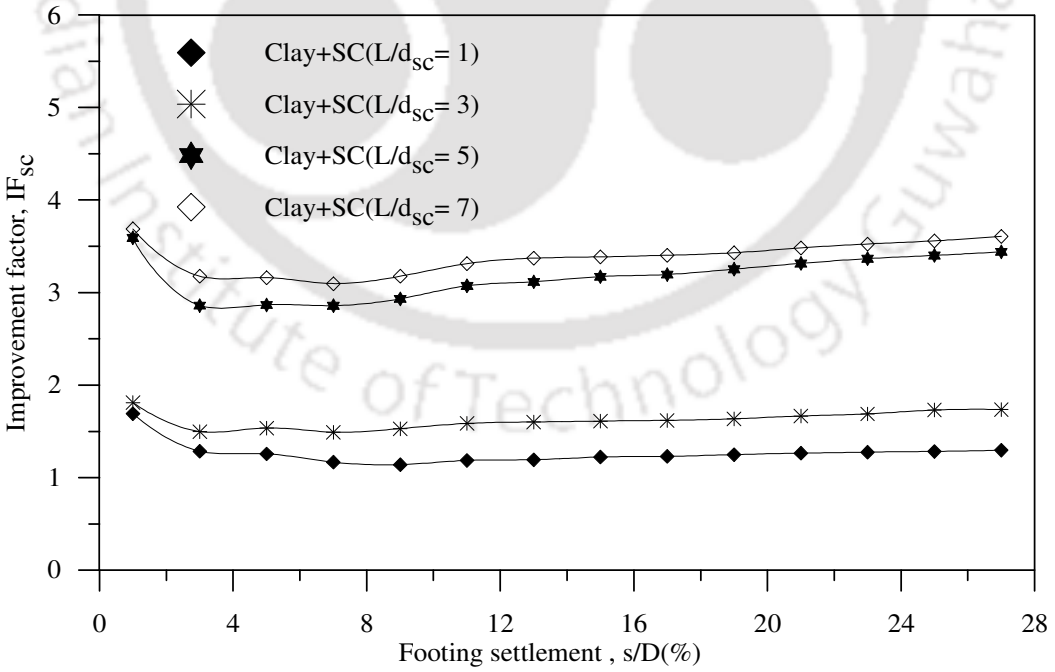

Fig.4.7: Variation of improvement factor with footing settlement for different length of stone columns (S/d_{sc} = 2.5) - Test series 2

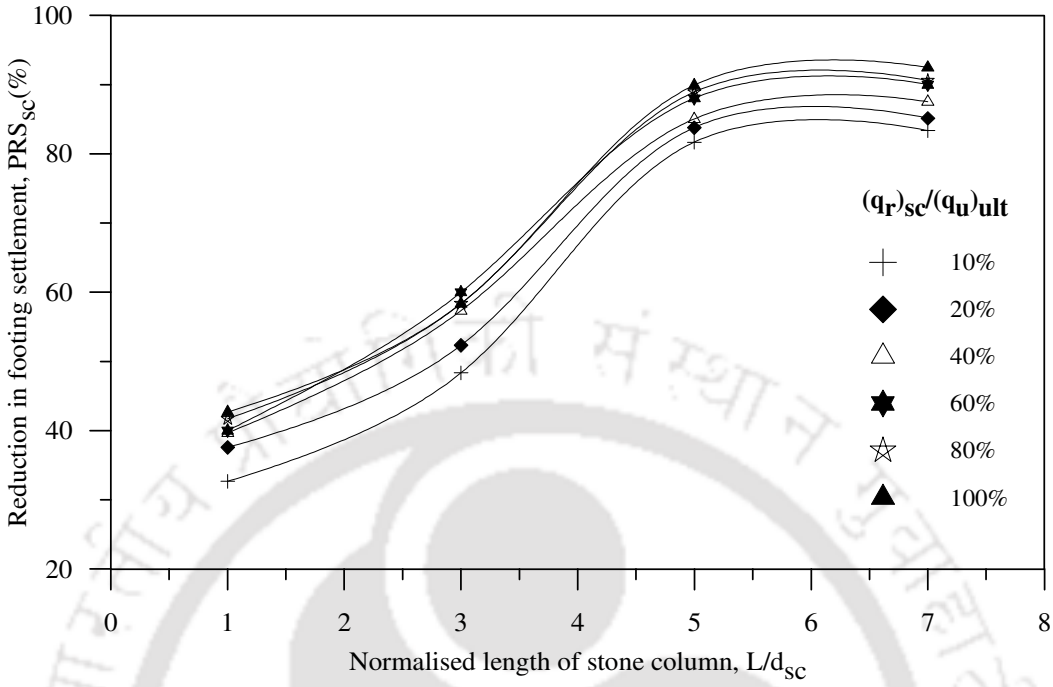

Fig.4.8: Variation of settlement reduction factor with length of stone columns ($S/d_{sc} = 2.5$) – Test series 2

The surface deformation profiles are presented in Figs. A_1-A_4 (Appendix I). The corresponding variations of surface deformation with footing settlement, at x = D, 2D and 3D are shown in Fig. 4.9, 4.10 and 4.11 respectively. From Fig. 4.9 it could be observed that the settlement on fill surface, at x = D, with stone column of $L/d_{sc}=1$ is comparable to that of the unreinforced clay bed. Being small in length and thereby having less peripherial area, the mobilised skin friction around the stone column is small. Besides, due to weak clay at base and shallow depth of embedment, the mobilized bearing capacity is very small. Therefore, the stone column, without offering much of resistance, just punches down under the footing loading leading to marginal reduction in surface settlement. Indeed the post test exhumed picture of stone column shape shows no bulging (Fig.4.12, $L/d_{sc}=1$). With increased length of stone

column the surface settlement (at x = D) is found to reduce indicating that the increased skin friction (due to increased peripherial area) and end bearing capacity (due to increased overburden) provides higher resistance against footing penetration leading to reduced settlement. The bulging in the stone columns ($L \geq 3d_{sc}$, Figs.4.12, 4.13, 4.14) indicates that the stone column, instead of getting punched down, has stood sustaining the footing pressure and hence has undergone radial volume expansion. Correspondingly, the surface deformation responses depicted in Figs. 4.10 and 4.11 show that the heaving is maximum for $L/d_{sc} = 1$ and continues to reduce with increase in length of the stone columns.

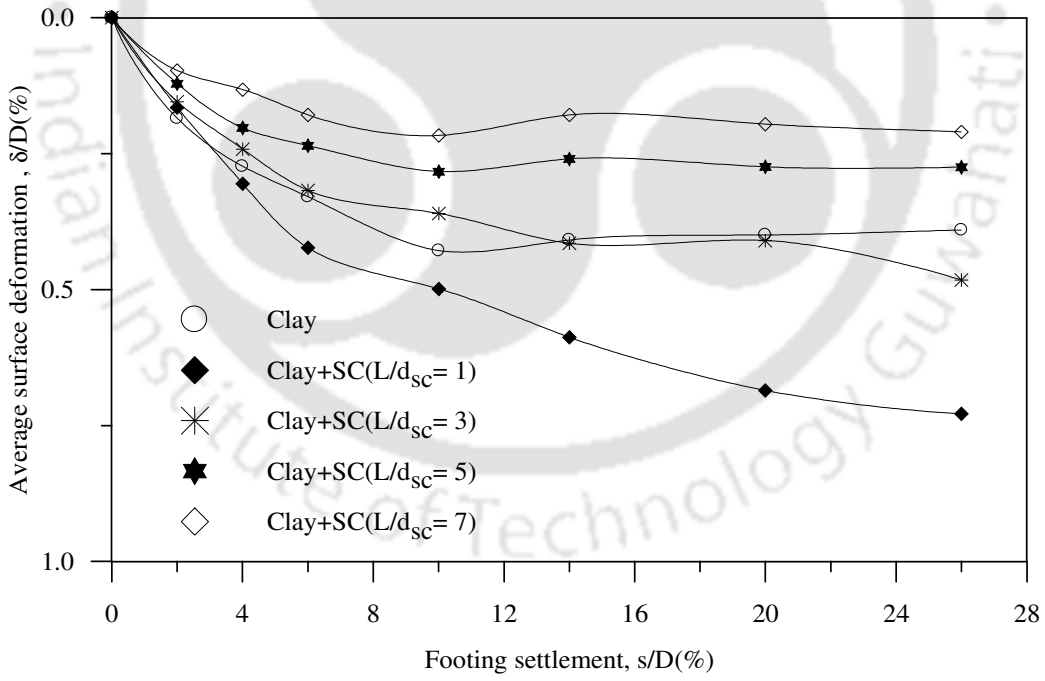

Fig.4.9: Variation of surface deformation, at x = D, with footing settlement for different lengths of stone columns ($S/d_{sc} = 2.5$) - Test series 2

.

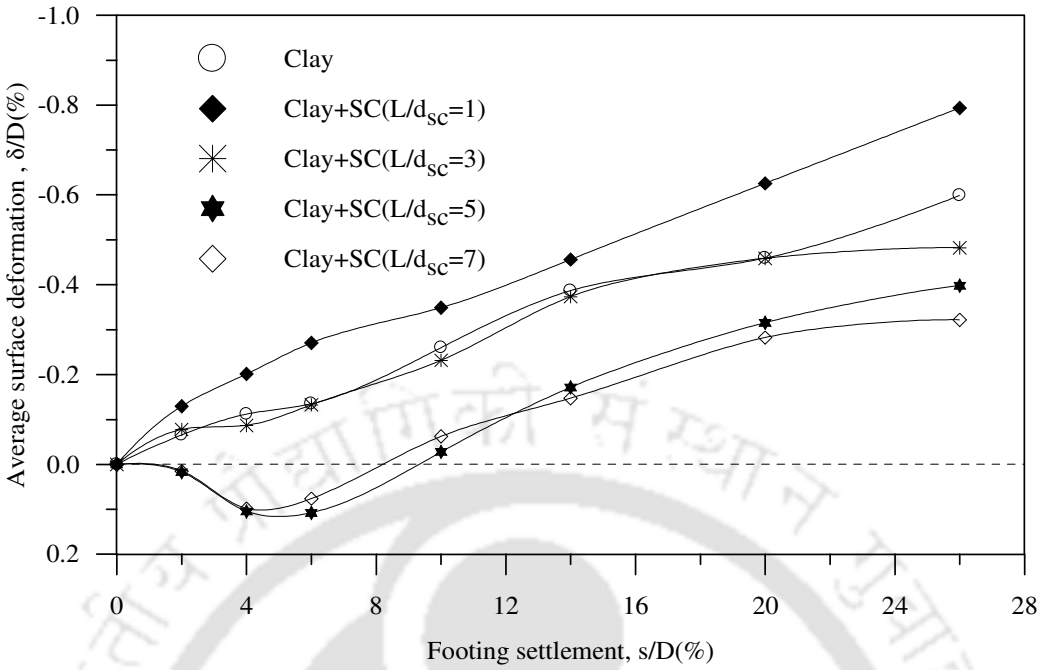

Fig.4.10: Variation of surface deformation, at x = 2D, with footing settlement for different lengths of stone columns (S/d_{sc} = 2.5) - Test series 2

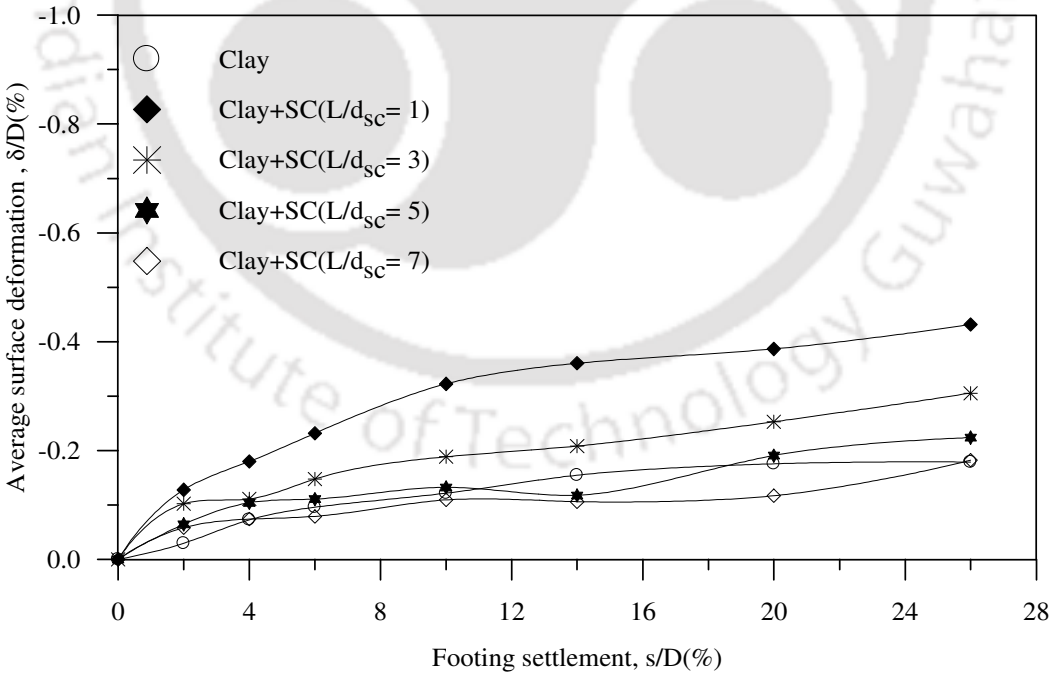

Fig.4.11: Variation of surface deformation, at x = 3D, with footing settlement for different lengths of stone columns (S/d_{sc} = 2.5) - Test series 2

The deformed shape of the stone columns depicted in Figs.4.13 and 4.14 indicate that bulging dies down to a practically negligible value for length of stone column greater than $4d_{sc}$. Similar observations have been reported by Rao et.al (1997) and Sharma et. al. (2004).

With increased length of stone column, it mobilizes higher end bearing due to high overburden pressure and greater skin friction due to increased peripheral area, therefore punches less and hence bulges more. A bulged stone column mobilises increased magnitude of soil passive resistance leading to increased load carrying capacity. However, beyond certain length (i.e. $L = 5d_{sc}$) though the resistance against punching continues to increase but the stone column reaches its maximum bulging capacity and hence further improvement in performance is marginal (Fig. 4.7). Hence, it can be concluded that the length of stone column (L) giving maximum performance improvement is about 5 times its diameter (d_{sc}).

$L/d_{sc} = 1$ $L/d_{sc} = 3$ $L/d_{sc} = 5$

Fig. 4.12: Photograph showing the post-test deformed shape of central stone column ($S/d_{sc} = 2.5$) - Test series 2

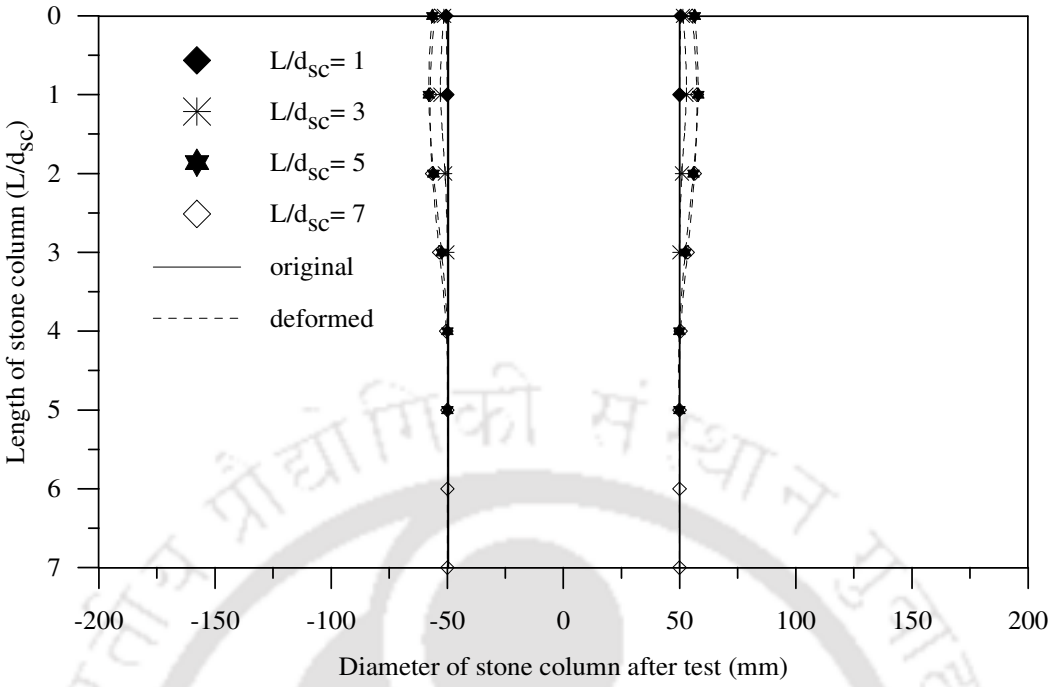

Fig. 4.13: Post-test longitudinal section of the central stone columns (S/d_{sc} = 2.5) - Test series 2

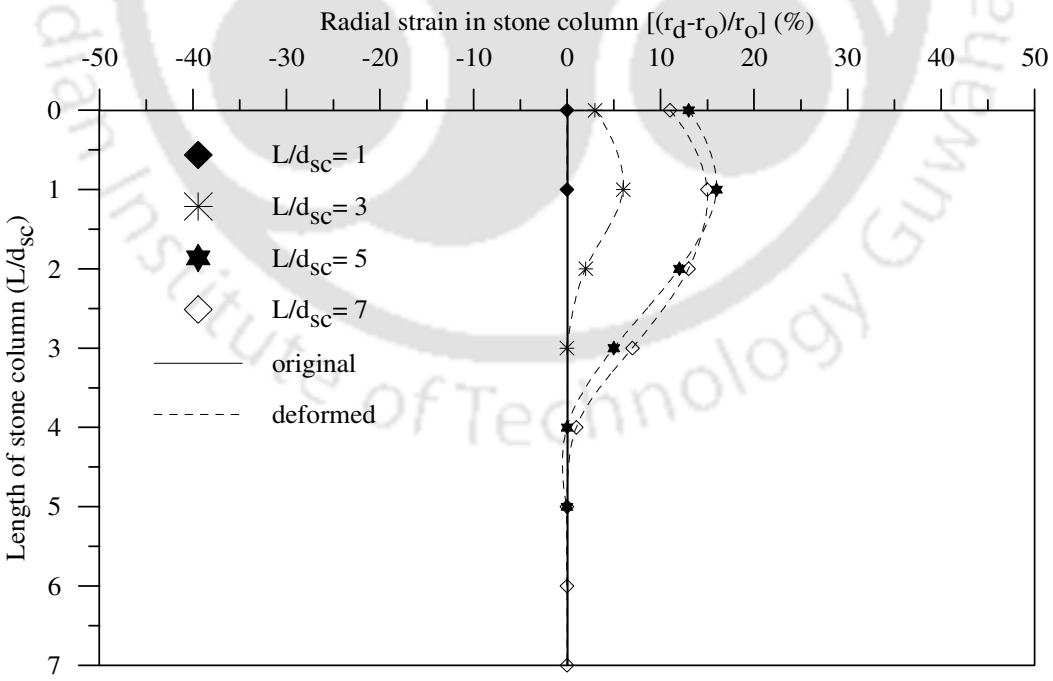

Fig. 4.14: Post-test radial strain in central stone columns (S/d_{sc} = 2.5) - Test series 2

4.3.2 Effect of spacing of stone columns

Fig.4.15 shows the bearing pressure versus footing settlement responses for different spacing of stone columns (S/d_{sc}). The corresponding variation of bearing capacity improvement factor (IF_{sc}) with footing settlement is depicted in Fig. 4.16. It could be observed that as the spacing of the stone columns decreases, the bearing pressure of the foundation bed increases. The increase in bearing pressure, when the spacing (S) reduces from $3.5d_{sc}$ to $2.5d_{sc}$ is substantially high beyond which further increase in bearing capacity is marginal. Hence the optimum spacing of the stone columns can be taken as $2.5d_{sc}$. The variation of settlement reduction factor PRS_{sc}, depicted in Fig.4.17 shows similar trends. This beahviour can better be explained through the surface settlement/heave responses and the stone column deformation profiles.

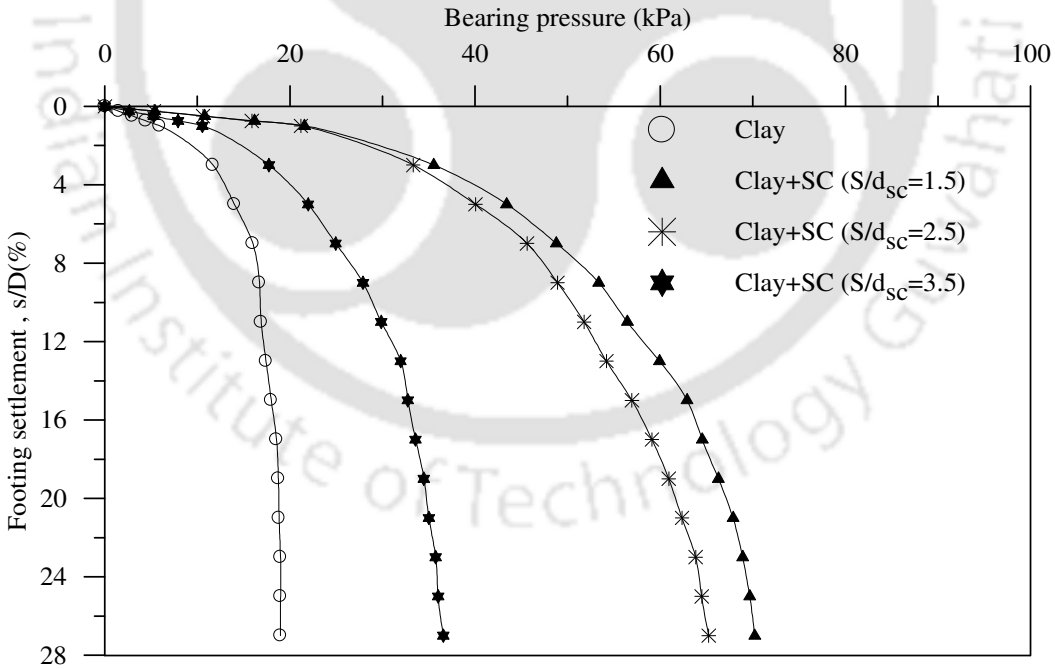

Fig. 4.15: Variation of bearing pressure with footing settlement for different spacing of stone columns (L/d_{sc} = 5) - Test series 3

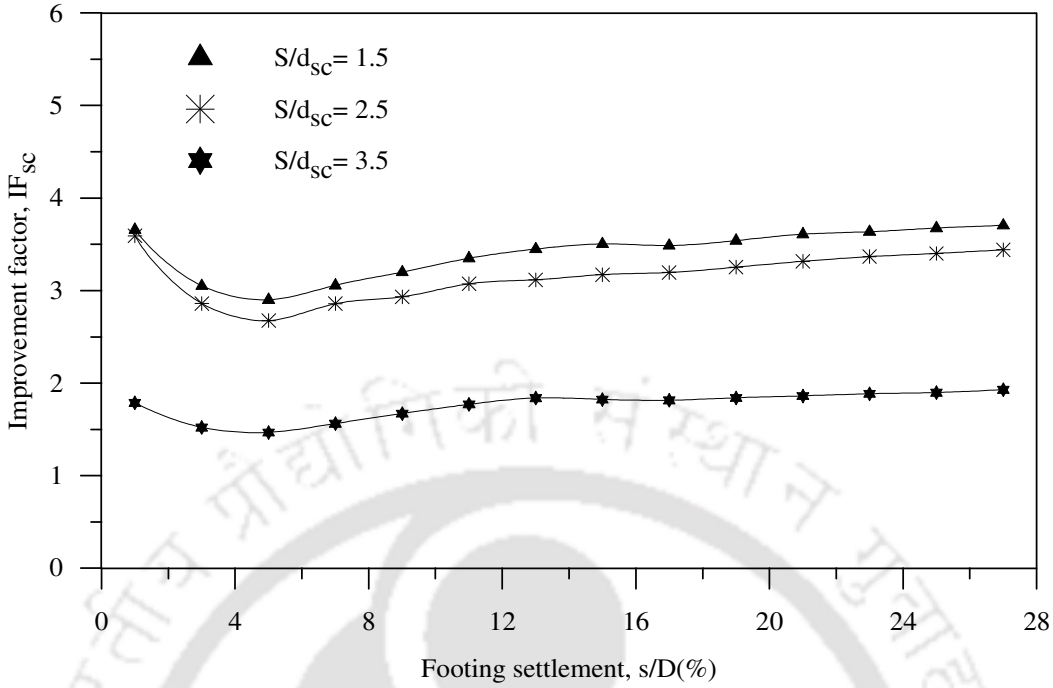

Fig.4.16: Variation of improvement factor with footing settlement for different spacing of stone columns (L/d_{sc} = 5) - Test series 3

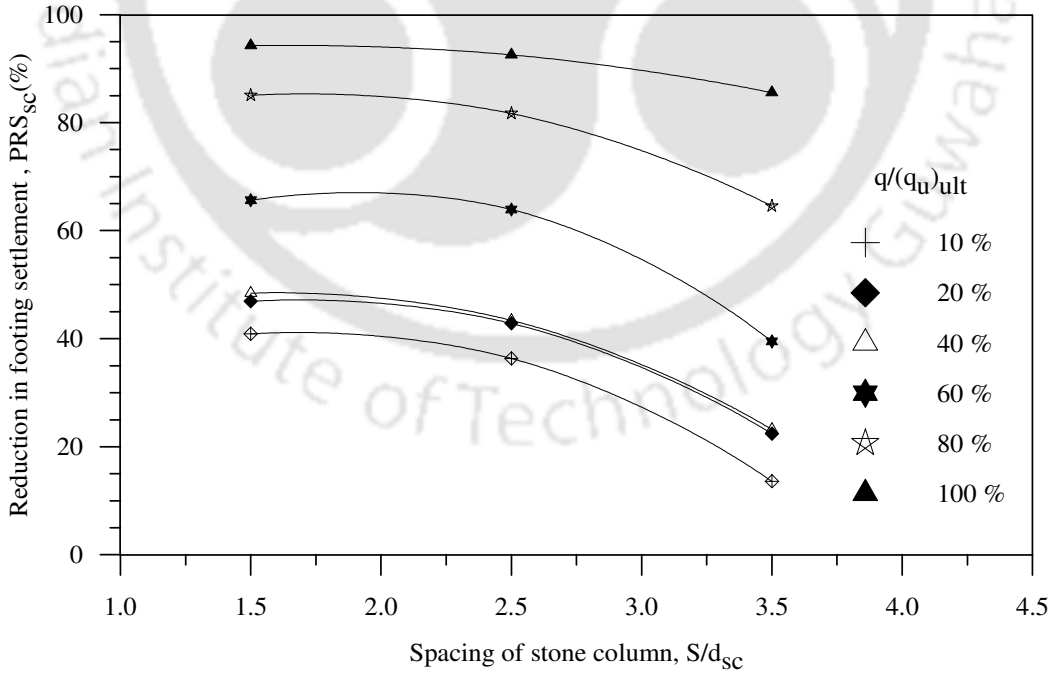

Fig. 4.17: Variation of settlement reduction factor with spacing of stone columns (L/d_{sc} = 5) - Test series 3

Fig. 4.18 shows that with stone column spacing (S) when kept at $1.5d_{sc}$, there is heaving on fill surface, at x = D. This is in contrary to the earlier cases wherein the fill surface around the footing generally has undergone settlement. With reduced spacing, the ring of stone columns tends to behave like a skirt around the footing, providing higher confinement to the foundation soil and hence increased performance improvement. The reduced bulging in the central stone column, with reduced spacing (Fig. 4.21-23), establishes the increased confinement effect of the surrounding peripheral stone columns. For too small spacing (i.e. S = $1.5d_{sc}$) the sidewise lateral movement of soil, due to footing penetration, gets substantially arrested by the ring of stone columns. In the event of the lateral movement getting restrained substantially, the encapsulated soil mass heaves up (Fig. 4.18). In fact, the peripheral stone columns (surrounding the footing) have undergone visible lateral buckling (Fig. 4.24) indicating that they have restrained the lateral thrust from the outward moving soil mass, sheared up under footing penetration.

However, for larger spacing of stone columns (S = 2.5 d_{sc} and 3.5 d_{sc}), there has taken place settlement, at x = D. With higher spacing the sheared soil mass easily passes through the wider clear spacing between the stone columns. In the absence of the surrounding obstruction and thereby the induced heaving, the fill surface has undergone the usual settlement, as takes place under footing loading. The settlement on fill surface for S = $2.5d_{sc}$ is lower compared to that with S = $3.5d_{sc}$. This attributed to the relatively higher confining effect of the stone columns with smaller spacing, inducing some amount of heaving that apparently has reduced the surface settlement.

Figs. 4.19 and 4.20 indicate that heaving reduces with decrease in spacing of the stone columns. With reduced spacing (S) the flow of soil is restrained to a greater degree by the ring of stone columns surrounding the footing. As a result which less soil flows to

the region outside leading to reduced heaving at, x = 2.5D and 3.5D. The relatively higher heaving with S = 3.5 d_{sc} than that with clay alone, is attributed to the constricted channeled flow of clay mass through the stone columns. As the clay mass now passes though the relatively narrow passage between the stone columns, it apparently produces higher heaving, along the path of flow, which is a local phenomenon.

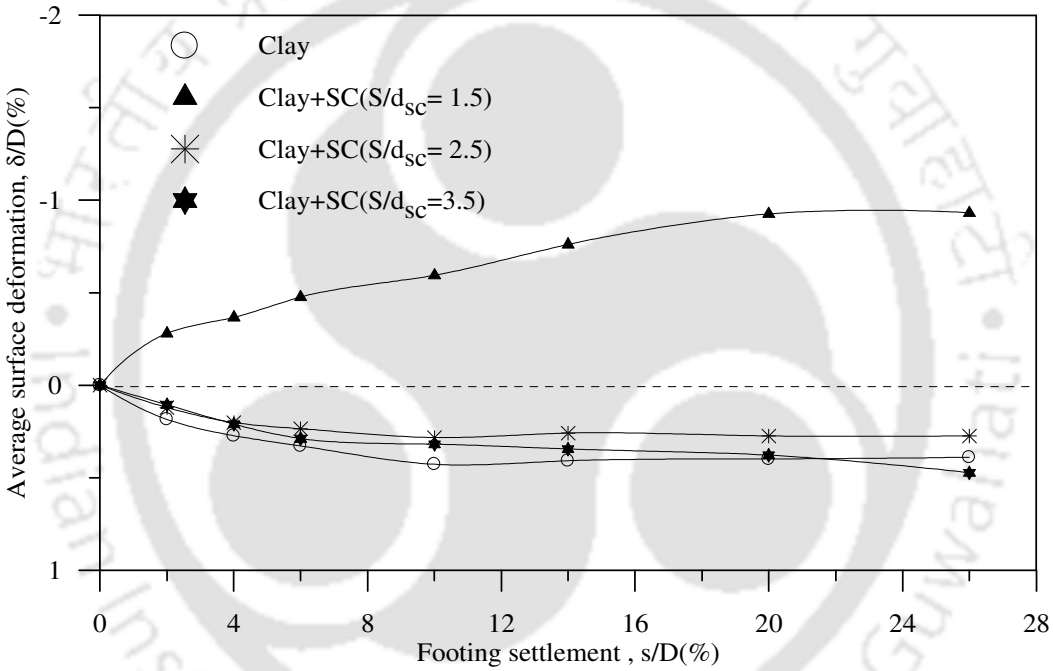

Fig.4.18: Variation of surface deformation, at x = D, with footing settlement for different spacing of stone columns (L/d_{sc} = 5) - Test series 3

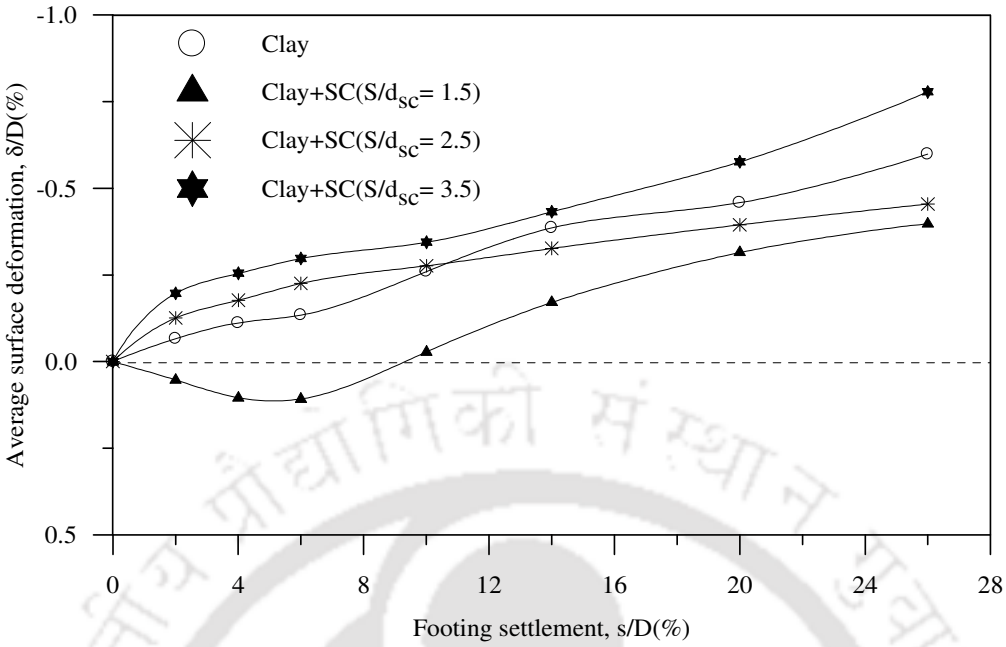

Fig. 4.19: Variation of surface deformation at, x = 2D, with footing settlement for different spacing of stone columns (L/d_{sc} = 5) - Test series 3

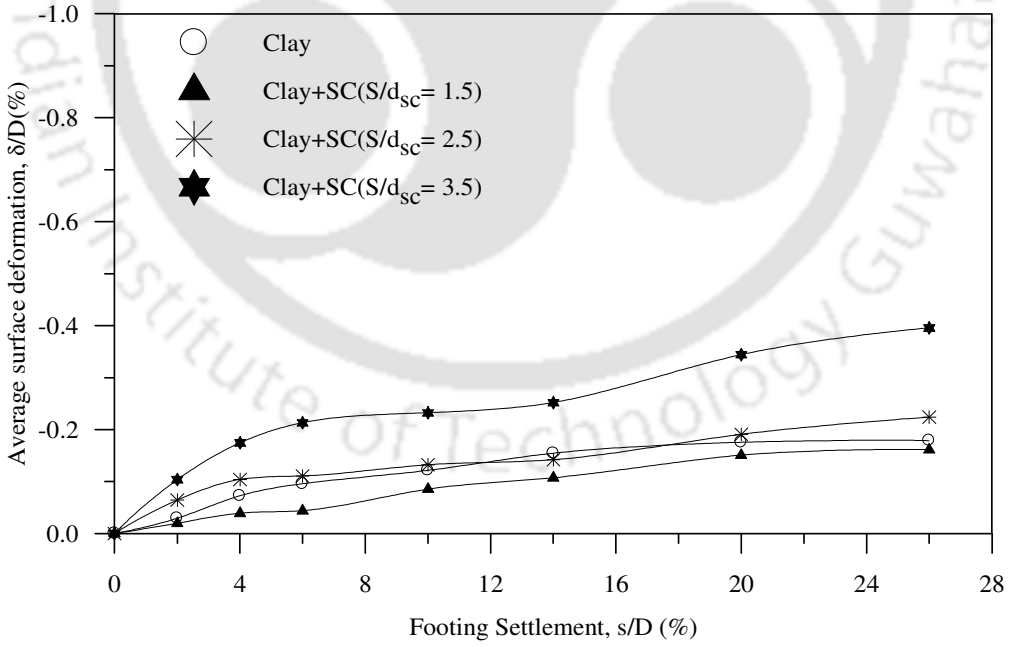

Fig.4.20: Variation of surface deformation, at x = 3D, with footing settlement for different spacing of stone columns (L/d_{sc} = 5) - Test series 3

$S/d_{sc} = 1.5$ $S/d_{sc} = 2.5$ $S/d_{sc} = 3.5$

Fig.4.21: Deformed shape of central stone columns after test ($L/d_{sc} = 5$) – Test series 3

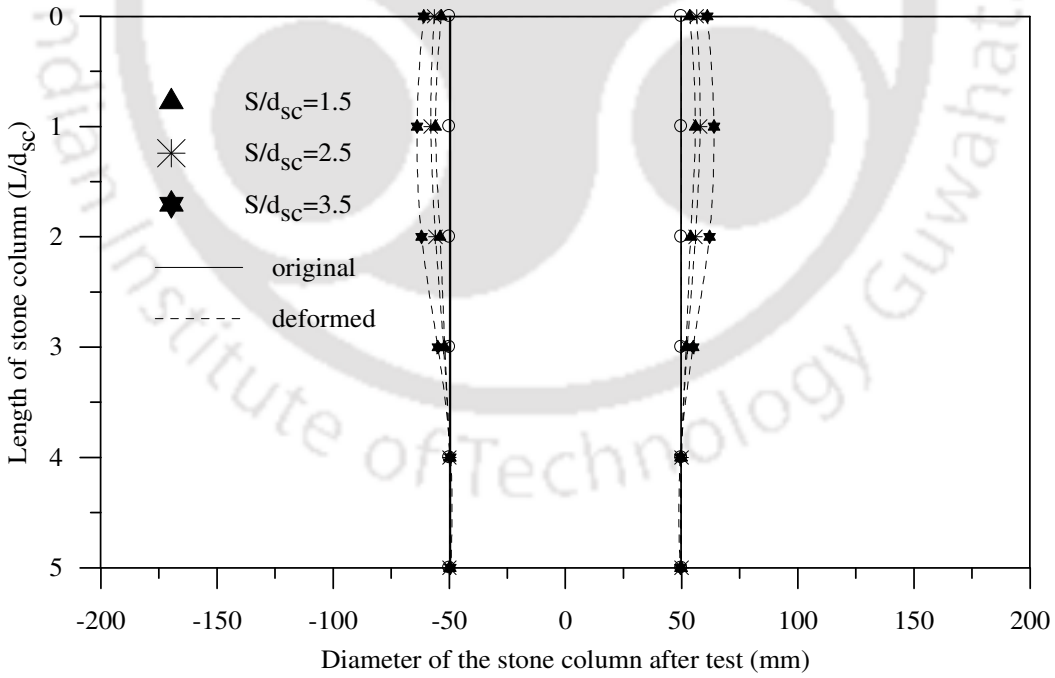

Fig.4.22: Post-test longitudinal section of the central stone column for varying spacing of stone columns ($L/d_{sc} = 5$) – Test series 3

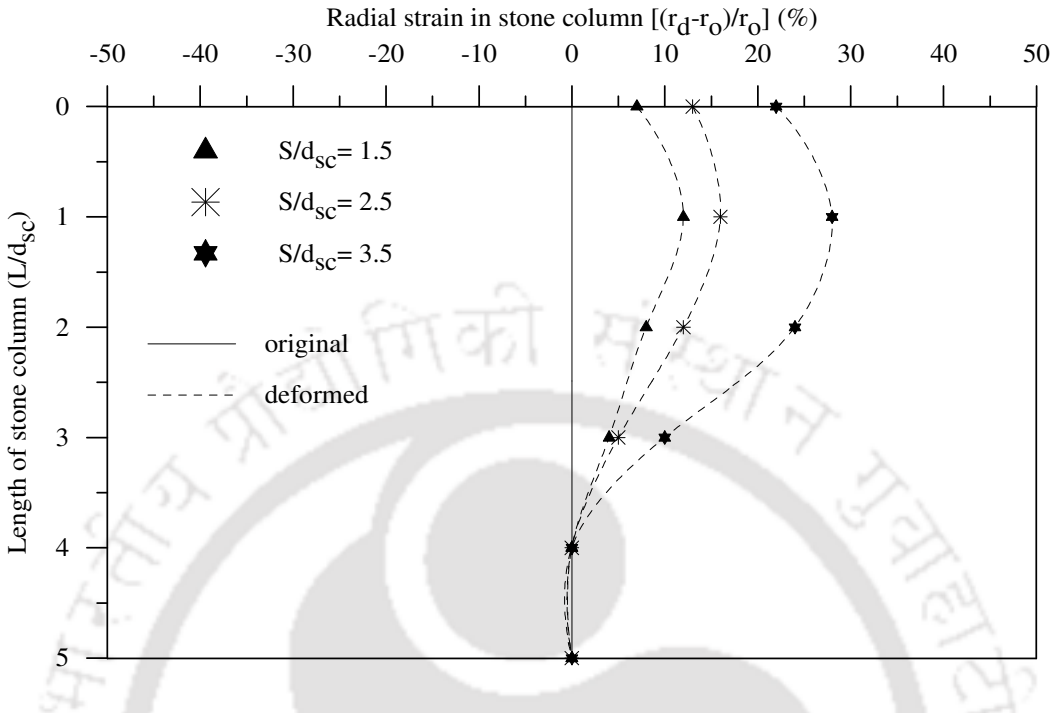

Fig.4.23: Radial strain in central stone columns for varying spacing of stone columns ($L/d_{sc} = 5$) - Test series 3

$S/d_{sc} = 1.5$ $S/d_{sc} = 2.5$ $S/d_{sc} = 3.5$

4.24: Post-test deformed shape of typical peripheral stone columns ($L/d_{sc} = 5$) – Test series 3

CHAPTER 5

GEOCELL SAND MATTRESS REINFORCED CLAY BED

5.1 INTRODUCTION

Under the present investigation five different series of tests (Test series 4-8, Table.3.1) have been carried out to study the behaviour of geocell reinforced sand mattress overlying clay bed under circular loading. The parameters varied are height of geocell mattress, density of infill soil and pocket size of geocells. The obtained test results are presented and discussed in this chapter.

Typical pressure-settlement responses depicted in Fig. 5.1 show that, while the unreinforced clay bed has undergone failure (i.e. the pressure settlement response tends to become nearly vertical) at a settlement about 10-12% of footing diameter, with geocell mattress the pressure settlement response is almost linear even at settlement as high as 25% of footing diameter. The continuous increase in bearing pressure with settlement indicates that shear failure has not taken place in the soil mass. Besides, the geocell mattress has reduced the settlement of the foundation bed substantially.

The performance improvement of the clay bed due to the provision of the geocell mattress is represented using the non dimensional improvement factors, IF_{gc} and PRS_{gc}, which are defined below.

$$IF_{gc} = \frac{\text{bearing pressure with geocell reinforcement } (q_r)_{gc}}{\text{bearing pressure of unreinforced clay bed } (q_u)} \tag{5.1}$$

Where, q_u and $(q_r)_{gc}$ are the bearing pressure of unreinforced and geocell reinforced clay bed, respectively, both taken at equal settlement (Fig. 5.1).

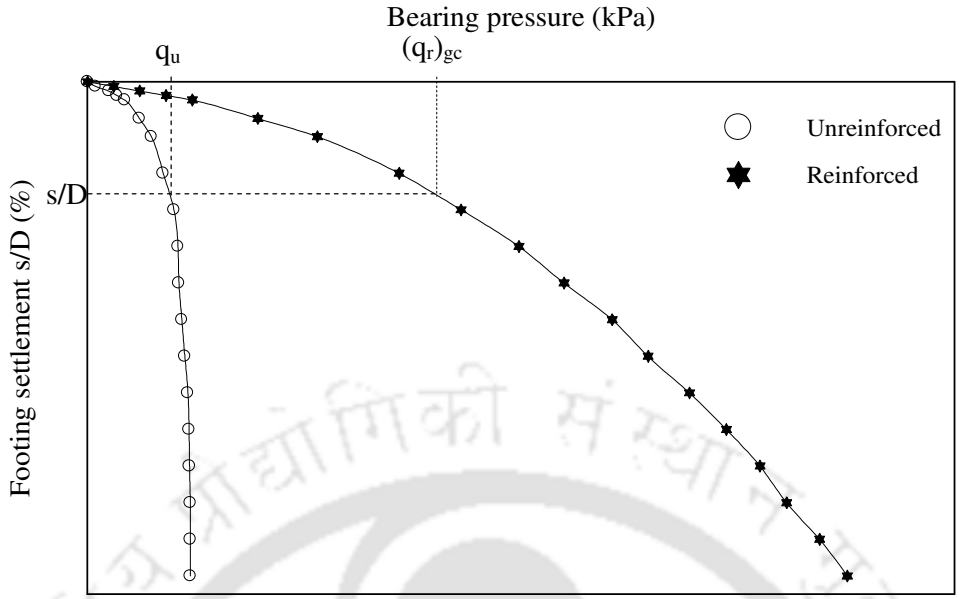

Fig.5.1: Definition sketch for bearing capacity improvement factor, IF_{gc}

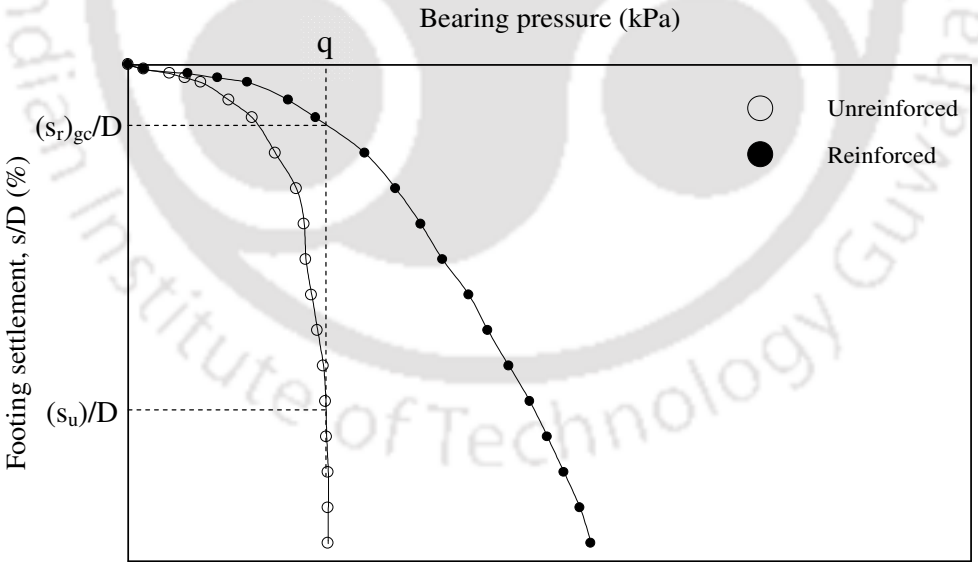

Fig.5.2: Definition sketch for Percentage Reduction in footing Settlement, PRS_{gc}

$$PRS_{gc} = \frac{s_u - (s_r)_{gc}}{s_u} \times 100 \qquad (5.2)$$

Where, s_u is footing settlement of the unreinforced clay bed and $(s_r)_{gc}$ is the settlement of the geocell reinforced clay bed, both taken at equal bearing pressure (Fig. 5.2).

The effect of different parameters of the geocell mattress, on the overall response of the foundation system are presented and discussed in the following sections.

5.2 EFFECT OF HEIGHT OF GEOCELL MATTRESS

The influence of the height of geocells (h/D) on the bearing pressure-settlement behaviour of the foundation system is shown in Fig. 5.3. It could be observed that both the bearing capacity and stiffness of the foundation bed increases with increase in height of the geocell mattress. The increased flexural rigidity, due to increased height, enables the geocell mattress to transmit the footing pressure more effectively and redistribute it over a wider area, thereby reduces the intensity of pressure on the soft soil below leading to overall performance improvement. The increased surcharge effect due to the geocell layer that increases with increase in its height (h/D) too is expected to have increased the bearing capacity of the clay subgrade.

The improvement in bearing capacity (IF_{gc}) and reduction in settlement $(PRS)_{gc}$ due to the geocell mattress are presented in Fig. 5.4 and Fig.5.5 respectively. It could be observed that there is significant improvement till h/D = 1.1, beyond, it is substantially less. The surface deformation profiles depicted in Figs. 5.6 – 5.9 indicate that with geocell mattress having shallow height (h/D < 1.1) there is substantial heave on fill surface, while with h/D > 1.1 heave has completely been subsided. The marginal heaving towards the ends of the geocell mattress (x = 3D) is attributed to the lifting up of the geocell mattress at its ends, being loaded at center.

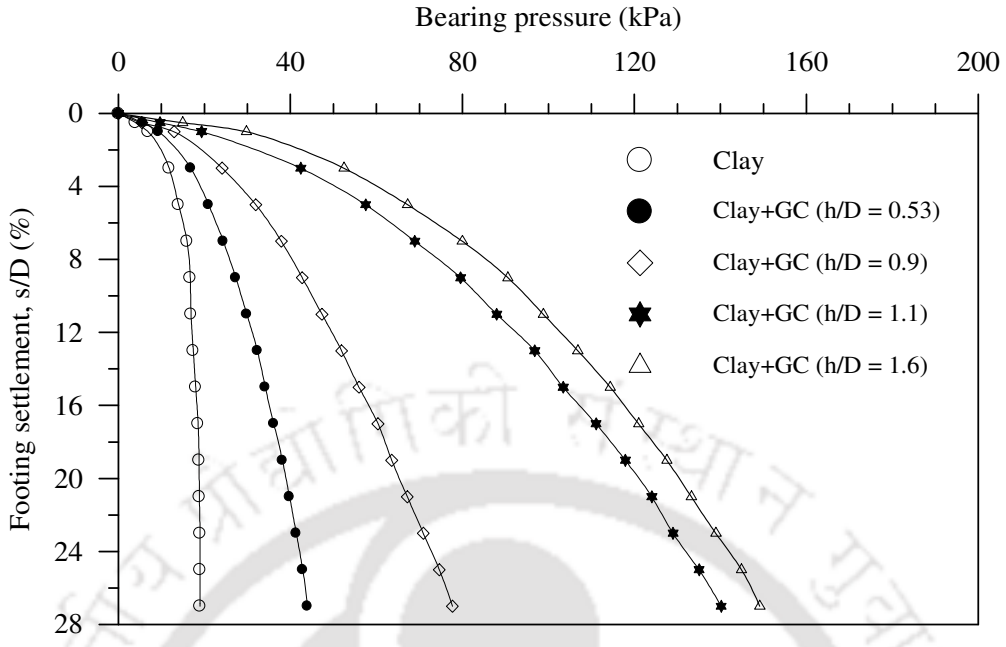

Fig.5.3: Variation of bearing pressure with footing settlement for different heights of geocell mattress (d_{gc}/D = 0.8, ID = 80%, u/D = 0.1) - Test series 4

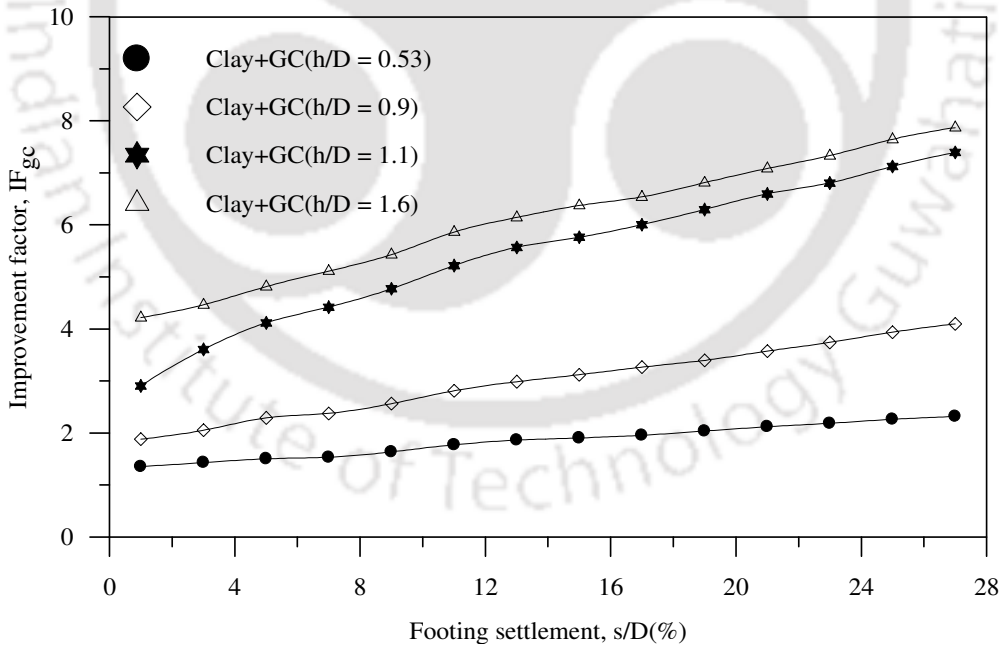

Fig.5.4: Variation of improvement factor with footing settlement for different heights of geocell mattress (d_{gc}/D = 0.8, ID = 80%, u/D = 0.1) - Test series 4

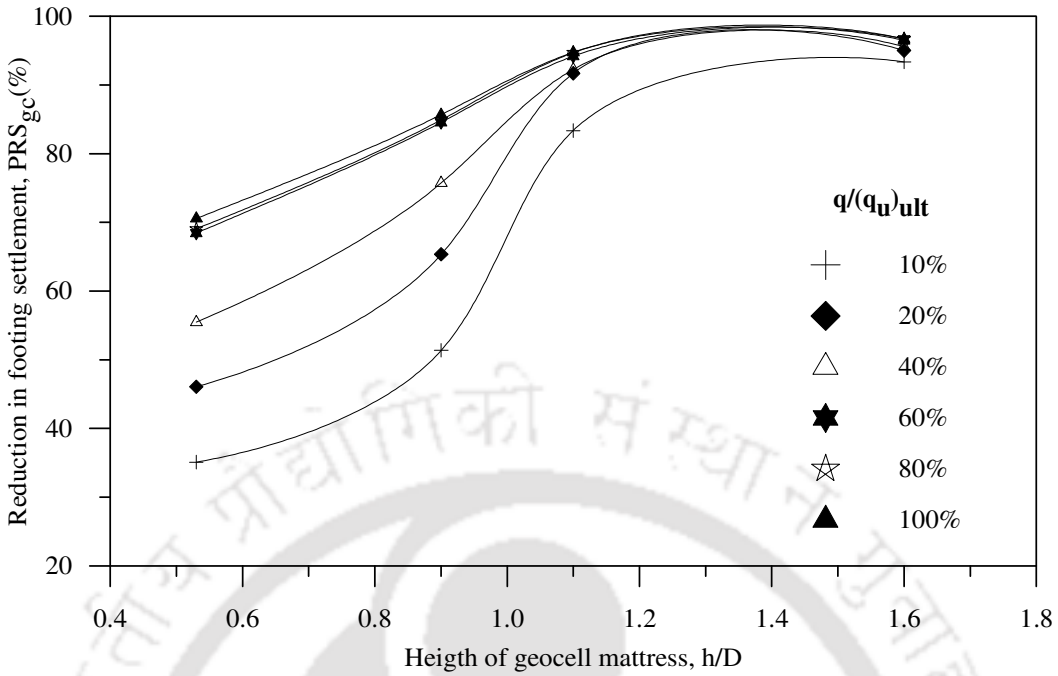

Fig. 5.5: Variation of settlement reduction factor with height of geocell mattress (d_{gc}/D = 0.8, ID = 80%, u/D = 0.1) - Test series 4

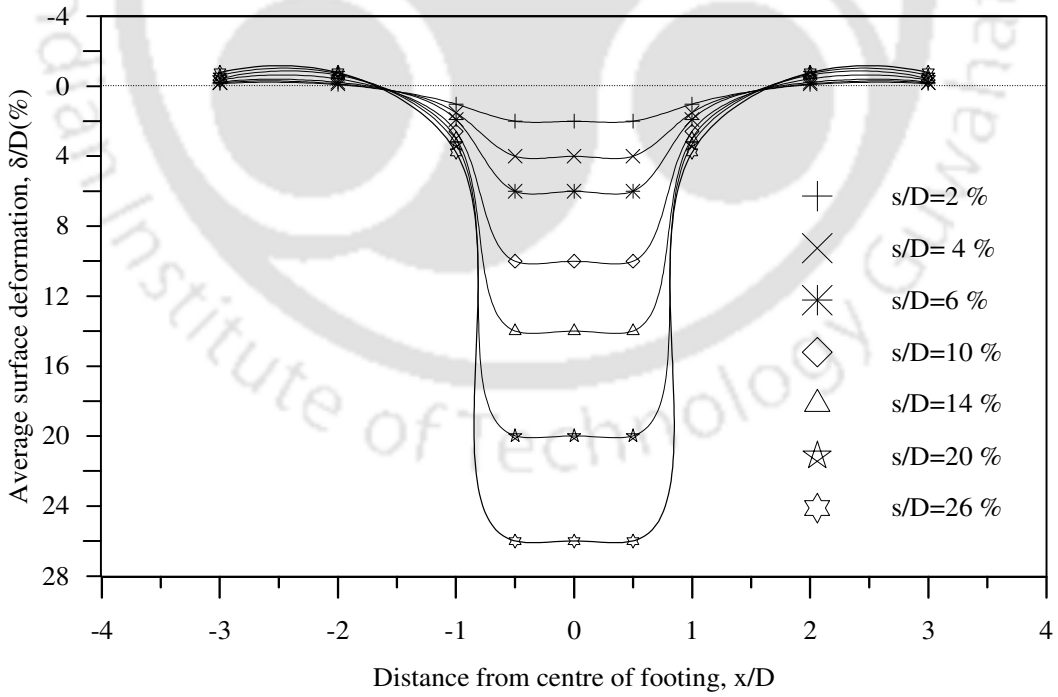

Fig. 5.6: Surface deformation profile, geocell mattress overlying clay (h/D = 0.53, d_{gc}/D = 0.8, ID = 80%, u/D = 0.1) - Test series 4

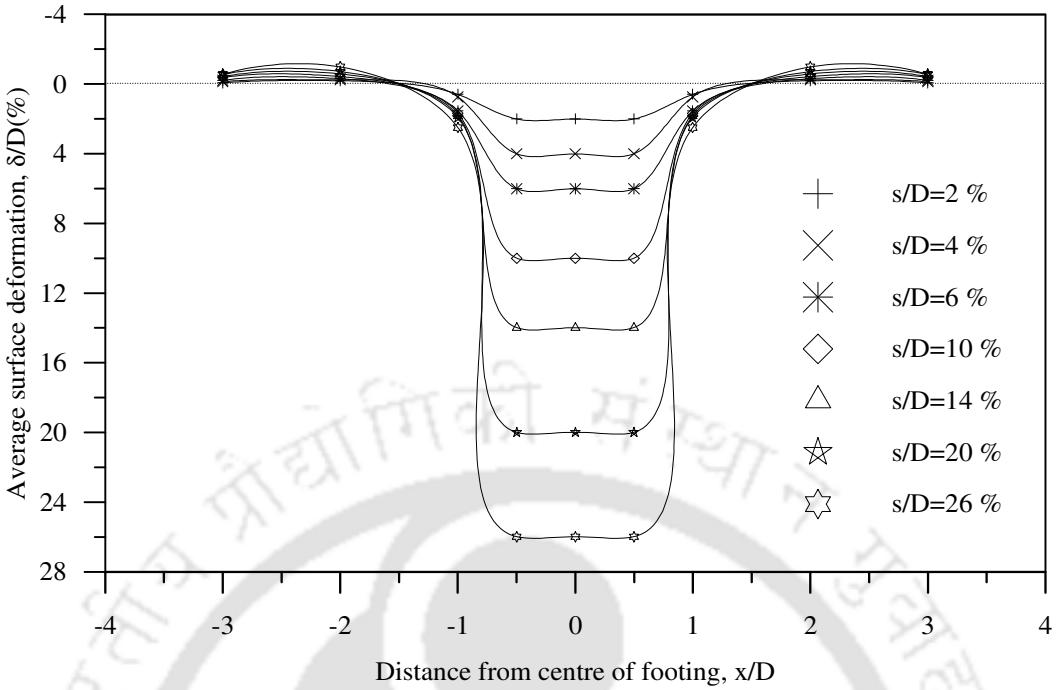

Fig. 5.7: Surface deformation profile, geocell mattress overlying clay (h/D = 0.9, d_{gc}/D = 0.8, ID = 80%, u/D = 0.1) - Test series 4

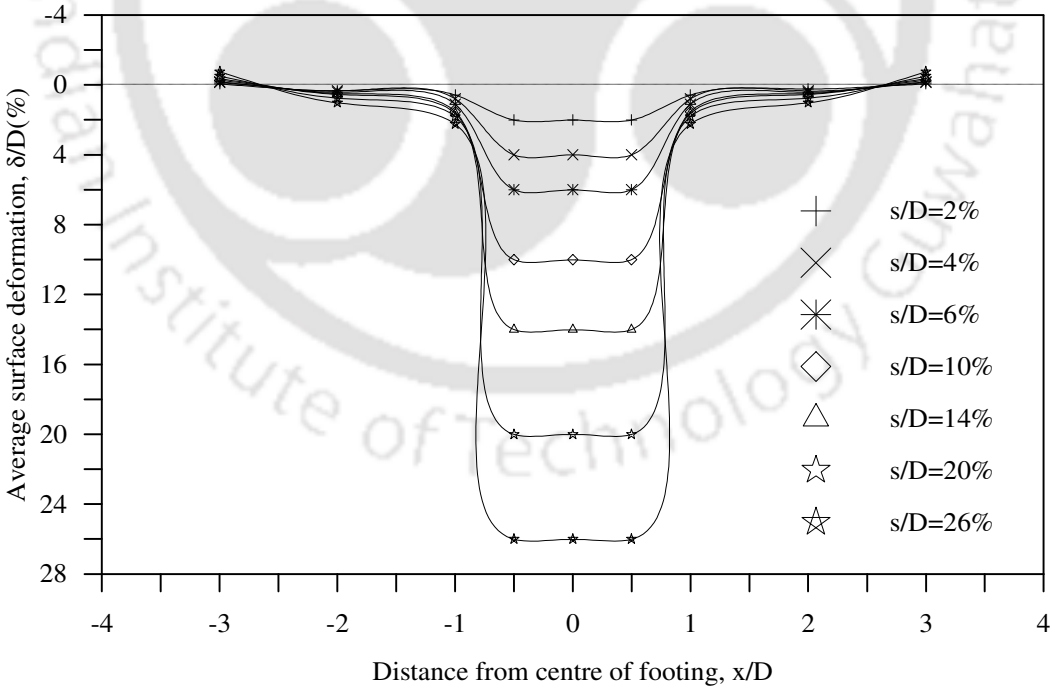

Fig. 5.8: Surface deformation profile, geocell mattress overlying clay (h/D = 1.1, d_{gc}/D = 0.8, ID = 80%, u/D = 0.1) - Test series 4

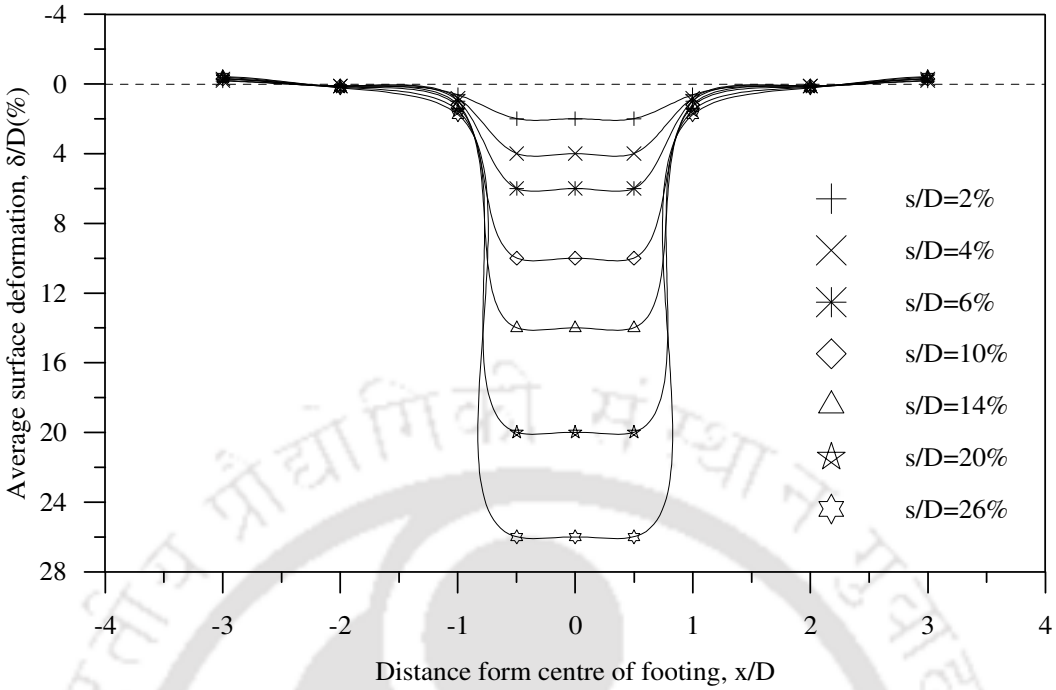

Fig. 5.9: Surface deformation profile, geocell mattress overlying clay (h/D = 1.6, d_{gc}/D = 0.8, ID = 80%, u/D = 0.1) - Test series 4

The geocell mattress through mobilization of anchorage via mobilization of interfacial friction and soil passive resistance stands against the footing penetration. For shallow depth (h) this resistance is small that, when overcome by the footing penetration, the geocell mattress punches down under the footing leading to heaving in the adjacent region. With increased height (h) the anchorage resistance increases and at one stage (h/D = 1.1) becomes sufficient enough to stand against the footing penetration leading to significant performance improvement. With further increase in height (h/D > 1.1) the performance improvement does not increase proportionately. This is attributed to local yielding of the geocell walls under footing, due to high contact pressure. From Fig. 5.5 it could be observed that at higher bearing pressure [i.e. q > 40% of $(q_u)_{ult}$] the responses almost superpose over each other indicating that the settlement reduction is proportional that the system behaves in elastic manner. This is because at higher bearing pressure the soil yields and the geocell reinforcement, which is relatively

elastic in nature, plays dominant role giving rise to a predominantly elastic response in the foundation system.

Fig. 5.10 shows that the settlement on fill surface, at x = D, reduces with increase in height of geocell mattress and correspondingly the heave at x = 2D and 3D (Fig. 5.11 and 5.12) too reduces with increase in height of the mattress. This is attributed to the increased rigidity of the geocell mattress as has been discussed earlier. The higher heaving at x = 2D and 3D, observed in case of geocell mattress of relatively shallow height (h/D = 0.53) is attributed to the lifting up of the geocell mattress owing to its centrally loaded beam like deflection. With increased height, the geocell mattress tends to behave as a deep beam that has relatively higher rigidity against bending, that it stands against the footing loading leading to reduced deflection and hence reduced heaving.

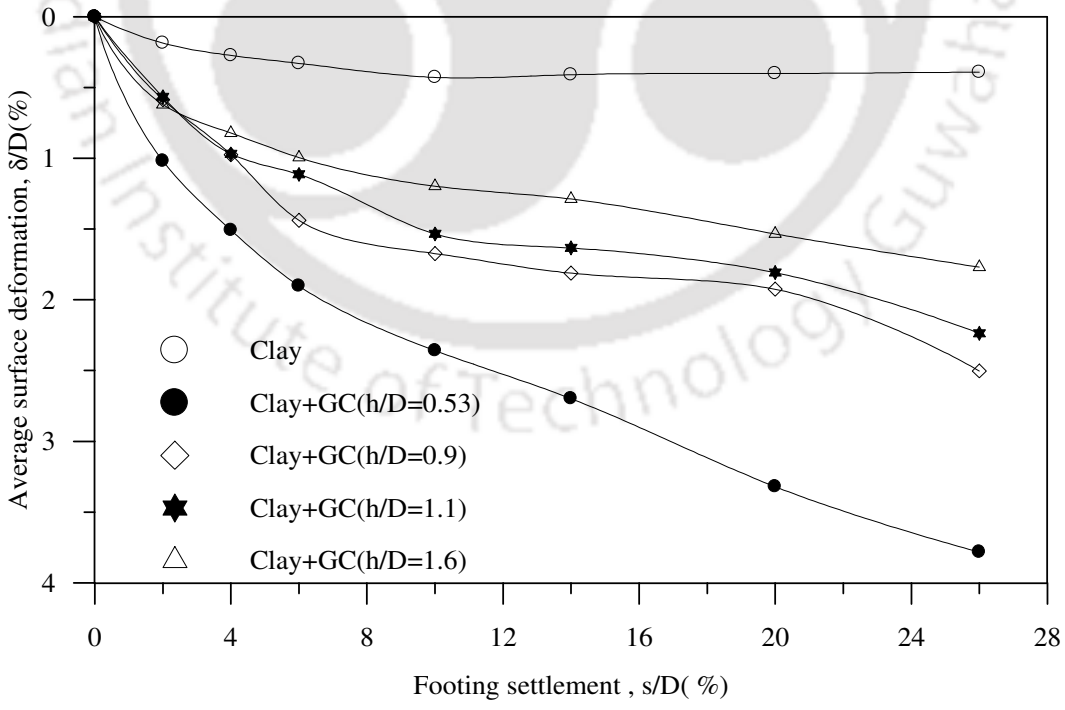

Fig.5.10: Variation of surface deformation, at x = D, with footing settlement for different heights of geocell mattress (d_{gc}/D = 0.8, ID = 80%, u/D = 0.1) - Test series 4

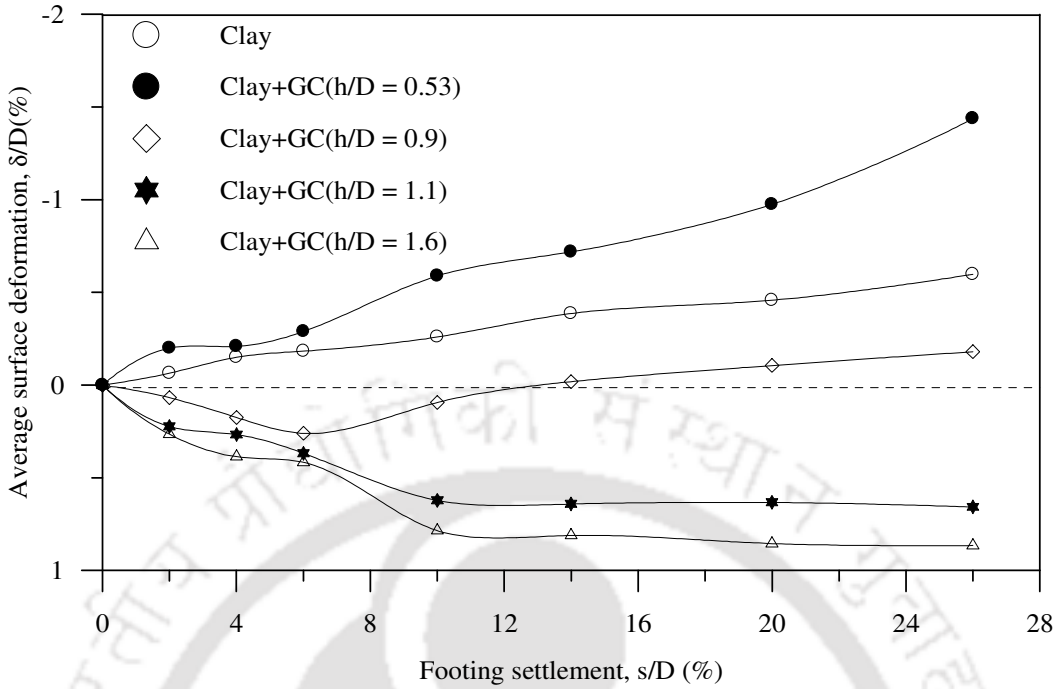

Fig.5.11: Variation of surface deformation, at x = 2D, with footing settlement for different heights of geocell mattress (d_{gc}/D = 0.8, ID = 80%, u/D = 0.1) - Test series 4

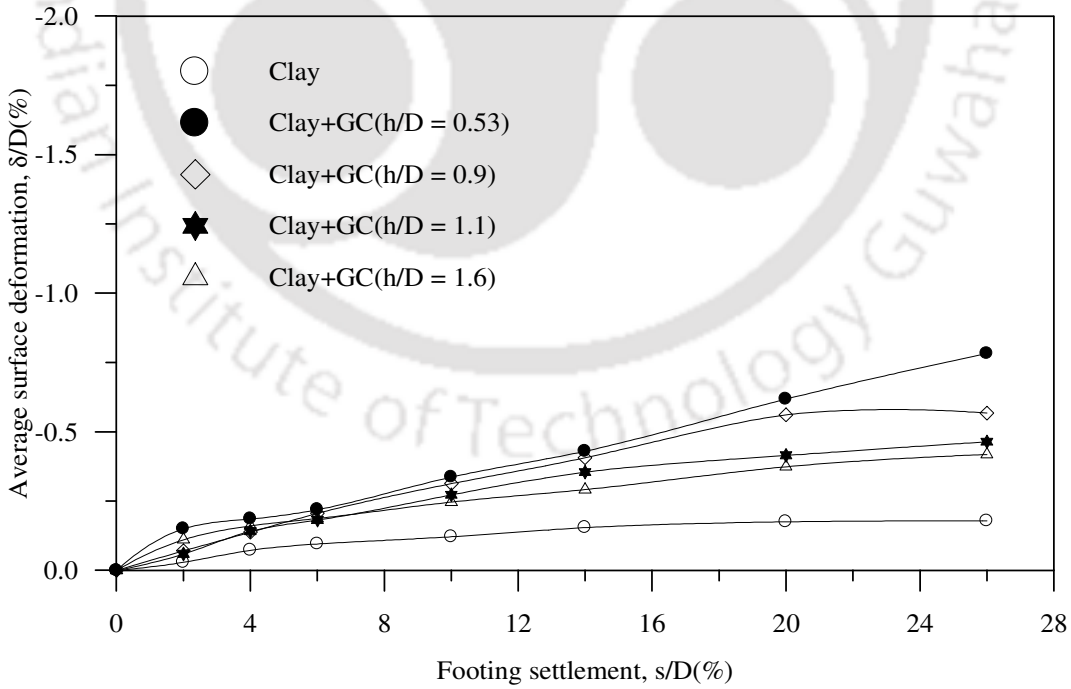

Fig.5.12: Variation of surface deformation, at x = 3D, with footing settlement for different heights of geocell mattress (d_{gc}/D = 0.8, ID = 80%, u/D = 0.1) - Test series 4

5.3 EFFECT OF RELATIVE DENSITY OF INFILL SOIL

The influence of relative density of infill sand in the geocells was studied for two different heights of geocell mattress i.e. h/D = 0.53 and 0.90, under test series 5 and 6 respectively.

The pressure-settlement responses depicted in Fig. 5.13 show that with increased density of infill soil the geocell mattress behaves stiffer (reduced slope of pressure-settlement response) and therefore is able to sustain increased loading. The bearing capacity improvement factors (IF_{gc}) are shown in Fig. 5.14. It could be observed that for the case with h/D = 0.53, the bearing capacity improvement due to the geocell reinforcement is more with higher relative density of infill soil. This indicates that, a denser soil matrix in the geocells derives increased benefit from the reinforcement. It has been observed that with increased density of soil the interfacial frictional resistance at the soil geogrid interface increases (Fig.3.22-3.25). As a result of which the anchorage against the downward deformation under footing penetration increases leading to better performance improvement. Besides, the dense soil tends to dilate which is restrained by the geocell walls, in turn; higher strength of reinforcement is mobilized. As the loose soil tends to contract under deformation, relatively large strain (i.e. large settlement) is required before it becomes dense enough to transfer stress onto the geocells. In other words, with loose soil infill the beneficial effect of geocell reinforcement remains substantially immobilised, leading to reduced performance improvement.

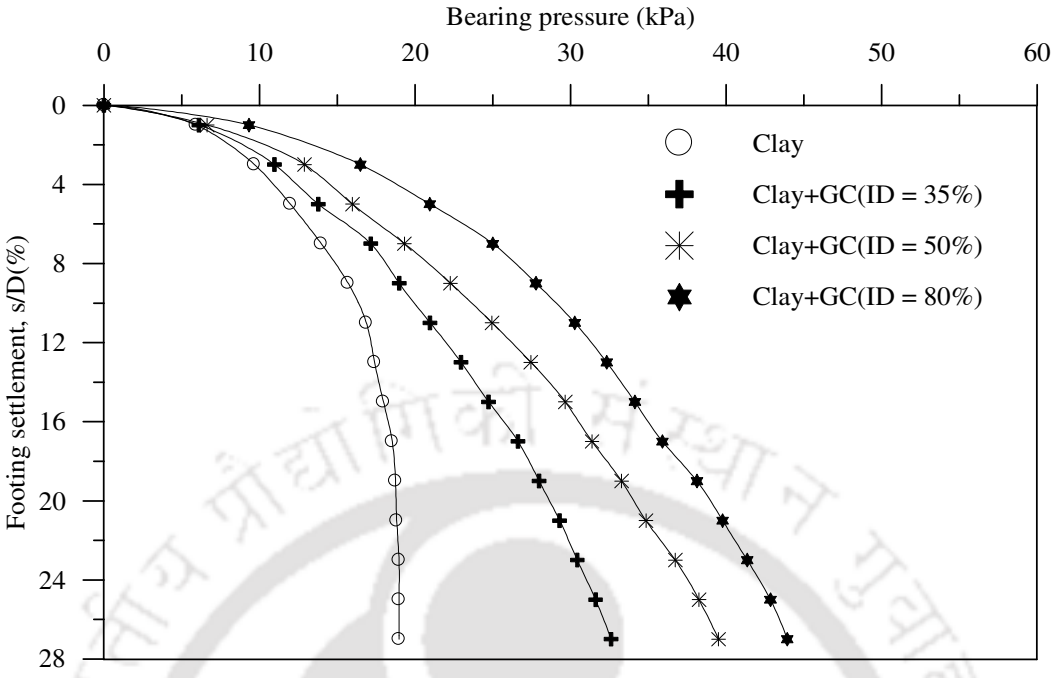

Fig. 5.13: Variation of bearing pressure with footing settlement for different relative density of infill soil (h/D = 0.53, d_{gc}/D = 0.8, u/D = 0.1) - Test series 5

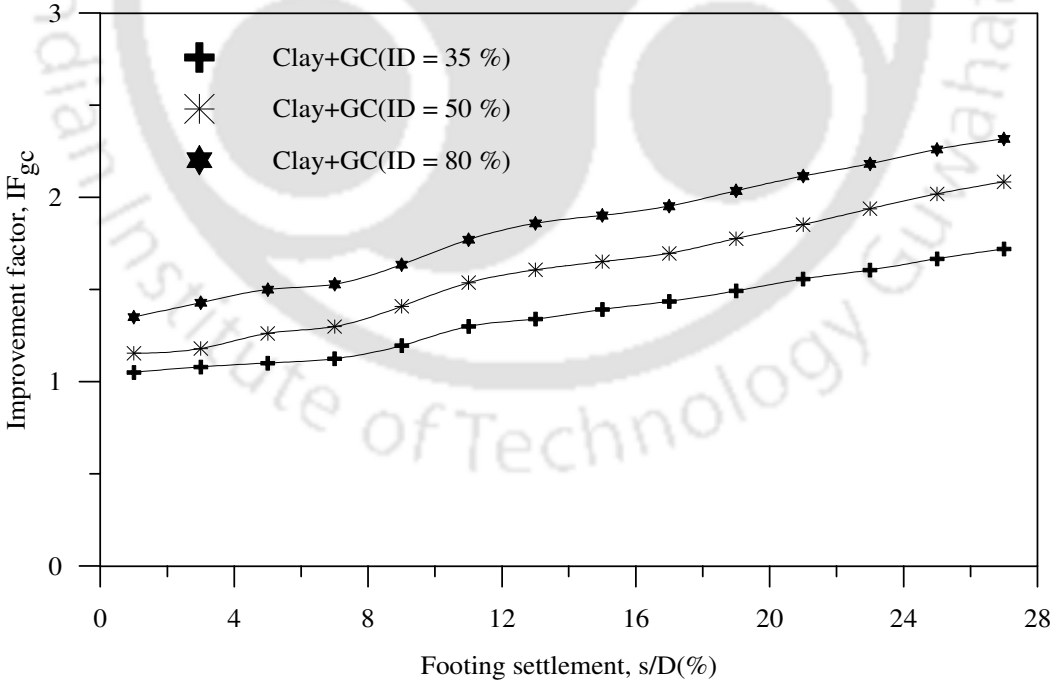

Fig.5.14: Variation of improvement factor with footing settlement for different relative density of infill soil (h/D = 0.53, d_{gc}/D = 0.8, u/D = 0.1) - Test series 5

The settlement reduction factor due to variation in relative density of soil, with geocell mattress of height 0.53D, is depicted in Fig.5.15. There is a sharp increase in PRS_{sc} with increase in relative density from 35% to 50%. Thereafter the reduction in settlement is relatively gradual with relative density increasing to 80%. This indicates that density of infill soil plays a major role in reducing the settlement of the geocell reinforced foundation system. It is of interest to note that with 80% relative density of infill soil, as high as 70% reduction in footing settlement is achieved.

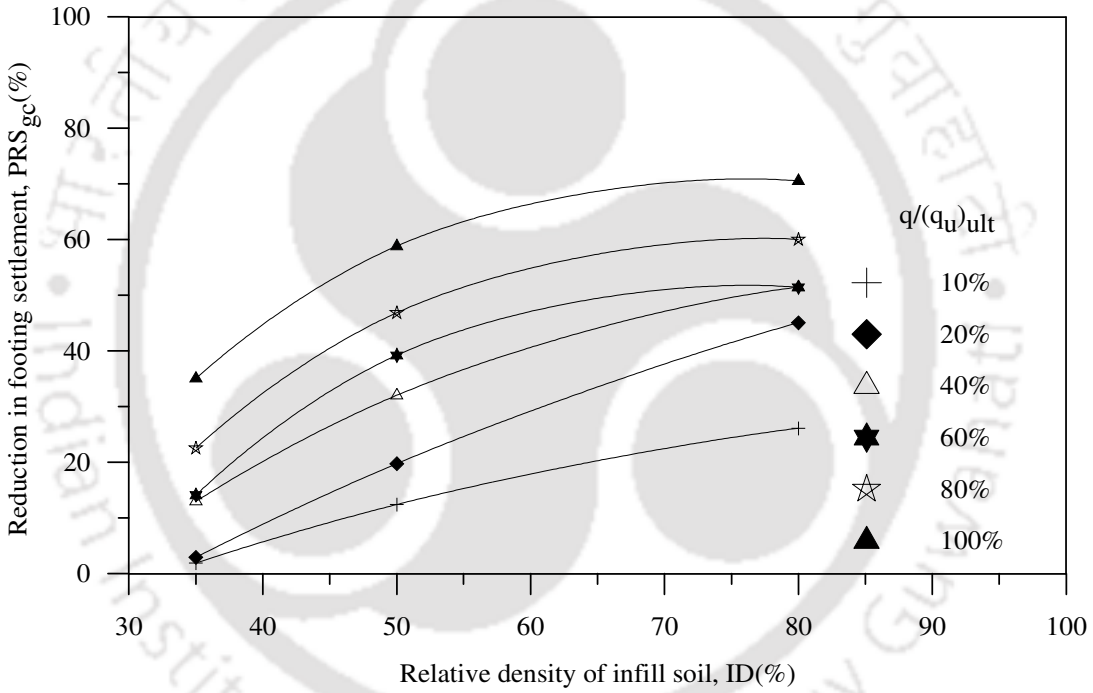

Fig. 5.15: Variation of settlement reduction factor with relative density of infill soil ($h/D = 0.53$, $d_{gc}/D = 0.8$, $u/D = 0.1$) - Test series 5

Fig. 5.16 shows that in the region near to the footing (i.e. x = D), with geocell mattress having dense soil, the settlement is more. The relatively flexible geocell mattress undergoes concave upward like deformation under and around the footing giving rise to settlement on fill surface. With increased density of infill soil, the geocell mattress behaves more coherently that it deflects more like a centrally loaded beam giving rise

to increased settlement on surface. Besides, with increased density of fill soil, the relatively rigid geocell mattress effectively restrains the heaving in the underlying clay mass leading to increased settlement on surface. Outside the loaded region the geocell mattress, owing to anchorage resistance at ends, deflects in convex upward shape (Fig. A_8-A_{10}) leading to heaving on fill surface (Fig. 5.17 and 5.18). The relatively higher heaving in case of ID = 35%, at x = 3D (at par with ID = 50%), is attributed to the lifting up of the geocell cage due to loose soil that offers anchorage resistance of very small magnitude.

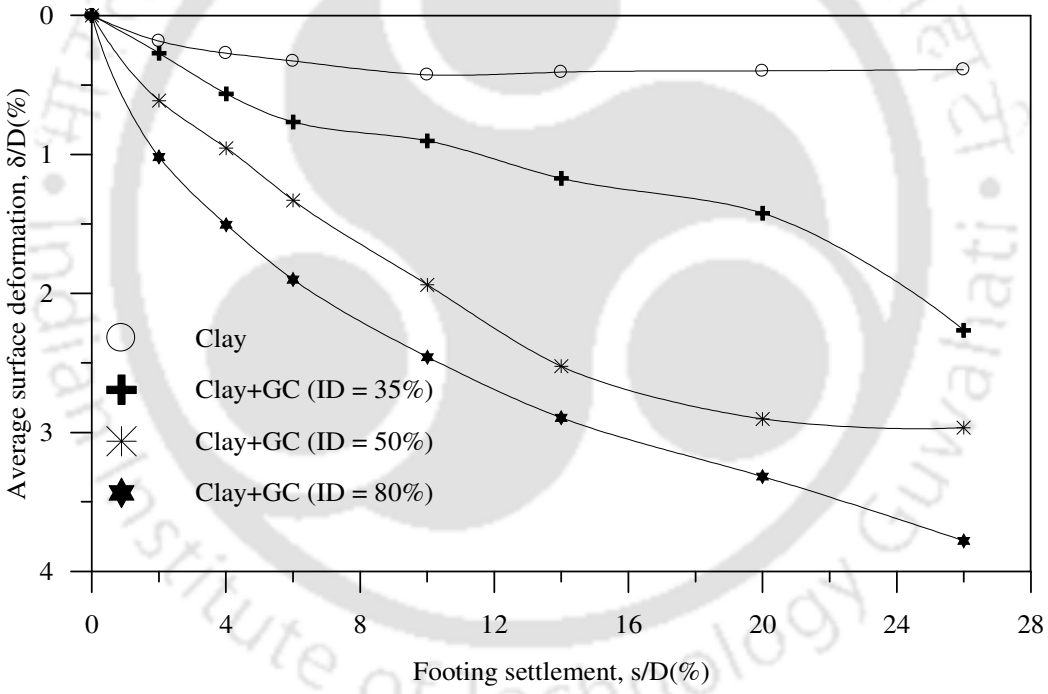

Fig.5.16: Variation of surface deformation, at x = D, with footing settlement for different relative density of infill soil (h/D = 0.53, d_{gc}/D = 0.8, u/D = 0.1) – Test series 5

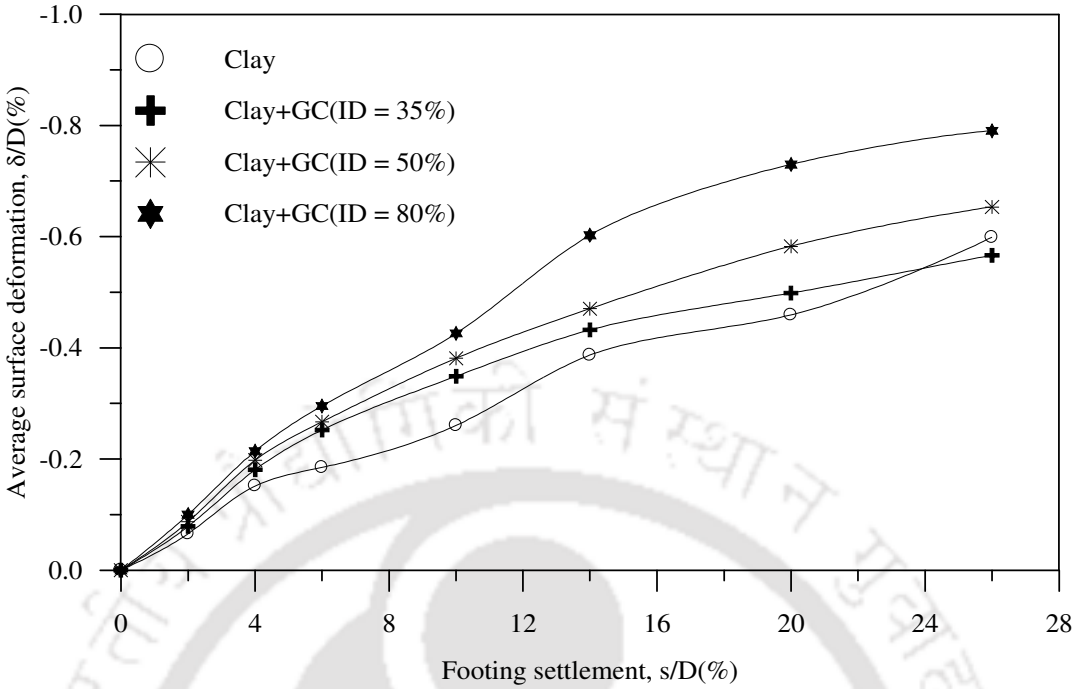

Fig.5.17: Variation of surface deformation, at x = 2D, with footing settlement for different relative density of infill soil (h/D = 0.53, d_{gc}/D = 0.8, u/D = 0.1) – Test series 5

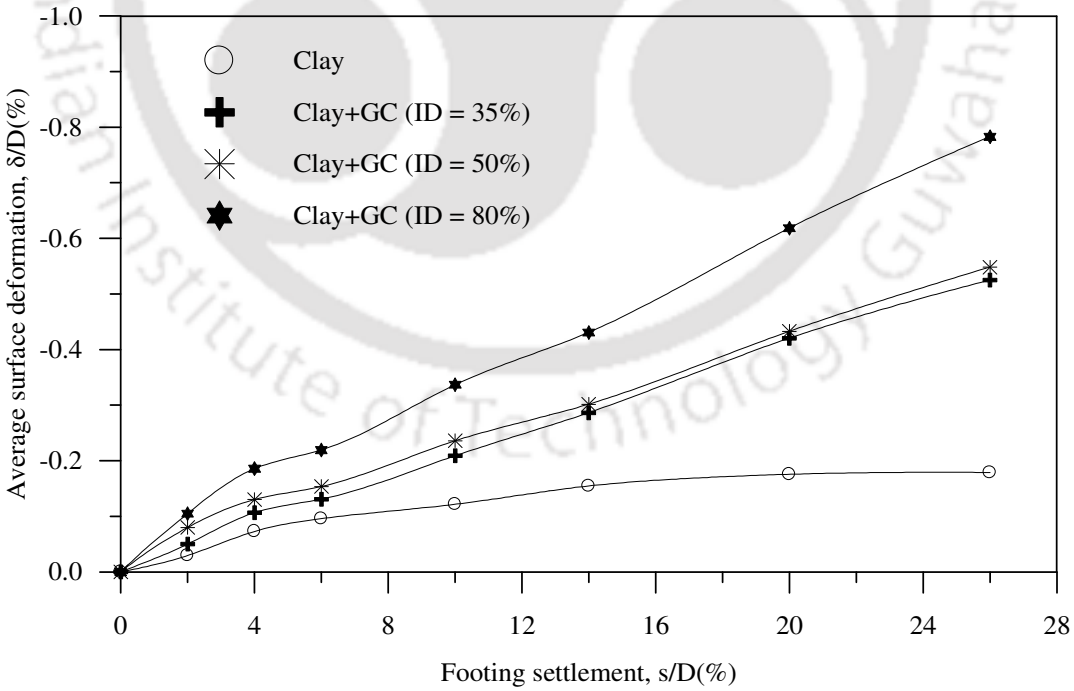

Fig.5.18: Variation of surface deformation, at x = 3D, with footing settlement for different relative density of infill soil (h/D = 0.53, d_{gc}/D = 0.8, u/D = 0.1) – Test series 5

With geocell mattress of relatively higher height (h/D = 0.9), similar trends too have been observed with respect to the relative density of infill soil (Fig. 5.19 - 5.23). However, compared to the case with geocell mattress of shallow height (h/D = 0.53, Fig. 5.14), the improvement factor (IF_{gc}) versus footing settlement responses, in the present case (i.e. h/D = 0.9) are relatively steeper. This is because with increased height, there develops large anchorage resistance at both the ends of the geocell mattress. As a result of which the geocell reinforcement, instead of getting pulled down, stands against footing penetration thereby mobilizes its strength and stiffness effectively, leading to increased performance improvement. With dense infill (ID = 80%), the fill surface at x = 2D has shown settlement. This indicates that, with increased height and dense infill, relatively larger area of geocell mattress participates in dispersing the footing load over a wider area leading to settlement over a larger area on the foundation bed.

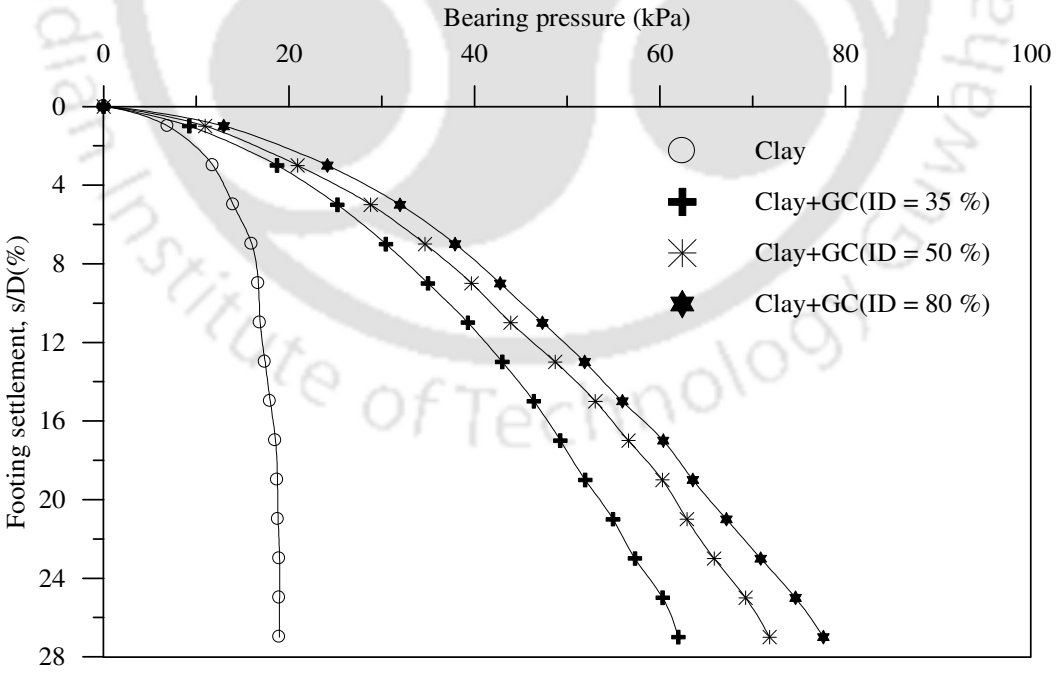

Fig.5.19: Variation of bearing pressure with footing settlement for different relative density of infill soil (h/D = 0.9, d_{gc}/D = 0.8, u/D = 0.1) - Test series 6

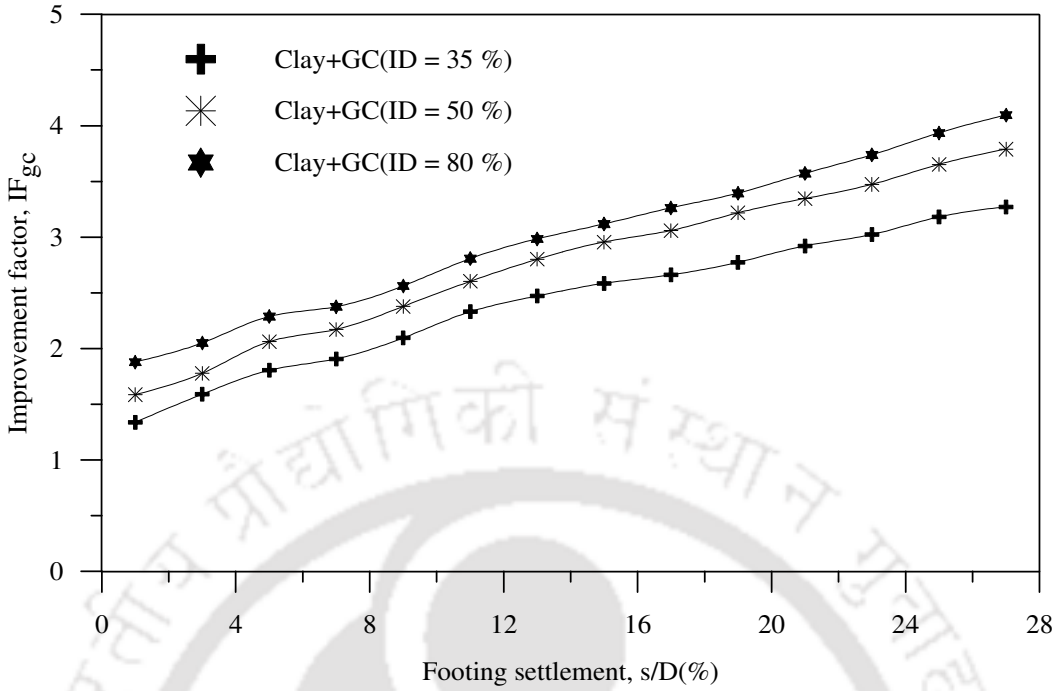

Fig.5.20: Variation of improvement factor with footing settlement for different relative density of infill soil (h/D = 0.9, d_{gc}/D = 0.8, u/D = 0.1) - Test series 6

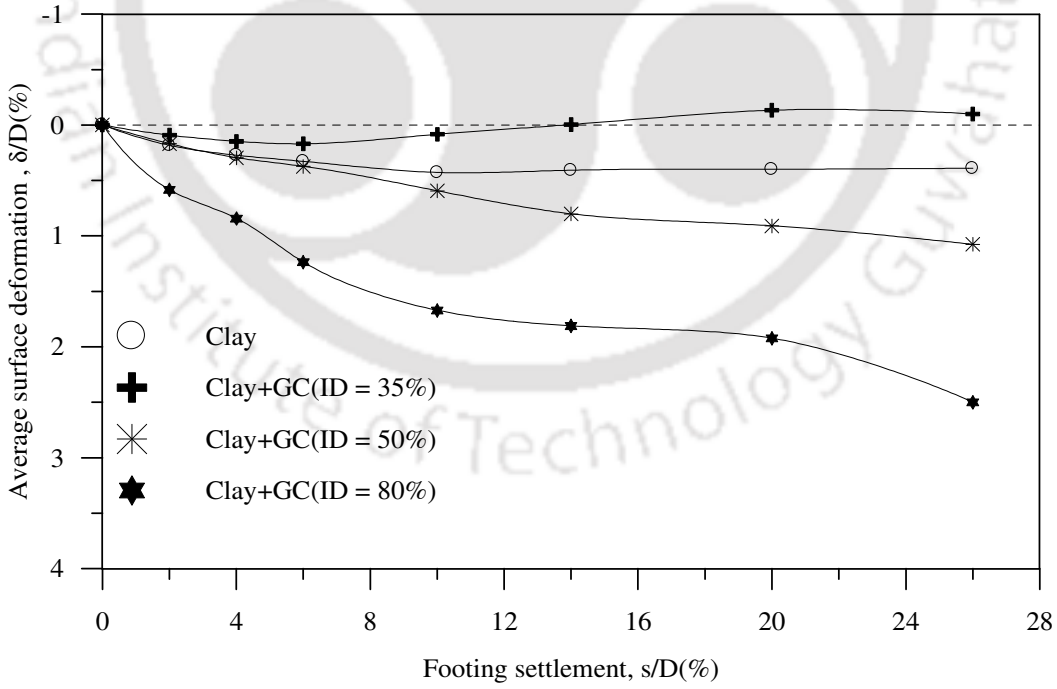

Fig.5.21: Variation of surface deformation, at x = D, with footing settlement for different relative density of infill soil (h/D = 0.9, d_{gc}/D = 0.8, u/D = 0.1)) – Test series 6

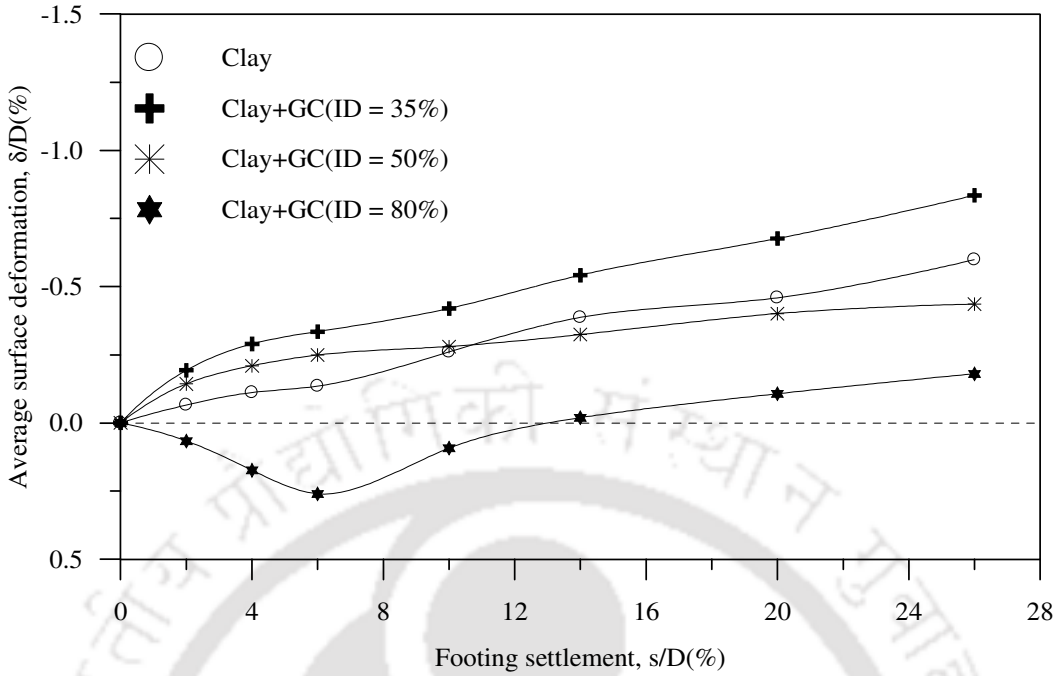

Fig.5.22: Variation of surface deformation, at x = 2D, with footing settlement for different relative density of infill soil (h/D = 0.9, d_{gc}/D = 0.8, u/D = 0.1) – Test series 6

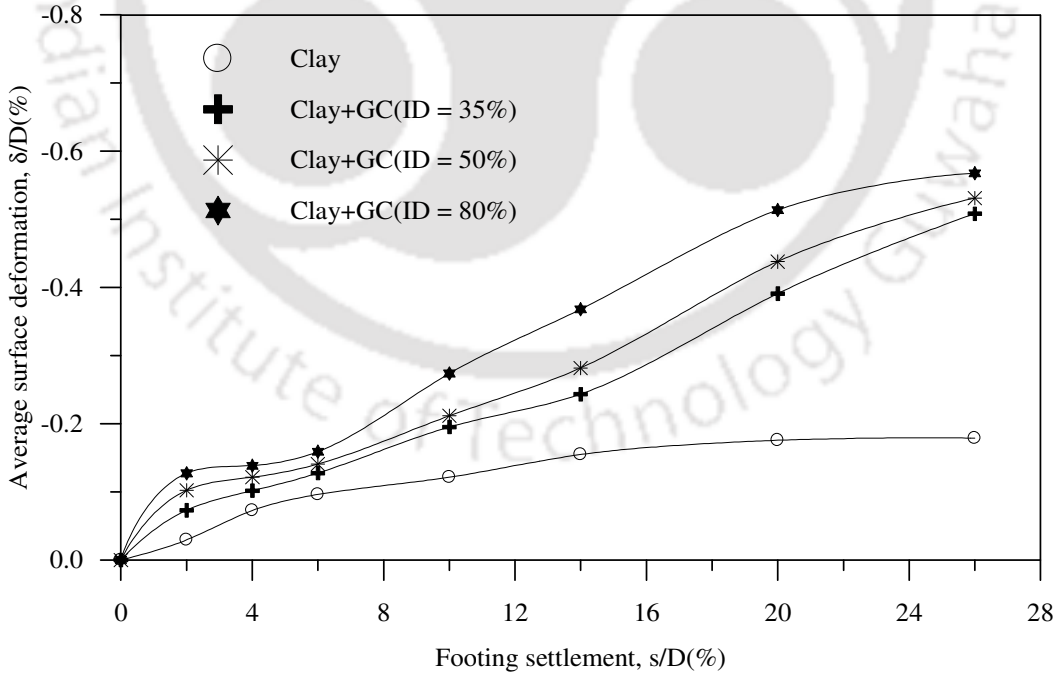

Fig.5.23: Variation of surface deformation at x = 3D with footing settlement for different relative density of infill soil (h/D = 0.9, d_{gc}/D = 0.8, u/D = 0.1) - Test series 6

5.4 EFFECT OF POCKET SIZE OF GEOCELLS

The variation of bearing pressure with footing settlement for different sizes of geocell pocket opening with h/D = 0.53 are depicted in Fig. 5.24. The corresponding variations in bearing capacity improvement factor (IF_{gc}) and settlement reduction factor $(PRS)_{gc}$ are presented in Fig. 5.25 and Fig. 5.26 respectively. The increased load carrying capacity and reduction in settlement with reduced pocket size is primarily due to two factors. First, with reduction in pocket size, the number of geocells and hence the joints per unit area of the mattress increases. Due to this the rigidity of the geocell cage increases leading to increase in the overall rigidity of the system against footing penetration. Second, with reduced pocket size, the confinement offered by the geocells per unit volume of soil increases, giving rise to a relatively stronger geocell mattress and hence a higher performance improvement of the system.

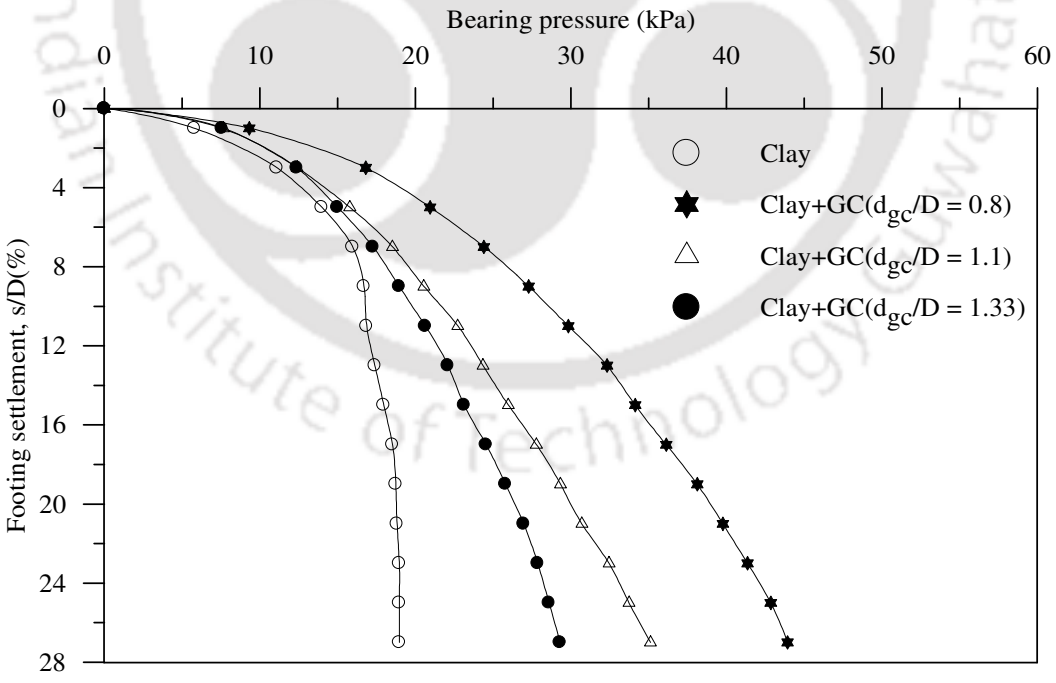

Fig.5.24: Variation of bearing pressure with footing settlement for different pocket size of the geocells (h/D = 0.53, ID = 80%, u/D = 0.1)) - Test series 7

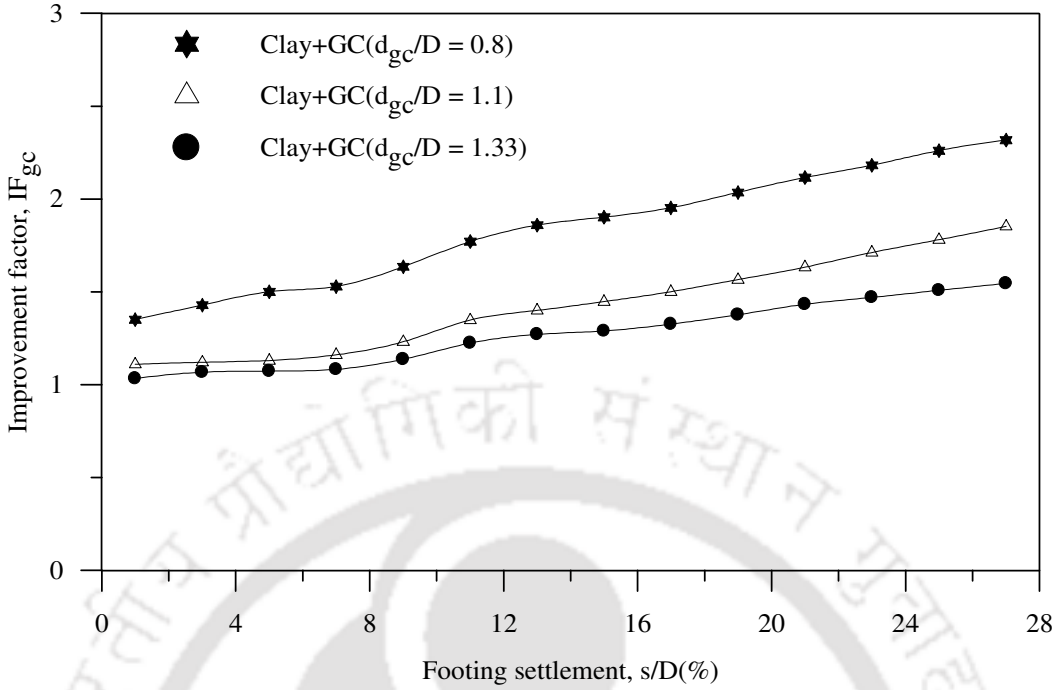

Fig.5.25: Variation of improvement factor with footing settlement for different pocket size of geocells (h/D = 0.53, ID = 80%, u/D = 0.1) - Test series 7

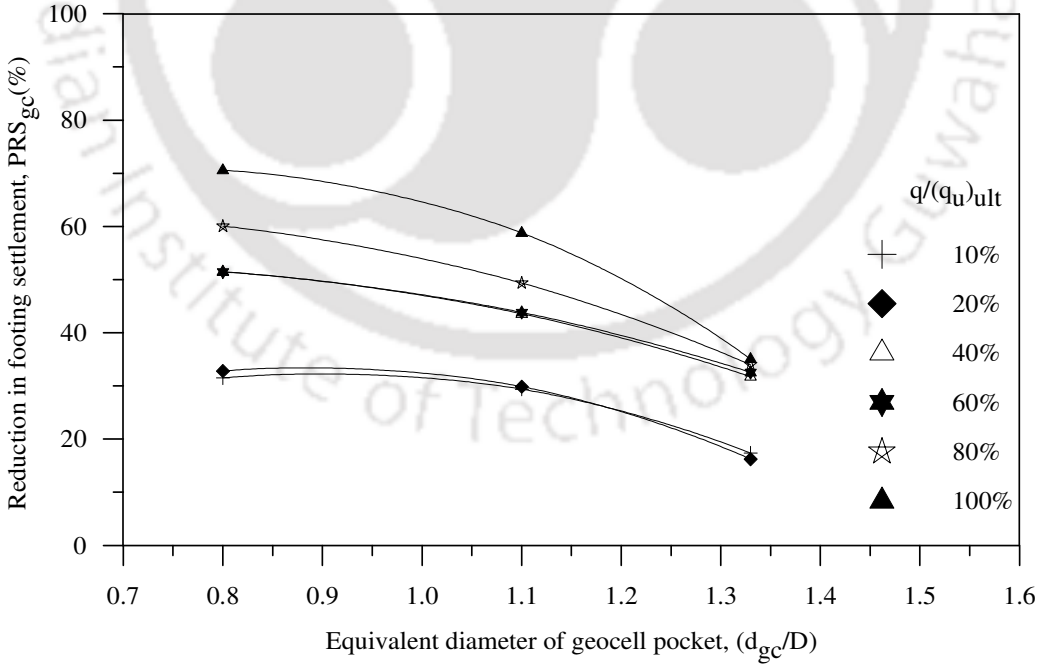

Fig. 5.26: Variation of settlement reduction factor with pocket size of geocells (h/D = 0.53, ID = 80%, u/D = 0.1) - Test series 7

The surface deformation profiles for pocket size of 0.8D and 1.1D are presented in Fig. 5.27 and Fig. 5.28 respectively. It can be seen that the heaving pattern is of hogging type in shape. This shape takes place due to anchorage at the ends that tries to hold the geocell mattress against footing settlement induced downward deformations. With very large pocket size of geocells (i.e. d_{gc} = 1.33D) the overall area of the geocell reinforcement reduces substantially. This reduces the mobilized interfacial frictional resistance and hence the end anchorage to a marginal value that the geocell reinforcement gets pulled down under footing penetration leading to reduced performance improvement (Fig. 5.25). Indeed, the surface deformation profile for d_{gc}/D = 1.33, presented in Fig. 5.29 shows that the end anchorage induced hogging type deformation of geocell mattress has ceased to manifest in this case.

.

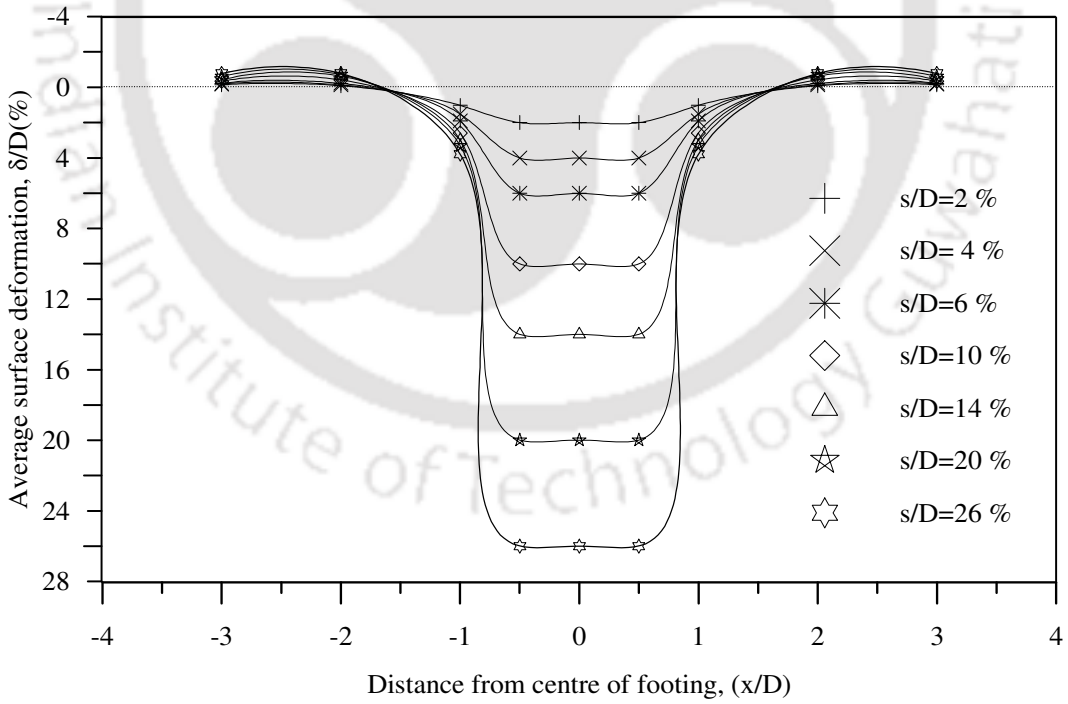

Fig. 5.27: Surface deformation profile, geocell mattress overlying clay (d_{gc}/D = 0.8, h/D = 0.53, ID = 80%, u/D = 0.1) - Test series 7

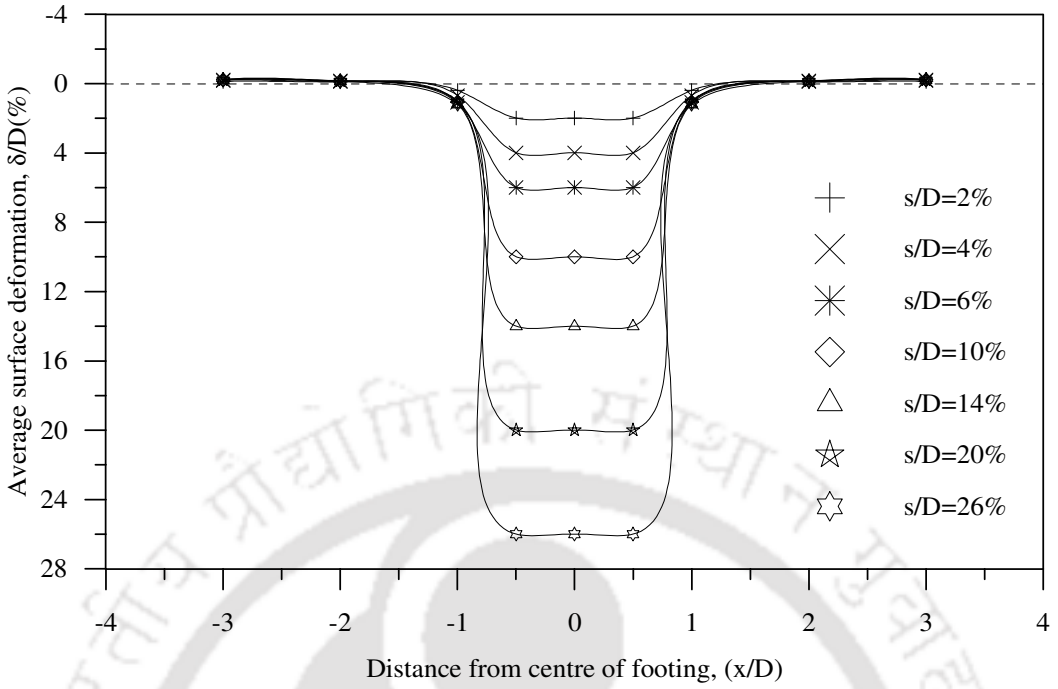

Fig. 5.28: Surface deformation profile, geocell mattress overlying clay (d_{gc}/D = 1.1, h/D = 0.53, ID = 80%, u/D = 0.1) -Test series 7

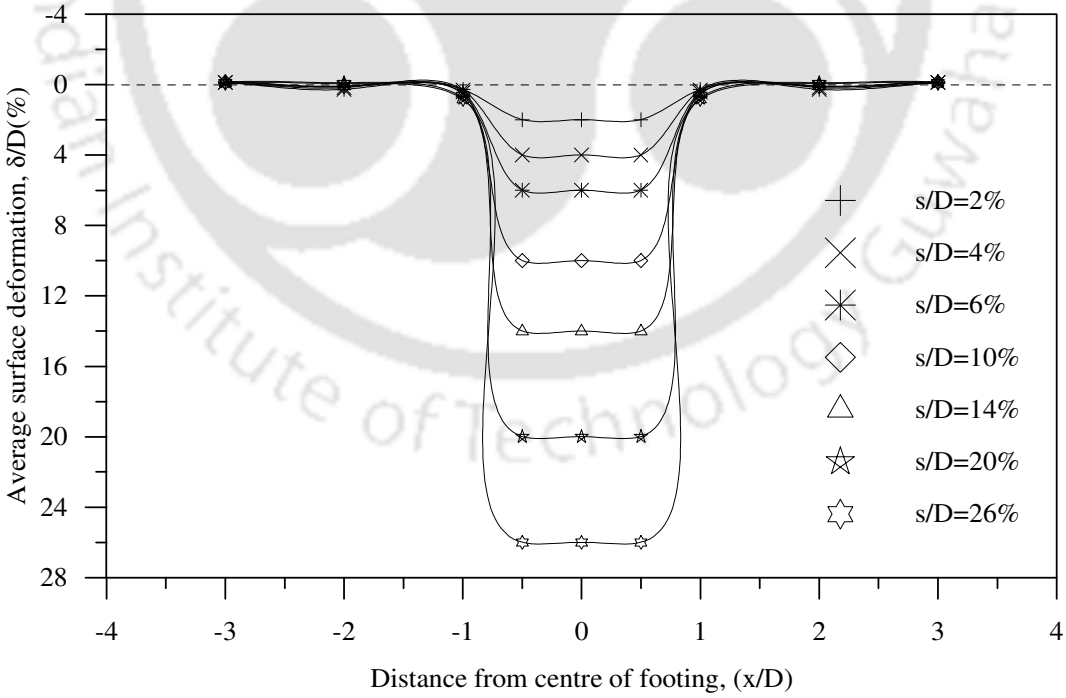

Fig. 5.29: Surface deformation profile, geocell mattress overlying clay (h/D = 0.53, d_{gc}/D = 1.33, ID = 80%, u/D = 0.1) - Test series 7

Fig. 5.30 shows that at x = D, the geocell mattress having smaller pocket size has undergone higher settlement. This indicates that with reduced pocket size the area of geocell mattress, which, participates actively in sharing the footing loading increases that the foundation bed settles over a wider area, along with the footing. This behaviour is attributed to the improved composite response of the geocell-soil structure, owing to the increased confinement offered by the geocell pockets to the encapsulated soil mass. Correspondingly, the heaving on fill surface, due to hogging type deformation of geocell mattress, is relatively higher with geocell mattress having smaller pocket size (Fig. 5.31 and Fig. 5.32). This is because with reduced pocket size, as the geocell mattress settles over larger area, it correspondingly displaces increased volume of clay mass underneath, which being accumulated in the adjacent region has produced higher heaving.

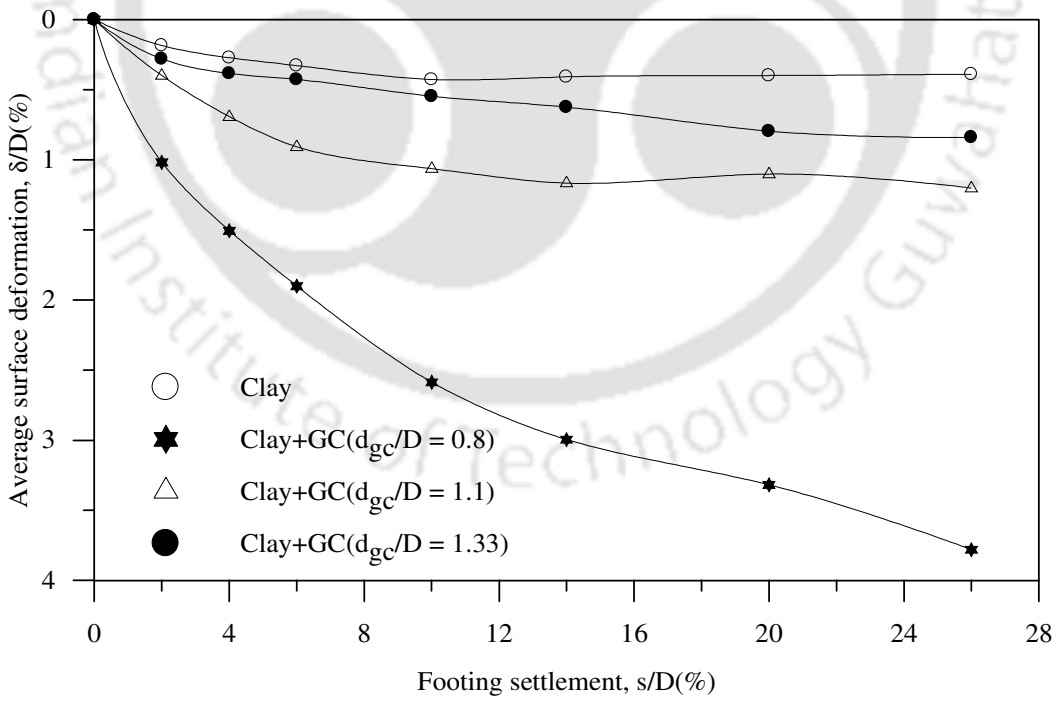

Fig.5.30: Variation of surface deformation at, x = D, with footing settlement for different pocket size of geocells (h/D = 0.53, ID = 80%, u/D = 0.1) - Test series 7

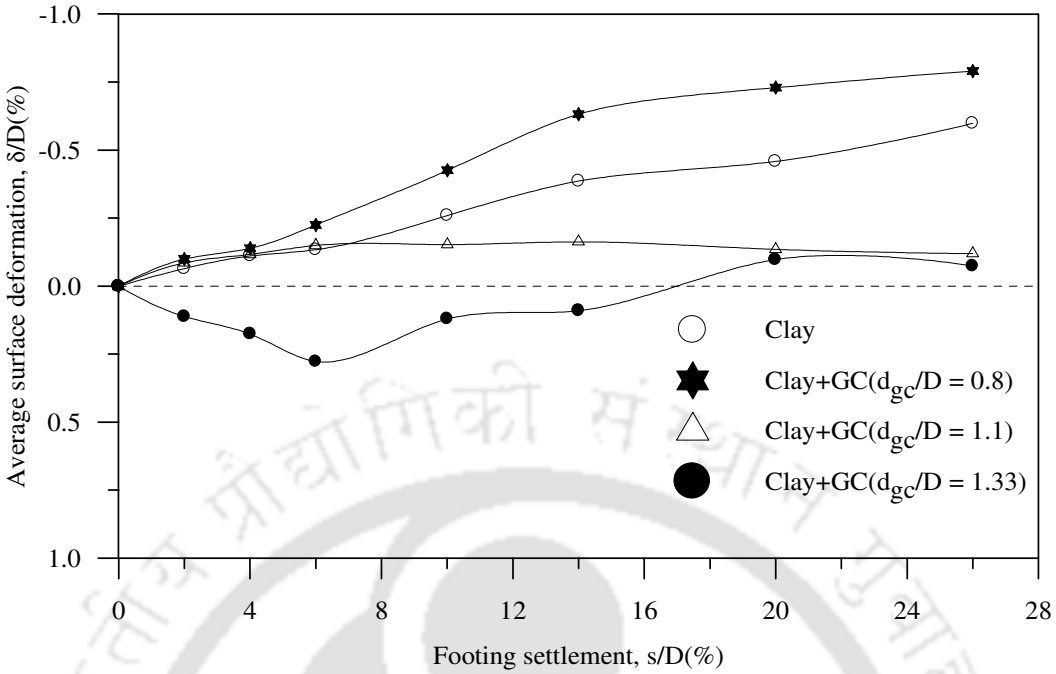

Fig.5.31: Variation of surface deformation, at x = 2D, with footing settlement for different pocket size of geocells (h/D = 0.53, ID = 80%, u/D = 0.1) - Test series 7

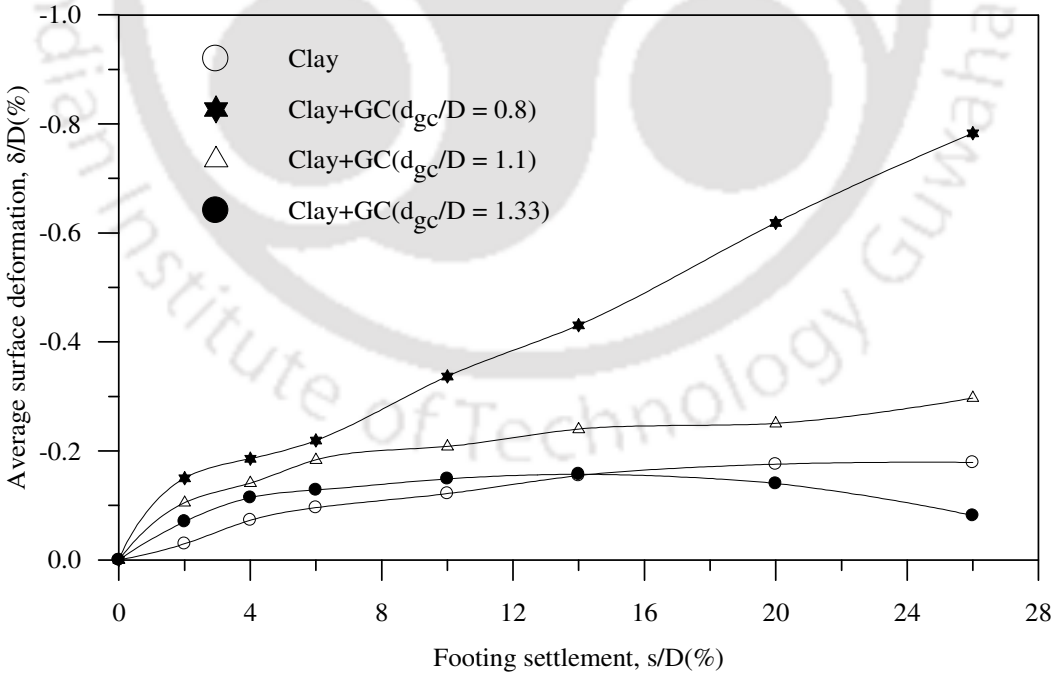

Fig.5.32: Variation of surface deformation, at x = 3D, with footing settlement for different pocket size of geocells (h/D = 0.53, ID = 80%, u/D = 0.1) - Test series 7

With increased height of geocell mattress (i.e. h/D = 0.9), the pressure settlement response (Fig. 5.33) and surface deformation responses (Fig. 5.36 - 5.38) for different pocket sizes (d_{gc}) show almost similar trend as that with h/D = 0.53. However, quantitatively the obtained improvement is higher for geocell mattress of larger height (Fig. 5.34 and Fig. 5.35 Vs. Fig. 5.26 and Fig. 5.27). Hence it can be said that the general behaviour of the geocell mattress, pertaining to the change in pocket size of the geocells, remains nearly same irrespective of the geocell mattress height i.e. shallow or deep.

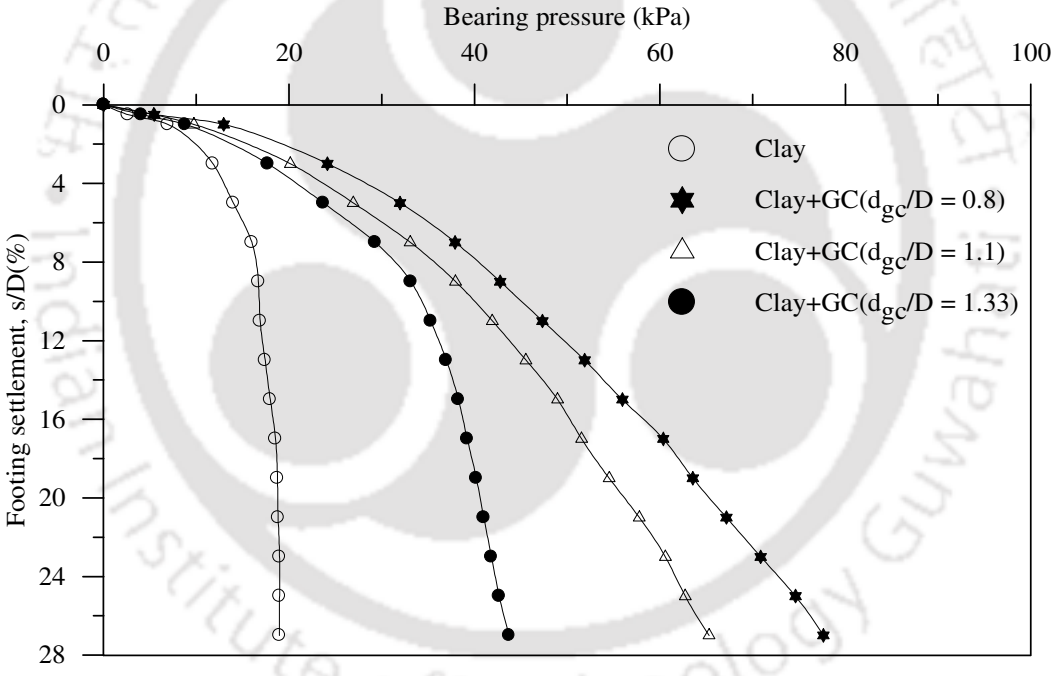

Fig.5.33: Variation of bearing pressure with footing settlement for different pocket size of the geocell (h/D = 0.9, ID = 80%, u/D = 0.1) - Test series 8

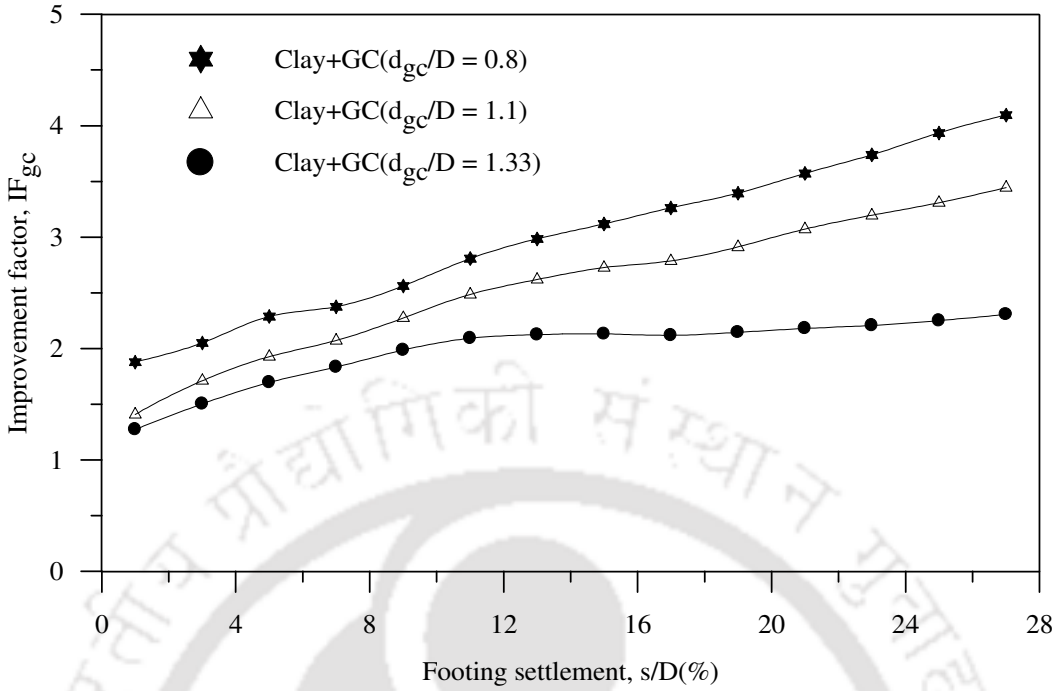

Fig.5.34: Variation of improvement factor with footing settlement for different pocket size of geocells (h/D = 0.9, ID = 80%, u/D = 0.1) - Test series 8

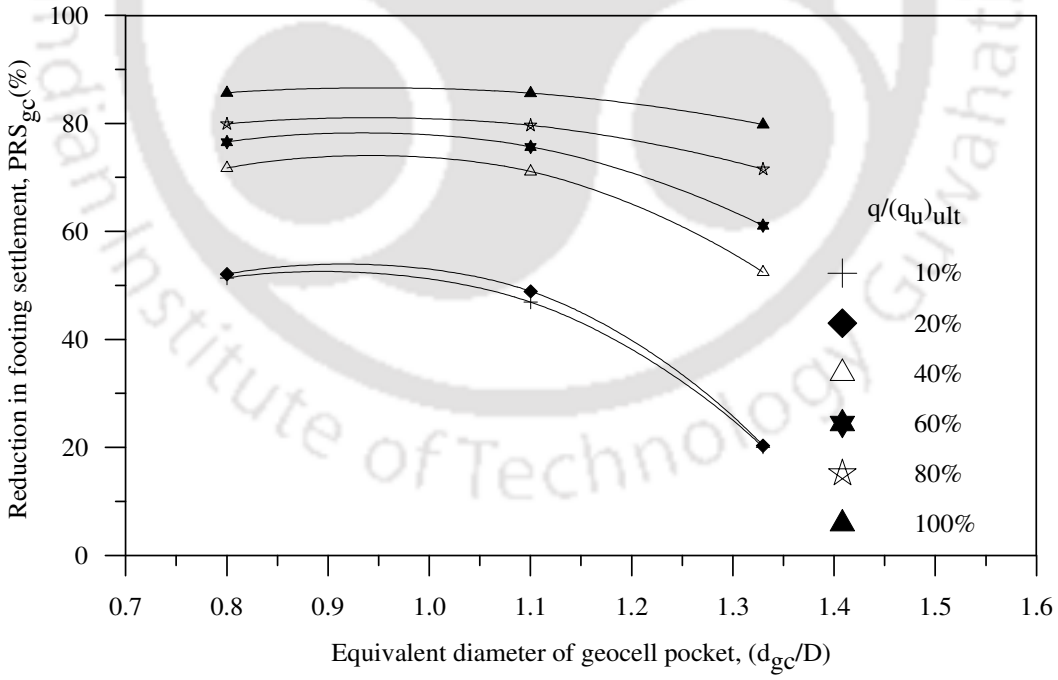

Fig. 5.35: Variation of settlement reduction factor with pocket size of geocells (h/D = 0.9, ID = 80%, u/D = 0.1) - Test series 8

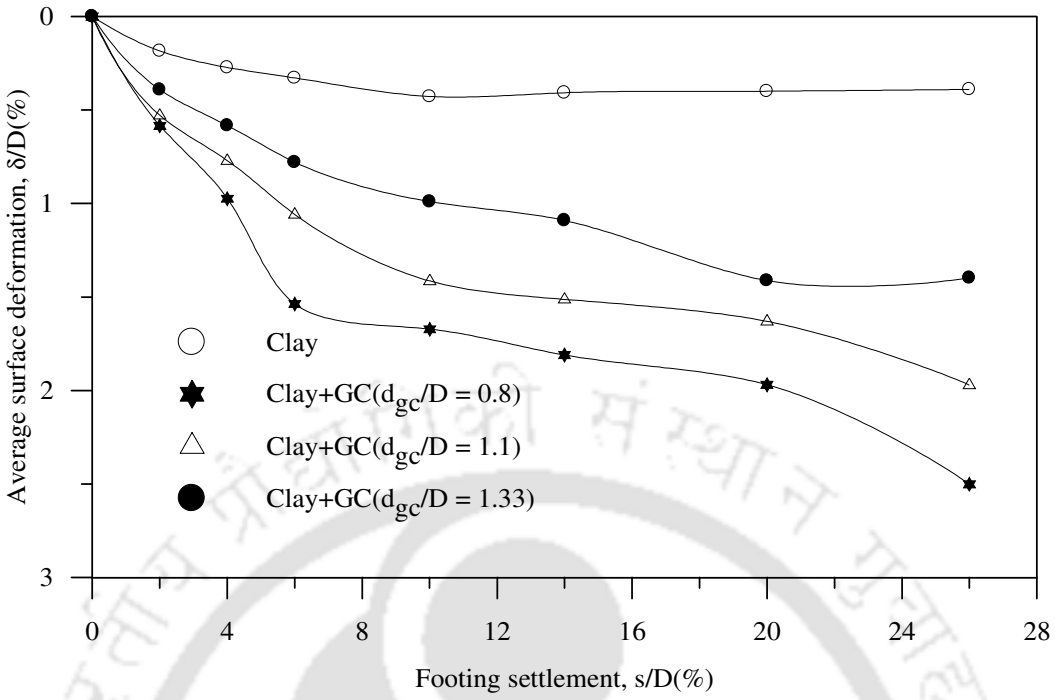

Fig.5.36: Variation of surface deformation, at x = D, with footing settlement for different pocket size of geocells (h/D = 0.9, ID = 80%, u/D = 0.1) – Test series 8

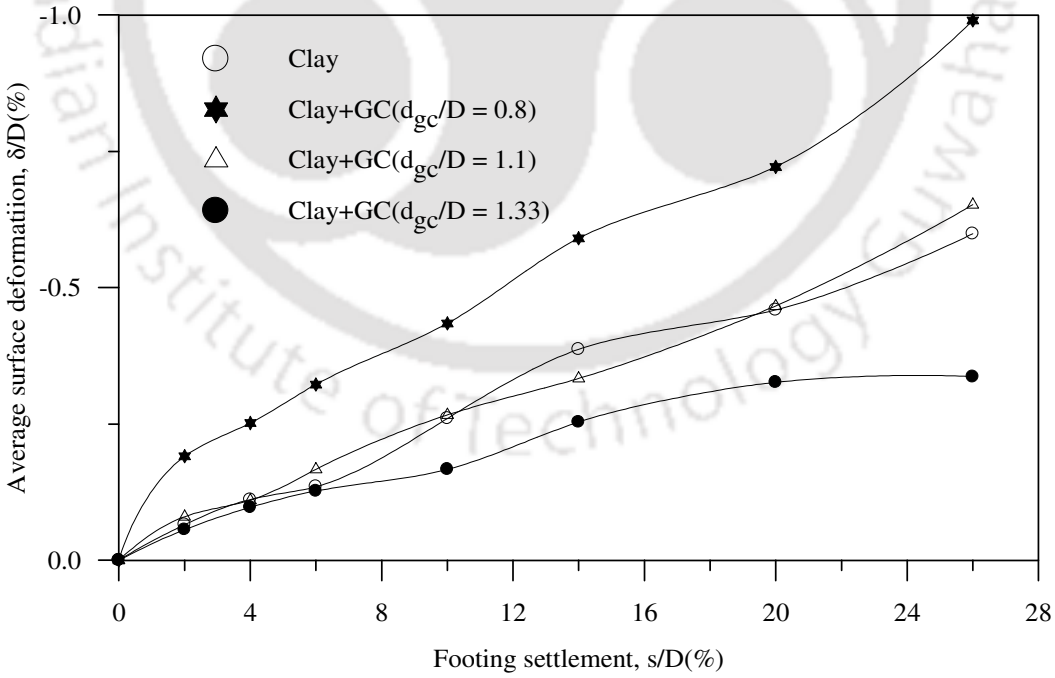

Fig.5.37: Variation of surface deformation, at x = 2D, with footing settlement for different pocket size of geocells (h/D = 0.9, ID = 80%, u/D = 0.1) – Test series 8

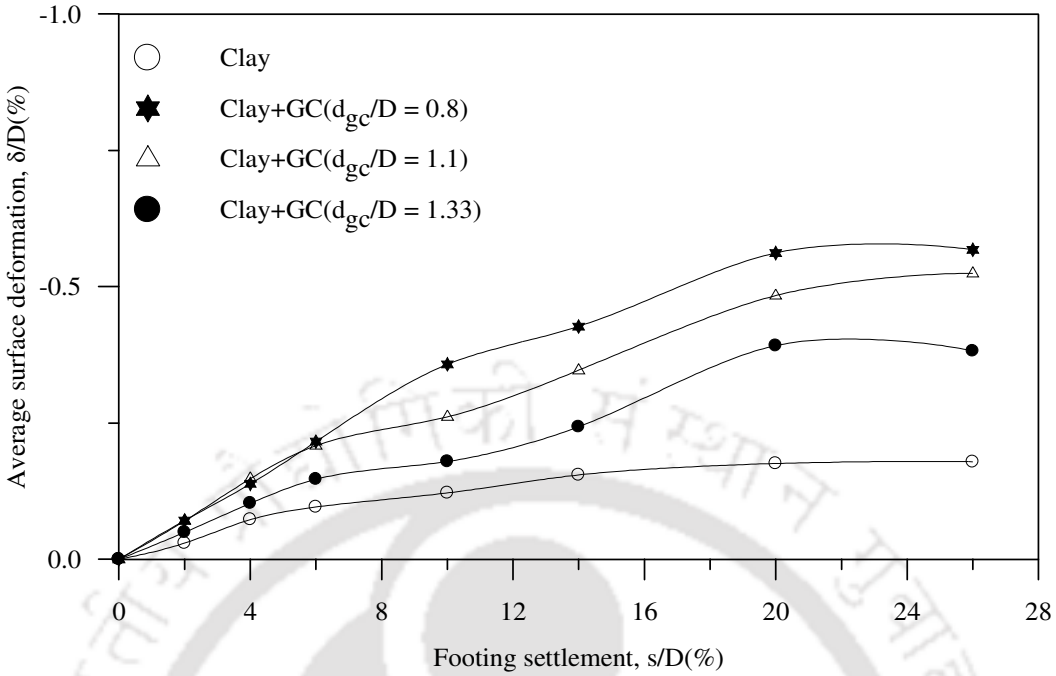

Fig.5.38: Variation of surface deformation, at x = 3D, with footing settlement for different pocket size of geocells (h/D = 0.9, ID = 80%, u/D = 0.1) – Test series 8

CHAPTER 6

GEOCELL MATTRESS-STONE COLUMN REINFORCED CLAY BED

6.1 INTRODUCTION

In the preceding two chapters the beneficial effects of stone column reinforcement (SC) and geocell mattress reinforcement (GC) placed individually, in the soft clay foundation have been studied. In this chapter the combined use of both these techniques i.e., stone columns and geocell mattress; has been brought out. Such type of foundation system (i.e. both stone column and geocell-sand mattress in clay bed) is referred to as *composite foundation bed* hereafter.

Typical bearing pressure-settlement responses depicted in Fig.6.1 shows that the stiffness (indicated through slope of pressure-settlement response) and load carrying capacity of the clay bed with composite reinforcement (i.e. Clay + GC + SC), is much higher as compared to that with the geocell mattress alone (i.e. Clay + GC). Similar behaviour is noticed in all other cases as well. This increased performance is attributed to the increased resistance against deformation induced by the stone columns that provide additional support to the geocell mattress, primarily, through mobilization of friction and stiffness of the stone aggregates. The performance improvement, due to the combined application of geocell mattress and stone column reinforcement, is quantified through non dimensional factors; bearing capacity improvement factor (IF_{gcsc}) and percentage reduction in footing settlement (PRS_{gcsc}) as defined below,

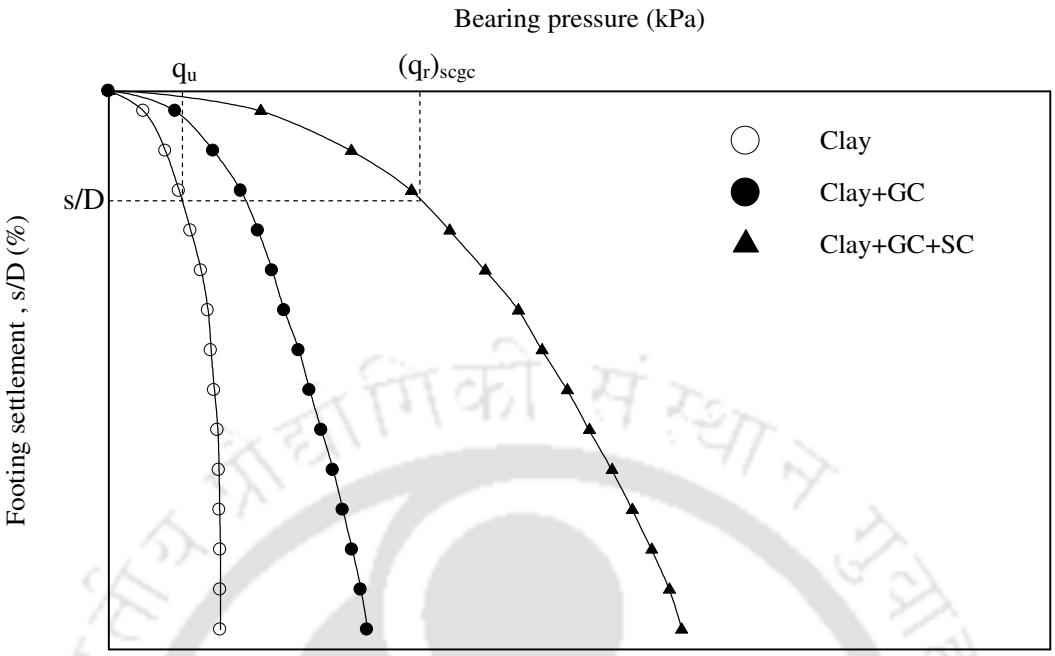

Fig.6.1: Definition sketch for bearing capacity Improvement factor, IF_{gcsc}

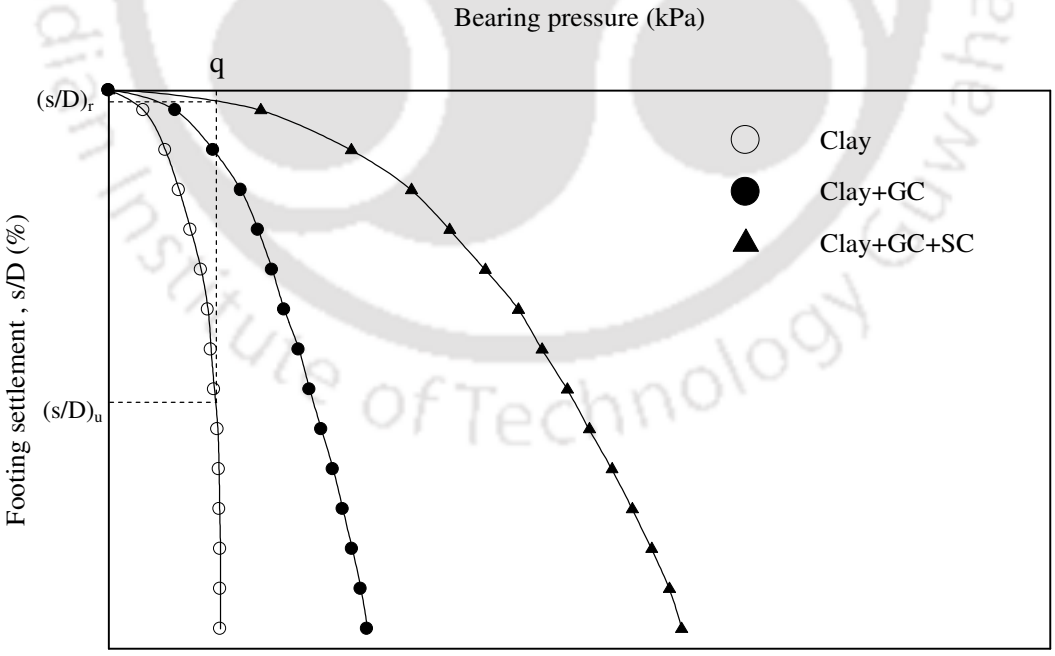

Fig.6.2: Definition sketch for settlement reduction factor, PRS_{gcsc}

$$IF_{gcsc} = \frac{(q_r)_{g\,csc}}{q_u} \tag{6.1}$$

$$PRS_{g\,csc} = \frac{s_u - (s_r)_{g\,csc}}{s_u} \tag{6.2}$$

Where, q_u and $(q_r)_{gcsc}$ are the bearing pressure of unreinforced and geocell mattress-stone column reinforced clay bed respectively, both taken at a given settlement of the footing (Fig. 6.1). Similarly, s_u and $(s_r)_{gcsc}$ are the settlement of unreinforced clay bed and geocell-stone column reinforced clay bed respectively, both at a given bearing pressure (q) as shown in Fig. 6.2.

The influence of different parameters such as, length and spacing of stone columns, height and pocket size of geocells, density of soil in the geocells; on the overall response of the composite foundation system are presented and discussed in the following sections.

6.2 EFFECT OF LENGTH OF STONE COLUMN

The influence of length (L) of stone columns on the overall performance of the composite foundation system has been studied for four different heights of geocell mattress (i.e. h = 0.53D, 0.9D, 1.1D and 1.6D; where D is the diameter of the footing). Tests were carried with for stone column lengths (L) of $1d_{sc}$, $3d_{sc}$, $5d_{sc}$ and $7d_{sc}$; where d_{sc} is the diameter of the stone columns. In all these tests (Test series 9-12), spacing of stone columns, pocket size of geocells, density of infill soil in geocells and depth of placement of geocell layer were kept constant as; S = $2.5d_{sc}$, d_{gc} = 0.8D, ID = 80%, u = 0.1D respectively. The obtained results, for different heights (h/D) of geocell mattress, are presented and discussed in the following subsections.

6.2.1 Height of geocell mattress (h/D) of 0.53

Fig. 6.3 shows the pressure-settlement responses of the composite foundation systems, for geocell mattress of height equal to 0.53D. The responses of clay bed alone and clay bed with geocell mattress (h = 0.53D) are also included in this figure, for purpose of comparison. The performance improvement of foundation bed, due to geocell-stone column reinforcement, quantified through the bearing capacity improvement factor, IF_{gcsc}, and settlement reduction factor, PRS_{gcsc}, are depicted in Fig. 6.4 and Fig. 6.5 respectively. It could be observed that with the composite reinforcement (i.e. geocell + stone column) the bearing capacity has gone up as high as 5 times the ultimate capacity of the unreinforced clay bed. While, with geocell reinforcement (h/D = 0.53) the bearing capacity was just 1.5 times (Fig. 5.4) and with stone column reinforcement (L/d_{sc} = 7) it was only 3.5 (Fig. 4.7) times that of the unreinforced clay bed. Fig 6.5 shows that the settlement reduction achieved with composite foundation bed is close to 100%.

With increase in length of stone columns from 3 to 5 times the diameter (i.e. L/d_{sc} = 3 to 5), there is sharp increase in performance, both in terms of increased bearing capacity (IF_{gcsc}) and reduced settlement (PRS_{gcsc}). This is attributed to the increased end bearing capacity due to increased embedment of stone columns and increased skin friction resistance mobilized over the increased length of stone columns. With further increase in length (L) to $7d_{sc}$, the additional improvement is much less. Hence it can be said that the optimum length of stone columns giving maximum performance improvement, in the composite foundation system, is about 5 times their diameter ($5d_{sc}$).

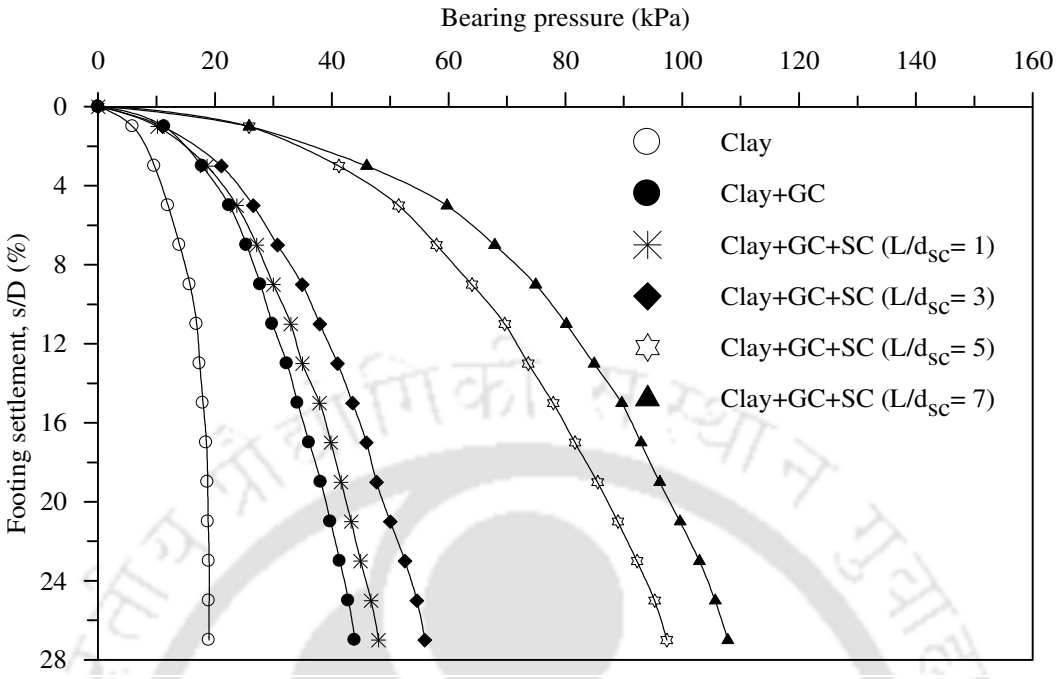

Fig.6.3: Variation of bearing pressure with footing settlement in composite foundation bed (h/D = 0.53, S/d_{sc} = 2.5) - Test series 9

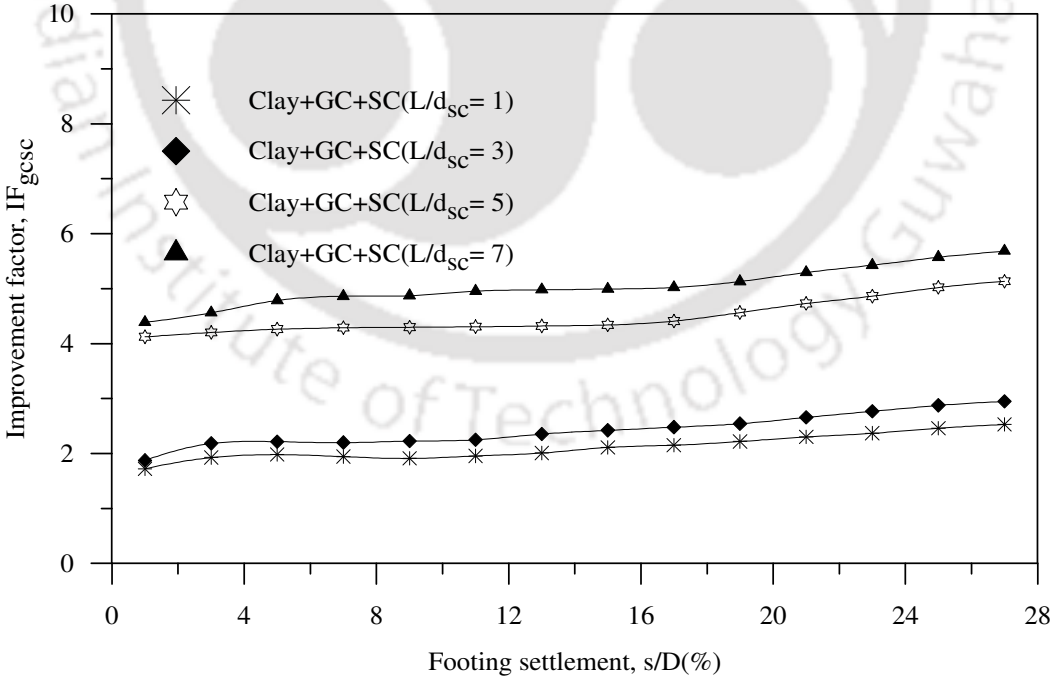

Fig.6.4: Variation of improvement factor with footing settlement in composite foundation bed for different lengths of stone columns (h/D = 0.53, S/d_{sc} = 2.5) – Test series 9

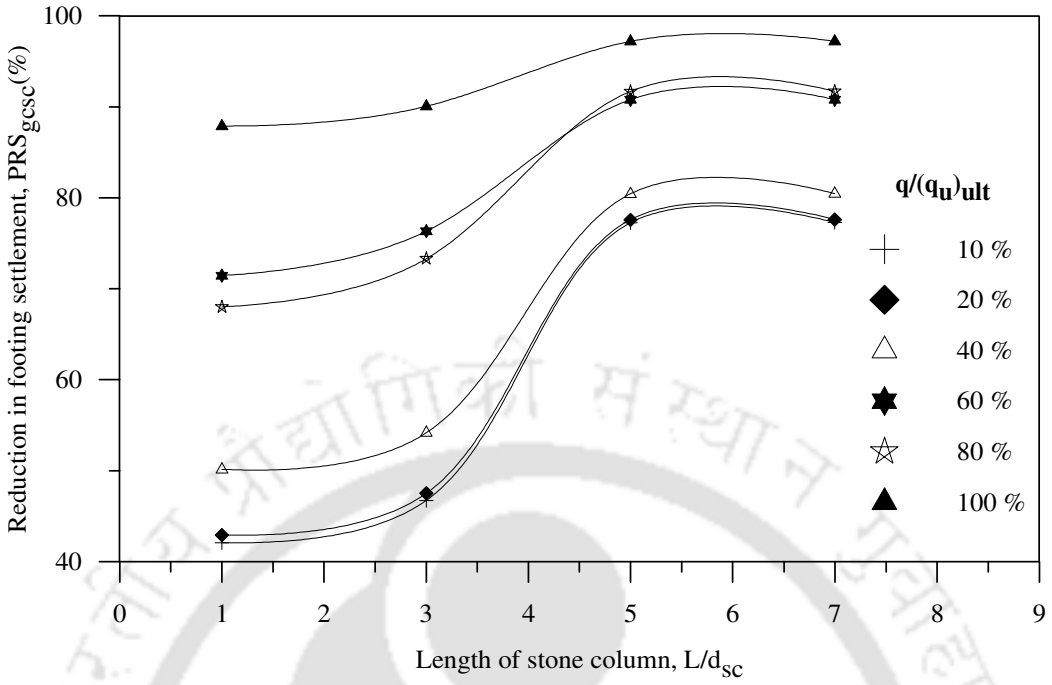

Fig.6.5: Variation of settlement reduction factor with length of stone column in composite foundation bed (h/D = 0.53, S/d_{sc} = 2.5) – Test series 9

Further increase in length of stone columns beyond the optimum, though increases the bearing capacity but this benefit remains unutilised due to excessive bulging of the stone columns, leading to marginal enhancement in performance improvement.

In order to decipher the contribution of individual reinforcement components (i.e. geocell sand mattress, stone columns) in the composite system, improvement factor ratios, IF_{gcsc}/IF_{gc} and IF_{gcsc}/IF_{sc}, have been made use of. Typical improvement factor ratios, IF_{gcsc}/IF_{gc} and IF_{gcsc}/IF_{sc}, for present case (h/D = 0.53) are depicted in Fig.6.6 and Fig. 6.7 respectively. The factor IF_{gcsc}/IF_{sc}, is the relative performance improvement due to the composite reinforcement, over the one with stone columns alone. This has been explained below,

$$\frac{IF_{g\,csc}}{IF_{sc}} = \frac{\frac{q_{g\,csc}}{q_u}}{\frac{q_{sc}}{q_u}} = \frac{q_{g\,csc}}{q_{sc}} \tag{6.3}$$

Thus, the factor (IF_{gcsc}/IF_{sc}) can be taken as the contribution of geocell mattress in sharing the surcharge loading applied onto the stone column-geocell reinforced foundation system. Similarly, the factor IF_{gcsc}/IF_{gc} (i.e.q_{gcsc}/q_{gc}) is the contribution of stone columns in the composite foundation system.

From Fig. 6.6, it could be observed that in case of L/d_{sc} of 5 and 7, the improvement factor ratios (IF_{gcsc}/IF_{gc}), initially, are of high magnitude. But it reduces sharply with settlement till (s/D) of about 3%, beyond which the rate of reduction is relatively gradual. The high value of IF_{gcsc}/IF_{gc} is attributed to the initial stiffened response of the compact granular columns. However, with increased settlement the stone columns undergo bulging giving rise to reduced compactness and hence the softened response. In case of stone columns with relatively small length (L/d_{sc}=1 and 3) such a stiffened response was not noticed. This is because; the short columns due to less end bearing and skin frictional resistance get punched down under the footing loading. In contrast, the long columns owing to large end bearing and skin friction resistance stand against the footing penetration giving rise to the stiff response of the foundation system. It can further be observed that the performance improvement due to the stone columns (IF_{gcsc}/IF_{gc}) increases with increase in length of stone columns and the increase is maximum for L/d_{sc} increasing from 3 to 5. This is typical of the stone column response as discussed in chapter 4 (section 4.3.1). This observation indicates that the stone column behaviour manifests well in the composite foundation bed with shallow height of geocell mattress (h = 0.53D).

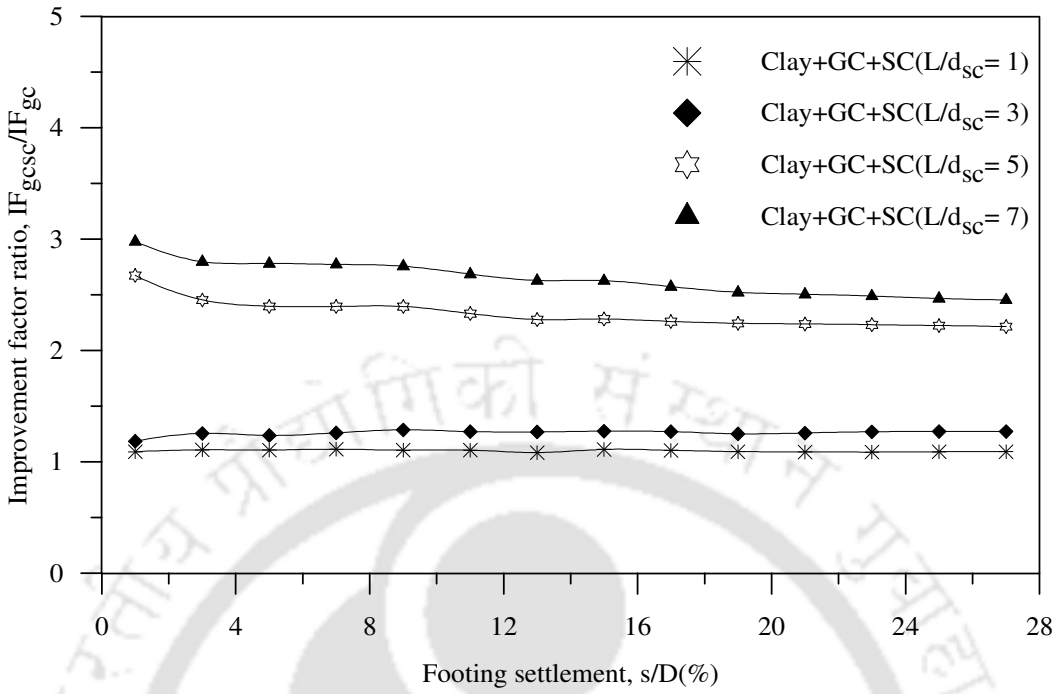

Fig.6.6: Improvement factor ratio vs. footing settlement, contribution of stone columns in composite foundation bed (h/D = 0.53, S/d_{sc} = 2.5) – Test series 9

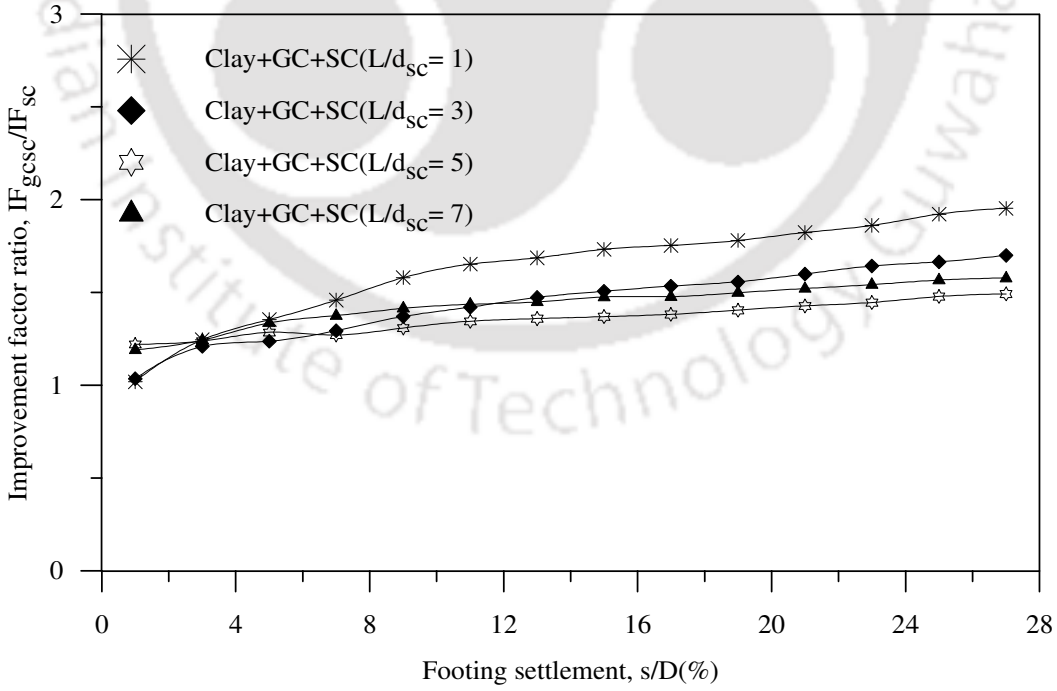

Fig.6.7: Improvement factor ratio vs. footing settlement, contribution of geocell mattress in composite foundation bed (h/D = 0.53, S/d_{sc} = 2.5) - Test series 9

From Fig.6.7, it is observed that the contribution of geocell mattress in performance improvement of the composite system (IF_{gcsc}/IF_{sc}) is maximum for stone columns having short length ($L/d_{sc} = 1$). The contribution of geocell reinforcement reduces with increase in length of stone columns and becomes almost constant for $L/d_{sc} \geq 5$. This is because, with increased length of stone columns the resistance against footing penetration increases leading to reduced settlement of the clay subgrade. With reduced settlement in the supporting clay foundation, the geocell reinforcement is now subjected to less deformation leading to reduced mobilization of its strength and hence reduced performance improvement. At initial stages (i.e. $s/D < 4\%$), when the stone columns share substantial portion of the surcharge load, the contribution of geocells is least. This indicates that, at this stage, the performance improvement due to the geocell mattress is just through dispersion of footing pressure over a wider area, rather than active participation of the reinforcement. This is attributed to the limited end anchorage due to shallow height of geocell mattress that it gets pulled down under the footing loading.

The surface deformation (δ) profiles, at different settlement levels of the footing, for stone column lengths (L/d_{sc}) of 1, 3, 5 and 7 are depicted in Figs. 6.8, 6.9, 6.10 and 6.11 respectively. It could be observed that with stone columns having short length ($L/d_{sc} = 1$), the foundation bed, under the loaded region has undergone sagging form of deformation and in the region outside has undergone hogging type deformation. With the geocell mattress pressing down, the clay mass, underneath, moves in the sidewise outward direction giving rise to heaving. As the geocell reinforcement through anchorage from soil tends to prevent this heaving, it undergoes the hogging form of bending and so is the observed surface deformation. With increased length of stone

columns the heaving of clay gets reduced leading to reduced hogging deformation in the geocell mattress (Fig. 6.8 - 6.11).

Fig. 6.12 shows that the settlement (s) on fill surface, at x = D, reduces with increased length of stone columns. This is attributed to the stiffening effect of the clay subgrade, brought about by the stone columns, that increases with increase in the length of stone columns. This in turn reduces the heaving of the foundation bed (Fig. 6.13 and 6.14). Little anomalies noticed in the initial stages could be due to some local effects.

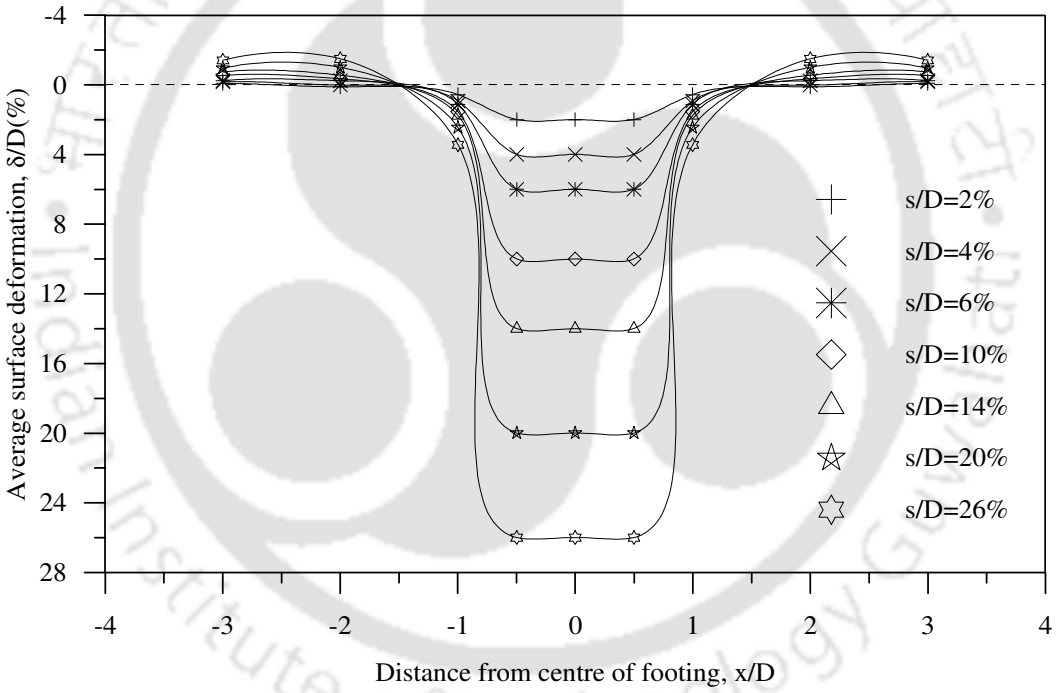

Fig. 6.8: Surface deformation profile, composite foundation bed

(h/D = 0.53, L/d_{sc} = 1, S/d_{sc} = 2.5) –Test series 9

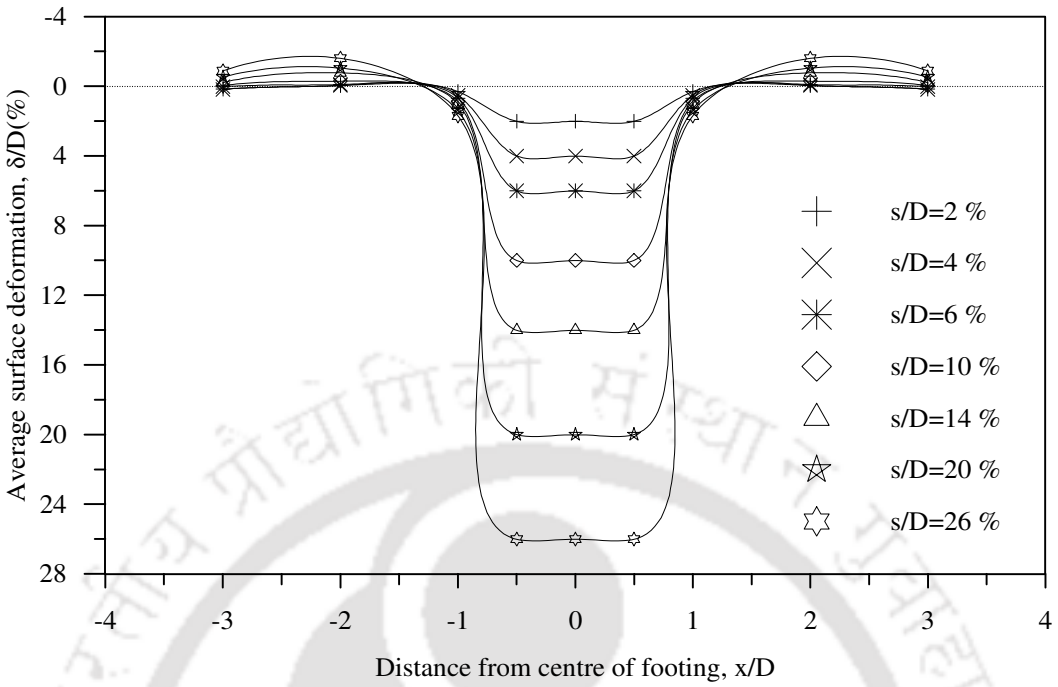

Fig.6.9: Surface deformation profile, composite foundation bed

(h/D = 0.53, L/d_{sc} = 3, S/d_{sc} = 2.5) – Test Series 9

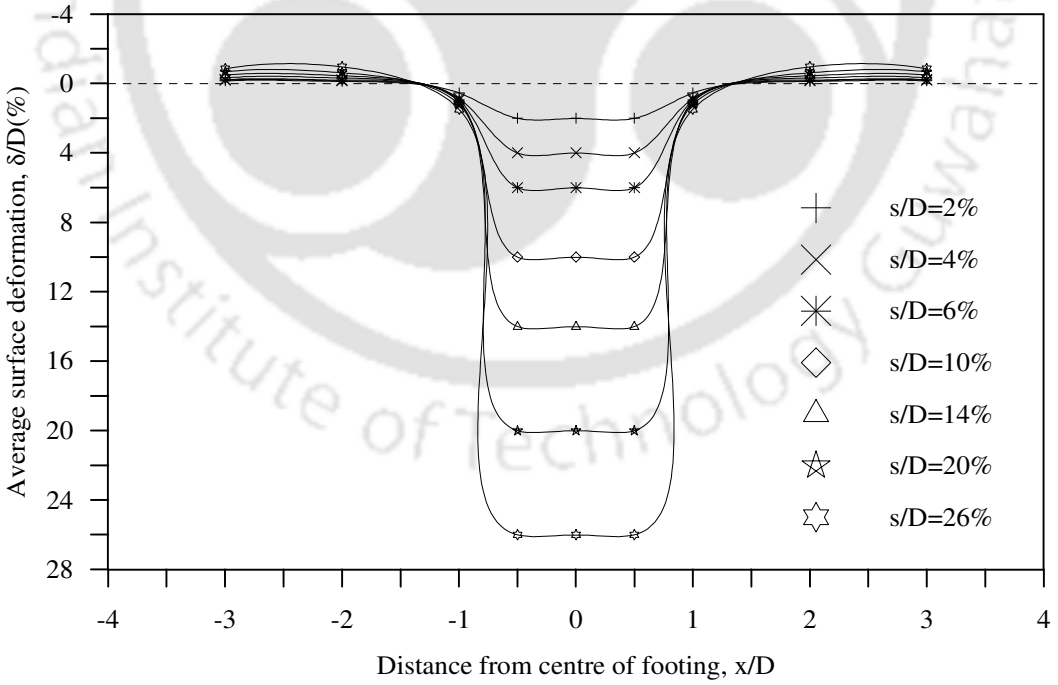

Fig.6.10: Surface deformation profile, composite foundation bed

(h/D = 0.53, L/d_{sc} = 5, S/d_{sc} = 2.5) – Test series 9

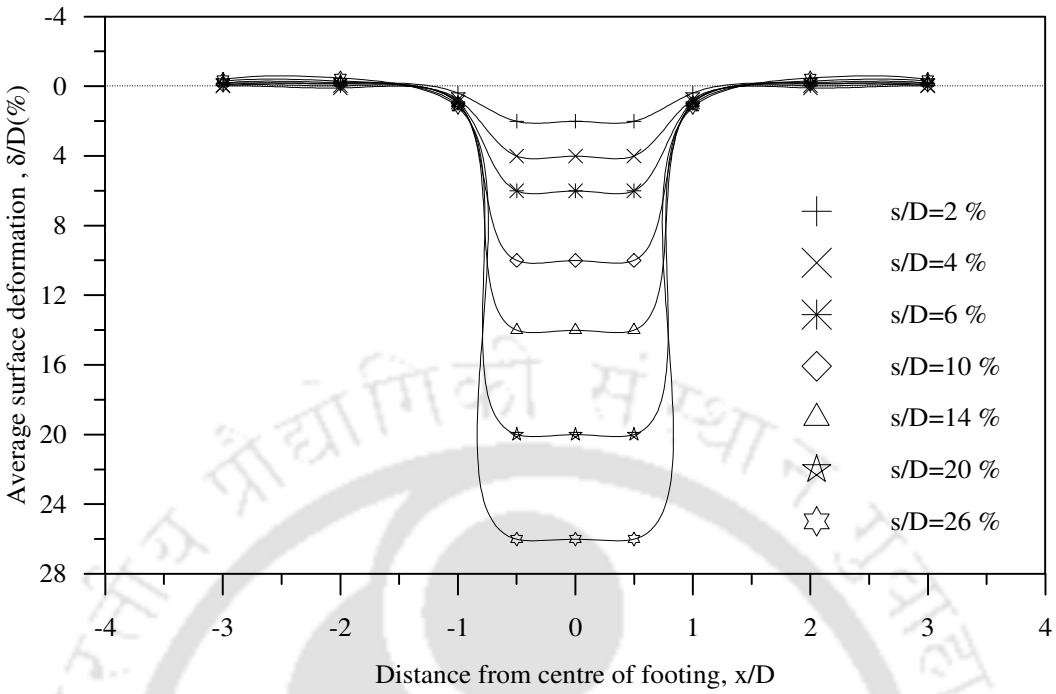

Fig.6.11: Surface deformation profile, composite foundation bed ($h/D = 0.53$, $L/d_{sc} = 7$, $S/d_{sc} = 2.5$) – Test Series 9

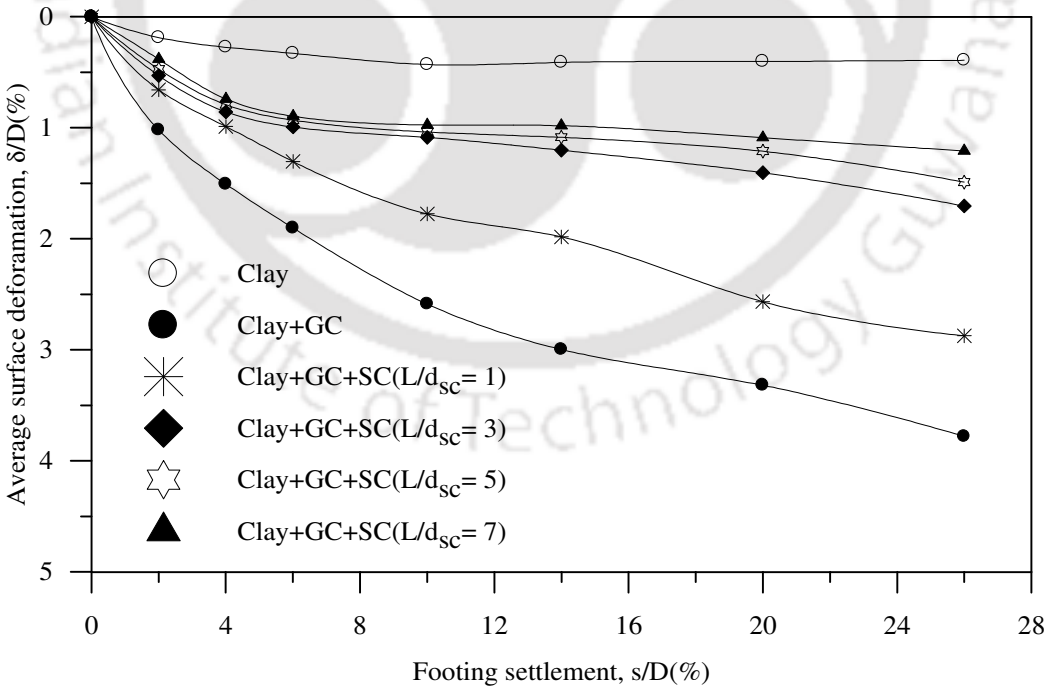

Fig.6.12: Variation of surface deformation, at x = D, with footing settlement in composite foundation bed ($h/D = 0.53$, $S/d_{sc} = 2.5$) – Test series 9

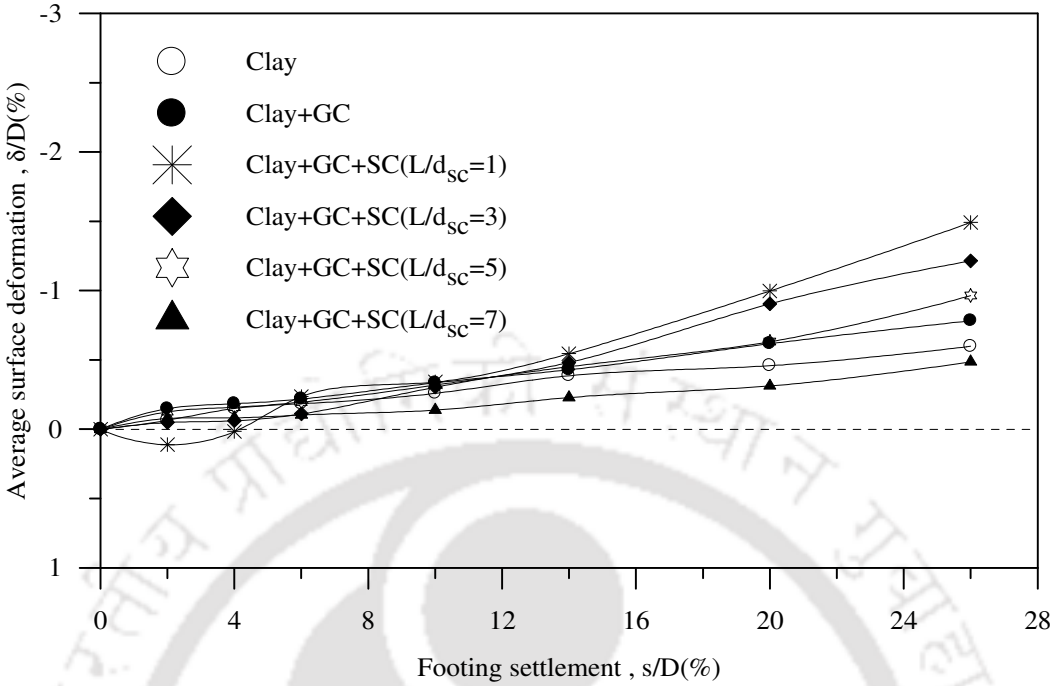

Fig.6.13: Variation of surface deformation, at x = 2D, with footing settlement, in composite foundation bed (h/D = 0.53, S/d_{sc} = 2.5) - Test series 9

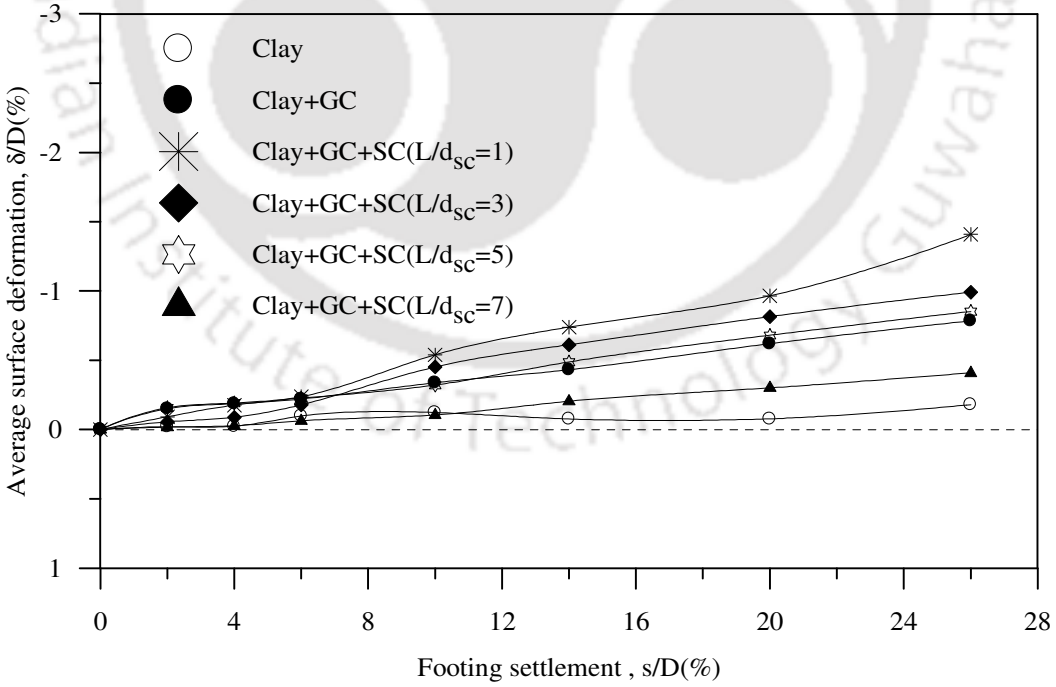

Fig.6.14: Variation of surface deformation, at x = 3D, with footing settlement, in composite foundation bed (h/D = 0.53, S/d_{sc} = 2.5) - Test series 9

The post test exhumed bulged shape of a typical central stone column is shown in Fig. 6.15. The radial strains in the central stone columns are depicted in Fig. 6.16. It could be observed that bulging increases with increase in length of stone columns. As the stone column bulges more, its cross sectional area increases that it can sustain increased loading. This testifies the earlier observation that the load carrying capacity of the foundation bed increases with increase in the length of stone columns (Fig. 6.3). It is of interest to note that maximum bulging has taken place at top of stone columns. Contrary to this, when the stone column was placed directly below the footing, maximum bulging took place at some depth below the top of the column (Fig. 4.13, 4.14, 4.22, 4.23). When placed directly below the footing, the friction on footing base restrains the stones to deform laterally. As this friction effect dies down with depth, maximum bulging takes place at some depth below the footing base. While in the present case the stone column being under the flexible geocell mattress, is free from such constraint and the bulging is proportional to the intensity of stress. As the stress intensity is maximum at top, so is the bulging.

Fig.6.15: Post-test deformed shape of a typical central stone column in composite foundation bed (L/d_{sc} = 5, h/D = 0.53, S/d_{sc} = 2.5) – Test series 9

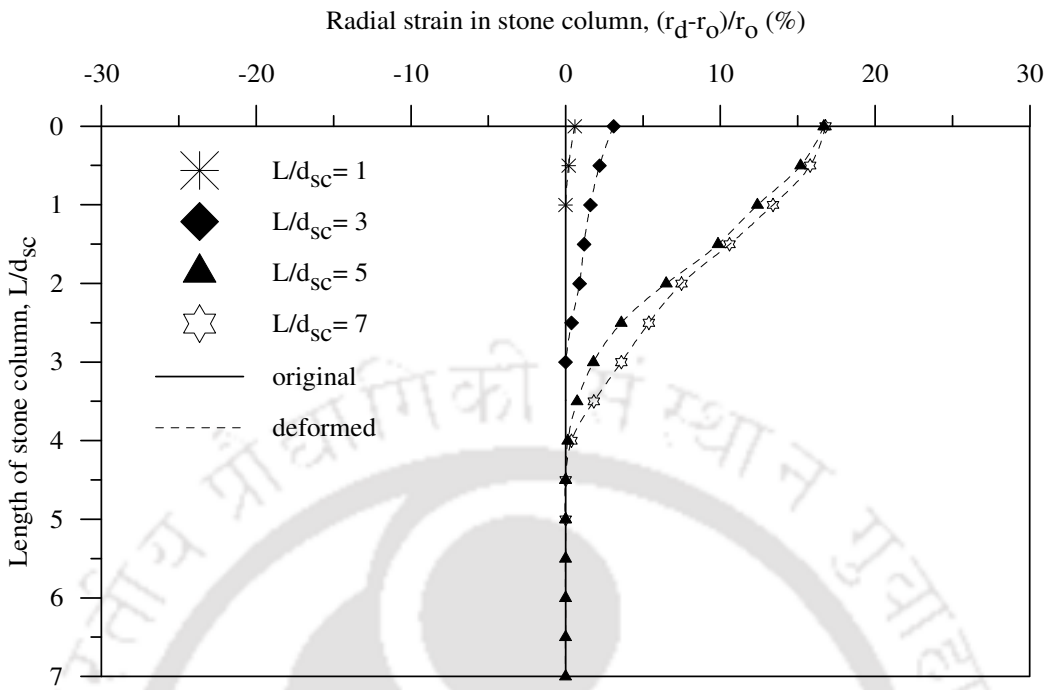

Fig.6.16: Radial strain in central stone column in composite foundation beds (h/D = 0.53, S/d_{sc} = 2.5) - Test series 9

6.2.2 Height of geocell mattress (h/D) of 0.9

Bearing pressure versus footing settlement responses for the composite foundation beds with geocell mattress of height equal to 0.9D and stone columns of varied lengths (i.e. L/d_{sc} = 1, 3 , 5, 7) are presented in Fig. 6.17. It could be observed that while with geocell reinforcement, the clay foundation can sustain bearing pressure of about 75 kPa, with the provision of stone columns in the clay bed (L/d_{sc} = 7) it has gone up to 140kPa. Fig 6.18 shows that with the provision of both geocell mattress (h = 0.9D) and stone columns (L = $7d_{sc}$), more than 6 fold increase in bearing capacity can be obtained (i.e. $IF_{gcsc} > 6$). Similar to the previous case (i.e. h = 0.53D), here too, there is a quantum jump in bearing capacity for length of stone column increasing from $3d_{sc}$ to $5d_{sc}$; beyond which further improvement is marginal (Fig. 6.18). The settlement reduction factor increases with increase in length of stone columns (Fig. 6.19) till

about $5d_{sc,}$ beyond which it remains nearly unchanged. Hence it can be said that, even with geocell mattress of moderate height (h = 0.9D), the influence of the stone columns on the behaviour of the composite foundation bed is still prominent and the optimum length of stone column is the same i.e. 5 times its diameter. From Figs. 6.20 and Fig. 6.21, it could be observed that as the contribution of stone columns (IF_{gcsc}/IF_{gc}) increases with increase in length of stone columns, correspondingly the contribution of geocells (IF_{gcsc}/IF_{sc}) reduces. However, the contribution of stone columns in the performance improvement is relatively less as compared to that with geocell mattress of height 0.53D. This can better be explained with the help of the surface deformation responses and deformations in stone columns.

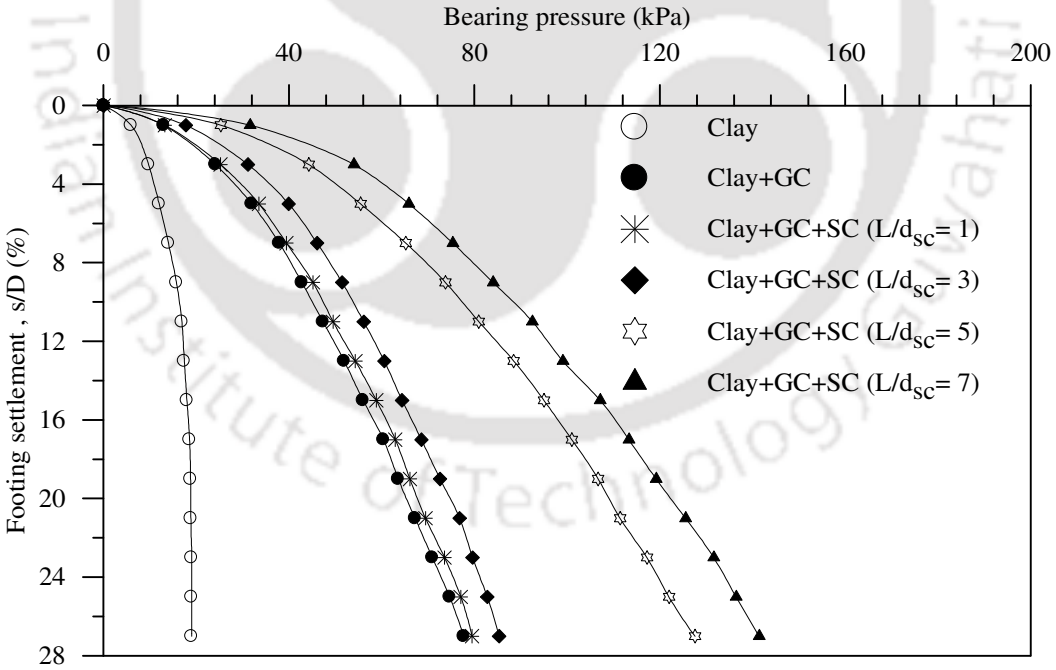

Fig.6.17: Variation of bearing pressure with footing settlement in composite foundation bed (h/D = 0.9, S/d_{sc} = 2.5) - Test series 10

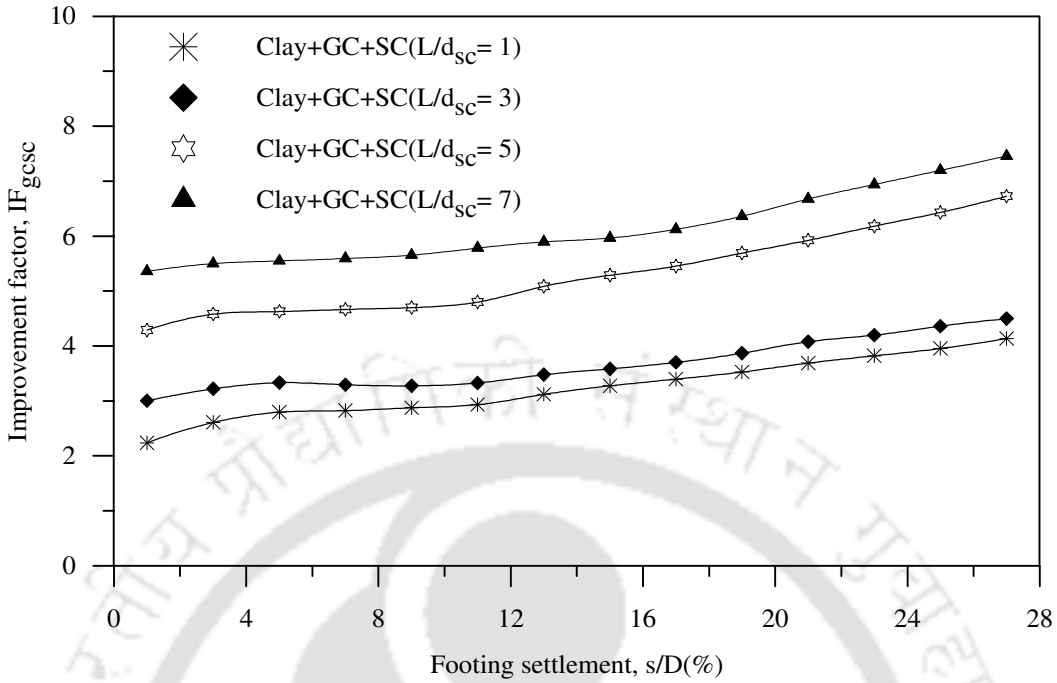

Fig.6.18: Variation of improvement factor with footing settlement in composite foundation (h/D = 0.9, S/d_{sc} = 2.5) – Test series 10

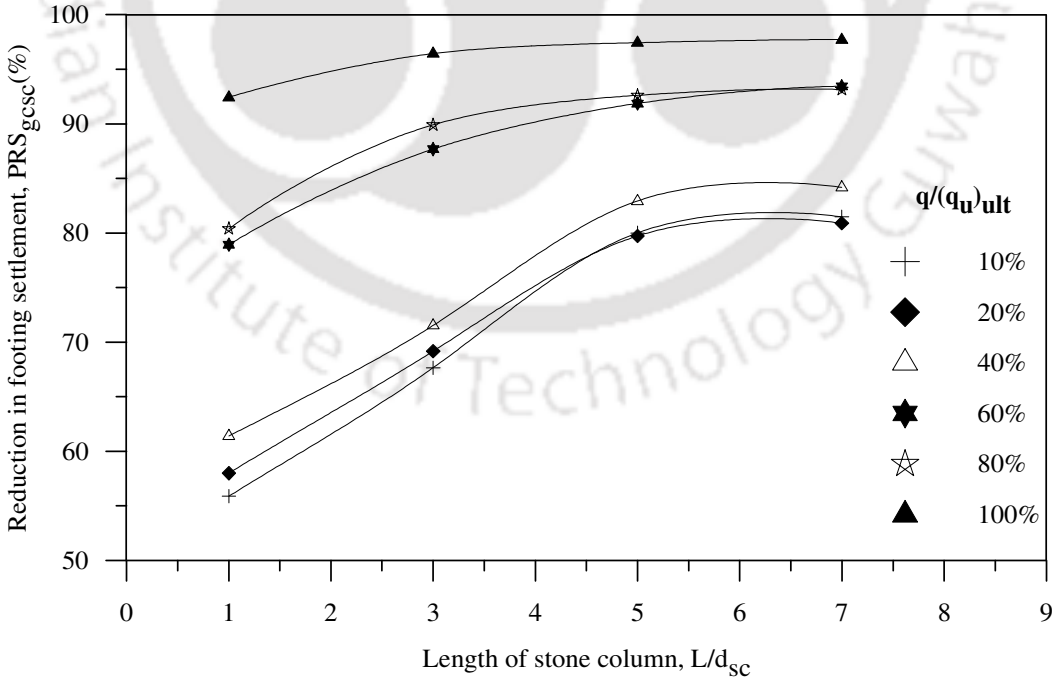

Fig.6.19: Variation of settlement reduction factor with length of stone column in composite foundation bed (h/D = 0.9, S/d_{sc} = 2.5) – Test series 10

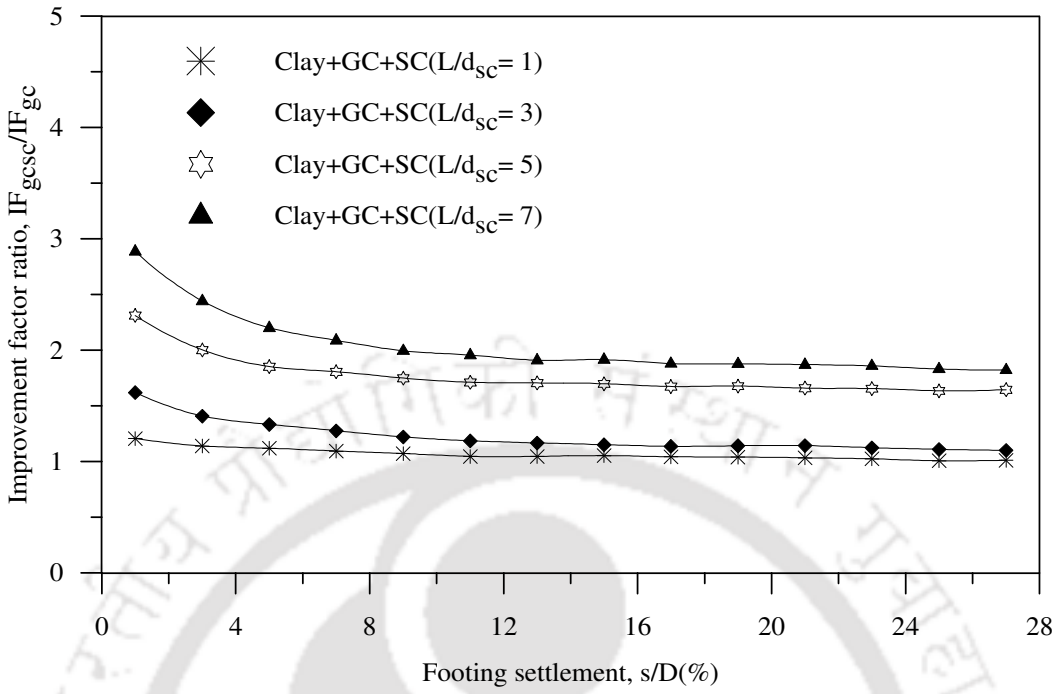

Fig.6.20: Improvement factor ration vs. footing settlement, showing the contribution of stone columns in composite foundation bed (h/D = 0.9, S/d_{sc} = 2.5) – Test series 10

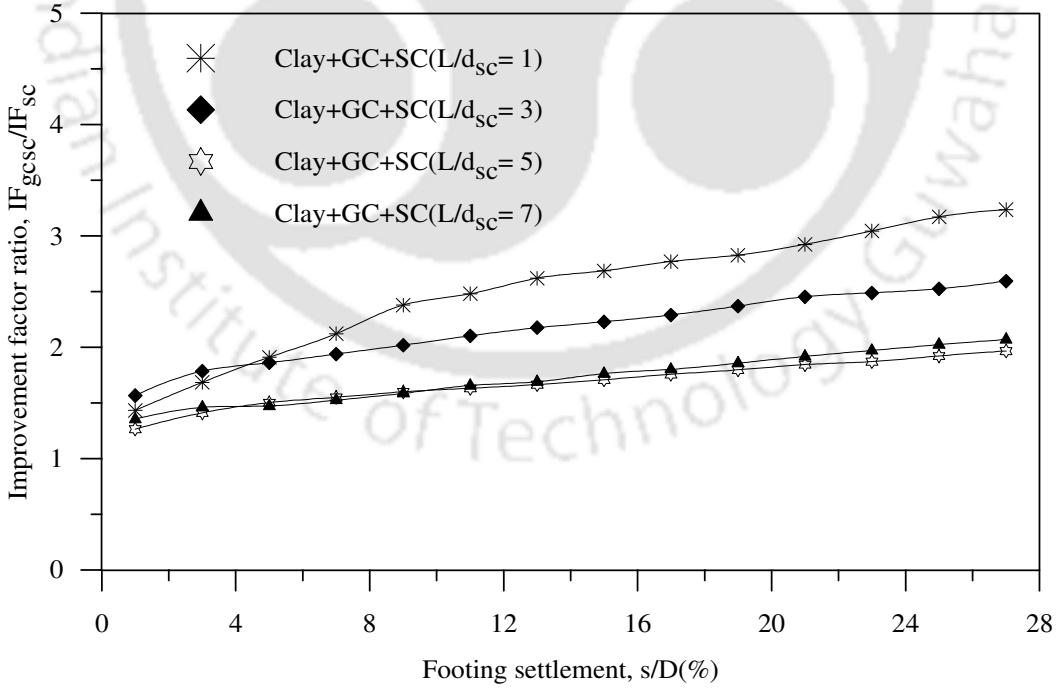

Fig.6.21: Improvement factor ratio vs. footing settlement, contribution of geocell mattress in composite foundation bed (h/D = 0.9, S/d_{sc} = 2.5) – Test series 10

The responses depicted in Figs. 6.22, 6.23 and 6.24 indicate that the surface settlement (at x = D) and heave (at x = 2D and 3D), for different lengths of stone columns fall in a relatively narrow band, indicating that the stone columns have relatively less influence on surface deformation responses. This is attributed to relatively larger depth of placement of stone columns from the footing base, as the geocell mattress is of higher height (h = 0.9D). Indeed, the maximum radial deformation in the stone columns (depicted in Fig. 6.25 and 6.26) is about 12% which is less than that with geocell mattress of shallow height (h = 0.53D), wherein, the maximum radial deformation was about 16% (Fig. 6.15 and Fig.6.16). This indicates that the mobilized strength of stone columns in the present case is relatively less leading to lower performance improvement. This is in agreement with the observation that the contribution of stone columns in the performance improvement (IF_{gcsc}/IF_{gc}) is relatively less when placed under geocell mattress of larger height (Fig.6.6 vs. Fig.6.20).

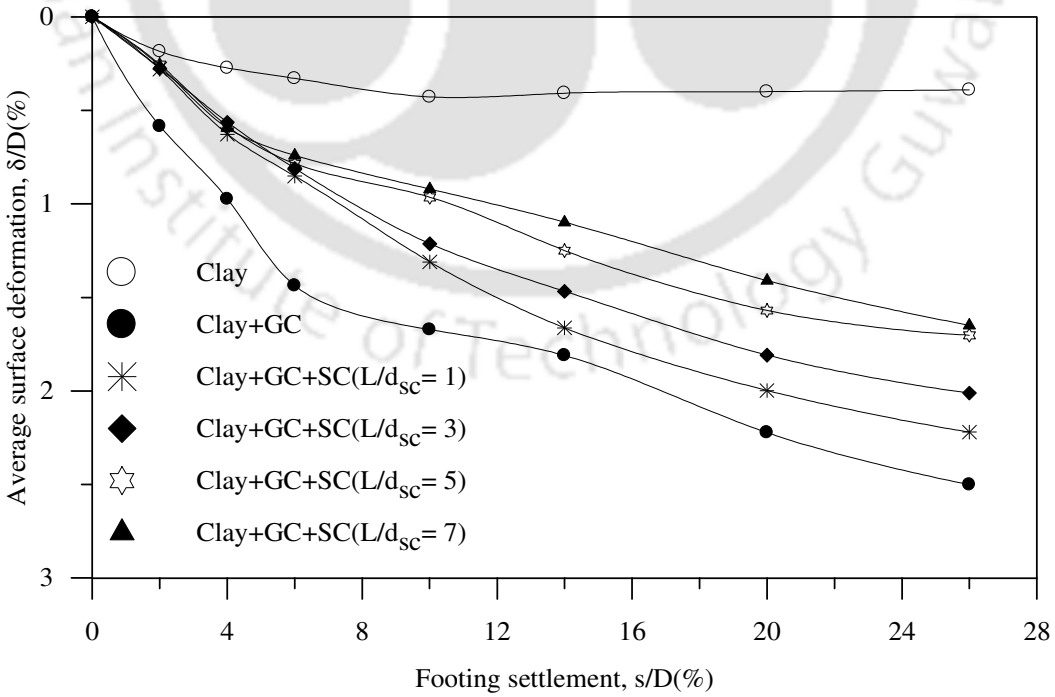

Fig.6.22: Variation of surface deformation, at x = D, with footing settlement in composite foundation bed (h/D = 0.9, S/d_{sc} = 2.5) – Test series 10

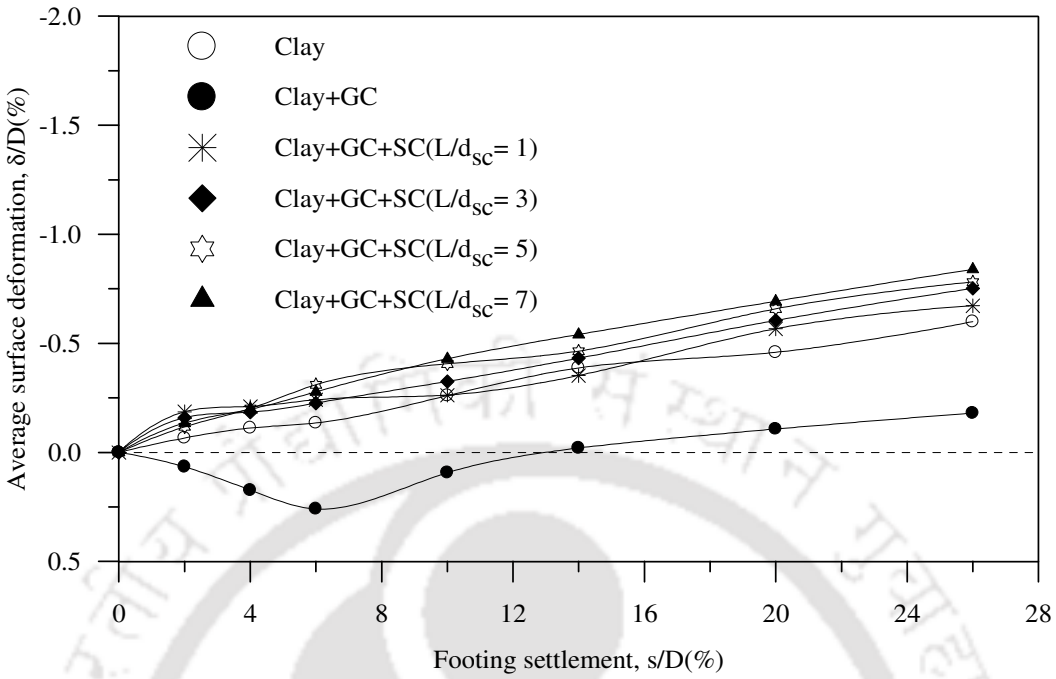

Fig.6.23: Variation of surface deformation, at x = 2D, with footing settlement in composite foundation bed (h/D = 0.9, S/d_{sc} = 2.5) – Test series 10

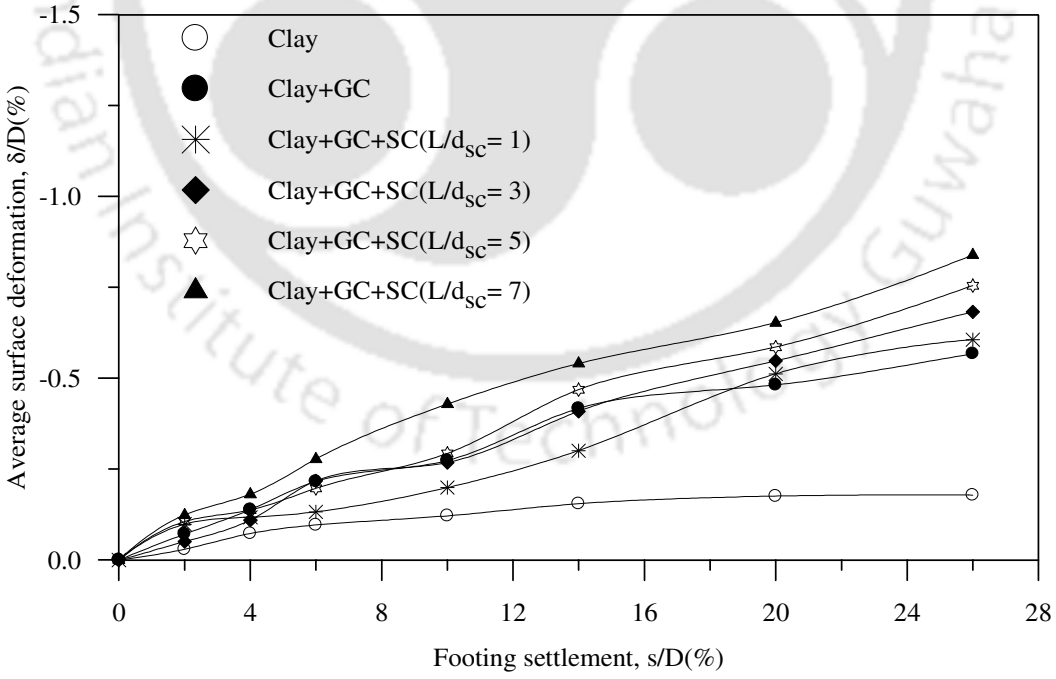

Fig.6.24: Variation of surface deformation, at x = 3D, with footing settlement in composite foundation bed (h/D = 0.9, S/d_{sc} = 2.5) – Test series 10

Fig.6.25: Post-test deformed shape of a typical central stone column in composite foundation bed (L/d_{sc} = 5, h/D = 0.9, S/d_{sc} = 2.5) – Test series 10

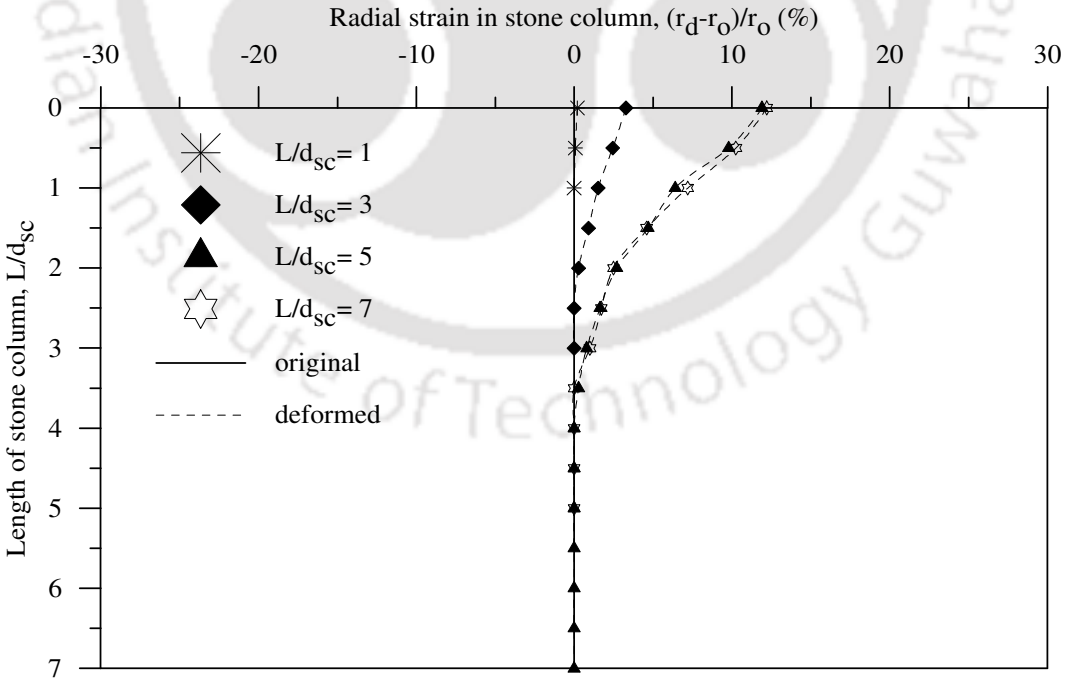

Fig.6.26: Radial strain in central stone columns in composite foundation bed (h/D = 0.9, S/d_{sc} = 2.5) - Test series 10

6.2.3 Height of geocell mattress (h/D) of 1.1

The bearing pressure-settlement responses of the footing on composite foundation bed with geocell mattress having height (h) of 1.1D and varied lengths of stone columns are depicted in Fig. 6.27. It could be observed that the increase in bearing capacity due to the stone columns is relatively less prominent. This is because the stone columns being placed at higher depth (h = 1.1D) are subjected to lower stress and deformation due to footing loading. This in turn mobilises lower strength and stiffness in the stone columns leading to lower performance improvement.

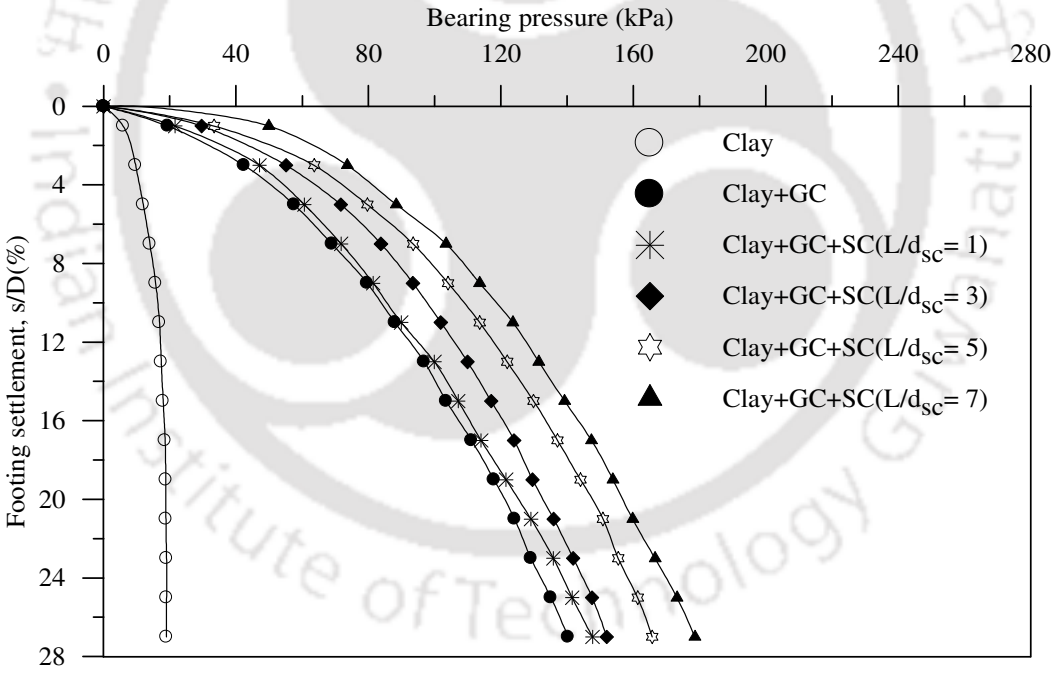

Fig.6.27: Variation of bearing pressure with footing settlement in composite foundation bed (h/D = 1.1, S/d_{sc} = 2.5) - Test series 11

The quantification of this performance improvement, due to the geocell-stone column reinforcement, is presented in Fig. 6.28. It could be observed that the composite

reinforcement, with h/D = 1.1 and L/d_{sc} = 7, can increase the bearing capacity as high as 9.8 times that of the unreinforced case (IF_{gcsc} = 9.8), while the settlement reduction is as high as 100% (Fig. 6.29). With increase in footing penetration the geocell mattress which now has higher height and therefore higher resistance against bending, bridges over the stone columns and hence carries most of the footing loading by itself. As the footing settles, the geocell reinforcement is subjected to increased deformation that it mobilises higher bending, shear and anchorage resistance. This enables it to carry increased proportion of the surcharge loading, relieving the stone columns lying underneath. Indeed, the contribution of stone columns, IF_{gcsc}/IF_{gc}, continues to reduce (Fig. 6.30), with increase in footing settlement, while that of geocell reinforcement, continues to increase (IF_{gcsc}/IF_{sc}, Fig. 6.31).

The contribution of stone columns continues to reduce sharply till footing settlement (s/D) equal to about 5%, beyond which the reduction rate is relatively less (Fig. 6.30). However, the contribution of geocell reinforcement is found to have increased steadily till large settlement (Fig. 6.31). This is because the geocell reinforcement being made of polypropylene geogrid needs relatively large amount of deformations for substantial part of its strength to get mobilized. Therefore, in the initial stages its contribution is less that it just transmits the footing pressure down onto the clay subgrade. Therefore, at this stage, the stone columns share major portion of the surcharge load. However, with increased deformation, the geocell mobilizes sufficient of its strength, as well as anchorage from soil, to stand against the footing that the pressure onto the stone columns reduces significantly. Therefore, the stone columns have contributed marginally towards the performance improvement of the composite foundation bed, indicated through low value of IF_{gcsc}/IF_{gc} (Fig.6.30).

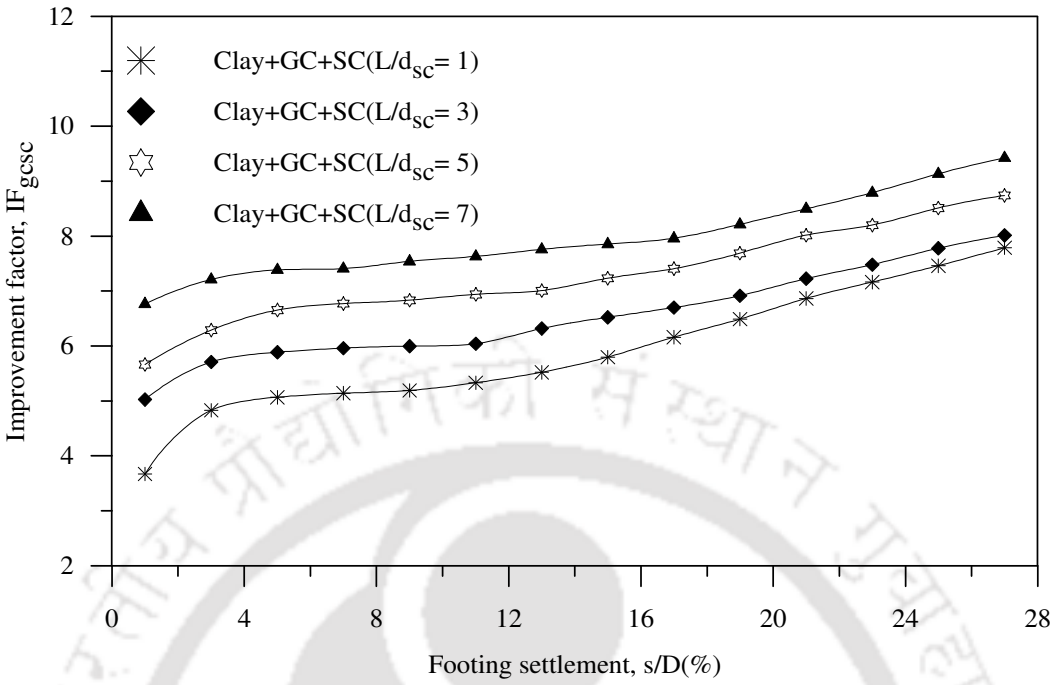

Fig.6.28: Improvement factor vs. footing settlement in composite foundation bed for different length of stone columns (h/D = 1.1, S/d_{sc} = 2.5) – Test series 11

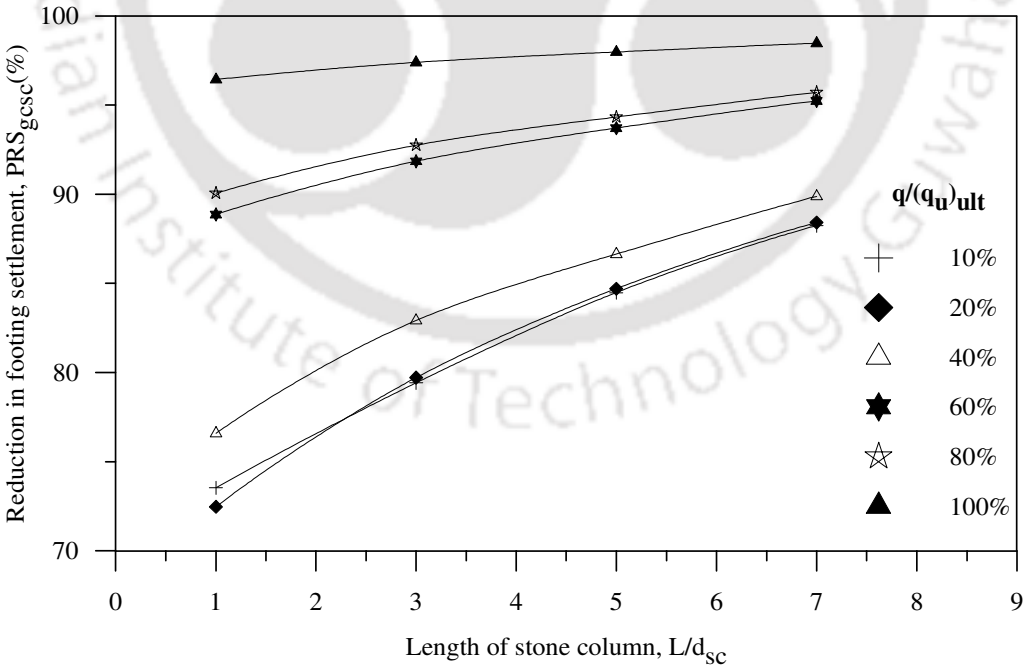

Fig.6.29: Variation of settlement reduction factor with length of stone columns in composite foundation bed (h/D = 1.1, S/d_{sc} = 2.5) – Test series 11

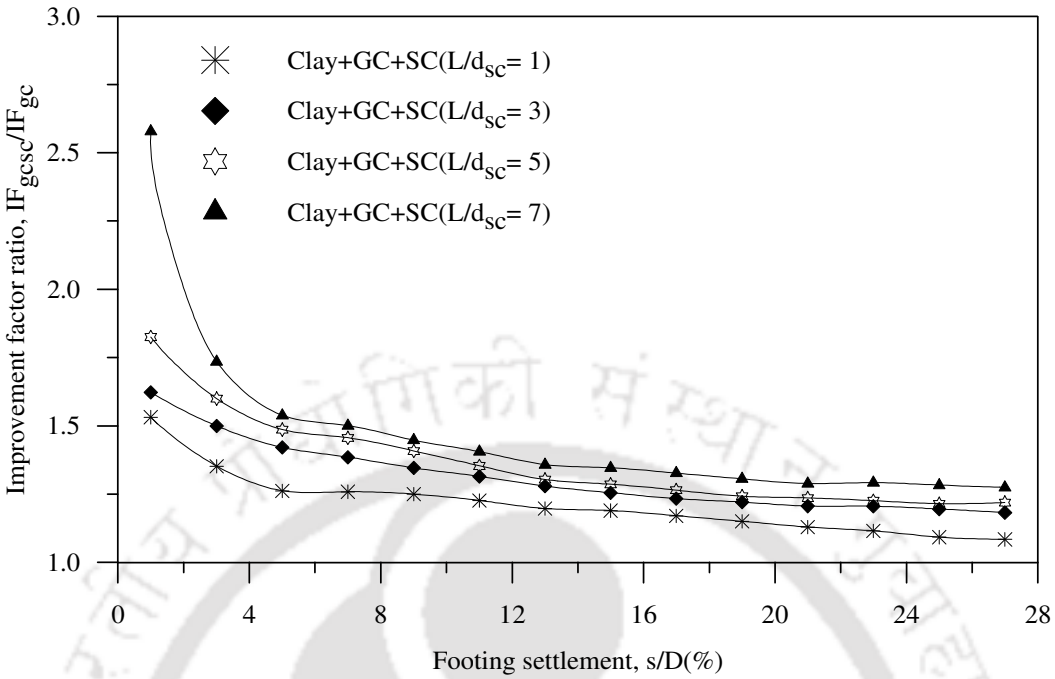

Fig.6.30: Improvement factor ratio vs. footing settlement, contribution of stone columns in composite foundation bed (h/D = 1.1, S/d_{sc} = 2.5) – Test series 11

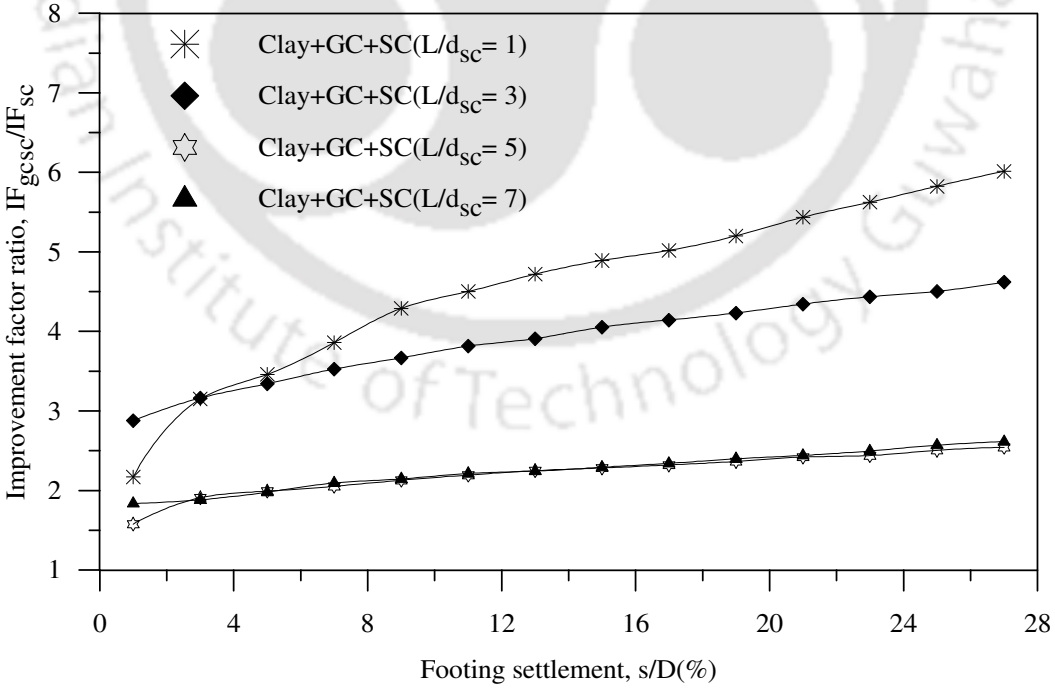

Fig.6.31: Improvement factor ratio vs. footing settlement, contribution of geocell mattress in composite foundation bed (h/D = 1.1, S/d_{sc} = 2.5) - Test series 11

The surface deformation responses in Fig. 6.32–Fig.6.34 show that, though the stone columns have reduced the surface settlement and heave but the responses with geocell-stone columns are close to that with geocell mattress alone. This indicates that the influence of stone columns in reducing settlement and heave on the composite foundation bed is relatively less.

Photograph of a typical post test exhumed stone column, from this series of tests, is shown in Fig. 6.35. The corresponding radial strains in the stone columns are presented in Fig. 6.36. It is of interest to note that the magnitude of this strain in the present case is relatively less than the earlier cases having comparatively smaller height of geocell mattress. This observation once again establishes that the mobilized strength of stone columns is less when height of geocell mattress provided above is more.

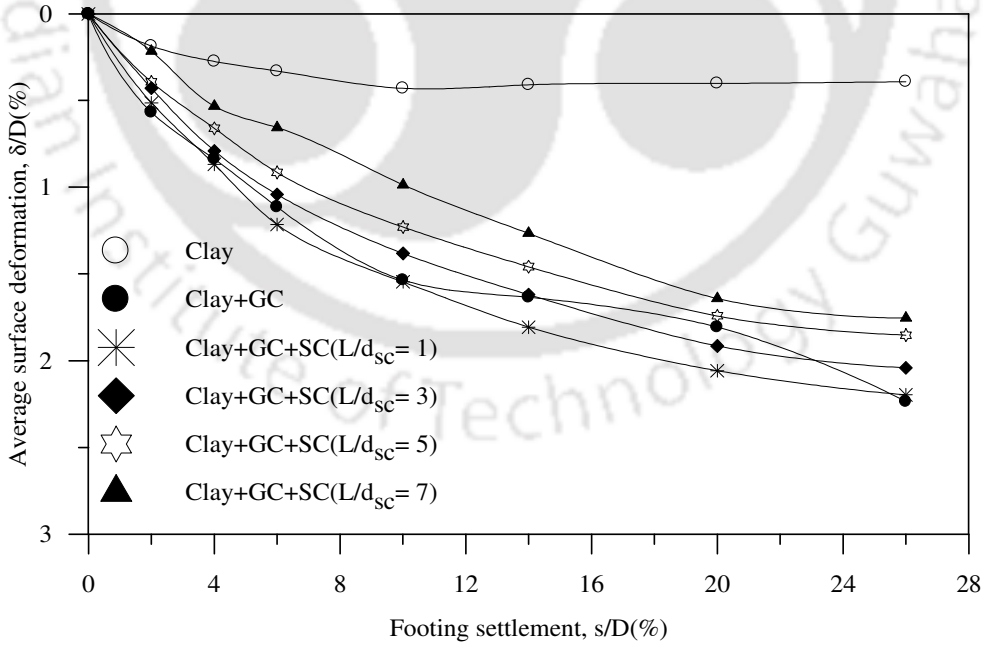

Fig.6.32: Variation of surface deformation, at x = D, with footing settlement in composite foundation bed (h/D = 1.1, S/d_{sc} = 2.5) – Test series 11

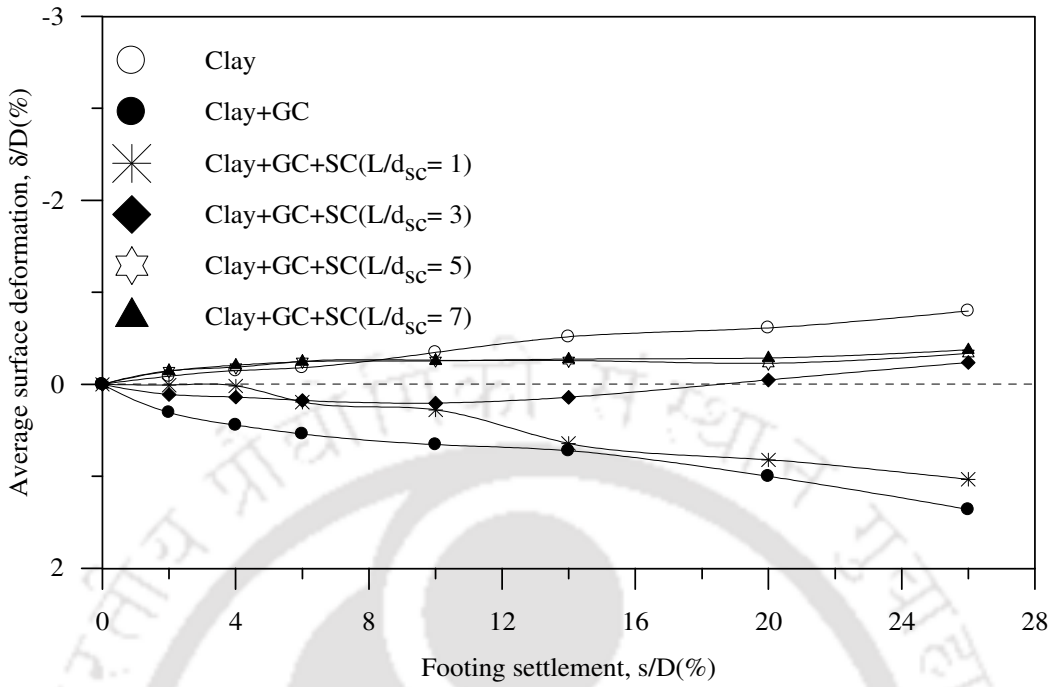

Fig.6.33: Variation of surface deformation, at x = 2D, with footing settlement in composite foundation bed (h/D = 1.1, S/d_{sc} = 2.5) – Test series 11

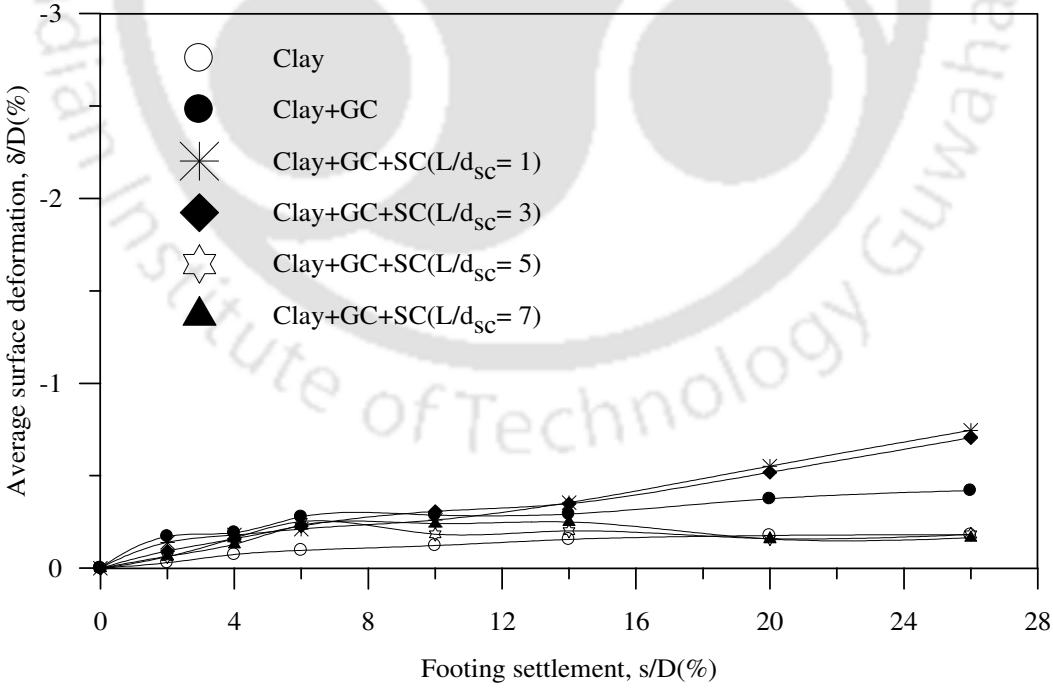

Fig.6.34: Variation of surface deformation, at x = 3D, with footing settlement in composite foundation bed (h/D = 1.1, S/d_{sc} = 2.5) – Test series 11

Fig.6.35: Post-test deformed shape of a typical central stone column in composite foundation bed (L/d_{sc} = 5, h/D = 1.1, S/d_{sc} = 2.5) – Test series 11

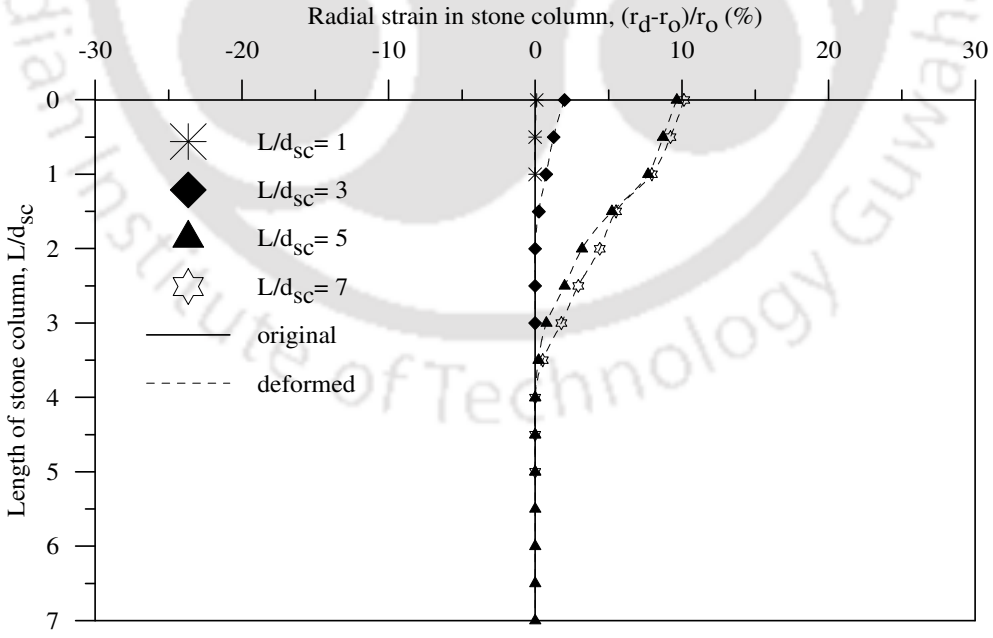

Fig.6.36: Radial strain in central stone column in composite foundation beds (h/D = 1.1, S/d_{sc} = 2.5) - Test series 11

6.2.4 Height of geocell mattress (h/D) of 1.6

The variation of bearing pressure with footing settlement for composite foundation bed with geocell mattress of height (h) equal to 1.6D is depicted in Fig. 6.37. It could be observed that with geocell mattress maximum bearing pressure achieved is about 150kPa while with stone column-geocell composite reinforcement it is about 170kPa. Fig. 6.38 shows that the maximum performance improvement due to the geocell-stone column reinforcement (h/D = 1.6, $L/d_{sc} = 7$) is about 10 times that of unreinforced case ($IF_{gcsc} = 10$). The maximum reduction in settlement at a pressure equal to the ultimate capacity of the unreinforced one is about 98% (Fig. 6.39).

Summarising along with the previous cases, it is observed that the maximum bearing capacity improvement due to the composite reinforcement system (IF_{gcsc}) with geocell mattress of height (h/D) = 0.53, 0.9, 1.1 and 1.6 is; 5.5, 7.5, 9.8 and 10 respectively. It could be observed that the increase in performance improvement with height of geocell mattress increasing beyond 1.1D is marginal. Hence it can be said that, height of geocell mattress equal to about the diameter of the footing is the optimum one giving maximum performance improvement in the composite foundation bed.

Fig. 6.40 shows that the improvement factor ratio, IF_{gcsc}/IF_{gc}, varies in the range of 1 to 1.2 indicating that the maximum contribution of stone columns in performance improvement is at the most 20% that of geocell mattress. Fig. 6.41 indeed shows such a response, wherein, the value of improvement factor ratio, IF_{gcsc}/IF_{sc}, is as high as 6 indicating that most of the footing pressure has been sustained by the geocell mattress. The geocell mattress being of large height (h = 1.6D) has high moment of inertia to stand against the footing penetration. Besides, with increase in height (h), the geocell area deriving anchorage from infill soil increases and so is the anchorage resistance. Therefore, the geocell mattress takes the footing loading on its own and hence major

portion of the stone columns lie dormant, leading to lower contribution to performance improvement.

The surface deformation responses are depicted in Figs. 6.42-6.44. It could be observed that, in general, the stone columns reduce settlement in and around the footing (x = D). But in the region away (x = 2D and 3D), the difference in the responses, with stone column length changing from shallow to deep, is relatively less. However, with increase in height of geocell mattress the heave on surface of the composite foundation beds, at x = 2D, gradually reduces and turns to be settlement for h = 1.6D (Fig.6.13 Vs. Fig. 6.43). Heave on fill surface is attributed to two factors; heaving of clay and lifting up of the geocell mattress. As with increased height, the geocell mattress suppresses the heaving in the underlying clay bed more effectively, apart from reducing its own lifting up at ends (owing to its increased rigidity); the overall heaving on fill surface is found to have reduced. Besides, the heaving on fill surface is found to have reduced with increase in length of stone columns (Fig.6.44). This is primarily due to the interception of slip surfaces in the clay bed by the relatively rigid stone columns leading to reduced heaving.

Fig. 6.45 and Fig. 6.46 show that the stone columns have undergone deformations of much lesser magnitude as compared to cases with lower height of geocell mattress (h/D = 0.53, Fig. 6.16; h/D = 0.9, Fig.6.26; h/D = 1.1, Fig. 6.36). With increased height the geocell mattress shares a relatively larger proportion of the surcharge loading and thereby the pressure transmitted unto the underlying stone columns reduces. This in turn reduces the mobilized strength in the stone columns. Hence, it can be said that the beneficial effect of stone columns, in the composite foundation system, remains under utilized for geocell mattress of very large height (h/D = 1.6).

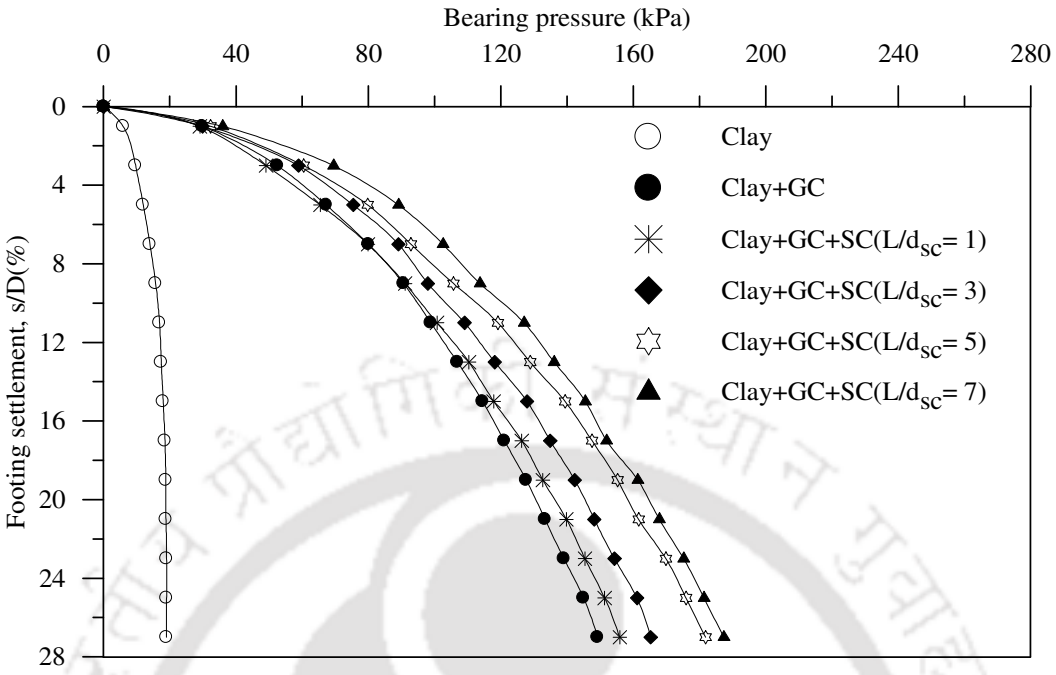

Fig.6.37: Variation of bearing pressure with footing settlement in composite foundation bed (h/D = 1.6, S/d$_{sc}$ = 2.5) - Test series 12

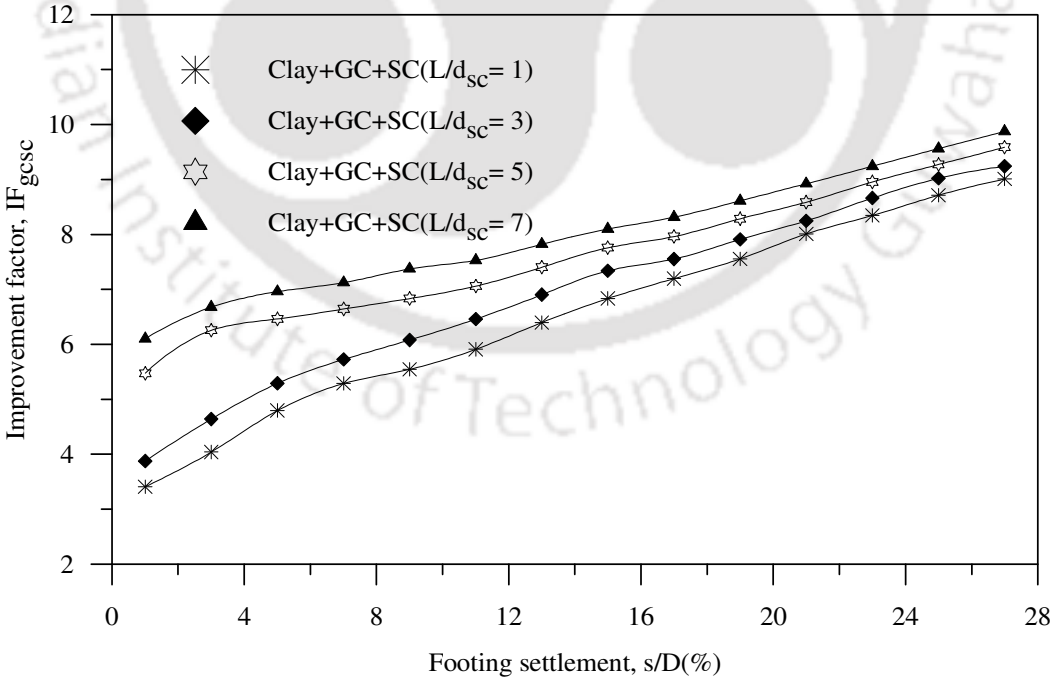

Fig.6.38: Variation of improvement factor with footing settlement in composite foundation bed (h/D = 1.6, S/d$_{sc}$ = 2.5) – Test series 12

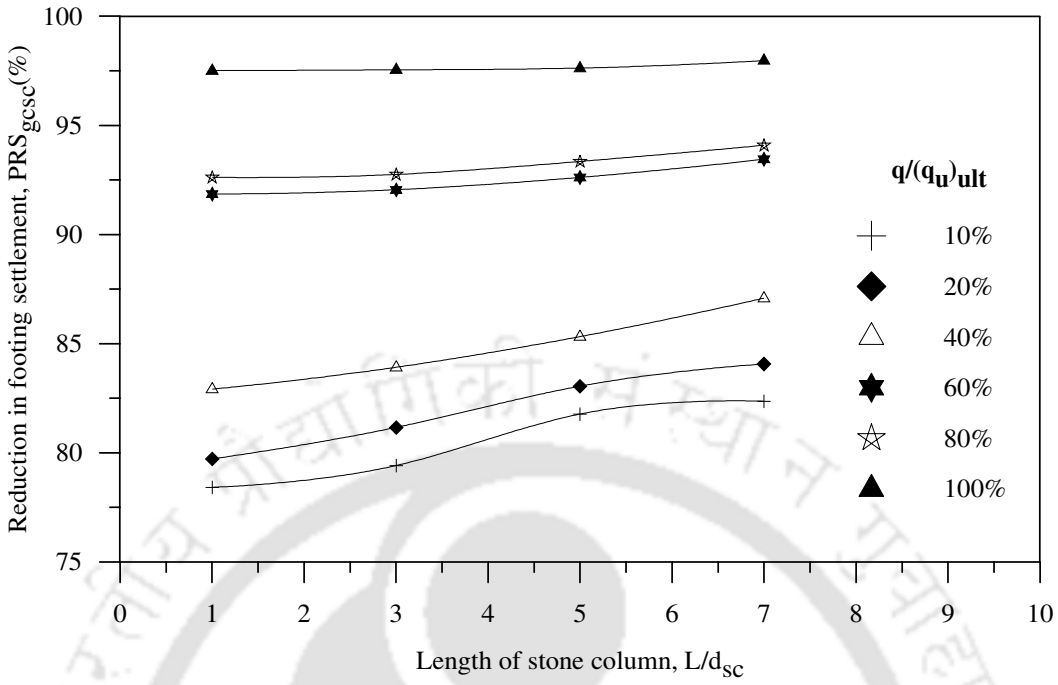

Fig.6.39: Variation of settlement reduction factor with length of stone columns, in composite foundation bed (h/D = 1.6, S/d_{sc} = 2.5) – Test series 12

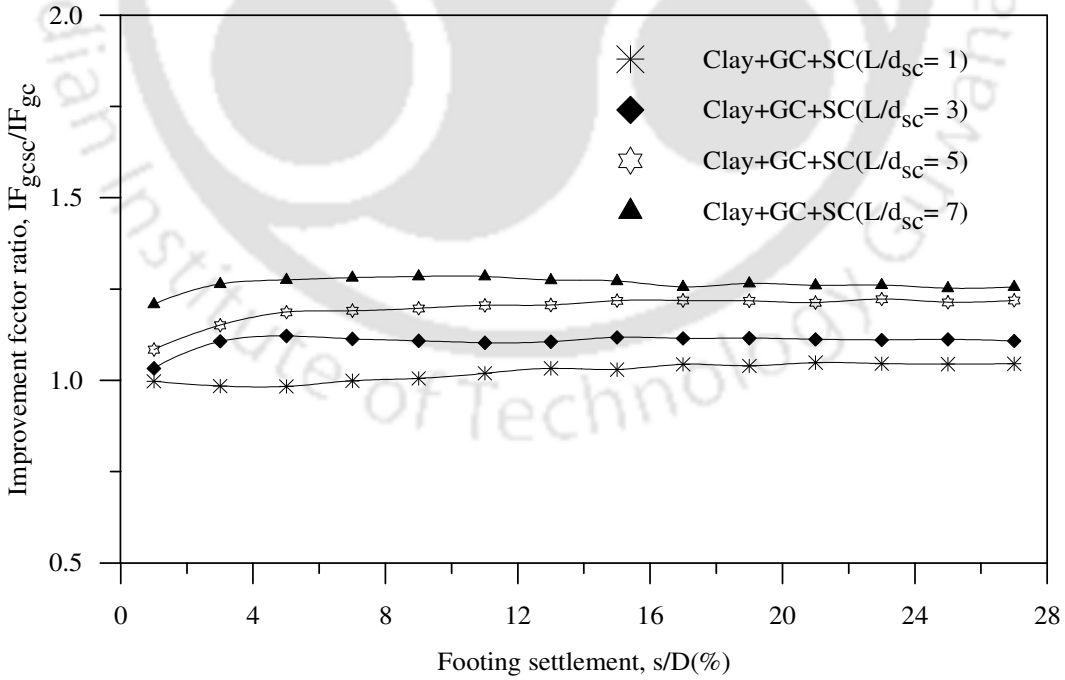

Fig.6.40: Improvement factor ratio vs. footing settlement, contribution of stone columns in composite foundation bed (h/D = 1.6, S/d_{sc} = 2.5) – Test series 12

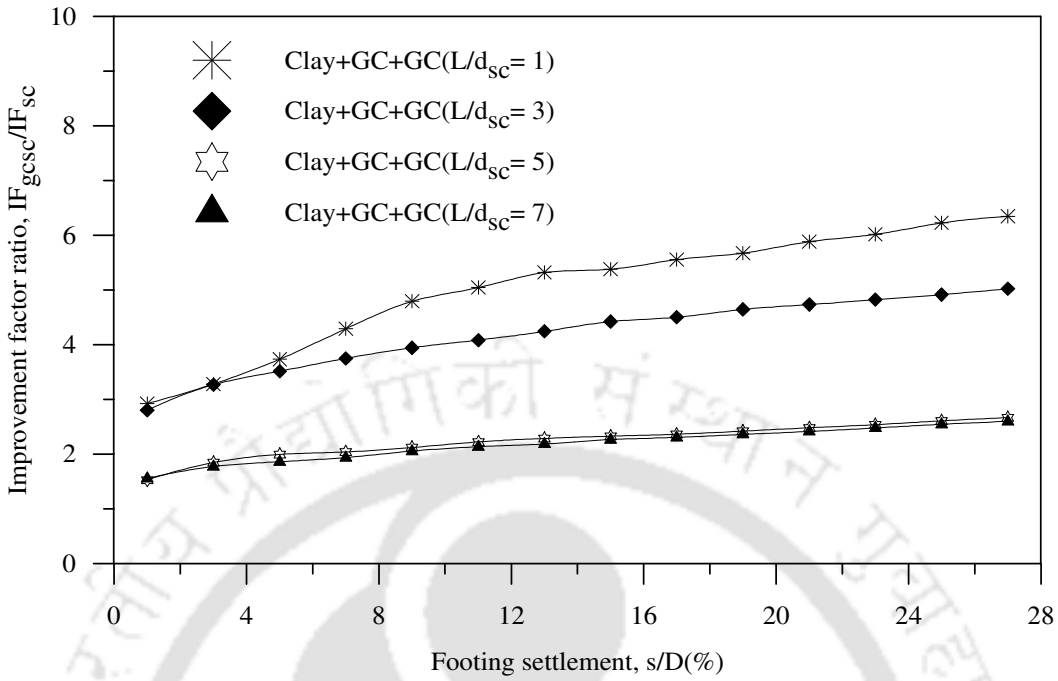

Fig.6.41: Improvement factor ratio vs. footing settlement, contribution of geocell mattress in composite foundation bed (h/D = 1.6, S/d_{sc} = 2.5) - Test series 12

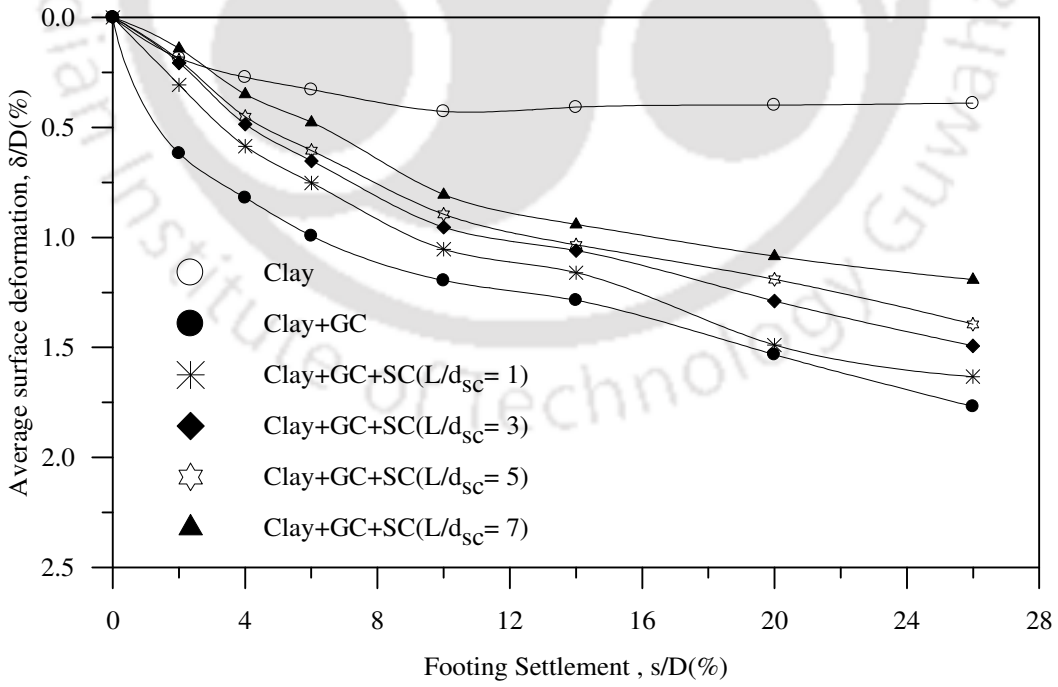

Fig.6.42: Variation of surface deformation, at x = D, with footing settlement in composite foundation bed (h/D = 1.60, S/d_{sc} = 2.5) – Test series 12

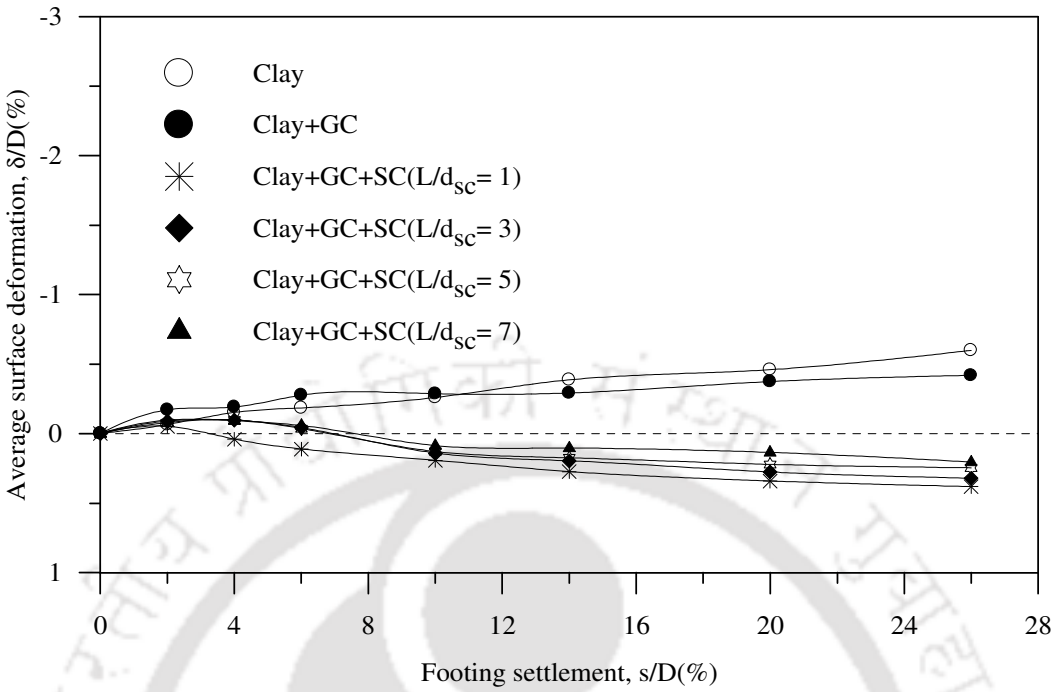

Fig.6.43: Variation of surface deformation at, x = 2D, with footing settlement in composite foundation bed (h/D = 1.6, S/d_{sc} = 2.5) – Test series 12

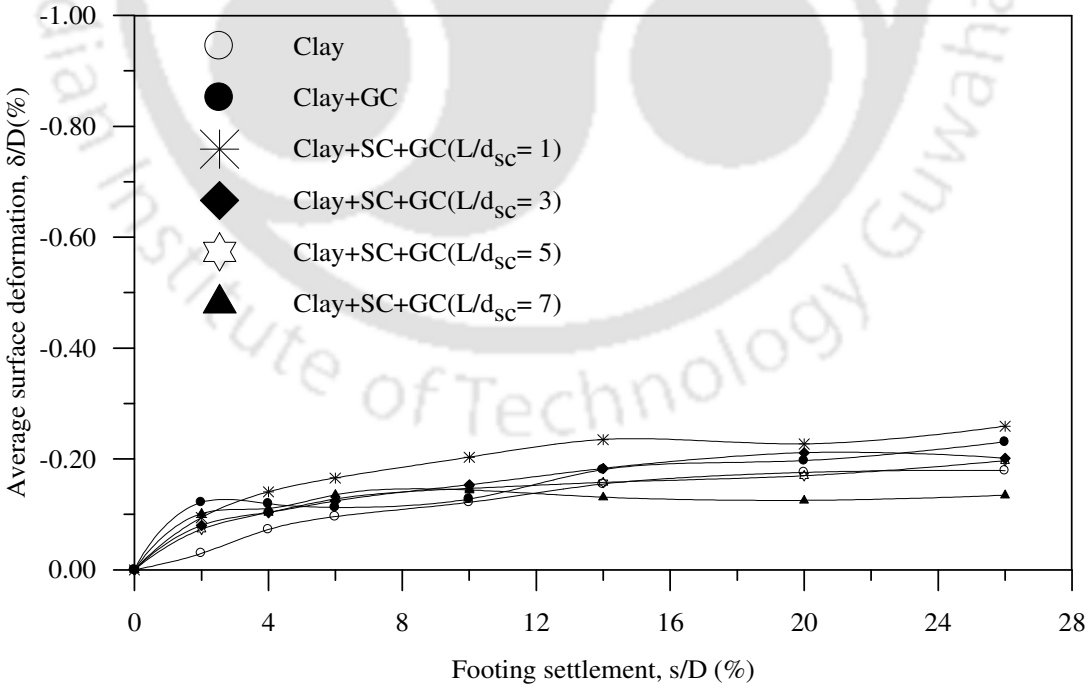

Fig.6.44: Variation of surface deformation, at x = 3D, with footing settlement in composite foundation bed (h/D = 1.6, S/d_{sc} = 2.5) – Test series 12

Fig.6.45: Post-test deformed shape of a typical central stone column in composite foundation bed (L/d_{sc} = 5, h/D = 1.6, S/d_{sc} = 2.5) – Test series 12

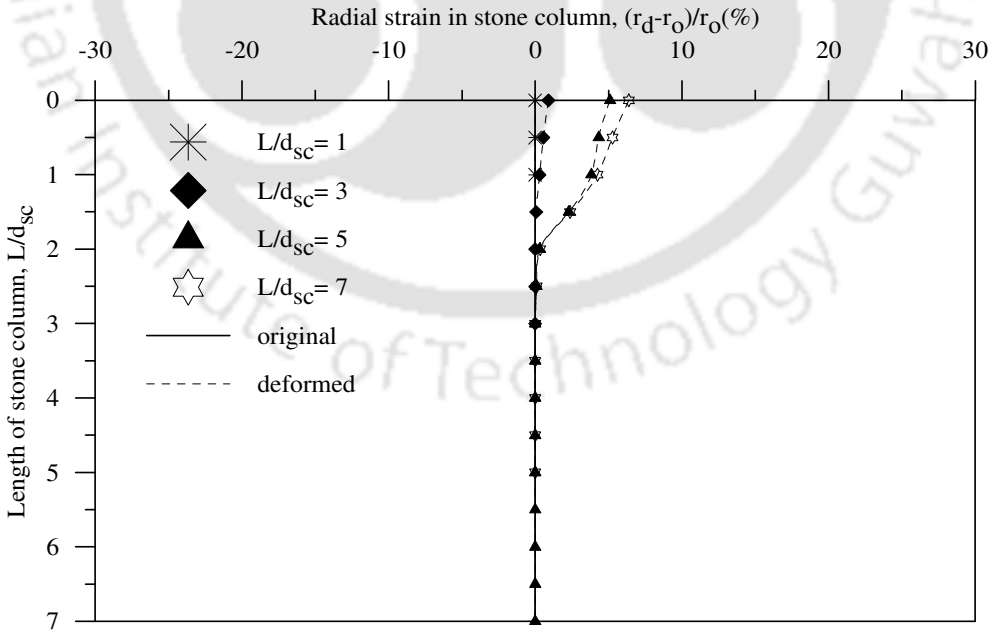

Fig.6.46: Radial strain in central stone column in composite foundation beds (h/D = 1.6, S/d_{sc} = 2.5) - Test series 12

6.3 EFFECT OF SPACING OF STONE COLUMNS

Effect of spacing (S) of stone columns on the performance of the clay bed with geocell-stone column composite reinforcement is studied for four different heights of geocell mattress (i.e., h = 0.53D, 0.9D, 1.1D and 1.6D). The different spacing of the stone columns, studied, are; $1.5d_{sc}$, $2.5d_{sc}$ and $3.5d_{sc}$, where d_{sc} is the diameter of the stone columns which is kept constant as 100 mm. In all these tests (test series 13-16), length of stone columns (L), pocket size of geocells (d_{gc}), density of infill soil (ID) and depth of placement of geocell layer (u) are kept constant as $5d_{sc}$, 0.8D, 80% and 0.1D respectively. The obtained results for different heights of geocell mattress are presented and discussed in the following sections.

6.3.1 Height of geocell mattress (h/D) of 0.53

Fig. 6.47 shows the bearing pressure-settlement responses of the footing on composite foundation bed for different spacing of stone columns (Test series 13). The height of geocell mattress and length of stone column in these tests, as mentioned earlier, were kept constant as 0.53D and $5d_{sc}$ respectively. The responses of clay bed and clay bed with geocell mattress are included for the purpose of comparison. It could be observed that in the initial stages (i.e. s/D < 5%) the slope of the pressure settlement responses with stone columns irrespective of their spacing, are much lesser than the case without stone columns. This indicates that the stone columns have provided additional stiffness to the foundation system. However, at higher settlements the slope of the pressure settlement response of composite foundation bed with stone columns having spacing of $3.5d_{sc}$, is comparable to that with geocell mattress alone (both the responses are nearly parallel). This is because at large spacing, the skirt like group action of the stone columns vanishes that they behave as individual entities. As a result of which the induced confinement by the peripheral stone columns reduces substantially. In the absence of adequate confinement from the surrounding stone columns, the central stone column right below the footing bulges prematurely (at relatively small settlement) and hence is unable to enhance the stiffness of the foundation system. However, with reduced spacing the group action of stone columns manifests that they

effectively induce confinement and hence stiffening effect in the foundation bed over large settlements. As a result of which the stone columns act in group that the surcharge pressure is transmitted over relatively large depth giving rise to increased load carrying of the foundation system. Besides when the spacing between the stone columns reduces the arching induced resistance against punching of soil between the stone columns reduces that the whole system behaves as a stiffened block which redistributes the surcharge pressure more uniformly onto the foundation bed leading to increased performance improvement.

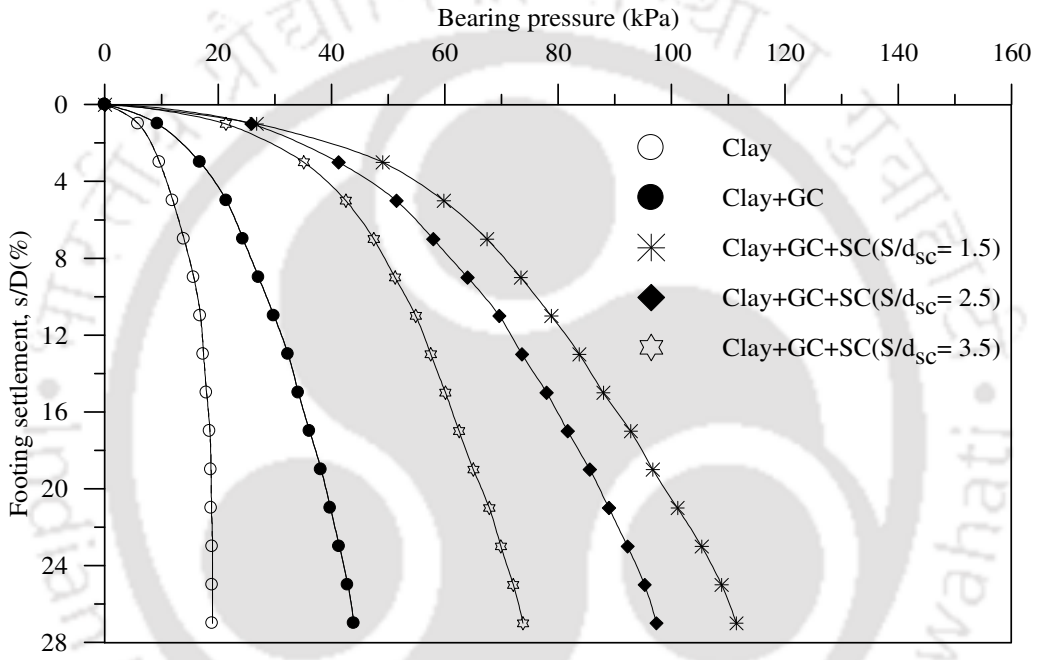

Fig.6.47: Variation of bearing pressure with footing settlement in composite foundation bed (h/D = 0.53, L/d_{sc} = 5) – Test series 13

The improvement factors (IF_{gcsc} and PRS_{gcsc}) presented in Figs.6.48 and 6.49, indicate that the performance improvement in terms of increase in bearing capacity and reduction in settlement, of the composite foundation system, increases with reduction in spacing of stone columns. However, the improvement with reduction in the spacing (S) from 3.5d_{sc} to 2.5d_{sc} is relatively larger as compared to the case with the spacing reducing from 2.5d_{sc} to 1.5d_{sc}. This observation once again establishes that when the spacing reduces from 3.5d_{sc} to 2.5d_{sc}, there is a significant change in the behaviour of stone columns that it shifts from near isolated response to an interacting response.

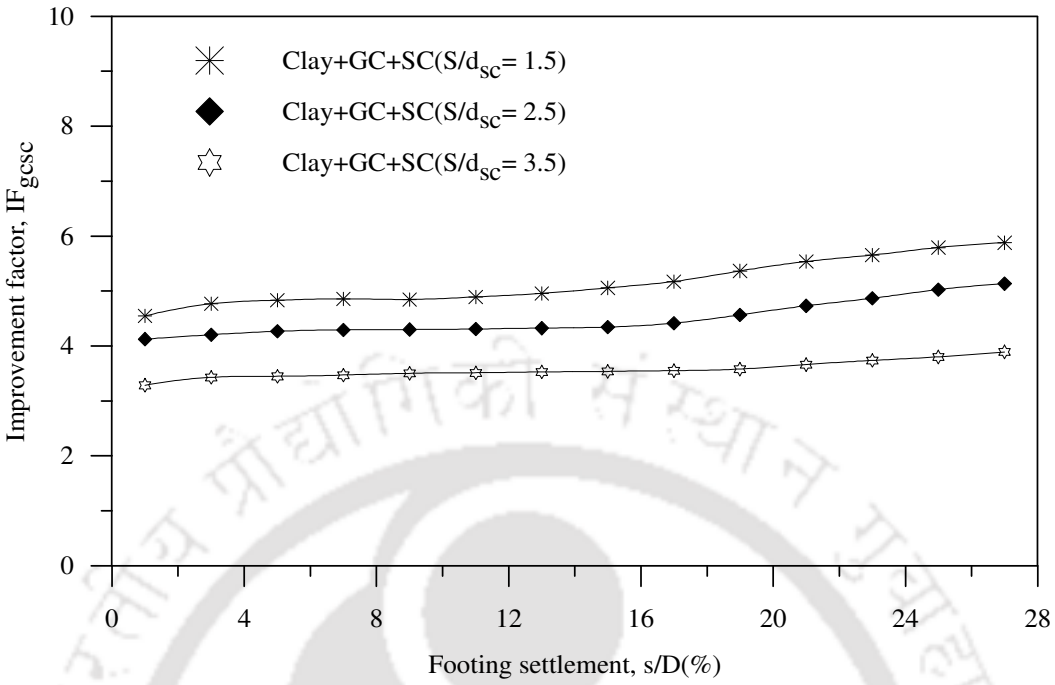

Fig.6.48: Variation of improvement factor with footing settlement in composite foundation bed (h/D = 0.53, L/d_{sc} = 5) – Test series 13

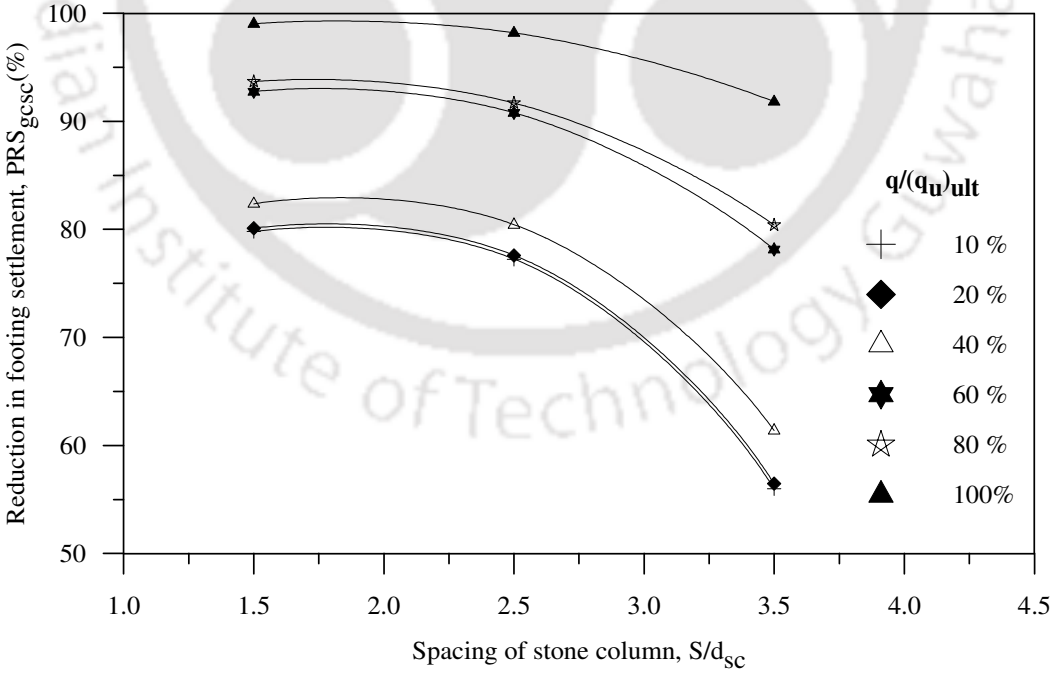

Fig.6.49: Variation of settlement reduction factor with spacing of stone columns in composite foundation bed (h/D = 0.53, L/d_{sc} = 5) – Test series 13

Fig. 6.50 shows that the relative contribution of stone columns in the composite system (IF_{gcsc}/IF_{gc}) is maximum for the closest spacing of stone columns ($S = 1.5d_{sc}$) and reduces with increase in the spacing. Correspondingly, the geocell mattress carried maximum load for large spacing of stone columns ($S = 3.5d_{sc}$, Fig. 6.51) while the contribution of geocell mattress with reduced spacing of stone columns ($S \leq 2.5d_{sc}$) is much smaller. When the spacing is large, the stone columns under and around the footing are subjected to relatively higher load and therefore are prone to yielding. Upon yielding of the stone columns under and around the footing, the geocell mattress bridges over leading to increased contribution in load sharing. The marginal difference in the IF_{gcsc}/IF_{sc} responses with the spacing (S) changing from $2.5d_{sc}$ to $1.5d_{sc}$ indicates that further change in the response of geocell mattress is practically marginal. This is because, increase in area replacement ratio of the stone columns (through decrease of the spacing) leads to increased uniformity in stress distribution in the clay-stone column bed that it yields less, giving rise to reduced straining in the geocell reinforcement leading to lower mobilisation of its strength. In such case the geocell mattress behaves more of like a load transmitting member while for larger spacing of stone columns ($S = 3.5d_{sc}$) it behaves as a load sustaining member, similar to a centrally loaded slab resting over columns. From the present observations it could be said that incase of practical constraints forcing to go for larger spacing of stone columns, additional required performance improvement can be met with the provision of geocell mattress.

Reduced surface settlement with reduced spacing of stone columns, in the region around the footing ($x = D$, Fig. 6.52) and correspondingly reduced heaving at $x = 2D$ and 3D (Fig. 6.53 and Fig. 6.54) testifies that the yield in foundation bed is reduced with reduced spacing of the stone columns.

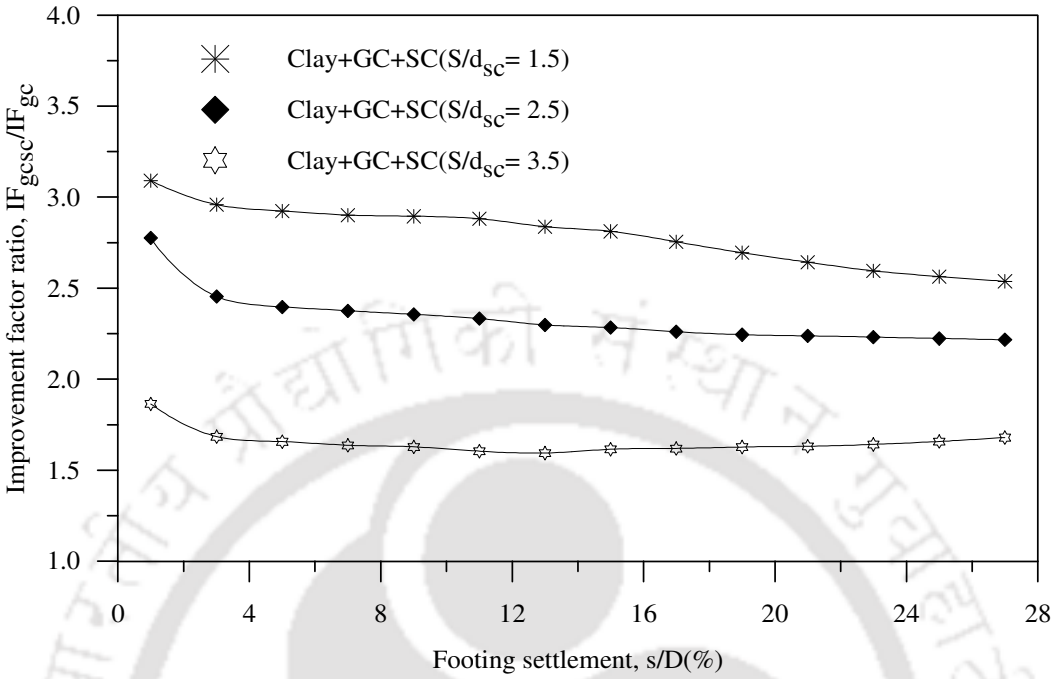

Fig.6.50: Improvement factor ratio vs. footing settlement, contribution of stone columns in composite foundation bed (h/D = 0.53, L/d_{sc} = 5) – Test series 13

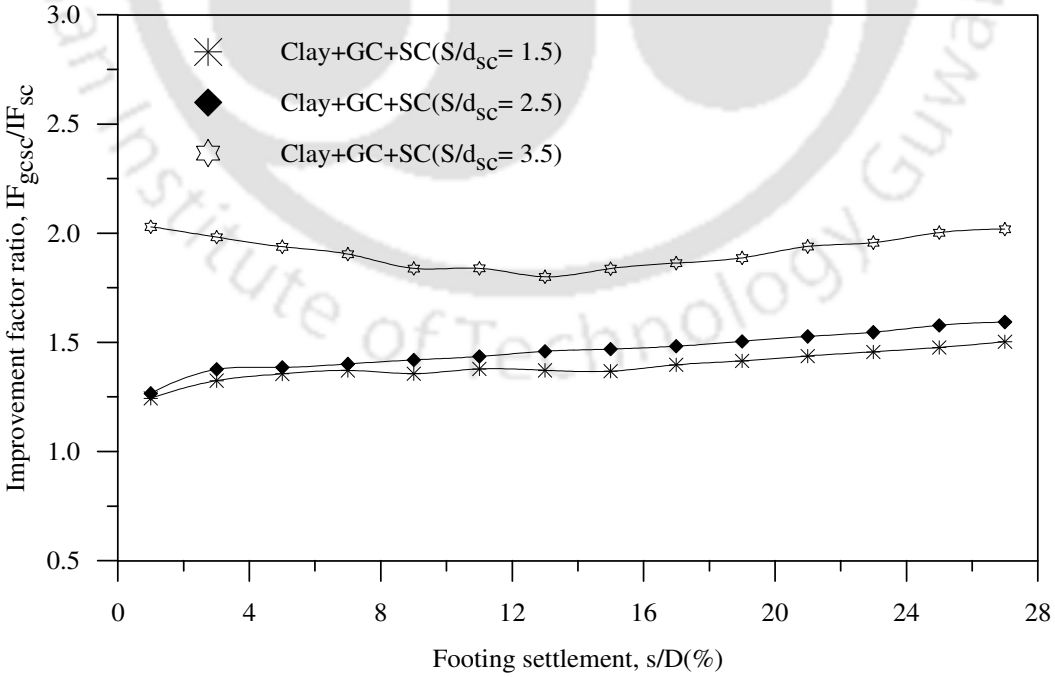

Fig.6.51: Improvement factor ratio vs. footing settlement, contribution of geocell mattress in composite foundation bed (h/D = 0.53, L/d_{sc} = 5) – Test series 13

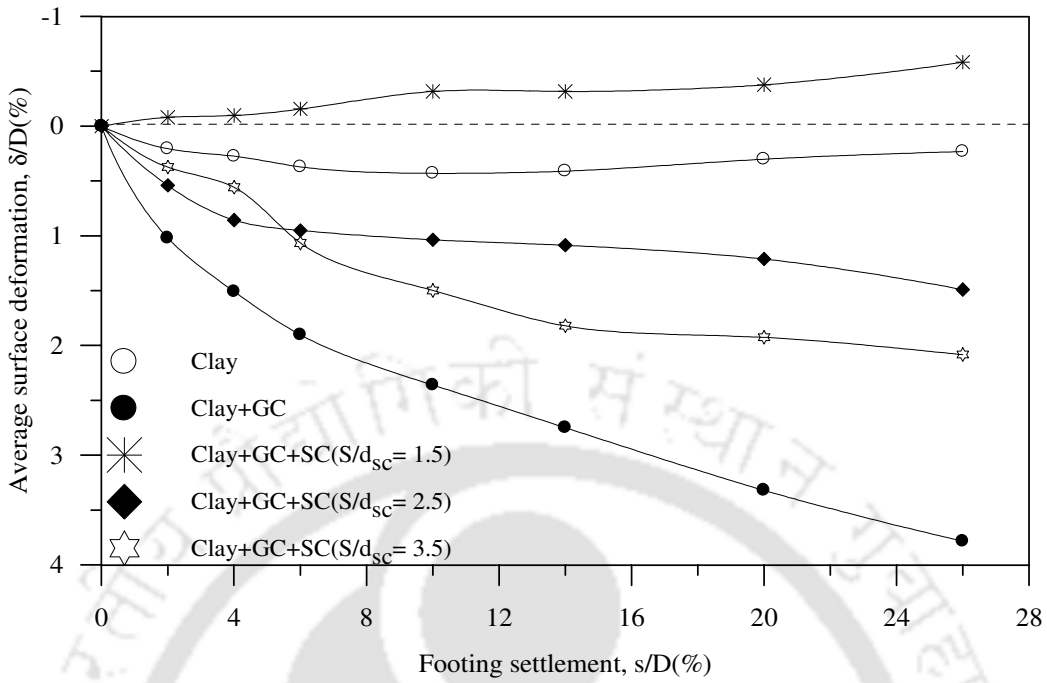

Fig.6.52: Variation of surface deformation, at x = D, with footing settlement in composite foundation bed (h/D = 0.53, L/d_{sc} = 5) – Test series 13

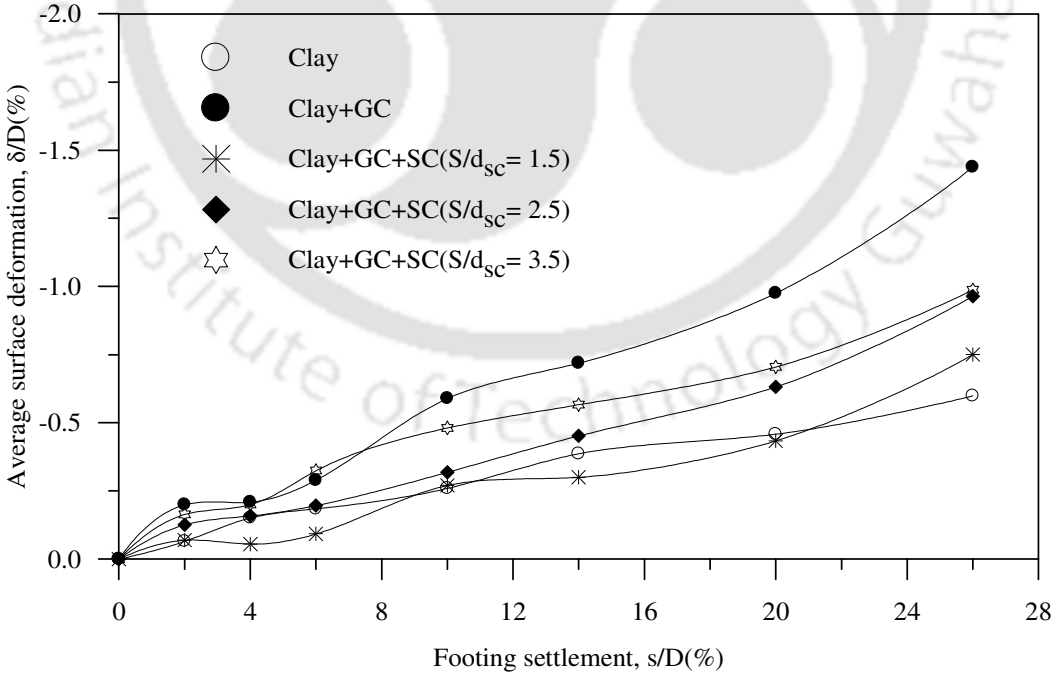

Fig.6.53: Variation of surface deformation, at x = 2D, with footing settlement in composite foundation bed (h/D = 0.53, L/d_{sc} = 5) – Test series 13

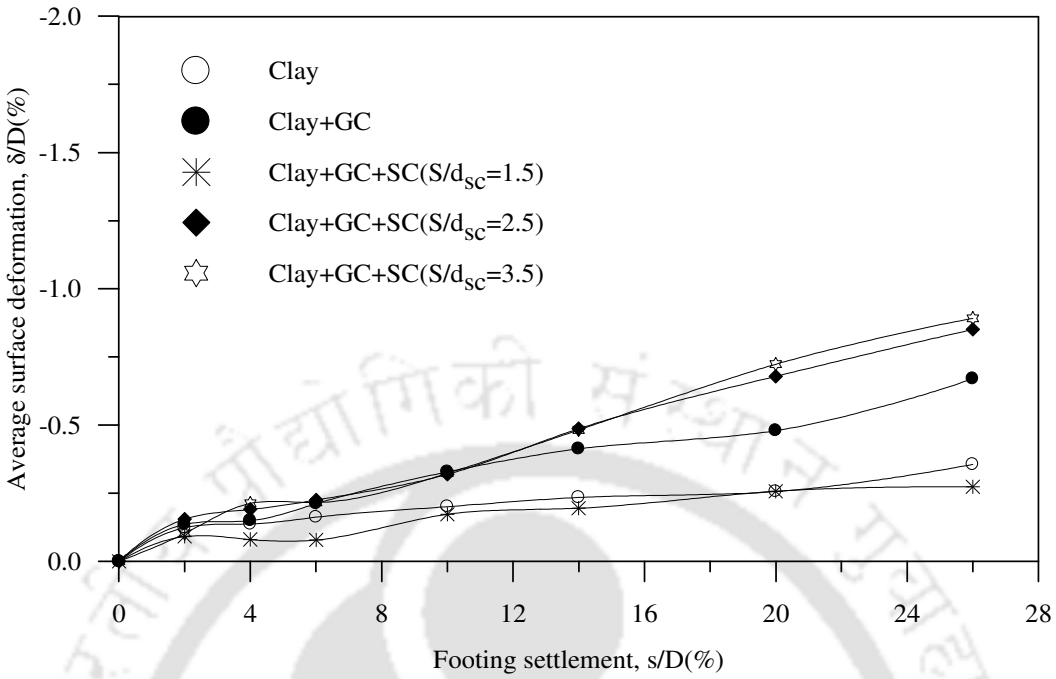

Fig.6.54: Variation of surface deformation, at x = 3D, with footing settlement in composite foundation bed (h/D = 0.53, L/d_{sc} = 5) – Test series 13

Typical post test exhumed shape of the central stone column (right below the footing) and the peripheral stone column (in the adjacent region) are shown in Fig. 6.55. It is of interest to note that the peripheral column has deformed as a laterally loaded pile. This establishes that the peripheral columns participate in restraining the central column against bulging. With increased spacing (S), as the group action and hence the restraining effect of the peripheral columns reduces, the central stone column bulges more (Fig. 6.56).

(a) Central column (b) Peripheral column

Fig. 6.55: Post-test deformed shape of stone columns in composite foundation bed (L/d_{sc} = 5, S/d_{sc} = 1.5, h/D = 0.53) – Test series 13

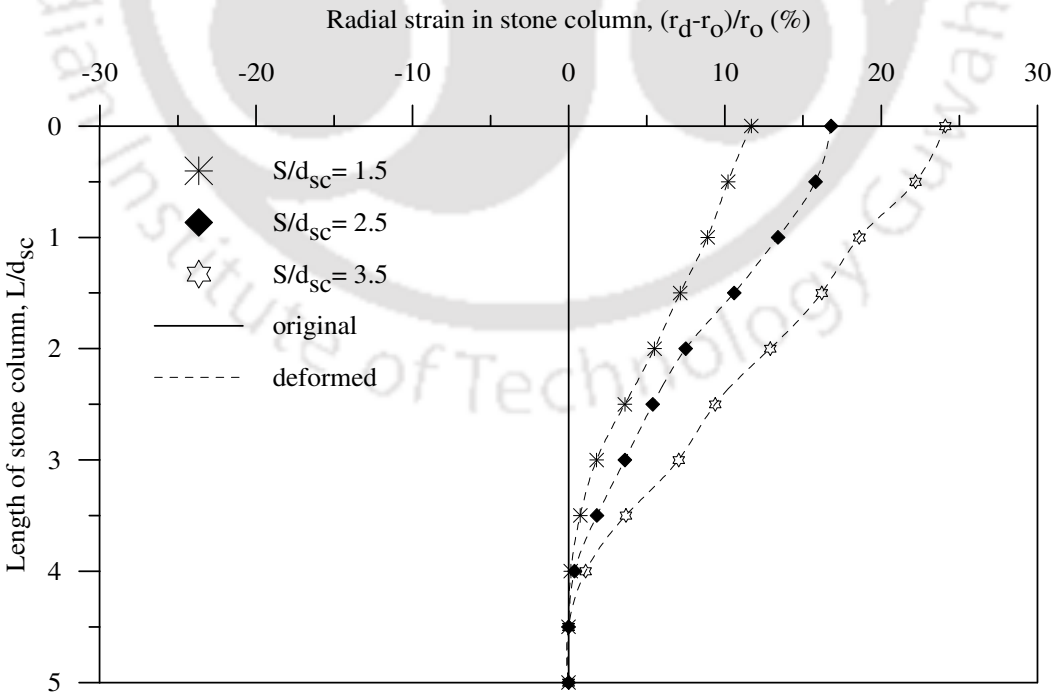

Fig.6.56 Radial strain in central stone columns in composite foundation bed (h/D = 0.53, L/d_{sc} = 5) – Test series 13

6.3.2 Height of geocell mattress (h/D) of 0.9

The variation of bearing pressure with footing settlement for different spacing of stone columns, in the composite foundation bed, with relatively higher height of geocell mattress (i.e. equal to 0.9D) is shown in Fig. 6.57. The quantification of the improvement in bearing capacity due to the geocell-stone column reinforcement (IF_{gcsc}) is depicted in Fig.6.58. In comparison to the case with h = 0.53D (Fig.6.48), the performance improvement in the present case is relatively higher. However, the contributions of the stone columns (IF_{gcsc}/IF_{gc}) in both the cases (Fig. 6.59 Vs. Fig. 6.50) are nearly the same indicating that the influence of stone columns, irrespective of their spacing, has not changed much with increase in height of the geocell mattress from 0.53D to 0.9D. Hence it can be said that the additional increase in performance improvement is mostly due to the increased contribution of geocell mattress owing to its increased height. Indeed, Fig. 6.60 shows a relatively increased contribution of geocell mattress in the overall load carrying capacity of the foundation system (IF_{gcsc}/IF_{sc}). The photograph of the deformed shape of the central stone columns, depicted in fig.6.61, clearly show that, with increased spacing the central stone column, right under the footing, has undergone higher bulging. This trend can more clearly be observed in the radial strain responses presented in Fig.6.62. Hence it can be said that with increased height of geocell mattress to 0.9D, the influence of variation of spacing of stone columns is still significant.

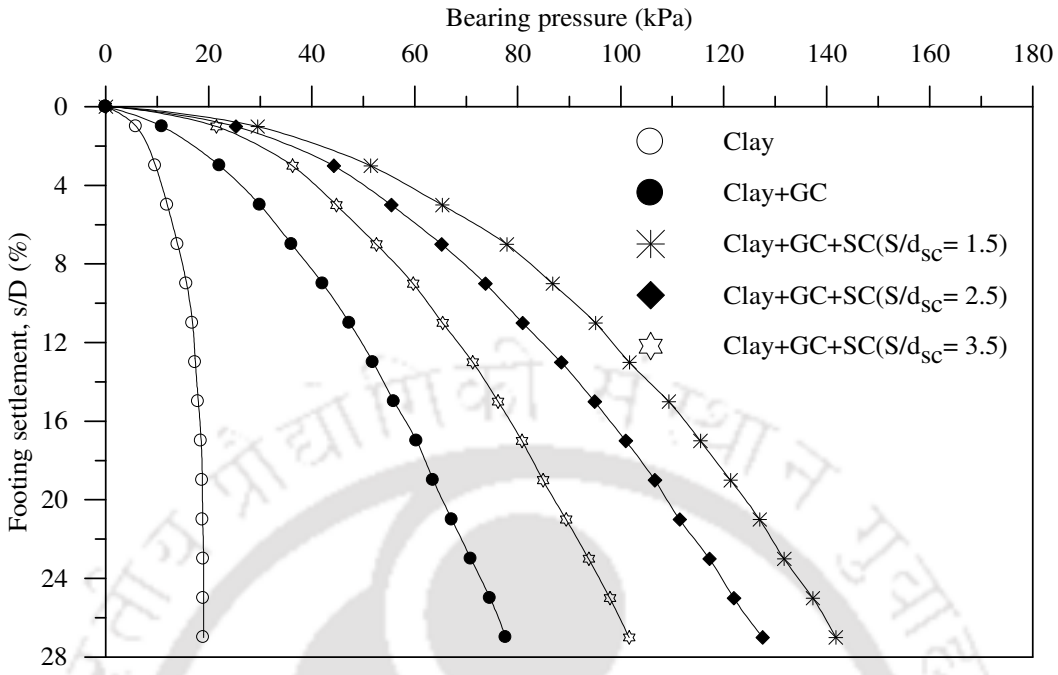

Fig.6.57: Variation of bearing pressure with footing settlement in composite foundation bed (h/D = 0.9, L/d_{sc} = 5) - Test series 14

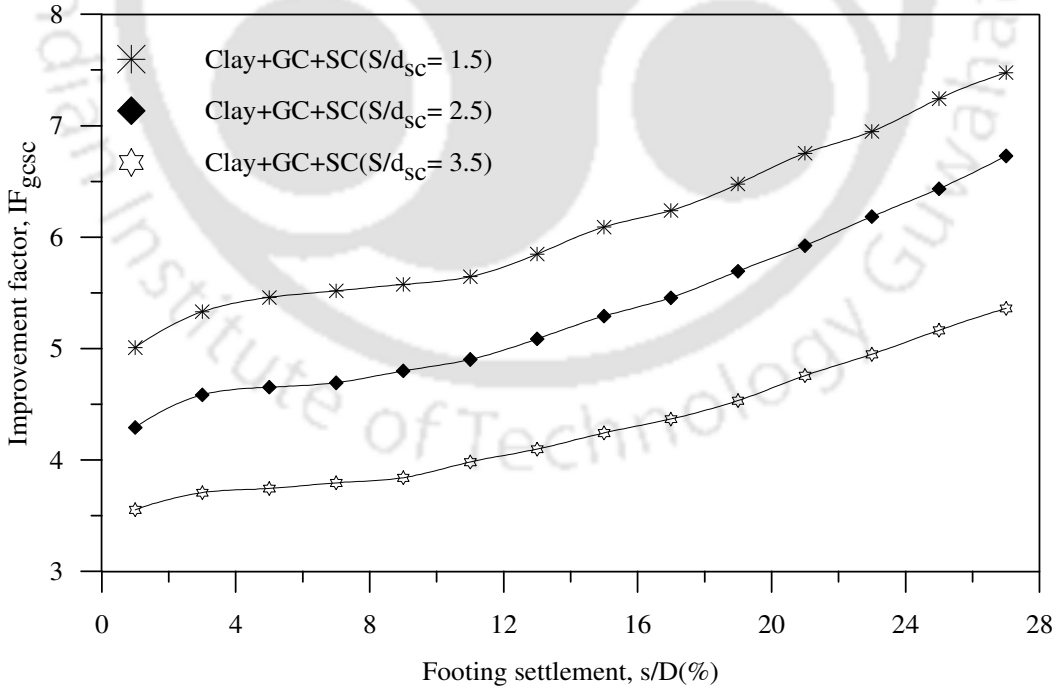

Fig.6.58: Variation of improvement factor with footing settlement in composite foundation bed (h/D = 0.9, L/d_{sc} = 5) – Test series 14

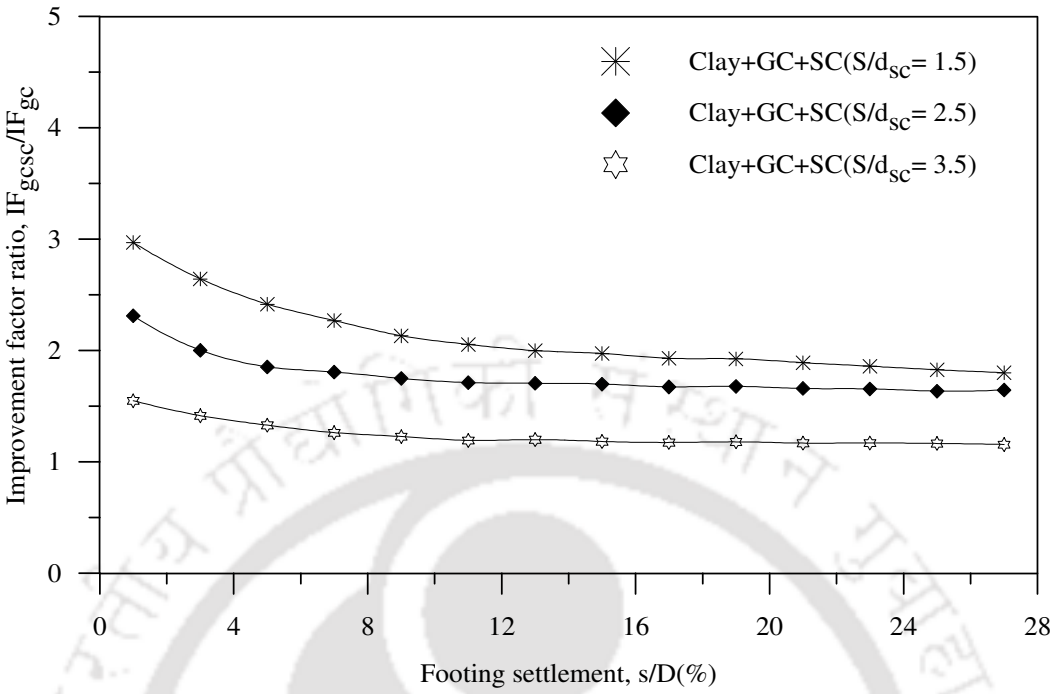

Fig.6.59: Improvement factor ratio vs. footing settlement, contribution of stone columns in composite foundation bed (h/D = 0.9, L/d_{sc} = 5) – Test series 14

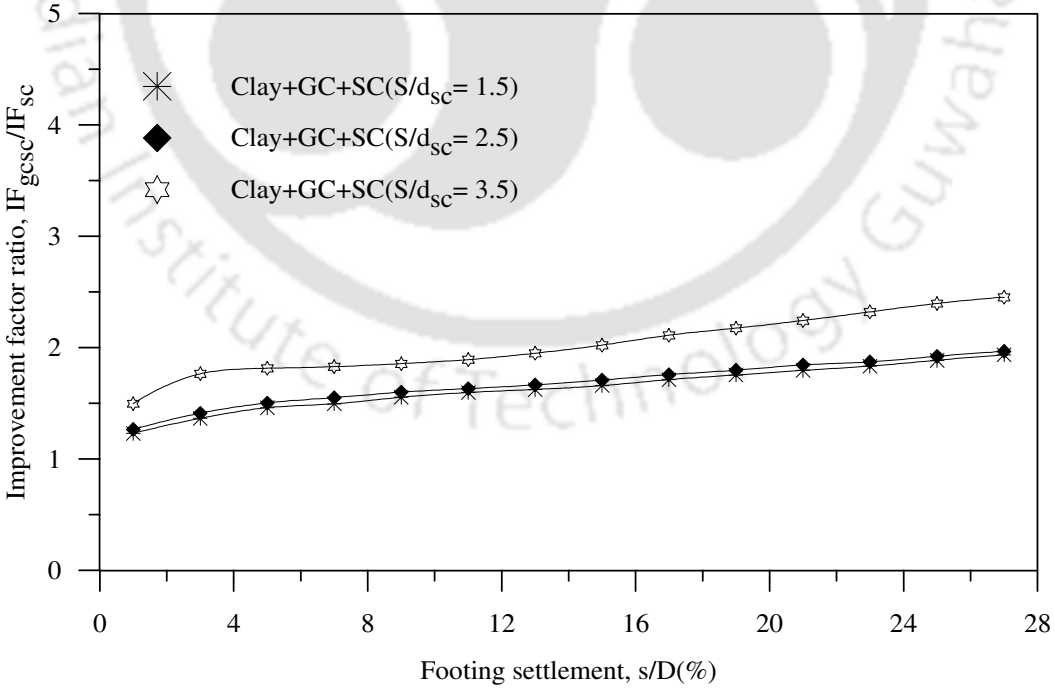

Fig.6.60: Improvement factor ratio vs. footing settlement, contribution of geocell mattress in composite foundation bed (h/D = 0.9, L/d_{sc} = 5) – Test series 14

(a) S/d_{sc} = 1.5 (b) S/d_{sc} = 2.5 (c) S/d_{sc} = 3.5

Fig. 6.61: Post-test deformed shape of central stone columns in composite foundation bed (h/D = 0.9, L/d_{sc} = 5) – Test series 14

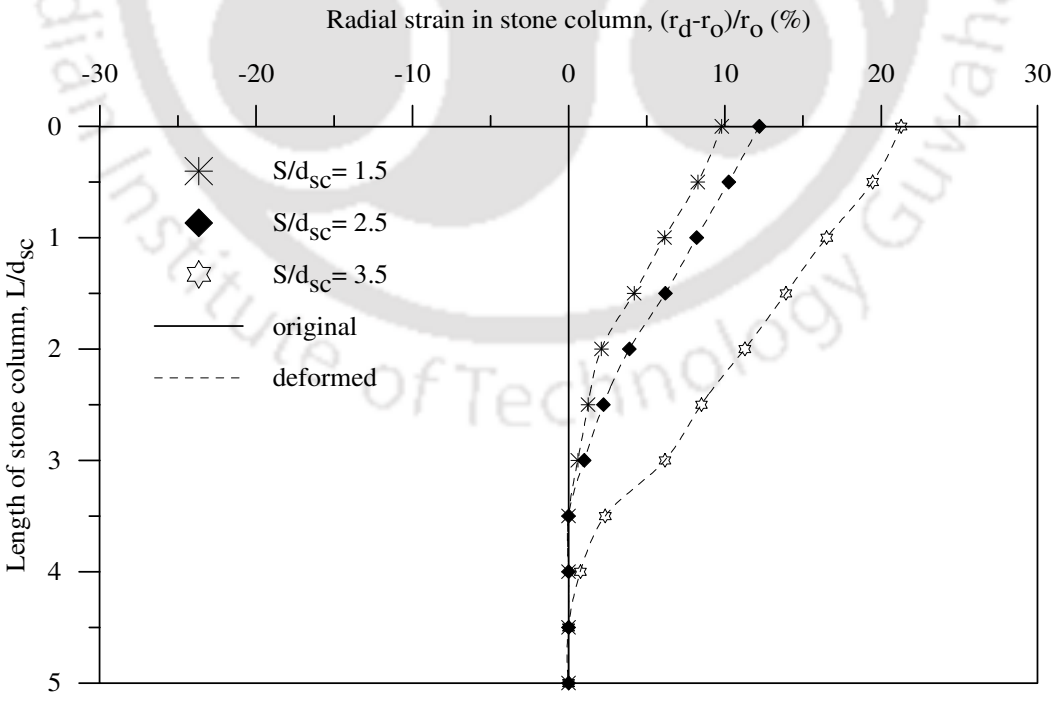

Fig.6.62: Radial strain in central stone column in composite foundation beds. (h/D = 0.9, L/d_{sc} = 5) - Test series 14

6.3.3 Height of geocell mattress (h/D) of 1.1

Fig. 6.63 depicting the responses for the case, h = 1.1D (Test series 15) shows that the pressure settlement responses of the composite foundation beds are close to the case with geocell mattress alone, indicating that the influence of stone columns is not prominent. However, the difference in the responses due to change in the spacing of the stone columns is still clearly visible. Fig. 6.64 shows that with stone columns having spacing of $1.5d_{sc,}$ the bearing capacity has gone up by 9.5 fold increase (IF_{gcsc} = 9.5). A comparison with the data presented in Figs. 6.48 and 6.58 it could be observed that with stone column spacing of $1.5d_{sc}$, the maximum bearing capacity improvement (IF_{gcsc}) is about 5.2 with geocell mattress of height = 0.53D, while, it is 7.5 (IF_{gcsc}) with geocell mattress of height = 0.9D.

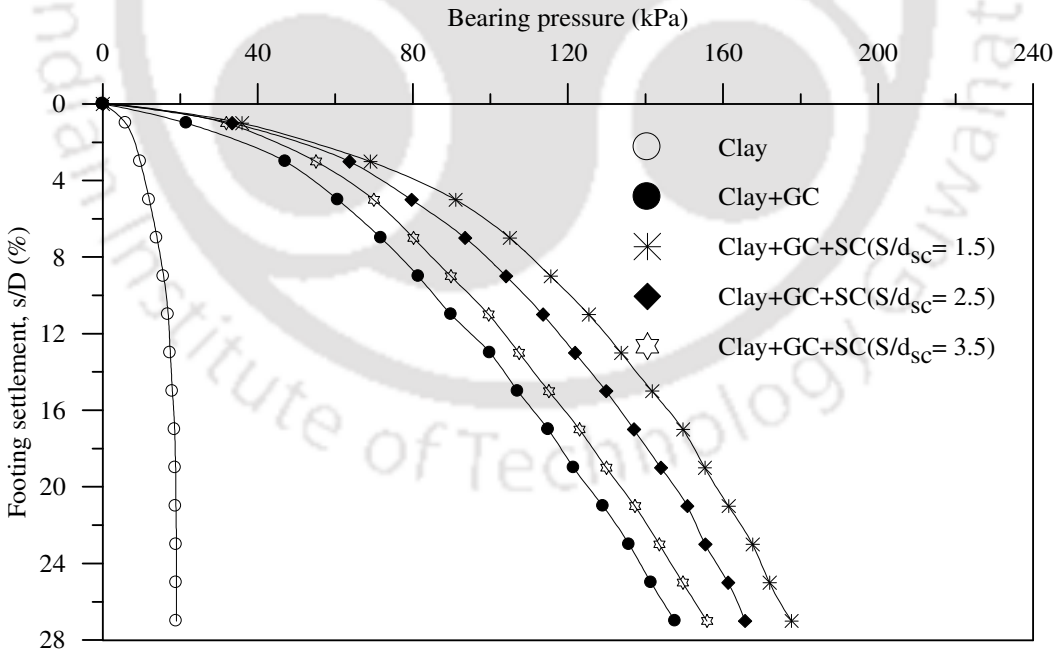

Fig.6.63: Variation of bearing pressure with footing settlement in composite foundation bed (h/D = 1.1, L/d_{sc} = 5) - Test series 15

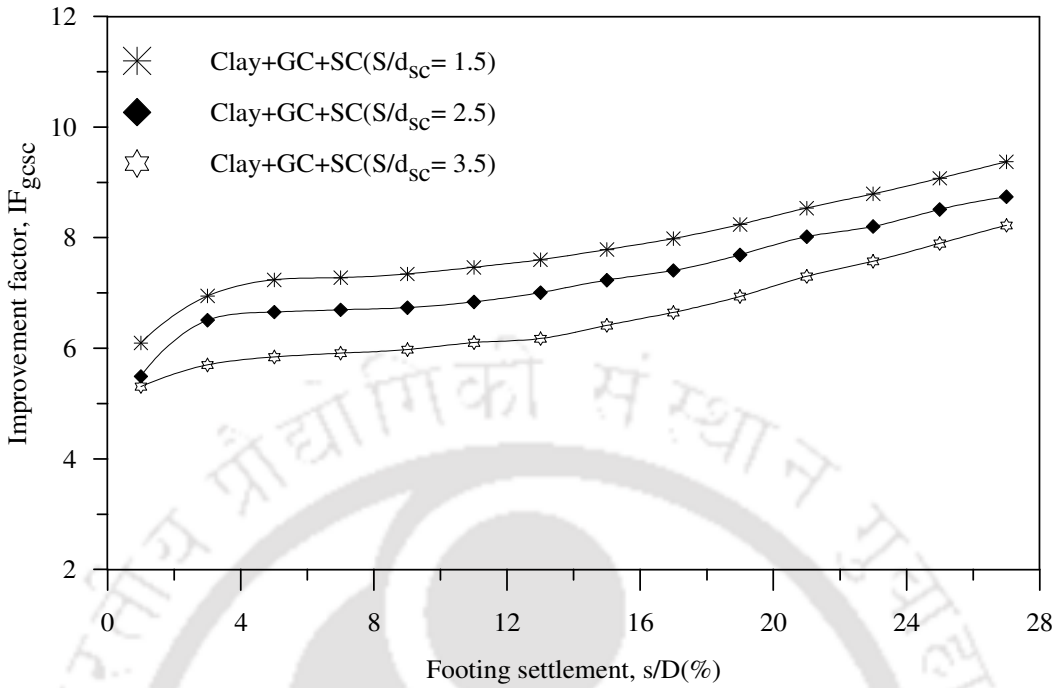

Fig.6.64: Variation of improvement factor with footing settlement in composite foundation bed (h/D = 1.1, L/d_{sc} = 5) – Test series 15

The settlement reduction responses (PRS_{gcsc}) for the case with h = 1.1D are shown in Fig. 6.65. It can be seen that the reduction in settlement (PRS_{gcsc}) with decrease in spacing of stone columns is almost linear. Contrary to this for relatively smaller height of geocell mattress it is nonlinear (h = 0.53D, Fig. 6.49). This is typical of stone column behaviour, as discussed in Chapter 4; that the rate of settlement increases with increase in spacing of stone columns. The present response with linear variation of the PRS_{gcsc} is typical of geocell mattress response (Chapter 5). Hence it can be said that for shallow height of geocell mattress (i.e. h = 0.53D and 0.9D) the stone columns play a dominant role in reducing settlement of the foundation bed. However, their role reduces for relatively higher height of geocell mattress (i.e. h ≥ 1.1D), wherein, the geocell mattress plays the dominant role. Indeed, Fig. 6.66 shows that the maximum observed value of the factor, IF_{gcsc}/IF_{gc}, in the present case is 2.1, while with relatively shallow height of geocell mattress (h = 0.9D) it was 3 (Fig. 6.59). This makes clear

that, with increase in height of geocell mattress, the relative contribution of stone columns in the composite foundation system has reduced. Correspondingly, Fig. 6.67 shows that, in the present case the maximum value of IF_{gcsc}/IF_{sc} is more than 4, while, in the previous case (h = 0.9D) it was only 2.8. This indicates that, with increase in height (h), the contribution of geocell mattress in the overall performance of the system has gone up. The deformation in the stone columns depicted in Fig 6.68 shows relatively lesser bulging compared to the case with geocell mattress of shallow heights (h = 0.9D, 0.53D; Fig. 6.62, 6.56) thus, testifying to the fact that with increase in height of geocell mattress the stone column strength has been mobilized to lesser degree.

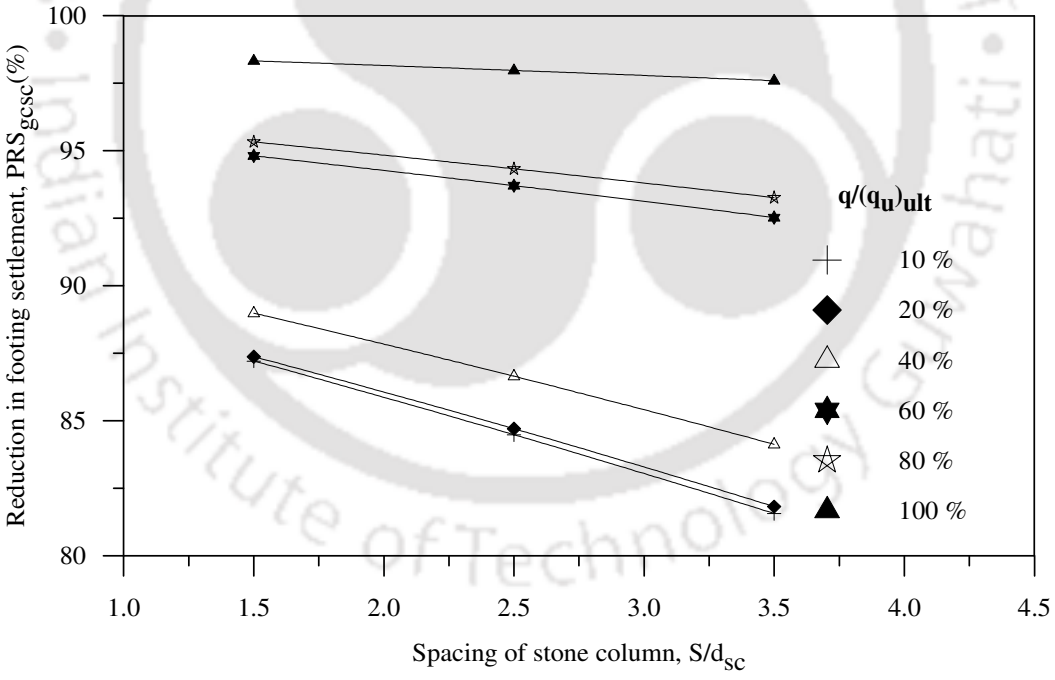

Fig.6.65: Variation of settlement reduction factor with spacing of stone column in composite foundation bed (h/D = 1.1, L/d_{sc} = 5) – Test series 15

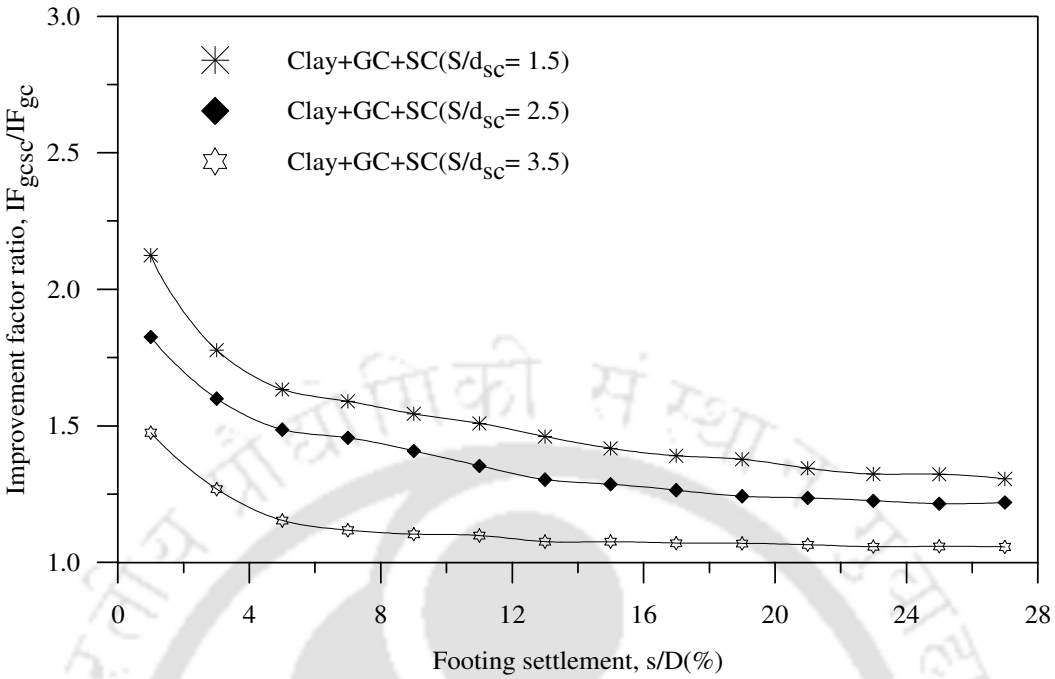

Fig.6.66: Improvement factor ratio vs. footing settlement, contribution of stone columns in composite foundation bed (h/D = 1.1, L/d_{sc} = 5) – Test series 15

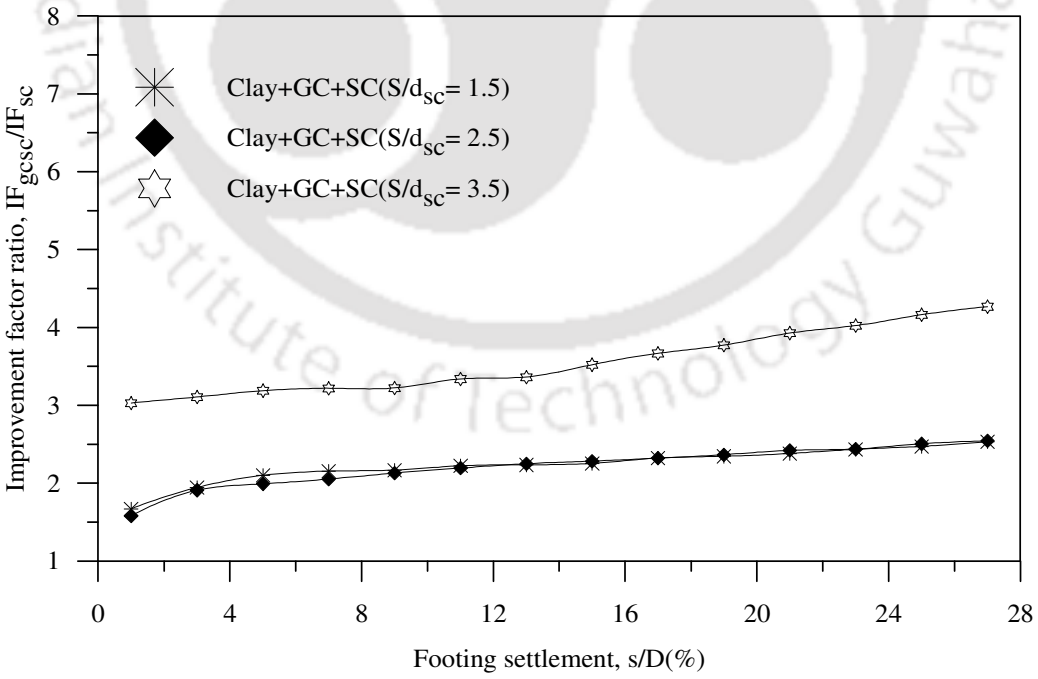

Fig.6.67: Improvement factor ratio vs. footing settlement, contribution of geocell mattress in composite foundation bed (h/D = 1.1, L/d_{sc} = 5) – Test series 15

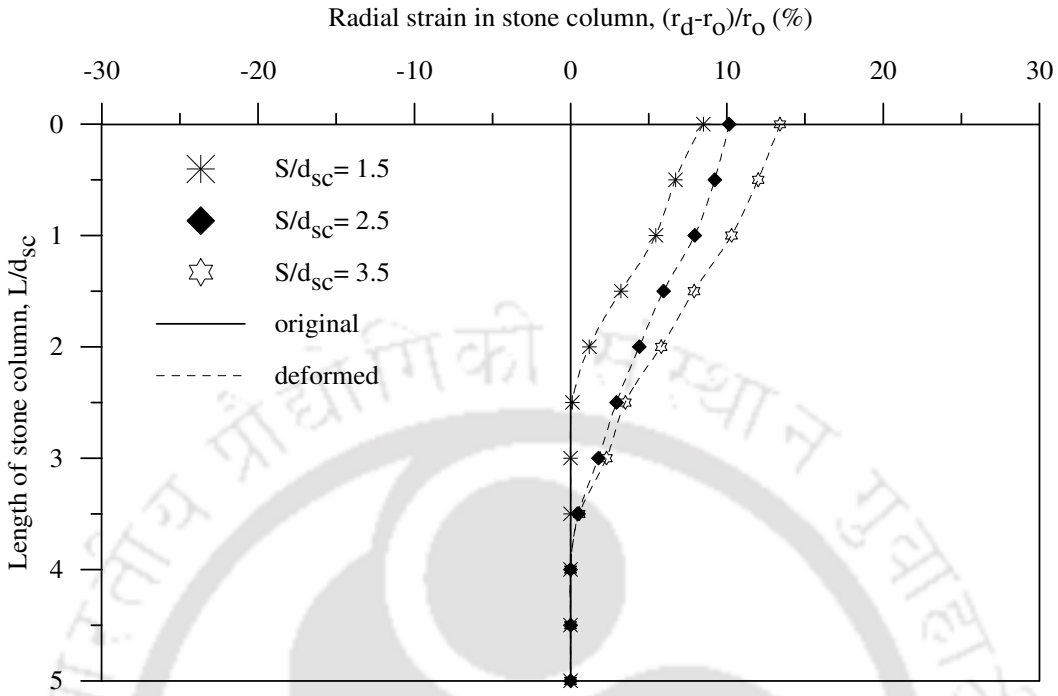

Fig.6.68: Radial strain in central stone column in composite foundation beds. ($h/D = 1.1$, $L/d_{sc} = 5$) - Test series 15

6.3.4 Height of geocell mattress (h/D) of 1.6

Variation of bearing pressure with footing settlement for different spacing of stone columns in composite foundation beds with h = 1.6D, is shown in Fig. 6.69. The corresponding variation of the bearing capacity improvement factor (IF_{gcsc}) is depicted in Fig. 6.70. It could be observed that the responses for different spacing of stone columns are very close to each other. This is attributed to the reduced influence of stone columns due to their increased proximity from the loading region (base of the footing), because of increased height of the geocell mattress. Indeed Fig.6.71 shows that the contribution of stone columns, in the performance improvement, is very less ($IF_{gcsc}/IF_{gc} < 1.3$).

Fig. 6.72 shows that the maximum contribution of geocell mattress (h = 1.6D) is about 4 times that of the stone columns. This is nearly same as the case with geocell mattress of height (h) equal to 1.1D (Fig. 6.67). Hence it can be said that beyond a certain stage, further increase in load carrying capacity with increase in height of geocell mattress in the composite foundation bed, is marginal. This is attributed to the local buckling and yielding of geocell walls that the global increase in strength and stiffness of the system due to increase in height of geocells (h) remains immobilized. Hence it could be said that, irrespective of the spacing of the stone columns, the critical height of geocell mattress (h) giving optimum performance improvement is nearly equal to the diameter of the footing. The visibly less bulging in the stone columns (Fig. 6.73) indicates that they have under performed, in sharing the surcharge loading.

Based on the above discussion it can be concluded that for optimum performance of the composite foundation bed, the geocell mattress height should be equal to the diameter of the footing and the stone column spacing should be 2.5 times the diameter of the stone column (d_{sc}).

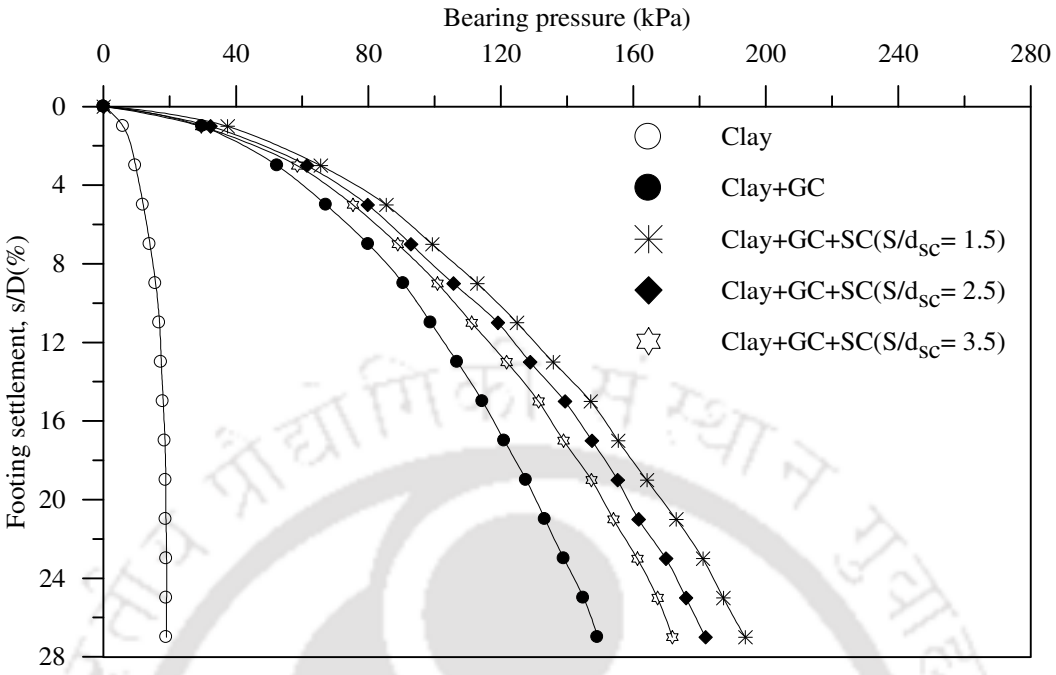

Fig.6.69: Variation of bearing pressure with footing settlement in composite foundation bed (h/D = 1.6, L/d_{sc} = 5) - Test series 16

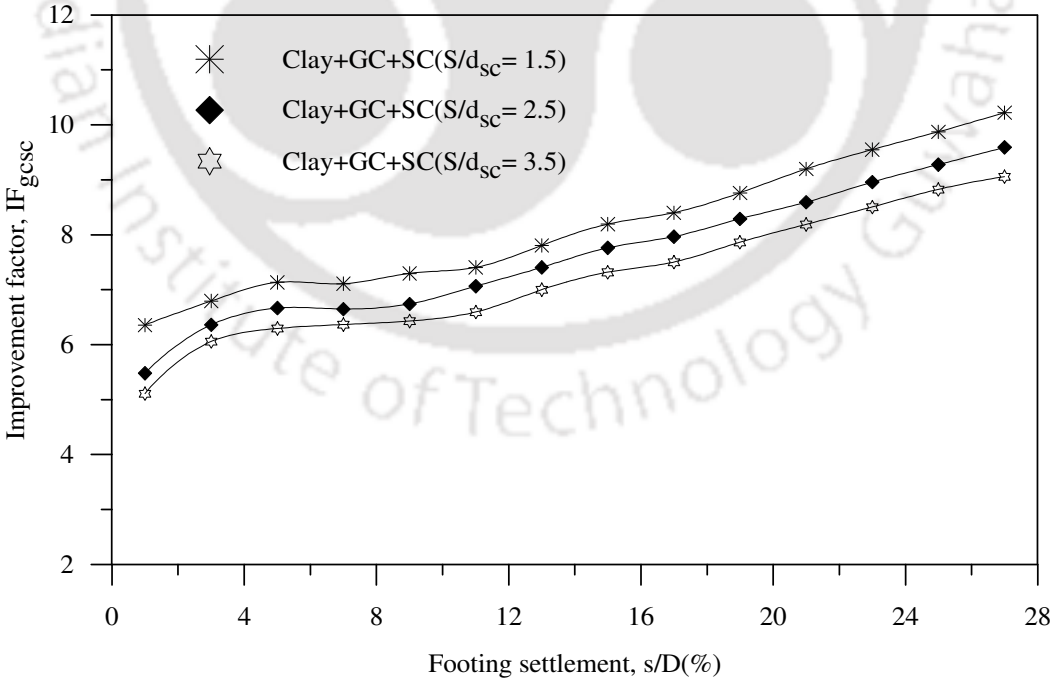

Fig.6.70: Variation of improvement factor with footing settlement in composite foundation bed (h/D = 1.6, L/d_{sc} = 5) – Test series 16

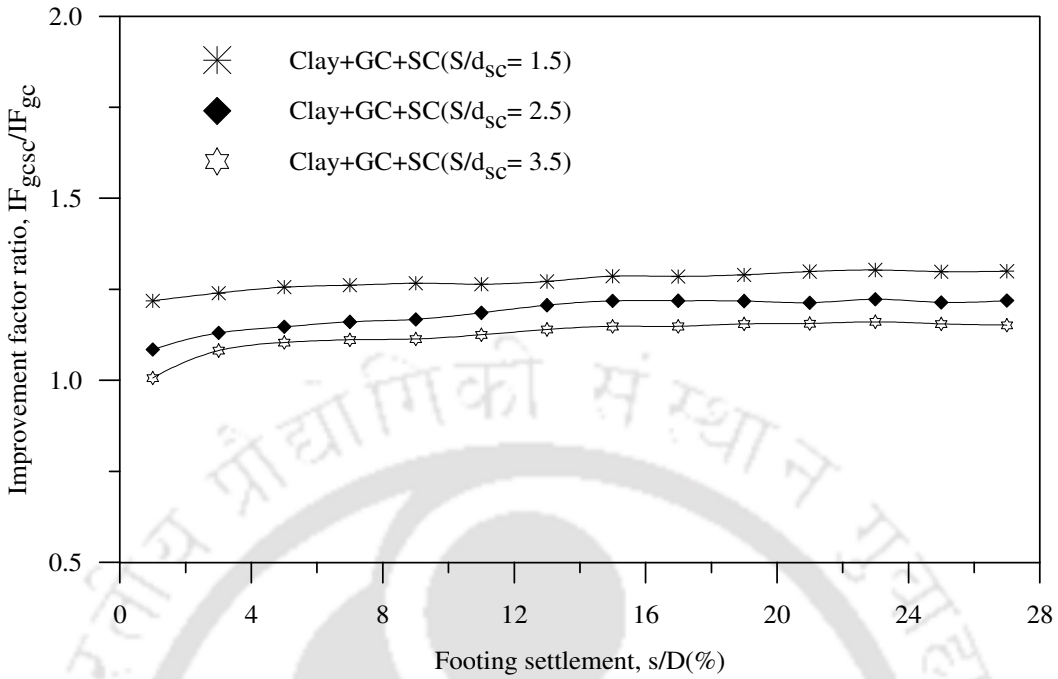

Fig.6.71: Improvement factor ratio vs. footing settlement, contribution of stone columns in composite foundation bed (h/D = 1.6, L/d_{sc} = 5) – Test series 16

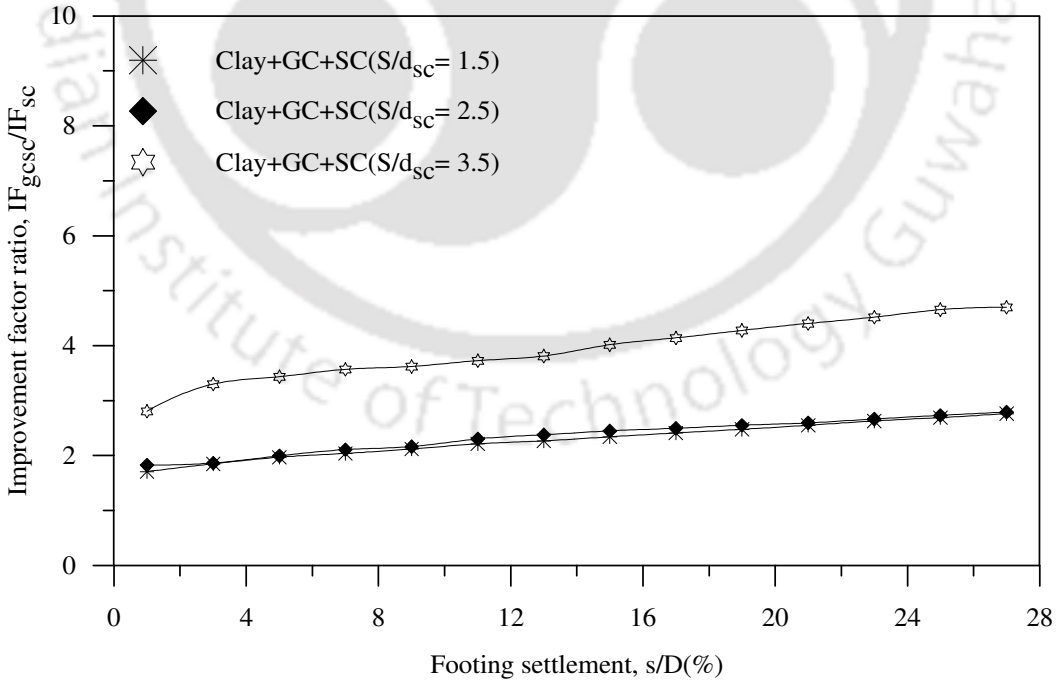

Fig.6.72: Improvement factor ratio vs. footing settlement, contribution of geocell mattress in composite foundation bed (h/D = 1.6, L/d_{sc} = 5) – Test series 16

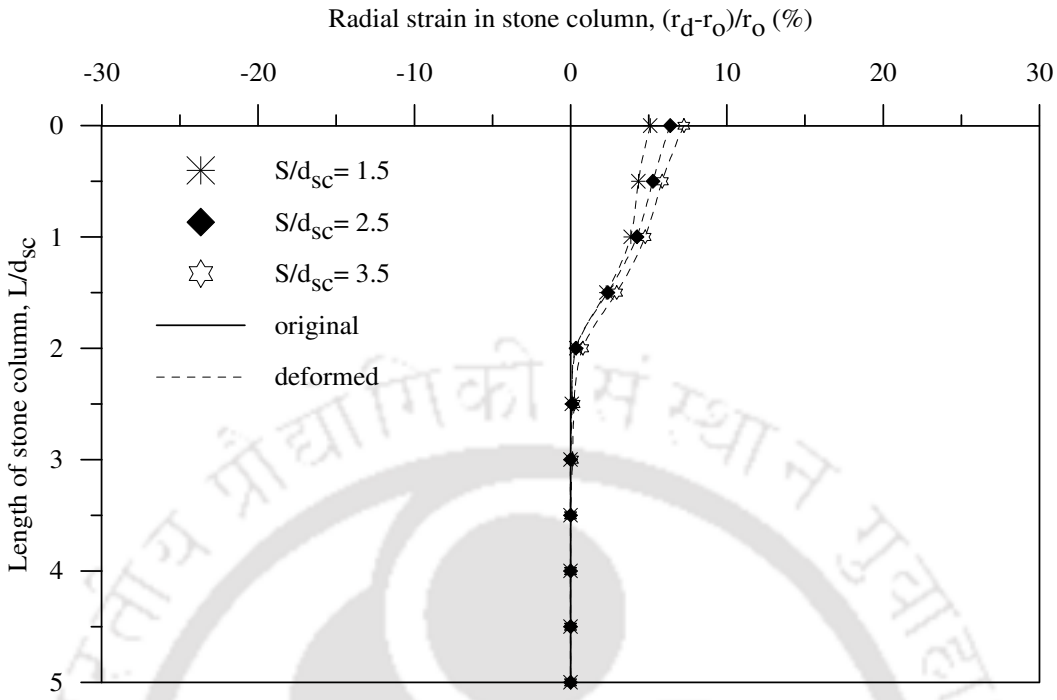

Fig.6.73: Radial strain in central stone columns in composite foundation bed (h/D = 1.6, L/d_{sc} = 5) – Test series 16

6.4 EFFECT OF POCKET SIZE OF GEOCELL (d_{gc}/D)

From the test data presented and discussed in the previous section it has been observed that the influence of stone columns in the composite foundation bed reduces with increase in height of geocell mattress (h). While the contribution of stone columns, in the composite bed, is substantial for h = 0.53D and 0.9D, it is much less for h = 1.1D and becomes marginal for h = 1.6D. In view of this further studies to understand the influence of parameters such as pocket size of geocells (d_{gc}) and relative density of infill soil, in the composite foundation beds, are carried out for h = 0.53D and 0.9D only.

The effect of pocket size (d_{gc}) of geocells on the overall performance of the geocell-stone column-clay bed, composite system, is brought in the following subsections. In these tests (Test series 17 and 18) the length of the stone columns (L), spacing of stone

columns (S), depth of placement of geocell mattress (u) and density of sand (ID) in the geocells, was kept constant as $5d_{sc}$, $2.5d_{sc,}$ 0.1D and 80% respectively.

6.4.1 Height of geocell mattress (h/D) of 0.53

Pressure-settlement response showing the influence of pocket size of geocells (d_{gc}/D) on the performance of the composite foundation bed (h = 0.53D) is depicted in Fig. 6.74. The corresponding responses of the geocell mattress reinforced clay beds and clay bed alone, are presented for the purpose of comparison. In general there is an increase in the bearing capacity with decrease in pocket size of the geocells. However, there is a visible difference in the trends for higher pocket size (d_{gc}/D = 1.33) compared to that with lower pocket size (d_{gc} = 1.1D and 0.8D). For d_{gc} = 1.33D, the pressure settlement response has almost become vertical for settlement beyond 20% of footing diameter, indicating that the composite foundation has undergone failure. While for smaller pocket sizes (i.e. d_{gc} = 1.1D and 0.8D) no such failure has been observed and the foundation bed continues to sustain increased surcharge pressure. In case of d_{gc} = 1.33D, the geocell pocket opening being 33% larger than that of the footing diameter; the footing directly rests on the encapsulated soil within the geocell pockets. Therefore, the improvement in performance is primarily due to the confinement and interfacial friction induced stiffening of the soil by the geocell walls. When the surcharge pressure exceeds the threshold value of this resistance, the footing along with the supporting sand, plunges into the underlying soft clay bed, leading to failure. However, for geocells with pocket sizes nearly equal to or smaller than the footing diameter (i.e. d_{gc} = 1.1D and 0.8D) the footing rests on the geocell-soil composite system with geocell walls under the footing, thereby deriving continuously increased resistance from the reinforcement leading to increased load carrying capacity.

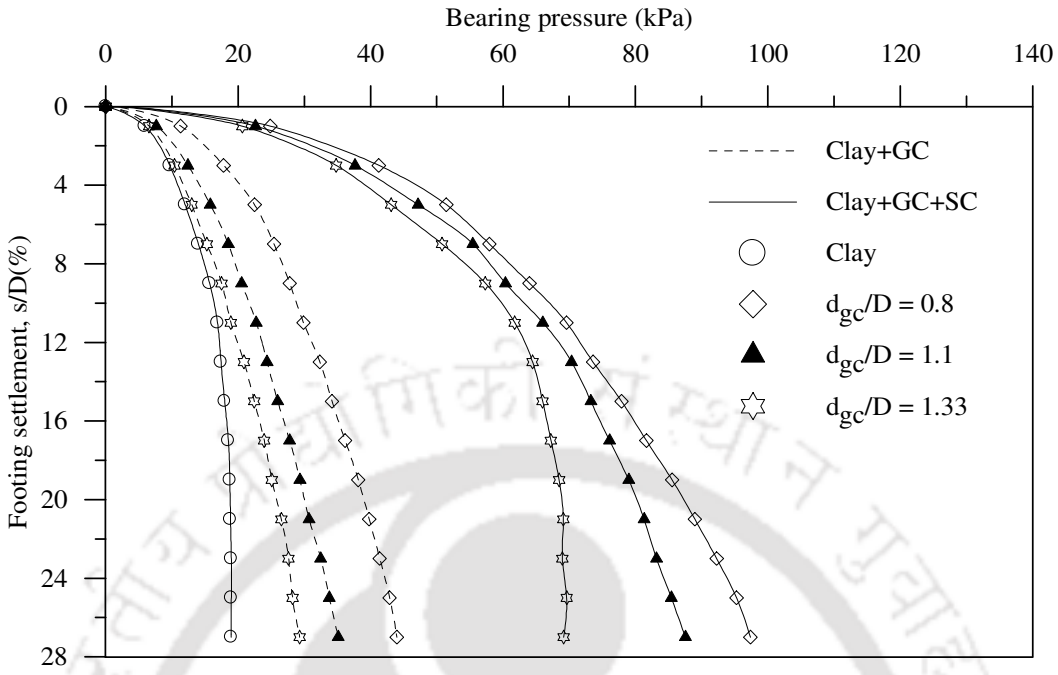

Fig.6.74: Variation of bearing pressure with footing settlement in composite foundation bed (h/D = 0.53, L/d_{sc} = 5, S/d_{sc} = 2.5) - Test series 17

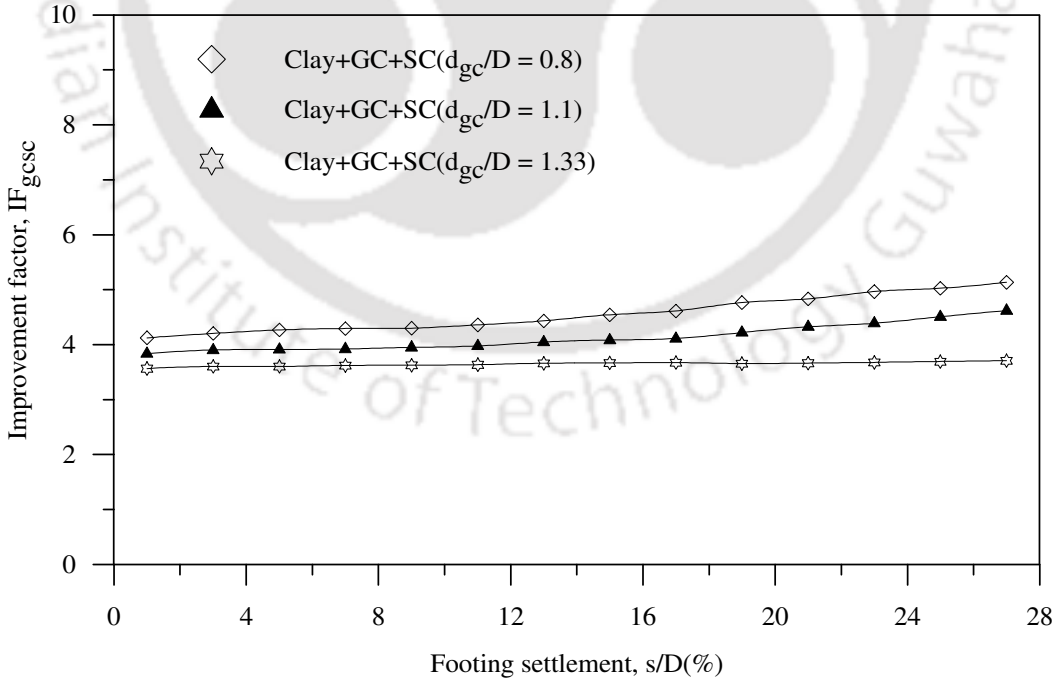

Fig.6.75: Variation of improvement factor with footing settlement in composite foundation bed (h/D = 0.53, L/d_{sc} = 5, S/d_{sc} = 2.5) – Test series 17

The settlement reduction factor depicted in Fig. 6.76 too shows much higher reduction in settlement for pocket size changing from 1.1D to 0.8D compared to that of 1.33D to 1.1D. Hence it could be said that the geocell pocket opening and the footing size should be designed such that the footing should completely cover at least one geocell pocket that the geocell reinforcement can actively participate leading to visible improvement in performance.

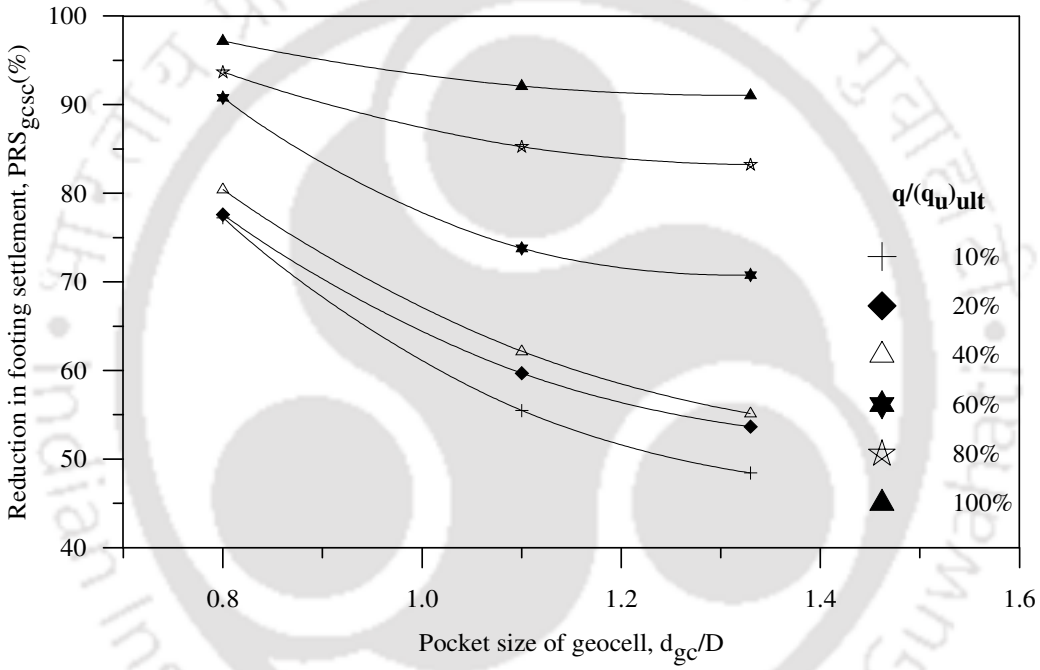

Fig.6.76: Variation of settlement reduction factor with pocket size of geocell mattress in composite foundation bed (h/D = 0.53, L/d_{sc} = 5, S/d_{sc} = 2.5) – Test series 17

Fig 6.77 shows that the share of the stone columns in sustaining the footing load (IF_{gcsc}/IF_{gc}) is the maximum for the case with geocells having the largest pocket size (1.33D). Correspondingly the contribution of geocell reinforcement is the least in this case (Fig. 6.78). With decrease in pocket size of geocells the contribution of stone columns is found to have reduced and that of geocell mattress has increased. This is because with reduced pocket size due to increased rigidity as well as anchorage resistance of the geocell system increases that it effectively bridges over the stone

columns and thereby sustains the footing loading. In case of geocells having pocket size larger than the footing diameter, as the footing directly rests on the soil over the central stone column, the stone column shares maximum load. Indeed, in this case the IF_{gcsc}/IF_{sc} factor is close to one indicating that the load sustained by the geocell reinforcement is marginal. As the soil supporting the footing overcomes the shear resistance of the supporting soil mass and the interfacial friction resistance on the geocell walls, it punches down breaking up the geocell-soil composite structure. Since the geocells remain as passive entities, in load sharing, the footing pressure is transmitted over relatively smaller area leading to lower settlement on the fill surface (Fig. 6.79). With reduced pocket opening size, as increased number of geocell walls come under the footing, the geocell mattress transmits the footing pressure, more effectively, over a wider area leading to increased settlement on the fill surface (Fig.6.79).

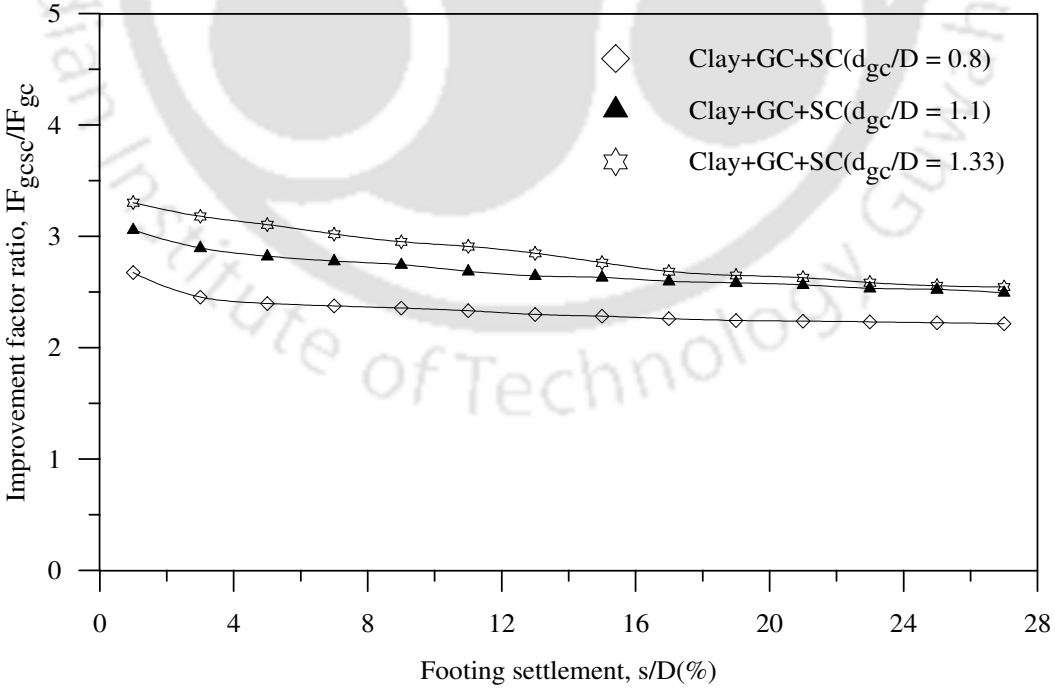

Fig.6.77: Improvement factor ratio vs. footing settlement, contribution of stone columns in composite foundation bed (h/D = 0.53, L/d_{sc} = 5, S/d_{sc} = 2.5) – Test series 17

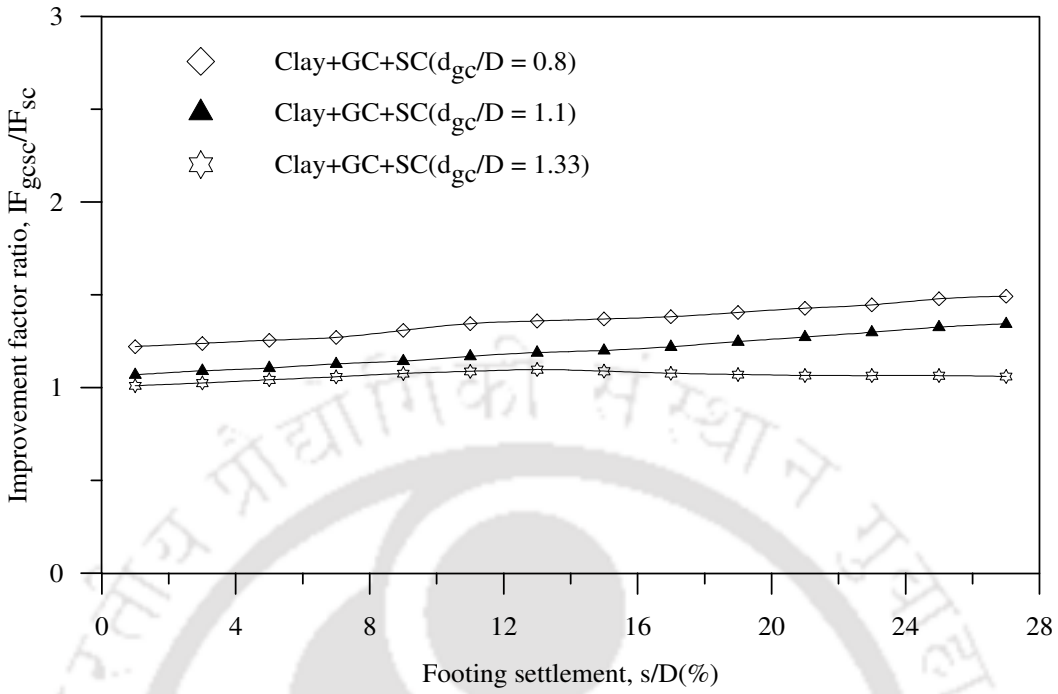

Fig.6.78: Improvement factor ratio vs. footing settlement, contribution of geocell mattress in composite foundation bed (h/D = 0.53, L/d_{sc} = 5, S/d_{sc} = 2.5) – Test series 17

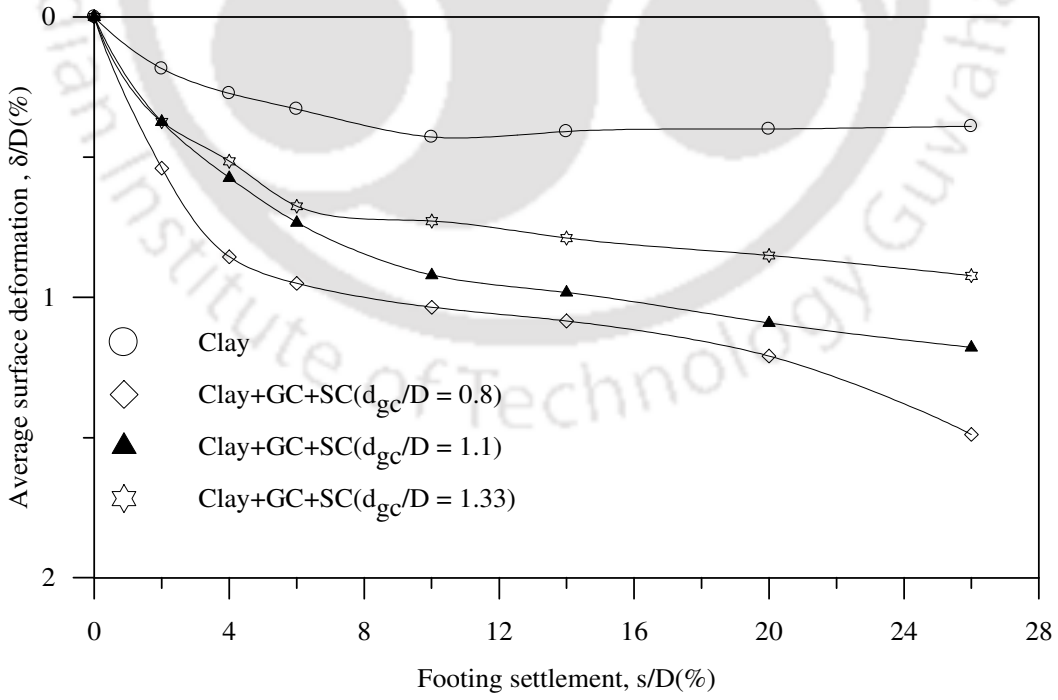

Fig.6.79: Variation of surface deformation, at x = D, with footing settlement in composite foundation bed (h/D = 0.53, L/d_{sc} = 5, S/d_{sc} = 2.5) – Test series 17

6.4.2 Height of geocell (h/D) of 0.9

The influence of pocket size of geocells on the pressure-settlement responses of the composite foundation bed with geocell mattress of 0.9D height (h) is shown in Fig. 6.80. The corresponding quantitative performance improvement (IF_{gcsc}) responses are presented in Fig. 6.81. Qualitatively, the responses are similar to the case with h = 0.53D (Fig. 6.74 and 6.75), however, quantitatively the bearing capacity improvement factor is relatively larger in the present case (h = 0.9D). This is attributed to the increased flexural rigidity of the geocell mattress due to increase in its height. Indeed the maximum contribution of the geocell reinforcement (IF_{gcsc}/IF_{sc}) with h = 0.53D, is about 1.5 (Fig.6.78) while with h = 0.9D it is more than 2 (Fig. 6.83).

The increased contribution of stone columns (IF_{gcsc}/IF_{gc}, Fig. 6.82) with increased pocket size (d_{gc}) of geocells is attributed to the increased deformations induced in the clay-stone column subgarde, under the footing penetration. With increased size of pocket openings, the geocell system turns more flexible that it deflects more and therefore transmits increased pressure onto the underlying stone columns, which in turn derives more passive resistance from the surrounding soil leading to increased performance improvement. Indeed the increased bulging in stone columns with increased pocket size of geocells, as shown in Fig.6.84 and Fig. 6.85, establishes that the stone columns have shared higher magnitude of surcharge loading.

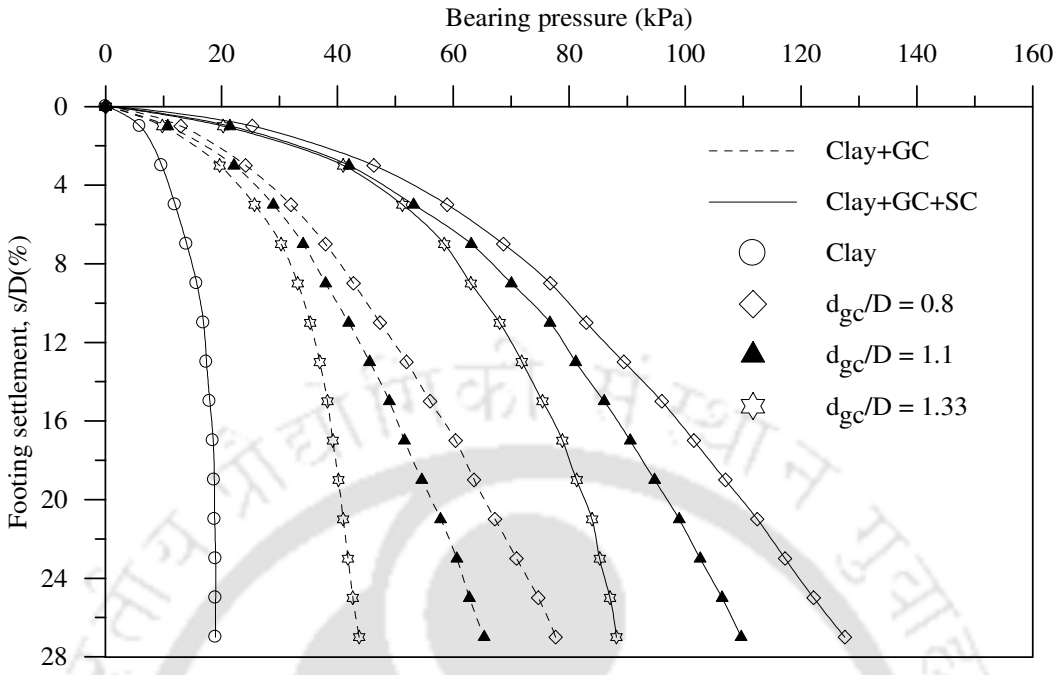

Fig.6.80: Variation of bearing pressure with footing settlement in composite foundation bed (h/D = 0.9, L/d_{sc} = 5, S/d_{sc} = 2.5) - Test series 18

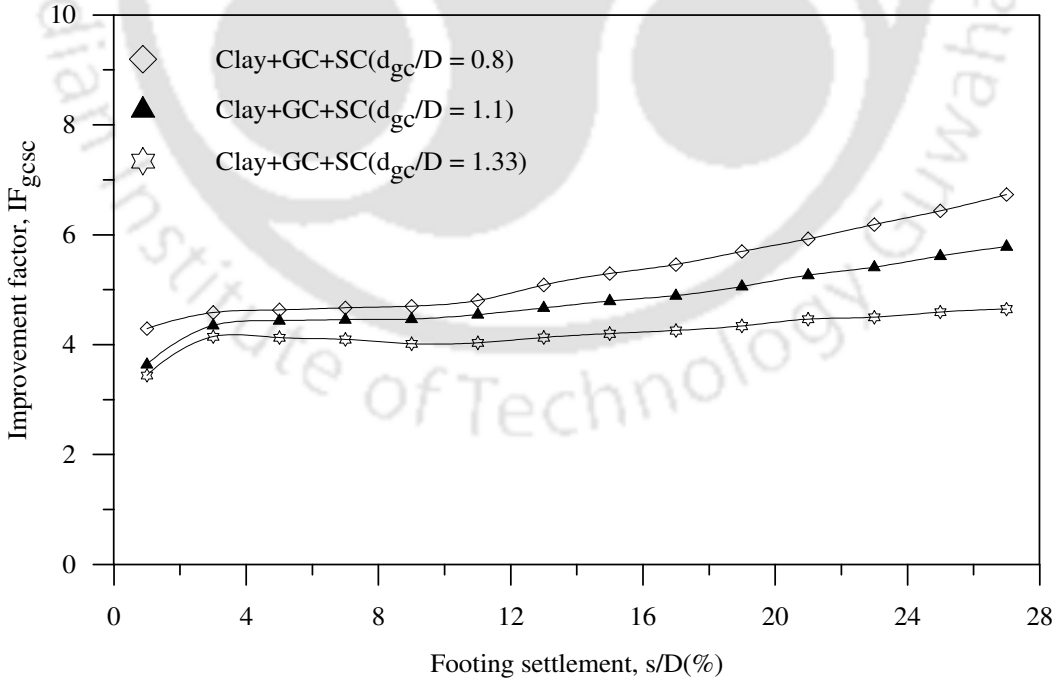

Fig.6.81: Variation of improvement factor with footing settlement in composite foundation bed (h/D = 0.9, L/d_{sc} = 5, S/d_{sc} = 2.5) – Test series 18

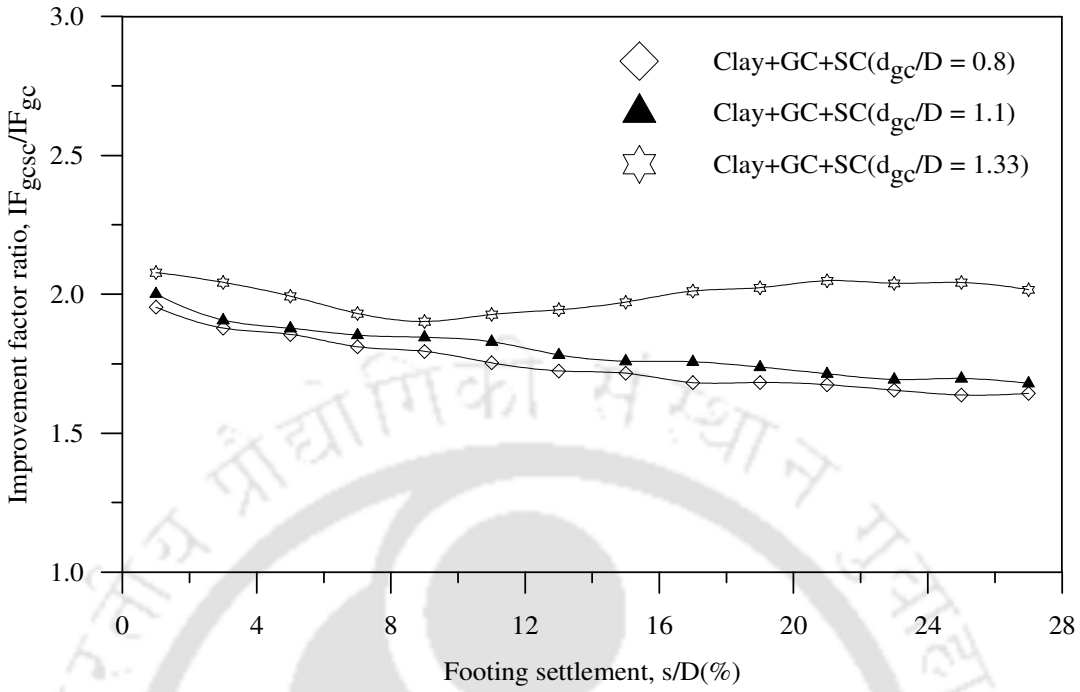

Fig.6.82: Improvement factor ratio vs. footing settlement, contribution of stone columns in composite foundation bed (h/D = 0.9, L/d_{sc} = 5, S/d_{sc} = 2.5) – Test series 18

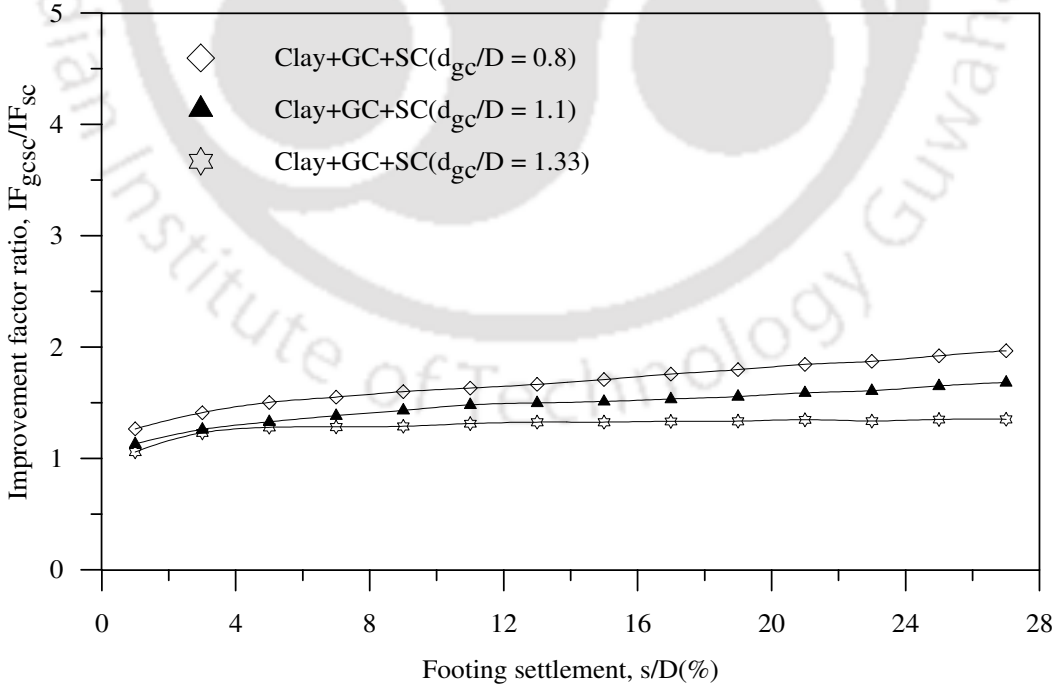

Fig.6.83: Improvement factor ratio vs. footing settlement, contribution of geocell mattress in composite foundation bed (h/D = 0.9, L/d_{sc} = 5, S/d_{sc} = 2.5) – Test series 18

(a) $d_{gc}/D = 0.8$ (b) $d_{gc}/D = 1.1$ (c) $d_{gc}/D = 1.33$

Fig. 6.84: Post-test deformed shape of central stone columns in composite foundation bed (h/D = 0.9, L/d_{sc} = 5, S/d_{sc} = 2.5) – Test series 18

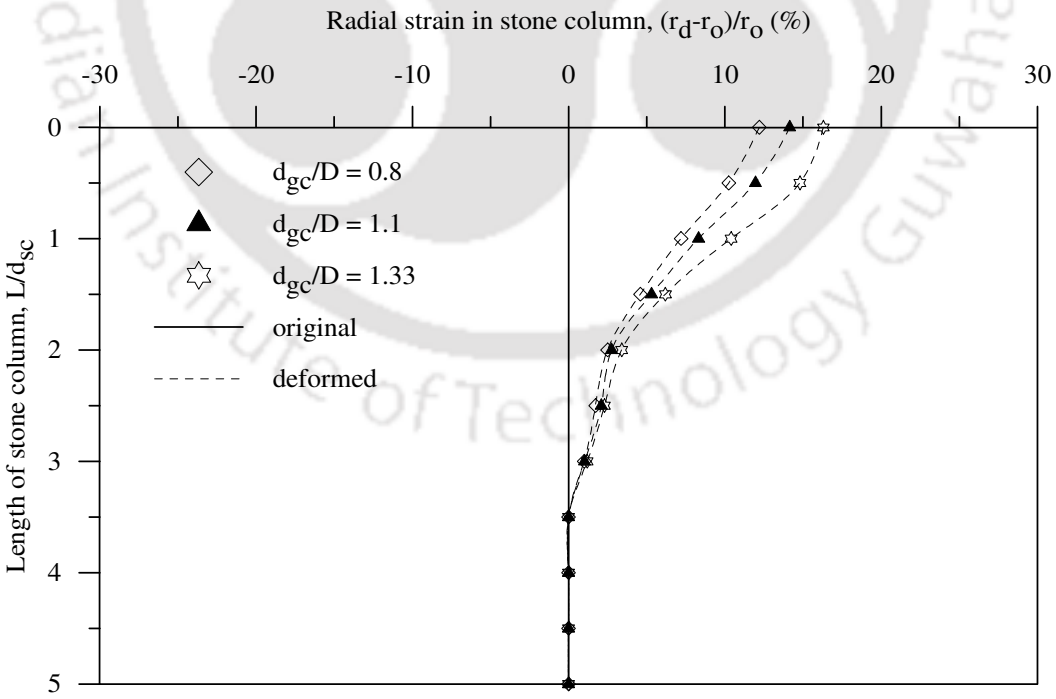

Fig.6.85: Radial strain in central stone column in composite foundation beds (h/D = 0.9, L/d_{sc} = 5, S/d_{sc} = 2.5) – Test series 18

6.5 EFFECT OF DENSITY OF INFILL SOIL (ID)

The influence of relative density (ID) of the infill sand in geocells, on the response of the composite foundation bed has been studied for two different heights of geocell mattress (i.e. h = 0.53D and h = 0.9D). The tests were carried out for relative densities of 35%, 50% and 80% (test series 19 and 20, Table 3.1). In all these tests the pocket size (d_{gc}) of geocells was kept as 0.8D and the length (L) and spacing (S) of the stone columns was kept as $5d_{sc}$ and $2.5d_{sc}$ respectively. The depth of placement (u) of the geocell layer, below the footing, was kept constant as 0.1D. The obtained results are presented and discussed separately for the two different heights in the following sections.

6.5.1 *Height of geocell mattress (h/D) of 0.53*

Fig. 6.86 illustrates the bearing pressure settlement responses of the footing for loose (ID = 35%), medium dense (ID = 50%) and dense (ID = 80%) sand in the geocells (h = 0.53D), for cases with and without stone columns in the underlying clay bed. The quantification of the performance improvement in terms of the factors IF_{gcsc} and PRS_{gcsc} is shown in Fig. 6.87 and 6.88 respectively.

It could be observed that the performance improvement, both in terms of increase in bearing capacity (IF_{gcsc}) and reduction in settlement (PRS_{gcsc}), increases with increase in density of fill soil in the geocells. Under footing penetration induced deformation the dense soil tends to expand, due to dilation. However, the three dimensional confinement of the geocells tend to suppress this volume expansion. Such an action, in turn, mobilizes higher strength in the geocell reinforcement leading to increased confinement to the encapsulated soil. As a result of which a better coherent geocell-soil structure is formed that redistributes the footing pressure more uniformly onto the

underlying clay subgrade, giving rise to increased load carrying capacity of the foundation system. Indeed Fig. 6.90 shows that the mobilized strength of geocell mattress (IF_{gcsc}/IF_{sc}) is the highest with dense soil. Fig. 6.89 shows that the contribution of stone columns (IF_{gcsc}/IF_{gc}) is the maximum, in case of loose soil in the geocells. With loose soil infill, the geocell mattress behaves as a flexible member that it undergoes increased deflection under footing loading, thereby, induces higher deformation in the underlying stone columns. With increased deformation the stone columns mobilize increased passive resistance from the surrounding soil and thereby sustain higher surcharge loading. The surface deformation responses shown in Fig. 6.91 are in good aggrement with the proposed mechanism that the geocell mattress with loose soil, being flexible is unable to transmit the footing pressure over larger area, leading to lower settlement in the region around.

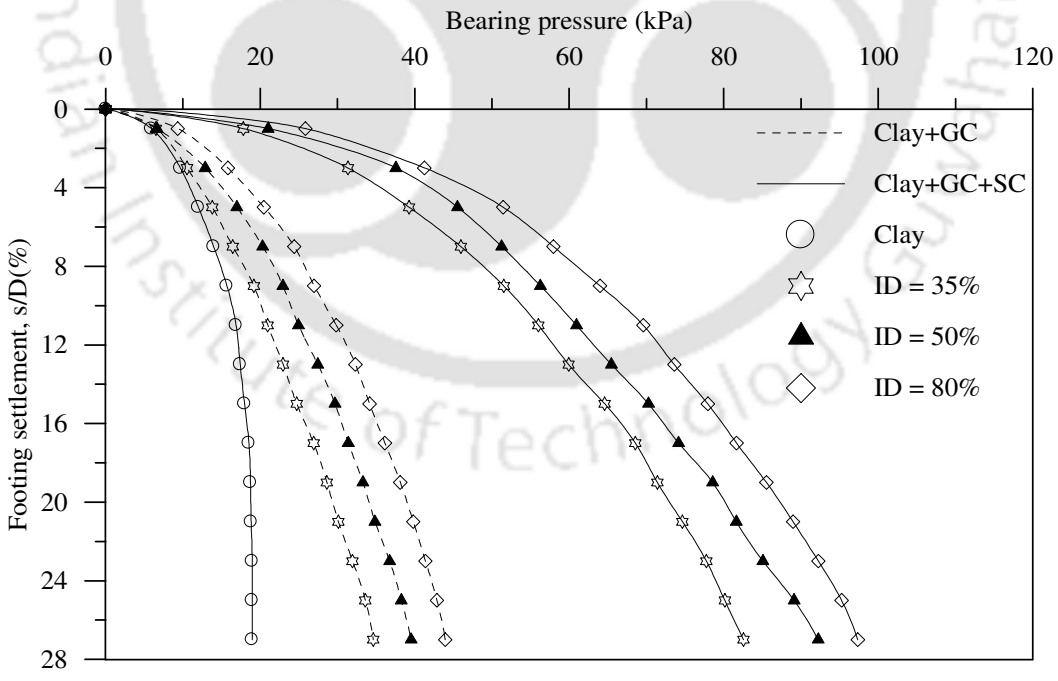

Fig.6.86: Variation of bearing pressure with footing settlement in composite foundation bed (h/D = 0.53, L/d_{sc} = 5, S/d_{sc} = 2.5) - Test series 19

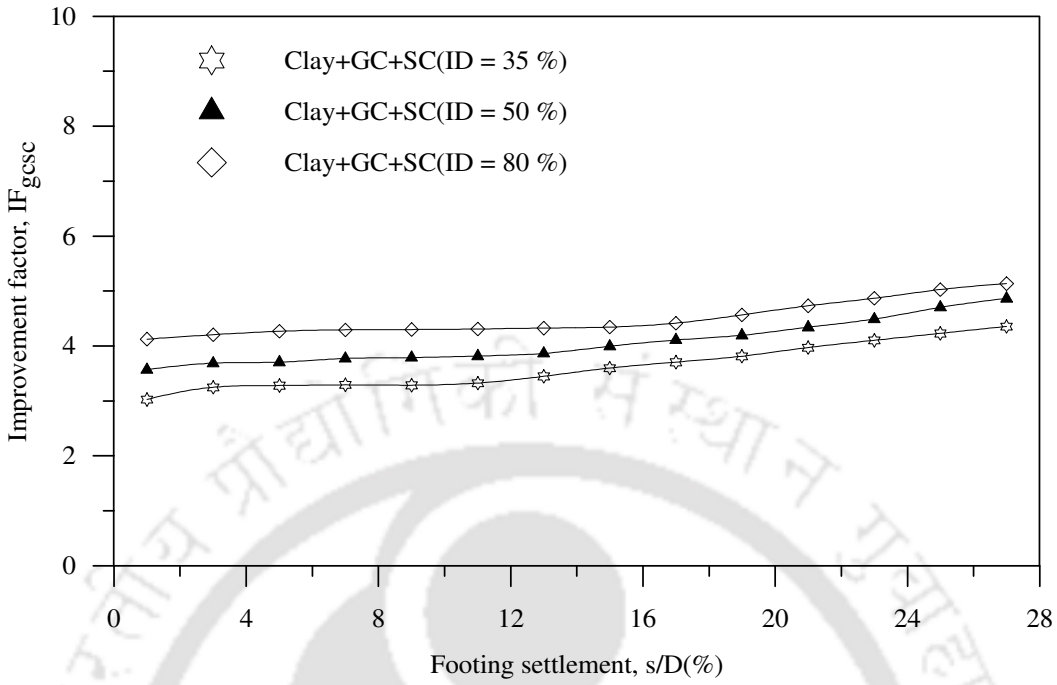

Fig.6.87: Variation of improvement factor with footing settlement in composite foundation bed (h/D = 0.53, L/d_{sc} = 5, S/d_{sc} = 2.5) – Test series 19

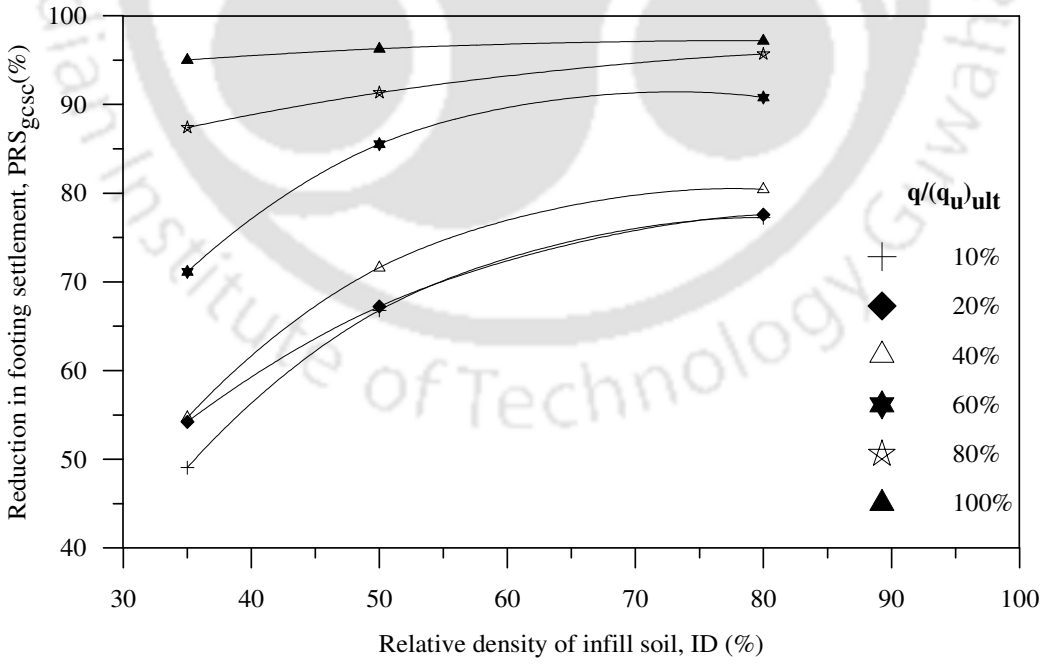

Fig.6.88: Variation of settlement reduction factor with relative density of infill soil in composite foundation bed (h/D = 0.53, L/d_{sc} = 5, S/d_{sc} = 2.5) – Test series 19

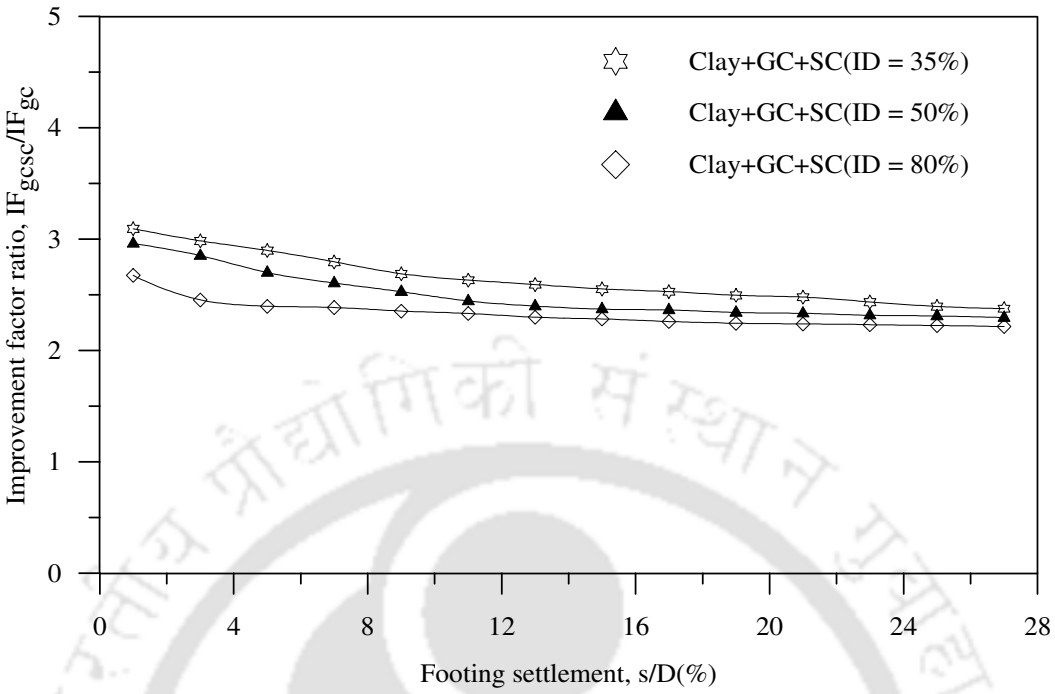

Fig.6.89: Improvement factor ratio vs. footing settlement, contribution of stone columns in composite foundation bed (h/D = 0.53, L/d_{sc} = 5, S/d_{sc} = 2.5) – Test series 19

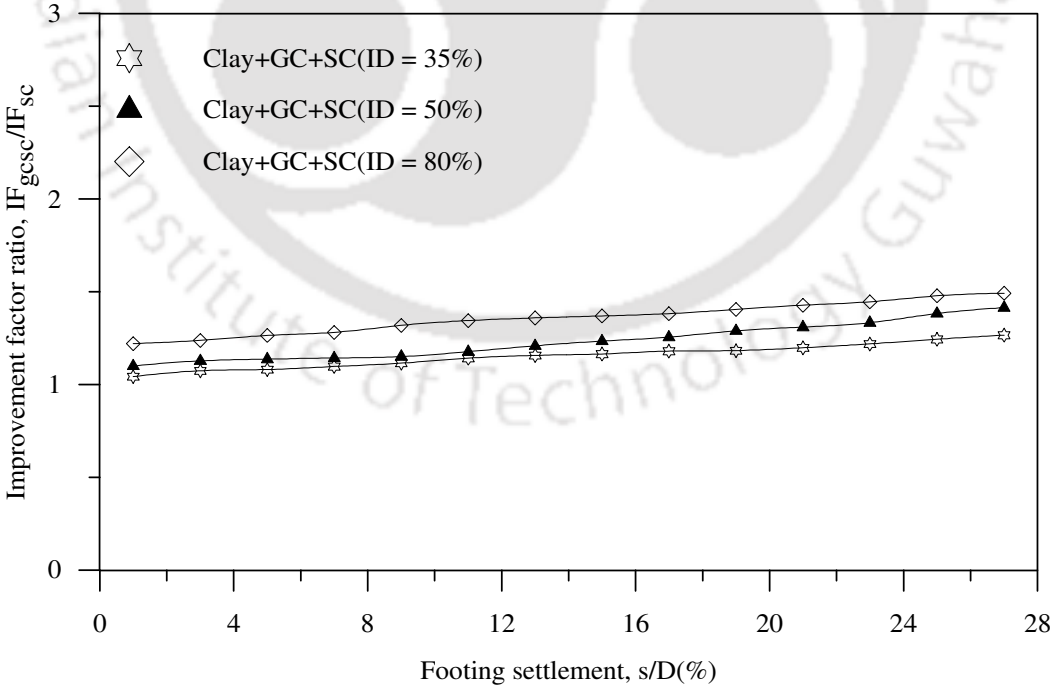

Fig.6.90: Improvement factor ratio vs. footing settlement, contribution of geocell mattress in composite foundation bed (h/D = 0.53, L/d_{sc} = 5, S/d_{sc} = 2.5) – Test series 19

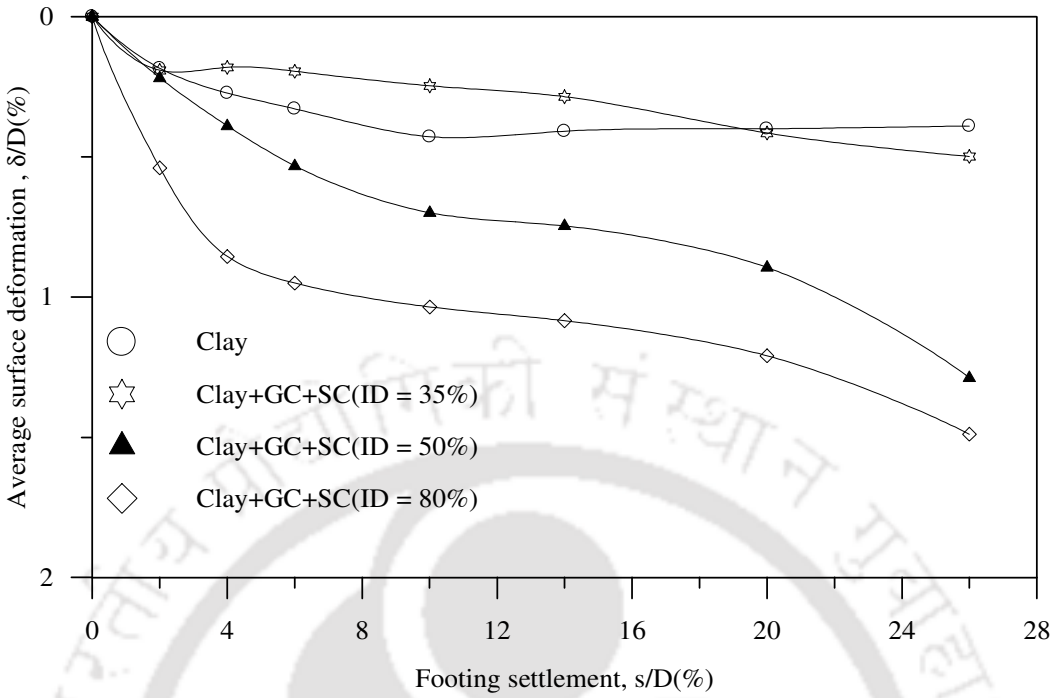

Fig.6.91: Variation of surface deformation, at x = D, with footing settlement in composite foundation bed (h/D = 0.53, L/d_{sc} = 5, S/d_{sc} = 2.5) – Test series 19

6.5.2 Height of geocell mattress (h/D) of 0.9

The influence of relative density of the soil fill in geocells, on the overall performance improvement of the composite foundation system with h = 0.9D, is depicted in Fig. 6.92 and Fig. 6.93. In comparison to the case with h = 0.53D, the quantitative improvement in bearing capacity is higher with h = 0.9D. This is because, in case of geocells having higher height (h), the cumulative frictional resistance at the geocell wall-soil interface is higher that the resistance against downward penetration of the encapsulated soil is more, leading to overall increase in performance improvement of the system.

The trend of increase in performance improvement with increase in relative density of the infill soil too has manifested in this case (h = 0.9D) as that with h = 0.53D. However, the contribution of stone columns (Fig.6.94), is nearly same irrespective of

the density of the fill soil. This is attributed to two different reasons. First, the geocells being of higher height sustain a larger portion of the footing loading and transmit relatively less to the stone columns lying below. Second, the stone columns being at a larger depth away from the base of the footing remain largely inactive. However, with increased settlement when the geocells start deforming the stone columns are subjected to increased deformation. This effect is relatively more in case of geocell mattress with loose soil infill. As a result, relatively higher contribution of the stone columns is mobilized, as reflected in the responses shown in Fig. 6.94. However, the difference is marginal as the geocells, owing to their increased height, have carried substantially higher portion of the footing load (Fig. 6.95). Increased strain in stone column incase with loose soil fill in geocells (Fig. 6.96), establishes that the stone columns have shared higher proportion of the surcharge loading.

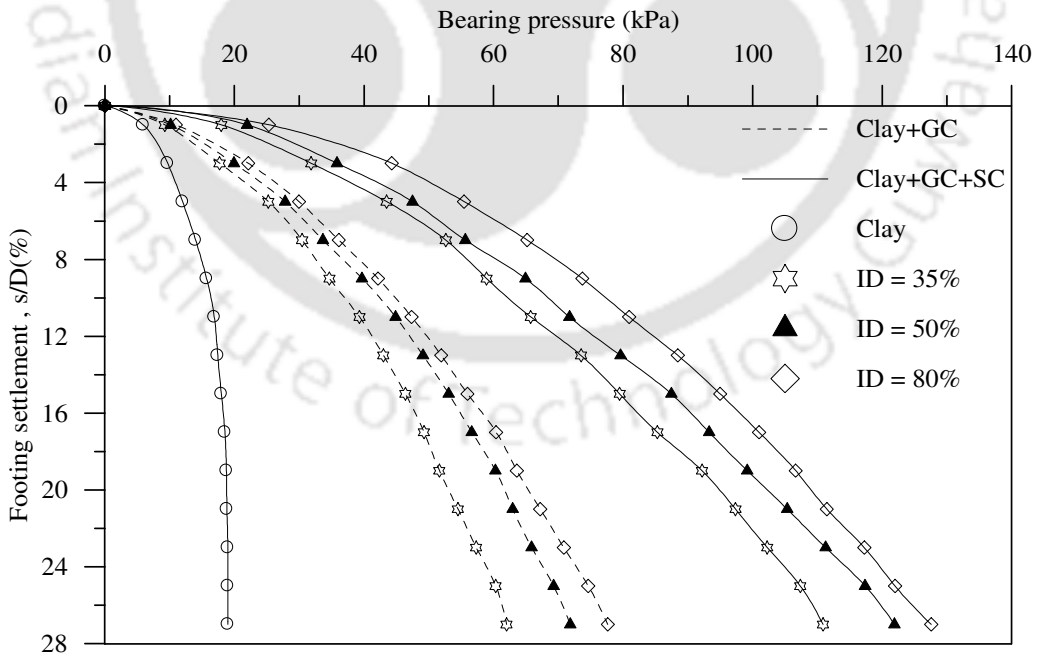

Fig.6.92: Variation of bearing pressure with footing settlement in composite foundation bed (h/D = 0.9, L/d_{sc} = 5, S/d_{sc} = 2.5) - Test series 20

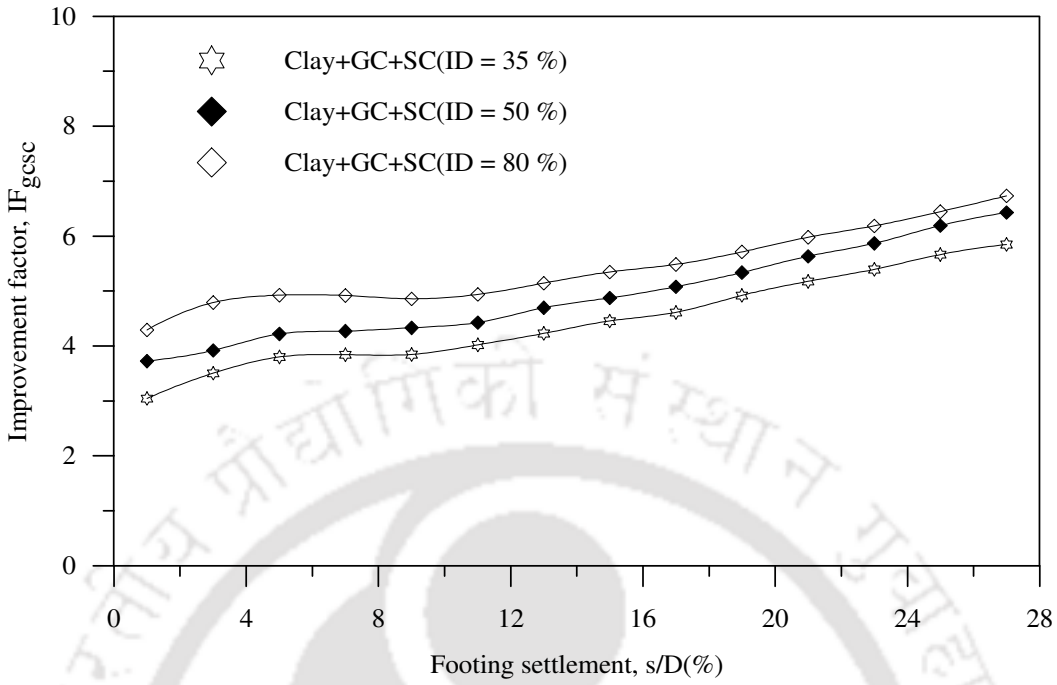

Fig.6.93: Variation of improvement factor with footing settlement in composite foundation bed (h/D = 0.9, L/d_{sc} = 5, S/d_{sc} = 2.5) – Test series 20

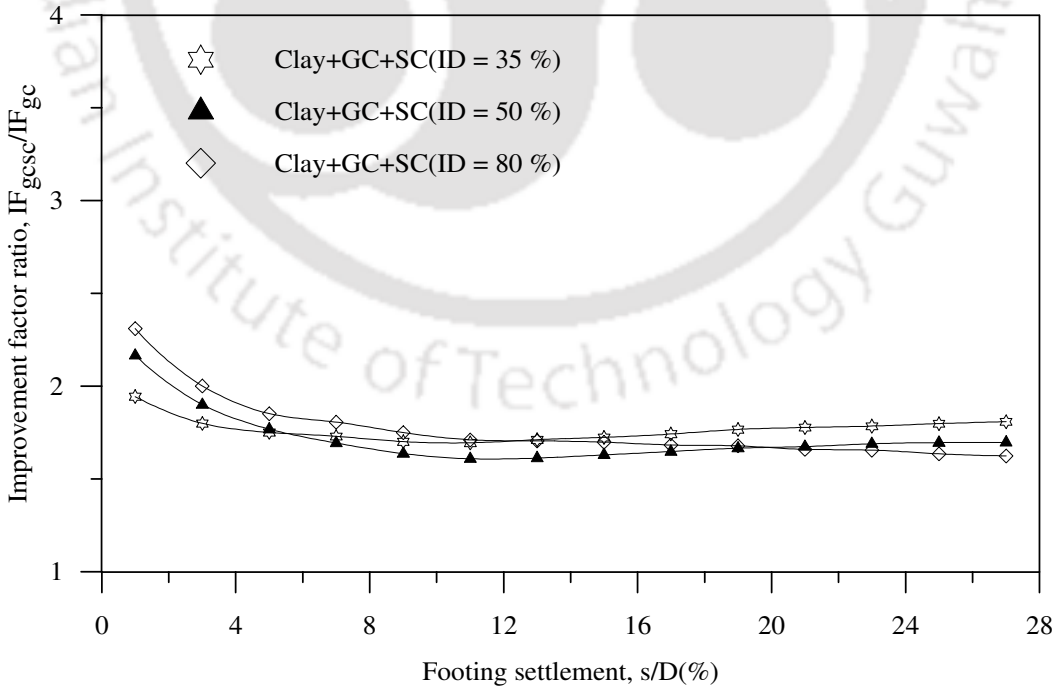

Fig.6.94: Improvement factor ratio vs. footing settlement, contribution of stone columns in composite foundation bed (h/D = 0.9, L/d_{sc} = 5, S/d_{sc} = 2.5) – Test series 20

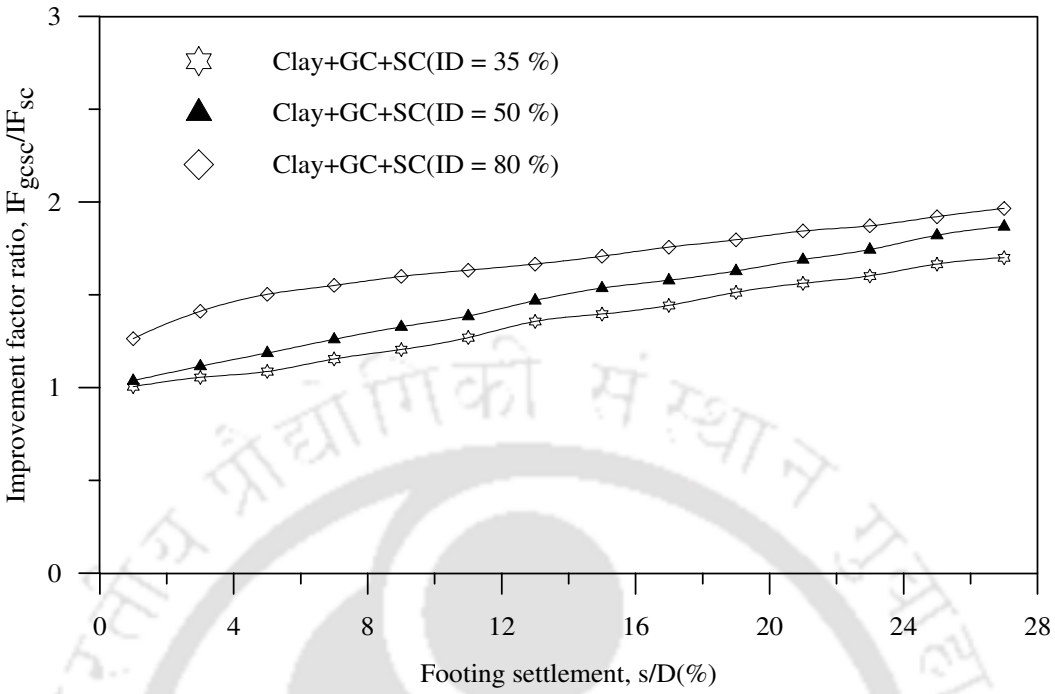

Fig.6.95: Improvement factor ratio vs. footing settlement, contribution of geocell mattress in composite foundation bed (h/D = 0.9, L/d_{sc} = 5, S/d_{sc} = 2.5) – Test series 20

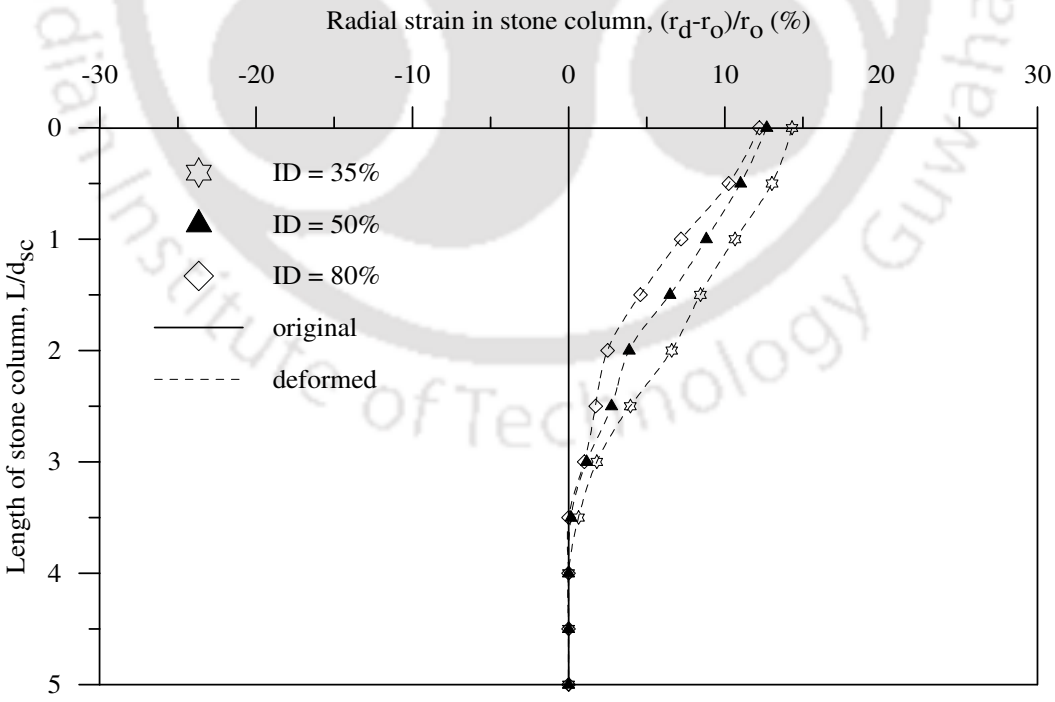

Fig. 6.96: Radial strain in central stone column in composite foundation beds (h/D = 0.9, L/d_{sc} = 5, S/d_{sc} = 2.5) – Test series 20

CHAPTER 7

GEOCELL MATTRESS-BASE GEOGRID-ENCASED STONE COLUMN REINFORCED CLAY BED

7.1 INTRODUCTION

In the previous chapters, it has been established that the geocell mattress-stone column composite reinforcement can provide remarkably high performance improvement in the clay foundation. In the literature (Ch. 2) it has been reported that a layer of planer geogrid at the base of geocell mattress can enhance the performance of the geocell mattress system. Similarly encasing of individual stone columns can produce increased performance improvement. In view of this it was envisaged that an additional layer of planer geogrid at the base of geocell mattress and encasement of stone columns would further enhance the performance of the geocell–stone column reinforced foundation system. This motivated to undertake five series of tests (Test series 21-25, Table 3.1, Ch. 3), the aim of which was to understand the influence of base geogrid and stone column encasement in the performance of the composite foundation bed. In all these tests the length and spacing of stone columns were kept as $5d_{sc}$ and $2.5d_{sc}$ respectively while the pocket size of geocells and relative density of infill soil was kept as 0.8D and 80% respectively. The depth of placement of the geocell layer from the base of the footing was kept as 0.1D. The obtained results are presented and discussed in the following sections.

7.2 EFFECT OF BASE GEOGRID

The influence of basal geogrid was studied for two different heights of geocell mattress (h = 0.53D and 0.9D) in the composite foundation bed. It should be mentioned here that for these two heights (h) of geocell mattress, the influence of

stone columns in the underlying clay subgrade, is prominent over the performance of the foundation bed as brought out in Chapter 6. The pressure settlement responses for these two cases (h = 0.53D and 0.9D) with and without base geogrid in the composite foundation bed are presented in Fig. 7.1. It could be observed that provision of an additional layer of geogrid at the base of geocell mattress, in the geocell-stone column composite foundation system, can further improve the performance of the foundation bed both in terms of increase in bearing capacity and reduction in settlement. The cumulative improvement in bearing capacity of the clay bed due to geocell-stone column-base geogrid reinforcements (IF_{gcscbg}) is summerised in Fig. 7.2. The bearing capacity improvement factor, IF_{gcscbg}, is defined as the ratio of bearing pressure with geocell-stone column-base geogrid reinforcement (q_{gcscbg}) to the bearing pressure (q_u) with unreinforced clay bed, both taken at equal settlement.

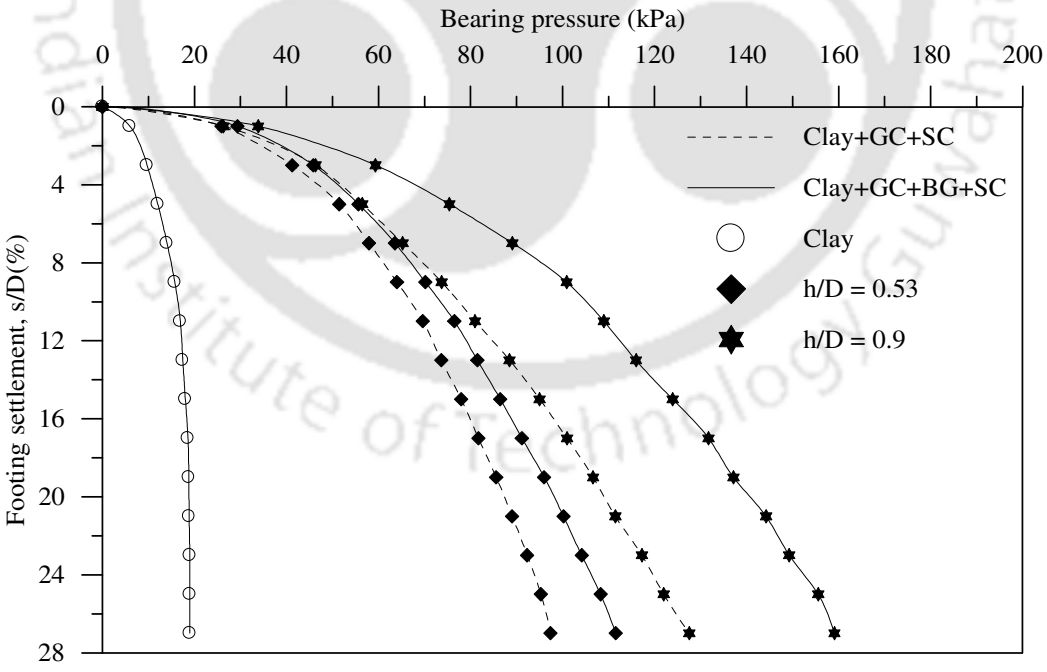

Fig.7.1: Variation of bearing pressure with footing settlement for composite foundation bed with base geogrid (L/d_{sc} = 5, S/d_{sc} =2.5, ID = 80%) – Test series 21

From fig.7.2, it could be observed that the performance improvement factor, with basal geogrid, for h = 0.53D and 0.9D, is as high as 5.7 and 8.5, while without the basal geogrid it (IF_{gcsc}) it was only about 5 and 6.5 respectively (Fig. 6.4, Fig. 6.18; L/d_{sc} = 5). Indeed the contribution of the base geogrid in the performance improvement, represented through the factor IF_{gcscbg}/IF_{gcsc} (Fig. 7.3), is about 1.1 for h = 0.53D and 1.3 for h = 0.9D. Hence a layer of planar geogrid at the interface between the geocell mattress and stone column reinforced clay bed can bring an improvement in bearing capacity as high as 30% more than the that with geocell-stone column alone.

It is of interest to note that, compared to the case with geocell mattress of shallow height (h = 0.53D), the basal geogrid induced increase in bearing capacity is higher in case of relatively deeper geocell mattress (h = 0.9D). This is attributed to the influence of stone columns. When placed at shallow depth (h = 0.53D) the stone columns share a substantially high proportion of the footing loading. As a result of which the basal geogrid remains relatively dormant leading to lower contribution in the performance improvement of the foundation system. While at relatively larger depth (h = 0.9D) major portion of the stone columns being outside the stressed zone, the basal geogrid shares a relatively larger portion of the surcharge load getting transmitted through the geocell mattress.

The other possible reason is the anchorage derived by the basal geogorid. The geocell mattress of shallow height gets pulled down and therefore unable to provide adequate anchorage to the base geogrid. But the geocell mattress of larger height being stable offers large anchorage to the base geogrid that the base geogrid effectively stands against footing penetration induced settlement leading increased contribution in the performance improvement.

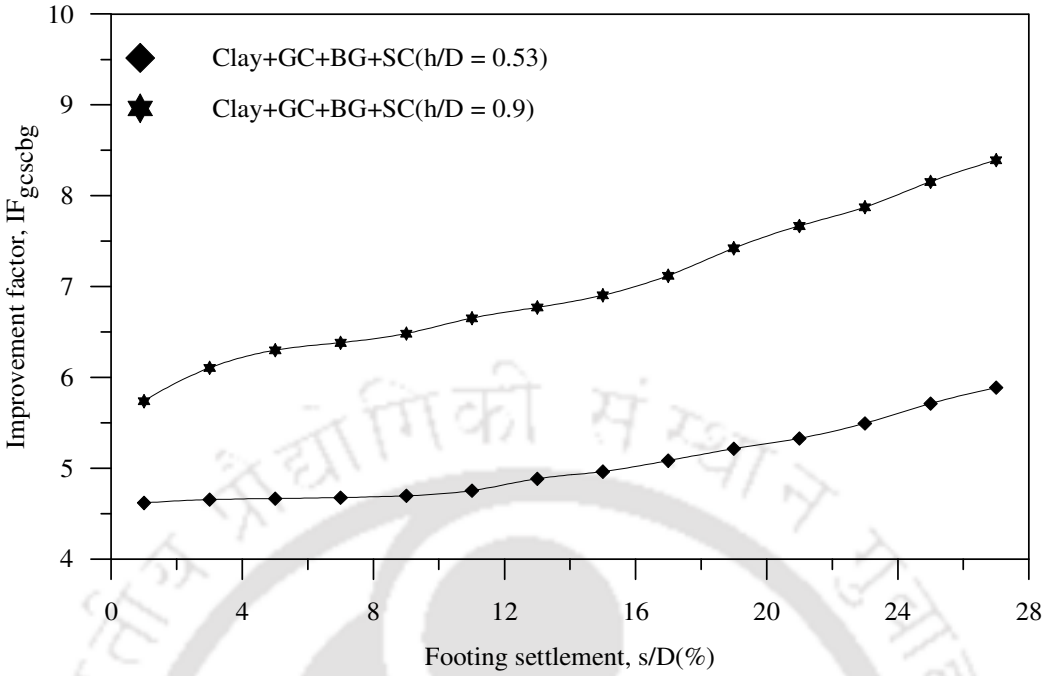

Fig.7.2: Variation of Improvement factor with footing settlement for composite foundation bed with base geogrid – Test series 21

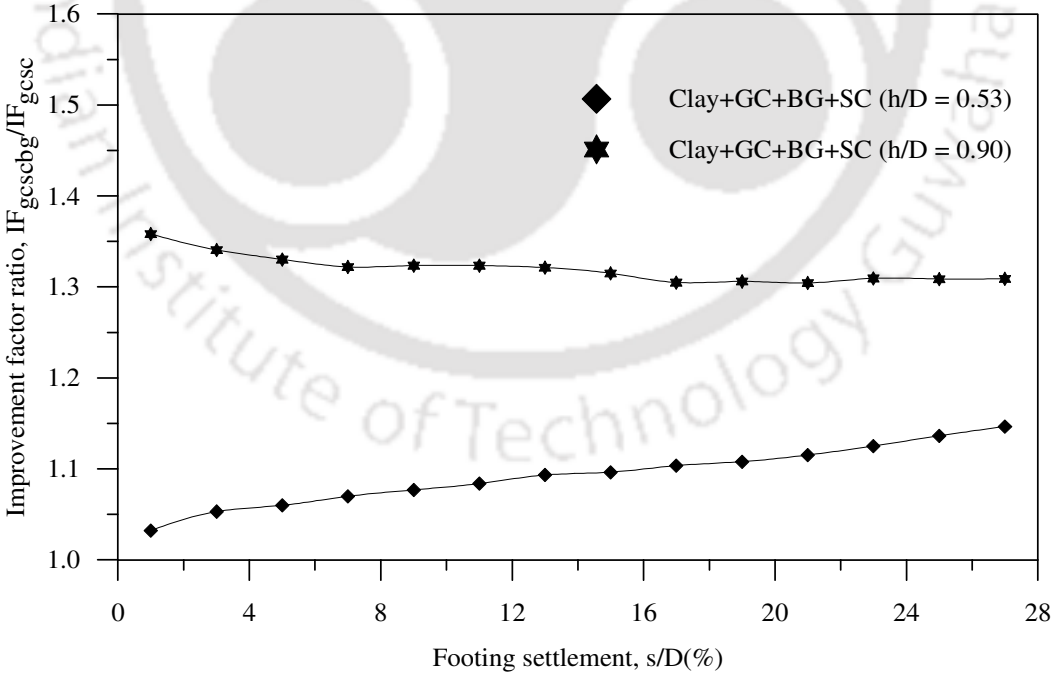

Fig.7.3: Variation of Improvement factor ratio with footing settlement for showing contribution of base geogrid in composite foundation bed– Test series 21

Fig. 7.4 shows that the settlement (at x = D) and heave (at x = 2D and 3D) on fill surface are reduced with the provision of the basal geogrid. The basal geogrid through mobilisation of its rigidity and anchorage from soil holds the geocell mattress against footing penetration that reduces the settlement near to the zone of loading (x = D). As a result of which relatively less stress is transferred to the soil below that it settles less. As this short term undrained settlement in clay bed, produces heaving in the adjacent regions, with reduction in settlement the heave too has reduced.

Fig. 7.7 shows that with the provision of basal geogrid at the geocell mattress-stone column interface, the stone columns have undergone reduced bulging. This establishes that with basal geogrid, the stress transmitted to the clay subgrade has reduced.

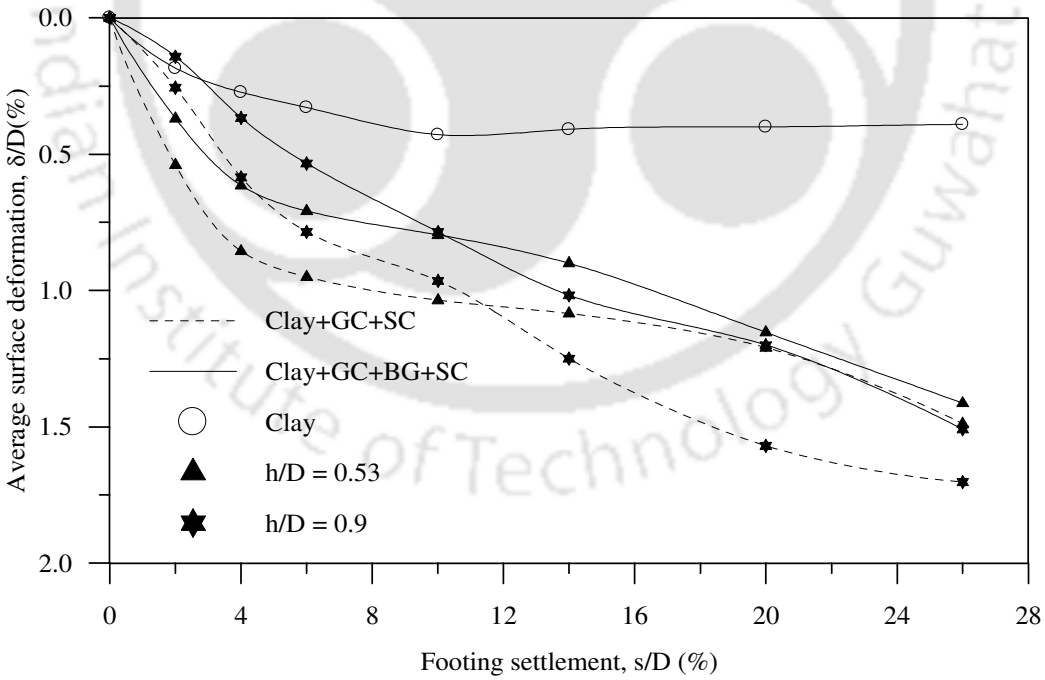

Fig.7.4: Variation of surface deformation, at x = D, with footing settlement for composite foundation bed with base geogrid -Test series 21

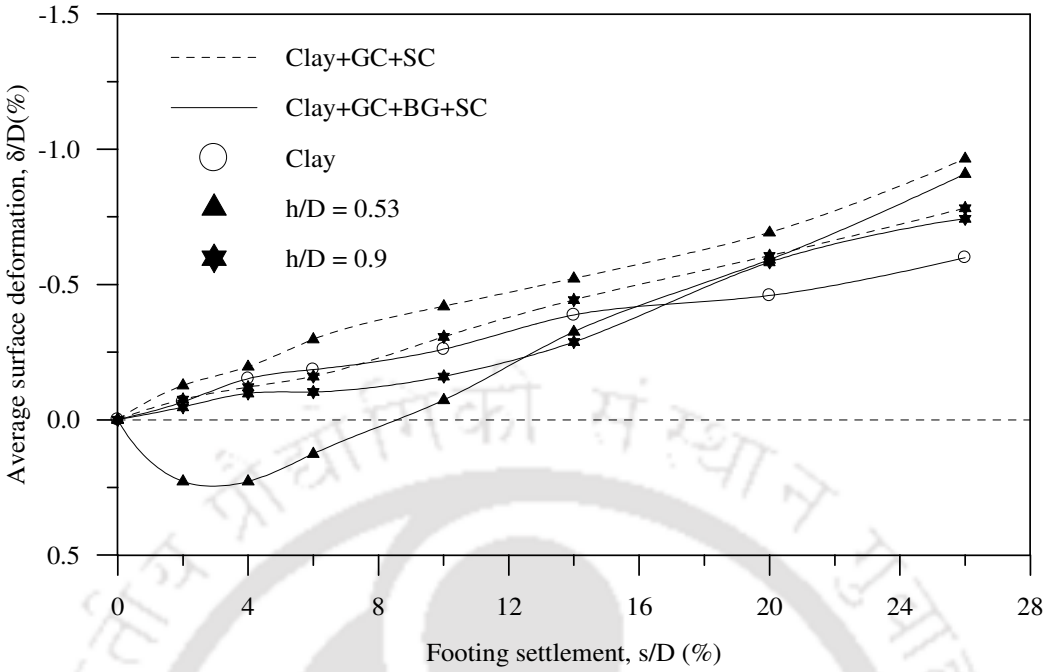

Fig.7.5: Variation of surface deformation, at x = 2D, with footing settlement for composite foundation bed with base geogrid - Test series 21

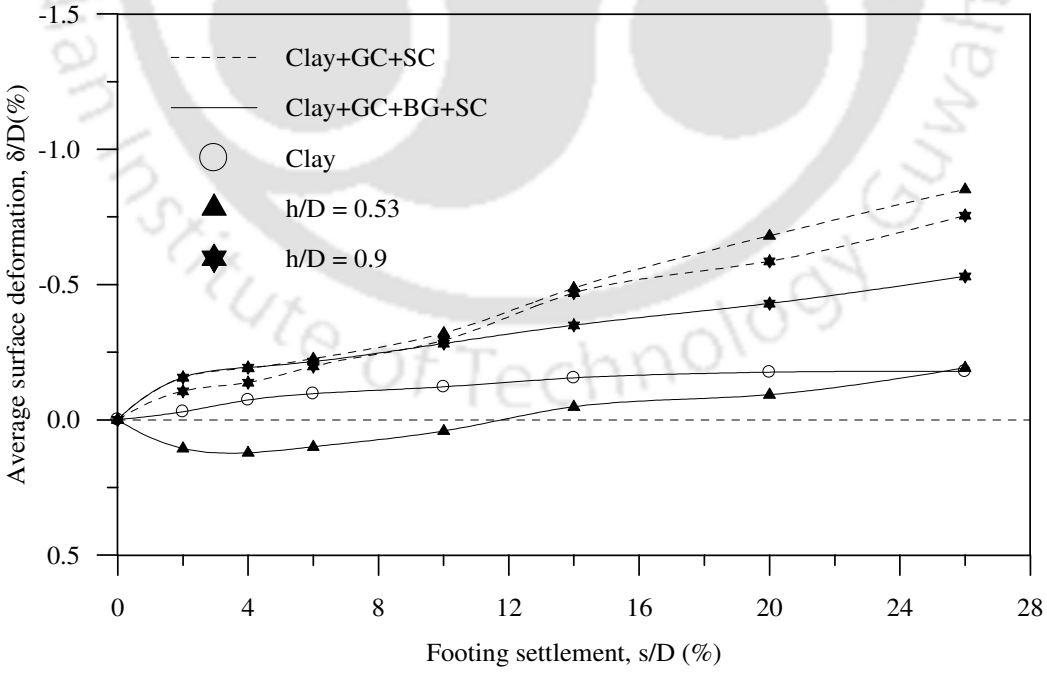

Fig.7.6: Variation of surface deformation, at x = 3D, with footing settlement for composite foundation bed with base geogrid - Test series 21

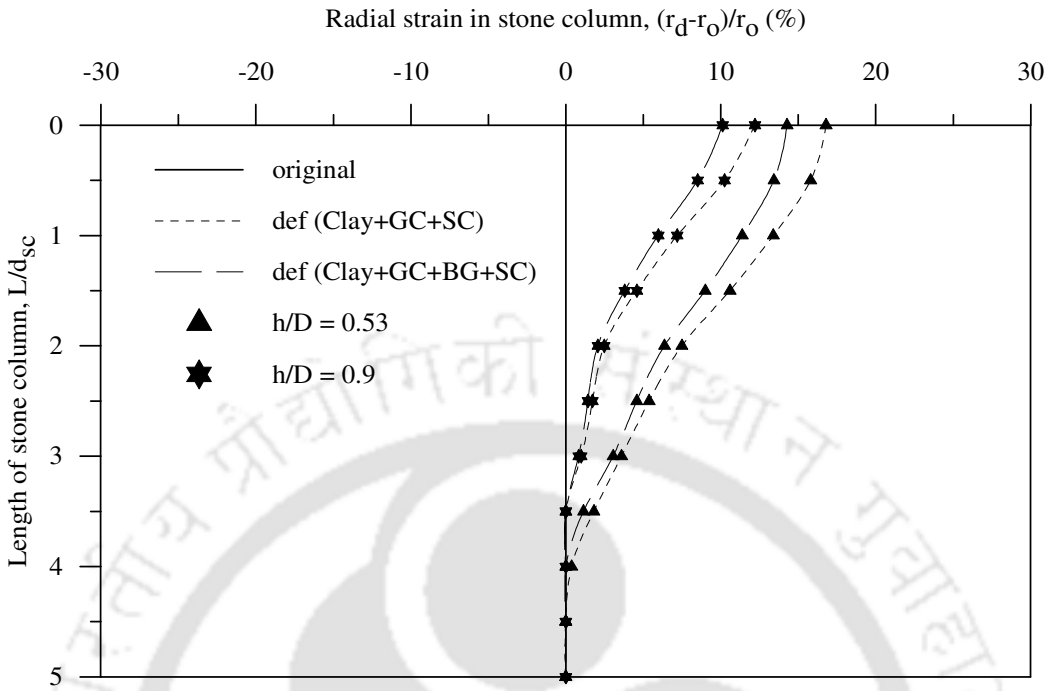

Fig.7.7: Radial strain in central stone column in composite foundation beds with base geogrid – Test series 21

7.3 EFFECT OF ENCASEMENT OF STONE COLUMNS

To understand the influence of geosynthetics encasement of stone columns, tests were carried out with encased stone column (ESC) in clay bed. The encasement length (L_{esc}) was varied as, equal to the diameter of stone column (d_{sc}), three times the diameter of stone column ($3d_{sc}$) and five times the diameter of stone column ($5d_{sc}$). Since in all these tests, the length of stone columns was kept constant as $5d_{sc}$, with encasement of $5d_{sc}$, the whole of the stone column was encased. Therefore, it is termed as fully encased stone column, ESC (full). The spacing of stone columns (S), too, was kept constant as $2.5d_{sc}$, in whole of this test program.

Subsequently, tests were carried out to study if the encasement of stone columns can bring further improvement in the performance of the composite foundation bed. These

tests were carried out for two different heights of geocell mattress (h = 0.53D and 0.9D) and stone column encasement lengths (L_{esc}) of d_{sc}, $3d_{sc}$ and full. The length (L) and spacing (S) of the stone columns were kept constant as $5d_{sc}$ and $2.5d_{sc}$ respectively. The results are presented and discussed in the following subsections.

7.3.1 Encased Stone columns in clay bed

Pressure-settlement responses of the clay beds with stone columns having varied lengths of encasement (L_{esc}) are shown in Fig. 7.8. The quantification of improvement in performance due to the encased stone columns, in terms of the bearing capacity improvement factor (IF_{esc}) and settlement reduction factor (PRS_{esc}), are brought out in Fig.7.9 and 7.10 respectively.

The factor, IF_{esc}, is defined as the ratio of bearing pressure with encased stone column at a given settlement, to the bearing pressure of clay bed alone at the same settlement. Correspondingly, PRS_{esc} is the ratio of the settlements of clay bed, with and without encased stone columns, both taken at equal bearing pressure.

It could be observed that compared to the case with the unencased stone columns (SC), the load carrying capacity of the clay bed is substantially higher with partially encased stone columns (L_{esc} = d_{sc} and $3d_{sc}$). The bearing capacity increases with increase in length of encasement. However, with fully encased stone columns (L_{esc} = full) the performance improvement has reduced substantially. In fact, the bearing pressures, in this case, are practically same as that with the unencased stone column (SC). Similar behaviour is noticed with settlement reduction (Fig. 7.10).

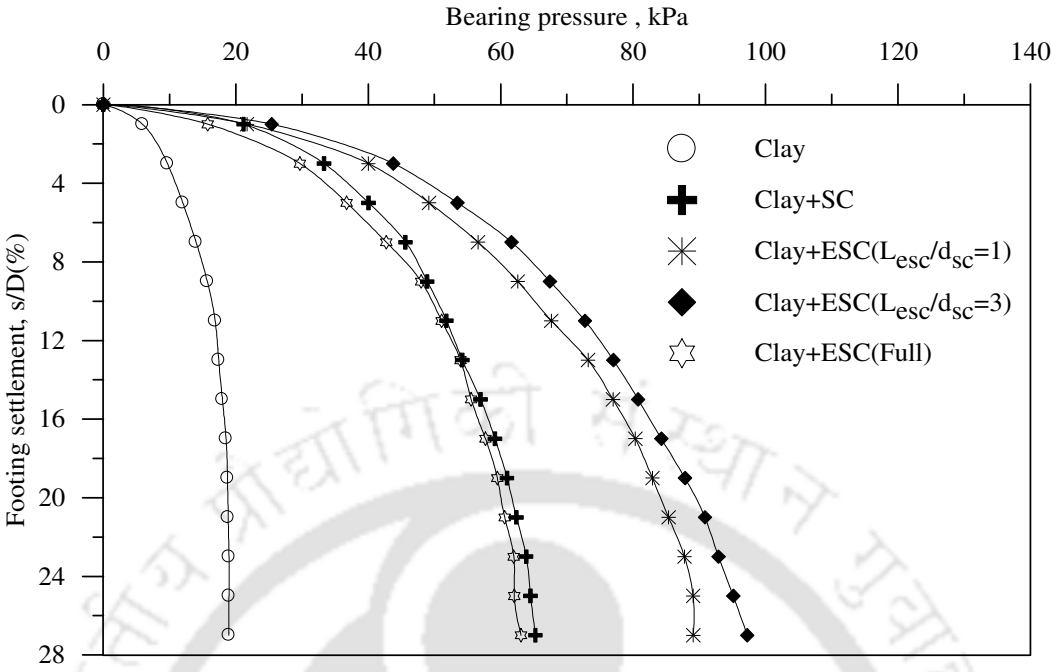

Fig.7.8: Variation of bearing pressure with footing settlement for encased stone column reinforced clay beds – Test series 22

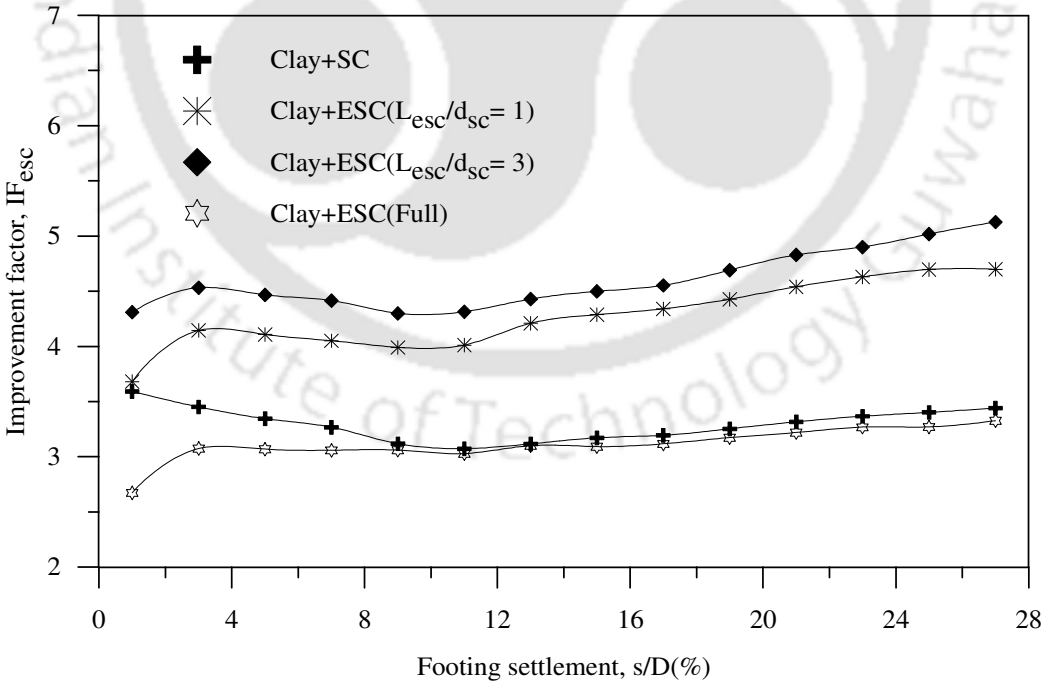

Fig.7.9: Variation of improvement factor with footing settlement for encased stone column reinforced clay beds – Test series 22

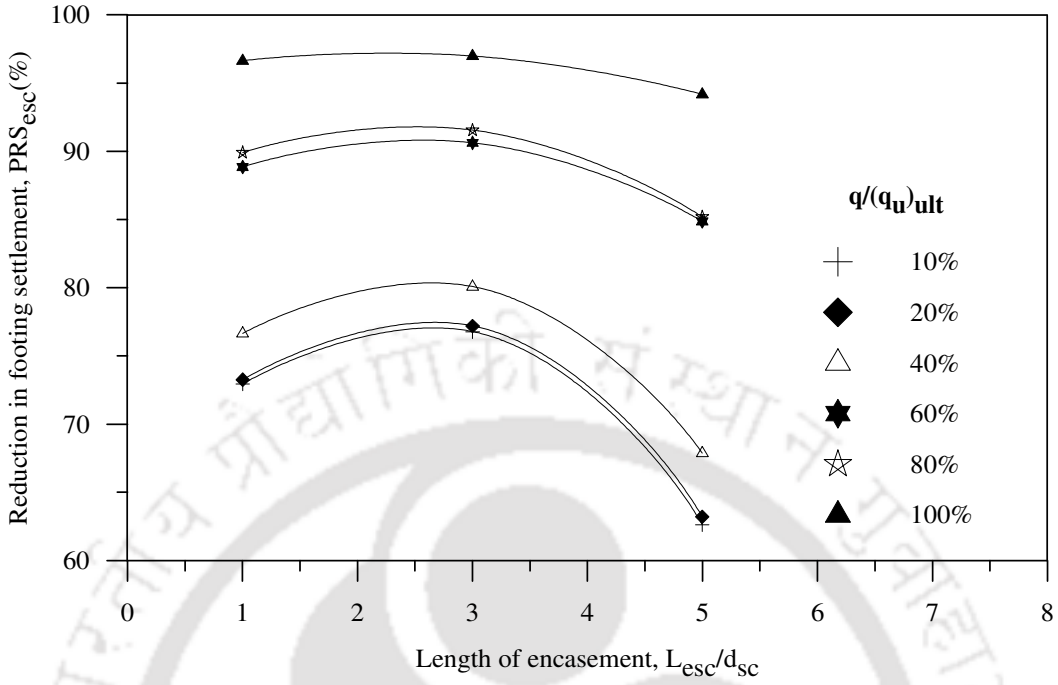

Fig.7.10: Variation of settlement reduction factor with length of encasement of stone columns – Test series 22

Fig. 7.11 shows that the fill surface, around the footing (x = D) has settled (δ) less with partially encased stone columns than that with fully encased stone columns. The reduced settlement (δ) on fill surface indicates that there is increased resistance of the foundation bed against footing loading. The results can further be analysed through the observed deformations in the post-test exhumed stone columns, shown in Fig. 7.12. It can be seen that in case of partial encasement, visible bulging has taken place in the region below the portion of encasement. The encased portion acts as a stiffened entity, that it transmits the surcharge load to the deeper zone below the encasement, leading to the bulging underneath. As the stone column now expands in the region of higher surcharge, the mobilized passive earth pressure from the soil is higher. Besides, the bulged portion serves as a bearing, that it mobilizes higher resistance

from soil, against footing loading. These two factors are believed to have produced the improved performance.

With encasement length (L_{esc}) of $3d_{sc}$, the bulge being at relatively larger depth, derives higher passive resistance from the soil leading to increased load carrying capacity than the case with encasement (L_{esc}) = $d_{sc.}$

With full encasement, the performance improvement has substantially reduced and is even less than that with unencased stone columns (Fig. 7.8). This is in contrary to the findings of Murugesan and Rajagopal (2007) in case of end bearing stone columns, wherein, full encasement has provided maximum improvement in the load carrying capacity. This is attributed to the difference in the boundary conditions. With end bearing, the fully encased stone column serves as a stiffened pile that it effectively transmits the surcharge pressure to the competent bed below, while in case of floating stone columns, as in the present investigation, the improved performance is mostly through passive pressure resistance from the surrounding soil mobilized through bulging and the interfacial shear resistance at the stone column-soil interface. Besides, the relatively smooth geosynthetics encasement reduces the interfacial shear resistance. These two factors are believed to have substantially reduced the resistance of the stone columns to stand against the applied loading. With the footing loading exceeding the limited available resistance, the stone column punches down reducing the encasement induced benefits to practically negligible value (Fig. 7.9).

Fig. 7.13 shows that the stone column, with length of encasement (L_{esc}) equal to diameter of stone column (d_{sc}) has bulged more than that having encasement length of $3d_{sc}$. This is because, in the former case (L_{esc}/d_{sc} = 1) the geosynthetics casing being of smaller length yields under the stress concentration and footing penetration induced expansion of the stone aggregates, leading to increased bulging. With increased length

of encasement, the stress concentration and footing penetration induced strains get distributed over larger area and thereby get reduced in their intensity leading to reduced bulging.

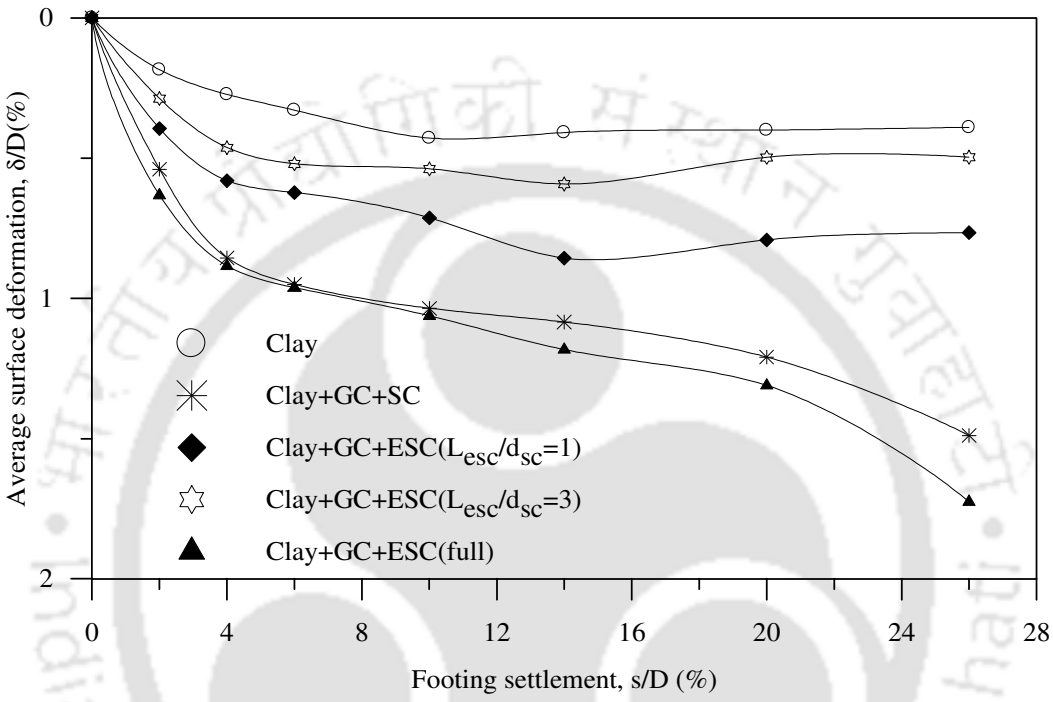

Fig.7.11: Variation of surface deformation, at x = D, with footing settlement for encased stone column reinforced clay beds - Test series 22

(a) L_{esc}/d_{sc} = 1 (b) L_{esc}/d_{sc} = 3 (c) L_{esc}/d_{sc} = full

Fig.7.12: Post test deformed shape of central stone columns with different length of encasement (L/d_{sc} = 5) – Test series 22

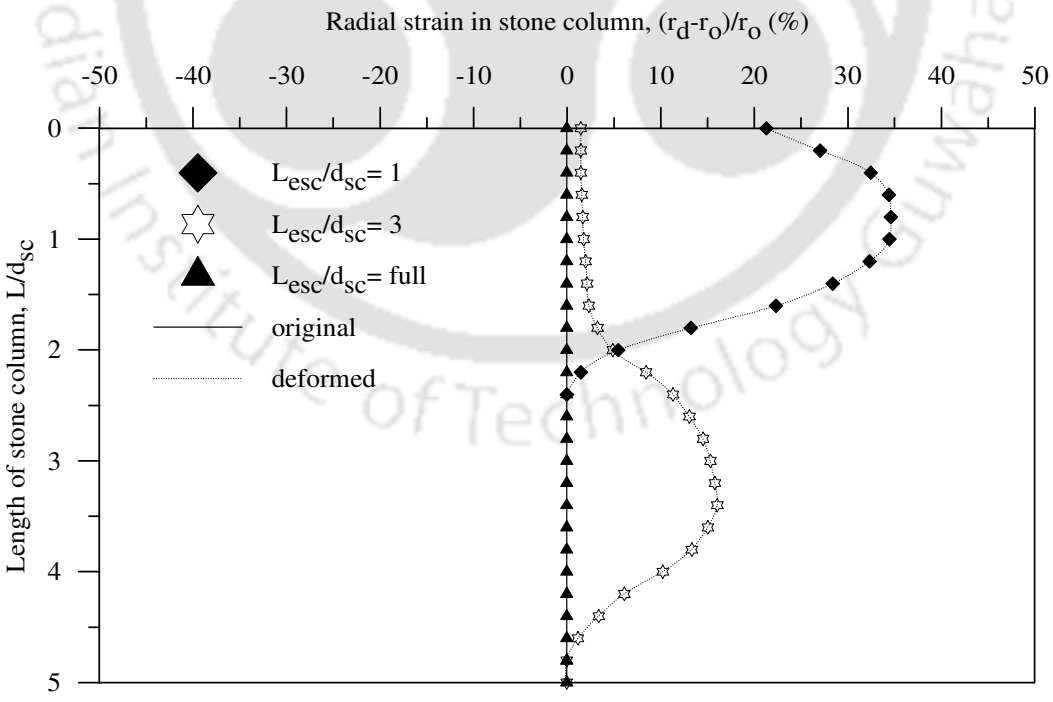

Fig. 7.13: Radial strain in central stone columns with different length of encasement (L/d_{sc} = 5, S/d_{sc} = 2.5) – Test series 22

7.3.2 Composite foundation bed (h/D = 0.53)

Fig. 7.14 shows the bearing pressure-settlement responses for different lengths of encasement of stone columns in composite foundation bed with geocell mattress of height (h) = 0.53D. It could be observed that encasement of stone columns has further improved the load carrying capacity of the composite foundation bed. With full length encasement, though the initial performance is at par with that having encasement length of $3d_{sc}$, however, at higher settlement the performance improvement has dropped down visibly.

The improvement in bearing capacity is quantified through the factor, IF_{gcesc}, is depicted in Fig. 7.15, where IF_{gcesc} is defined as the bearing pressure of geocell-encased stone column reinforced clay bed (q_{gcesc}) to the bearing pressure of unreinforced clay bed (q_u), both at equal footing settlement. It can be seen that with encasement of stone columns the bearing capacity of the clay bed has increased by 6.5 times while with unencased stone columns it stood at about 4 only (IF_{gcsc} = 4, Fig.6.4). It is of interest to note that with $L_{esc} = d_{sc}$, the bearing capacity improvement factor (IF_{gcesc}) has continuously increased with increase in footing settlement. But with $L_{esc} = 3d_{sc}$, there is an initial decrease after which the bearing capacity improvement factor (IF_{gcesc}) continues to increase with increase in footing settlement. With full length encasement, there is continues decrease of the improvement factor with increased settlement of the footing; however the rate of reduction tends to be nearly asymptotic for settlements beyond 15% of footing diameter (i.e. s/D >15%). This result can better be explained by deciphering the contribution of the stone columns and the geocell mattress, individually.

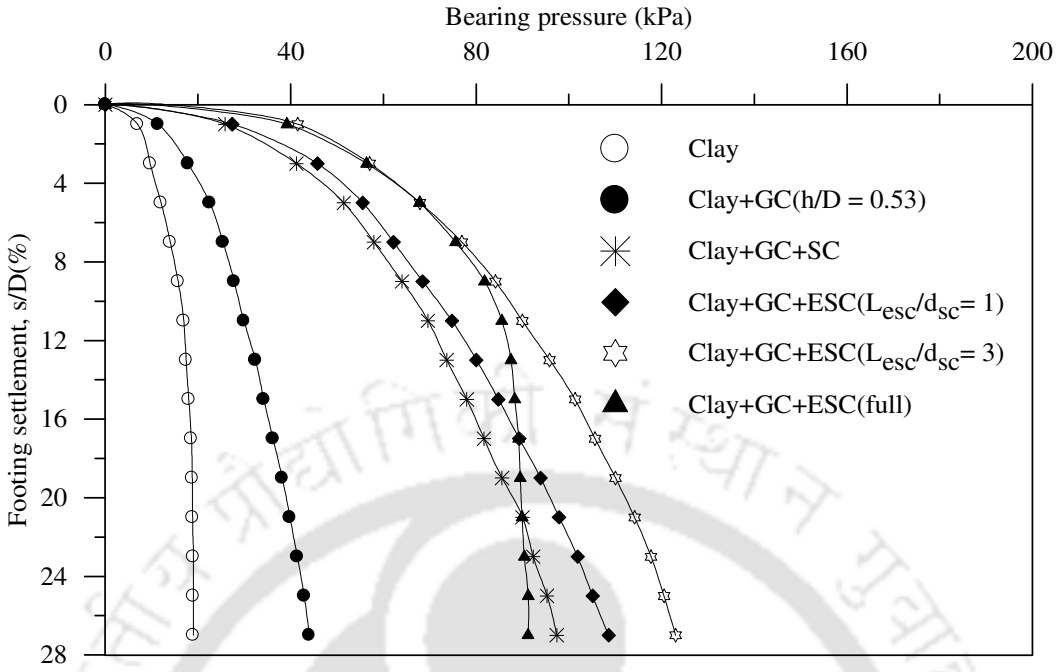

Fig.7.14: Bearing pressure vs. footing settlement, encased stone columns in composite foundation bed (h/D = 0.53, L/d_{sc} = 5, S/d_{sc} = 2.5) – Test series 23

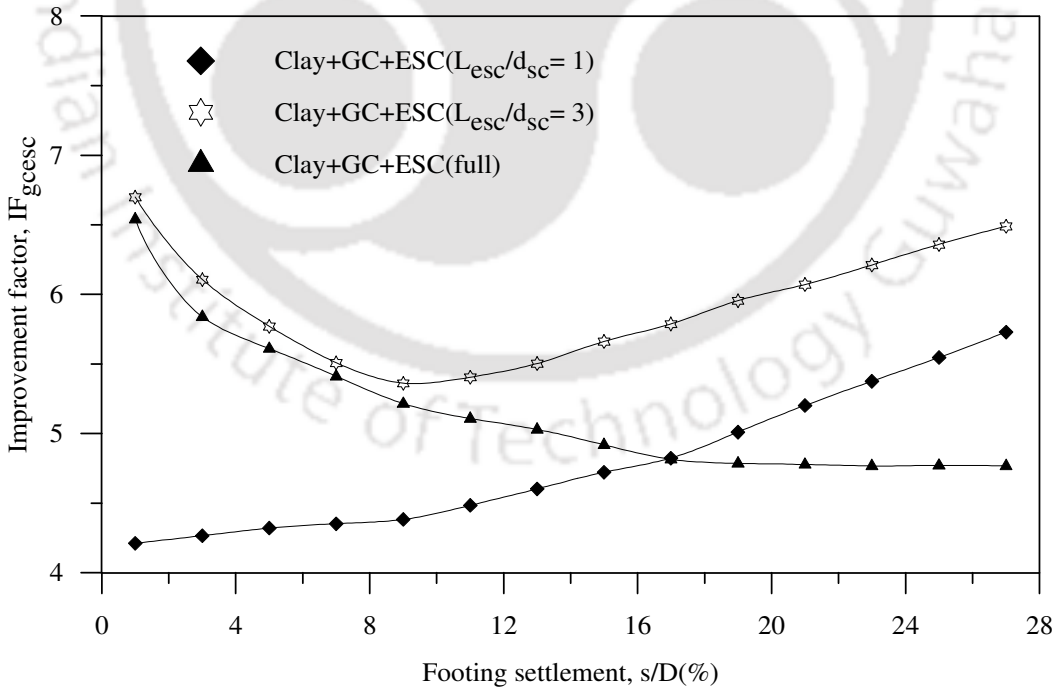

Fig.7.15: Improvement factor vs. footing settlement, encased stone columns in composite foundation bed (h/D = 0.53, L/d_{sc} = 5, S/d_{sc} = 2.5) – Test series 23

Fig. 7.16 shows that with encasement length (L_{esc}) equal to d_{sc}, the contribution of stone columns (IF_{gcesc}/IF_{gc}) continues to increase till settlement of about 12% of footing diameter, beyond which further improvement is marginal. However, at higher settlement range the geocell mattress has shown an increased contribution (IF_{gcesc}/IF_{esc}). As a result of which the combined performance improvement (IF_{gcesc}) has shown a continuously increasing trend (Fig. 7.15, $L_{esc}/d_{sc} = 1$).

Fig.7.16 shows that with encasement length of '$3d_{sc}$' the stone columns have induced maximum performance improvement and the reduction in the performance improvement with increase in settlement is mild. In view of this it could be said that the maximum performance improvement (IF_{gcesc}) noticed in this case ($L_{esc} = 3d_{sc}$, Fig. 7.15) is due to the enhanced contribution of the encased stone columns. The visible reduction in the contribution of the stone columns, with full length encasement is in aggrement with the trend observed in Fig. 7.15 (IF_{gcesc}). This is attributed to the punching down of the fully encased stones columns, under footing loading. Correspondingly, the geocell mattress has shared higher loading as shown in Fig.7.17. However, the contribution of geocell mattress has reduced with increase in settlement of footing. This is attributed to the relatively shallow height of the geocell mattress (h = 0.53D), that the end anchorage is less. As a result of which the geocell mattress yields under footing penetration leading to reduced performance improvement.

Fig. 7.18 shows that settlement on fill surface at x = D, is more with fully encased stone columns and is the least with partially encased stone columns having encasement (L_{ess}) of $3d_{sc}$. This establishes that maximum resistance has been offered by the stone columns with $L_{esc} = 3d_{sc}$ and the fully encased stone columns have offered least resistance against footing loading. The load carrying mechanism of the encased stone columns in the composite foundation bed can more clearly be

understood through the deformation patterns noticed in the post-test exhumed stone columns (Fig. 7.19 and Fig. 7.20). Unlike the case with partially encased stone columns alone, wherein, bulging takes place below the encasement (Fig. 7.12), no such distinct bulging in stone columns has been noticed in the present case, with the composite reinforcement. This is because in the previous case, as the footing directly rests over the stone column, the stone pieces are pushed down under loading giving rise to substantial bulging under the casing. While in the present case with geocell mattress, in between, the concentrated footing loading gets dispersed and is much uniformly distributed, leading to reduced intensity of stress over the stone columns. Therefore, the stone columns have undergone a more uniformly distributed pattern of deformation over their length.

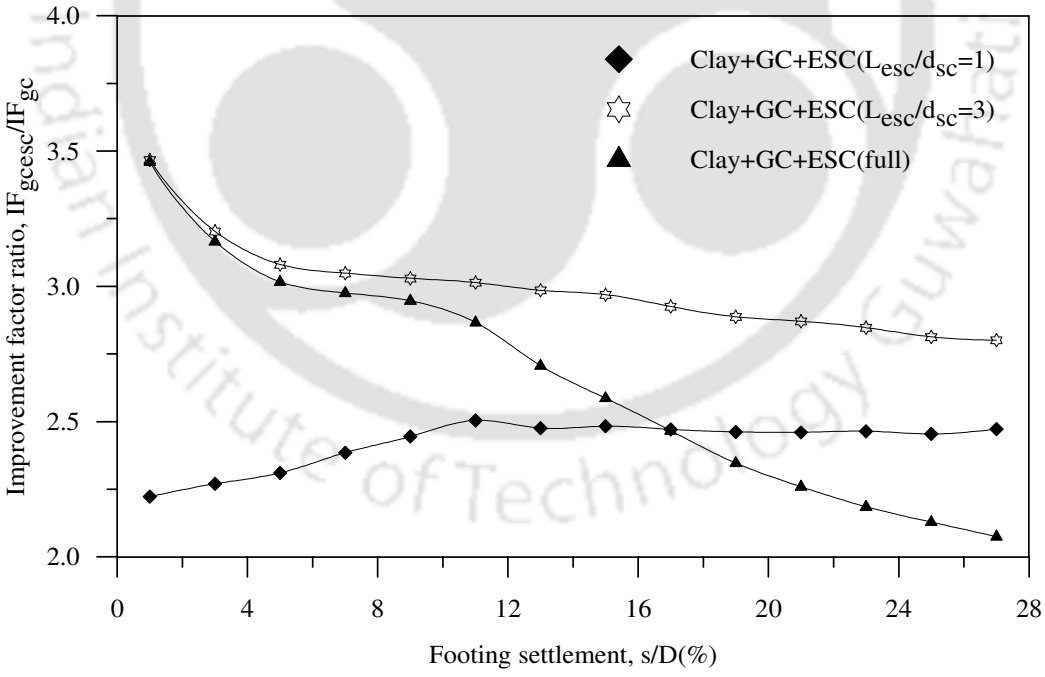

Fig.7.16: Improvement factor ratio vs. footing settlement, contribution of encased stone columns in the composite foundation bed (h/D = 0.53) – Test series 23

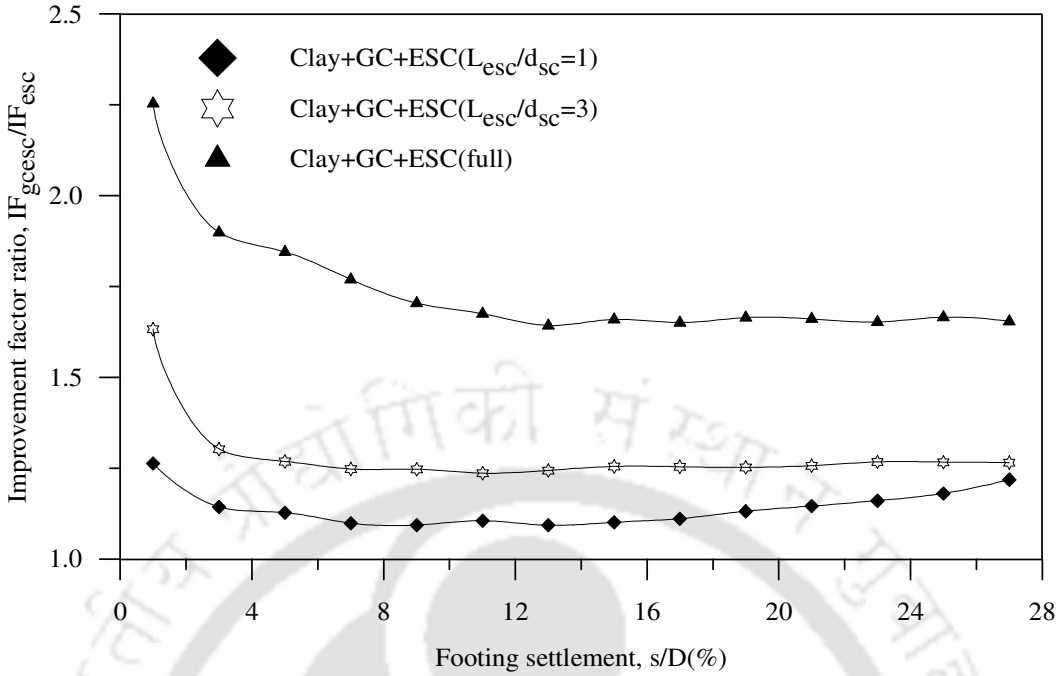

Fig.7.17: Improvement factor ratio vs. footing settlement, contribution of geocell mattress in encased stone column reinforced composite foundation beds (h/D = 0.53) – Test series 23

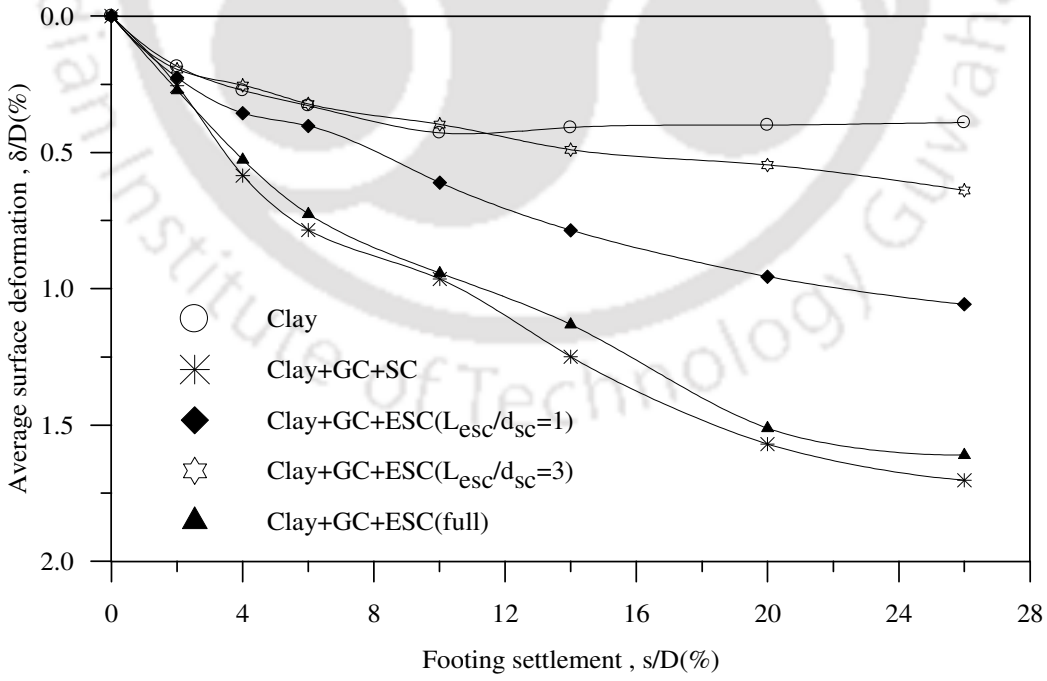

Fig.7.18: Variation of surface deformation, at x = D, with footing settlement for encased stone columns in composite foundation bed (h/D = 0.53) – Test series 23

(a) L_{esc}/d_{sc} = 1 (b) Lesc/d_{sc} = 3 (c) L_{esc}/d_{sc} = full

Fig. 7.19: Post-test deformed shape of the encased central stone column in composite foundation beds (h/D = 0.53) – Test series 23

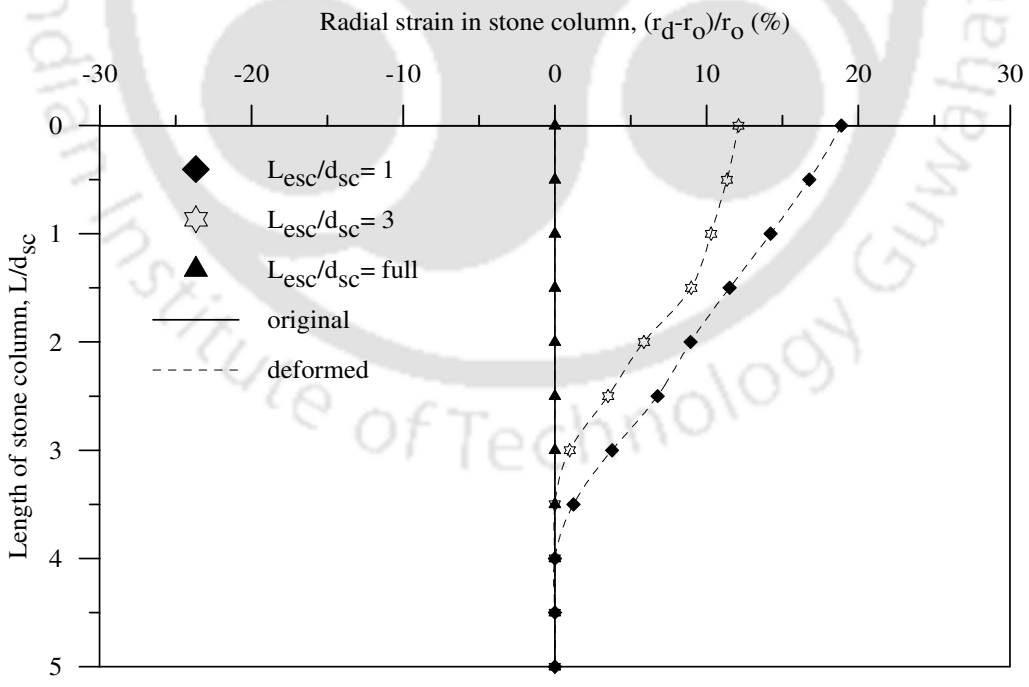

Fig. 7.20: Radial strain in the encased central stone column in composite foundation beds (h/D = 0.53) - Test series 23

7.3.3 Composite foundation bed (h/D = 0.9)

The pressure-settlement response and the corresponding bearing capacity improvement factor (IF_{gcesc}) for different encasement length of stone columns, in composite foundation bed with geocell mattress of height, h/D = 0.9, are depicted in Fig. 7.21 and Fig. 7.22 respectively. The contribution of encased stone columns (IF_{gcesc}/IF_{gc}) and that of geocell mattress (IF_{gcesc}/IF_{esc}) are shown in Fig. 7.23 and Fig. 7.24 respectively. It could be observed that the trends are similar to the earlier case, with h/D = 0.53. However, the difference due to different lengths of encasement is relatively less. This is attributed to the larger depth of placement of the stone columns owing to increased height of geocell mattress (h/D = 0.9). As the stone columns move away from the footing, the intensity of pressure on the stone columns reduces. This in turn causes less deformation in the stone aggregates. Indeed, Fig. 7.25 and Fig. 7.26 show that deformation in the stone columns is relatively less in magnitude and more uniform in distribution. With reduced deformation, the encased geogrid strength is undermobilised leading to reduced performance improvement. As the beneficial effect of the encasing reinforcement remains substantially unmobilised, the difference in performance improvement with varying length of encasement is found to be marginal.

It is of interest to note that, in the present case (i.e. h = 0.9D) with fully encased stone columns, the improvement factor (IF_{gsesc}) has shown an increasing trend with footing settlement. While with geocell mattress of height (h) equal to 0.53D, it has decreased with increase in footing settlement (Fig. 7.15). This is attributed to the difference in height of geocell mattress. As geocell mattress of shallow height (h = 0.53D) has less resistance, with the underlying stone columns punching down, the geocell mattress too punches down, leading to reduced performance improvement (IF_{gcesc}). While with increased height, the geocell mattress owing to increased rigidity and anchorage resistance stands against the footing penetration leading to overall increase in load carrying capacity of the foundation bed (IF_{gcesc}). Indeed, the results depicted in Fig. 7.24 indicate that with increase in settlement, the geocell mattress has shared increased proportion of surcharge loading (IF_{gcesc}/IF_{esc}).

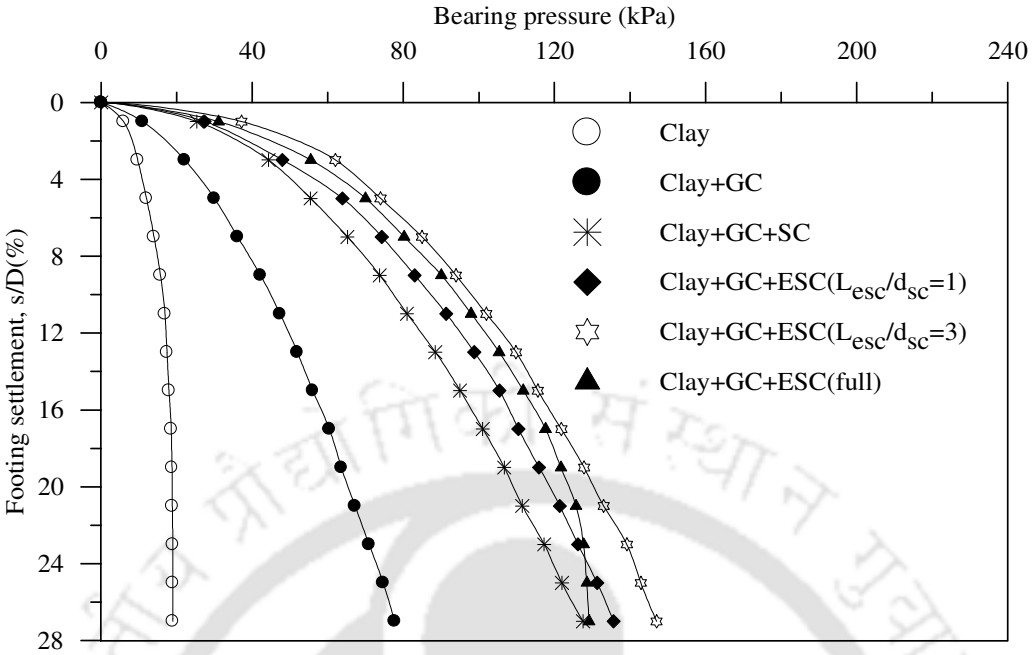

Fig.7.21: Variation of bearing pressure with footing settlement, encased stone columns in composite foundation bed (h/D = 0.9) – Test series 24

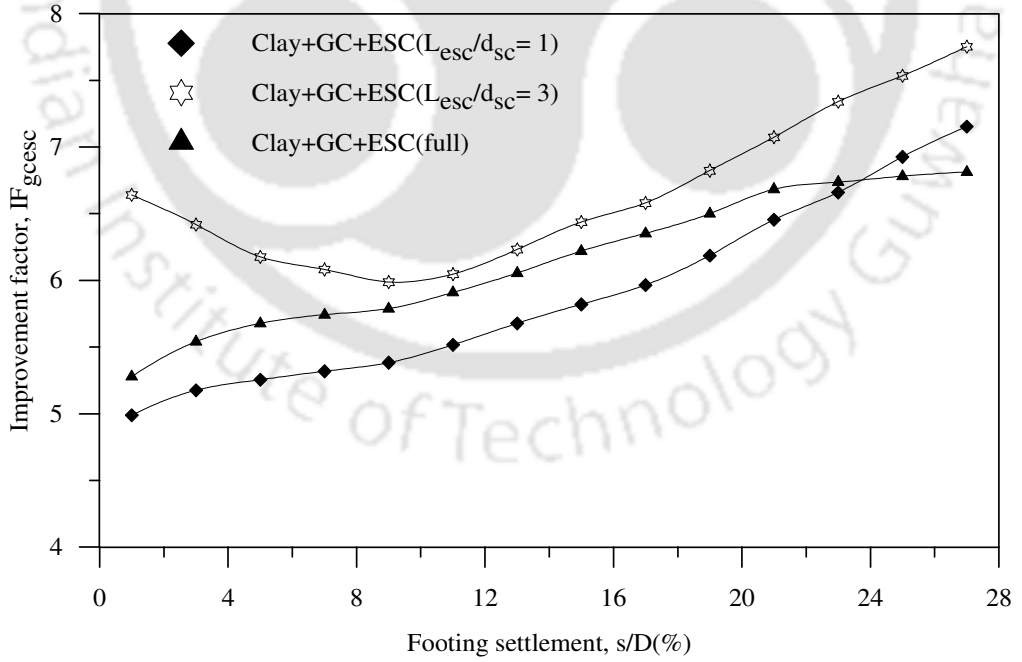

Fig.7.22: Improvement factor vs. footing settlement, encased of stone columns in composite foundation bed (h/D = 0.9) - Test series 24

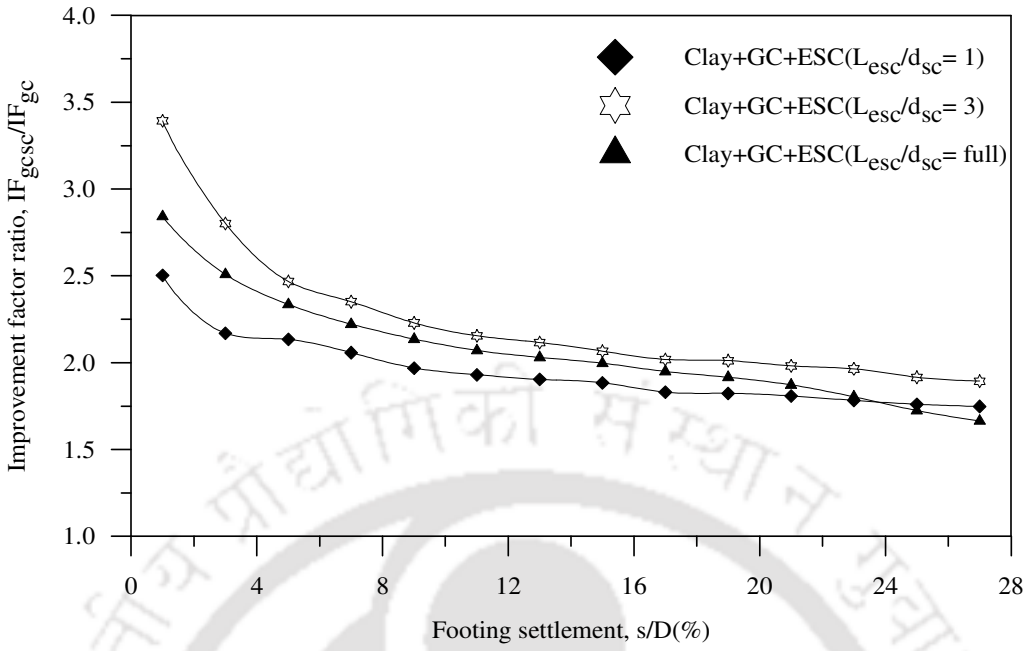

Fig.7.23: Improvement factor ratio vs. footing settlement, contribution of encased stone columns in composite foundation bed (h/D = 0.9) –Test series 24

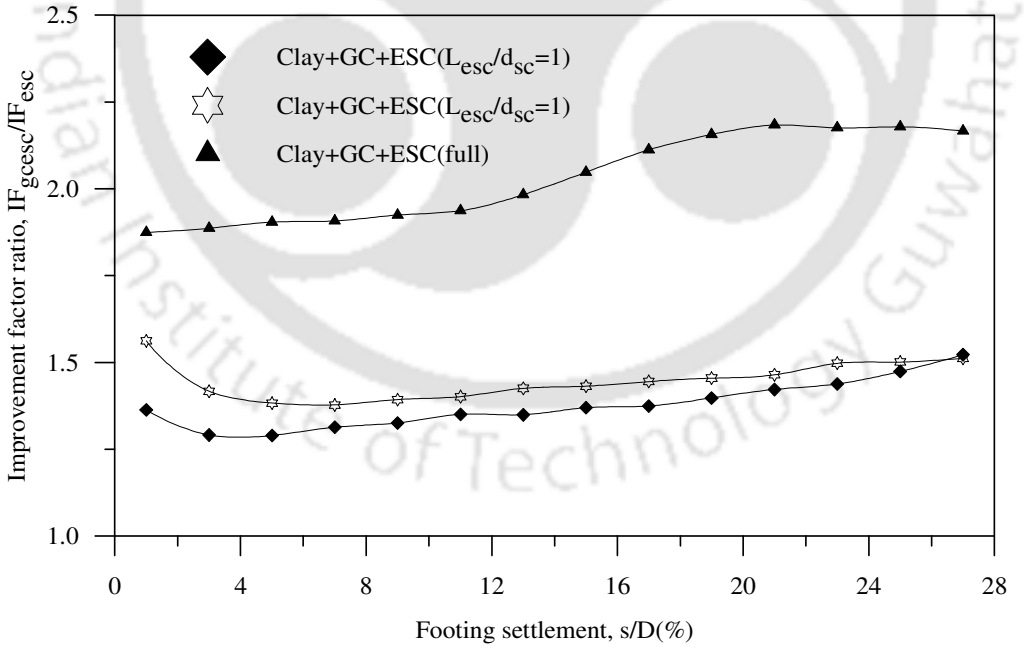

Fig.7.24: Improvement factor ratio vs. footing settlement, contribution of geocell mattress in encased stone column reinforced composite foundation bed (h/D = 0.9) – Test series 24

(a) L_{esc}/d_{sc} = 1 (b) L_{esc}/d_{sc} = 3 (c) L_{esc}/d_{sc} = full

Fig. 7.25: Post-test deformed shape of the encased central stone column in composite foundation beds (h/D = 0.9) – Test series 24

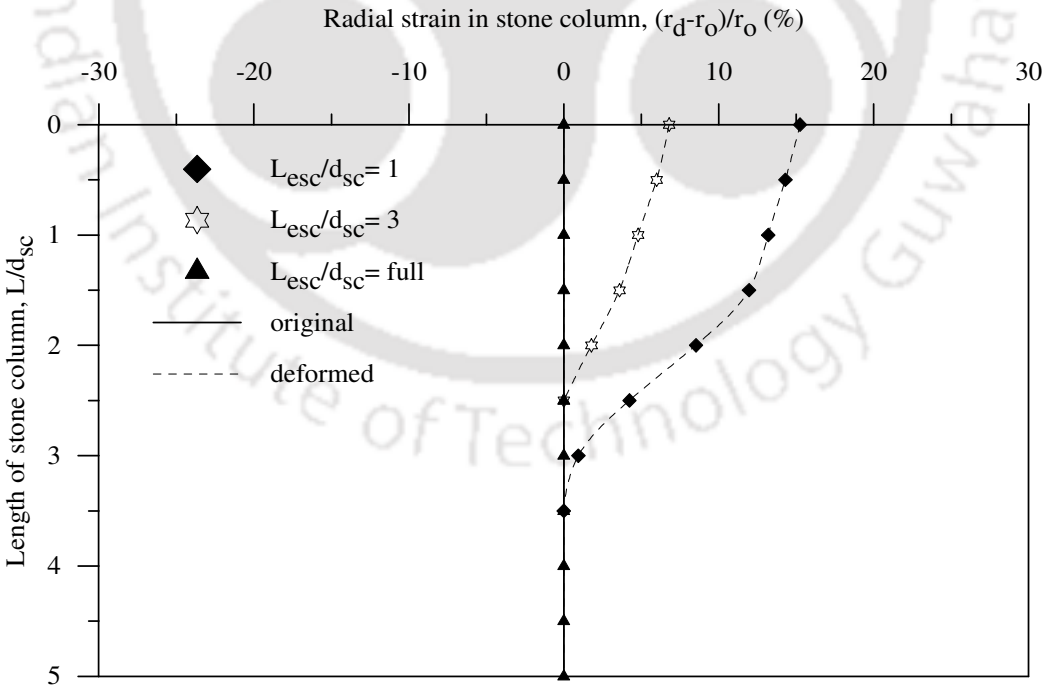

Fig. 7.26: Radial strain in the encased central stone columns in composite foundation beds (h/D = 0.9) – Test series 24

7.4 COMBINED EFFECT OF BASE GEOGRID AND ENCASEMENT OF STONE COLUMNS

From the results presented in the previous sections, it has been observed that either provision of basal geogrid or encasement of stone columns can further increase the performance of stone column-geocell reinforced clay bed. At this stage it was envisaged that if both the techniques, basal geogrid and encasement of stone columns, are applied simultaneously; the performance of the composite foundation bed would increase further. Therefore, tests were carried out under series 25 (Table 3.1, Ch.3). As the length of encasement (L_{esc}) = $3d_{sc}$, gives maximum performance improvement, the same has been adopted in this test series. From the obtained results presented in Fig. 7.27 it can be seen that, with encasement of stone columns, the performance improvement of the basal geogrid reinforced composite foundation bed has further been increased.

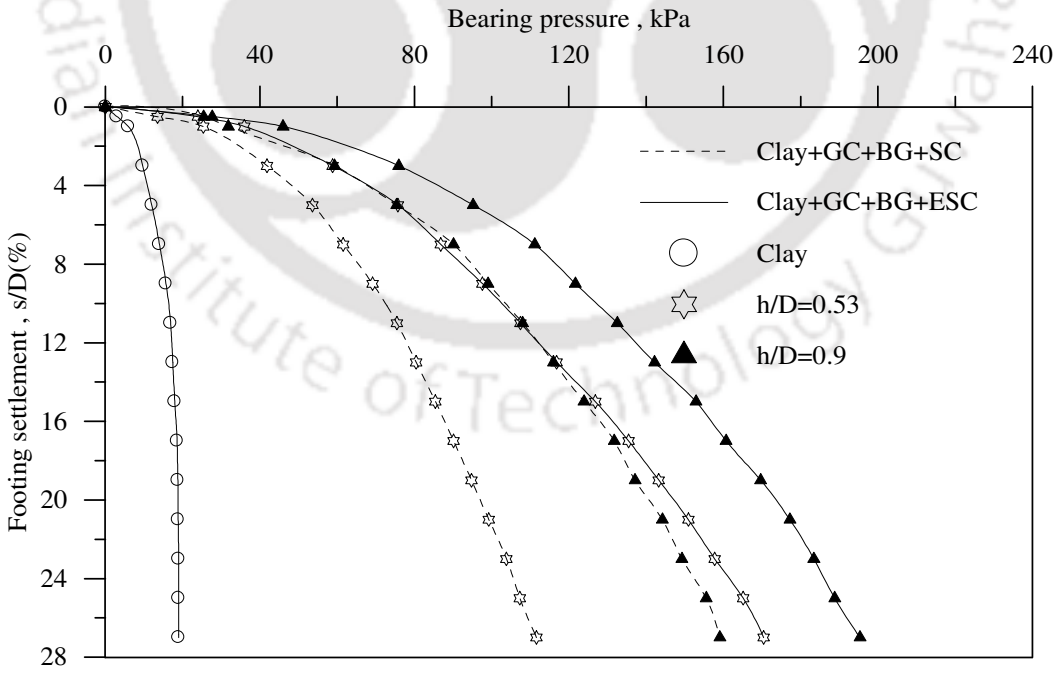

Fig.7.27: Variation of bearing pressure with footing settlement for composite foundation bed with encased stone columns and base geogrid (L_{esc}/d_{sc} = 3) - Test series 25

Fig 7.28 shows that nearly 9 fold increase in bearing capacity of the clay bed can be obtained with provision of geocell-base geogrid-encased stone column reinforcement ($IF_{gcescbg}$ = 8.9), wherein, the geocell mattress height (h) is 0.53D. Whereas with geocell mattress of height 0.9D the improvement is as high as 10 fold ($IF_{gcescbg}$ = 10.2). It is of interest to note that, the improvement due to geocell-stone column reinforcement alone (IF_{gcsc}), with h = 0.53D, is only 5 and that with h = 0.9D is 6.5 (Fig.6.4, Fig. 6.18; L/d_{sc} = 5).

From the surface deformation responses depicted in Fig. 7.29, it could be observed that there is not much change in the settlement on the fill surface due to encasement of stone columns. However, at higher settlement of footing, the fill surface with encased stone columns has shown relatively larger settlement than that without encasement. Since the encasement arrests bulging of stone columns, the associated heaving too reduces. As this heaving used to counter balance the settlement on fill surface, with its reduction, surface settlement has apparently increased.

The deformation pattern of the encased central stone column, with base geogrid in the composite foundation beds, depicted in Fig. 7.30 and Fig. 7.31 are nearly similar to the case without the basal geogrid (Fig.7.20, 7.26; L_{esc}/d_{sc} = 3). However, the strain in stone columns in the present case is comparatively higher. This is attributed to the increased bearing pressure that has been applied on to the foundation in the present case.

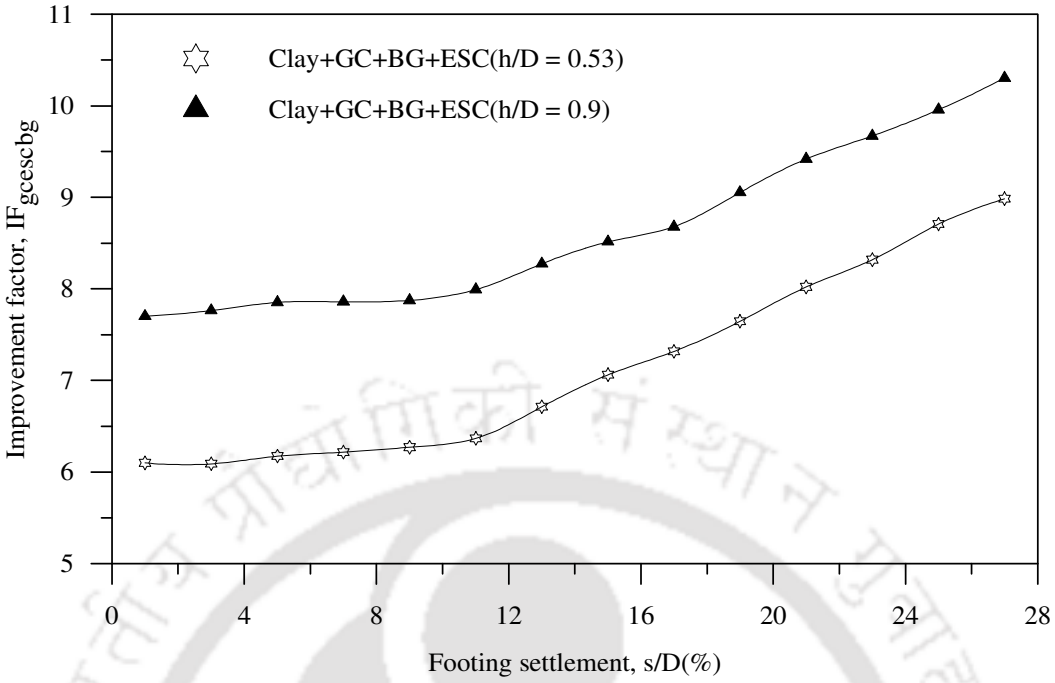

Fig. 7.28: Variation of improvement factor with footing settlement for composite foundation bed with encased stone columns and base geogrid - Test series 25

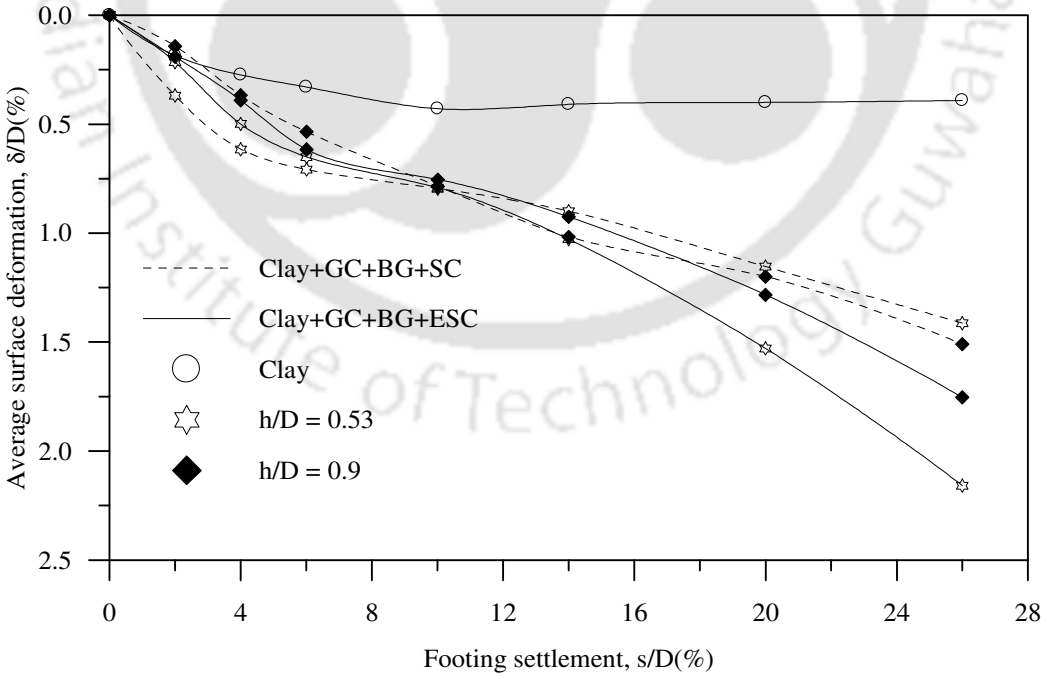

Fig.7.29: Variation of surface deformation with footing settlement, at x = D, for composite foundation bed with encased stone columns and base geogrid - Test series 25

(a) h/D = 0.53 (b) h/D = 0.9

Fig. 7.30: Post-test deformed shape of the central encased stone columns in composite foundation bed with base geogrid (L_{esc}/d_{sc} = 3) - Test series 25

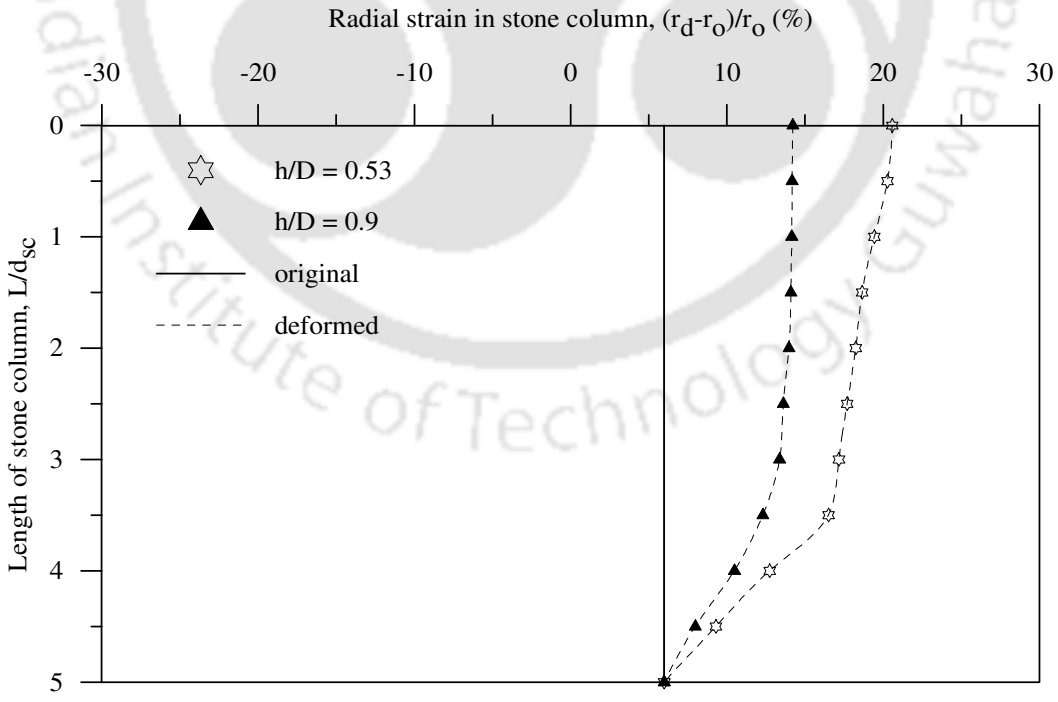

Fig. 7.31: Radial strain in encased central stone column in composite foundation beds with base geogrid (L_{esc}/d_{sc} = 3) - Test series 25

7.5 COMPARATIVE ANALYSIS

In this section a comparison of performance improvements for all forms of reinforcements studied under this investigation is presented and discussed. The bearing capacity improvement factors pertaining to different forms of reinforcement (IF_{sc}, IF_{gc}, IF_{gcsc}, IF_{gcesc}, $IF_{gcescbg}$) with varied parameters (h, d_{gc}, ID, L, S, d_{sc}, L_{esc}; Test series 2-25) are summarised in Table 7.1. It could be observed that with provision of stone column reinforcement, the bearing capacity of soft clay beds can be increased by 3.7 fold (Test series 3; S/d_{sc} = 1.5, L/d_{sc} = 5). Whereas, with geocell reinforcement of very large height and with dense infill (h/D = 1.6, ID = 80%, Test series 4) the performance improvement increases by 7.87 times (IF_{gc} = 7.87). When coupled together; stone columns with spacing of $1.5d_{sc}$, length of $5d_{sc}$ and geocell mattress of height (h) 1.6D with dense infill (ID = 80%); the bearing capacity has increased by 10 fold (IF_{gcsc} = 10.22, Test series 16). This is substantially high performance improvement. However, with geocell mattress of much less height, h = 0.9D, similar order of performance improvement can be achieved if the stone columns are partially encased (L_{esc} = $3d_{sc}$) and a layer of planar geogrid is provided at the base of the geocell mattress ($IF_{gcescbg}$ = 10.3, Test series 25). Even with geocell mattress of shallow height (h = 0.53) the improvement in bearing capacity is as high as 9 times that of unreinfoced case ($IF_{gcescbg}$ = 8.99). This is because, the stone columns are more effective, when the geocell height is relatively less, as has been brought out in Chapter 6. At times, due to practical constraints, larger height geocell mattress may not be possible to be accommodated. In such situations provision of encased stone columns and base geogrid, are the viable alternatives to manage with geocell mattress of relatively smaller height. Besides, with reduced height of geocell mattress the overall cost is expected to reduce down.

Table 7.1 Bearing capacity Improvement Factors (IF: IF_{sc}, IF_{gc}, IF_{gcsc}, IF_{gcesc}, $IF_{gcescbg}$)

Test series	Reinforcement	Variable parameter	Bearing capacity Improvement Factor (IF)							
			s/D 1%	s/D 5%	s/D 9%	s/D 13%	s/D 17%	s/D 21%	s/D 25%	s/D 27%
2	SC	L/d_{sc} = 1	1.69	1.25	1.14	1.19	1.23	1.26	1.28	1.30
	SC	L/d_{sc} = 3	1.81	1.54	1.53	1.60	1.62	1.66	1.73	1.73
	SC	L/d_{sc} = 5	3.59	2.87	2.93	3.12	3.19	3.31	3.40	3.44
	SC	L/d_{sc} = 7	3.69	3.20	3.17	3.37	3.40	3.48	3.56	3.60
3	SC	S/d_{sc} = 1.5	3.66	2.90	3.20	3.45	3.49	3.61	3.67	**3.70**
	SC	S/d_{sc} = 2.5	3.59	2.87	2.93	3.12	3.19	3.31	3.40	3.44
	SC	S/d_{sc} = 3.5	1.79	1.47	1.67	1.84	1.81	1.86	1.90	1.93
4	GC	h/D = 0.53	1.34	1.50	1.64	1.86	1.95	2.11	2.26	2.32
	GC	h/D = 0.9	1.86	2.00	2.53	2.98	3.26	3.57	3.94	4.09
	GC	h/D = 1.1	2.90	4.10	4.77	5.57	6.00	6.60	7.12	7.39
	GC	h/D = 1.6	4.20	4.81	5.43	6.14	6.54	7.08	7.64	**7.87**
5	GC	ID = 35%	1.05	1.07	1.16	1.32	1.45	1.60	1.77	1.83
	GC	ID = 50%	1.15	1.33	1.42	1.58	1.70	1.85	2.02	2.08
	GC	ID = 80%	1.34	1.50	1.64	1.86	1.95	2.11	2.26	2.32
6	GC	ID = 35%	1.34	2.11	2.21	2.47	2.66	2.90	3.18	3.27
	GC	ID = 50%	1.60	2.10	2.40	2.82	3.06	3.35	3.65	3.79
	GC	ID = 80%	1.86	2.00	2.53	2.98	3.26	3.57	3.94	4.09
7	GC	d_{gc}/D = 0.8	1.34	1.50	1.64	1.86	1.95	2.11	2.26	2.32
	GC	d_{gc}/D = 1.1	1.13	1.12	1.23	1.40	1.50	1.63	1.78	1.85
	GC	d_{gc}/D = 1.33	1.06	1.08	1.12	1.20	1.29	1.41	1.49	1.54
8	GC	d_{gc}/D = 0.8	1.86	2.00	2.53	2.98	3.26	3.57	3.94	4.09
	GC	d_{gc}/D = 1.1	1.40	1.92	2.27	2.62	2.78	3.07	3.31	3.44
	GC	d_{gc}/D = 1.33	1.27	1.70	1.98	2.12	2.12	2.17	2.24	2.31
9	GC + SC	L/d_{sc} = 1	1.72	1.98	1.91	2.01	2.15	2.30	2.46	2.53
	GC + SC	L/d_{sc} = 3	1.87	2.22	2.23	2.36	2.48	2.66	2.88	2.95
	GC + SC	L/d_{sc} = 5	4.12	4.26	4.29	4.32	4.41	4.73	5.02	5.13
	GC + SC	L/d_{sc} = 7	4.39	4.79	4.87	4.98	5.02	5.30	5.57	5.69
10	GC + SC	L/d_{sc} = 1	2.24	2.80	2.88	3.12	3.40	3.69	3.96	4.14
	GC + SC	L/d_{sc} = 3	3.00	3.33	3.28	3.48	3.70	4.08	4.36	4.50
	GC + SC	L/d_{sc} = 5	4.29	4.63	4.70	5.09	5.45	5.92	6.43	6.73
	GC + SC	L/d_{sc} = 7	5.36	5.55	5.65	5.89	6.12	6.68	7.20	7.46
11	GC + SC	L/d_{sc} = 1	3.66	5.06	5.18	5.74	6.15	6.86	7.46	7.78
	GC + SC	L/d_{sc} = 3	5.02	5.98	5.94	6.31	6.69	7.22	7.77	8.01
	GC + SC	L/d_{sc} = 5	5.66	6.65	6.63	7.00	7.40	8.01	8.50	8.74
	GC + SC	L/d_{sc} = 7	7.00	7.38	7.24	7.55	7.98	8.50	9.13	9.42
12	GC + SC	L/d_{sc} = 1	3.41	4.80	5.55	6.40	7.20	8.01	8.72	9.01
	GC + SC	L/d_{sc} = 3	3.88	5.29	6.00	7.00	7.55	8.25	9.02	9.24
	GC + SC	L/d_{sc} = 5	5.48	6.46	6.84	7.41	7.96	8.59	9.28	9.59
	GC + SC	L/d_{sc} = 7	6.10	7.00	7.38	7.82	8.32	8.93	9.56	9.88

Table 7.1 (continued…)

Test series	Reinforcement	Variable parameter	Bearing capacity Improvement factor (IF)							
			s/D 1%	s/D 5%	s/D 9%	s/D 13%	s/D 17%	s/D 21%	s/D 25%	s/D 27%
13	GC + SC	S/d_{sc} = 1.5	4.54	4.82	4.84	4.95	5.16	5.53	5.79	5.88
	GC + SC	S/d_{sc} = 2.5	4.12	4.26	4.29	4.32	4.41	4.73	5.02	5.13
	GC + SC	S/d_{sc} = 3. 5	3.28	3.44	3.50	3.52	3.54	3.65	3.79	3.89
14	GC + SC	S/d_{sc} = 1.5	5.01	5.46	5.57	5.85	6.24	6.75	7.24	7.47
	GC + SC	S/d_{sc} = 2.5	4.29	4.63	4.70	5.09	5.45	5.92	6.43	6.73
	GC + SC	S/d_{sc} = 3.5	3.55	3.74	3.84	4.09	4.36	4.75	5.16	5.36
15	GC + SC	S/d_{sc} = 1.5	6.10	7.23	7.34	7.60	7.97	8.53	9.07	9.37
	GC + SC	S/d_{sc} = 2.5	5.66	6.65	6.63	7.00	7.40	8.01	8.50	8.74
	GC + SC	S/d_{sc} = 3. 5	5.30	5.84	5.97	6.17	6.65	7.30	7.89	8.22
16	GC + SC	S/d_{sc} = 1.5	6.35	7.13	7.29	7.81	8.40	9.20	9.87	**10.22**
	GC + SC	S/d_{sc} = 2.5	5.48	6.46	6.84	7.41	7.96	8.59	9.28	9.59
	GC + SC	S/d_{sc} = 3. 5	5.10	6.29	6.43	7.00	7.50	8.19	8.82	9.06
17	GC + SC	d_{gc}/D = 0.8	4.12	4.26	4.29	4.32	4.41	4.73	5.02	5.13
	GC + SC	d_{gc}/D= 1.1	3.87	3.90	3.94	4.04	4.11	4.32	4.50	4.61
	GC + SC	d_{gc}/D = 1.33	3.56	3.60	3.62	3.65	3.67	3.66	3.69	3.70
18	GC + SC	d_{gc}/D = 0.8	4.29	4.63	4.70	5.09	5.45	5.92	6.43	6.73
	GC + SC	d_{gc}/D = 1.1.	3.64	4.44	4.46	4.66	4.89	5.26	5.61	5.78
	GC + SC	d_{gc}/D = 1.33	3.44	4.12	4.01	4.13	4.25	4.46	4.59	4.64
19	GC + SC	ID = 35%	3.03	3.28	3.28	3.45	3.70	3.97	4.23	4.35
	GC + SC	ID = 50%	3.57	3.70	3.79	3.86	4.10	4.34	4.69	4.86
	GC + SC	ID = 80%	4.12	4.26	4.29	4.32	4.41	4.73	5.02	5.13
20	GC + SC	ID = 35%	3.04	3.80	3.84	4.22	4.61	5.17	5.66	5.85
	GC + SC	ID = 50%	3.72	4.21	4.33	4.70	5.07	5.63	6.19	6.43
	GC + SC	ID = 80%	4.29	4.63	4.70	5.09	5.45	5.92	6.43	6.73
21	GC+SC+BG	h/D = 0.53	4.62	4.66	4.70	4.88	5.08	5.33	5.71	5.88
	GC+SC+BG	h/D = 0.9	5.74	6.30	6.48	6.77	7.12	7.67	8.15	8.39
22	ESC	L_{esc}/d_{sc} = 1	3.68	4.10	4.00	4.21	4.34	4.54	4.70	4.70
	ESC	L_{esc}/d_{sc} = 3	4.31	4.46	4.30	4.42	4.55	4.83	5.01	5.13
	ESC	L_{esc}/d_{sc} = 5 (Full)	2.67	3.06	3.06	3.09	3.11	3.21	3.26	3.32
23	GC + ESC	L_{esc}/d_{sc} = 1	4.24	4.38	4.42	4.60	4.82	5.20	5.54	5.72
	GC + ESC	L_{esc}/d_{sc} = 3	6.70	5.67	5.36	5.51	5.71	6.07	6.36	6.49
	GC + ESC	L_{esc}/d_{sc} = 5(Full)	6.53	5.52	5.21	5.02	4.81	4.77	4.80	4.80
24	GC + ESC	L_{esc}/d_{sc} = 1	4.99	5.25	5.38	5.68	5.96	6.45	6.93	7.15
	GC + ESC	L_{esc}/d_{sc} = 3	6.64	6.17	5.99	6.23	6.58	7.07	7.53	7.75
	GC + ESC	L_{esc}/d_{sc} = 5	5.28	5.68	5.79	6.05	6.35	6.68	6.78	6.81
25	GC+ESC+ BG	h/D = 0.53	6.10	6.18	6.27	6.71	7.32	8.02	8.71	8.99
	GC+ESC+BG	h/D = 0.9	7.70	7.86	7.88	8.28	8.68	9.42	9.96	**10.30**

CHAPTER 8

REGRESSION MODEL AND DIMENSIONAL ANALYSIS

8.1 REGRESSION ANALYSIS

Analytical formulation for estimation of the bearing capacity of geocell-stone column reinforced foundation beds is very difficult. This is due mainly to the complex stress-dependent nature of the encapsulated soil in geocells, difficulty in mathematically modeling the three-dimensional behaviour of geocells and the non-linear interaction between geocell mattress and stone columns. Therefore, there arises need of a simple formulation that can predict well the bearing capacity of such complex system. Regression model is a statistical tool for obtaining quantitative functional relationship between a dependent variable and a set of independent variables. This method is widely used in Geotechnical Engineering practice for fitting of empirical equations from test data.

From the experimentally obtained pressure settlement responses, presented in the previous chapters (Ch.4-7), extensive data on bearing pressure at different settlements of footing, for various parameters pertaining to the clay subgrade, stone columns and geocell mattress are obtained. These data provided a large database for the regression analysis. Seventy percent of the total data, sampled over the whole range, was used for the regression analysis and the rest was kept aside for validation of the model. Multiple nonlinear regression analysis has been carried out to develop empirical relationships for predicting the bearing pressures of stone column reinforced clay beds, geocell mattress reinforced clay beds, geocell mattress-stone column reinforced composite foundation beds, and composite reinforced foundation beds along with base geogrid; the details of which are presented below.

8.1.1 Stone column reinforced clay bed

In Chapter 4, it has been brought out that the bearing pressure of stone column reinforced soft clay bed (q_{sc}) is dependent on, bearing capacity of unreinforced clay bed (q_u); settlement (s) and diameter (D) of footing; length (L), diameter (d_{sc}) and spacing (S) of stone columns. Through a series of trial and error, the following functional form is fitted to the experimental data.

$$q_{sc} = (q_u)^{c_1}\left(\frac{s}{D}\right)^{c_2}\left(\frac{L}{d_{sc}}\right)^{c_3}\left(\frac{S}{d_{sc}}\right)^{c_4} \tag{8.1}$$

Where, c_1, c_2, c_3 and c_4 are the regression coefficients. These coefficients were found out through nonlinear regression analysis (Dielman, 2001). The final form of the proposed model, for predicting the bearing capacity of soft clay foundation bed with stone column reinforcement (q_{sc}), is expressed by the following equation.

$$q_{sc} = (q_u)^{1.66}\left(\frac{s}{D}\right)^{0.17}\left(\frac{L}{d_{sc}}\right)^{0.57}\left(\frac{S}{d_{sc}}\right)^{-1.36} \tag{8.2}$$

This model was validated using the data samples which were not used in the regression analysis. The predictive performance of the model is measured through the coefficient of determination (R^2). The coefficient of determination (R^2) for this model is found to be 0.9, which indicates that the model can predict well. The correlation between the measured and predicted values of the bearing pressure (q_{sc}) is shown in Fig.8.1. It is observed that there is a close match between the two.

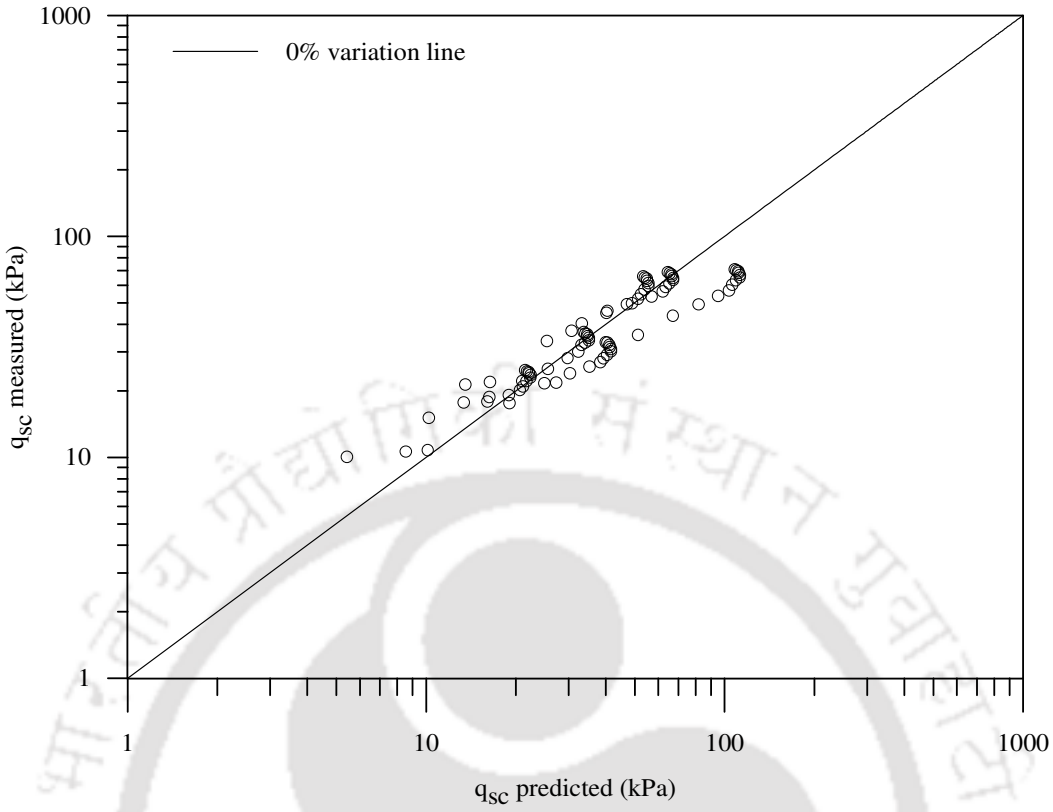

Fig. 8.1 Predicted vs. measured bearing pressure, stone column reinforced clay bed.

8.1.2 Geocell mattress overlying clay bed

The test data, presented in Chapter 5, shows that the bearing pressure of geocell-sand mattress reinforced clay bed (q_{gc}) is influenced by parameters such as; bearing pressure on unreinforced clay bed (q_u); settlement (s) and size of footing (D); pocket opening size of geocells (d_{gc}), height of geocell layer (h), angle of friction of infill soil in geocells (φ), angle of interfacial friction between infill soil and geocell wall (δ). Through trial and error, the following nonlinear relationship between the dependent and the independent variables is proposed to model the experimental trends.

$$q_{gc} = (q_u)^{c_1}\left(\frac{s}{D}\right)^{c_2}\left(\frac{d_{gc}}{D}\right)^{c_3}(c_4)^{\frac{h}{D}}(c_5)^{\frac{\delta}{\phi}} \tag{8.3}$$

Having obtained the regression coefficients; c_1, c_2, c_3, c_4 and c_5 through nonlinear regression analysis and substituting the same in the above model, the equation for determining the bearing capacity, q_{gc}, can be written as,

$$q_{gc} = (q_u)^{0.46}\left(\frac{s}{D}\right)^{0.38}\left(\frac{d_{gc}}{D}\right)^{-0.49}(3.39)^{\frac{h}{D}}(1.61)^{\frac{\delta}{\Phi}} \qquad (8.4)$$

The R^2 value for this model is found to be 0.97. From Fig. 8.2, it could be observed that the observed and predicted values of bearing pressures fall within a narrow band, very close to the zero error line.

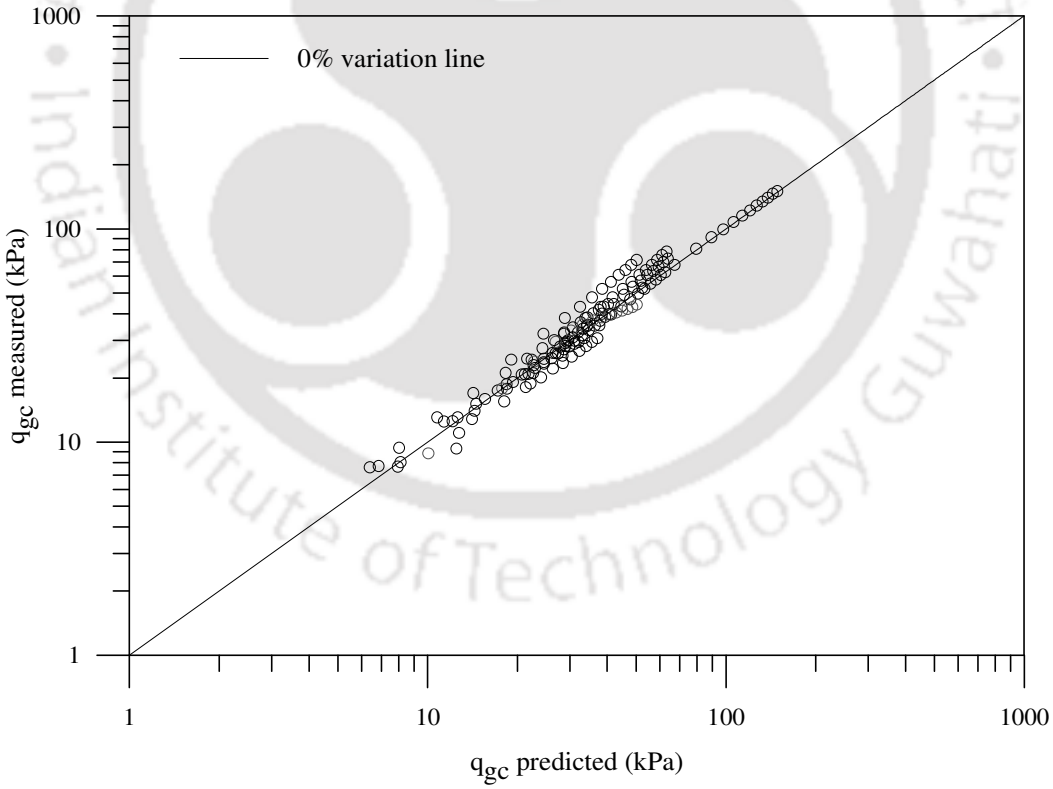

Fig. 8.2 Predicted vs. measured bearing pressure, geocell mattress overlying clay bed.

8.1.3 Geocell-stone column composite foundation bed

The influence of both geocell mattress and stone columns, govern the response of the geocell mattress-stone column reinforced composite foundation beds. Therefore, the parameters that influence the beahaviour of stone column reinforced clay foundation bed and the geocell mattress reinforced clay foundation bed are expected to govern the performance of the composite foundation system (q_{gcsc}). Considering these parameters, the following functional form is fitted to the test data.

$$q_{g\,csc} = (q_u)^{c_1}\left(\frac{s}{D}\right)^{c_2}(c_3)^{\frac{d_{gc}}{D}}(c_4)^{\frac{h}{D}}(c_5)^{\frac{\delta}{\phi}}\left(\frac{L}{d_{sc}}\right)^{c_6}\left(\frac{S}{d_{sc}}\right)^{c_7} \tag{8.5}$$

The constants c_1, c_2, c_3, c_4, c_5, c_6 and c_7 are found to be; 0.11, 0.43, 0.65, 1.69, 72.64, 0.18 and -0.15, respectively. Substituting these values in Eq. 8.5, the relationship for predicting the bearing capacity, q_{gcsc}, can be written as follows,

$$q_{g\,csc} = (q_u)^{0.11}\left(\frac{s}{D}\right)^{0.43}(0.65)^{\frac{d_{gc}}{D}}(1.69)^{\frac{h}{D}}(72.64)^{\frac{\delta}{\Phi}}\left(\frac{L}{d_{sc}}\right)^{0.18}\left(\frac{S}{d_{sc}}\right)^{-0.15} \tag{8.6}$$

The regression co-efficient (R^2) for this equation is found out to be 0.92. From fig.8.3, it could be observed that, there exists a good agreement between the measured and the estimated bearing capacity (q_{gcsc}) values. Since, in order to use this model one has to obtain the bearing capacity of the unreinforced clay bed (q_u), through field tests, the factors such as; type of soil, its in situ strength and stiffness, footing size etc. are taken care of. Besides, the friction parameters, δ and φ, are to be evaluated from laboratory tests (direct shear, pull out), the reinforcement mechanism of geocell-sand system is

well taken care of. Since the model can incorporate the actual filed conditions, it can be considered to be relatively more reliable.

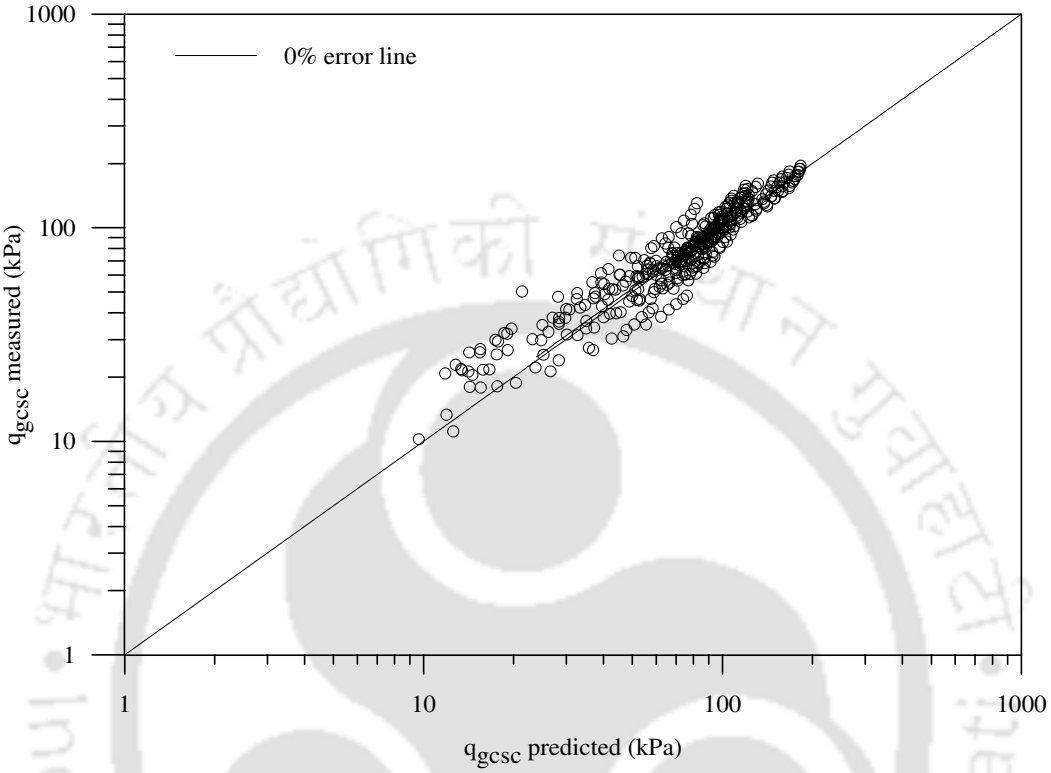

Fig. 8.3 Predicted vs. measured bearing pressure, composite foundation beds.

8.1.4 Composite foundation bed with base geogrid and encased stone columns

The regression model for predicting the improved bearing capacity, q_{gcscbg} , due to additional planar reinforcement at base of the geocell mattress of height, h, overlying stone column reinforced clay bed is found to be,

$$q_{g\,csc\,bg} = \left(q_{g\,csc}\right)^{1.05}\left(\frac{s}{D}\right)^{0.04}(1.01)^{\frac{h}{D}} \tag{8.7}$$

The regression co-efficient (R^2) for this model is found to be 0.99, therefore the predicted and measured value of q_{gcscbg} are very close to the zero error line (Fig.8.4).

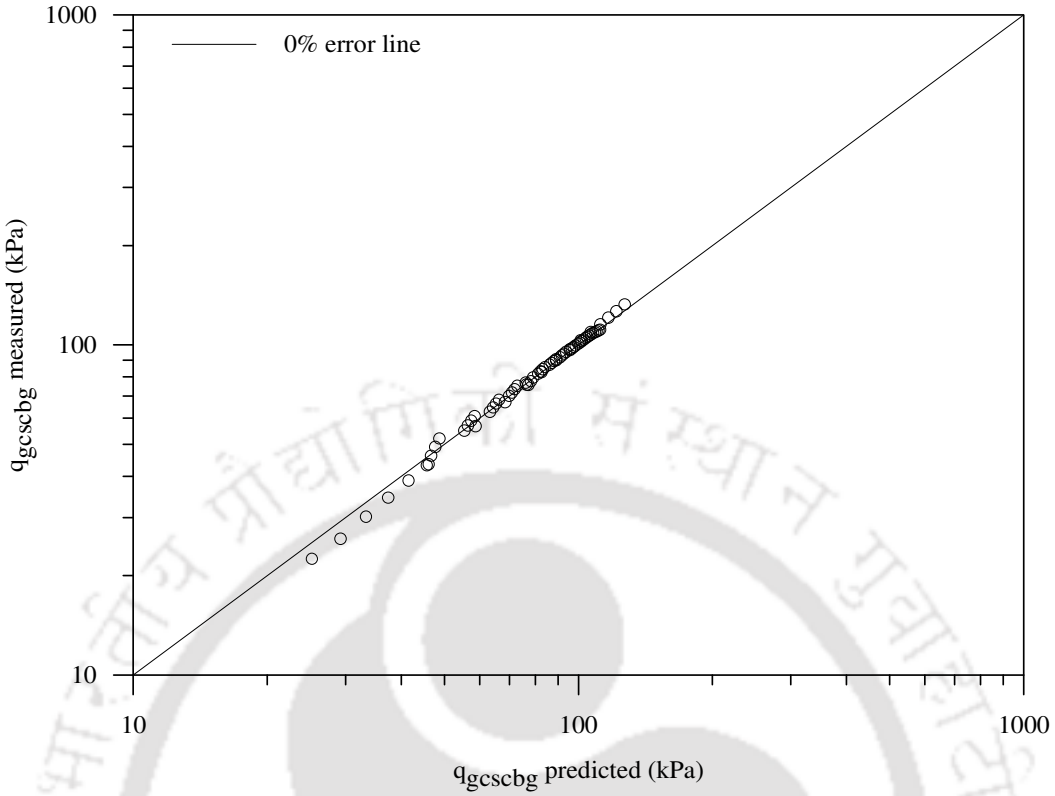

Fig. 8.4 Predicted vs. measured bearing pressure, composite foundation bed with base geogrid.

The regression model for predicting the bearing capacity of geocell mattress cum stone column reinforced clay bed with basal geogrid, $q_{gcescbg}$, is found to be,

$$q_{gcescbg} = \left(q_{gcesc}\right)^{1.29}\left(\frac{s}{D}\right)^{0.16}(0.01)^{\frac{h}{D}} \tag{8.8}$$

The value of coefficient of determination (R^2) being 0.97, the model is able to predict well (Fig. 8.5).

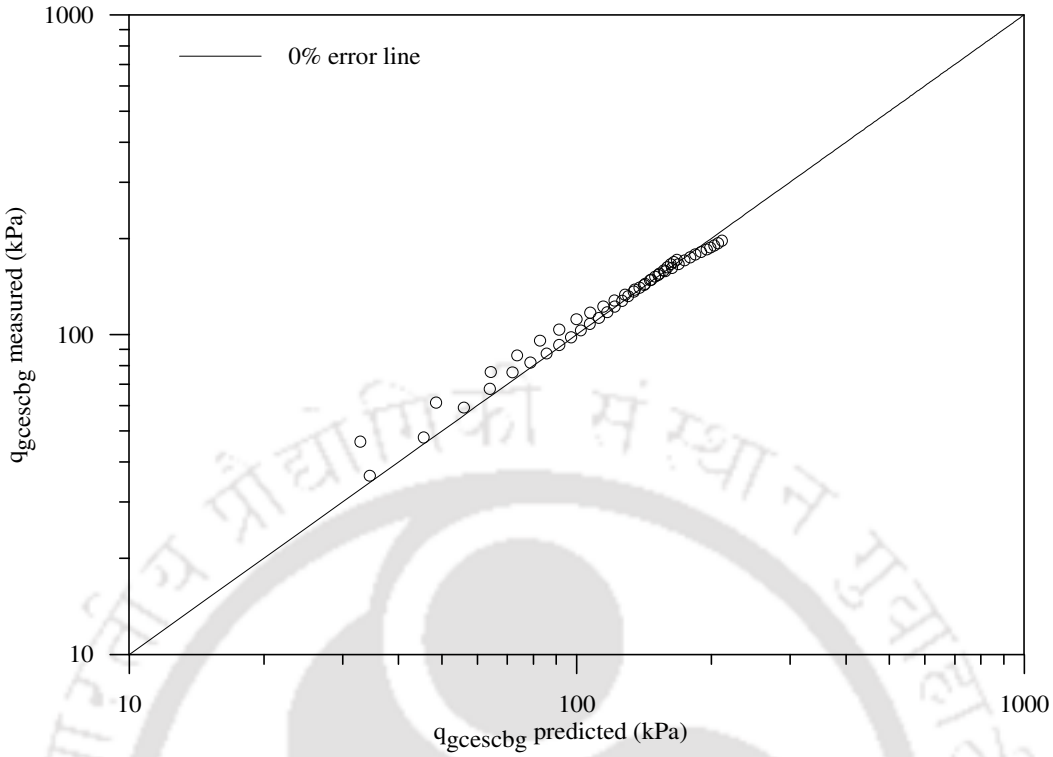

Fig.8.5 Predicted vs. measured bearing pressure, composite foundation bed with encased stone columns and base geogrid.

8.2 DIMENSIONAL ANALYSIS

Dimensional analysis can be used to study the scale effect of various parameters on the performance of reinforced foundation beds (Love, 1984, Fakher and Jones 1996). In the present investigations, the various parameters that contribute towards the performance improvement of composite foundation beds can be summerised as D, h, d_{gc}, S_t, d_{sc}, L, S, φ, c_u, γ, G ; where φ is the angle of internal friction of soil, S_t is the stiffness of the reinforcement, γ is the unit weight of soil, G is the shear modulus of the soil. The governing function for the composite foundation system can be written as:

$$f(D, h, d_{gc}, S_t, d_{sc}, L, S, c_u, \gamma, G, \varphi, s, q_{gcsc}, q_u) = 0 \qquad (8.9)$$

The equation (8.1) comprises of 14 parameters and got two fundamental dimensions (i.e. length and force) and hence can be studied by 12 (i.e. 14 - 2) independent parameters (Langhaar 1951). The independent parameters can be written as $\pi_1, \pi_2, \pi_3, \pi_4 \ldots\ldots\ldots \pi_{14}$ as per Buckingham Pi Theorem. Hence the Eq. 8.1 can be written as

$$g(\pi_1, \pi_2, \pi_3, \pi_4 \ldots\ldots\ldots \pi_{12}) =$$

$$g\left[\left(\frac{s}{D}\right),\left(\frac{h}{D}\right),\left(\frac{d_{gc}}{D}\right),\left(\frac{h}{d_{gc}}\right)\left(\frac{d_{sc}}{D}\right)\left(\frac{L}{D}\right),\left(\frac{S}{D}\right),\left(\frac{G}{D\gamma}\right)\left(\frac{S_t\gamma}{G^2}\right),\left(\frac{c_u}{D\gamma}\right),\left(\frac{q_{g\,\mathrm{csc}}}{q_u}\right),\varphi\right]$$

$$= 0 \tag{8.10}$$

For a prototype footing (p) with diameter N times than that of the model (m)

$$\frac{D_p}{D_m} = N \tag{8.11}$$

For similarity to be satisfied all the π terms should be equal, both for model and prototype.

$$(\pi_8)_p = (\pi_8)m$$

$$\frac{G_p}{D_p\gamma_p} = \frac{G_m}{D_m\gamma_m} \tag{8.12}$$

In the case of soils in model and prototype to be of equal density, the equation (8.12) boils down to,

$$\frac{G_p}{G_m} = \frac{D_p}{D_m} = N \tag{8.13}$$

$$(\pi_9)_p = (\pi_9)_m$$

$$\frac{S_{tp}\gamma_p}{G_p^{\ 2}} = \frac{S_{tm}\gamma_m}{G_m^{\ 2}}$$

$$\frac{S_{tp}}{S_{tm}} = \frac{G_p^{\ 2}}{G_m^{\ 2}} = N^2 \qquad (8.14)$$

Hence, for the 1g model test results such as the present one, to be valid quantitatively, the strength of the prototype geocell should be of N^2 times the strength of the model geocells, where N is the model scale. In the present model tests the strength of the geocell joints is much lower, compared to that of the geocell wall material (i.e. geogrid). Therefore, the performance improvement due to geocell reinforcement will be proportionate to the strength of the geocell joints rather than the geogrid used to make the geocells. Hence, the results of the present study to be applicable in practice, the prototype geocell (both joint and geogrid) should have a minimum strength of N^2 times the strength of the geocell joints, in the model tests. For example, for a prototype foundation of diameter 3 times that of model footing (i.e. N = 3), the geocell material should have a minimum tensile strength of 42.75 kN/m (i.e. 4.75 kN/m × 9). It could be observed that all other parameters have a linear variation.

CHAPTER 9

SUMMARY AND CONCLUSIONS

9.1 SUMMARY

In view of increased construction activity over weak soils, requirement for in situ treatment for the same to improve its performance is in ever increasing demand. Among the various ground improvement techniques used for improving the in-situ ground conditions, geosynthetics reinforcement and stone column technique are very popular, in the present days. This is primarily due to several advantages viz. ease of construction, economy, saving construction time and unique suitability under certain circumstances; that finds favour with the practicing engineers. The three dimensional geocells are the latest adaptation in the avenues of geosynthetic reinforcements. A general over view of these techniques is presented in Chapter 1.

Review of literature presented, in Chapter 2, shows that both geocell-sand mattress and stone columns are effective means for performance improvement of soft clay foundations. Their individual applications though have been intensely studied, by many researchers, but combined application of both has remained unexplored. Therefore, in the present research work a series of experiments have been carried out to develop an understanding of the behaviour of foundation systems having geocell-sand mattress overlying stone column reinforced clay beds.

The model tests were conducted in a test bed-cum-loading frame assembly in the laboratory. To prepare the test bed, the moist clay soil was placed in the test box and compacted in 0.05 m thick layers till the desired height was reached. The stone columns were constructed by replacement method. The diameter of the stone columns in the model tests was kept as 100mm. The geocell layer, which is a continuous

cellular structure, was prepared by cutting the biaxial geogrids to required length and height from full rolls and placing them in transverse and diagonal directions with bodkin joints at the connections. Then the geocell pockets were filled with sand, using sand raining technique. The model foundation used is made of a steel plate of 150mm in diameter and 30 mm in thickness. The footing was loaded with a computer controlled motorised hydraulic system. Loading was applied on the footing through the computer controlled hydraulic system. The load deformation data was acquired by the computerised data acquisition system. In total 25 different series of model load tests were conducted to establish the influence of the various parameters pertaining to the stone column-clay-geocell mattress foundation system, the details of which are presented in Chapter 3.

In Chapter 4, results of the model load tests on stone column reinforced clay beds are presented and discussed. The influence of various parameters of stone columns on the overall performance of the stone column reinforced clay foundation system has been brought out.

The results of load tests on geocell reinforced sand beds overlying soft clay subgrade are presented and discussed in Chapter 5. Parameters such as height of geocell mattress, pocket opening size of geocells and density of infill soil in geocells are found to have visible influence on the performance of the geocell reinforced foundation system.

In chapter 4 and 5 it was observed that both geocell reinforcement and stone column technique can enhance the load carrying capacity of soft clay bed markedly. It was therefore envisaged that combination of both theses techniques can further enhance the performance improvement, which has been studied under Chapter 6. A series of experiments have been carried out to study the influence of various parameters such

as; length and spacing of stone columns; height and pocket size of geocells; density of fill soil in geocells; on the overall performance of the composite foundation beds.

9.2 CONCLUSIONS

Based on the experiments and parametric studies carried out in this investigation, the following specific conclusions, of practical significance, can be drawn.

1. With the provision stone columns, of adequate length and spacing, 3.5 fold increases in bearing capacity of soft clay foundations can be achieved.
2. With increased length of stone column, it mobilizes higher end bearing through increased overburden pressure and greater skin friction resistance through increased peripheral area; therefore it punches less leading to increased bearing capacity. However, beyond certain length (i.e. $L = 5d_{sc}$) though the resistance against punching continues to increase but the stone column bulges excessively and hence further improvement in performance is marginal. Hence, it can be concluded that, for the present range of test conditions, the length of stone column (L) giving maximum performance improvement is about five times its diameter ($5d_{sc}$).
3. With reduced spacing, the stone columns induce increased confinement onto the foundation soil, leading to increased performance improvement. The increase in bearing pressure, when the spacing of stone columns reduces from $3.5d_{sc}$ to $2.5d_{sc}$ is substantially high beyond which further increase in bearing capacity is marginal. Hence the critical spacing of the stone columns can be taken as $2.5d_{sc}$.
4. The bulging in stone columns dies down to practically negligible value for length of stone column greater than four times its diameter (i.e. $L > 4d_{sc}$).
5. While the unreinforced clay bed undergoes failure at a settlement of about 10-12% of footing diameter (i.e. the pressure settlement response tends to become nearly

vertical), with geocell mattress the pressure settlement response is almost linear even at settlement as high as 25% of footing diameter. This indicates that the geocell reinforcement, owing to its three dimensional confinement, substantially reduces the shear failure in the foundation soil.

6. The bearing capacity of the foundation bed increases, significantly, with increase in the height of geocell mattress till about 1.1.D, beyond which further improvement is marginal.

7. With reduced pocket size, the overall rigidity as well as the confinement offered by the geocells per unit volume of soil increases, giving rise to a relatively stronger geocell mattress and hence a higher performance improvement of the system. However, the general behaviour of the geocell mattress, pertaining to the change in pocket size of the geocells, remains nearly same irrespective of the geocell mattress height i.e. shallow or deep.

8. With increased density of infill soil in geocells, the interfacial frictional resistance at the soil geogrid interface increases. As a result of which the anchorage against downward deformation under footing penetration increases leading to better performance improvement. Besides, as the dense soil tends to dilate it is restrained by the geocell walls, in turn; higher strength of reinforcement is mobilized leading to increased performance improvement.

9. With geocell mattress of optimum geometry and dense soil infill, seven fold increase in bearing capacity of the clay foundation can be achieved.

10. The stiffness and load carrying capacity of the clay bed with composite reinforcement (i.e. Clay + GC + SC) is much higher as compared to that with the geocell mattress alone (i.e. Clay + GC). This is due to the increased resistance

against deformation induced by the stone columns through mobilization of friction and stiffness of the stone aggregates.

11. The load carrying capacity of the composite (i.e. geocell-stone column reinforced) foundation bed increases with increase in length of stone columns till $5d_{sc}$, beyond which further improvement is marginal.

12. The critical spacing of stone columns in composite foundation beds, giving maximum performance improvement, is $2.5d_{sc}$. Further reduction in spacing of the stone columns does not produce much of additional performance improvement.

13. The influence of stone columns in the composite foundation beds reduces with increase in height of geocell mattress (h). With h/D ratio increasing beyond 1.1, the stone column influence over the foundation response has visibly been reduced indicating that the critical height of geocell mattress in composite foundation bed is nearly equal to the diameter of the footing.

14. The geocell pocket opening and the footing size should be designed such that the footing should completely cover at least one geocell pocket that the geocell reinforcement can actively participate leading to visible improvement in the performance of the composite foundation system.

15. The geocell mattress-stone column composite reinforcement can increase the bearing capacity of clay bed by ten fold.

16. An additional layer of planar geogrid at the interface between the geocell mattress and stone column reinforced clay bed can bring an improvement in bearing capacity as high as 30% more than that with geocell mattress-stone column reinforcement alone.

17. Encasement of stone columns further improves the performance improvement, with the bearing capacity increasing with the increase in the length of encasement.

However, with full length encasement, of the floating stone columns, the performance improvement reduces substantially. This is attributed to the absence of bulge formation and reduced skin friction resistance due to the relatively smooth surface of the encasement.

18. Combined use of base geogrid and encasement of stone columns is an added advantage that brings further improvement in load carrying capacity of the composite foundation bed. Nearly 9 fold increase in bearing capacity of the clay bed can be obtained with provision of geocell-base geogrid-encased stone column reinforcement, even with geocells of shallow height (h = 0.53D).

19. Dimensional analysis shows that, the results of the present study to be applicable in practice, the strength of the prototype geocell should be of N^2 times the strength of the model geocells, where N is the model scale.

REFERENCES

1. **Abdullah, C.H.** and **Edil, T.B.** (2007). "Behaviour of geogrid-reinforced load transfer platforms for embankment on rammed aggregate piers." *Geosynthetic International,* 14(3), 141-153.
2. **Alamgir, M., Miura, N., Poorooshasb, H.B.** and **Madhav, M.R.** (1996). "Deformation analysis of soft ground reinforced by columnar inclusions." *Computer and Geotechnics,* 18(4), 267-290.
3. **Ambily, A.P.** and **Gandhi, S.R.** (2007). "Behaviour of Stone Columns Based on Experimental and FEM Analysis." *Journal of Geotechnical and Geoenvironmental Engineering,* ASCE, 133(4), 405-515.
4. **Arulrajah, A., Abdullah, A.,** and **Bouzza, A.**, (2009). "Ground improvement technique for railway embankments." *Ground Improvement,* 162(G11), 3-14.
5. **ASTM Standard** D0854, 2006, **"**Test Methods for specific Gravity of Soil solids by Water Pycnometer." *ASTM International*, West Conshohocken, PA, 2006, 10.1520/D0854-05.
6. **ASTM Standard** D2487, 2006, "Standard practice for classification of soils for engineering purposes (Unified Soil Classification System)." *ASTM International*, West Conshohocken, PA, 2006, 10.1520/D2487-06E01.
7. **ASTM Standard** D2850, 2003, "Standard test method for unconsolidated-undrained triaxial compression test on cohesive soils." *ASTM International*, West Conshohocken, PA, 2007, 10.1520/D2850-03AR07.
8. **ASTM Standard** D4221, 2005, "Standard test methods for dispersive characteristics of clay soil by double hydrometer." *ASTM International*, West Conshohocken, PA, 10.1520/D4221-99R05.
9. **ASTM Standard** D4253**,** 2006, **"**Standard test methods for maximum index density and unit weight of soils and calculation of relative density." *ASTM International*, West Conshohocken, PA, 10.1520/D4253-00R06
10. **ASTM Standard** D4254, 2006, **"**Standard test methods for minimum index density and unit weight of soils and calculation of relative density." *ASTM International,* West Conshohocken, PA, 10.1520/D4254-00R06E01.

11. **ASTM Standard** D4318, 2005, "Standard Test Methods for Liquid Limit, Plastic Limit, and Plasticity Index of Soils." *ASTM International*, West Conshohocken, PA, 2005, 10.1520/D4318-05

12. **ASTM Standard** D4884, 2009, "Standard Test method for strength of strewn thermally bonded seams of Geotextiles." *ASTM International*, West Conshohocken, PA, 10.1520/D4884-09.

13. **ASTM Standard** D5311**,** 2004, **"**Standard Test Methods for Load Controlled Cyclic Triaxial Strength of Soil." *ASTM International*, West Conshohocken, PA, 10.1520/D5311-92R04E01.

14. **ASTM Standard** D6528, 2007, "Standard Test Methods for Consolidated Undrained Direct Simple Shear Testing of Cohesive Soils." *ASTM International*, West Conshohocken, PA, 10.1520/D6528-07.

15. **ASTM Standard** D6637**,** 2009. "Standard Test Methods for Determining Tensile Properties of Geogrid by Single or Multi-Rib Tensile Methods." *ASTM International,* West Conshohocken, PA, 10.1520/D6637-01R09.

16. **ASTM Standard** D6706, 2007, "Standard Test Method for Measuring Geosynthetic Pullout Resistance in Soil." *ASTM International*, West Conshohocken, PA, 10.1520/D6706-01R07.

17. **ASTM Standard** D6913, 2004, **"**Standard Test Methods for Particle-Size Distribution (Gradation) of Soils Using Sieve Analysis." *ASTM International*, West Conshohocken, PA, 2004, 10.1520/D6913-04R09.

18. **Ayadat, T.** and **Hanna, A.M.** (2005). **"**Encapsulated stone column as a soil improvement technique for collapsible soil." *Ground Improvement,* 9(4), 137-147.

19. **Ayadat, T.** and **Hanna, A.M.** (2008). "Soil improvement by internally reinforced stone columns." *Ground Improvement,* 6(GI2), 55-63.

20. **Bae, W.S., Shin, B.W.** and **An, B.C.** (2002). **"**Behaviours of Foundation System Improved with Stone Columns." *Proceedings of the Twelfth International Offshore and Polar Engineering Conference,* Kitakyushu, Japan, 675-678.

21. **Bathurst, R.J.** and **Crowe, R.E.** (1994). "Recent case histories of flexible geocell retaining walls in North America." *Recent Case Histories of Permanent Geosynthetic-Reinforced Soil Retaining Walls*. Eds. Tatsuoka, F., Leshchinsky, Balkema, Rotterdam, pp. 3–19.

22. **Bathurst R.J.** and **Knight M.A.** (1998). "Analysis of geocell reinforced-soil covers over large span conduits." *Computer and Geotechnics,* 22(3–4), 205–219.

23. **Black, J., Sivakumar, V.** and **MeKinley, J.D.** (2007). **"**Performance of clay samples reinforced with vertical granular columns." *Canadian Geotechnical Journal, 44*, 89-95.

24. **Black, J.A., Sivakumar, V., Madhav, M.R.** and **McCabe, B.A.** (2007a). "Reinforced stone column in weak deposits: Laboratory Model Study." *Journal of Geotechnical and Geoenvironmental Engineering,* ASCE, 133, 1254-1161.

25. **Broms, B.B.** and **Massarch, K.R.** (1977). "Grid Mats - A New Foundation Method." *Proceeding of the ninth International Conference on Soil Mechanics and Foundation Engineering,* Tokyo. 433-438.

26. **Bush, D.I., Jenner, C.G.** and **Bassett, R.H.** (1990). **"**The Design and Construction of Geocell Foundation Mattresses Supporting Embankments over Soft Ground." *Geotextiles and Geomembranes,* 9, 83-98.

27. **Buckingham, E.** (1914). "On Physically Similar Systems; Illustrations of the Use of Dimensional Equations." *Bureau of Standards,* Second Series, 345-376.

28. **Carroll Jr., R.G.** and **Curtis, V.C.** (1990). "Geogrid connections." *Geotextiles and Geomembranes,* 9, 515-530.

29. **Chritoulas, S., Bouckvalaas, G.,** and **Giannaros, C.** (2000). **"**An experimental Study on the Model Stone Columns." *Soils and Foundations,* 40(6), 11-22.

30. **Chummer, A.V.** (1972). **"**Bearing Capacity theory from experimental results." *Journal of the Soil Mechanics and foundations Division,* ASCE 98 (12), 1311-1324.

31. **Cowland, J.W.** and **Wong, S.C.K.** (1993). **"**Performance of a Road Embankment on Soft Clay Supported on a Geocell Mattress Foundation." *Geotextiles and Geomembranes,* 22, 687-705.

32. **Das, B. M.** and **Khing K. H.** (1994) "Foundation on layered soil with geogrid reinforcement - effect of a void." *Geotextiles and Geomembranes*, 13, 545-553.

33. **Das, B.M.**, **Puri**, **V.K., Omar, M.T.** and **Evgin, E.** (1996) "Bearing capacity of strip foundation on geogrid-reinforced sand - scale effects in model tests." Proceedings of *6th International Conference on Offshore and Polar Engineering*, Los Angles, May, 527-530.

34. **Dash, S.K., Krishnaswamy, N.R.** and **Rajagopal, K.** (2001a). **"**Bearing capacity of strip footing supported on geocell-reinforced sand." *Geotextiles and Geomembranes,* 19, 235- 256.
35. **Dash, S.K., Krishnaswamy, N.R.,** and **Rajagopal, K.** (2001b). "Strip footing on geocell reinforced sand beds with additional planar reinforcement." *Geotextiles and Geomembranes,* 19, 529-538.
36. **Dash, S.K., Sireesh, S.** and **Sitharam, T.G.** (2003a). **"**Model studies on circular footing supported on geocell reinforced sand underlain by soft clay." *Geotextiles and Geomembranes,* 21, 197-219.
37. **Dash, S.K., Sireesh, S.** and **Sitharam, T.G.** (2003b). "Behaviour of geocell-reinforced sand beds under circular footing." *Ground Improvement,* 7(3), 111-115.
38. **Dash, S.K., Rajagopal, K.** and **Krishnaswamy, N.R**. (2004). **"**Performance of different geosynthetic reinforcement materials in sand foundations." *Geosynthetics International,* 11(1), 35-42.
39. **Dash, S.K., Reddy, P.D.T.** and **Raghukanth, S.T.G.** (2008). **"**Subgrade modulus of geocell-reinforced sand foundations." *Ground Improvement*, G12, 79-87.
40. **De Garldel, R.** and **Morel, G.** (1986). "New strengthening techniques by textile elements for low-volume roads." *Proceedings of Third International Conference on Geotextiles.* Vienna, Austria. 1027-1032
41. **Dean, R.** and **Lothian, E.** (1990). **"**Embankment construction problems over deep variable soft deposits using a geocell mattress." *Performance of Reinforced Soil Structures.,* Eds. McGown, A., Yeo, K.C., and Andrawes, K.Z., British Geotechnical Society, Thomas Telford Ltd., London, 443-447.
42. **Deb, K., Chandra, S.** and **Basudhar, P.K.** (2007). "Generalised model for Geosynthetic-Reinforced Granular Fill-Soft Soil with Stone Columns." *International Journal of Geomechanics,* ASCE, 7(4), 266-276
43. **Dewer, S.** (1962). "The Oldest Roads in Britain." *The countryman,* 59(3). 547-555
44. **Dielman, T.E.** (2001). "Applied regression analysis for Business and Economics." *Duxbury, Thomson Learning Inc*. USA
45. **Fakher, Ali Jones, Colins, J.F.P.** (1996). " Bearing capacity of Rectangular Footings on Geogrid-Reinforced Sand" *Journal of Geotechnical Engineering,* ASCE( ), 326-327
46. **Forsman, J., Slunga, E.** and **Lahtinen, P.** (1998). "Geogrid and Geocell Reinforced Secondary Road over Deep Peat Deposit." *Proceedings of the 6th International Conference on Geosynthetics,* Atlanta 2, 773-778

47. **Gibson, R.E.** (1953). **"**Experimental Determination of the True Cohesion and True Angle of Internal Friction in Clays." *Proceedings, 3rd International Conference,* ISSMFE, Zurich, 1, 126-130.

48. **Gniel, J.,** and **Bouazza, A.** (2008). "Improvement of soft soils using geogrid encased stone columns." *Geotextiles and Geomembranes,* 27, 167-175.

49. **Guido, V.A., Chang, D.K.,** and **Sweeny, M.A.** (1989). "Comparison of geogrid and geotextile reinforced slabs." *Canadian Geotechnical Journal*, 23(1), 435-440.

50. **Gupta, P.** and **Somnath, B.** (1994). **"**Bearing capacity improvement using geogrids." *Journal of Civil Engineering and Construction Review*, **7**, 12-13.

51. **Han, J.** and **Gabr, M.A.** (2002). "Numerical Analysis of Geosynthetic-Reinforced and Pile-Supported Earth Platforms over Soft Soil." *Journal of Geotechnical and Geoenvironmental Engineering,* ASCE, 128, 44-53.

52. **Hughes, J.M.O.** and **Withers, N.J.** (1974). **"**Reinforcing of soft cohesive soils with stone columns." *Ground Engineering,* 7(3), 42-49.

53. **Jenner, C.G., Bassett, R.H.** and **Bush, D.I.** (1988). "The use of slip line fields to assess improvement in bearing capacity of soft ground by cellular foundation mattress installed at the base of an embankment." *Proceedings of International Geotechnical Symposium on Theory and Practice of Earth Reinforcement,* Kyhshu, ed. Yamanouchi, T., Miura, N., and Ochiai, H. Belkema, Rotterdam, 209-214

54. **Johnson, J.E.** (1982). "Bridge and Tidal Waters." *Municipal Engineers.* 109, 104-107

55. **Johnson W.** and **Mellor P.B.** (1983). *Engineering Plasticity*., Ellis Marwood Ltd., Chichester (UK).

56. **Juran, I.,** and **Guermazi, A.** (1988). **"**Settlement response of soft soils Reinforced by Compacted sand columns." *Journal of Geotechnical Engineering,* ASCE, 114(8), 930-942.

57. **Juran, I.,** and **Riccobono, O.** (1991). "Reinforcing Soft Soils with Artificially Cemented Compacted Sand Columns." *Journal of Geotechnical Engineering*, ASCE, 117(7), 1042-1060.

58. **Khay, M.**, **Morel, G.** and **Perrier H.** (1986) "Use of geotextiles in construction of low cost highways: an experiment." Proceedings of *Third International Conference on Geotextiles*, Vienna, 957-961.

59. **Knight, M. A.** and **Bathurst R. J.** (1997). **"**Finite element analysis of reinforced geocell-soil covers over large span conduits." *Proceedings of the 6th International Symposium on Numerical Models in Geomechanics,* Montreal. A. A. Balkema, Rotterdam, 269-274.

60. **Koerner, R. M.** (1990). *Designing with geosynthetics.* 2nd Edition. Prentice Hall, Englewood Cliffs, N.J.

61. **Krishnaswamy, N. R., Rajagopal, K. and Madhavi Latha, G** (1998) "Geocell Reinforcement for Construction of Embankments over Soft Clay Foundation," *Proc. of 2nd Int. Conf. on Ground Improvement Techniques*, October 8-9, Singapore, 251-258,

62. **Krishnaswamy, N.R., Rajagopal, K.** and **Latha, G.M.** (2000). **"**Model studies on geocell supported embankments constructed over soft clay foundation." *Geotechnical Testing Journal*, 23(1), 45-54.

63. **Langhaar, J.L.** (1951), "Dimensional analysis and theory of models" *John Wiley & Sons,* New York, N.Y.

64. **Madhav, M.R., Sharma, J.K.** and **Sivakumar, V.** (2009). **"**Settlement of and load distribution in a granular piled raft." *Geomechanics and Engineering,* 1(1), 97-112.

65. **Madhavi Latha, G., Rajagopal, K.** and **Krishnaswamy, N.R.** (2006). "Experimental and Theoretical Investigations on Geocell-Supported Embankments." *International Journal of Geomechanics,* ASCE, 6(1), 30-35.

66. **Malarvizhi, S.N. and Ilamparuthi, K.** (2007). "Comparative Study on the Behaviour of Encased Stone Column and Conventional Stone Column." *Soils and Foundations,* .47(5), 873-885.

67. **Mandal, J.N.** and **Gupta, P.** (1994). **"**Stability of geocell-reinforced soil." *Construction and Building Materials*. 8(1), 55-62.

68. **Mayerhof, G.G.** and **Sastry, V.V.R.N.** (1978). "Bearing Capacity of piles in layered soils." Part I, *Canadian Geotechnical Journal,* 15, 171-182.

69. **Mayerhof, G.G.** and **Sastry, V.V.R.N.** (1978). **"**Bearing capacity of piles in layered soils." Part II, *Canadian Geotechnical Journal,* 15, 183-189.

70. **McKelvey, D., Sivakumar, V., Bell, A.** and **Graham, J.** (2004). "Modeling vibrated Stone columns on soft clay." *Journal of Geotechnical Engineering* 157(GE3), 137–149.

71. **Mhaiskar, S.Y.** and **Mandal, J.N.** (1996). "Investigations on soft clay subgrade strengthening using geocells." *Construction and Building Materials*. 10(4), 281–286.

72. **Mitchell, J.K., Kao, T.C.** and **Kavazanjiam, E.Jr.** (1979). "Analysis of grid cell reinforced pavement bases." *US Army Engineers Waterways Experiment Station.* Technical Report GL-79–8,

73. **Mitchell, J.K.** and **Huber, T.R.** (1985). "Performance of a stone column foundation." *Journal of Geotechnical Engineering,* ASCE, 111(2), 205-223.

74. **Moreau, Neil** and **Marry** (1835). "Foundations-emploi du sable." *Annales des Ponts and Chaussees,* Memoirs, No. 224, 171-214.

75. **Murugesan, S.** and **Rajagopal, K.** (2006). "Geosynthetic-encased stone columns: Numerical evaluation." *Geotextiles and Geomembranes,* 24, 349-358.

76. **Murugesan, S.** and **Rajagopal, K.** (2007). "Model tests on geosynthetic-encased stone columns." *Geosynthetics International,* 14(6), 346-354.

77. **Murugesan, S.** and **Rajagopal, K.** (2008). "Shear Load Tests on Stone Columns with and Without Geosynthetic Encasement." *Geotechnical Testing Journal,* 32(1), 1-10.

78. **Murugesan, S.** and **Rajagopal, K.** (2010). "Studies on the behaviour of single and group of geosynthetic encased stone columns." *Journal of Geotechnical and Geoenvironmental Engineering,* ASCE, 136 (1), 129-139.

79. **Panda, B.C.** (2000). **"**Structural behaviour of concrete block pavement." PhD thesis submitted to *Indian Institute of Technology Kharagpur*, India.

80. **Poorooshasb, H. B.** and **Meyorhof, G. G.** (1997). "Analysis of Behavior of Stone Columns and Lime Columns." *Computers and Geotechnics,* 20(1), 47-70.

81. **Puppala, A. J.** and **Musenda, C.** (2007) "Effects of Fiber Reinforcement on Strength and Volume Change in Expansive Soils" Journal of the Transportation Research Board, Vol. 1736 / 2000, 134-140.

82. **Rao, S.N., Reddy, K.M.** and **Kumar, P.H.** (1997). "Studies on Groups of Stone Columns in Soft Clays."*Proceedings of Symposium on Ground Improvement Techniques for Practising Engineers,* Chennai, India, 165-182.

83. **Rao, A.S., Phanikumar, B.R.** and **Suresh, K.** (2008). "Response of granular pile-anchors under compression." *Ground Improvement,* 6 (GI3), 121-129.

84. **Rea, C.** and **Mitchell, J.K.** (1978). "Sand reinforcement using paper grid cells." *Proceedings, Symposium on Earth Reinforcement,* ASCE Annual Convention, 3130, Pittsburgh, P.A., 644-663.

85. **Robertson, J.** and **Gilchrist, A.J.T.** (1987). "Design and construction of a reinforced embankment across soft lakebed deposits." *Proceedings International Conference on Foundations and Tunnels,* London, 2, ed. M. C. Forde. Engineering Technics Press, Edinburgh, 84-92.

86. **Selig, E.T** and **McKee, K.E.** (1961). "Static and Dynamic behaviour of small footings." *Journal of Soil Mechanics and Foundation Engineering,* ASCE, 87(6), 29-47.

87. **Sharma, R.S., Phanikumar, B.R.** and **Nagendra, G.** (2004). **"**Compressive load response of granular piles reinforced with geogrids." *Canadian Geotechnical Journal,* 41, 187-192.

88. **Sridharan A.** *Bearing capacity improvement* pp. 175-196 In **G.V. Rao** and **G.V.V.S. Raju**(ed.) *Engineering with Geosynthetics*, Tata McGraw-Hill, New Delhi, 1990.

89. **Simac, M.R.** (1990). **"**Connections for geogrid systems." *Geotextiles and Geomembranes,* 9, 537-546.

90. **Sireesh, S., Sithram, T.G.** and **Dash, S. K.** (2009). **"**Bearing capacity of circular footing on geocell–sand mattress overlying clay bed with void." *Geotextiles and Geomembranes,* 27, 89-98.

91. **Sitharam, T.G., Sireesh, S.** and **Dash, S.K.** (2005). "Model studies of a circular footing supported on geocell-reinforced clay." *Canadian Geotechnical Journal,* 42, 693-703.

92. **Sitharam, T.G., Sireesh, S.** and **Dash, S.K.** (2007). **"**Performance of surface footing on geocell-reinforced soft clay beds." *Geotechnical and Geological Engineering,* 25, 509-524.

93. **Terzaghi, K.,** (1943). *Theoretical Soil Mechanics,* John Willey and Sons Inc., New York, N.Y.

94. **Terzaghi, K.,** (1967). *Soil Mechanics in Engineering Practice,* John Willey and Sons Inc, New York, N.Y.

95. **Vidal, H.** (1969) The Principle of reinforced earth, *Highway Research Record*, No. 282, Washington, D.C.

96. **Webster, S. L.** and **Watkins, J. E.** (1977). "Investigation of Construction Techniques for Tactical Bridge Approach Roads across Soft Ground." *Technical Report S-77-1,* United States Army Corps of Engineers, Waterways Experiment Station, Mississippi, USA.

97. **Webster, S. L.** and **Alford, S. J.** (1978). "Investigation of Construction Concepts for Pavements across Soft Ground." *Technical Report S-78-6*, United States Army Corps of Engineers, Waterways Experiment Station, Mississippi, USA.

98. **Wesseloo, J., Vissar, A.T.** and **Rust, E.** (2009). "The stress–strain behaviour of multiple cell geocell packs." *Geotextiles and Geomembranes,* 27, 31-38.

99. **Wood, D.M., Hu, W.** and **Nash, D.F.T**. (2000). "Group effects in stone column foundations: model tests." *Geotechnique,* 50(6), 689-698.

100. **Wu, C. S., Hong, Y. S.** and **Lin, H.C.** (2009). "Axial stress relation of encapsulated granular columns." *Computer and Geotechnics,* 35, 226-240.

101. **Wu, C. S.,** and **Hong, Y. S.** (2009). "Laboratory tests on geosynthetic-encapsulated sand columns." *Geotextiles and Geomembranes,* 27, 107-120.

102. **Zhou, H.,** and **Wen, X.** (2008). "Model studies on geogrid or geocell-reinforced sand cushion on soft soil." *Geotextiles and Geomembranes,* 26, 231-238.

103. **Zhang, L., Zhao, M., Zou, X.,** and **Zhao, H.** (2009). "Deformation analysis of geocell reinforcement using Winkler model." *Computers and Geotechnics*, 36, 977-983.

APPENDIX I

SURFACE DEFORMATION RESPONSES

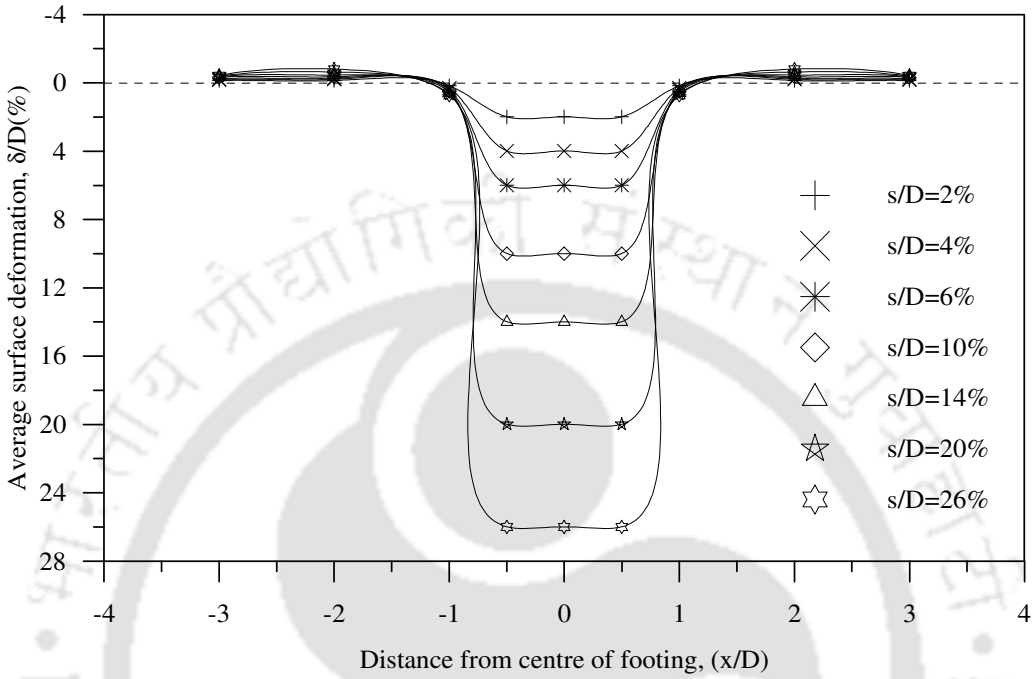

Fig.A1.1: Surface deformation profile, stone column reinforced clay bed ($L/d_{sc} = 1$) - Test series 2

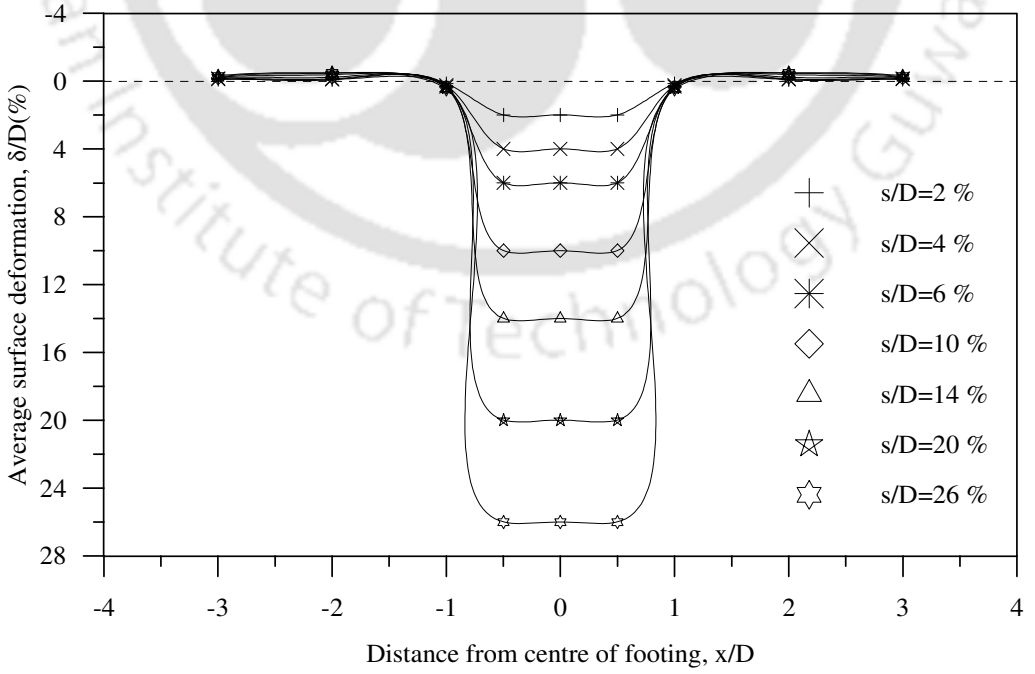

Fig.A1.2: Surface deformation profile, stone column reinforced clay bed ($L/d_{sc} = 3$) -Test series 2

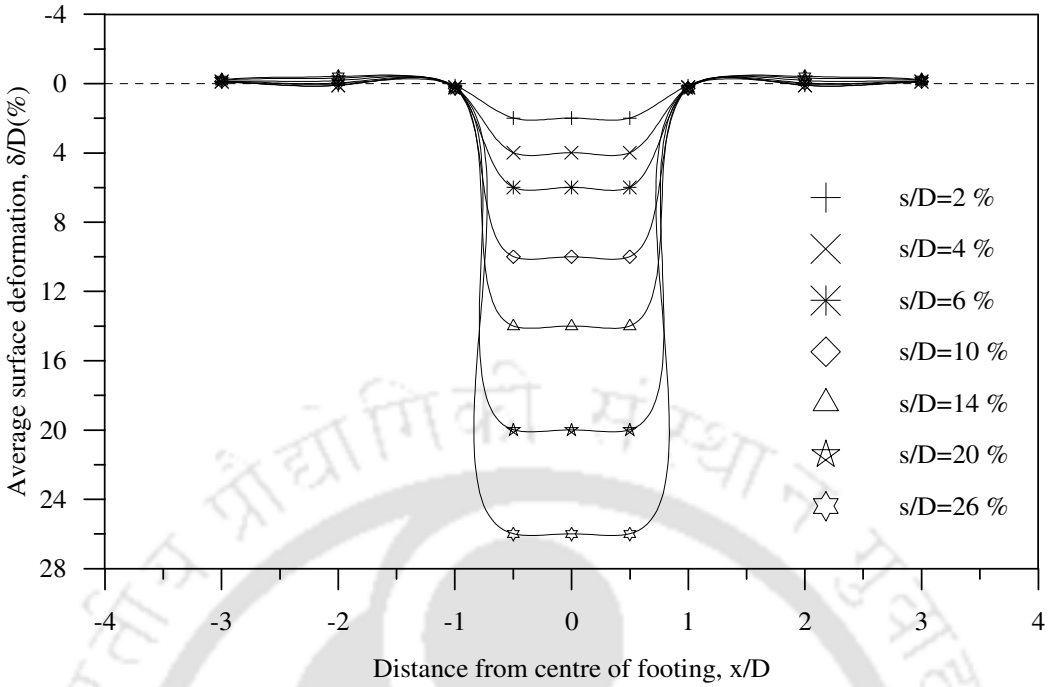

Fig.A1.3: Surface deformation profile, stone column reinforced clay bed ($L/d_{sc} = 5$) - Test series 2

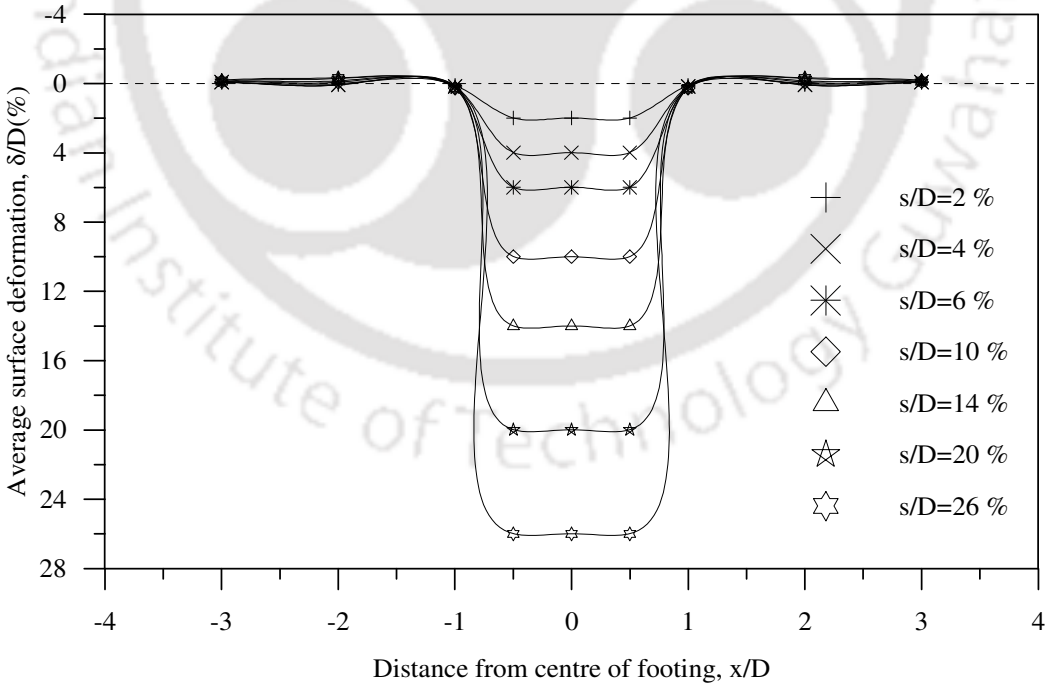

Fig.A1.4: Surface deformation profile, stone column reinforced clay bed ($L/d_{sc} = 7$) - Test series 2

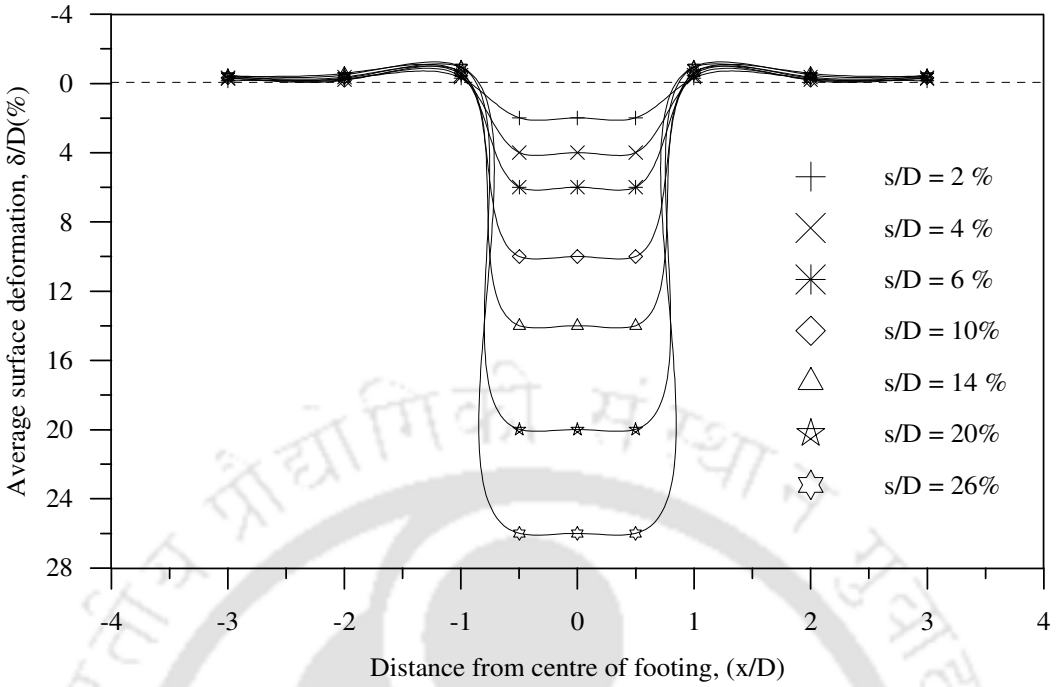

Fig.A1.5: Surface deformation profile, stone column reinforced clay bed (S/d_{sc} = 1.5) - Test series 3

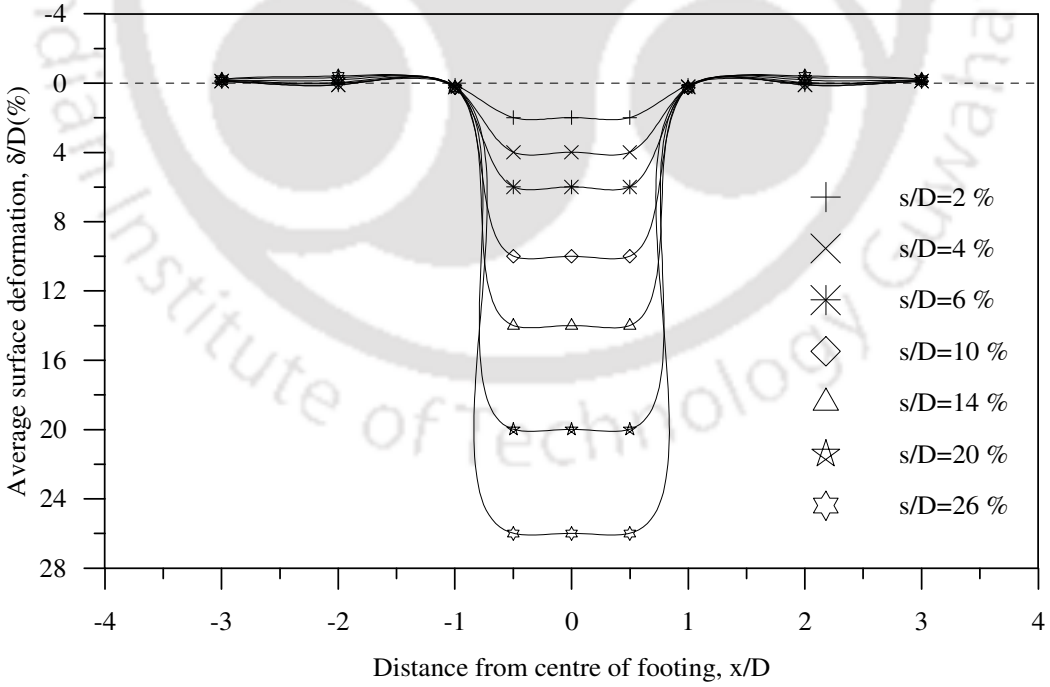

Fig.A1.6: Surface deformation profile, stone column reinforced clay bed (S/d_{sc} = 2.5) - Test series 3

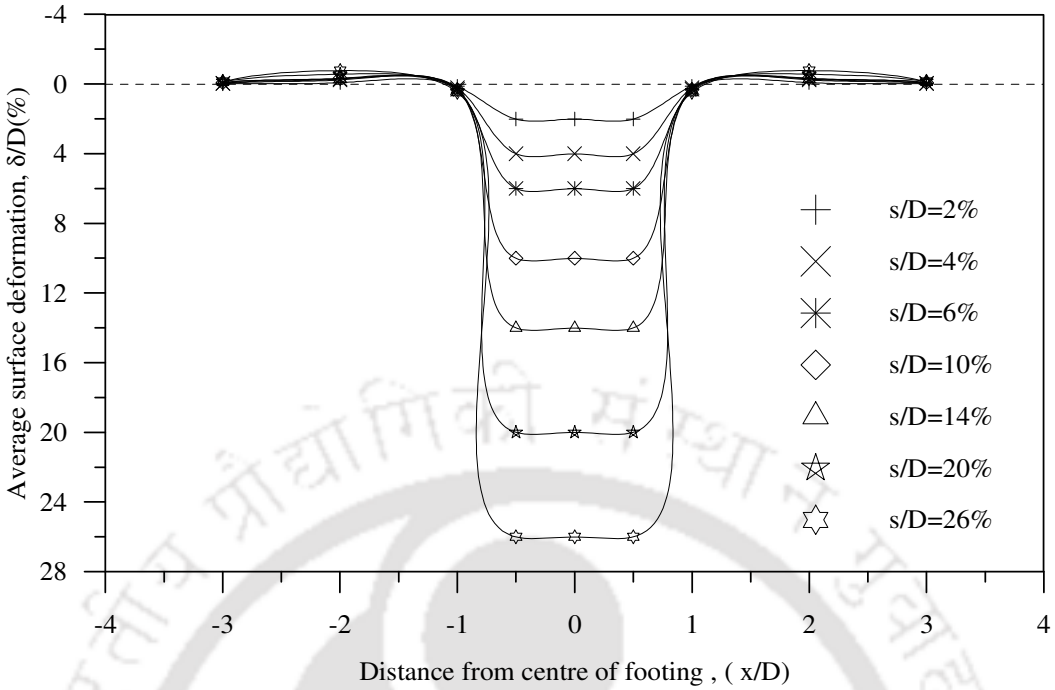

Fig.A1.7: Surface deformation profile, stone column reinforced clay bed ($S/d_{sc} = 3.5$) - Test series 3

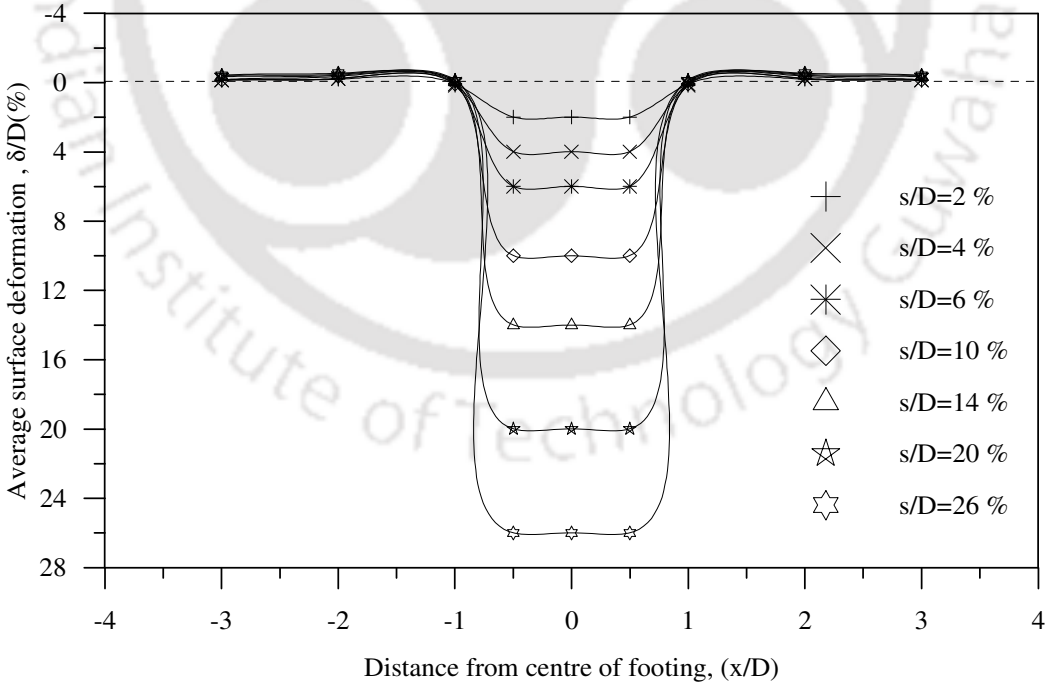

Fig.A1.8: Surface deformation profile, geocell-sand mattress reinforced clay bed (ID = 35%) – Test series 5

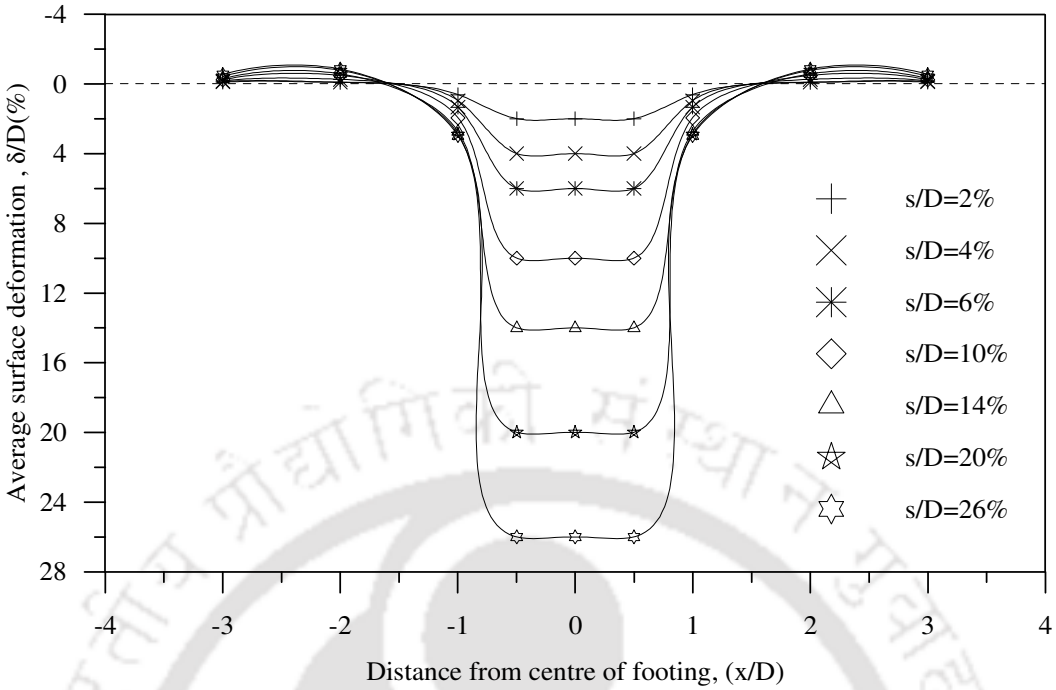

Fig.A1.9: Surface deformation profile, geocell-sand mattress reinforced clay bed (ID = 50%) – Test series 5

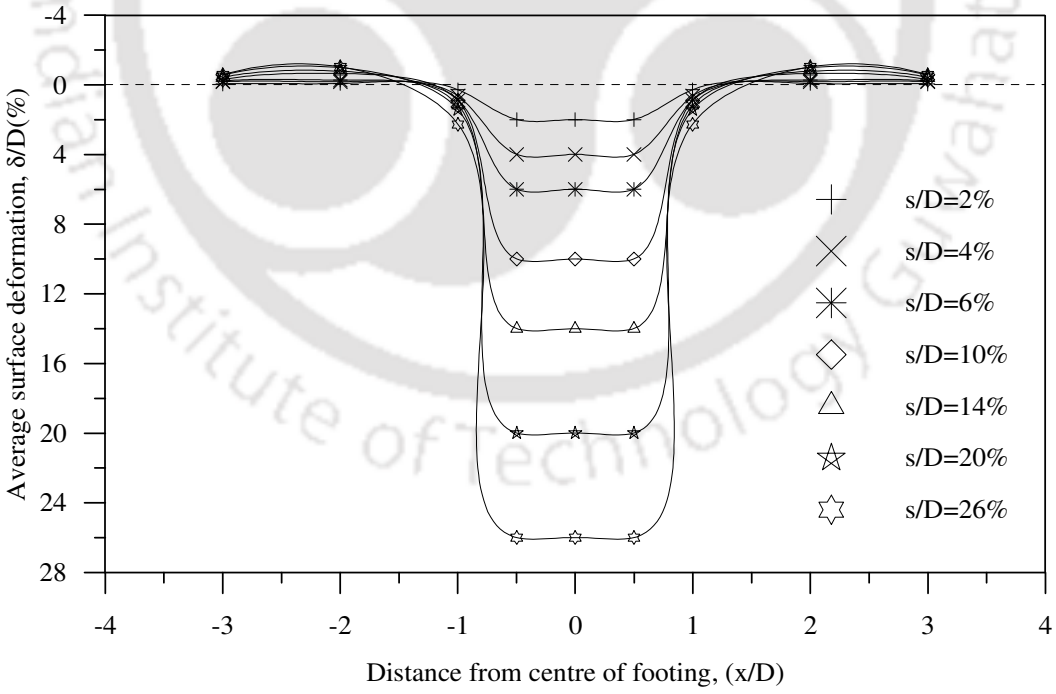

Fig.A1.10: Surface deformation profile, geocell-sand mattress reinforced clay bed (ID = 80%) – Test series 5

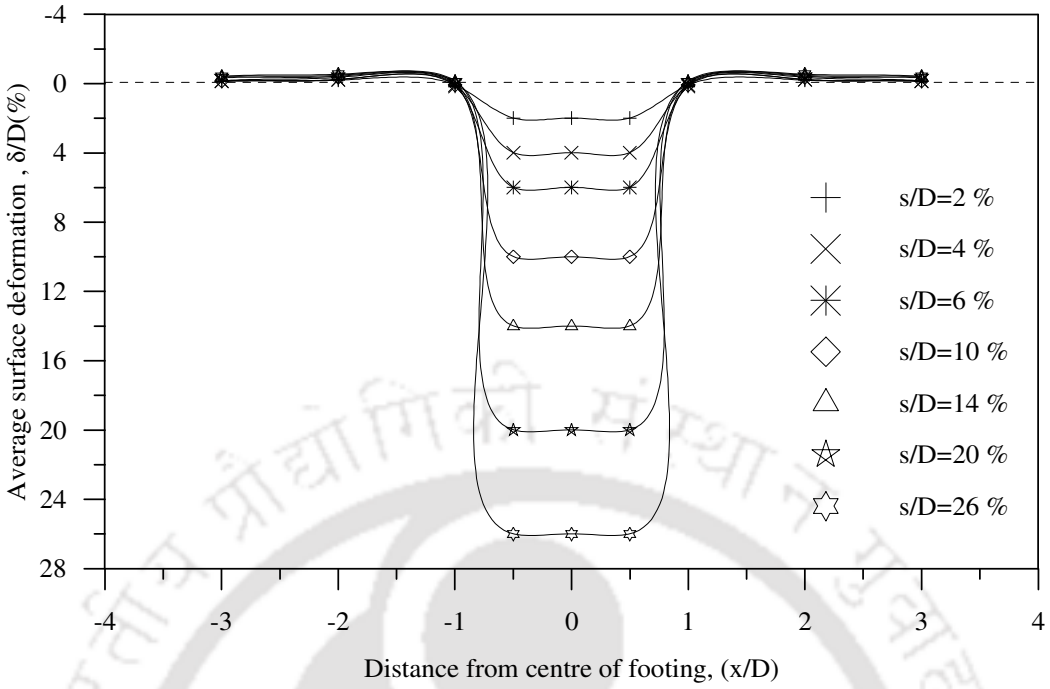

Fig.A1.11: Surface deformation profile, geocell-sand mattress reinforced clay bed (ID = 35%) – Test series 6

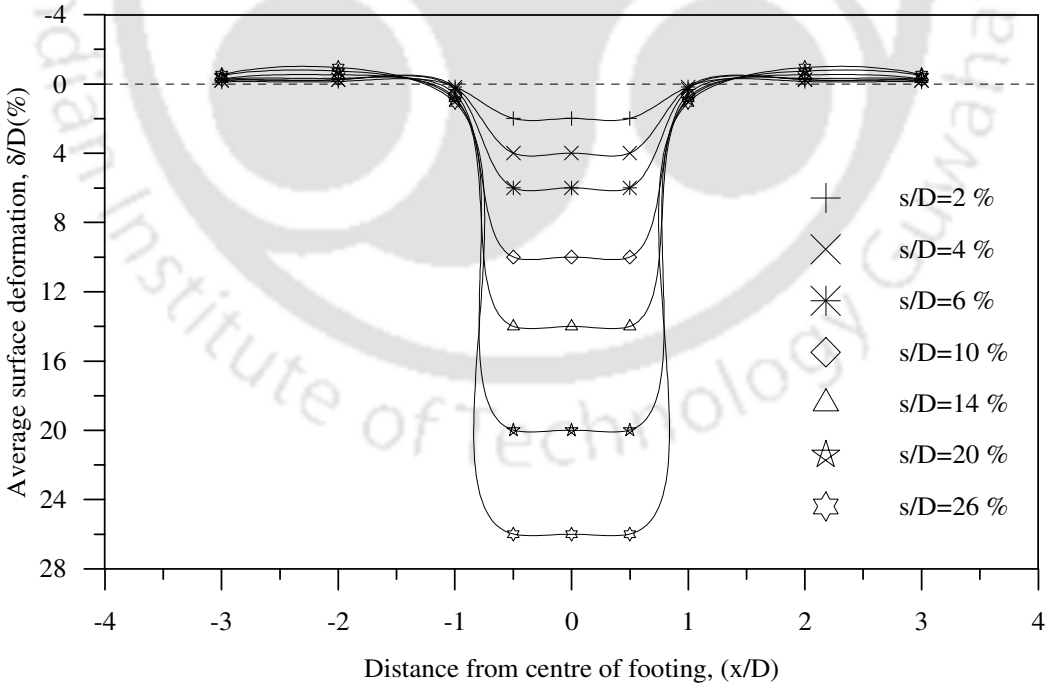

Fig.A1.12: Surface deformation profile, geocell-sand mattress reinforced clay bed (ID = 50%) – Test series 6

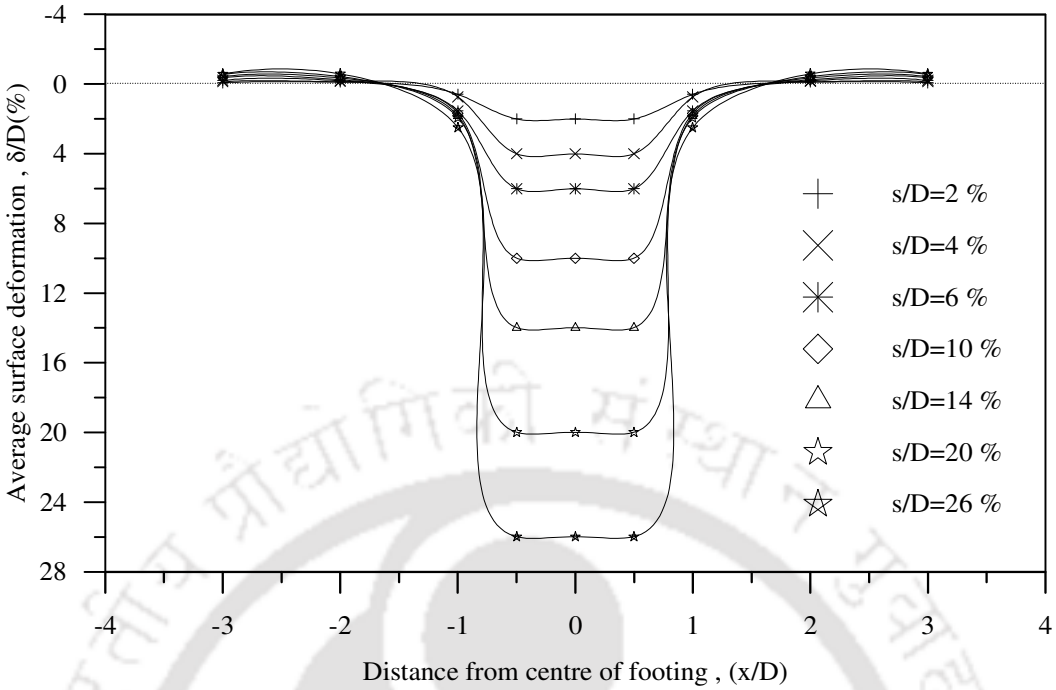

Fig.A1.13: Surface deformation profile, geocell-sand mattress reinforced clay bed (ID = 80%) – Test series 6

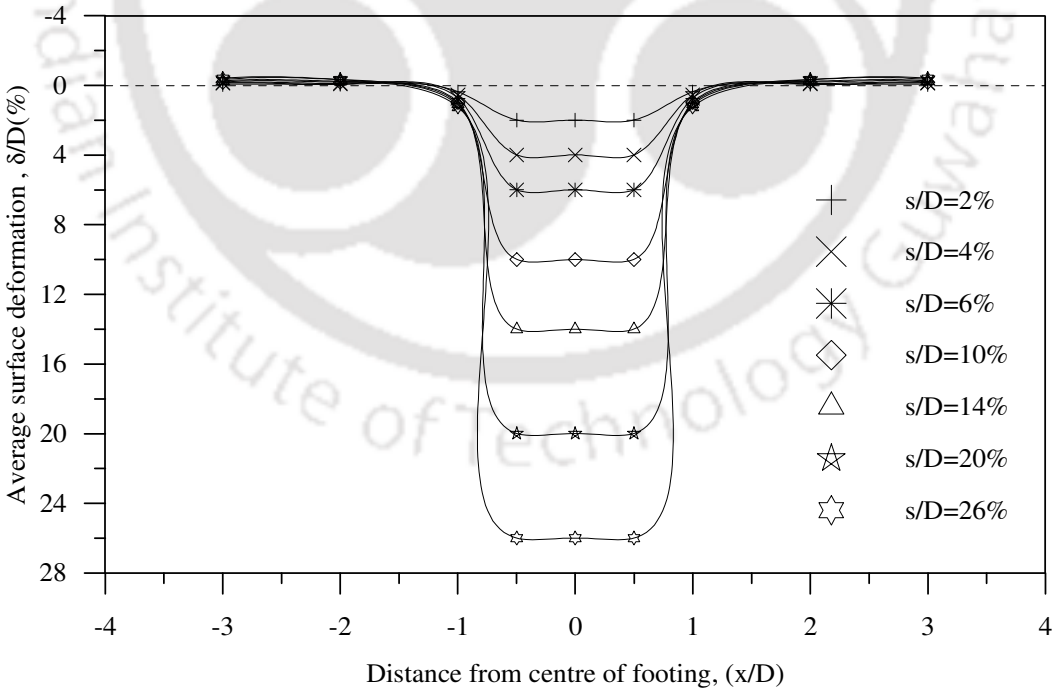

Fig.A1.14: Surface deformation profile, geocell-sand mattress reinforced clay bed (d_{gc}/D = 0.8) – Test series 8

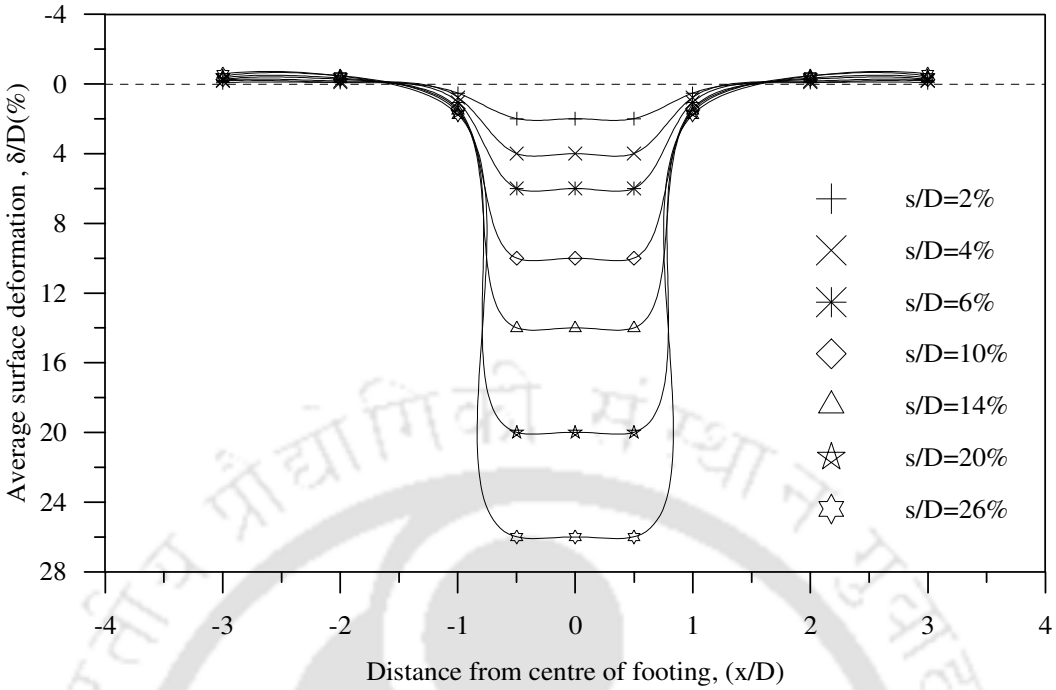

Fig.A1.15: Surface deformation profile, geocell-sand mattress reinforced clay bed (d_{gc}/D = 1.1) – Test series 8

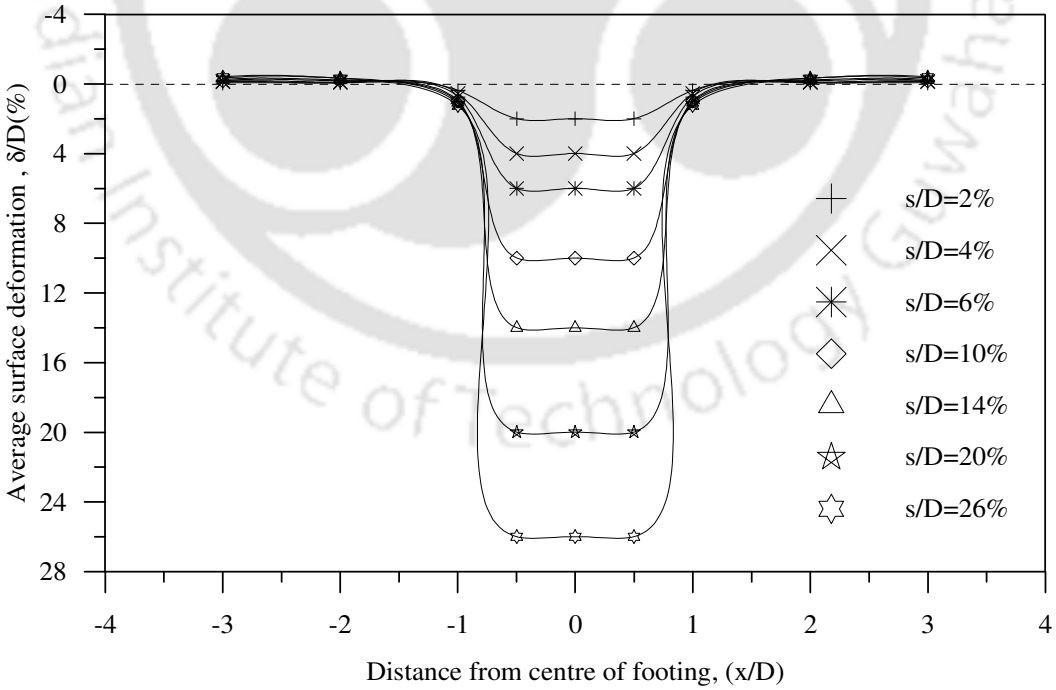

Fig.A1.16: Surface deformation profile, geocell-sand mattress reinforced clay bed (d_{gc}/D = 1.33) – Test series 8

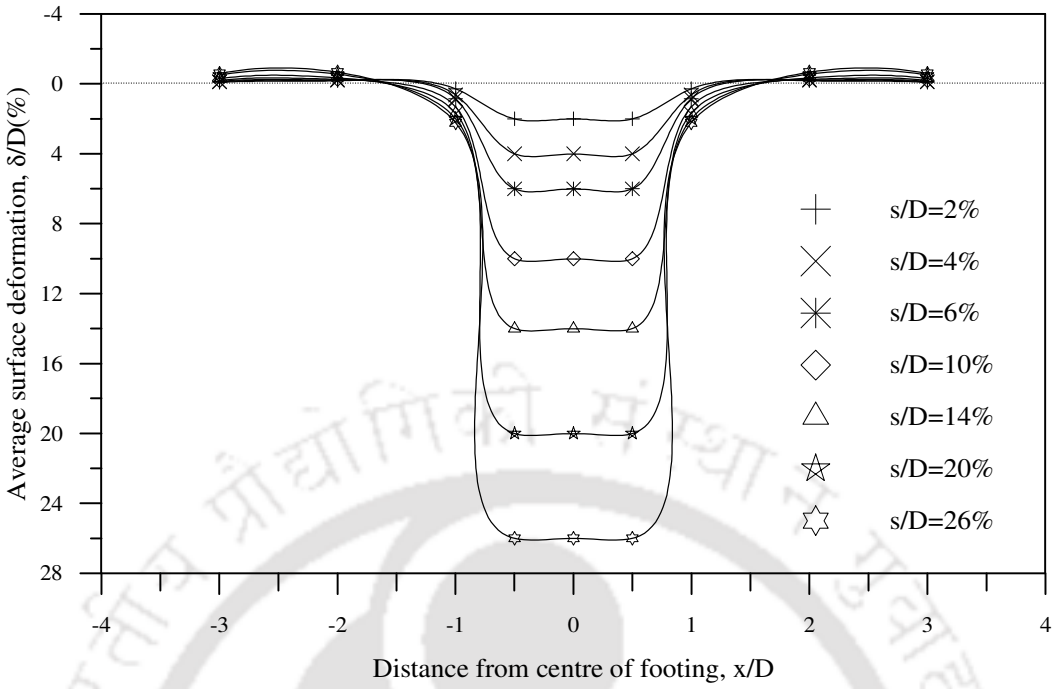

Fig. A1.17: Surface deformation profile, composite foundation bed

(h/D = 0.9, L/d_{sc} = 1) – Test series 10

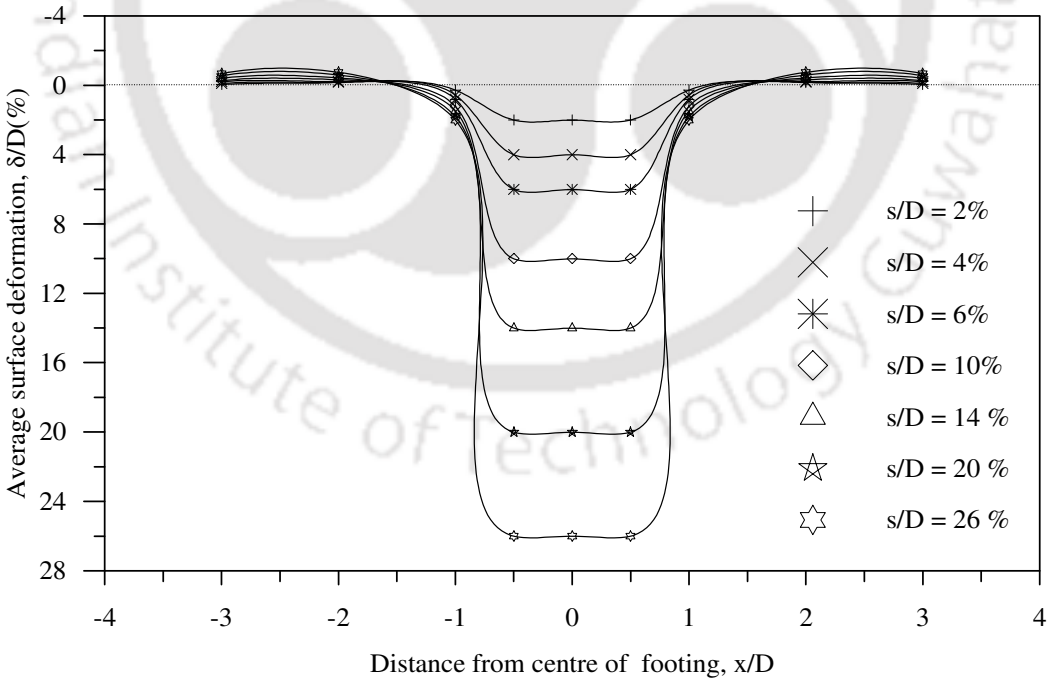

Fig.A1.18: Surface deformation profile, composite foundation bed

(h/D = 0.9, L/d_{sc} = 3) – Test series 10

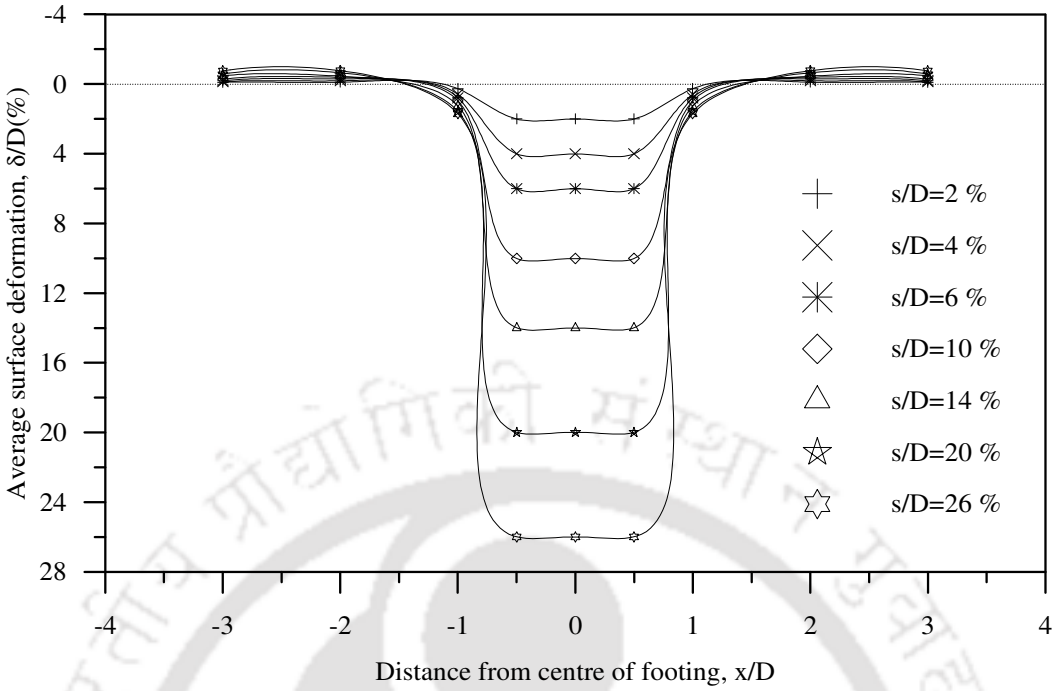

Fig.A1.19: Surface deformation profile, composite foundation bed
(h/D = 0.9, L/d_{sc} = 5) – Test series 10

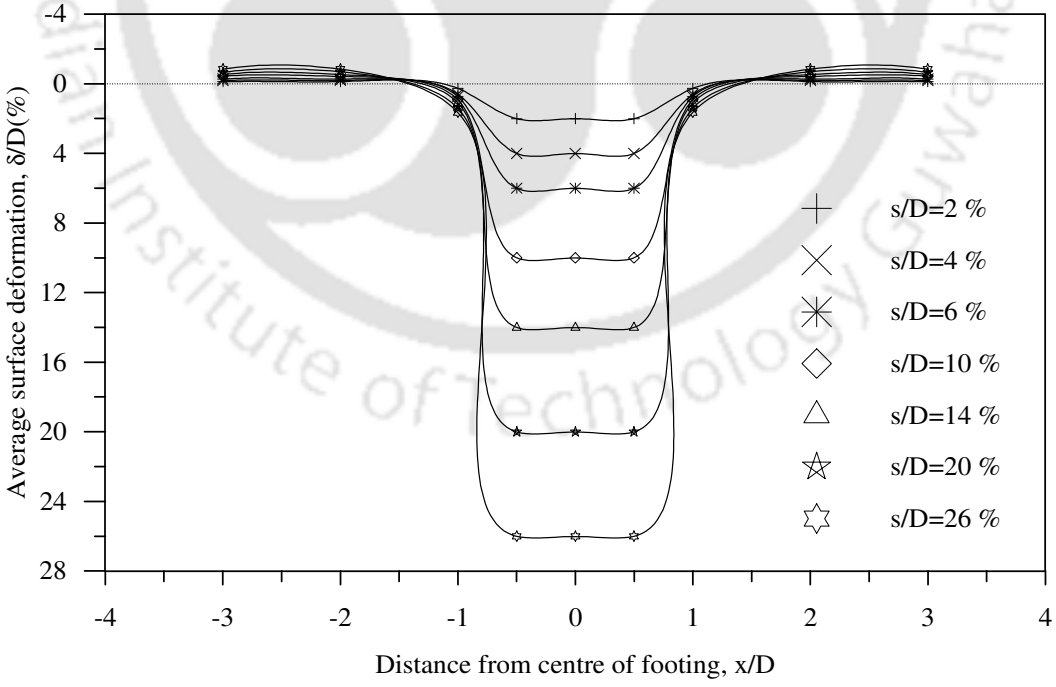

Fig.A1.20: Surface deformation profile, composite foundation bed
(h/D = 0.9, L/d_{sc} = 7) – Test series 10

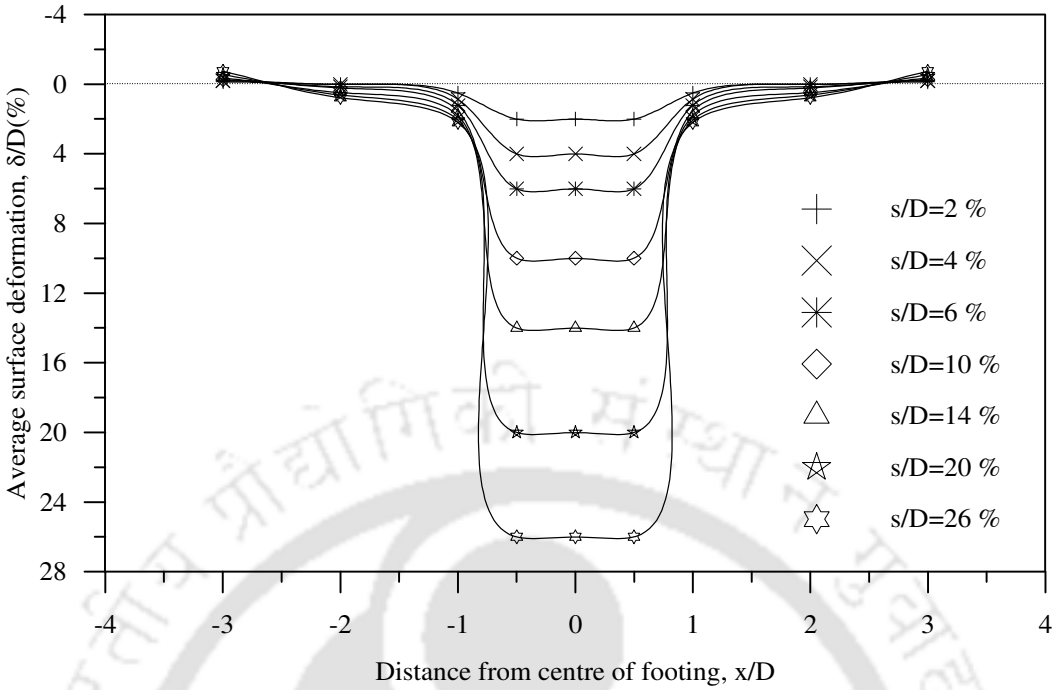

Fig.A1.21: Surface deformation profile, composite foundation bed

(h/D = 1.1, L/d_{sc} = 1) – Test series 11

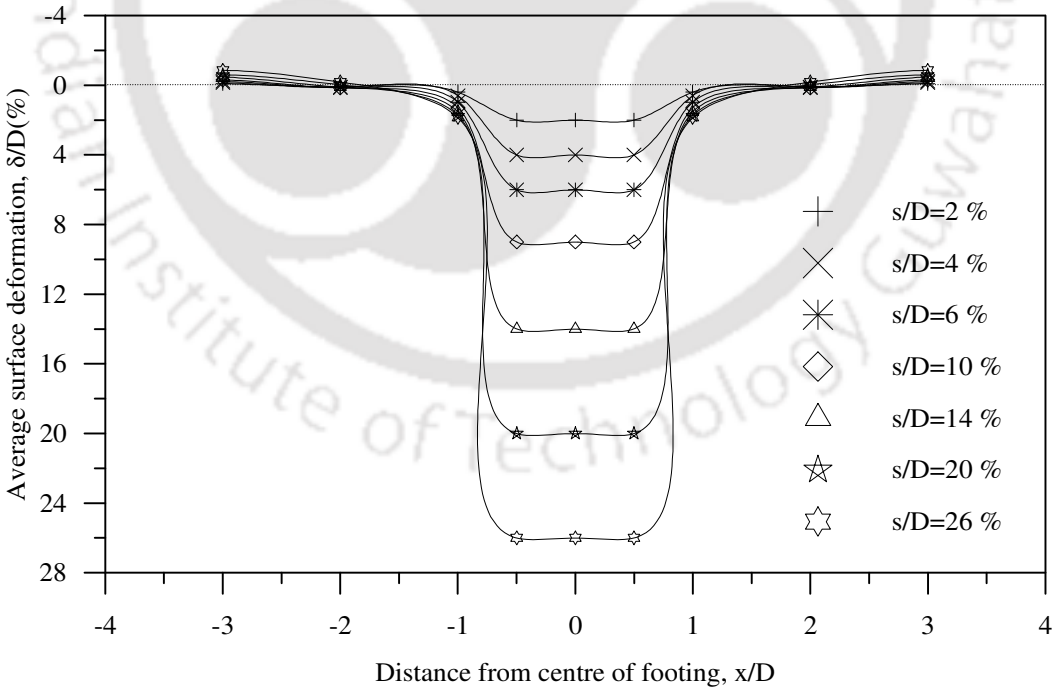

Fig.A1.22: Surface deformation profile, composite foundation bed

(h/D = 1.1, L/d_{sc} = 3) – Test series 11

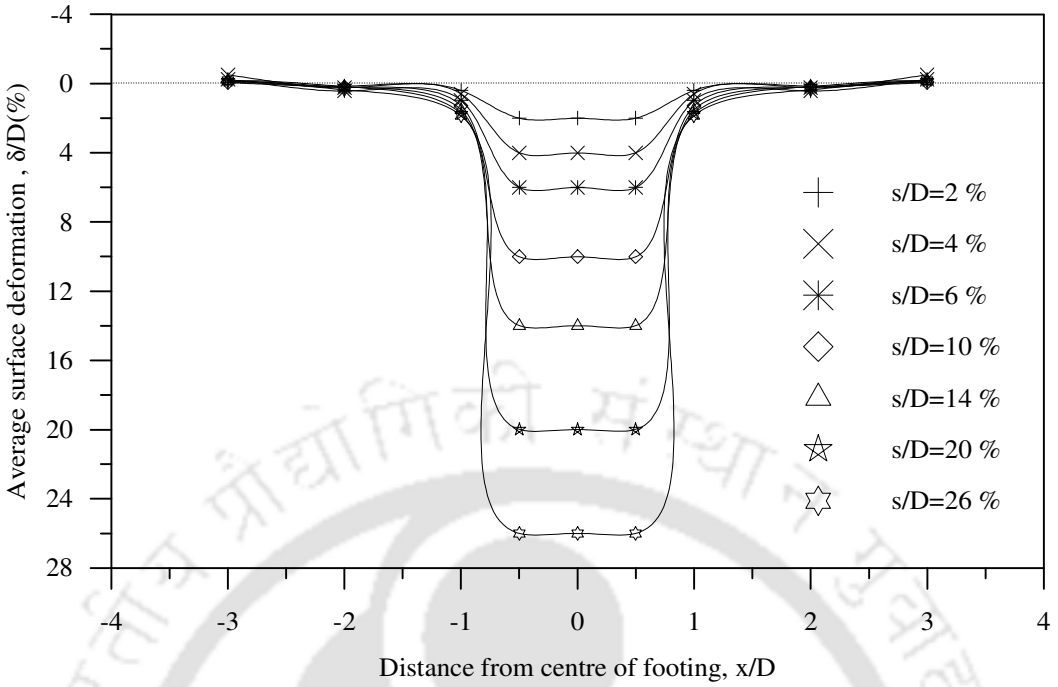

Fig.A1.23: Surface deformation profile, composite foundation bed

(h/D = 1.1, L/d_{sc} = 5) – Test series 11

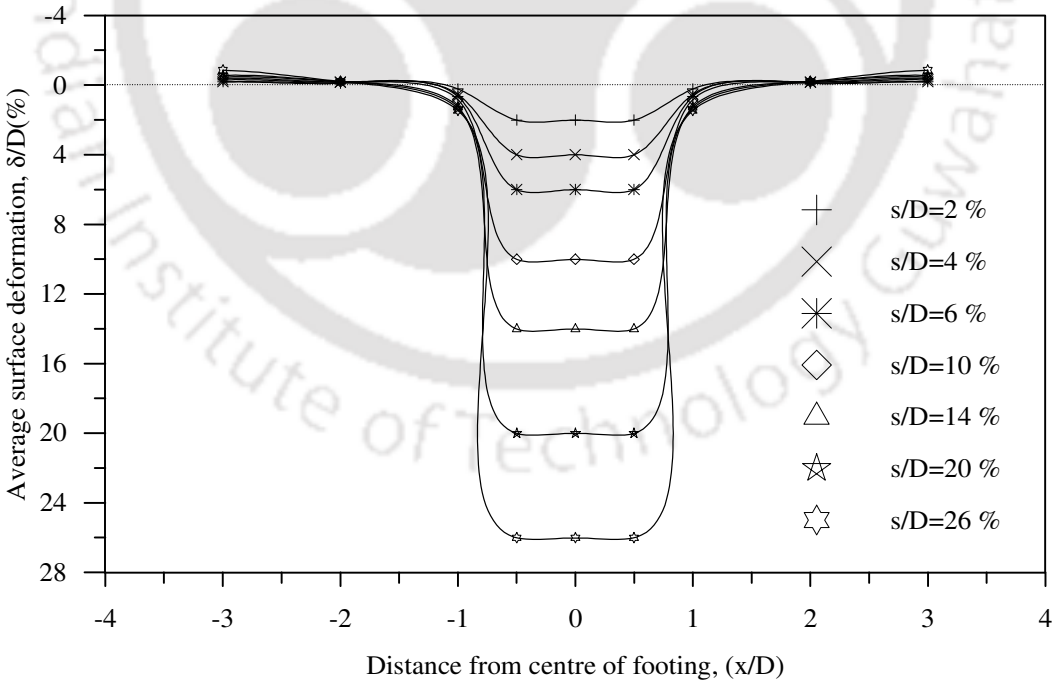

Fig.A1.24: Surface deformation profile, composite foundation bed

(h/D = 1.1, L/d_{sc} = 7) – Test series 11

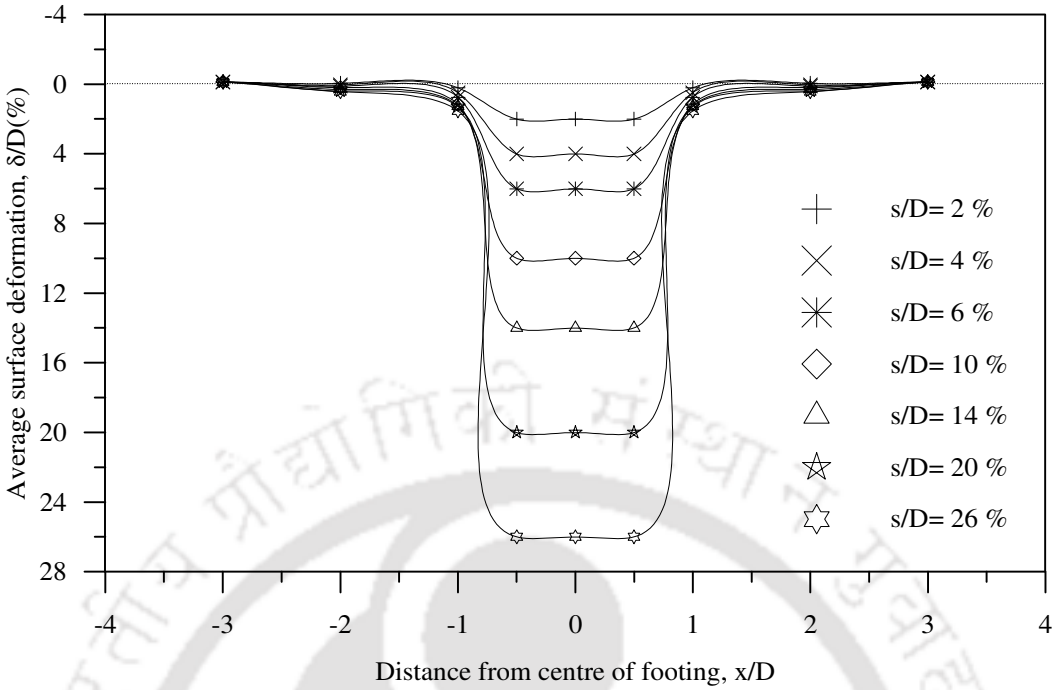

Fig.A1.25: Surface deformation profile, composite foundation bed

(h/D = 1.6, L/d_{sc} = 1) – Test series 12

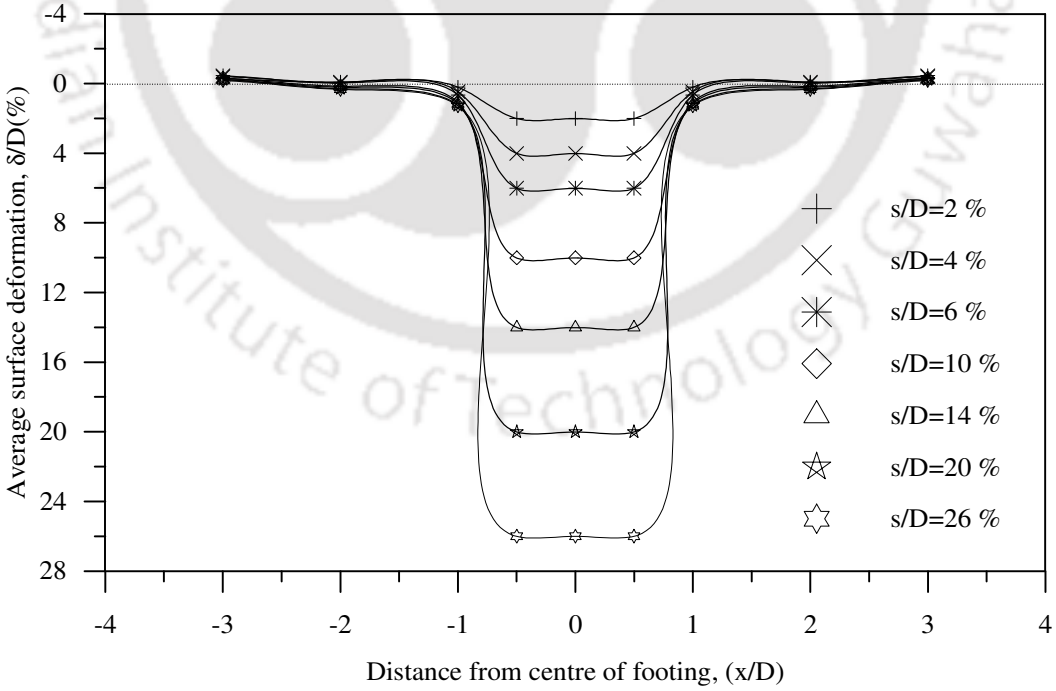

Fig.A1.26: Surface deformation profile, composite foundation bed

(h/D = 1.6, L/d_{sc} = 3) – Test series 12

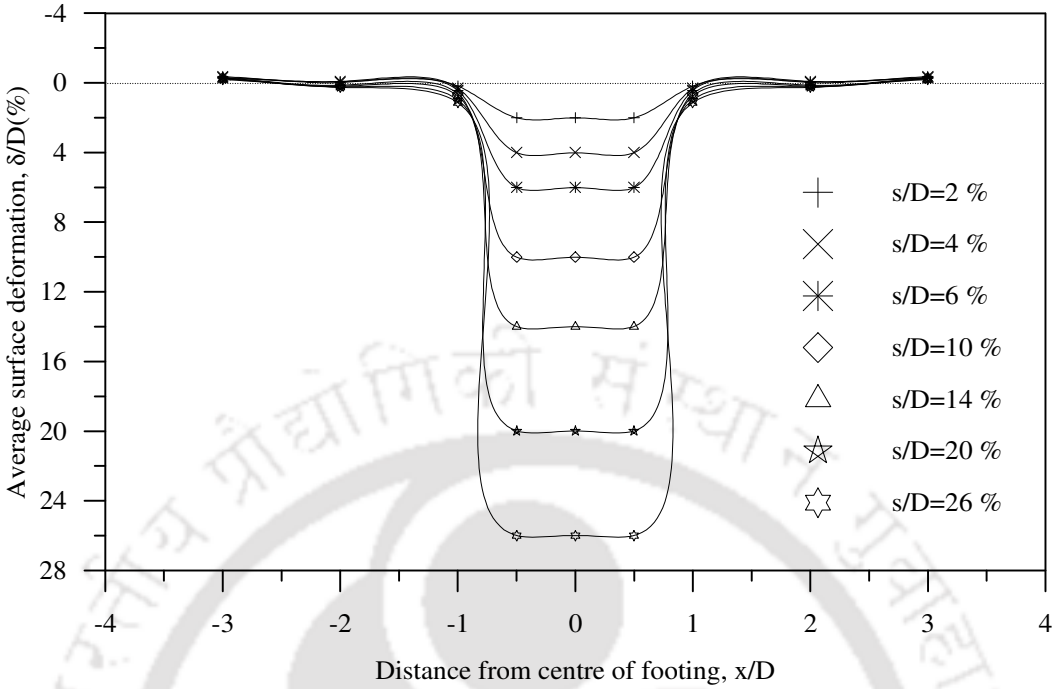

Fig.A1.27: Surface deformation profile, composite foundation bed

(h/D = 1.6, L/d_{sc} = 5) – Test series 12

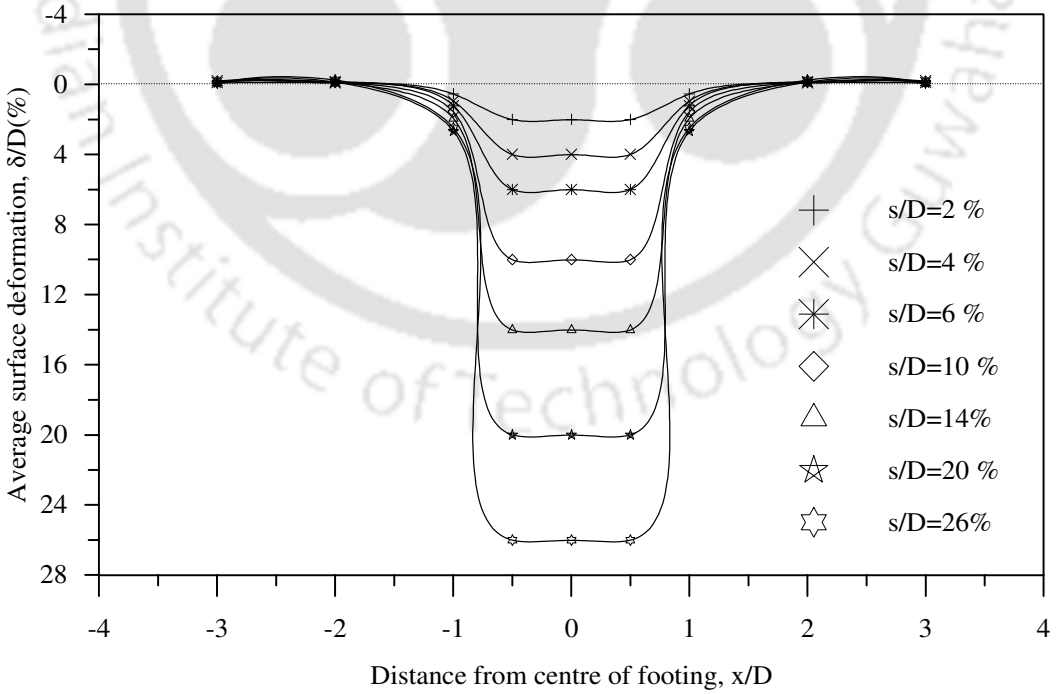

Fig.A1.28: Surface deformation profile, composite foundation bed

(h/D = 1.6, L/d_{sc} = 7) – Test series 12

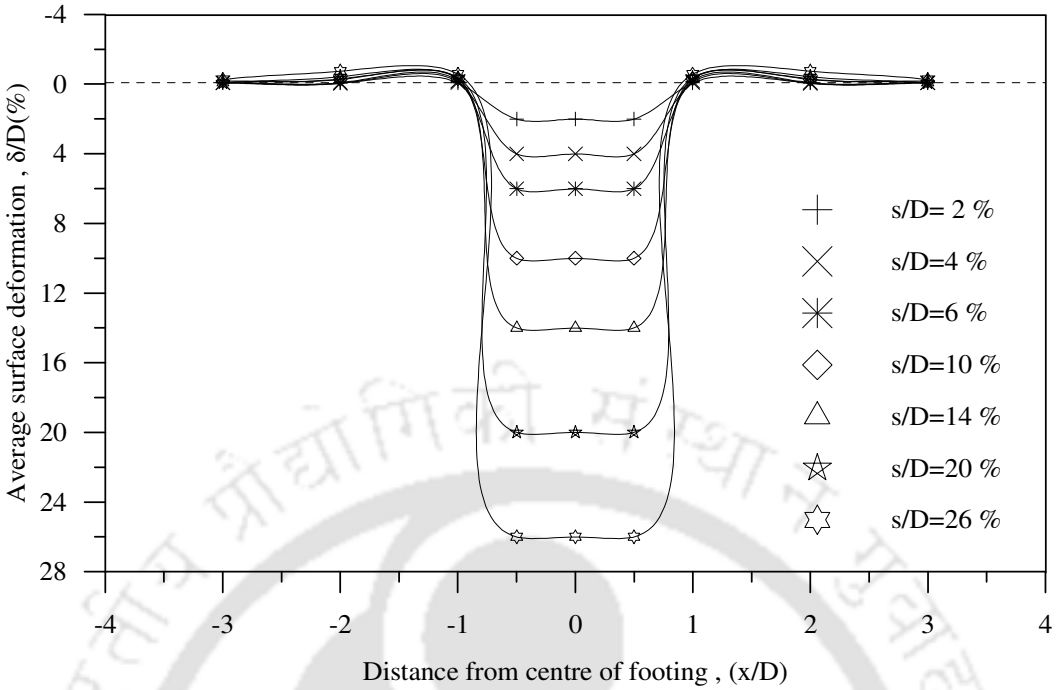

Fig.A1.29: Surface deformation profile, composite foundation bed

(h/D = 0.53, S/d_{sc} = 1.5) - Test series 13

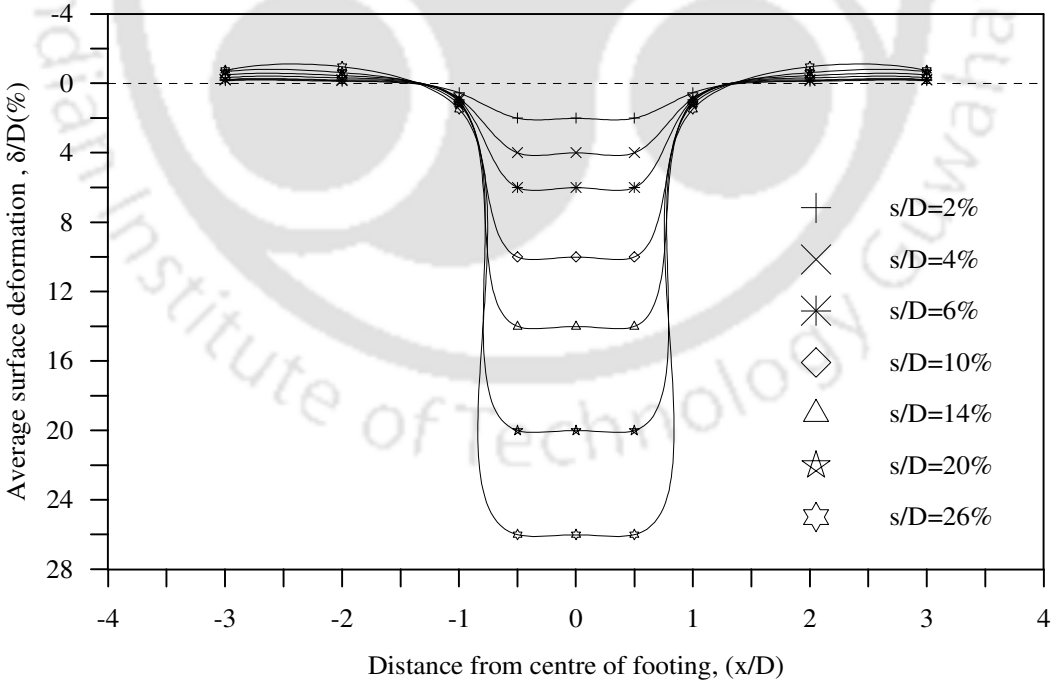

Fig.A1.30: Surface deformation profile, composite foundation bed

(h/D = 0.53, S/d_{sc} = 2.5) - Test series 13

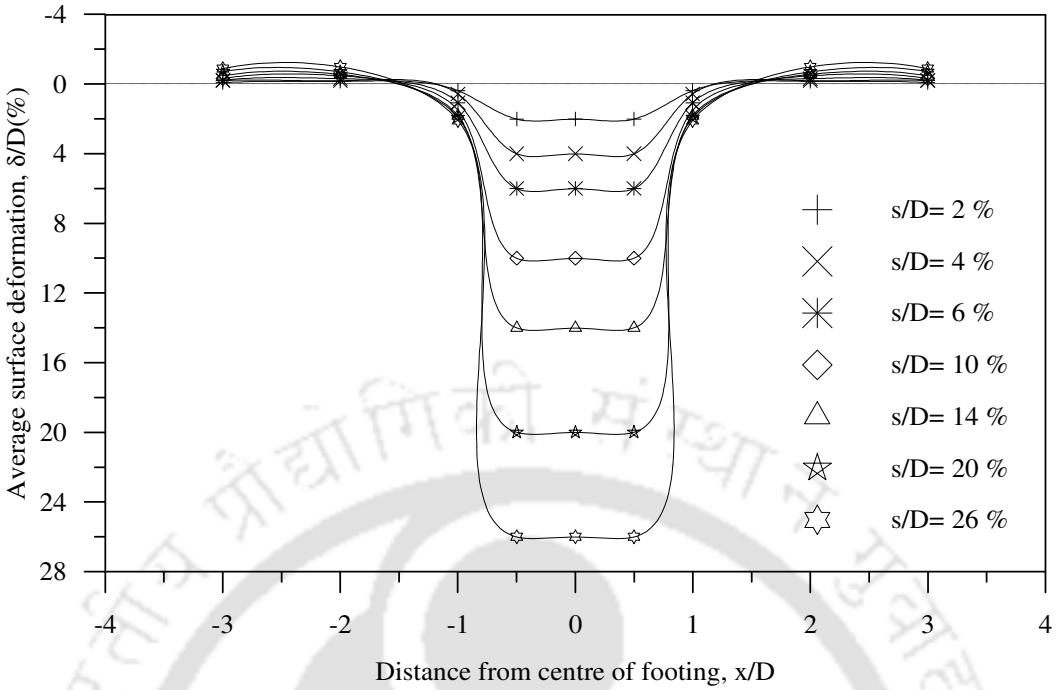

Fig. A1.31: Surface deformation profile, composite foundation bed
($h/D = 0.53$, $S/d_{sc} = 3.5$) - Test series 13

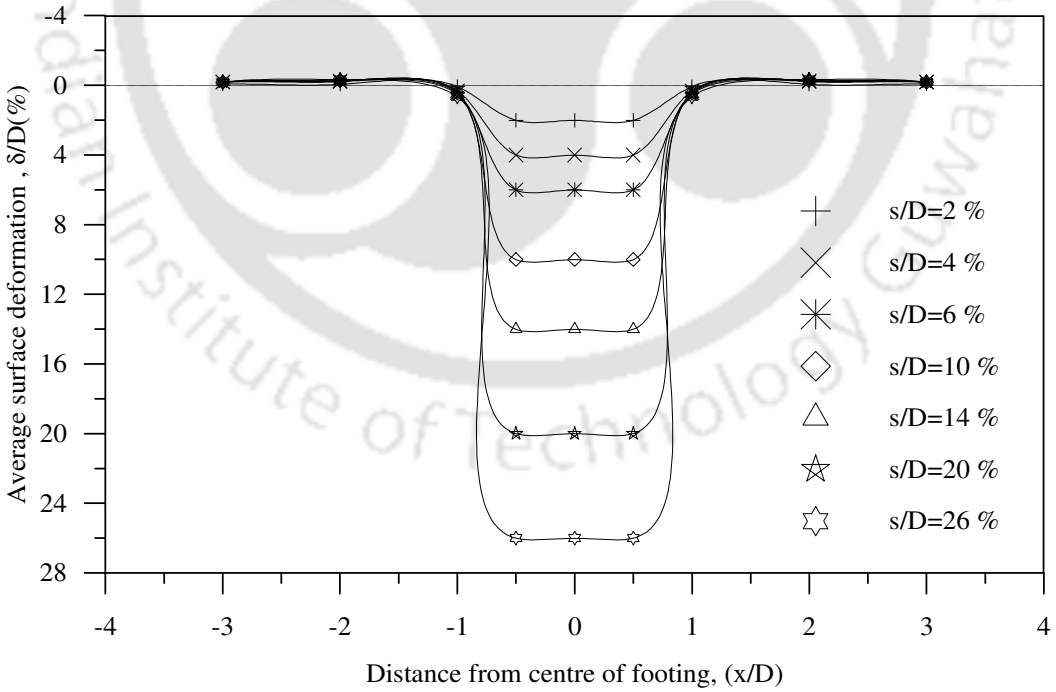

Fig. A1.32: Surface deformation profile, composite foundation bed
($h/D = 0.9$, $S/d_{sc} = 1.5$) - Test series-14

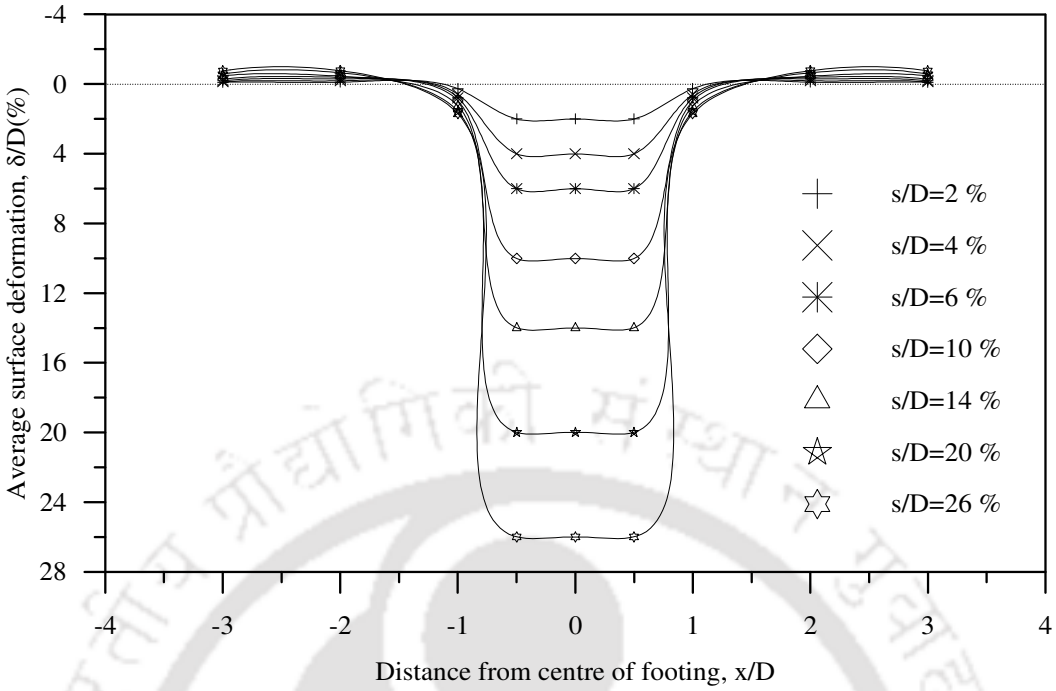

Fig. A1.33: Surface deformation profile, composite foundation bed ($h/D = 0.9$, $S/d_{sc} = 1.5$) - Test series-14

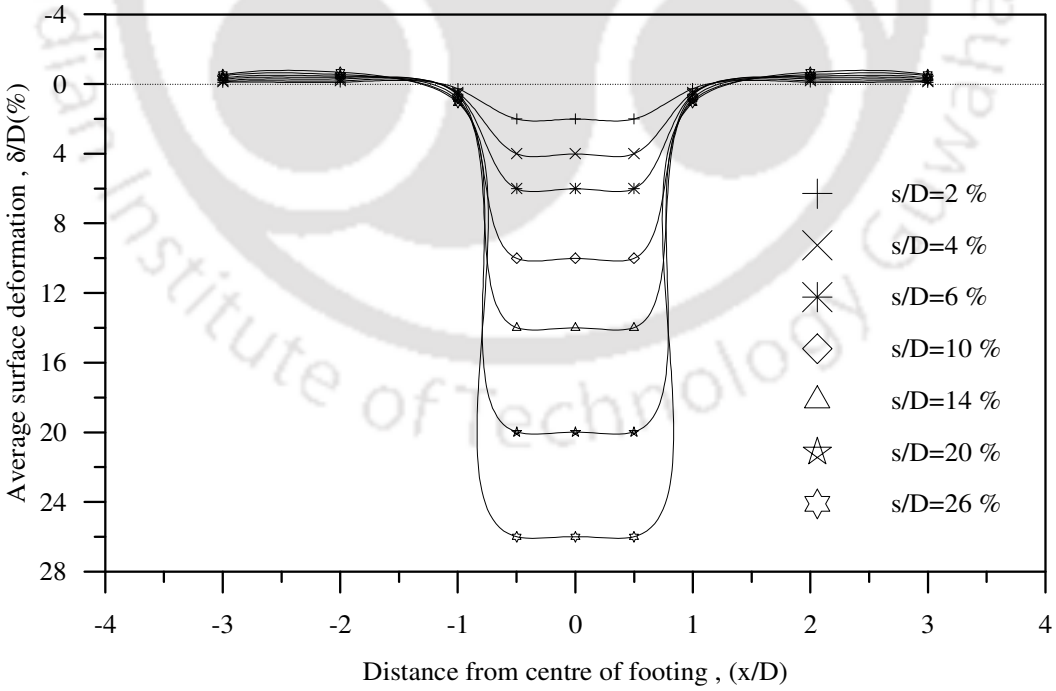

Fig. A1.34: Surface deformation profile, composite foundation bed ($h/D = 0.9$, $S/d_{sc} = 3.5$) - Test series-14

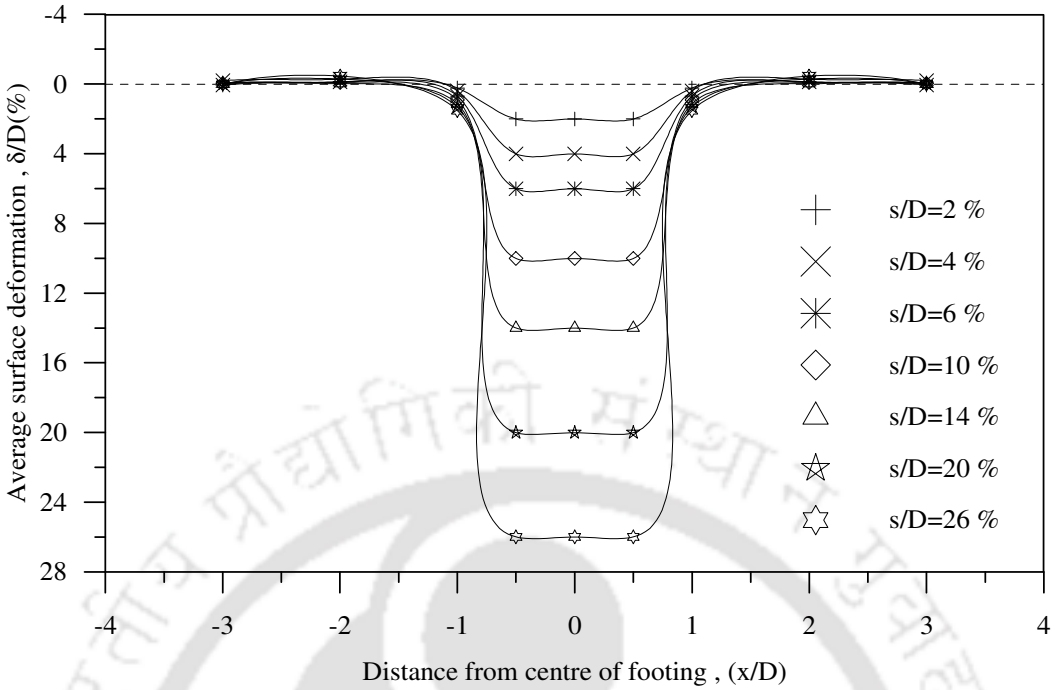

Fig.A1.35: Surface deformation profile, composite foundation bed

(h/D = 1.1, S/d_{sc} = 1.5) – Test series 15

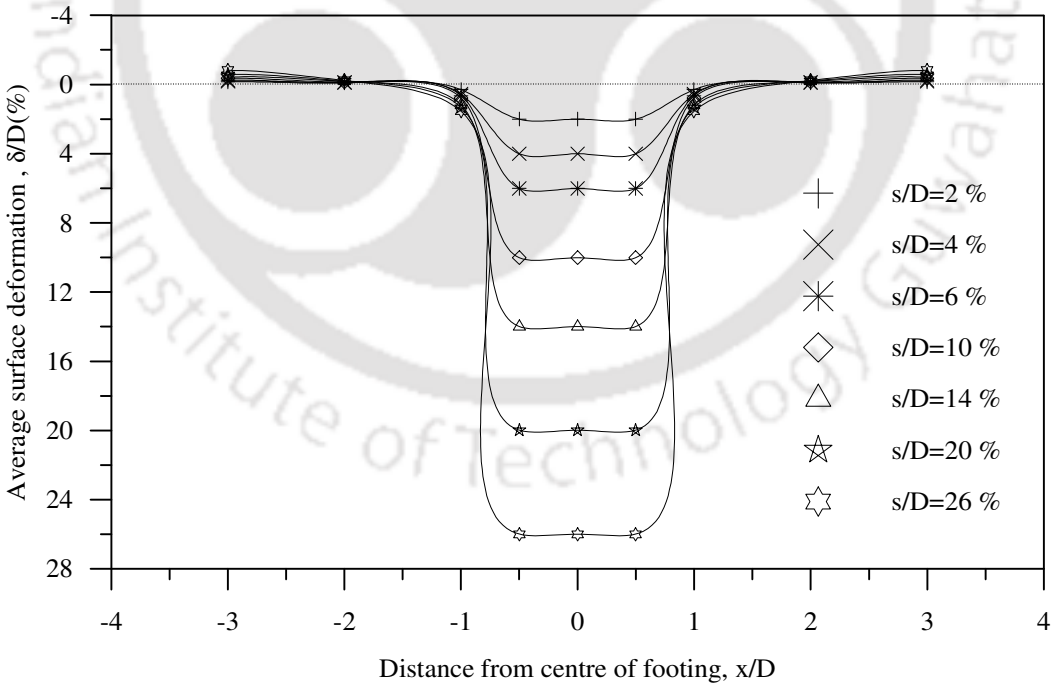

Fig.A1.36 Surface deformation profile, composite foundation bed

(h/D = 1.1, S/d_{sc} = 2.5) – Test series 15

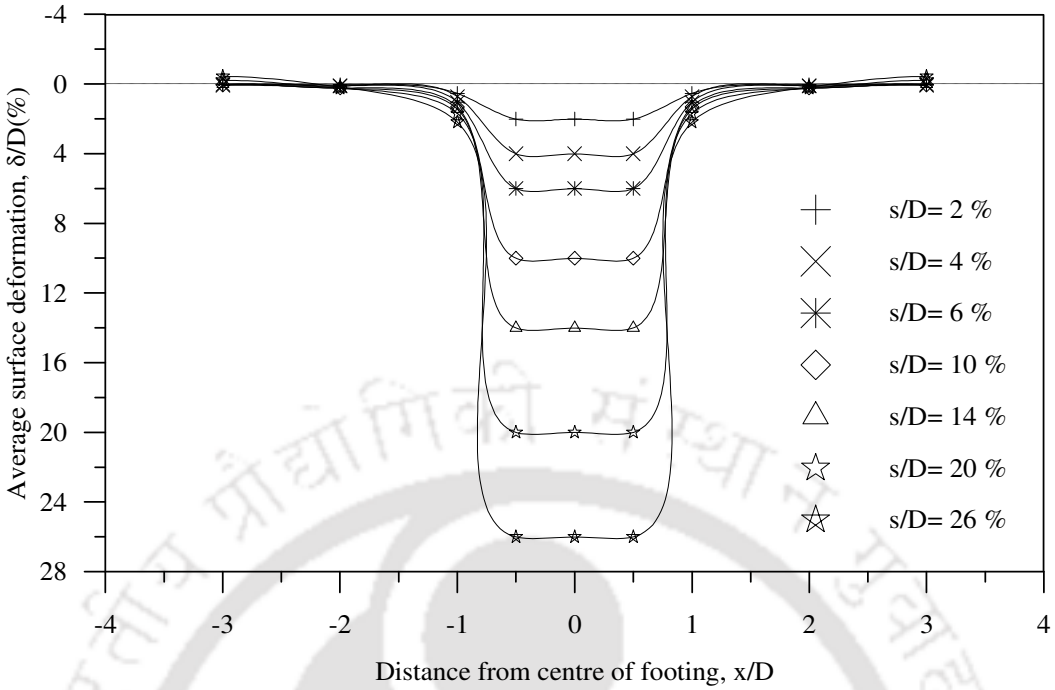

Fig. A1.37: Surface deformation profile, composite foundation bed

(h/D = 1.1, S/d_{sc}=3.5) – Test series 15

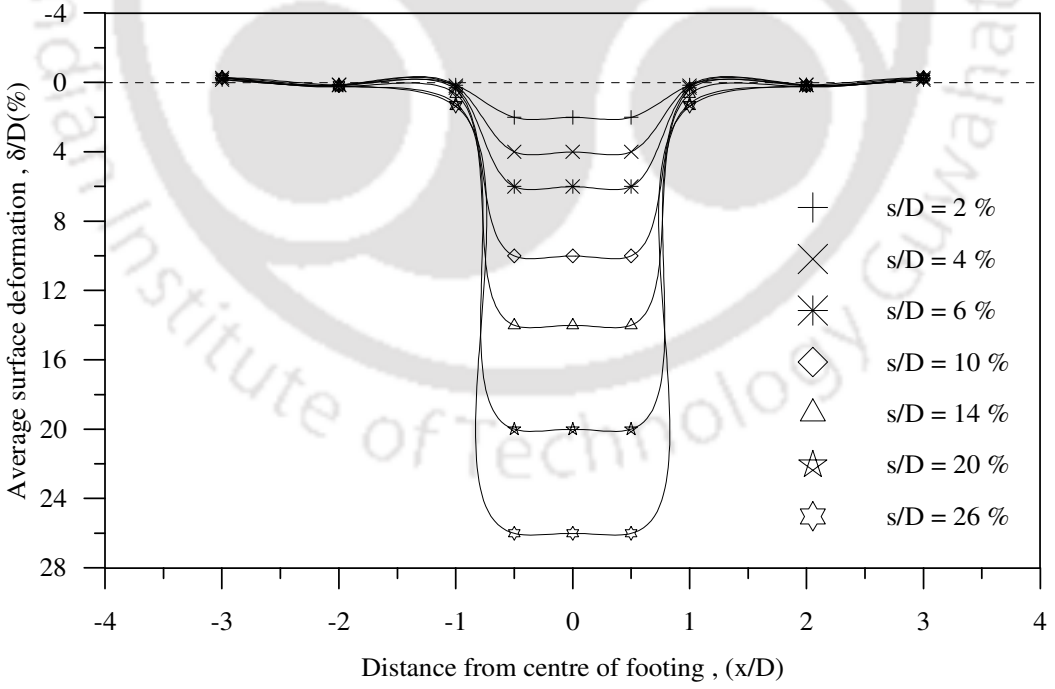

Fig. A1.38: Surface deformation profile, composite foundation bed

(h/D = 1.6, S/d_{sc} = 1.5) - Test series 16

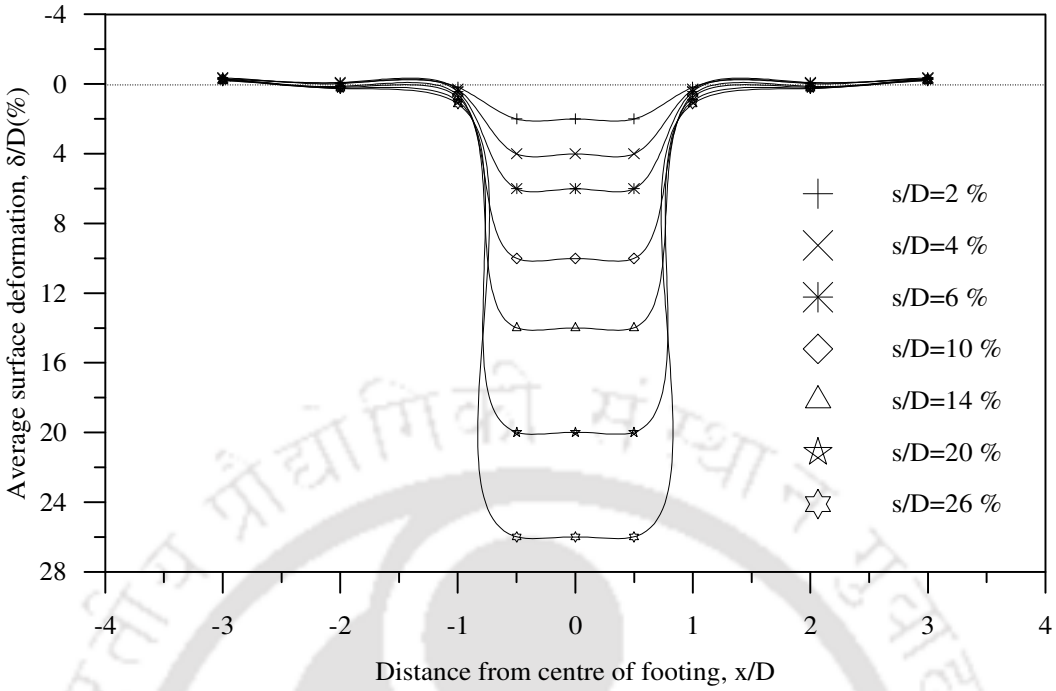

Fig. A1.39: Surface deformation profile, composite foundation bed ($h/D = 1.6$, $S/d_{sc} = 2.5$) – Test series 16

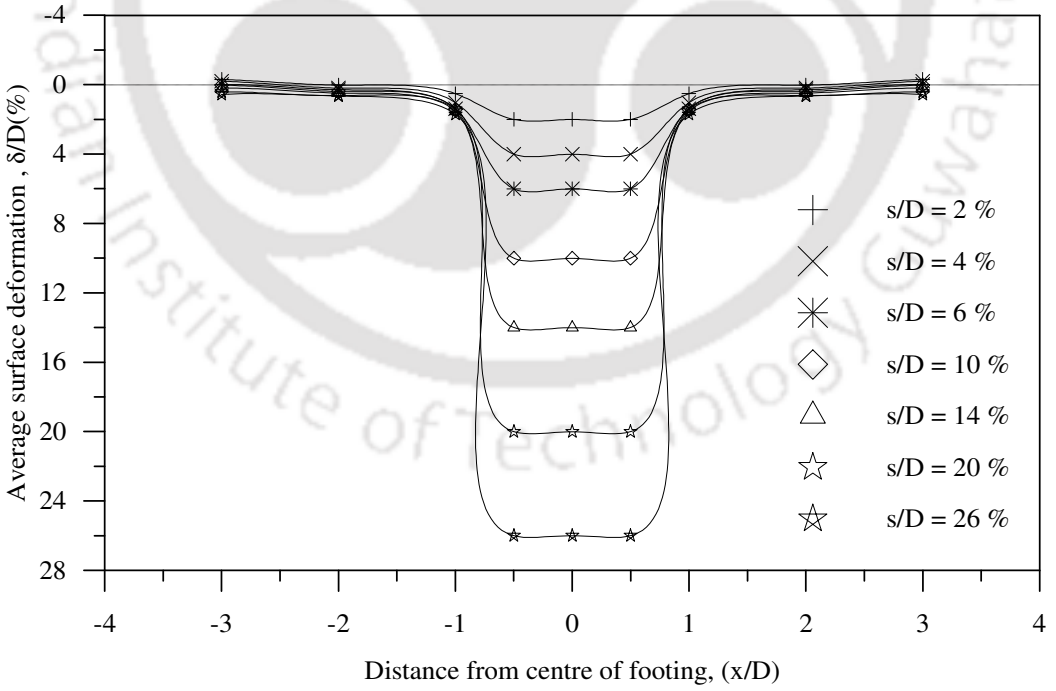

Fig. A1.40: Surface deformation profile, composite foundation bed ($h/D = 1.6$, $S/d_{sc} = 3.5$) – Test series 16

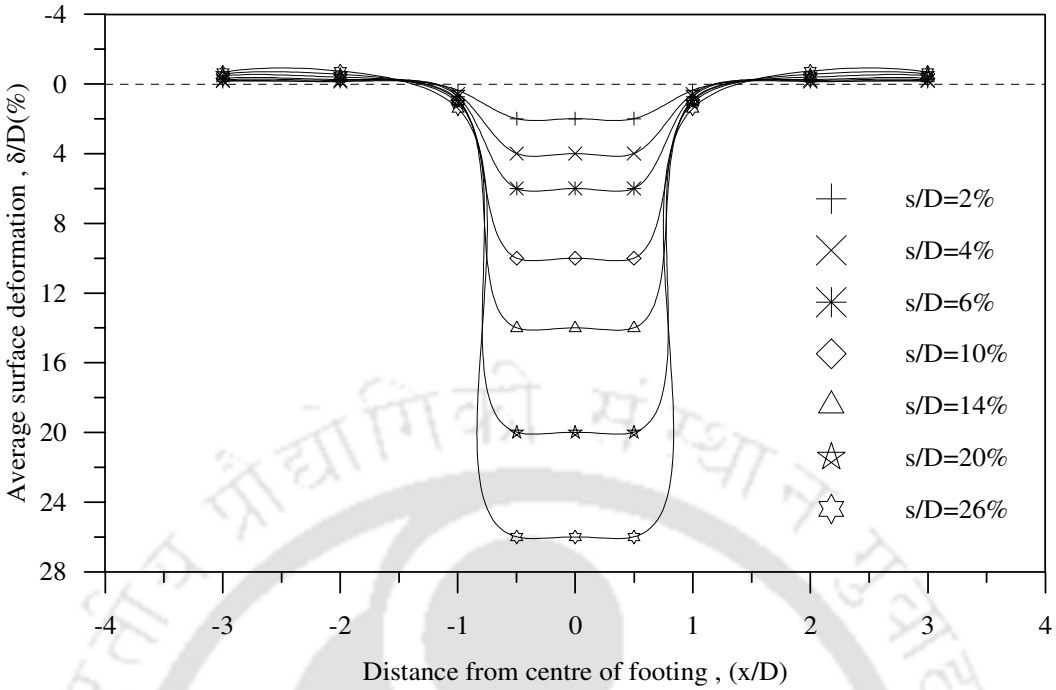

Fig.A1.41: Surface deformation profile, composite foundation bed

(h/D = 0.53, d_{gc}/D = 1.1) – Test series 17

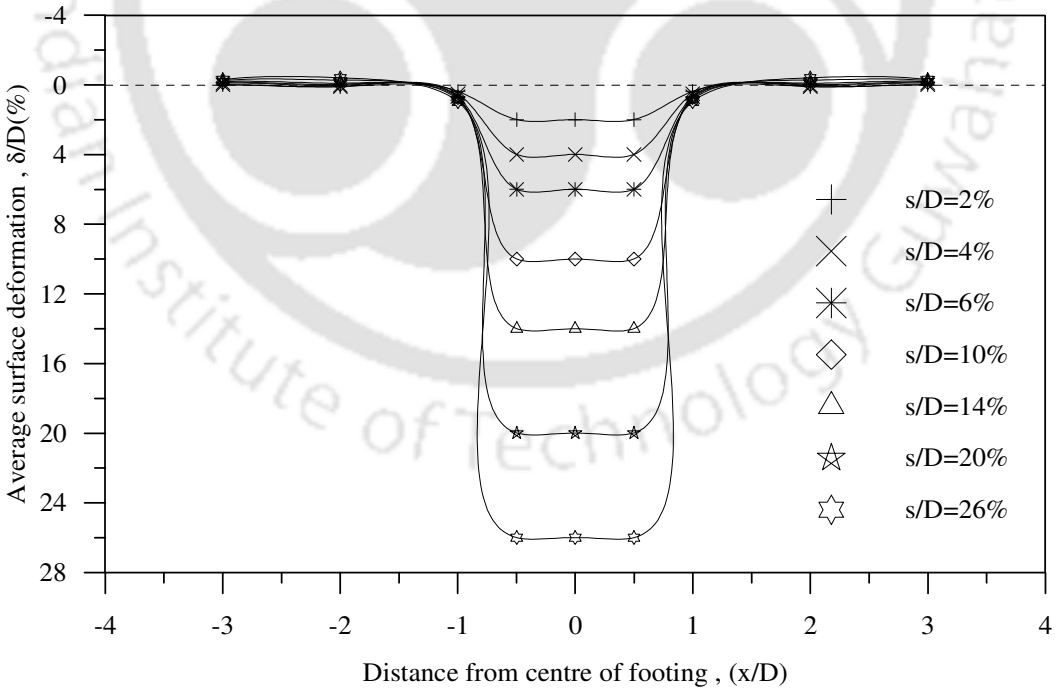

Fig.A1.42: Surface deformation profile, composite foundation bed

(h/D = 0.53, d_{gc}/D = 1.33) – Test series 17

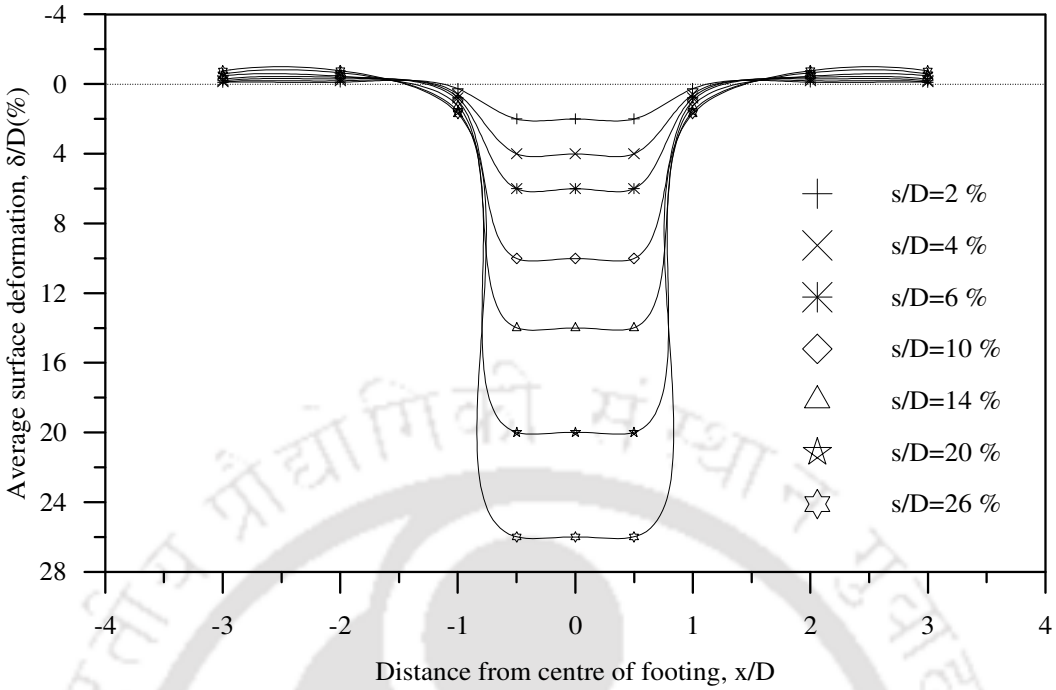

Fig.A1.43: Surface deformation profile, composite foundation bed

(h/D = 0.9, d_{gc}/D = 0.8) – Test series 18

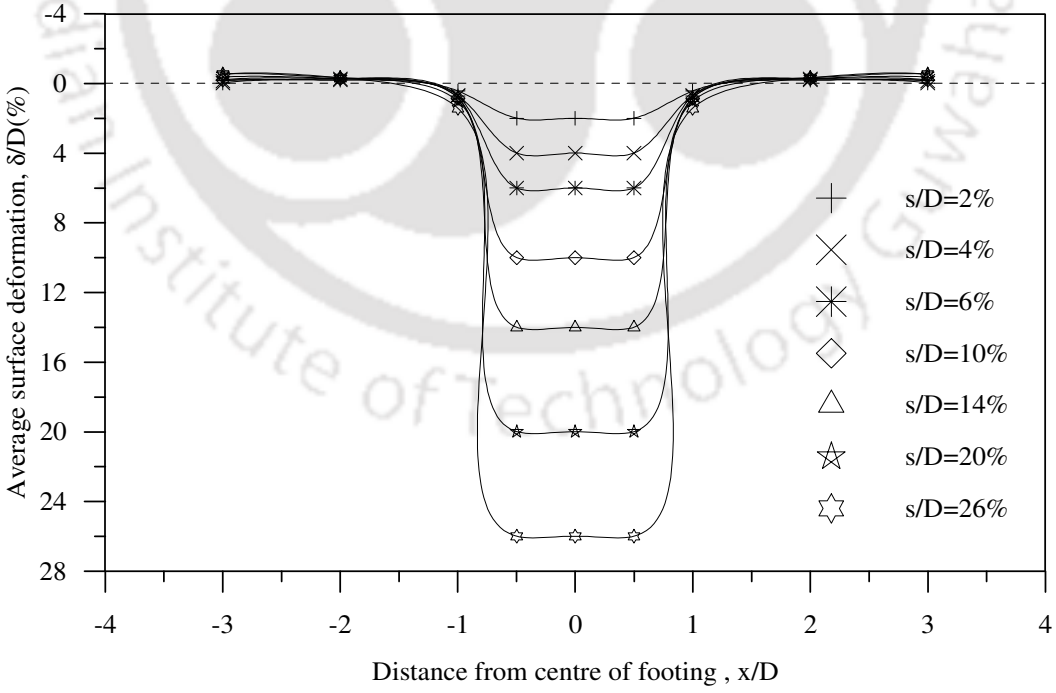

Fig.A1.44: Surface deformation profile, composite foundation bed

(h/D = 0.9, d_{gc}/D = 1.1) – Test series 18

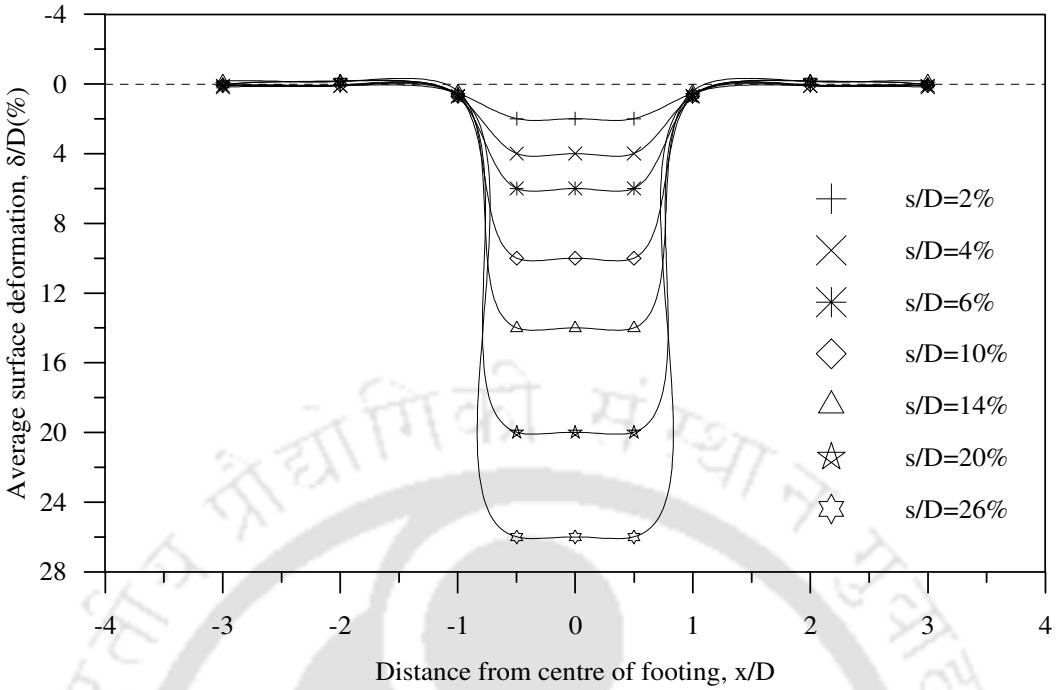

Fig.A1.45: Surface deformation profile, composite foundation bed
(h/D = 0.9, d_{gc}/D = 1.33) – Test series 18

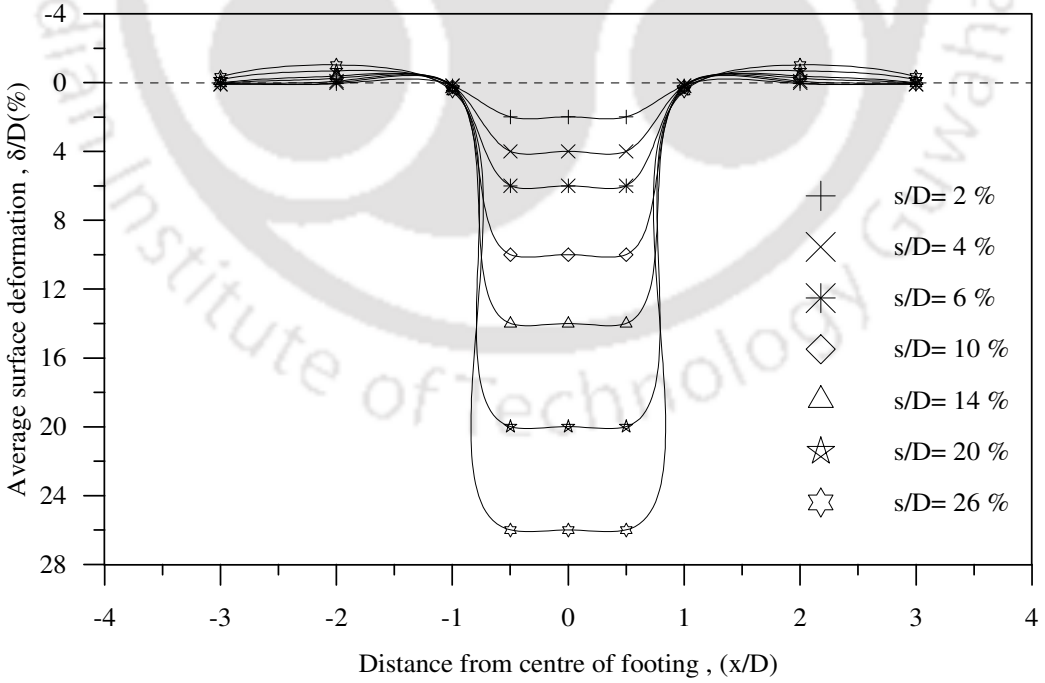

Fig.A1.46: Surface deformation profile, composite foundation bed
(h/D = 0.9, ID = 35%) – Test series 19

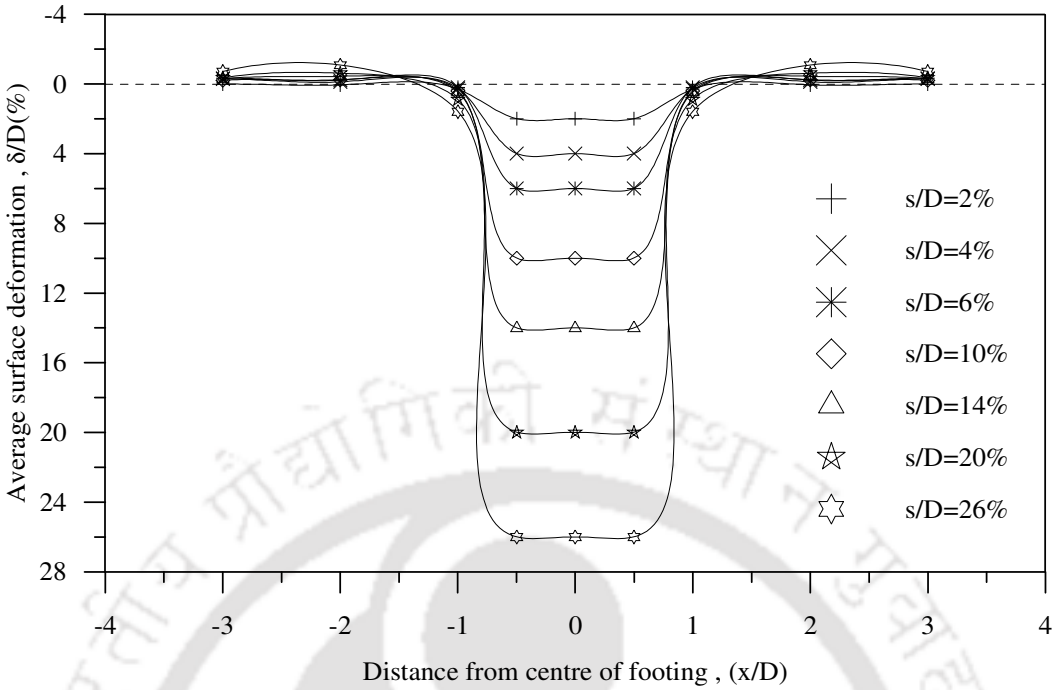

Fig.A1.47: Surface deformation profile, composite foundation bed (h/D = 0.9, ID = 50%) – Test series 19

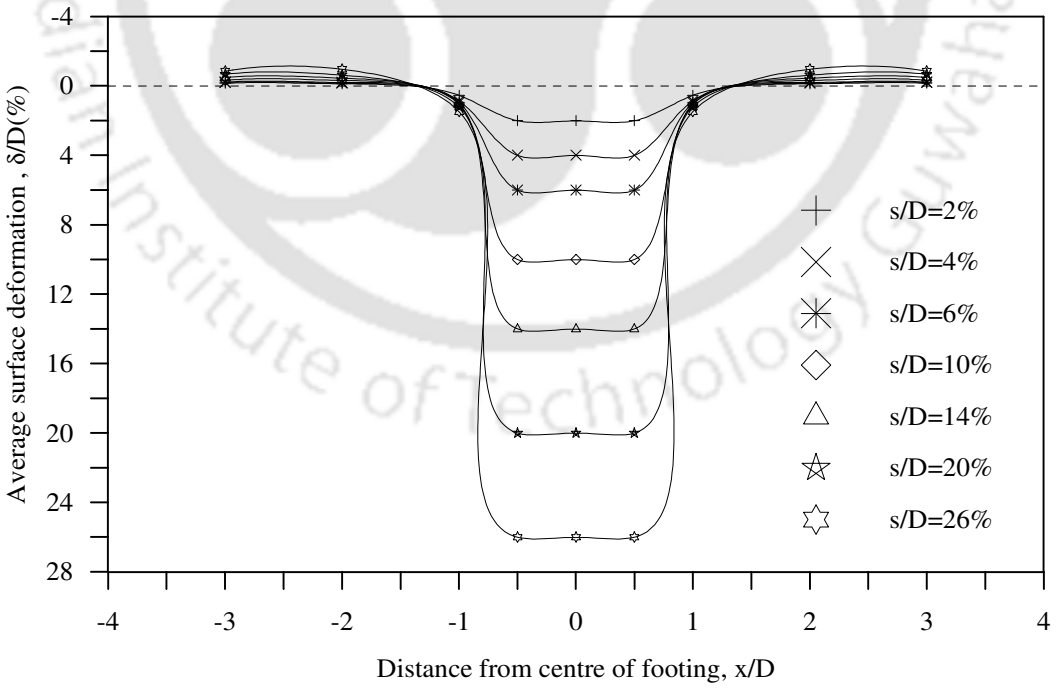

Fig.A1.48: Surface deformation profile, composite foundation bed (h/D = 0.9, ID = 80%) – Test series 19

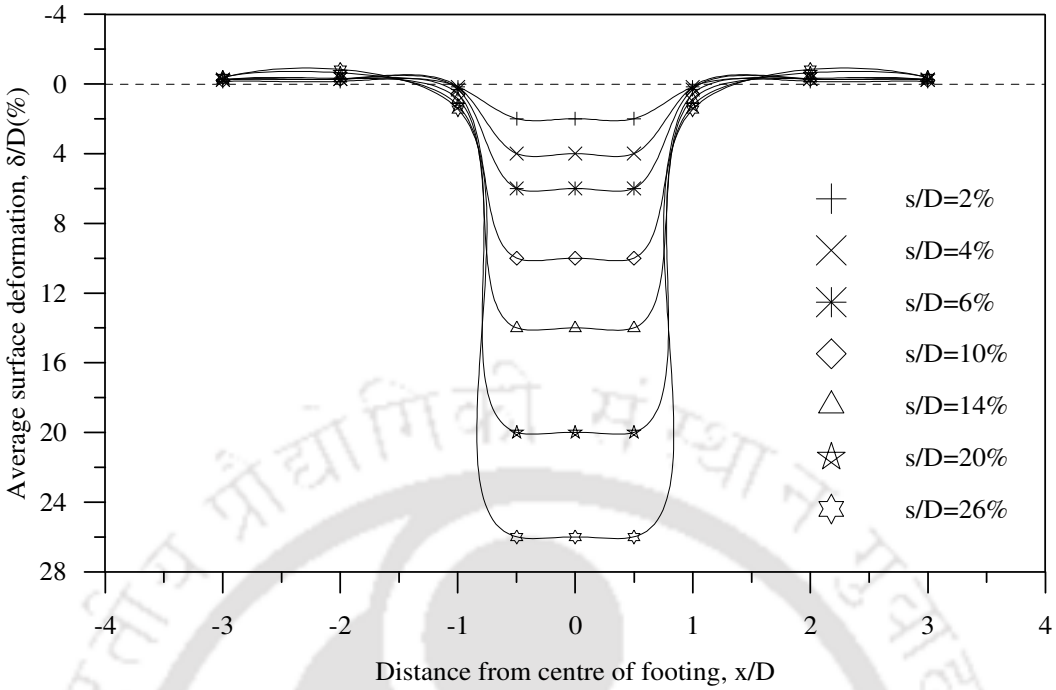

Fig.A1.49: Surface deformation profile, composite foundation bed (h/D = 0.9, ID = 35%) – Test series 20

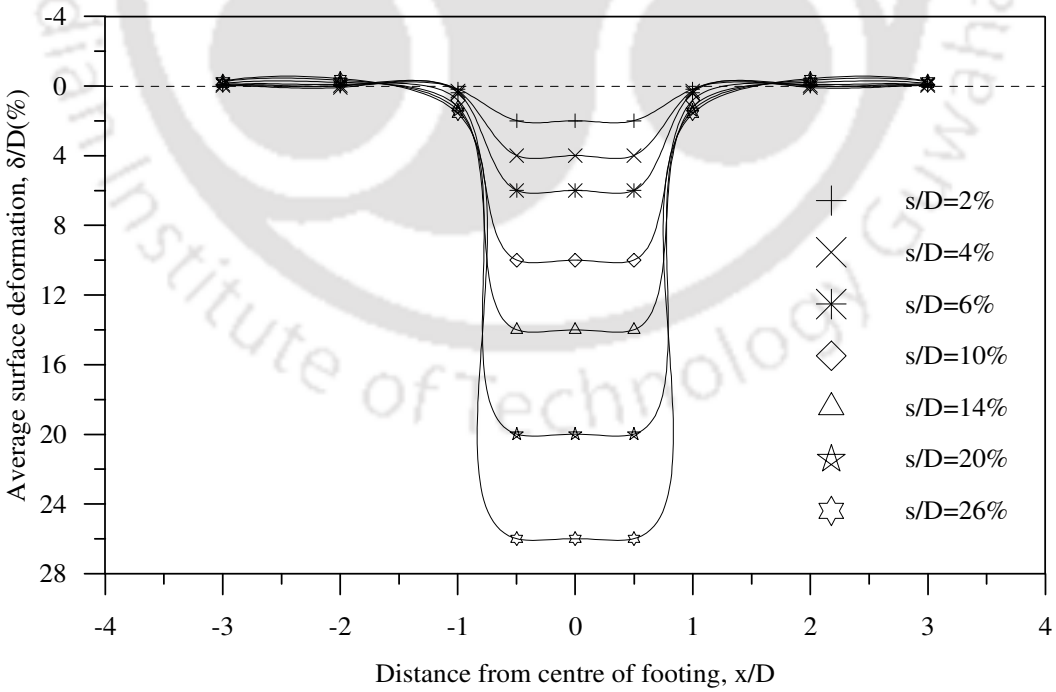

Fig.A1.50: Surface deformation profile, composite foundation bed (h/D = 0.9, ID = 50%) – Test series 20

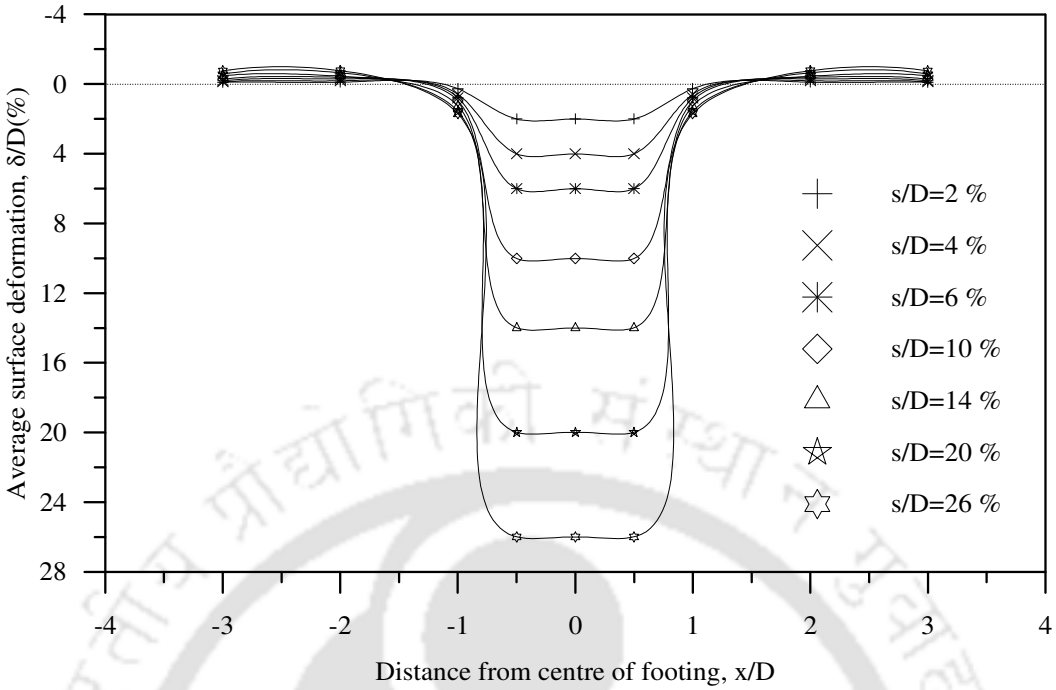

Fig.A1.51: Surface deformation profile, composite foundation bed (h/D = 0.9, ID = 80%) – Test series 20

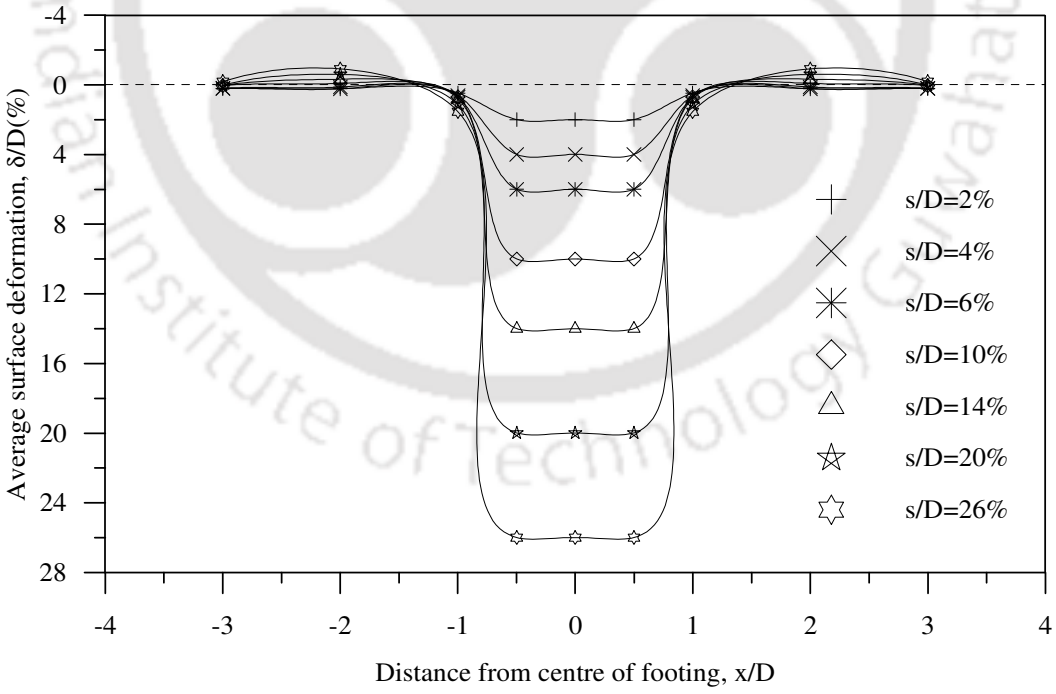

Fig.A1.52: Surface deformation profile, composite foundation bed with base geogrid (h/D = 0.53) - Test series 21

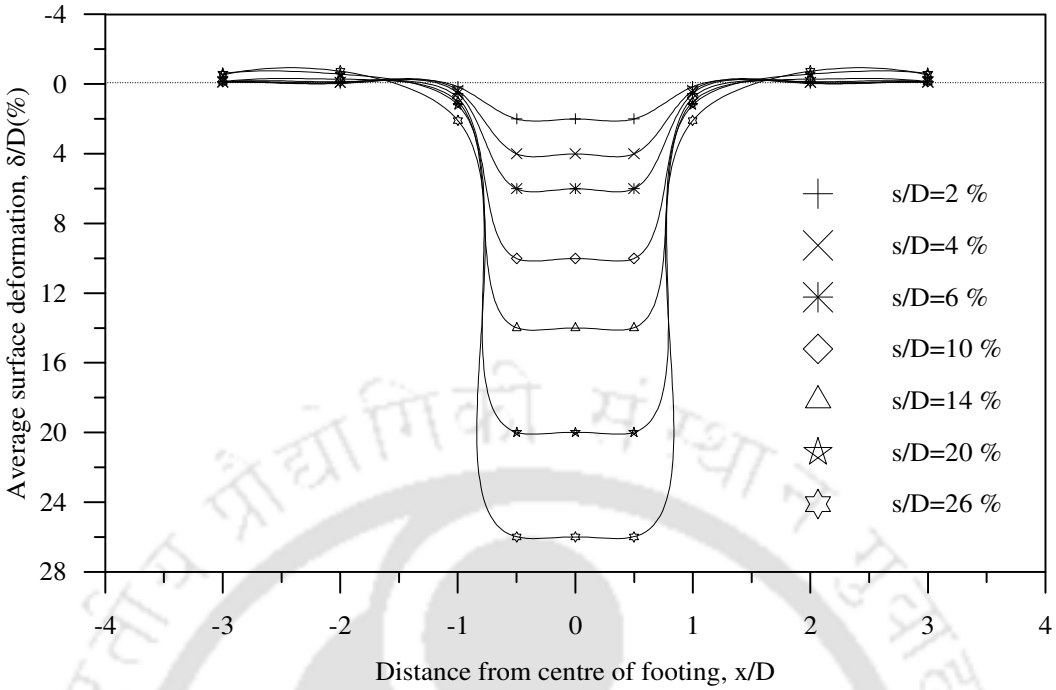

Fig.A1.53: Surface deformation profile, composite foundation bed with base geogrid (h/D = 0.9) - Test series 21

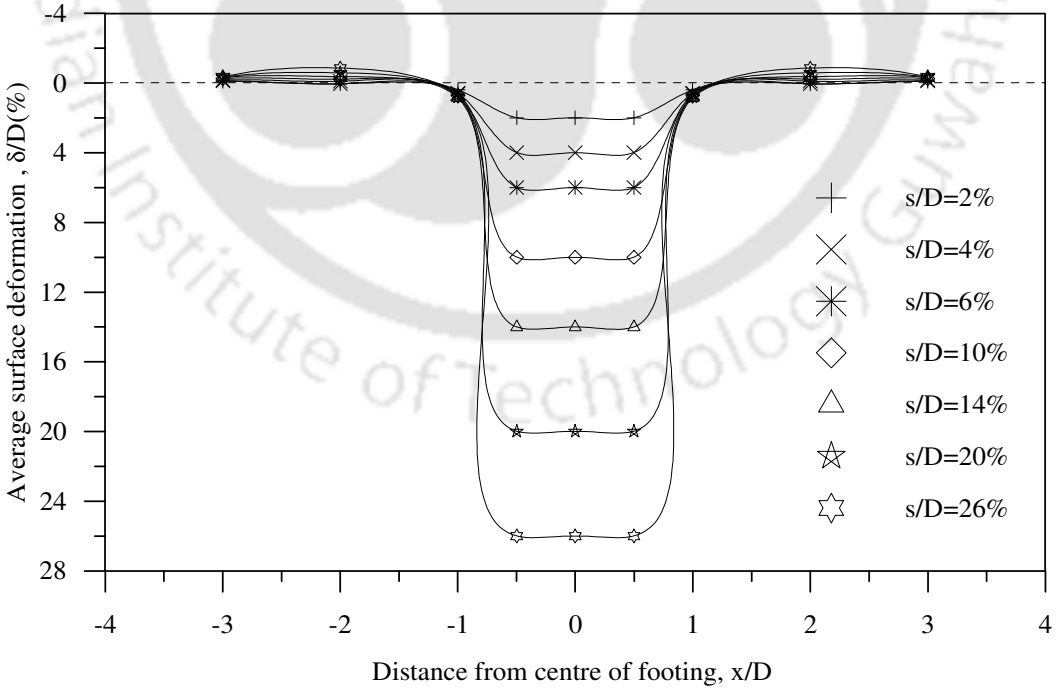

Fig.A1.54: Surface deformation profile, encased stone column reinforced clay bed (L_{esc}/d_{sc} = 1, S/d_{sc} = 2.5) - Test series 22

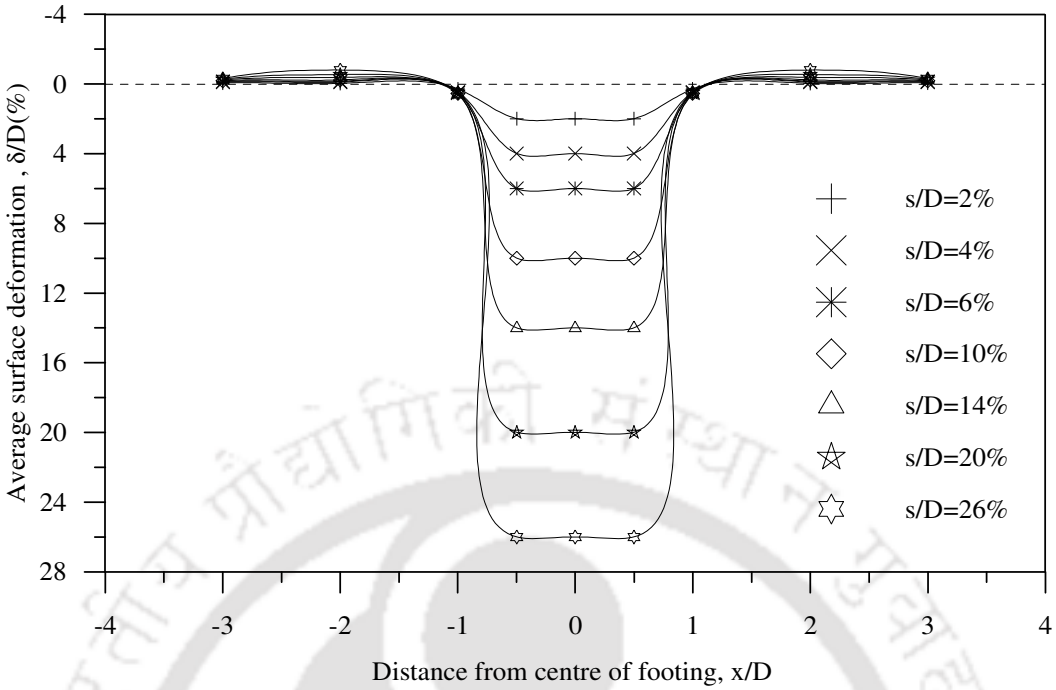

Fig.A1.55: Surface deformation profile, encased stone column reinforced clay bed (L_{esc}/d_{sc} = 3, S/d_{sc} = 2.5) - Test series 22

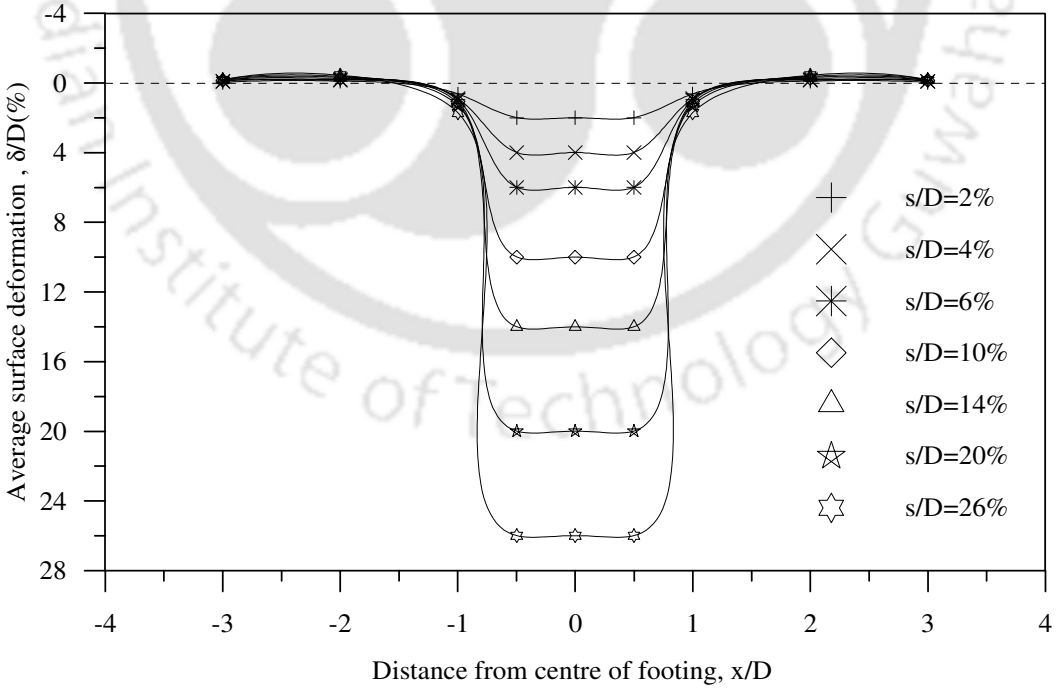

Fig.A1.56: Surface deformation profile, encased stone column reinforced clay bed (Full length encasement, S/d_{sc} = 2.5) - Test series 22

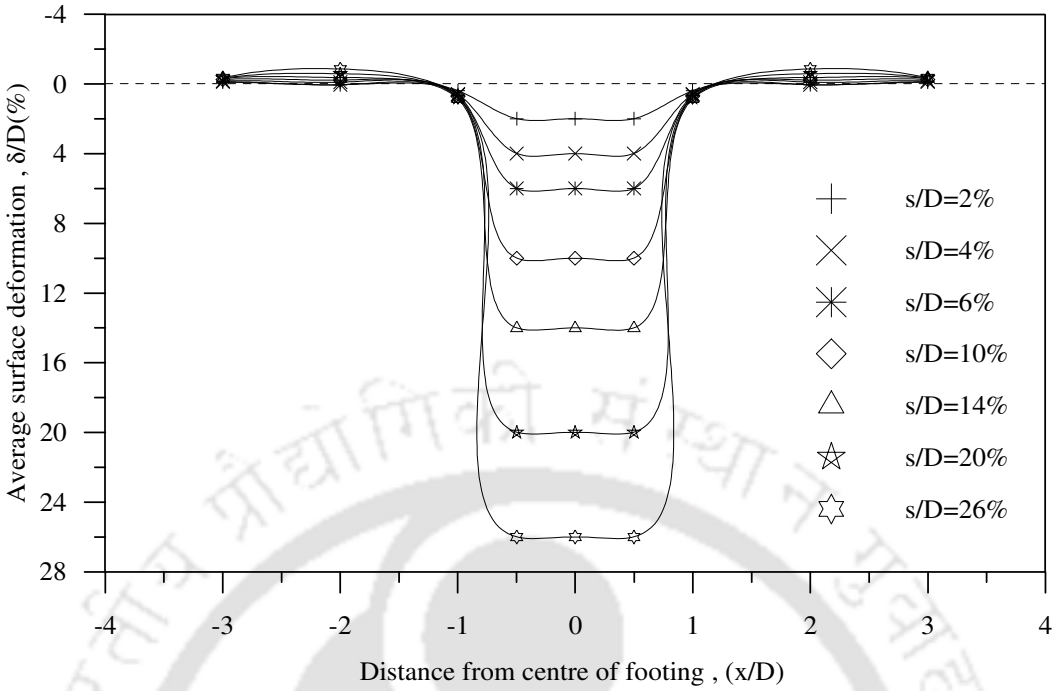

Fig. A1.57: Surface deformation profile, composite foundation bed with encased stone columns (L_{esc}/d_{sc} = 1, h/D = 0.53) – Test series 23

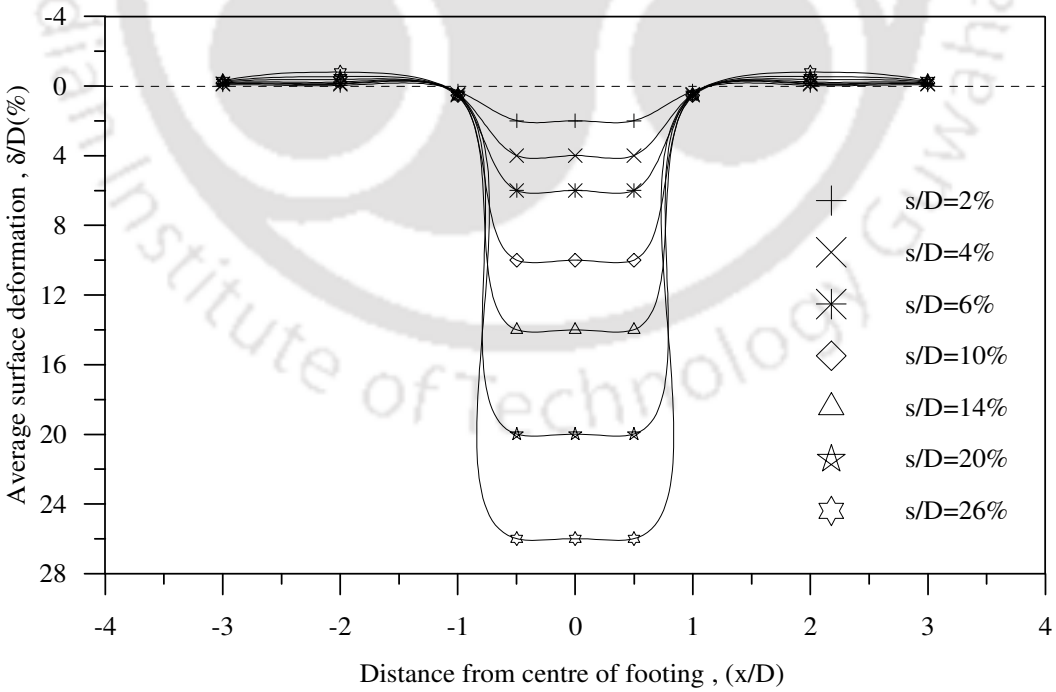

Fig.A1.58: Surface deformation profile, composite foundation bed with encased stone columns (L_{esc}/d_{sc} = 3, h/D = 0.53) – Test series 23

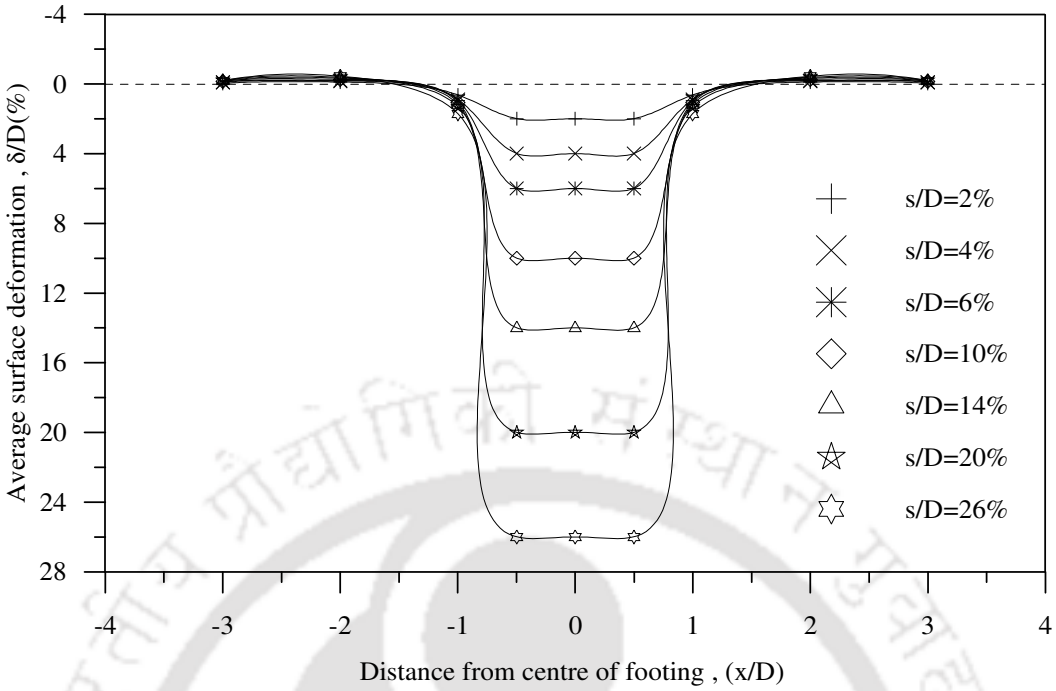

Fig.A1.59: Surface deformation profile, composite foundation bed with encased stone columns (Full length encasement, h/D = 0.53) – Test series 23

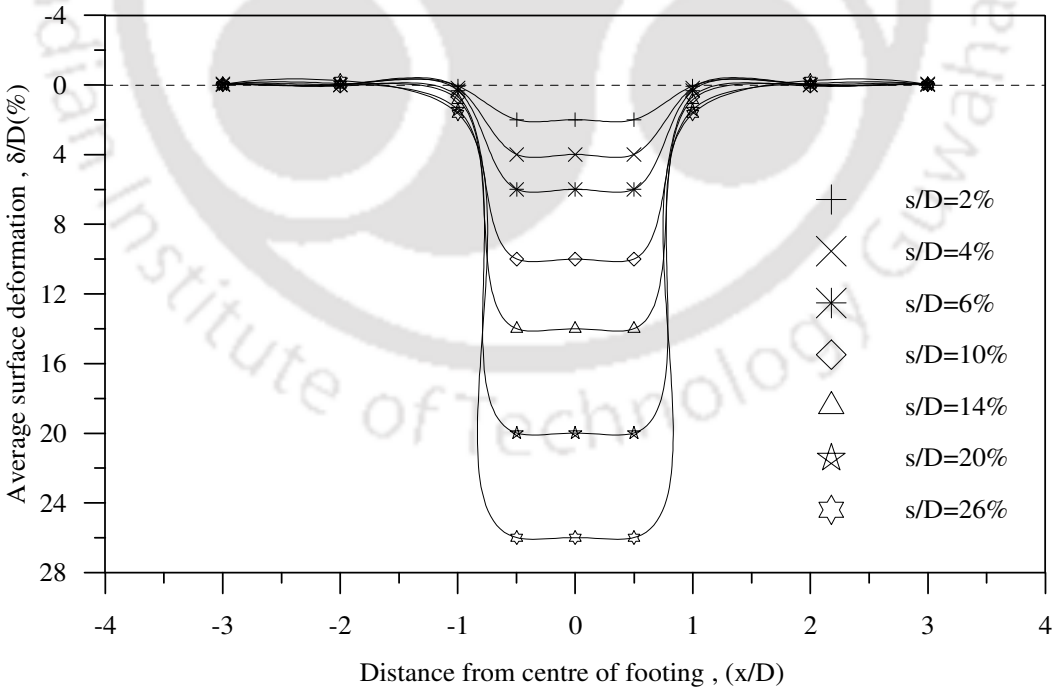

Fig. A1.60: Surface deformation profile, composite foundation bed with partially encased stone columns (L_{esc}/d_{sc} = 1, h/D = 0.9) -Test series 24

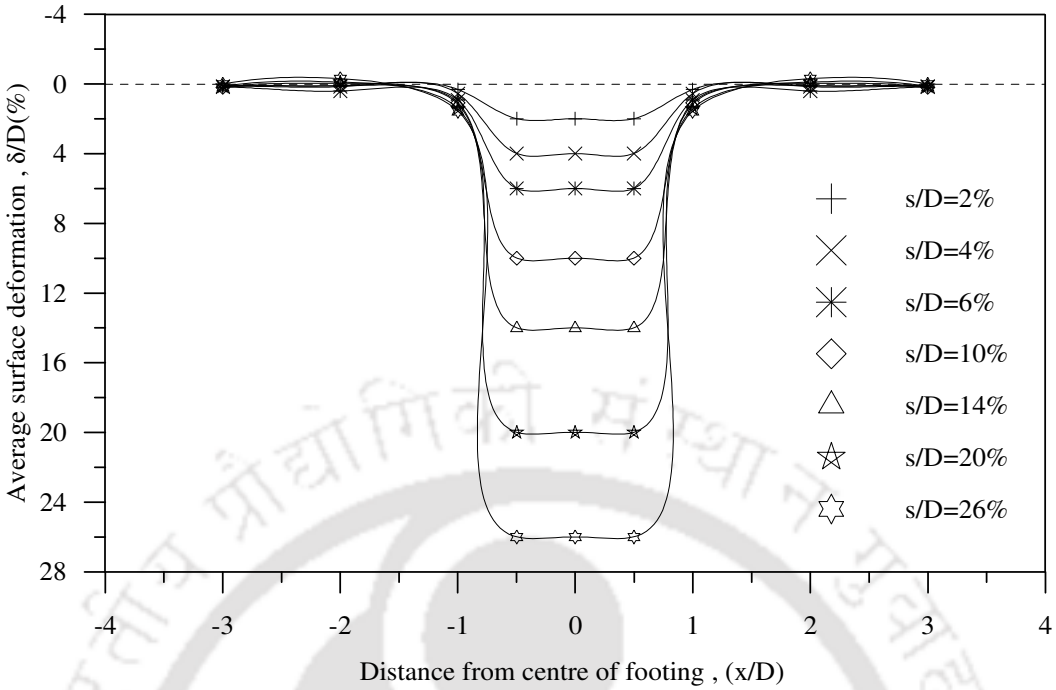

Fig. A1.61: Surface deformation profile, composite foundation bed with partially encased stone columns (L_{esc}/d_{sc} = 3, h/D = 0.9) - Test series 24

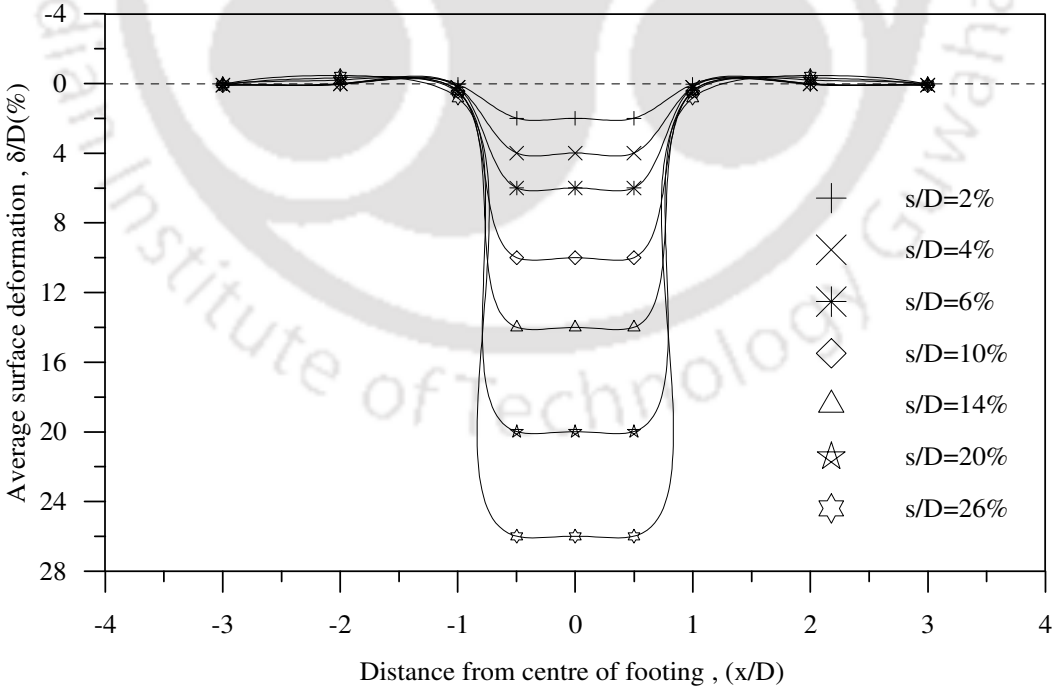

Fig. A1.62: Surface deformation profile, composite foundation bed with encased stone columns (Full length encasement, h/D = 0.9) -Test series 24

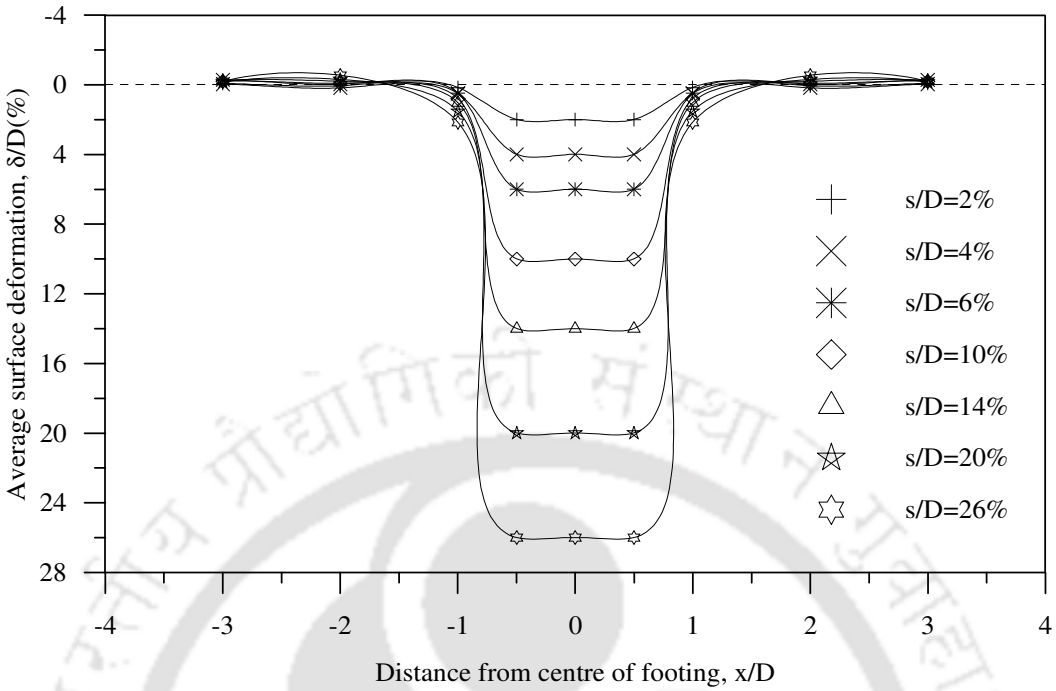

Fig.A1.63: Surface deformation profile, composite foundation bed with encased stone columns and base geogrid (L_{esc}/d_{sc} = 3, h/D = 0.53) - Test series 25

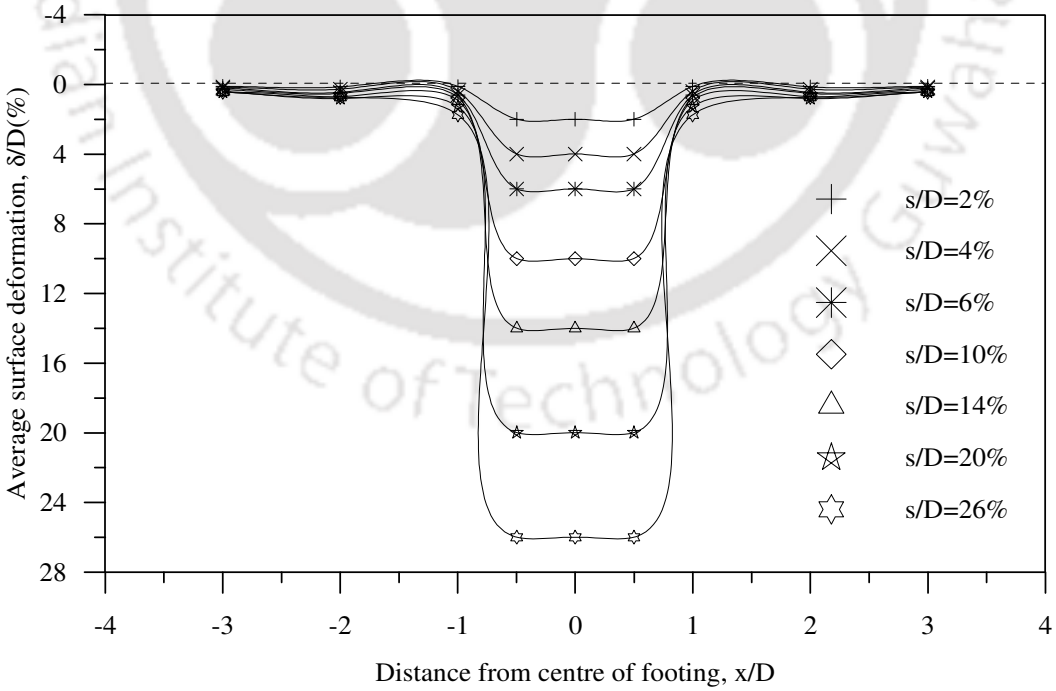

Fig.A1.64: Surface deformation profile, composite foundation bed with encased stone columns and base geogrid (L_{esc}/d_{sc} = 3, h/D = 0.9) - Test series 25

APPENDIX II

PERFORMANCE IMPROVEMENT FACTORS

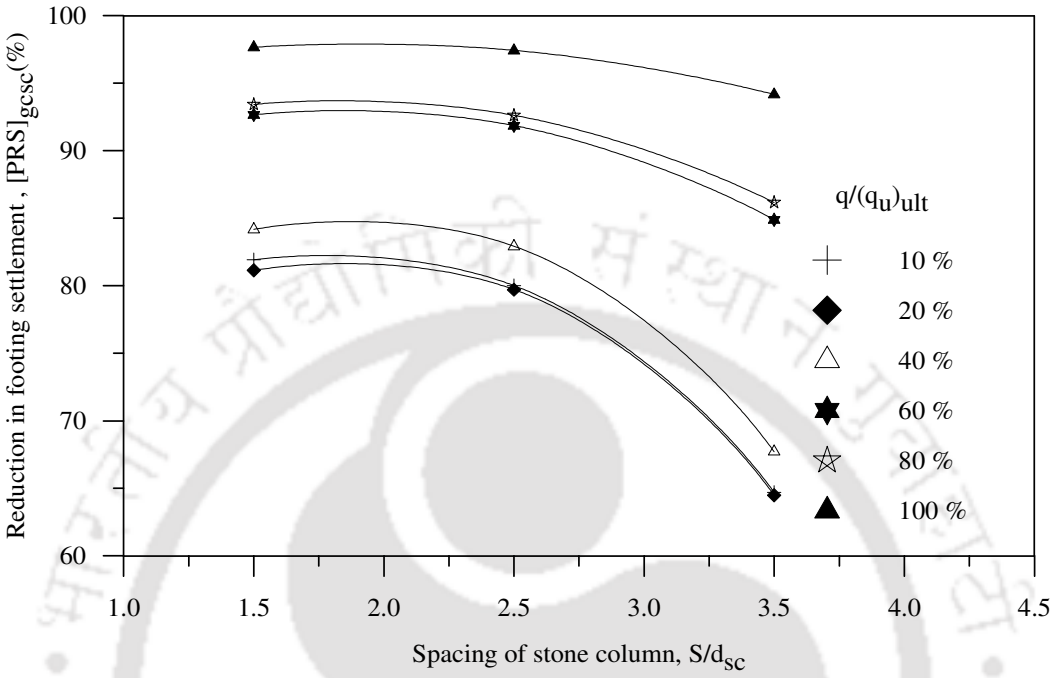

Fig.A2.1: Settlement reduction factor vs. spacing of stone columns, composite foundation bed (h/D = 0.9, L/d_{sc} = 5) – Test series 14

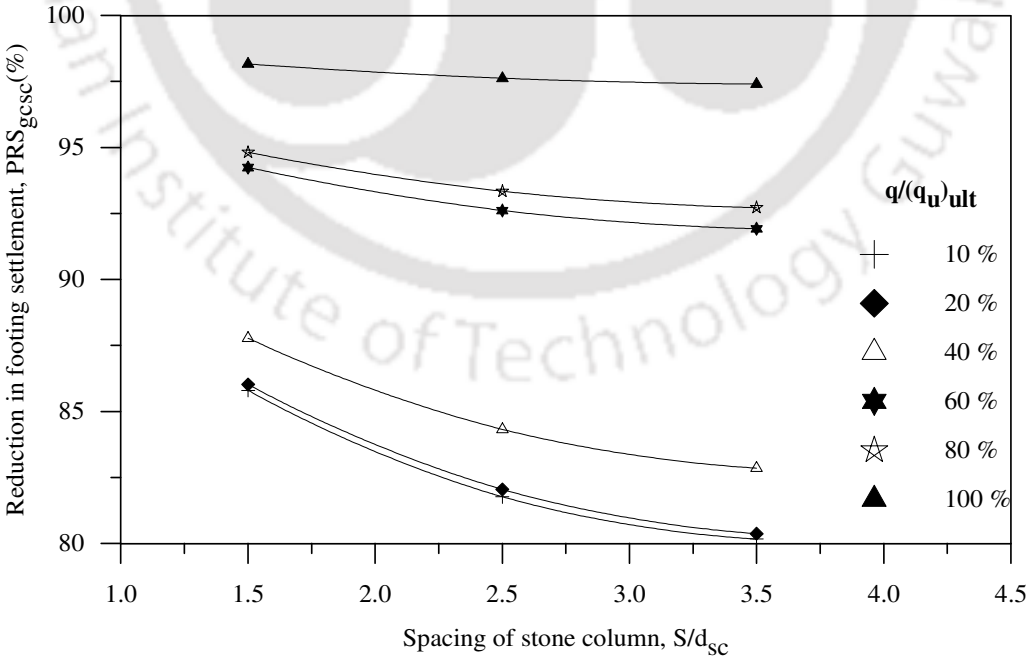

Fig.A2.2: Settlement reduction factor vs. spacing of stone columns, composite foundation bed (h/D = 1.6, L/d_{sc} = 5) – Test series 16

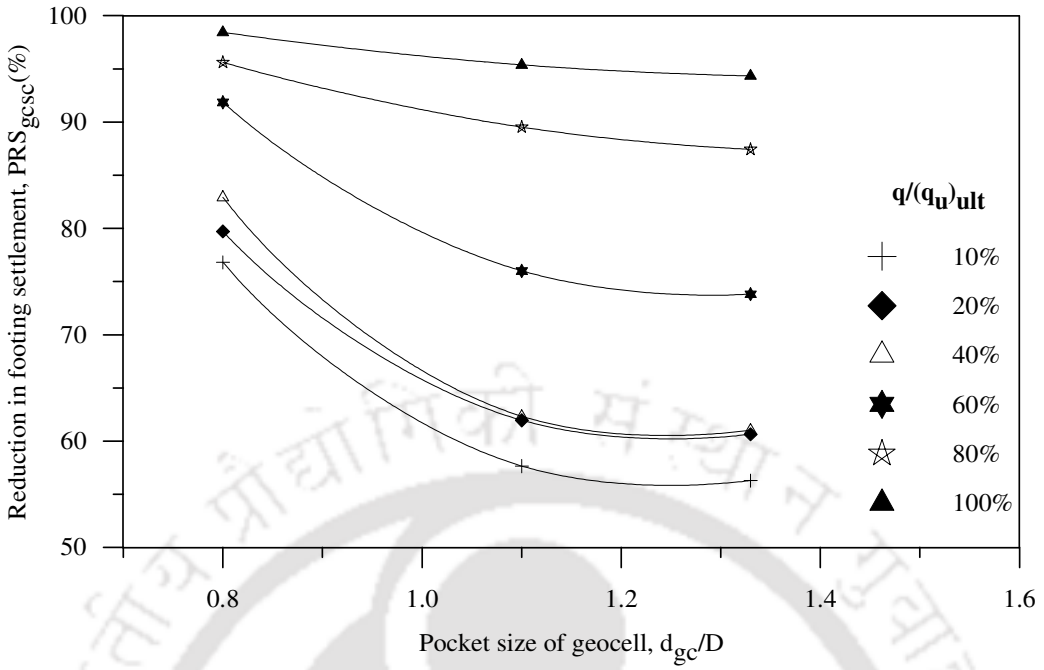

Fig.A2.3: Settlement reduction factor vs. pocket size of geocells, composite foundation bed (h/D = 0.9, S/d_{sc} = 2.5) – Test series 18

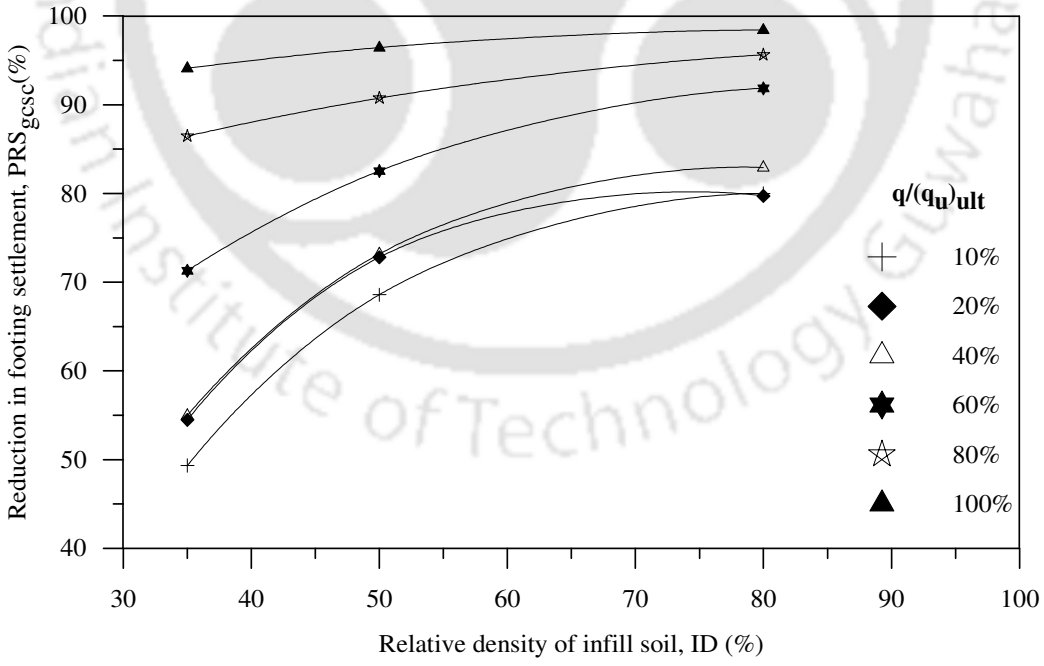

Fig.A2.4: Settlement reduction factor vs. relative density of infill soil, composite foundation bed (h/D = 0.9, S/d_{sc} = 2.5) – Test series 20

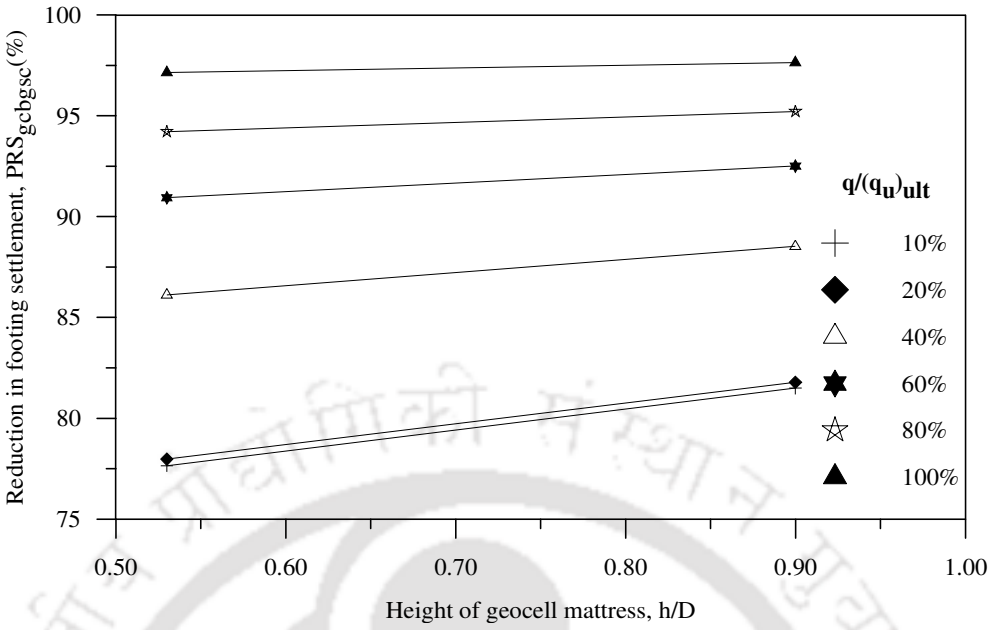

Fig.A2.5: Settlement reduction factor vs. height of geocell mattress, composite foundation bed with base geogrid layer – Test series 21

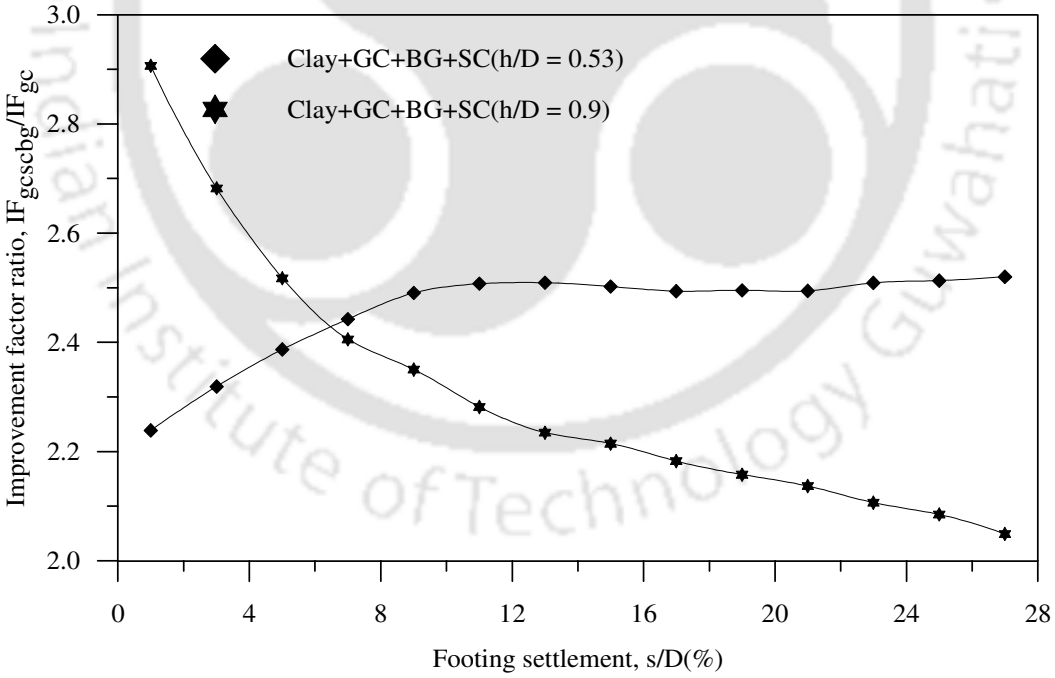

Fig.A2.6: Bearing capacity improvement factor ratio vs. footing settlement, contribution of stone columns and base geogrid in composite foundation bed – Test series 21

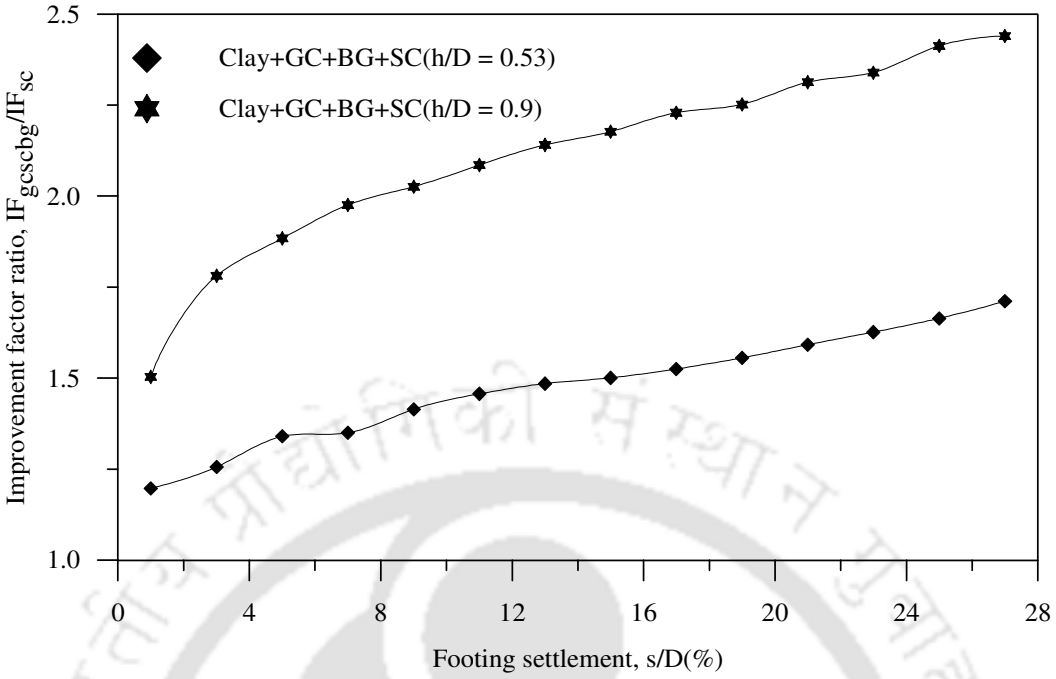

Fig.A2.7: Improvement factor ratio vs. footing settlement, contribution of geocell and base geogrid in composite foundation bed – Test series 21

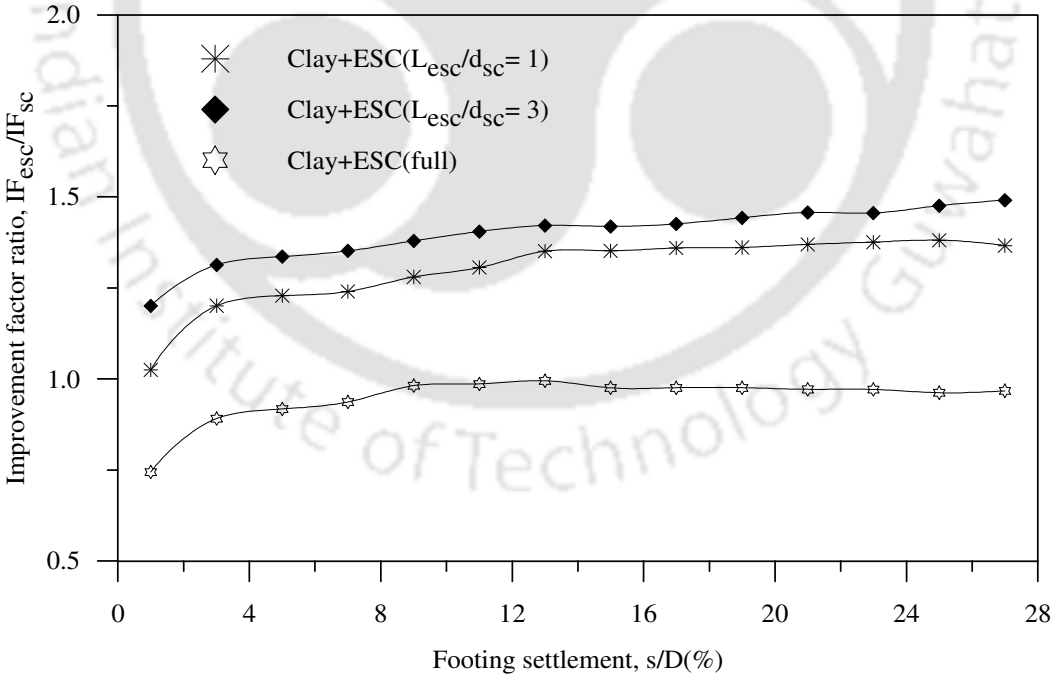

Fig.A2.8: Improvement factor ratio vs. footing settlement, contribution of encasement of stone columns – Test series 22

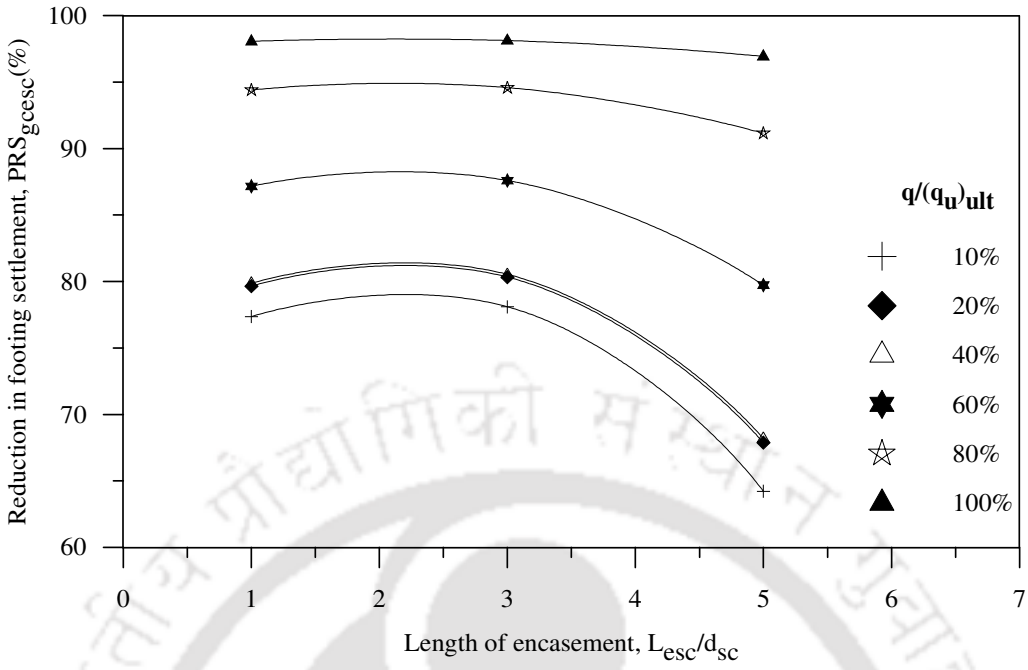

Fig.A2.9: Settlement reduction factor vs. length of encasement, composite foundation bed with encased stone columns (h/D = 0.53) – Test series 23

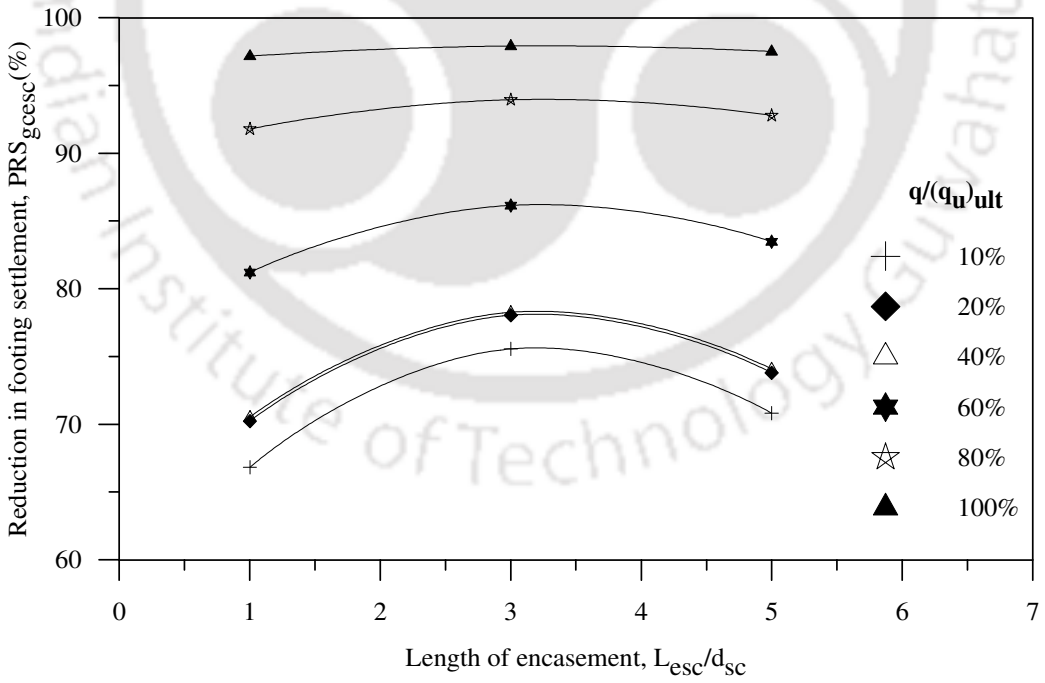

Fig.A2.10: Settlement reduction factor vs. length of encasement of stone columns, composite foundation bed with encased stone columns (h/D = 0.9) – Test series 24

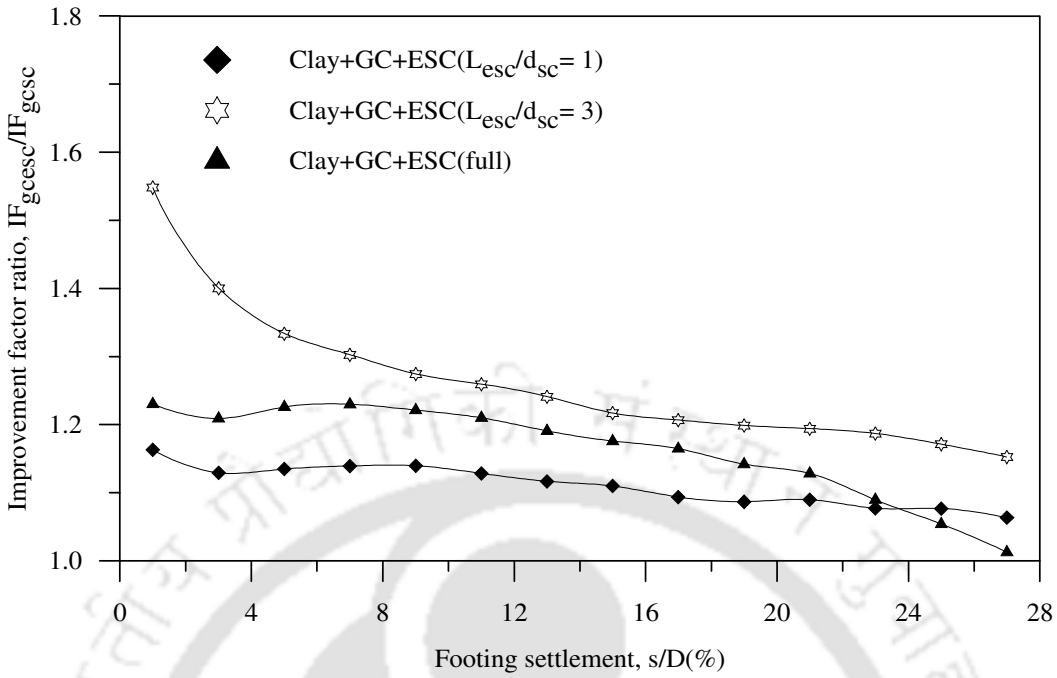

Fig.A2.11: Improvement factor ratio vs. footing settlement, contribution of encasement of stone columns in composite foundation bed (h/D = 0.9) – Test series 24

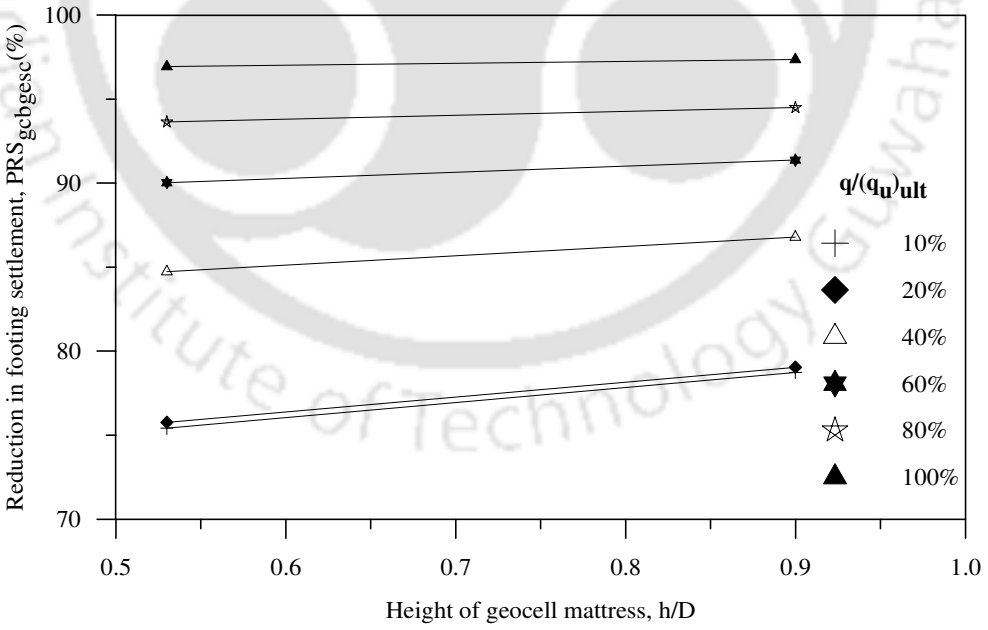

Fig.A2.12: Settlement reduction factor vs. height of geocell mattress, composite foundation bed with base grid and encased stone columns (L_{esc}/d_{sc} = 3) – Test series 25